

UNIVERSIDADE FEDERAL DE SÃO CARLOS

CENTRO DE CIÊNCIAS EXATAS E DE TECNOLOGIA

DEPARTAMENTO DE QUÍMICA

PROGRAMA DE PÓS-GRADUAÇÃO EM QUÍMICA

**“SYNTHESIS OF *N*-HETEROCYCLES AND BUILDING
BLOCKS USING MULTICOMPONENT,
PHOTOCHEMICAL AND ELECTROCHEMICAL
APPROACHES”**

Aloisio de Andrade Bartolomeu*

Tese apresentada como parte dos
requisitos para obtenção do título de
DOUTOR EM CIÊNCIAS, área de
concentração: QUÍMICA ORGÂNICA.

Orientador: Prof. Dr. Kleber Thiago de Oliveira

***Bolsista FAPESP**

**São Carlos - SP
2020**

Approval Sheet



UNIVERSIDADE FEDERAL DE SÃO CARLOS

Centro de Ciências Exatas e de Tecnologia
Programa de Pós-Graduação em Química

Folha de Aprovação

Assinaturas dos membros da comissão examinadora que avaliou e aprovou a Defesa de Tese de Doutorado do candidato Aloisio de Andrade Bartolomeu, realizada em 17/02/2020:

Kleber Thiago de Oliveira

Prof. Dr. Kleber Thiago de Oliveira
UFSCar

Ronaldo Aloise Pili

Prof. Dr. Ronaldo Aloise Pili
UNICAMP

Márcio Weber Paixão

Prof. Dr. Márcio Weber Paixão
UFSCar

Giovanni Wilson Amarante

Prof. Dr. Giovanni Wilson Amarante
UFJF

Timothy John Brocksom

Prof. Dr. Timothy John Brocksom
UFSCar

I dedicate this work to my family, and especially to my father, Salvador Bartolomeu, who is my example of strength, honesty, and joy for life.

Acknowledgments

First of all, I would like to thank God for giving me the gift of life, good health, strength, and wisdom to conduct this research.

I would like to thank my family for believing in me, supporting my choices, and helping me to overcome all obstacles.

I am forever grateful to my supervisor, Prof. Dr. Kleber Thiago de Oliveira, for his guidance, enthusiasm, friendship, support, patience, and the opportunity to perform research in his laboratory.

My special thanks to Prof. Dr. Luiz Carlos da Silva Filho for his friendship and collaboration in the first chapter of this thesis.

I would also like to express my profound gratitude to Prof. Dr. Timothy Noël (TU/e, The Netherlands) for giving me the opportunity to work in his research group and live in the Netherlands.

I am grateful to Ph.D. student Gabriele Laudadio for his help and fruitful collaboration during my time at the Eindhoven University of Technology (TU/e).

I am also grateful to Ph.D. student Rodrigo Costa e Silva for his help and discussions; without him the JOC paper would not have been published in time.

I also thank Prof. Dr. Timothy John Brocksom, an exceptional organic chemist, for all his teachings, fruitful discussions, and scientific contributions.

My sincere thanks to all members, past and present, of Laboratório de Química Bio-Orgânica (LQBO/UFSCar) for the friendly atmosphere and interesting discussions about the ups and downs of research and graduate student life over coffee breaks. Similarly, I need to thank the members of the Noël group who kindly devoted time and effort to help me on numerous occasions. Thank you, guys! You've made my days so much more enjoyable.

Special thanks to the former laboratory technician Vinícius Wellington dos Santos de Souza for his willingness to always keep the lab functioning.

Thanks to Prof. Dr. Rose Maria Carlos from Laboratório de Fotoquímica Inorgânica e Bioinorgânica (LaFIB/DQ/UFSCar) for the fluorimeter facilities.

Thanks to Prof. Dr. Quezia Bezerra Cass from Núcleo de Pesquisa em Cromatografia (Separare/DQ/UFSCar) for HRMS analyses.

Thanks to Prof. Dr. Norberto Peporine Lopes and technician Jacqueline Nakau Mendonça from Núcleo de Pesquisa em Produtos Naturais e Sintéticos (NPPNS/FCFRP/USP) for MALDI-TOF analyses of phthalocyanines.

Thanks to Prof. Dr. Antonio Gilberto Ferreira and technician Luciana Vizotto from Laboratório de Ressonância Magnética Nuclear (DQ/UFSCar) for NMR analyses.

Thanks to the Companhia Brasileira de Metalurgia e Mineração (CBMM) for NbCl₅ samples.

A very special thanks to the Fundação de Amparo à Pesquisa do Estado de São Paulo (FAPESP) for their financial support and for providing a Ph.D. scholarship [Grant number: 2014/24506-3], and a research internship abroad scholarship (BEPE) [Grant number: 2018/08772-6].

Thanks to the Coordenação de Aperfeiçoamento de Pessoal de Nível Superior (Capes) for granting a Ph.D. scholarship for a period of two months.

I would like to thank the Federal University of São Carlos (UFSCar) and the Graduate Program in Chemistry (PPGQ/UFSCar) for their support during this journey. Similarly, I need to thank the Eindhoven University of Technology (TU/e) and the Chemical Engineering and Chemistry department for their support.

This study was financed in part by the Coordenação de Aperfeiçoamento de Pessoal de Nível Superior - Brasil (CAPES) - Finance Code 001.

Thank you!

“Success is not [an] accident. It is hard work, perseverance, learning, studying, sacrifice, and most of all, love of what you are doing or learning to do.”—

Pelé, King of Soccer

List of Abbreviations

- TLC – Thin layer chromatography
- FT-IR – Fourier transform infrared spectroscopy
- HRMS – High-resolution mass spectrometry
- MALDI-TOF – Matrix-assisted laser desorption/ionization time-of-flight
- ESI-TOF – Electrospray ionization time-of-flight
- GC-MS – Gas chromatography coupled with mass spectrometry
- GC-FID – Gas chromatography with flame ionization detection
- ^1H NMR – Proton nuclear magnetic resonance
- ^{13}C NMR – Carbon-13 nuclear magnetic resonance
- DEPT-135 – Distortionless enhancement of polarization transfer (135° decoupling pulse)
- ^{19}F NMR – Fluorine-19 nuclear magnetic resonance
- UV-Vis – Ultraviolet-visible spectroscopy
- CV – Cyclic voltammetry
- Φ_{F} – Fluorescence quantum yield
- r.t. – Room temperature
- PTFE – Polytetrafluoroethylene
- PTFA – Perfluoroalkoxy alkane
- TEMPO – 2,2,6,6-Tetramethyl-1-piperidinyloxy free radical
- BHT – 2,6-Di-*tert*-butyl-*p*-cresol
- HMDS – Hexamethyldisilazane
- DBU – 1,8-Diazabicyclo[5.4.0]undec-7-ene
- DBN – 1,5-Diazabicyclo[4.3.0]non-5-ene
- DDQ – 2,3-Dichloro-5,6-dicyano-*p*-benzoquinone
- Dyad – a supramolecular structure consisting of two distinct linked components or subunits

PCs – Phthalocyanines

MPCs – Metallophthalocyanines

ZnPC – Zinc phthalocyanine

H₂PC – Metal-free phthalocyanine

Zn(OTf)₂ – Zinc trifluoromethanesulfonate

PDT – Photodynamic therapy

MCRs – Multicomponent reactions

S_NAr – Nucleophilic aromatic substitution reaction

S_{NR}1 – Monomolecular radical nucleophilic substitution reaction

Ru(bpy)₃Cl₂·6H₂O – Tris(2,2'-bipyridyl)dichlororuthenium(II) hexahydrate

SET – Single electron transfer

CT band – Charge transfer band

EDA complex – Electron donor-acceptor complex

Pd₂(dba)₃ – Tris(dibenzylideneacetone)dipalladium(0)

dppf – 1,1'-Bis(diphenylphosphino)ferrocene

TBAF – Tetrabutylammonium fluoride

PyFluor – 2-Pyridinesulfonyl fluoride

Selectfluor – 1-Chloromethyl-4-fluoro-1,4-diazoniabicyclo[2.2.2]octane bis(tetrafluoroborate)

(*n*-Bu)₃NMeO₃SOMe – Tributylmethylammonium methyl sulfate

DMAP – 4-(Dimethylamino)pyridine

GC – Glassy carbon

SCE – Saturated calomel electrode

RVC – Reticulated vitreous carbon

HFIP – 1,1,1,3,3,3-Hexafluoroisopropanol

DHFR inhibitor – Dihydrofolate reductase inhibitor

DcpS inhibitor – Scavenger mRNA-decapping enzyme inhibitor

HOMO – Highest occupied molecular orbital

LUMO – Lowest unoccupied molecular orbital

SuFEx – Sulfur(VI) fluoride exchange

DABSO – 1,4-Diazabicyclo[2.2.2]octane bis(sulfur dioxide) adduct

PTSA – *p*-Toluenesulfonic acid

18-Crown-6 – 1,4,7,10,13,16-Hexaoxacyclooctadecane

List of Tables

Table 1.1 – Results obtained and reported for the synthesis of compounds 1.75-1.77	19
Table 1.2 – Synthesis of phthalonitriles 1.80a-i	20
Table 1.3 – Synthesis of phthalonitriles 1.80j-p	22
Table 1.4 – Photophysical parameters of ZnPCs 1.81a-c in THF.....	28
Table 1.5 – Data for obtainment of Φ_F for ZnPCs 1.81a-c	50
Table 1.6 – Data for obtainment of ϵ for ZnPC 1.81a	51
Table 1.7 – Data for obtainment of ϵ for ZnPC 1.81b	52
Table 1.8 – Data for obtainment of ϵ for ZnPC 1.81c	52
Table 2.1 – Screening of the reaction conditions.....	72
Table 3.1 – Preliminary experiments.....	131
Table 3.2 – Amount of pyridine.....	132
Table 3.3 – Additive screening.....	133
Table 3.4 – Fluorine sources.....	134
Table 3.5 – Evaluation of the total amount of KF.....	135
Table 3.6 – Influence of supporting electrolyte.....	135
Table 3.7 – Constant current screening.....	136
Table 3.8 – Further optimization screening.....	137
Table 3.9 – Thiophenol quenching experiment.....	172
Table 3.10 – Diphenyl disulfide quenching experiment.....	173

List of Figures

Figure 1.1 – Chemical structure and nomenclature of the phthalocyanine core.	1
Figure 1.2 – Phthalocyanine precursors.	2
Figure 1.3 – (a) UV-Vis spectra of H ₂ PC(<i>t</i> -butyl) ₈ (blue line) and ZnPC(<i>t</i> -butyl) ₈ (red line) in EtOAc. (b) Schematic representation of the energy levels and transitions (Q- and B-bands) in a metallated phthalocyanine.	3
Figure 1.4 – Phthalocyanine core functionalizations.	5
Figure 1.5 – Some isolated intermediates in PC synthesis.	8
Figure 1.6 – ¹ H NMR (400 MHz) spectra in CDCl ₃ of 1.80c (a) and 1.80q (b).	25
Figure 1.7 – Comparison of HRMS spectra of 1.80c (a) and 1.80q (b).	25
Figure 1.8 – Aggregation behavior of ZnPc 1.81a in THF at different concentrations.	27
Figure 1.9 – Normalized emission spectra for Std-ZnPc (black line), 1.81a (red line), 1.81b (blue line) and 1.81c (green line).	28
Figure 1.10 – Photobleaching study of ZnPc 1.81a in THF.	29
Figure 1.11 – Aggregation behavior of ZnPC 1.81b in THF at different concentrations.	48
Figure 1.12 – Aggregation behavior of ZnPC 1.81c in THF at different concentrations.	49
Figure 1.13 – Emission spectra of ZnPCs 1.81a-c and standard ZnPC.	50
Figure 1.14 – Experimental setup used in the photobleaching studies.	53
Figure 1.15 – Photobleaching study of ZnPC 1.81b in THF.	54
Figure 1.16 – Photobleaching study of ZnPC 1.81c in THF.	54
Figure 2.1 – Structures of drugs that contain the pyridine nucleus directly linked to aryl or heteroaryl units.	69
Figure 2.2 – Unsuccessful substrates in our photochemical approach.	76
Figure 2.3 – Mechanistic studies by UV-Vis spectroscopy.	79
Figure 2.4 – ¹ H NMR spectrum for 2.20a , 2.21a , and their mixture in D ₂ O.	81
Figure 2.5 – ¹ H NMR spectrum for 2.20a' , 2.21a , and their mixture in D ₂ O.	82
Figure 2.6 – Components of the photoreactor.	86
Figure 2.7 – Step-by-step photoreactor assembly.	87
Figure 2.8 – Aggregation studies by ¹ H NMR spectroscopy.	100
Figure 2.9 – (a) Chromatogram of the crude reaction mixture in the absence of Ru(bpy) ₃ Cl ₂ . (b) GC-MS spectrum of <i>O</i> -arylated-TEMPO product.	101

Figure 2.10 – (a) Chromatogram of the crude reaction mixture in the presence of Ru(bpy) ₃ Cl ₂ . (b) GC-MS spectrum of <i>O</i> -arylated-TEMPO product.	102
Figure 2.11 – Correlation map ¹ H- ¹⁵ N HMBC.....	105
Figure 3.1 – Typical glass cells used for electrosynthesis.	118
Figure 3.2 – Schematic diagram of the electron transfer on the surface of the electrode.	119
Figure 3.3 – Different operation modes of electrodes in electrochemical processes.	120
Figure 3.4 – Representative sulfonyl fluorides and their function.	128
Figure 3.5 – List of unsuccessful substrates in our electrochemical approach.	141
Figure 3.6 – Mechanistic investigation of the electrochemical sulfonyl fluoride synthesis..	142
Figure 3.7 – Mechanistic studies by GC-MS.	146
Figure 3.8 – Right: Assembled electrochemical flow reactor. Left: Components of the flow reactor.....	150
Figure 3.9 – Top: Assembled electrochemical batch reactor. Bottom: Components of the batch reactor.....	151
Figure 3.10 – Kinetic experiment at constant potential conditions. 1D ¹⁹ F NMR stacked spectra for the time course array of the reaction from 0 to 9 h reaction time. Top: Full range stacked spectra. Bottom: Zoom from -63.0 to -60.0 ppm.	165
Figure 3.11 – Kinetic experiment at constant potential conditions. Top: Integration of peaks of the ¹⁹ F NMR plot. Bottom: Current intensity over time.....	166
Figure 3.12 – Kinetic experiment at constant current conditions. 1D ¹⁹ F NMR stacked spectra for the time course array of the reaction from 0 to 24 h reaction time. Top: Full range stacked spectra. Bottom: Zoom from -63.0 to -60.0 ppm.	168
Figure 3.13 – Kinetic experiment at constant current conditions. Top: Integration of peaks of the ¹⁹ F NMR plot. Bottom: Applied voltage over time.....	168
Figure 3.14 – Kinetic experiment at constant current under an inert atmosphere. 1D ¹⁹ F NMR stacked spectra for the time course array of the reaction from 0 to 12 h reaction time. Top: Full range stacked spectra. Bottom: Zoom from -63.0 to -60.0 ppm.	170
Figure 3.15 – Kinetic experiment at constant current under an inert atmosphere. Top: Integration of peaks of the ¹⁹ F NMR plot. Bottom: Applied voltage over time.....	171
Figure 3.16 – Cyclic voltammogram of blank solution.....	177
Figure 3.17 – Cyclic voltammograms of thiophenol.....	177
Figure 3.18 – Cyclic voltammogram of KF.	178
Figure 3.19 – Cyclic voltammogram of diphenyl disulfide.	178
Figure 3.20 – Cyclic voltammogram of pyridine.	179

Figure 3.21 – Cyclic voltammograms of mixture of pyridine with KF.	179
Figure 3.22 – Cyclic voltammograms of reaction mixture (Py + KF + PhSH).....	180
Figure 3.23 – Cyclic voltammograms of reaction mixture (Py + KF + PhSSPh).	180
Figure 3.24 – Cyclic voltammograms of Et ₃ N.	181
Figure 3.25 – Cyclic voltammograms of reaction mixture (Et ₃ N + KF + PhSSPh).	182
Figure 3.26 – Formation of fluorinating species via anion exchange.	183
Figure 4.1 – ¹ H NMR spectrum of compound 1.77 in CDCl ₃	193
Figure 4.2 – ¹³ C NMR spectrum of compound 1.77 in CDCl ₃	194
Figure 4.3 – ¹³ C DEPT-135 NMR spectrum of compound 1.77 in CDCl ₃	194
Figure 4.4 – ¹ H NMR spectrum of compound 1.78g in CDCl ₃	195
Figure 4.5 – ¹³ C NMR spectrum of compound 1.78g in CDCl ₃	196
Figure 4.6 – ¹³ C DEPT-135 NMR spectrum of compound 1.78g in CDCl ₃	196
Figure 4.7 – ¹ H NMR spectrum of compound 1.80a in CDCl ₃	197
Figure 4.8 – ¹³ C NMR spectrum of compound 1.80a in CDCl ₃	198
Figure 4.9 – ¹³ C DEPT-135 NMR spectrum of compound 1.80a in CDCl ₃	198
Figure 4.10 – ¹ H NMR spectrum of compound 1.80b in CDCl ₃	199
Figure 4.11 – ¹³ C NMR spectrum of compound 1.80b in CDCl ₃	200
Figure 4.12 – ¹³ C DEPT-135 NMR spectrum of compound 1.80b in CDCl ₃	200
Figure 4.13 – ¹ H NMR spectrum of compound 1.80c in CDCl ₃	201
Figure 4.14 – ¹³ C NMR spectrum of compound 1.80c in CDCl ₃	202
Figure 4.15 – ¹³ C DEPT-135 NMR spectrum of compound 1.80c in CDCl ₃	202
Figure 4.16 – ¹ H NMR spectrum of compound 1.80d in CDCl ₃	203
Figure 4.17 – ¹³ C NMR spectrum of compound 1.80d in CDCl ₃	204
Figure 4.18 – ¹³ C DEPT-135 NMR spectrum of compound 1.80d in CDCl ₃	204
Figure 4.19 – ¹ H NMR spectrum of compound 1.80e in CDCl ₃	205
Figure 4.20 – ¹³ C NMR spectrum of compound 1.80e in CDCl ₃	206
Figure 4.21 – ¹³ C DEPT-135 NMR spectrum of compound 1.80e in CDCl ₃	206
Figure 4.22 – ¹ H NMR spectrum of compound 1.80f in CDCl ₃	207
Figure 4.23 – ¹³ C NMR spectrum of compound 1.80f in CDCl ₃	208
Figure 4.24 – ¹³ C DEPT-135 NMR spectrum of compound 1.80f in CDCl ₃	208
Figure 4.25 – ¹ H NMR spectrum of compound 1.80g in CDCl ₃	209
Figure 4.26 – ¹³ C NMR spectrum of compound 1.80g in CDCl ₃	210
Figure 4.27 – ¹³ C DEPT-135 NMR spectrum of compound 1.80g in CDCl ₃	210
Figure 4.28 – ¹ H NMR spectrum of compound 1.80h in CDCl ₃	211

Figure 4.29 – ^{13}C NMR spectrum of compound 1.80h in CDCl_3 .	212
Figure 4.30 – ^{13}C DEPT-135 NMR spectrum of compound 1.80h in CDCl_3 .	212
Figure 4.31 – ^1H NMR spectrum of compound 1.80i in CDCl_3 .	213
Figure 4.32 – ^{13}C NMR spectrum of compound 1.80i in CDCl_3 .	214
Figure 4.33 – ^{13}C DEPT-135 NMR spectrum of compound 1.80i in CDCl_3 .	214
Figure 4.34 – ^1H NMR spectrum of compound 1.80j in CDCl_3 .	215
Figure 4.35 – ^{13}C NMR spectrum of compound 1.80j in CDCl_3 .	216
Figure 4.36 – ^{13}C DEPT-135 NMR spectrum of compound 1.80j in CDCl_3 .	216
Figure 4.37 – ^1H NMR spectrum of compound 1.80k in CDCl_3 .	217
Figure 4.38 – ^{13}C NMR spectrum of compound 1.80k in CDCl_3 .	218
Figure 4.39 – ^{13}C DEPT-135 NMR spectrum of compound 1.80k in CDCl_3 .	218
Figure 4.40 – ^1H NMR spectrum of compound 1.80l in CDCl_3 .	219
Figure 4.41 – ^{13}C NMR spectrum of compound 1.80l in CDCl_3 .	220
Figure 4.42 – ^{13}C DEPT-135 NMR spectrum of compound 1.80l in CDCl_3 .	220
Figure 4.43 – ^1H NMR spectrum of compound 1.80m in CDCl_3 .	221
Figure 4.44 – ^1H NMR spectrum of compound 1.80n in CDCl_3 .	222
Figure 4.45 – ^{13}C NMR spectrum of compound 1.80n in CDCl_3 .	223
Figure 4.46 – ^{13}C DEPT-135 NMR spectrum of compound 1.80n in CDCl_3 .	223
Figure 4.47 – ^1H NMR spectrum of compound 1.80o in CDCl_3 .	224
Figure 4.48 – ^1H NMR spectrum of compound 1.80p in CDCl_3 .	225
Figure 4.49 – ^{13}C NMR spectrum of compound 1.80p in CDCl_3 .	226
Figure 4.50 – ^{13}C DEPT-135 NMR spectrum of compound 1.80p in CDCl_3 .	226
Figure 4.51 – ^1H NMR spectrum of compound 1.80q in CDCl_3 .	227
Figure 4.52 – ^{13}C NMR spectrum of compound 1.80q in CDCl_3 .	228
Figure 4.53 – ^{13}C DEPT-135 NMR spectrum of compound 1.80q in CDCl_3 .	228
Figure 4.54 – ^1H NMR spectrum of compound 1.81a in $\text{CDCl}_3/\text{DMSO-}d_6$ (2:1).	229
Figure 4.55 – ^1H NMR spectrum of compound 1.81b in $\text{CDCl}_3/\text{DMSO-}d_6$ (2:1).	230
Figure 4.56 – ^1H NMR spectrum of compound 1.81c in $\text{CDCl}_3/\text{DMSO-}d_6$ (2:1).	231
Figure 4.57 – ^1H NMR spectrum of compound 2.22a – 2 aryl in CDCl_3 .	232
Figure 4.58 – ^{13}C NMR spectrum of compound 2.22a – 2 aryl in CDCl_3 .	233
Figure 4.59 – ^1H NMR spectrum of compound 2.22a – 4 aryl in CDCl_3 .	234
Figure 4.60 – ^{13}C NMR spectrum of compound 2.22a – 4 aryl in CDCl_3 .	235
Figure 4.61 – ^1H NMR spectrum of compound 2.22b – 2 aryl in CDCl_3 .	236
Figure 4.62 – ^{13}C NMR spectrum of compound 2.22b – 2 aryl in CDCl_3 .	237

Figure 4.63 – ^1H NMR spectrum of compound 2.22b – 4 aryl in CDCl_3	238
Figure 4.64 – ^{13}C NMR spectrum of compound 2.22b – 4 aryl in CDCl_3	239
Figure 4.65 – ^1H NMR spectrum of compound 2.22c – 2 aryl in CDCl_3	240
Figure 4.66 – ^{13}C NMR spectrum of compound 2.22c – 2 aryl in CDCl_3	241
Figure 4.67 – ^1H NMR spectrum of compound 2.22c – 4 aryl in CDCl_3	242
Figure 4.68 – ^{13}C NMR spectrum of compound 2.22c – 4 aryl in CDCl_3	243
Figure 4.69 – ^1H NMR spectrum of compound 2.22d – 2 aryl in CDCl_3	244
Figure 4.70 – ^{13}C NMR spectrum of compound 2.22d – 2 aryl in CDCl_3	245
Figure 4.71 – ^1H NMR spectrum of compound 2.22d – 4 aryl in CDCl_3	246
Figure 4.72 – ^{13}C NMR spectrum of compound 2.22d – 4 aryl in CDCl_3	247
Figure 4.73 – ^1H NMR spectrum of compound 2.22e – 2 aryl in $(\text{CD}_3)_2\text{CO}$	248
Figure 4.74 – ^{13}C NMR spectrum of compound 2.22e – 2 aryl in $(\text{CD}_3)_2\text{CO}$	249
Figure 4.75 – ^1H NMR spectrum of compound 2.22e – 4 aryl in CDCl_3	250
Figure 4.76 – ^{13}C NMR spectrum of compound 2.22e – 4 aryl in CDCl_3	251
Figure 4.77 – ^1H NMR spectrum of compound 2.22f – 2 aryl in $(\text{CD}_3)_2\text{CO}$	252
Figure 4.78 – ^{13}C NMR spectrum of compound 2.22f – 2 aryl in $(\text{CD}_3)_2\text{CO}$	253
Figure 4.79 – ^1H NMR spectrum of compound 2.22f – 4 aryl in $(\text{CD}_3)_2\text{CO}$	254
Figure 4.80 – ^{13}C NMR spectrum of compound 2.22f – 4 aryl in $(\text{CD}_3)_2\text{CO}$	255
Figure 4.81 – ^1H NMR spectrum of compound 2.22g – 2 aryl in CDCl_3	256
Figure 4.82 – ^{13}C NMR spectrum of compound 2.22g – 2 aryl in CDCl_3	257
Figure 4.83 – ^1H NMR spectrum of compound 2.22g – 4 aryl in CDCl_3	258
Figure 4.84 – ^{13}C NMR spectrum of compound 2.22g – 4 aryl in CDCl_3	259
Figure 4.85 – ^1H NMR spectrum of compound 2.22h – 2 aryl in CDCl_3	260
Figure 4.86 – ^{13}C NMR spectrum of compound 2.22h – 2 aryl in CDCl_3	261
Figure 4.87 – ^1H NMR spectrum of compound 2.22i – 2 aryl in CDCl_3	262
Figure 4.88 – ^{13}C NMR spectrum of compound 2.22i – 2 aryl in CDCl_3	263
Figure 4.89 – ^1H NMR spectrum of compound 2.22i – 4 aryl in CDCl_3	264
Figure 4.90 – ^{13}C NMR spectrum of compound 2.22i – 4 aryl in CDCl_3	265
Figure 4.91 – ^1H NMR spectrum of compound 2.22j – 2 aryl in CDCl_3	266
Figure 4.92 – ^{13}C NMR spectrum of compound 2.22j – 2 aryl in CDCl_3	267
Figure 4.93 – ^1H NMR spectrum of compound 2.22j – 4 aryl in CDCl_3	268
Figure 4.94 – ^{13}C NMR spectrum of compound 2.22j – 4 aryl in CDCl_3	269
Figure 4.95 – ^1H NMR spectrum of compound 2.22k – 2 aryl in CDCl_3	270
Figure 4.96 – ^{13}C NMR spectrum of compound 2.22k – 2 aryl in CDCl_3	271

Figure 4.97 – ^1H NMR spectrum of compound 2.22k – 4 aryl in CDCl_3 .	272
Figure 4.98 – ^{13}C NMR spectrum of compound 2.22k – 4 aryl in CDCl_3 .	273
Figure 4.99 – ^1H NMR spectrum of compound 2.22l – 2 aryl in CDCl_3 .	274
Figure 4.100 – ^{13}C NMR spectrum of compound 2.22l – 2 aryl in CDCl_3 .	275
Figure 4.101 – ^1H NMR spectrum of compound 2.22l – 4 aryl in CDCl_3 .	276
Figure 4.102 – ^{13}C NMR spectrum of compound 2.22l – 4 aryl in CDCl_3 .	277
Figure 4.103 – ^1H NMR spectrum of compound 2.22m – 2 aryl in CDCl_3 .	278
Figure 4.104 – ^{13}C NMR spectrum of compound 2.22m – 2 aryl in CDCl_3 .	279
Figure 4.105 – ^1H NMR spectrum of compound 2.22m – 4 aryl in CDCl_3 .	280
Figure 4.106 – ^{13}C NMR spectrum of compound 2.22m – 4 aryl in CDCl_3 .	281
Figure 4.107 – ^1H NMR spectrum of compound 2.22n – 2 aryl in CDCl_3 .	282
Figure 4.108 – ^{13}C NMR spectrum of compound 2.22n – 2 aryl in CDCl_3 .	283
Figure 4.109 – ^1H NMR spectrum of compound 2.22n – 4 aryl in CDCl_3 .	284
Figure 4.110 – ^{13}C NMR spectrum of compound 2.22n – 4 aryl in CDCl_3 .	285
Figure 4.111 – ^1H NMR spectrum of compound 2.22o – 2 aryl in CDCl_3 .	286
Figure 4.112 – ^{13}C NMR spectrum of compound 2.22o – 2 aryl in CDCl_3 .	287
Figure 4.113 – ^1H NMR spectrum of compound 2.22o – 4 aryl in CDCl_3 .	288
Figure 4.114 – ^{13}C NMR spectrum of compound 2.22o – 4 aryl in CDCl_3 .	289
Figure 4.115 – ^1H NMR spectrum of compound 2.22r – 2 aryl in CDCl_3 .	290
Figure 4.116 – ^{13}C NMR spectrum of compound 2.22r – 2 aryl in CDCl_3 .	291
Figure 4.117 – ^1H NMR spectrum of compound 2.22s – 2 aryl in CDCl_3 .	292
Figure 4.118 – ^{13}C NMR spectrum of compound 2.22s – 2 aryl in CDCl_3 .	293
Figure 4.119 – ^1H NMR spectrum of compound 2.22t – 2 aryl in CDCl_3 .	294
Figure 4.120 – ^{13}C NMR spectrum of compound 2.22t – 2 aryl in CDCl_3 .	295
Figure 4.121 – ^1H NMR spectrum of compound 2.22u – 2 aryl in CDCl_3 .	296
Figure 4.122 – ^{13}C NMR spectrum of compound 2.22u – 2 aryl in CDCl_3 .	297
Figure 4.123 – ^1H NMR spectrum of compound 2.22u – 4 aryl in CDCl_3 .	298
Figure 4.124 – ^{13}C NMR spectrum of compound 2.22u – 4 aryl in CDCl_3 .	299
Figure 4.125 – ^1H NMR spectrum of compound 2.22v in CDCl_3 .	300
Figure 4.126 – ^{13}C NMR spectrum of compound 2.22v in CDCl_3 .	301
Figure 4.127 – ^1H NMR spectrum of compound 2.22w – 2 aryl in CDCl_3 .	302
Figure 4.128 – ^{13}C NMR spectrum of compound 2.22w – 2 aryl in CDCl_3 .	303
Figure 4.129 – ^1H NMR spectrum of compound 2.22w – 4 aryl in CDCl_3 .	304
Figure 4.130 – ^{13}C NMR spectrum of compound 2.22w – 4 aryl in CDCl_3 .	305

Figure 4.131 – ^1H NMR spectrum of compound 2.22x in CDCl_3	306
Figure 4.132 – ^{13}C NMR spectrum of compound 2.22x in CDCl_3	307
Figure 4.133 – ^1H NMR spectrum of compound 3.26a in CDCl_3	308
Figure 4.134 – ^{13}C NMR spectrum of compound 3.26a in CDCl_3	309
Figure 4.135 – ^{19}F NMR spectrum of compound 3.26a in CDCl_3	309
Figure 4.136 – ^1H NMR spectrum of compound 3.26a-der in CDCl_3	310
Figure 4.137 – ^{13}C NMR spectrum of compound 3.26a-der in CDCl_3	311
Figure 4.138 – ^1H NMR spectrum of compound 3.26b in CDCl_3	312
Figure 4.139 – ^{13}C NMR spectrum of compound 3.26b in CDCl_3	313
Figure 4.140 – ^{19}F NMR spectrum of compound 3.26b in CDCl_3	313
Figure 4.141 – ^1H NMR spectrum of compound 3.26c in CDCl_3	314
Figure 4.142 – ^{13}C NMR spectrum of compound 3.26c in CDCl_3	315
Figure 4.143 – ^{19}F NMR spectrum of compound 3.26c in CDCl_3	315
Figure 4.144 – ^1H NMR spectrum of compound 3.26d in CDCl_3	316
Figure 4.145 – ^{13}C NMR spectrum of compound 3.26d in CDCl_3	317
Figure 4.146 – ^{19}F NMR spectrum of compound 3.26d in CDCl_3	317
Figure 4.147 – ^1H NMR spectrum of compound 3.26e in CDCl_3	318
Figure 4.148 – ^{13}C NMR spectrum of compound 3.26e in CDCl_3	319
Figure 4.149 – ^{19}F NMR spectrum of compound 3.26e in CDCl_3	319
Figure 4.150 – ^1H NMR spectrum of compound 3.26f in CDCl_3	320
Figure 4.151 – ^{13}C NMR spectrum of compound 3.26f in CDCl_3	321
Figure 4.152 – ^{19}F NMR spectrum of compound 3.26f in CDCl_3	321
Figure 4.153 – ^1H NMR spectrum of compound 3.26g in CDCl_3	322
Figure 4.154 – ^{13}C NMR spectrum of compound 3.26g in CDCl_3	323
Figure 4.155 – ^{19}F NMR spectrum of compound 3.26g in CDCl_3	323
Figure 4.156 – ^1H NMR spectrum of compound 3.26h in CDCl_3	324
Figure 4.157 – ^{13}C NMR spectrum of compound 3.26h in CDCl_3	325
Figure 4.158 – ^{19}F NMR spectrum of compound 3.26h in CDCl_3	325
Figure 4.159 – ^1H NMR spectrum of compound 3.26i in CDCl_3	326
Figure 4.160 – ^{13}C NMR spectrum of compound 3.26i in CDCl_3	327
Figure 4.161 – ^{19}F NMR spectrum of compound 3.26i in CDCl_3	327
Figure 4.162 – ^{19}F NMR spectrum of compound 3.26j in CDCl_3	328
Figure 4.163 – ^{13}C NMR spectrum of compound 3.26j in CDCl_3	329
Figure 4.164 – ^1H NMR spectrum of compound 3.26j-der in CDCl_3	330

Figure 4.165 – ^{13}C NMR spectrum of compound 3.26j-der in CDCl_3 .	331
Figure 4.166 – ^{19}F NMR spectrum of compound 3.26j-der in CDCl_3 .	331
Figure 4.167 – ^1H NMR spectrum of compound 3.26k in CDCl_3 .	332
Figure 4.168 – ^{13}C NMR spectrum of compound 3.26k in CDCl_3 .	333
Figure 4.169 – ^{19}F NMR spectrum of compound 3.26k in CDCl_3 .	333
Figure 4.170 – ^1H NMR spectrum of compound 3.26l in CDCl_3 .	334
Figure 4.171 – ^{13}C NMR spectrum of compound 3.26l in CDCl_3 .	335
Figure 4.172 – ^{19}F NMR spectrum of compound 3.26l in CDCl_3 .	335
Figure 4.173 – ^1H NMR spectrum of compound 3.26m in CDCl_3 .	336
Figure 4.174 – ^{13}C NMR spectrum of compound 3.26m in CDCl_3 .	337
Figure 4.175 – ^{19}F NMR spectrum of compound 3.26m in CDCl_3 .	337
Figure 4.176 – ^1H NMR spectrum of compound 3.26n in CDCl_3 .	338
Figure 4.177 – ^{13}C NMR spectrum of compound 3.26n in CDCl_3 .	339
Figure 4.178 – ^{19}F NMR spectrum of compound 3.26n in CDCl_3 .	339
Figure 4.179 – ^1H NMR spectrum of compound 3.26o in CDCl_3 .	340
Figure 4.180 – ^{13}C NMR spectrum of compound 3.26o in CDCl_3 .	341
Figure 4.181 – ^{19}F NMR spectrum of compound 3.26o in CDCl_3 .	341
Figure 4.182 – ^1H NMR spectrum of compound 3.26p in CDCl_3 .	342
Figure 4.183 – ^{13}C NMR spectrum of compound 3.26p in CDCl_3 .	343
Figure 4.184 – ^{19}F NMR spectrum of compound 3.26p in CDCl_3 .	343
Figure 4.185 – ^1H NMR spectrum of compound 3.26q in CDCl_3 .	344
Figure 4.186 – ^{13}C NMR spectrum of compound 3.26q in CDCl_3 .	345
Figure 4.187 – ^{19}F NMR spectrum of compound 3.26q in CDCl_3 .	345
Figure 4.188 – ^1H NMR spectrum of compound 3.26r-der in CDCl_3 .	346
Figure 4.189 – ^{13}C NMR spectrum of compound 3.26r-der in CDCl_3 .	347
Figure 4.190 – ^1H NMR spectrum of compound 3.26s-der in CDCl_3 .	348
Figure 4.191 – ^{13}C NMR spectrum of compound 3.26s-der in CDCl_3 .	349
Figure 4.192 – ^1H NMR spectrum of compound 3.26t-der in CDCl_3 .	350
Figure 4.193 – ^{13}C NMR spectrum of compound 3.26t-der in CDCl_3 .	351
Figure 4.194 – ^1H NMR spectrum of compound 3.26u in CDCl_3 .	352
Figure 4.195 – ^{13}C NMR spectrum of compound 3.26u in CDCl_3 .	353
Figure 4.196 – ^{19}F NMR spectrum of compound 3.26u in CDCl_3 .	353
Figure 4.197 – ^1H NMR spectrum of compound 3.26v-der in CDCl_3 .	354
Figure 4.198 – ^{13}C NMR spectrum of compound 3.26v-der in CDCl_3 .	355

Figure 4.199 – ^1H NMR spectrum of compound 3.26w in CDCl_3	356
Figure 4.200 – ^{13}C NMR spectrum of compound 3.26w in CDCl_3	357
Figure 4.201 – ^{19}F NMR spectrum of compound 3.26w in CDCl_3	357
Figure 4.202 – ^1H NMR spectrum of compound 3.26x in CDCl_3	358
Figure 4.203 – ^{13}C NMR spectrum of compound 3.26x in CDCl_3	359
Figure 4.204 – ^{19}F NMR spectrum of compound 3.26x in CDCl_3	359
Figure 4.205 – ^1H NMR spectrum of compound 3.26y in CDCl_3	360
Figure 4.206 – ^{13}C NMR spectrum of compound 3.26y in CDCl_3	361
Figure 4.207 – ^{19}F NMR spectrum of compound 3.26y in CDCl_3	361
Figure 4.208 – ^1H NMR spectrum of compound 3.26z in CDCl_3	362
Figure 4.209 – ^{13}C NMR spectrum of compound 3.26z in CDCl_3	363
Figure 4.210 – ^{19}F NMR spectrum of compound 3.26z in CDCl_3	363
Figure 4.211 – ^1H NMR spectrum of compound 3.26aa in CDCl_3	364
Figure 4.212 – ^{13}C NMR spectrum of compound 3.26aa in CDCl_3	365
Figure 4.213 – ^{19}F NMR spectrum of compound 3.26aa in CDCl_3	365

List of Schemes

Scheme 1.1 – Formation of PC macrocycle by a stepwise mechanism.....	7
Scheme 1.2 – Formation of PC macrocycle by a concerted mechanism.	8
Scheme 1.3 – Synthesis of 4,5-dichlorophthalonitrile.....	9
Scheme 1.4 – Synthesis of 4-trimethylsilyl-phthalonitrile.	10
Scheme 1.5 – Synthesis of 1-alkyl-5,6-dicyanobenzoimidazoles.....	11
Scheme 1.6 – Synthesis of tetrasubstituted phthalonitriles via Diels-Alder chemistry.	11
Scheme 1.7 – Synthesis of acetylenic phthalonitriles via Diels-Alder chemistry.	12
Scheme 1.8 – Synthesis of 3-(4-methyloxycarbonyl)butylphthalonitrile.....	13
Scheme 1.9 – Preparation of dendritic phthalonitriles.....	14
Scheme 1.10 – Preparation of functionalized phthalonitriles 1.57 and 1.58	15
Scheme 1.11 – Pd-Catalyzed Sonogashira coupling reaction of 3-ethynylthiophene with 4,5-dichlorophthalonitrile.....	16
Scheme 1.12 – Pd-Catalyzed Suzuki coupling reaction of phenylboronic acids with 4,5-dichlorophthalonitrile.....	16
Scheme 1.13 – Pd-catalyzed Stille coupling reaction of organostannanes with 4-iodophthalonitrile.....	16
Scheme 1.14 – Pd-Catalyzed Heck–Cassar coupling reaction of terminal alkynes with 4,5-diiodophthalonitrile.....	17
Scheme 1.15 – Synthetic route of 4-formylphthalonitrile.	18
Scheme 1.16 – a) Mechanism proposed by Cao et al. b) Our mechanistic proposal based on experimentation.....	24
Scheme 1.17 – Synthesis of zinc phthalocyanine-quinoline dyads (1.81a-c).	26
Scheme 2.1 – EDA complex formation and its synthetic use enabled by light.	64
Scheme 2.2 – Exciplex complex formation and its synthetic use enabled by light.	65
Scheme 2.3 – EDA complex-photoinduced arylation of pyrroles with diaryliodonium salts.	66
Scheme 2.4 – Photoarylation of 3-hydroxypyridine with aryldiazonium salts.....	67
Scheme 2.5 – Photoarylation of (halo)benzenes with aryldiazonium salts.	68
Scheme 2.6 – Approaches for the synthesis of biaryls containing the pyridine nucleus.	70
Scheme 2.7 – Evaluation of the reaction scope..	74
Scheme 2.8 – Mechanistic investigations.	78

Scheme 2.9 – Proposed mechanism for the visible-light-induced direct C–H arylation of <i>N</i> -heterocycles.....	83
Scheme 3.1 – Indirect electrochemical allylic C–H oxidation.	124
Scheme 3.2 – Electrochemically induced C–C (a), C–N (b), C–O (c), and C–S (d) bonds formation from C–H bonds.....	125
Scheme 3.3 – Electrochemical synthesis of natural products.....	126
Scheme 3.4 – Electrochemical sulfonamide synthesis by direct anodic coupling of thiols and amines.....	127
Scheme 3.5 – Established synthetic routes to prepare sulfonyl fluorides.....	130
Scheme 3.6 – Substrate scope for the electrochemical sulfonyl fluoride synthesis..	139
Scheme 3.7 – Electrochemical synthesis of sulfonyl fluoride from thiosulfonate..	145
Scheme 3.8 – Proposed mechanism 2.....	147
Scheme 3.9 – Kinetic experiment at constant potential conditions.	164
Scheme 3.10 – Kinetic experiment at constant current conditions.....	167
Scheme 3.11 – Kinetic experiment at constant current under an inert atmosphere.....	169
Scheme 3.12 – 1-Fluoropyridinium tetrafluoroborate experiment.	174
Scheme 3.13 – Pyridinium chloride experiment.....	175
Scheme 3.14 – Triethylamine experiment.	176

Resumo

“SÍNTESE DE *N*-HETEROCICLOS E BLOCOS DE CONSTRUÇÃO USANDO ABORDAGENS MULTICOMPONENTE, FOTOQUÍMICA E ELETROQUÍMICA.”

Reações multicomponentes e protocolos mediados por luz e eletroquímica são ferramentas poderosas para a síntese orgânica moderna. Além disso, elas obedecem a vários princípios da química verde, tais como: economia atômica, catálise, redução de resíduos, eficiência energética, condições brandas de reação, etc. Portanto, o desenvolvimento de novas metodologias sintéticas, empregando essas ferramentas poderosas, é altamente desejável e desafiador. O capítulo 1 descreve a eficiência do NbCl_5 para a promoção de RMCs entre 4-formilftalonitrilo, anilinas e fenilacetilenos através de um processo pericíclico de hetero-Diels-Alder. Essa abordagem multicomponente exibiu um amplo escopo de substrato e, para demonstrar a versatilidade da biblioteca de ftalonitrilos, três novos derivados ftalocianínicos foram sintetizados e caracterizados. O capítulo 2 aborda uma metodologia livre de metais para a fotoarilação de piridinas e outros heterociclos (tais como quinolina e quinoxalina) com sais de arenodiazônio, em água, usando um fotorreator construído de forma artesanal. Essa abordagem fotoquímica demonstrou um amplo escopo de substrato em relação ao componente sal de diazônio e investigações adicionais do mecanismo reacional suportam um mecanismo através de um complexo EDA. Finalmente, o capítulo 3 apresenta a síntese de fluoretos de sulfonila através do acoplamento oxidativo eletroquímico de tióis e fluoreto de potássio. Essa abordagem também mostrou um amplo escopo de substrato, incluindo uma variedade de alquil, benzil, aril e heteroaril tióis ou dissulfetos. Além disso, estudos cinéticos e outros estudos adicionais foram realizados na tentativa de esclarecer o mecanismo dessa reação eletroquímica.

Palavras-chave: reações multicomponentes, ftalonitrilo, fotocatálise, eletrossíntese, sal de arenodiazônio, complexo EDA, fluoreto de sulfonila.

Abstract

“SYNTHESIS OF *N*-HETEROCYCLES AND BUILDING BLOCKS USING MULTICOMPONENT, PHOTOCHEMICAL AND ELECTROCHEMICAL APPROACHES.” Multicomponent reactions and protocols mediated by light and electrochemistry are powerful tools for modern organic synthesis. Moreover, they obey several principles of green chemistry such as atom economy, catalysis, waste reduction, energy efficiency, mild reaction conditions, etc. Therefore, the development of new synthetic methodologies employing these powerful tools is highly desirable and challenging. Chapter 1 describes the efficiency of NbCl₅ for the promotion of MCRs between 4-formylphthalonitrile, anilines, and phenylacetylenes through a pericyclic hetero-Diels-Alder process. This multicomponent approach exhibited a wide substrate scope and, to demonstrate the versatility of the phthalonitrile library, we synthesized and characterized three new phthalocyanine derivatives. Chapter 2 covers a metal-free methodology for the photoarylation of pyridines and other heterocycles (such as quinoline and quinoxaline) with aryldiazonium salts in water using a homemade photoreactor. This photochemical approach displayed a broad scope regarding the diazonium salt component and further mechanistic investigations support a mechanism through an EDA complex. Finally, chapter 3 outlines the synthesis of sulfonyl fluorides through electrochemical oxidative coupling of thiols and potassium fluoride. This approach also showed a wide substrate scope, including a variety of alkyl, benzyl, aryl, and heteroaryl thiols or disulfides. Furthermore, kinetic and other additional studies were performed in an attempt to clarify the mechanism of this electrochemical reaction.

Keywords: multicomponent reactions, phthalonitrile, photocatalysis, electrosynthesis, aryldiazonium salt, EDA complex, sulfonyl fluoride.

Summary

1	Chapter 1	1
1.1	Introduction	1
1.1.1	Phthalocyanines.....	1
1.1.2	Proposed mechanism for the formation of PC macrocycle	6
1.1.3	Phthalonitriles	8
1.2	Results and discussion	18
1.2.1	Synthesis of 4-formylphthalonitrile (1.77).....	18
1.2.2	Synthesis of phthalonitrile derivatives (1.80a-q)	19
1.2.3	Synthesis of ZnPCs 1.81a-c	26
1.2.4	Aggregation, photobleaching and photophysical properties of ZnPCs 1.81a-c	27
1.3	Conclusion	30
1.4	Experimental	31
1.4.1	Chemicals and materials.....	31
1.4.2	Equipment	31
1.4.3	Procedure for synthesis of 4-Formylphthalonitrile (1.77)	32
1.4.4	Procedure for synthesis of 4-(Decyloxy)aniline (1.78g)	33
1.4.5	General procedure for the synthesis of phthalonitriles	34
1.4.6	Characterization data of phthalonitrile-quinoline dyads	35
1.4.7	General procedure for the synthesis of ZnPCs 1.81a-c	45
1.4.7.1	Zinc phthalocyanine-quinoline 1.81a	46
1.4.7.2	Zinc phthalocyanine-quinoline 1.81b	46
1.4.7.3	Zinc phthalocyanine-quinoline 1.81c	47
1.4.8	Aggregation studies.....	48
1.4.9	Fluorescence measurements	49
1.4.10	Molar absorption coefficient (ϵ)	50
1.4.11	Photobleaching studies	53
	Reference	55
2	Chapter 2	63
2.1	Introduction	63
2.1.1	Electron donor-acceptor complex	63
2.1.2	Pyridines.....	68
2.2	Results and discussion	71
2.2.1	Photoarylation of <i>N</i> -heterocycles	71
2.2.2	Mechanistic insights and counterpoints with Ru-photocatalyzed reactions	77

2.3	Conclusion	84
2.4	Experimental.....	85
2.4.1	General information	85
2.4.2	Photochemical reactor	85
2.4.3	General procedure for the synthesis of aryldiazonium salts	88
2.4.4	General procedure for the photoarylation of <i>N</i> -heterocycles	88
2.4.5	Characterization data of arylated <i>N</i> -heterocycles.....	89
2.4.6	NMR spectra for checking aggregation at high concentration	100
2.4.7	Radical quenching experiments.....	101
2.4.8	¹ H- ¹⁵ N HMBC analyses.....	103
	Reference	106
3	Chapter 3	117
3.1	Introduction	117
3.1.1	Basic concepts in organic electrochemistry	117
3.1.2	Organic electrosynthesis	122
3.1.3	Sulfonyl fluorides.....	127
3.2	Results and discussion	130
3.2.1	Additional studies after the publication.....	144
3.3	Conclusion	148
3.4	Experimental.....	149
3.4.1	General information	149
3.4.2	Electrochemical reactor.....	150
3.4.3	Reaction optimization	152
3.4.4	General procedures.....	152
3.4.4.1	Cleaning procedures	152
3.4.4.2	General procedure for electrochemical synthesis of sulfonyl fluorides.....	153
3.4.4.3	General procedure for derivatization of volatile sulfonyl fluorides.....	154
3.4.4.4	Procedure for the scale-up experiment	154
3.4.4.5	Procedure for the kinetic experiment in batch conditions	155
3.4.4.6	Procedure for the kinetic experiment in flow conditions.....	155
3.4.5	Characterization data of sulfonyl fluorides	156
3.5	Mechanistic studies.....	164
3.5.1	Kinetic experiments.....	164
3.5.2	Radical quenching experiments.....	171
3.6	Fluorination step.....	173
3.6.1	1-Fluoropyridinium	174
3.6.2	Pyridinium chloride.....	175
3.6.3	Triethylamine	175

3.7	Cyclic voltammetry analyses	176
3.7.1	Starting materials	177
3.7.2	Reaction mixture	179
3.7.3	Experiment with Et ₃ N	181
3.8	Faraday efficiency.....	183
	Reference	184
4	NMR Data.....	193
4.1	Spectra of Chapter 1.....	193
4.1.1	¹ H, ¹³ C and DEPT-135 NMR spectra of compound 1.77	193
4.1.2	¹ H, ¹³ C and DEPT-135 NMR spectra of compound 1.78g	195
4.1.3	¹ H, ¹³ C and DEPT-135 NMR spectra of compound 1.80a	197
4.1.4	¹ H, ¹³ C and DEPT-135 NMR spectra of compound 1.80b	199
4.1.5	¹ H, ¹³ C and DEPT-135 NMR spectra of compound 1.80c	201
4.1.6	¹ H, ¹³ C and DEPT-135 NMR spectra of compound 1.80d	203
4.1.7	¹ H, ¹³ C and DEPT-135 NMR spectra of compound 1.80e	205
4.1.8	¹ H, ¹³ C and DEPT-135 NMR spectra of compound 1.80f	207
4.1.9	¹ H, ¹³ C and DEPT-135 NMR spectra of compound 1.80g	209
4.1.10	¹ H, ¹³ C and DEPT-135 NMR spectra of compound 1.80h	211
4.1.11	¹ H, ¹³ C and DEPT-135 NMR spectra of compound 1.80i	213
4.1.12	¹ H, ¹³ C and DEPT-135 NMR spectra of compound 1.80j	215
4.1.13	¹ H, ¹³ C and DEPT-135 NMR spectra of compound 1.80k	217
4.1.14	¹ H, ¹³ C and DEPT-135 NMR spectra of compound 1.80l	219
4.1.15	¹ H NMR spectrum of compound 1.80m	221
4.1.16	¹ H, ¹³ C and DEPT-135 NMR spectra of compound 1.80n	222
4.1.17	¹ H NMR spectrum of compound 1.80o	224
4.1.18	¹ H, ¹³ C and DEPT-135 NMR spectra of compound 1.80p	225
4.1.19	¹ H, ¹³ C and DEPT-135 NMR spectra of compound 1.80q	227
4.1.20	¹ H NMR spectrum of compound 1.81a	229
4.1.21	¹ H NMR spectrum of compound 1.81b	230
4.1.22	¹ H NMR spectrum of compound 1.81c	231
4.2	Spectra of Chapter 2.....	232
4.2.1	¹ H and ¹³ C NMR spectra of compound 2.22a – 2 aryl	232
4.2.2	¹ H and ¹³ C NMR spectra of compound 2.22a – 4 aryl	234
4.2.3	¹ H and ¹³ C NMR spectra of compound 2.22b – 2 aryl	236
4.2.4	¹ H and ¹³ C NMR spectra of compound 2.22b – 4 aryl	238
4.2.5	¹ H and ¹³ C NMR spectra of compound 2.22c – 2 aryl	240
4.2.6	¹ H and ¹³ C NMR spectra of compound 2.22c – 4 aryl	242
4.2.7	¹ H and ¹³ C NMR spectra of compound 2.22d – 2 aryl	244
4.2.8	¹ H and ¹³ C NMR spectra of compound 2.22d – 4 aryl	246
4.2.9	¹ H and ¹³ C NMR spectra of compound 2.22e – 2 aryl	248
4.2.10	¹ H and ¹³ C NMR spectra of compound 2.22e – 4 aryl	250
4.2.11	¹ H and ¹³ C NMR spectra of compound 2.22f – 2 aryl	252
4.2.12	¹ H and ¹³ C NMR spectra of compound 2.22f – 4 aryl	254
4.2.13	¹ H and ¹³ C NMR spectra of compound 2.22g – 2 aryl	256

4.2.14	¹ H and ¹³ C NMR spectra of compound 2.22g – 4 aryl	258
4.2.15	¹ H and ¹³ C NMR spectra of compound 2.22h – 2 aryl	260
4.2.16	¹ H and ¹³ C NMR spectra of compound 2.22i – 2 aryl	262
4.2.17	¹ H and ¹³ C NMR spectra of compound 2.22i – 4 aryl	264
4.2.18	¹ H and ¹³ C NMR spectra of compound 2.22j – 2 aryl	266
4.2.19	¹ H and ¹³ C NMR spectra of compound 2.22j – 4 aryl	268
4.2.20	¹ H and ¹³ C NMR spectra of compound 2.22k – 2 aryl	270
4.2.21	¹ H and ¹³ C NMR spectra of compound 2.22k – 4 aryl	272
4.2.22	¹ H and ¹³ C NMR spectra of compound 2.22l – 2 aryl	274
4.2.23	¹ H and ¹³ C NMR spectra of compound 2.22l – 4 aryl	276
4.2.24	¹ H and ¹³ C NMR spectra of compound 2.22m – 2 aryl	278
4.2.25	¹ H and ¹³ C NMR spectra of compound 2.22m – 4 aryl	280
4.2.26	¹ H and ¹³ C NMR spectra of compound 2.22n – 2 aryl	282
4.2.27	¹ H and ¹³ C NMR spectra of compound 2.22n – 4 aryl	284
4.2.28	¹ H and ¹³ C NMR spectra of compound 2.22o – 2 aryl	286
4.2.29	¹ H and ¹³ C NMR spectra of compound 2.22o – 4 aryl	288
4.2.30	¹ H and ¹³ C NMR spectra of compound 2.22r – 2 aryl	290
4.2.31	¹ H and ¹³ C NMR spectra of compound 2.22s – 2 aryl	292
4.2.32	¹ H and ¹³ C NMR spectra of compound 2.22t – 2 aryl	294
4.2.33	¹ H and ¹³ C NMR spectra of compound 2.22u – 2 aryl	296
4.2.34	¹ H and ¹³ C NMR spectra of compound 2.22u – 4 aryl	298
4.2.35	¹ H and ¹³ C NMR spectra of compound 2.22v	300
4.2.36	¹ H and ¹³ C NMR spectra of compound 2.22w – 2 aryl	302
4.2.37	¹ H and ¹³ C NMR spectra of compound 2.22w – 4 aryl	304
4.2.38	¹ H and ¹³ C NMR spectra of compound 2.22x	306

4.3 Spectra of Chapter 3..... 308

4.3.1	¹ H, ¹³ C and ¹⁹ F NMR spectra of compound 3.26a	308
4.3.2	¹ H and ¹³ C NMR spectra of compound 3.26a-der	310
4.3.3	¹ H, ¹³ C and ¹⁹ F NMR spectra of compound 3.26b	312
4.3.4	¹ H, ¹³ C and ¹⁹ F NMR spectra of compound 3.26c	314
4.3.5	¹ H, ¹³ C and ¹⁹ F NMR spectra of compound 3.26d	316
4.3.6	¹ H, ¹³ C and ¹⁹ F NMR spectra of compound 3.26e	318
4.3.7	¹ H, ¹³ C and ¹⁹ F NMR spectra of compound 3.26f	320
4.3.8	¹ H, ¹³ C and ¹⁹ F NMR spectra of compound 3.26g	322
4.3.9	¹ H, ¹³ C and ¹⁹ F NMR spectra of compound 3.26h	324
4.3.10	¹ H, ¹³ C and ¹⁹ F NMR spectra of compound 3.26i	326
4.3.11	¹⁹ F and ¹³ C NMR spectra of compound 3.26j	328
4.3.12	¹ H, ¹³ C and ¹⁹ F NMR spectra of compound 3.26j-der	330
4.3.13	¹ H, ¹³ C and ¹⁹ F NMR spectra of compound 3.26k	332
4.3.14	¹ H, ¹³ C and ¹⁹ F NMR spectra of compound 3.26l	334
4.3.15	¹ H, ¹³ C and ¹⁹ F NMR spectra of compound 3.26m	336
4.3.16	¹ H, ¹³ C and ¹⁹ F NMR spectra of compound 3.26n	338
4.3.17	¹ H, ¹³ C and ¹⁹ F NMR spectra of compound 3.26o	340
4.3.18	¹ H, ¹³ C and ¹⁹ F NMR spectra of compound 3.26p	342
4.3.19	¹ H, ¹³ C and ¹⁹ F NMR spectra of compound 3.26q	344
4.3.20	¹ H and ¹³ C NMR spectra of compound 3.26r-der	346
4.3.21	¹ H and ¹³ C NMR spectra of compound 3.26s-der	348
4.3.22	¹ H and ¹³ C NMR spectra of compound 3.26t-der	350
4.3.23	¹ H, ¹³ C and ¹⁹ F NMR spectra of compound 3.26u	352
4.3.24	¹ H and ¹³ C NMR spectra of compound 3.26v-der	354
4.3.25	¹ H, ¹³ C and ¹⁹ F NMR spectra of compound 3.26w	356

4.3.26	¹ H, ¹³ C and ¹⁹ F NMR spectra of compound 3.26x	358
4.3.27	¹ H, ¹³ C and ¹⁹ F NMR spectra of compound 3.26y	360
4.3.28	¹ H, ¹³ C and ¹⁹ F NMR spectra of compound 3.26z	362
4.3.29	¹ H, ¹³ C and ¹⁹ F NMR spectra of compound 3.26aa	364
5	Appendix	366
A	List of publications	366
B	Participation in events	368
C	Disciplines	369

Chapter 1: Multicomponent reactions mediated by NbCl₅ for the synthesis of phthalonitrile-quinoline dyads: methodology, scope, mechanistic insights and applications in phthalocyanine synthesis

Reproduced with permission of **BARTOLOMEU, A. A.**; BROCKSOM, T. J.; DA SILVA-FILHO, L. C. & DE OLIVEIRA, K. T. “Multicomponent reactions mediated by NbCl₅ for the synthesis of phthalonitrile-quinoline dyads: methodology, scope, mechanistic insights and applications in phthalocyanine synthesis”. *Dyes Pigm.*, 151: 391, 2018. Copyright 2018 Elsevier.

1 Chapter 1

Chapter 1 is based on our paper published in *Dyes and Pigments* in 2018, and it presents the results obtained on the development of an MCR approach for the one-pot synthesis of a library of phthalonitrile-quinoline dyads. Examples of phthalocyanine syntheses were performed to demonstrate the versatility of the new functionalized building blocks.

1.1 Introduction

1.1.1 Phthalocyanines

The name phthalocyanine was coined by Patrick Linstead and is a combination of the prefix *phthal*, originally from the Greek *naphtha* (rock oil), and the word *cyanine*, from the Greek *kyanos* (blue).¹

Phthalocyanines (tetrabenzotetraazaporphyrins or tetrabenzoporphyrazines) are planar aromatic macrocycles consisting of four isoindole units linked together through nitrogen atoms. They possess an 18 π -electron aromatic cloud delocalized over an arrangement of alternated carbon and nitrogen atoms (Figure 1.1).²

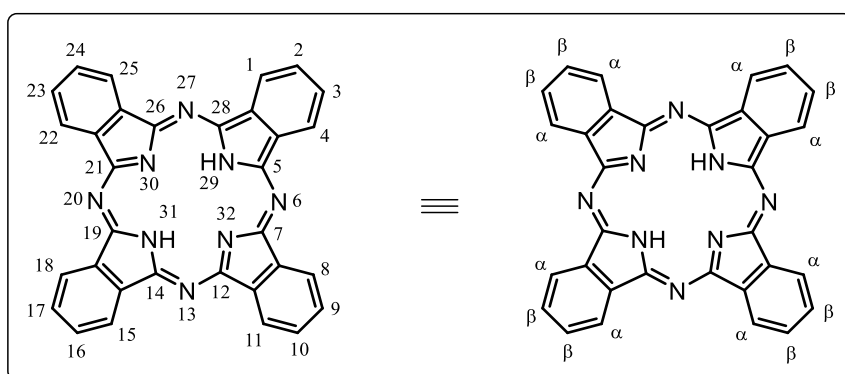


Figure 1.1 – Chemical structure and nomenclature of the phthalocyanine core.

The preparation of phthalocyanines has traditionally been carried out by cyclotetramerization of phthalonitriles (**a**), but also of various other precursors, such as phthalic anhydrides (**b**), phthalimides (**c**), 1,3-diiminoisoindolines (**d**), and phthalamides (**e**) (Figure 1.2).³

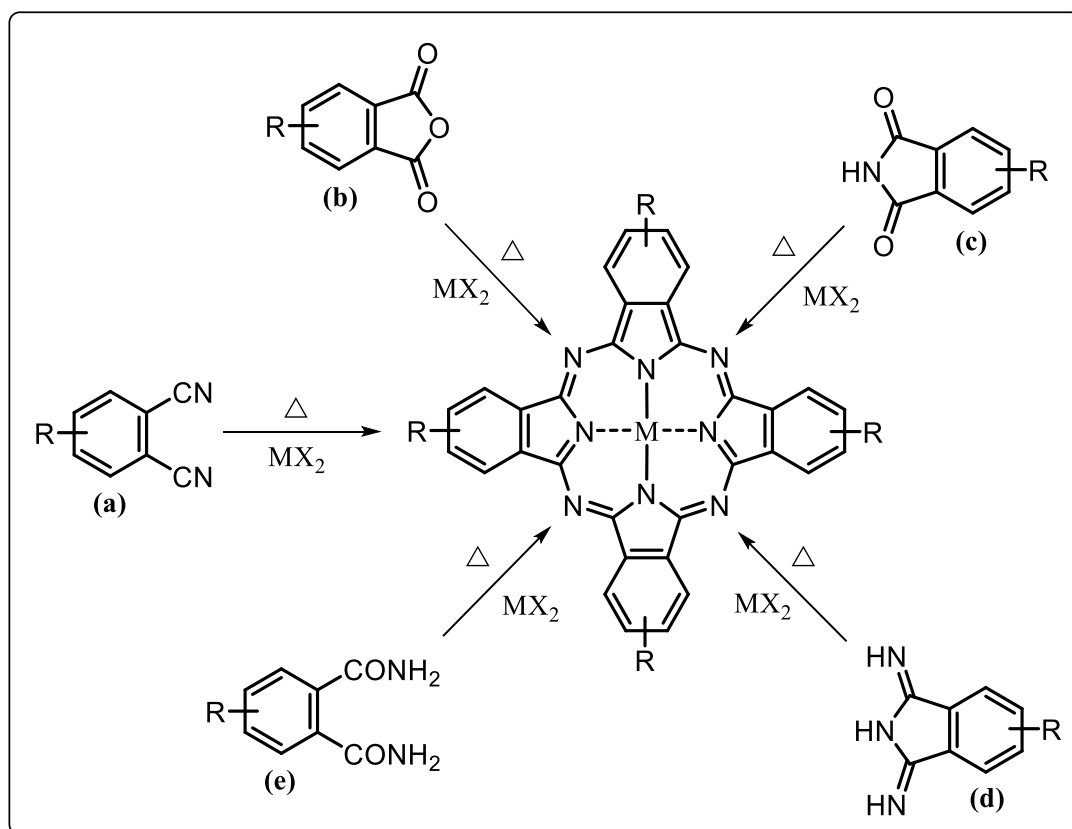


Figure 1.2 – Phthalocyanine precursors: **(a)** phthalonitrile, **(b)** phthalic anhydrides, **(c)** phthalimides, **(d)** 1,3-diiminoisoindolines, and **(e)** phthalamides.

An intense Q-band at 650-700 nm is present in the UV-Vis spectrum of metallated phthalocyanines (Figure 1.3a – red curve), which is associated with π - π^* doubly degenerated transition $1a_{1u} \rightarrow 1e_g$ (Figure 1.3b).^{2,4} For metal-free phthalocyanines, the Q-band is split into two components (see Figure 1.3a – blue curve) due to possessing lower symmetry (D_{2h}) than planar MPCs (D_{4h}).^{2,4} The UV-vis spectrum also presents a broadband near 350 nm

(the so-called Soret or B-band) due to two $\pi\text{-}\pi^*$ transitions ($1a_{2u}\rightarrow 1e_g$ and $1b_{2u}\rightarrow 1e_g$) (see Figure 1.3a and 1.3b). Moreover, a series of vibrational components is observed near the Q-band.⁴

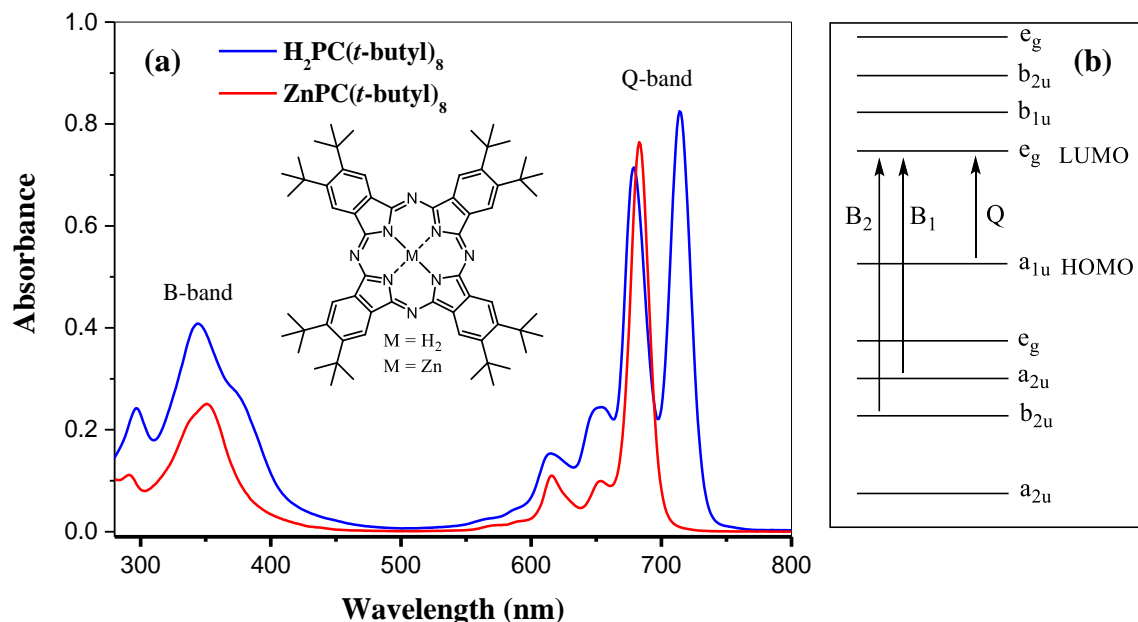


Figure 1.3 – (a) UV-Vis spectra of H₂PC(*t*-butyl)₈ (blue line) and ZnPC(*t*-butyl)₈ (red line) in EtOAc.⁵ (b) Schematic representation of the energy levels and transitions (Q- and B-bands) in a metallated phthalocyanine.^{2,4}

Obviously, it is noteworthy that the electronic characteristics can be influenced by parameters such as the nature and position of the peripheral substituents, the nature and oxidation state of the central atom, the extent of the conjugation in the macrocycle system, and deviations from planarity.^{4,6} For example, Furuyama et al. (2014) synthesized a series of PCs that absorb and emit in the near-infrared region using chalcogen elements (S, Se, and Te) and pnictogen elements (P, As, and Sb) as peripheral and central (core) substituents, respectively.⁷

Due to their remarkable properties, PCs have applications in many different fields. Initially, these compounds were used as dyes and pigments in the textile, printing, and paint industries due to their high thermal stability and low reactivity and solubility.^{8,9} PCs and MPCs have been used more recently in high-tech applications such as semiconductor

materials,¹⁰⁻¹² solar cells,¹³ liquid crystals,^{14,15} catalysis,^{16,17} and others.¹⁸⁻²² Moreover, these compounds have also been studied and employed as photosensitizers in photodynamic therapy.^{21,23-25}

Unsubstituted PCs in the α - and β -positions of the macrocycle (see Figure 1.1) have negligible solubility in the most common organic solvents (DMSO, THF, DMF, etc.) and in water. In fact, even highly aromatic organic solvents such as 1-chloronaphthalene and quinoline do not yield solutions with concentrations greater than 10^{-5} M. Sulfuric acid (> 8 M) is the only effective solvent to solubilize these compounds. However, protonation of the aza-nitrogens alters the properties of the macrocycle and limits the usefulness of these solutions. For example, a strong bathochromic shift in the Q-band (ca. 80–120 nm) can be observed when the aza-nitrogens are protonated.³

The low solubility of unsubstituted PCs can be mainly attributed to the extreme hydrophobicity of the aromatic core and planarity of the PC,³ which favors the occurrence of non-covalent attractive interactions (especially π - π stacking interactions, but also van de Waals forces and, in particular cases more specific interactions, such as hydrogen bonds) between the electronic clouds of the aromatic system, leading to the formation of dimers, trimers and higher-order structures in solution, a phenomenon well-known as aggregation.²⁶ This phenomenon depends on concentration, temperature, nature of the substituents and solvents, and complexed metal ions.²⁶

The structure of PCs can be modified by the replacement of the central atom, introduction of substituents into the peripheral and non-peripheral positions of the macrocycle, replacement of the *meso*-atoms, and substitution of the core isoindole nitrogen(s) by other elements (Figure 1.4).^{8,9,27} Obviously, the modification of the PC core allows the tuning of their properties, e.g., chemical, optical, electrochemical, coordination, etc.^{4,28}

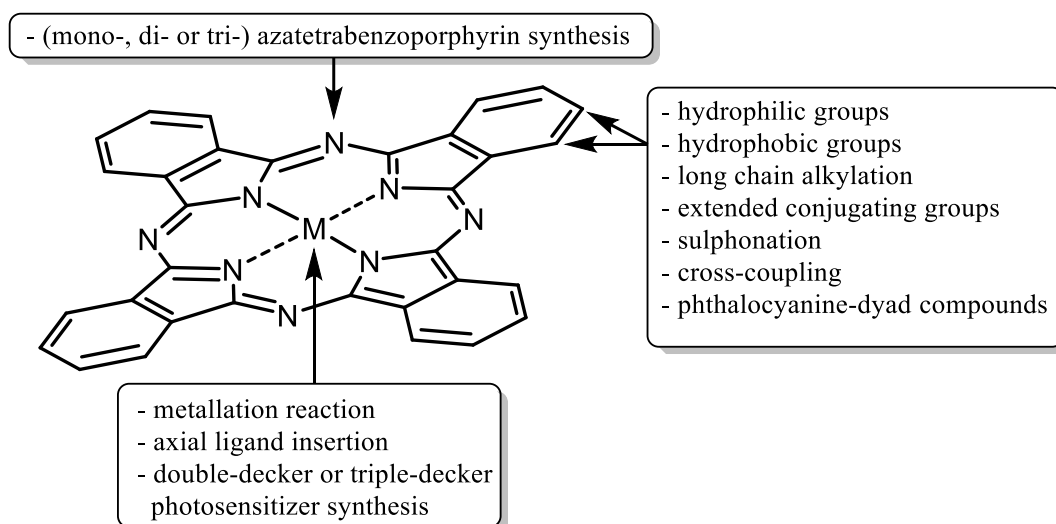


Figure 1.4 – Phthalocyanine core functionalizations.

Among the above-mentioned strategies, the introduction of substituents at the peripheral (β) and/or non-peripheral (α) positions of the macrocycle, and the use of transition metal cations of octahedral coordination geometry are the most effective manners of not only reducing aggregation but also increasing the solubility of PC compounds.²⁹

Peripheral substituents can be introduced into the PC core by using two approaches: direct modification of the macrocycle (e.g., electrophilic aromatic substitution reactions) or cyclotetramerization of an already substituted precursor.⁹

The first approach usually results in the formation of complex regioisomeric mixtures from which the desired product can be isolated only with considerable difficulty and also in low yield, which is due to the drastic reaction conditions employed.³ However, such problems have been circumvented through the use of cross-coupling chemistry.³⁰⁻³³

The second approach permits the introduction of a controlled number of substituents into the phthalocyanine core. Thus, through this approach, it is possible to obtain functionalized PCs in the peripheral (β) and/or non-peripheral (α) positions of the macrocycle and these analogs have improved photophysical, photochemical, and biological properties.⁹ In this context, multicomponent reactions should be very useful for the synthesis of these PC

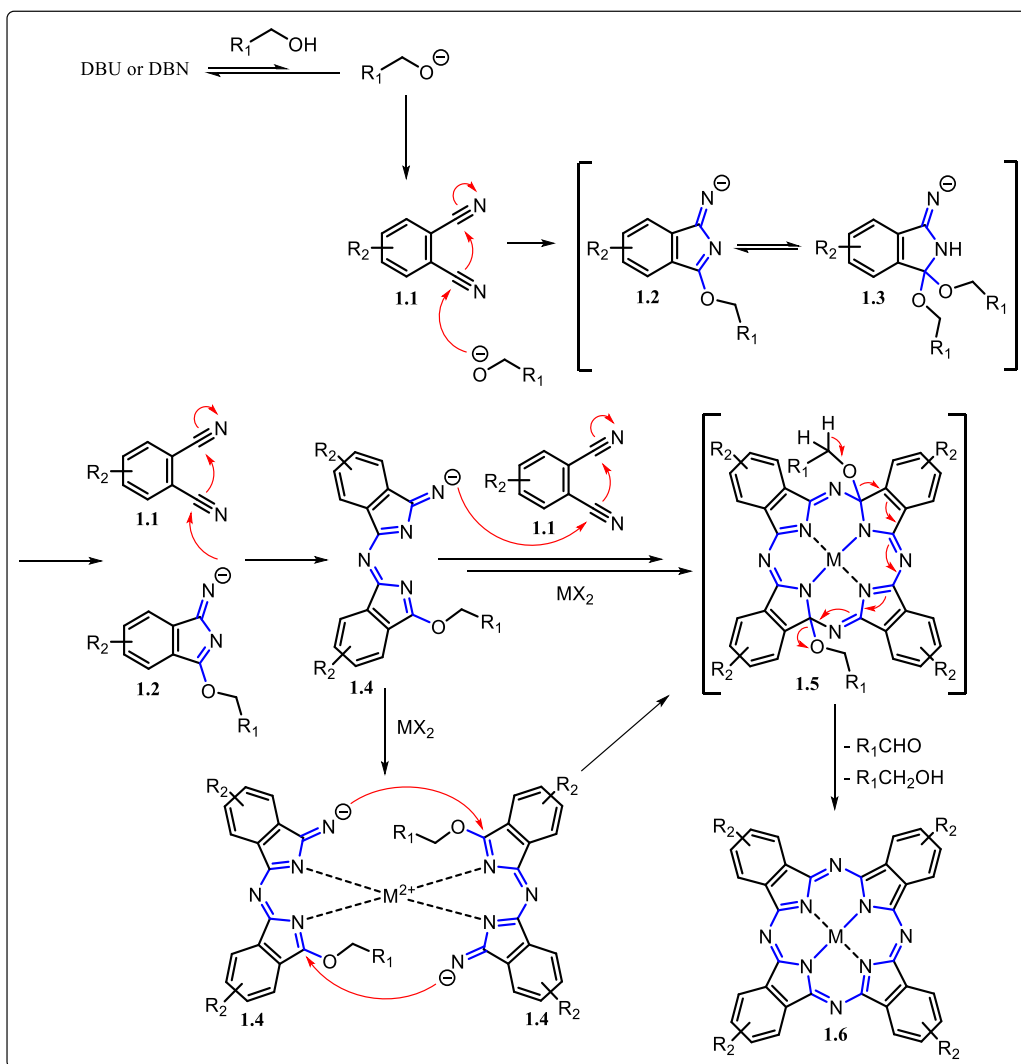
precursors (building blocks), providing extended conjugation and, at the same time, functionalities that can help to decrease or suppress aggregation.

1.1.2 Proposed mechanism for the formation of PC macrocycle

Although it is difficult to gain a detailed understanding of the reaction mechanism due to the different conditions employed in the synthesis of these compounds, in some synthetic routes the intermediates were isolated and their structures characterized by spectroscopic and spectrometric analyses including IR, X-ray diffraction, ^1H and ^{13}C -NMR, and MS.³⁴⁻³⁸

A proposed mechanism to explain the formation of PC macrocycle from phthalonitriles in a reaction medium containing an alcohol and its alkoxide is presented in Scheme 1.1.^{35,36,39}

In this stepwise mechanism, alcohol is first deprotonated by a non-nucleophilic base, such as DBU or DBN, to give alkoxide ions (nucleophile), which carries out a nucleophilic attack at the cyano group of the phthalonitrile **1.1**, thus giving the isoindole derivative **1.2** (monomeric intermediate),⁴⁰ which is in equilibrium with intermediate **1.3**. Then, intermediate **1.2** (nucleophile) reacts with another molecule of phthalonitrile **1.1** to form the dimeric intermediate **1.4**, which can coordinate with metal cations and self-condense or react sequentially with two other molecules of phthalonitrile **1.1** to produce intermediate **1.5**. Finally, intermediate **1.5** is subsequently aromatized with the loss of alkoxy groups giving aldehydes or alcohol forms (identified by mass spectrometry),⁴¹ to produce phthalocyanine **1.6**.



Scheme 1.1 – Formation of PC macrocycle by a stepwise mechanism.

It is noteworthy that the monomeric intermediate **1.7**, the dimeric lithium salt **1.8**, and the nickel complexes **1.9-1.11** were also isolated and identified in methodologies in which the solvent used was an alcohol (Figure 1.5),^{34,35,41,42} supporting the proposed mechanism.

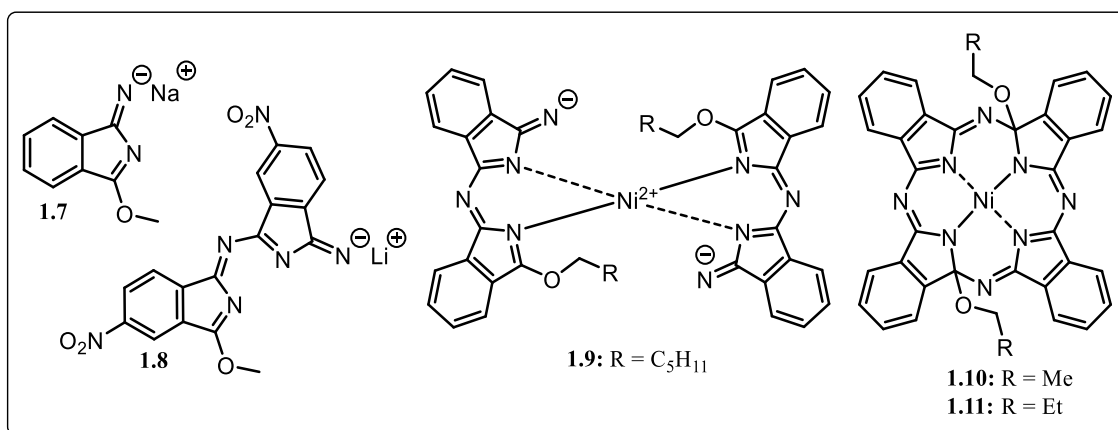
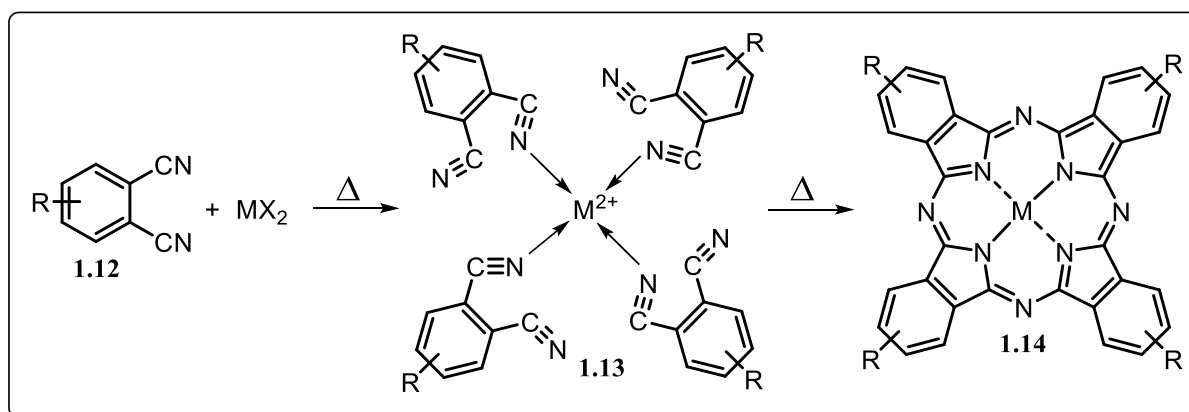


Figure 1.5 – Some isolated intermediates in PC synthesis.

A concerted mechanism has also been proposed to explain the formation of PC macrocycle in solid-state reactions (without solvent or other additives) (Scheme 1.2).⁴³ In this mechanism, initially, four units of phthalonitrile (**1.12**) coordinate with the metal ion forming a complex (**1.13**), which leads to the formation of the macrocycle (**1.14**).



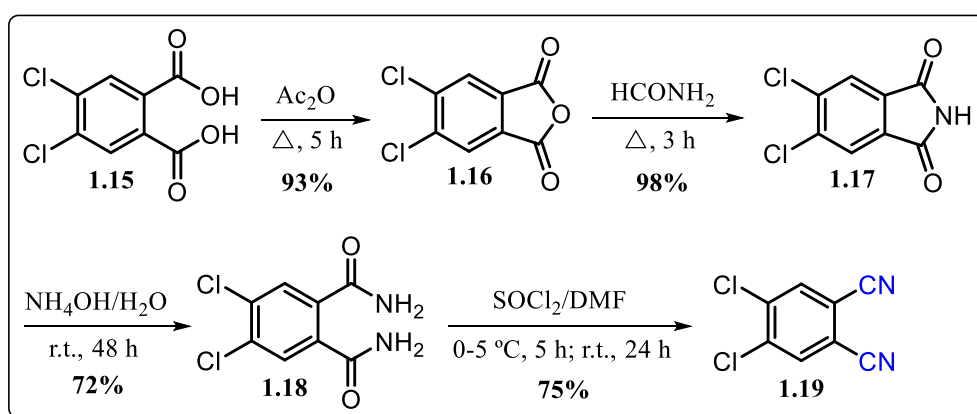
Scheme 1.2 – Formation of PC macrocycle by metal-induced coordination of the four phthalonitrile units (a concerted mechanism).

1.1.3 Phthalonitriles

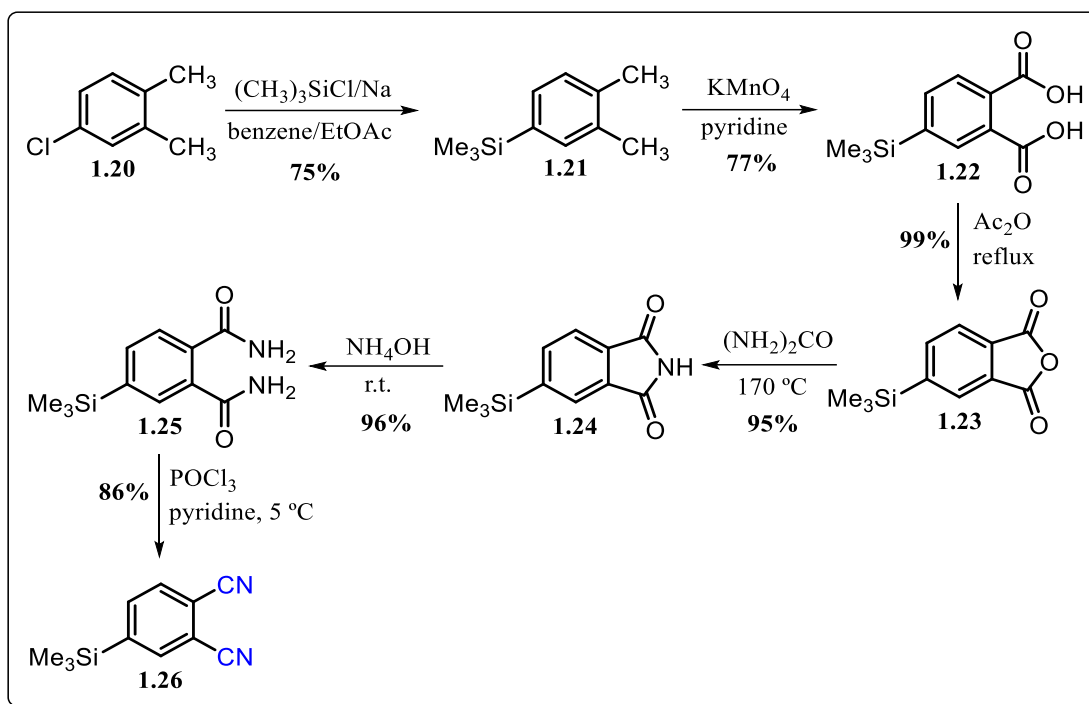
Phthalonitriles (1,2-dicyanobenzenes) are mainly known to be phthalocyanine precursors,³ but also have several desirable physical and chemical properties for technological

applications. Phthalonitrile-based resins have applications such as adhesives, thin films, composite matrices, high-performance polymers, and electrical conductors.⁴⁴⁻⁴⁹ Recently, it has also been reported that a series of C4-substituted phthalonitriles are potent reversible inhibitors of recombinant human monoamine oxidase B (MAO-B).^{50,51} Also, two other phthalonitrile derivatives containing pharmacophore groups like morpholine and triazole in the same molecule or an aminopyrazole group showed interesting inhibition profiles against enzymes (or isozymes) such as xanthine oxidase (XO) and the human carbonic anhydrases I and II (hCA-I and hCA-II), respectively.^{52,53}

Phthalonitriles can be synthesized from the other *ortho*-phthalic acid derivatives. A stepwise progression from the dicarboxylic acid is as follows: dicarboxylic acid → anhydride → imide → diamide → phthalonitrile (the so-called acidic route to substituted phthalonitriles).³ The reaction pathway involves the ammonolysis of dicarboxylic acid followed by dehydration of the resulting diamide to give the phthalonitrile.⁵⁴ Examples of the application of this synthetic approach are shown in Schemes 1.3 and 1.4 for the synthesis of 4,5-dichlorophthalonitrile (**1.19**) and 4-trimethylsilyl-phthalonitrile (**1.26**), respectively.⁵⁵



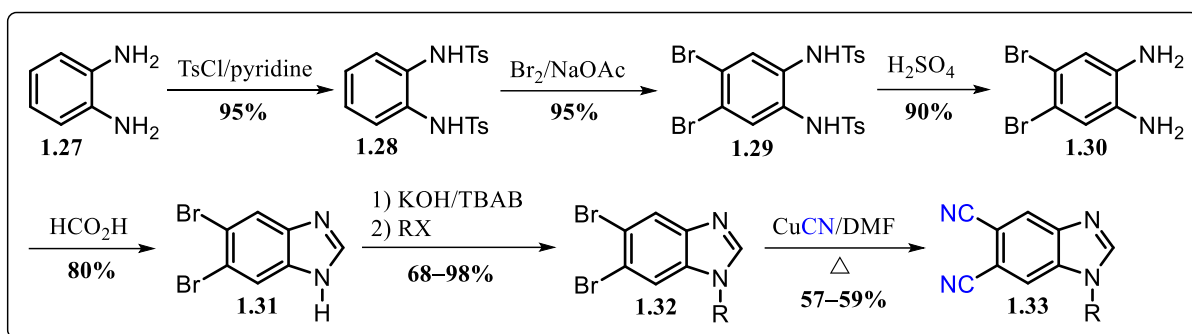
Scheme 1.3 – Synthesis of 4,5-dichlorophthalonitrile.



Scheme 1.4 – Synthesis of 4-trimethylsilyl-phthalonitrile.

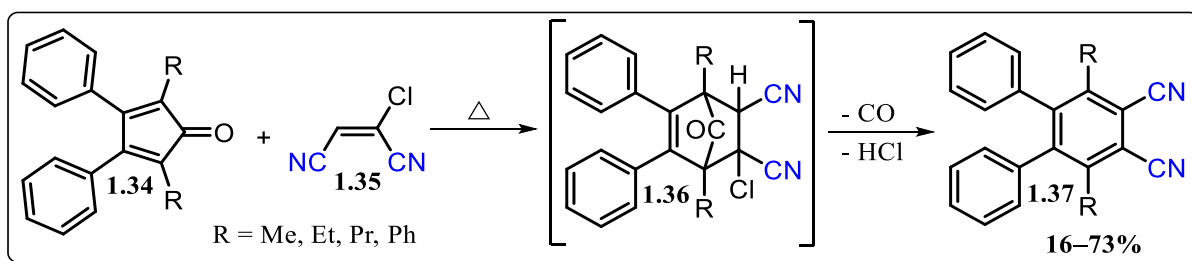
The Rosenmund-von Braun reaction is a very popular method for preparing nitriles such as phthalonitriles.³ In these reactions, phthalonitriles are obtained by refluxing aromatic vicinal dihalides (usually 1,2-dibromobenzenes) in the presence of an excess of CuCN in a polar high-boiling point solvent such as *N,N*-dimethylformamide, pyridine or nitrobenzene. However, the reaction conditions employed to obtain these compounds favor the formation of the corresponding CuPCs as a by-product, as well as other by-products that can be formed with the other functionalities present in the dihalides, which explains the low yields observed in the synthesis of many phthalonitriles by this method.^{3,54}

As shown in Scheme 1.5 below, the Rosenmund-von Braun reaction was used in the last step of the synthetic route to convert 1-alkyl-5,6-dibromobenzoimidazoles (**1.32**) to 1-alkyl-5,6-dicyanobenzoimidazoles (**1.33**).⁵⁶



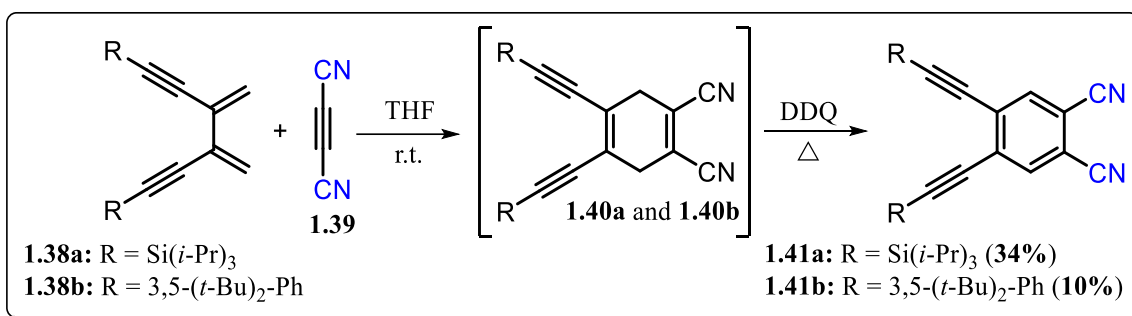
Scheme 1.5 – Synthesis of 1-alkyl-5,6-dicyanobenzoimidazoles.

Phthalonitriles, naphthalonitriles or other aromatic *ortho*-dinitriles can also be synthesized by the Diels-Alder reaction or other cycloaddition reactions.³ Although not widely used for this purpose, the Diels-Alder reaction is suitable for the synthesis of polysubstituted six-membered rings, such as phthalonitriles. For example, tetrasubstituted phthalonitriles **1.37** were obtained by the reaction between tetrasubstituted cyclopentadienones (**1.34**) (dienes) and 2-chloromaleonitrile (**1.35**) (dienophile). This Diels-Alder reaction affords the intermediate **1.36** which aromatizes after CO extrusion and HCl elimination (Scheme 1.6).^{3,57}



Scheme 1.6 – Synthesis of tetrasubstituted phthalonitriles via Diels-Alder chemistry.

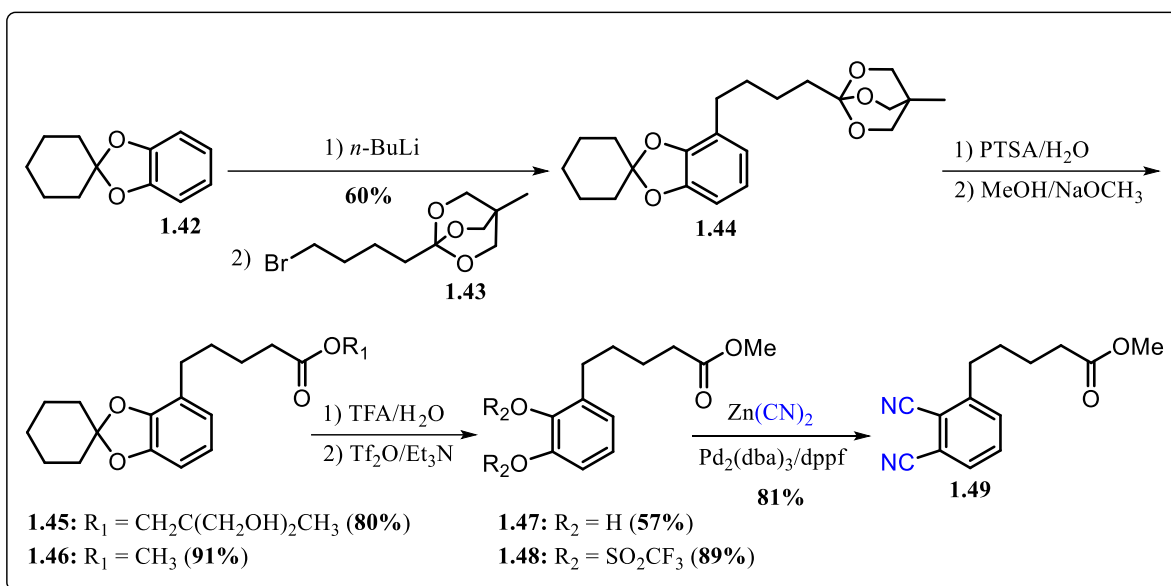
A Diels-Alder reaction has also been used in the preparation of acetylenic phthalonitriles (**1.41a** and **1.41b**), as shown in Scheme 1.7 below. This cycloaddition reaction between dicyanoacetylene (**1.39**) (dienophile) and conjugated dimethylenehexadiynes (**1.38a** and **1.38b**) (dienes) leads to the intermediates **1.40a** and **1.40b** which are oxidized in the presence of DDQ to give the phthalonitriles **1.41a** and **1.41b**, respectively.^{3,58,59}



Scheme 1.7 – Synthesis of acetylenic phthalonitriles via Diels-Alder chemistry.

A recent approach for the synthesis of phthalonitriles involves the transition metal-catalyzed cyanation of aryl triflates/nonaflates.³ In these reactions, the reagent system is comprised of a cyanide source (usually KCN or Zn(CN)₂) and a palladium(0) or nickel(0) catalyst in the presence of a ligand.³

In a study by Drechsler et al. (1999), the synthesis of phthalonitrile **1.49** was performed from the protected catechol **1.42** (Scheme 1.8).^{3,60} Initially, **1.42** was converted to protected alkyl catechol **1.44** using *n*-BuLi and the alkyl bromide **1.43** (directed *ortho* metalation). Then the *ortho* ester group in the resulting alkyl catechol **1.44** was converted into the methyl ester **1.46** in two steps, the first being an acid-catalyzed ring-opening of the bicyclic system to the dihydroxy ester **1.45**, and the second being a re-esterification in methanol to give **1.46**. Next, the ketal group of **1.46** was cleaved at r.t. using a TFA/H₂O mixture (95: 5), leading to the formation of the catechol **1.47**. Finally, the hydroxyl groups of **1.47** were first converted to triflates and subsequently replaced by cyanide using Zn(CN)₂ and a Pd₂(dba)₃/dppf catalyst to give the phthalonitrile **1.49**.

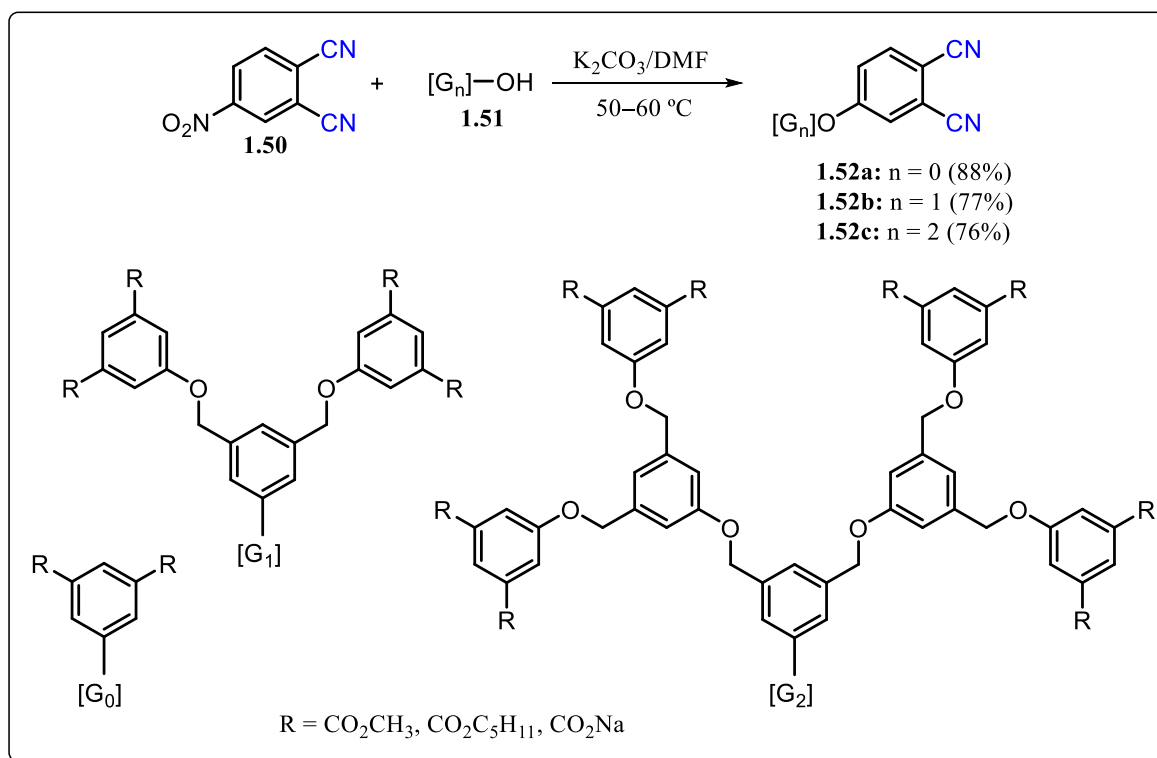


Scheme 1.8 – Synthesis of 3-(4-methyloxycarbonyl)butylphthalonitrile.

Functionalized phthalonitriles can also be prepared by modification of preexisting phthalonitrile molecules.³ This approach is relevant because a considerable number of substituted phthalonitriles and naphthalonitriles bearing chemically versatile groups are commercially available.³ In addition, simpler phthalonitriles can be easily synthesized from inexpensive commercially available starting materials using one of the aforementioned methods.

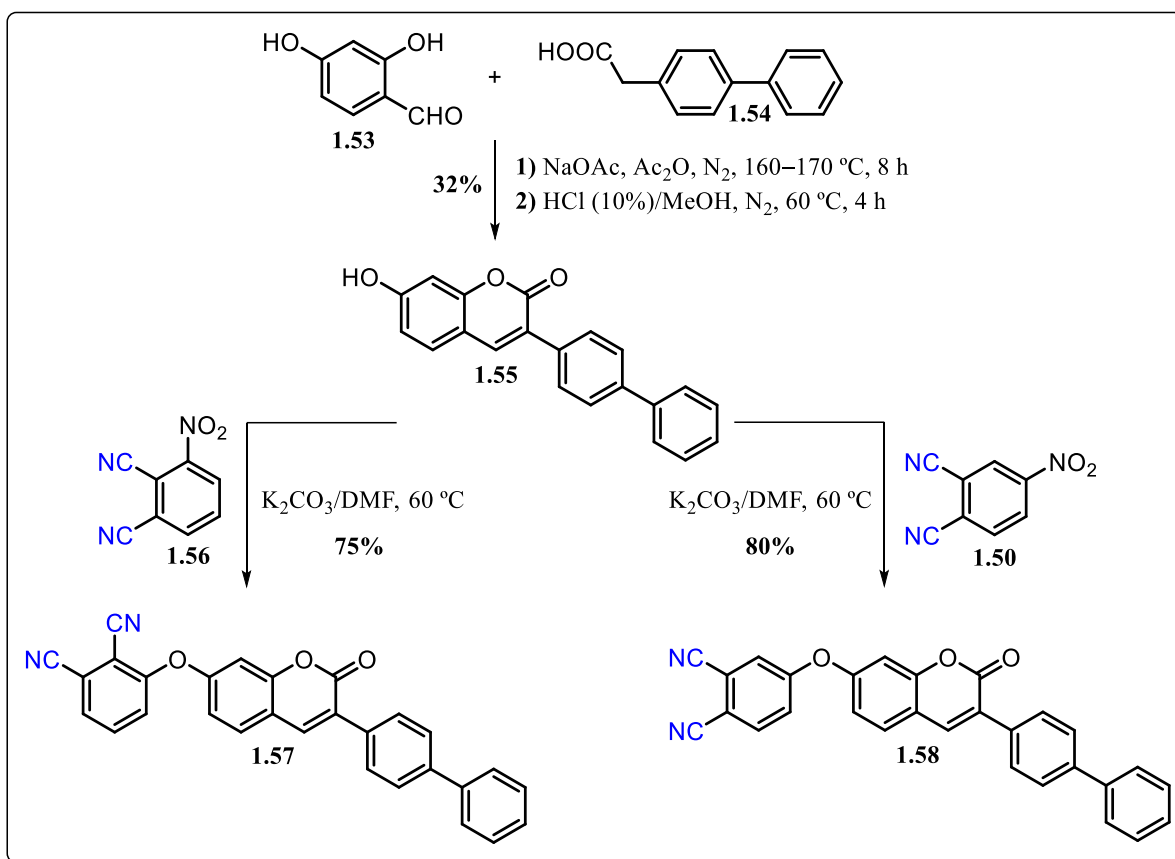
The most widely used reactions employed in the modification of substituted phthalonitriles and naphthalonitriles are nucleophilic aromatic substitution reactions.³

An example of an efficient $\text{S}_{\text{N}}\text{Ar}$ reaction was reported by Ng et al. (1999) (Scheme 1.9).⁶¹ Treatment of phenols **1.51** with 4-nitrophthalonitrile (**1.50**) in dry DMF in the presence of anhydrous K_2CO_3 resulted in the formation of desired dendritic phthalonitriles (**1.52a-c**) in 76–88% yields. These phthalonitriles were later cyclotetramerized to PCs that are essentially non-aggregated in organic solvents.⁶¹



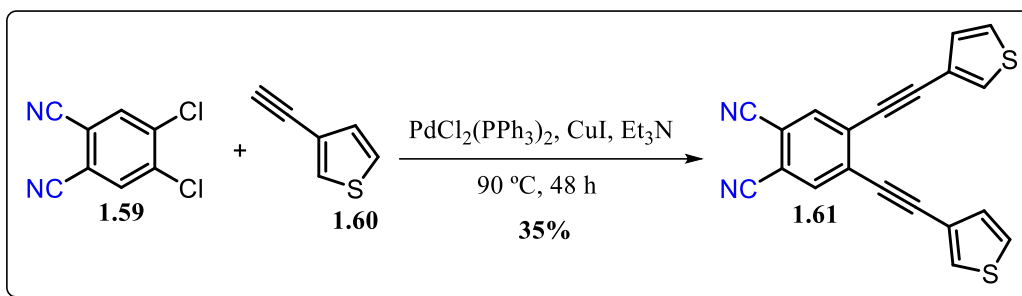
Scheme 1.9 – Preparation of dendritic phthalonitriles.

Gök et al. (2016) also reported the functionalization of nitrophthalonitriles with a hydroxycoumarin employing $\text{S}_{\text{N}}\text{Ar}$ reactions (Scheme 1.10).⁶² The authors first synthesized 7-hydroxy-3-biphenylcoumarin (**1.55**) via Perkin-Oglialoro condensation of 4-biphenylacetic acid (**1.54**) with 2,4-dihydroxybenzaldehyde (**1.53**) in the presence of $\text{NaOAc}/\text{Ac}_2\text{O}$. Treatment of coumarin **1.55** with nitrophthalonitriles **1.50** and **1.56** in dry DMF in the presence of anhydrous K_2CO_3 resulted in the formation of functionalized phthalonitriles **1.57** and **1.58** in 75 and 80% yields, respectively. These phthalonitriles were later cyclotetramerized to H_2PCs and MPCs (Zn, Co, and InCl).⁶²

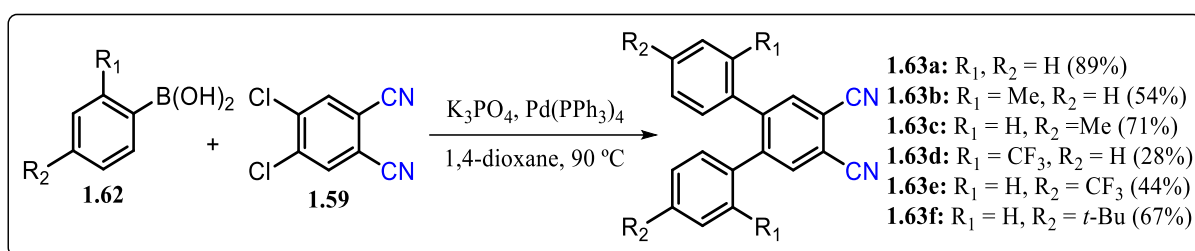


Scheme 1.10 – Preparation of functionalized phthalonitriles **1.57** and **1.58**.

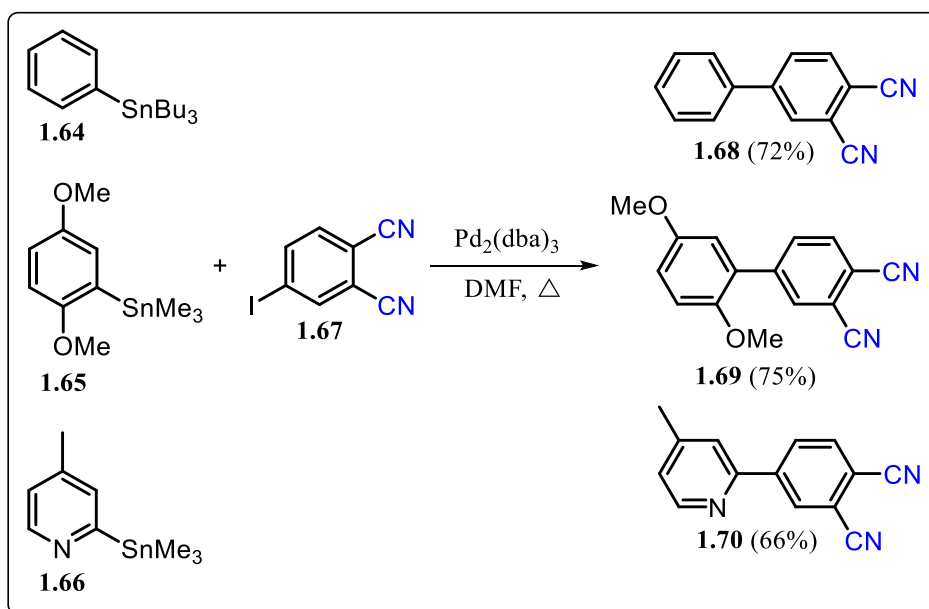
An alternative approach for functionalizing phthalonitriles is through palladium-catalyzed cross-coupling reactions such as Sonogashira, Suzuki, Stille, and Heck–Cassar (also known as the Heck alkynylation or Cu-free Sonogashira reaction).³ These coupling reactions are advantageous because they often proceed with high yield and are tolerant to a variety of functional groups present in the starting phthalonitriles. Examples of such reactions are illustrated in Schemes 1.11–1.14.^{63–66}



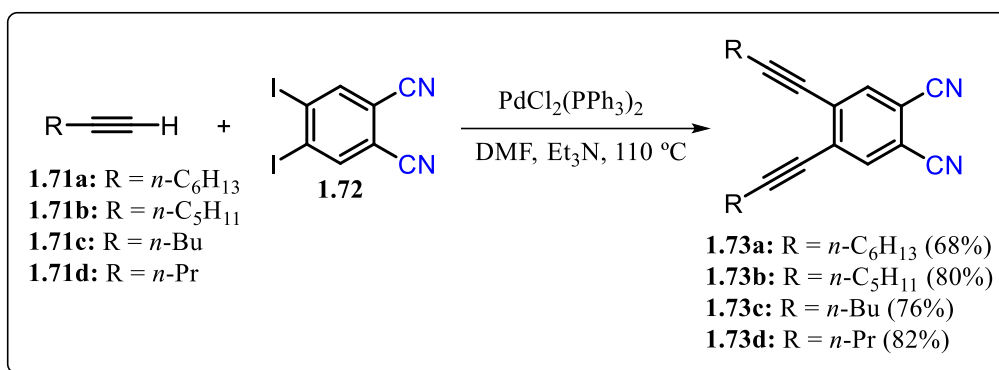
Scheme 1.11 – Pd-Catalyzed Sonogashira coupling reaction of 3-ethynylthiophene with 4,5-dichlorophthalonitrile.



Scheme 1.12 – Pd-Catalyzed Suzuki coupling reaction of phenylboronic acids with 4,5-dichlorophthalonitrile.



Scheme 1.13 – Pd-catalyzed Stille coupling reaction of organostannanes with 4-iodophthalonitrile.



Scheme 1.14 – Pd-Catalyzed Heck–Cassar coupling reaction of terminal alkynes with 4,5-diiodophthalonitrile.

It is clear from the above examples that cross-coupling reactions are a powerful tool for functionalizing phthalonitriles. However, these methodologies are not always cost-competitive and not easily scalable.

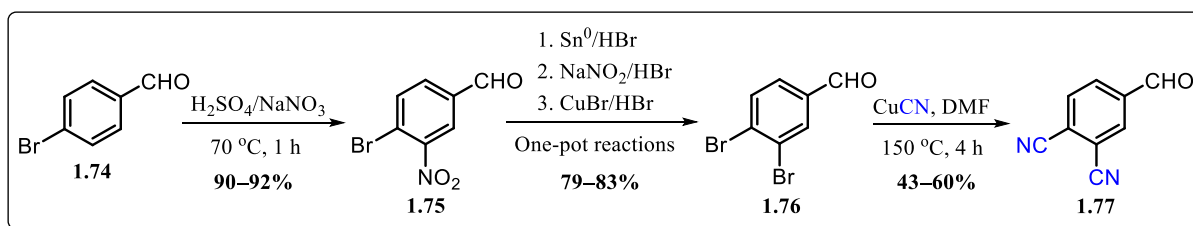
Functionalized phthalonitriles can also be prepared by halogenation of a commercially available substrate followed by S_NAr reactions or transition metal-catalyzed cross-coupling reactions. In addition, functionalized phthalonitriles can be prepared by modifying sulfonated phthalonitriles or 2,3-dicyanohydroquinone derivatives.³

Finally, there are a variety of methods that can be used to synthesize or functionalize phthalonitriles. However, the functionalization of these compounds through MCRs, as described in this thesis, was not previously reported in the literature. The synthetic route established here for the preparation of functionalized phthalonitriles should be useful for the synthesis of these important building blocks.

1.2 Results and discussion

1.2.1 Synthesis of 4-formylphthalonitrile (1.77)

Initially, the synthesis of 4-formylphthalonitrile (**1.77**) was planned as described in Scheme 1.15,⁶⁷⁻⁶⁹ starting from 4-bromobenzaldehyde (**1.74**) which was nitrated at the 3-position with sodium nitrate in a mixture of concentrated sulfuric acid at 70 °C to give 4-bromo-3-nitrobenzaldehyde (**1.75**). In the next step, reduction of the nitro group of **1.75** with an SnBr₂ solution (generated *in situ* from Sn⁰ and HBr) followed by diazotization and reaction with CuBr (Sandmeyer reaction) gave **1.76**. Finally, compound **1.76** was transformed into the 4-formylphthalonitrile (**1.77**) by the Rosenmund-von Braun reaction.



Scheme 1.15 – Synthetic route of 4-formylphthalonitrile.

The results obtained in our study together with those reported previously are summarized in Table 1.1.⁶⁷⁻⁶⁹

Analyzing the results shown in Table 1.1, it is evident that compounds **1.75-1.77** were synthesized with similar and optimized yields over those previously reported in the literature. Moreover, the synthetic route used herein could be scaled-up without loss of yield.

Table 1.1 – Results obtained and reported for the synthesis of compounds **1.75-1.77**.

Entry	Compound	Starting material (g)	Product (g)	Yield (%) ^[a]	Reference
1		10	11.5	93	Swoboda et al. ⁶⁹
2	1.75	4	4.5	90	This study
3		10.1	11.6	92	This study
4		10.5	8.1	68	Swoboda et al. ⁶⁹
5	1.76	2.1	1.9	79	This study
6		10.6	10.1	83	This study
7		4.3	1.15	46	Schweikart et al. ⁶⁷
8		4.3	1.3	53	An et al. ⁶⁸
9	1.77	1	0.26	43	This study
10		4.4	1.57	60	This study

^[a]Isolated yields.

1.2.2 Synthesis of phthalonitrile derivatives (1.80a-q)

After the synthesis and characterization of phthalonitrile **1.77**, it was used together with substituted anilines (**1.78a-g**) and phenylacetylenes (**1.79a,b**) in MCRs promoted by NbCl₅ to obtain the phthalonitriles **1.80a-i** (Table 1.2).

Table 1.2 – Synthesis of phthalonitriles **1.80a-i**.^[a]

1.79a: R₂ = H
1.79b: R₂ = *n*-pentyl
1.78a: R₁ = H
1.78b: R₁ = F
1.78c: R₁ = Cl
1.78d: R₁ = OMe
1.78e: R₁ = NO₂
1.78f: R₁ = Et
1.78g: R₁ = O-*n*-Dec
1.80a: R₁, R₂ = H
1.80b: R₁ = F; R₂ = H
1.80c: R₁ = Cl; R₂ = H
1.80d: R₁ = OMe; R₂ = H
1.80e: R₁ = NO₂; R₂ = H
1.80f: R₁ = Et; R₂ = H
1.80g: R₁ = O-*n*-Dec; R₂ = H
1.80h: R₁ = OMe; R₂ = *n*-pentyl
1.80i: R₁ = O-*n*-Dec; R₂ = *n*-pentyl

Entry	Aniline	Product	R ₁	R ₂	Yield (%) ^[f]
1 ^[b]	1.78a	1.80a	H	H	0
2 ^[c]	1.78a	1.80a	H	H	26
3 ^[d]	1.78a	1.80a	H	H	29
4	1.78a	1.80a	H	H	40
5 ^[d]	1.78b	1.80b	F	H	42
6	1.78b	1.80b	F	H	76
7 ^[e]	1.78c	1.80c	Cl	H	6
8 ^[d]	1.78c	1.80c	Cl	H	49
9	1.78c	1.80c	Cl	H	80
10 ^[d]	1.78d	1.80d	OMe	H	52
11	1.78d	1.80d	OMe	H	75
12 ^[d]	1.78e	1.80e	NO ₂	H	41
13	1.78e	1.80e	NO ₂	H	55
14	1.78f	1.80f	Et	H	75
15	1.78g	1.80g	O- <i>n</i> -Dec	H	76
16	1.78d	1.80h	OMe	<i>n</i> -pentyl	70
17	1.78g	1.80i	O- <i>n</i> -Dec	<i>n</i> -pentyl	81

^[a]Conditions: 4-formylphthalonitrile (**1.77**) (0.5 mmol), aniline derivatives (**1.78a-g**) (0.5 mmol), phenylacetylenes (**1.79a,b**) (0.55 mmol), NbCl₅ (50 mol%), *p*-chloranil (0.55 mmol) in CH₃CN (5 mL) were heated in a glass pressure tube at 100 °C for 24 h.

^[b]The reaction was carried out in the absence of NbCl₅ and *p*-chloranil at room temperature.

^[c]The reaction was carried out in the absence of *p*-chloranil at r.t. for 96 h.

^[d]The reaction was carried out in the absence of *p*-chloranil.

^[e]The reaction was carried out in the absence of NbCl₅.

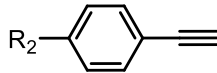
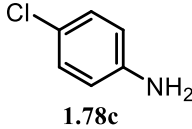
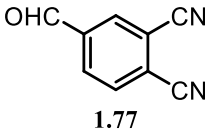
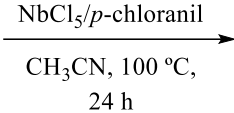
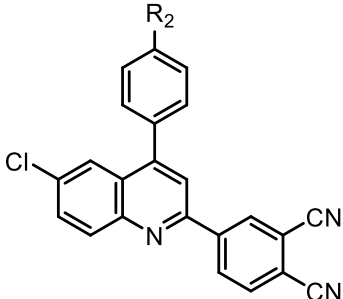
^[f]Isolated yields.

We initially tested 4-formylphthalonitrile (**1.77**) and phenylacetylene (**1.79a**) as model substrates to explore the aniline scope. When the MCR was carried out with aniline (**1.78a**) in the absence of NbCl₅ and *p*-chloranil at r.t. for 24 h, the desired phthalonitrile (**1.80a**) was not obtained (Table 1.2, entry 1). The formation of an imine (an intermediate isolable in this MCR) was detected. When the same MCR was carried out in the presence of NbCl₅ at r.t. for 96 h, the phthalonitrile **1.80a** was obtained in 26% yield (entry 2). A similar result (29%) was observed when the MCR was performed at 100 °C for 24 h (entry 3). However, when NbCl₅ and *p*-chloranil were used together also at 100 °C for 24 h, the compound **1.80a** was obtained in 40% yield (entry 4). Interestingly, when the MCR was carried out with aniline **1.78c** and *p*-chloranil (without NbCl₅), the phthalonitrile **1.80c** was obtained in 6% yield (entry 7). Similar results had already been reported by Nanni and co-workers (1992, 1993) for the synthesis of 2,4-diphenylquinolines from imines and phenylacetylene under oxidizing conditions.^{70,71}

It is also clear from Table 1.2 that anilines which contain either electron-donating or electron-withdrawing groups can be tolerated in this MCR (entries 5, 6, and 8–17) with no evident changes in yield. For example, the MCRs carried out with the substituted anilines **1.78b-e** in the presence of the NbCl₅/*p*-chloranil system at 100 °C for 24 h provided the phthalonitriles **1.80b-e** in yields ranging from 55 to 80% (entries 6, 9, 11, and 13). These results are better than those obtained using only NbCl₅ under the same conditions (41–52%, Table 1.2, entries 5, 8, 10, and 12). In addition, the MCRs carried out with the anilines **1.78f,g** and phenylacetylene (**1.79a**) or **1.78d,g** and 1-ethynyl-4-pentylbenzene (**1.79b**) in the presence of the NbCl₅/*p*-chloranil system at 100 °C for 24 h afforded the compounds **1.80f-i** in 70–81% yields (entries 14–17).

Subsequently, we used 4-formylphthalonitrile (**1.77**) and 4-chloroaniline (**1.78c**) as model substrates to explore the phenylacetylene scope (Table 1.3).

Table 1.3 – Synthesis of phthalonitriles **1.80j-p**.^[a]

				
1.79b : R ₂ = <i>n</i> -pentyl	1.79f : R ₂ = Me			
1.79c : R ₂ = <i>n</i> -butyl	1.79g : R ₂ = F			
1.79d : R ₂ = <i>tert</i> -butyl	1.79h : R ₂ = CO ₂ Me			
1.79e : R ₂ = OMe				
	+			
1.78c		1.77		1.80j : R ₂ = <i>n</i> -pentyl 1.80k : R ₂ = <i>n</i> -butyl 1.80l : R ₂ = <i>tert</i> -butyl 1.80m : R ₂ = OMe 1.80n : R ₂ = Me 1.80o : R ₂ = F 1.80p : R ₂ = CO ₂ Me
Entry	Acetylene	Product	R ₂	Yield (%) ^[b]
1	1.79b	1.80j	<i>n</i> -pentyl	80
2	1.79c	1.80k	<i>n</i> -butyl	73
3	1.79d	1.80l	<i>tert</i> -butyl	79
4	1.79e	1.80m	OMe	78
5	1.79f	1.80n	Me	80
6	1.79g	1.80o	F	79
7	1.79h	1.80p	CO ₂ Me	57

^[a]Conditions: NbCl₅ (50 mol%), *p*-chloranil (0.55 mmol), 4-formylphthalonitrile (**1.77**) (0.5 mmol), 4-chloroaniline (**1.78c**) (0.50 mmol) and phenylacetylene derivatives (**1.79b-h**) (0.55 mmol) in CH₃CN (5 mL) at 100 °C for 24 h.

^[b]Isolated yields.

Aniline **1.78c** was selected due to its efficiency in the MCR, as previously demonstrated (80%, Table 1.2, entry 9). It was found that substituted phenylacetylenes (**1.79b-g**) were suitable substrates for this MCR (Table 1.3), and the expected phthalonitriles (**1.80j-o**) were obtained in 73–80% yields (entries 1–6) using the NbCl₅/*p*-chloranil system at 100 °C for 24 h. Notably, when phenylacetylene **1.79h** (R₂ = CO₂Me) was used in the MCR under the same conditions, the phthalonitrile **1.80p** was obtained in only 57% yield (entry 7), possibly due to the strong electron-withdrawing and mesomeric effect of the ester group. Furthermore, we have successfully performed a scaled-up experiment of **1.77** (2.5 mmol) with

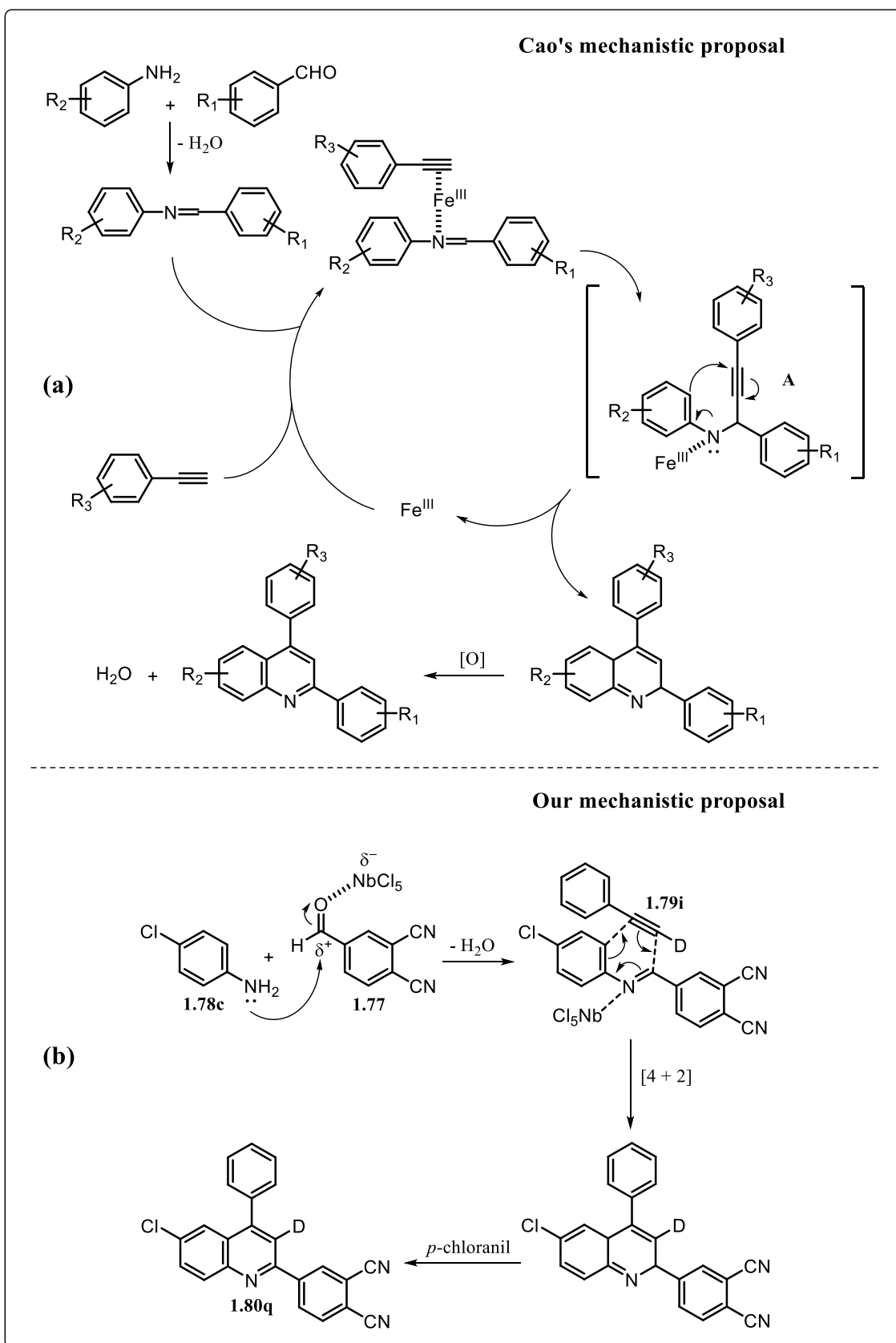
1.78c and **1.79a** using the same conditions established in Table 1.2 (entry 9), and obtained 640.2 mg of **1.80c** in 70% yield (see Section 1.4.6).

Intriguingly, the literature suggests that these reactions proceed through a stepwise pathway involving the propargylamine **A** as a key intermediate (Scheme 1.16a),⁷²⁻⁷⁹ or by a concerted pathway (not proven).^{70,80}

To obtain our own insight into the mechanism of this MCR, a deuterium labeling experiment using phenylacetylene-*d* (99% atom D) (**1.79i**) with 4-formylphthalonitrile (**1.77**) and 4-chloroaniline (**1.78c**) was carried out under the same reaction conditions, as described in Table 1.3. To our delight, the deuterated phthalonitrile **1.80q** was obtained as a single product in 74% yield, showing that C–D bond rupture does not occur during the MCR. Unsurprisingly, the same reaction with anhydrous FeCl₃ (50 mol%) also provided the deuterated phthalonitrile **1.80q** as single product (66% yield), thus supporting a concerted pericyclic mechanism and refuting a stepwise mechanism as shown in Scheme 1.16a. Thereby, we propose the initial formation of an imine between formylphthalonitrile **1.77** and the substituted anilines **1.78** promoted by NbCl₅. This is followed by a hetero-Diels-Alder reaction with the phenylacetylenes **1.79** also promoted by NbCl₅. Finally, the dihydroquinoline intermediate is oxidized by *p*-chloranil to the phthalonitrile-quinoline dyads **1.80** (Scheme 1.16b).

As illustrated in the ¹H NMR spectrum of phthalonitrile **1.80c** (Figure 1.6a), the H-3 signal of the quinoline nucleus appearing at δ 7.86 ppm (singlet, 1H) is absent in the spectrum of the deuterium-labeled phthalonitrile **1.80q** (Figure 1.6b). The structure of **1.80q** was confirmed by HRMS with a molecular ion peak at m/z 367.0865 [M (deuterated) + H]⁺ (Figure 1.7b).

After optimizing the methodology, testing the scope, and elucidating the mechanism of this NbCl₅ mediated MCR, we demonstrated the versatility of selected phthalonitrile-quinoline dyads as precursors to synthesize novel phthalocyanines (see Section 1.2.3 below).



Scheme 1.16 – (a) Mechanism proposed by Cao et al.⁷² (b) Our mechanistic proposal based on experimentation.

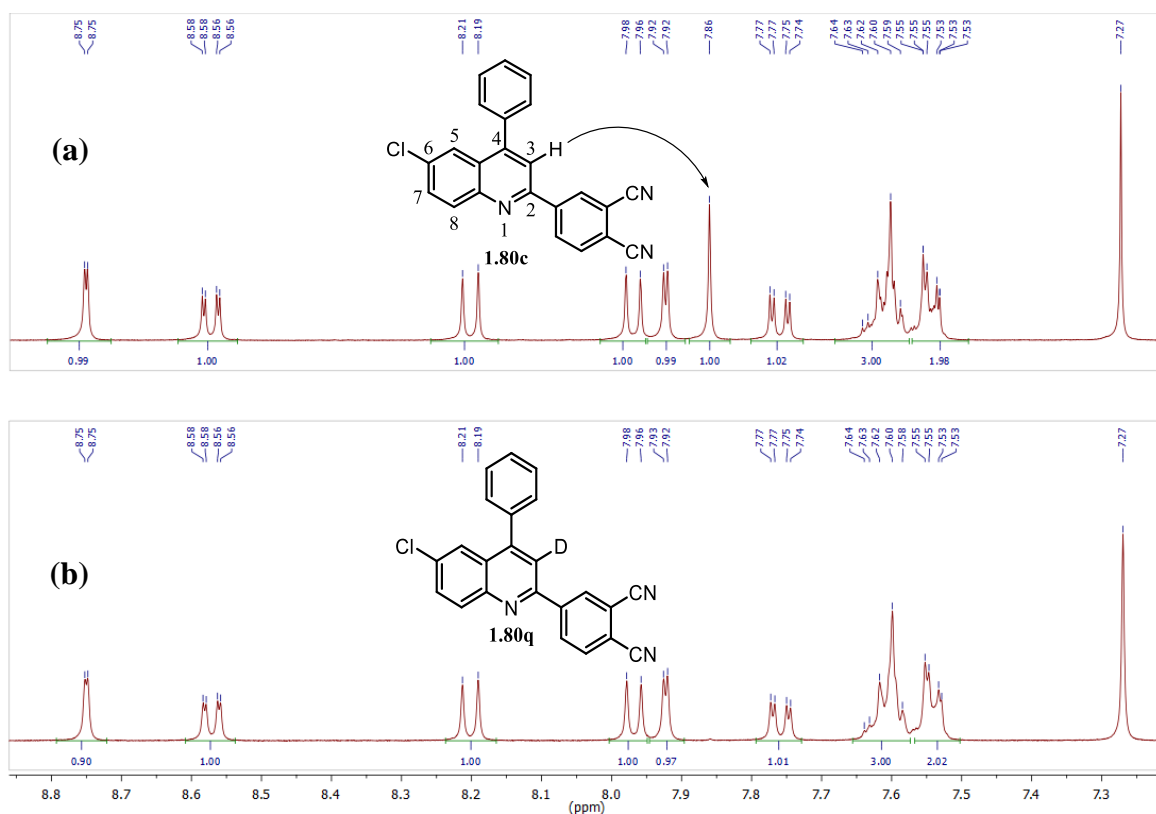


Figure 1.6 – ^1H NMR (400 MHz) spectra in CDCl_3 of **1.80c** (a) and **1.80q** (b).

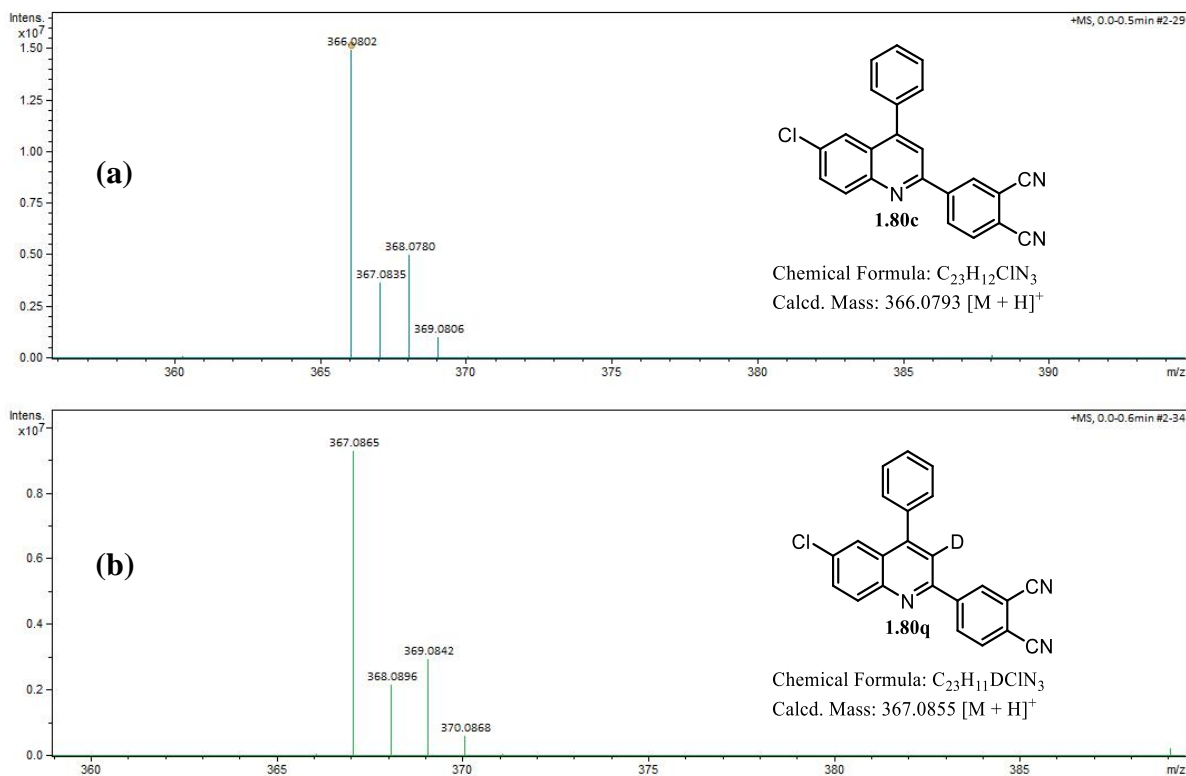
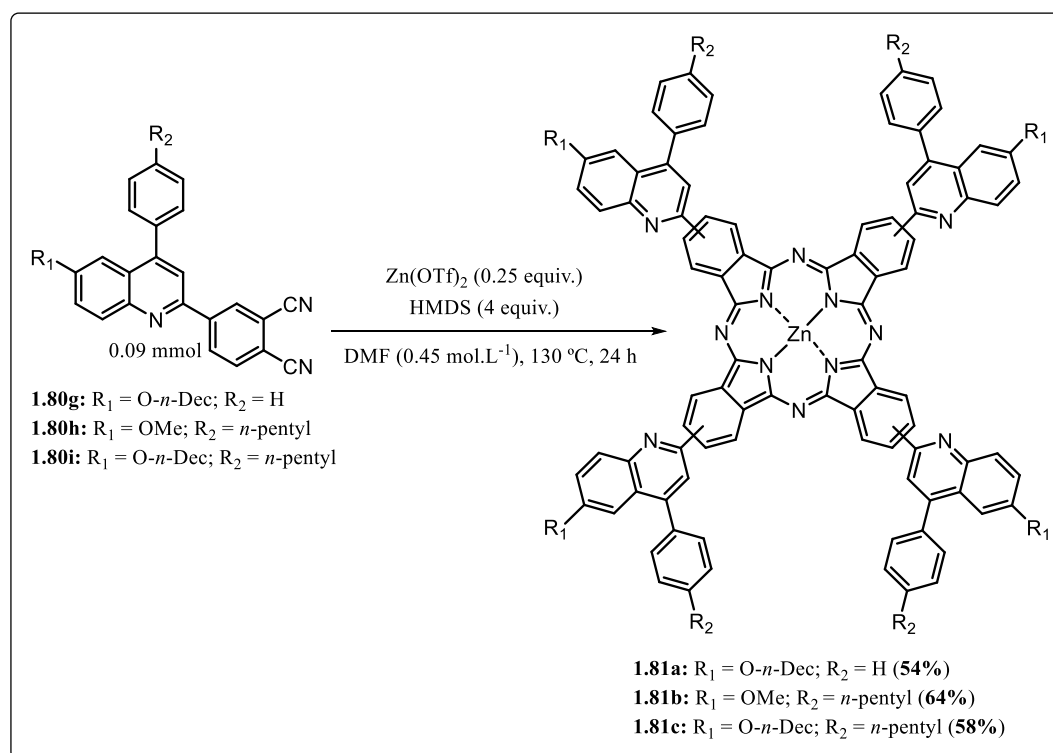


Figure 1.7 – Comparison of HRMS spectra of **1.80c** (a) and **1.80q** (b).

1.2.3 Synthesis of zinc phthalocyanine-quinoline dyads (**1.81a-c**)

ZnPCs **1.81a-c** were prepared by cyclotetramerization of phthalonitriles **1.80g-i**, respectively, in the presence of Zn(OTf)₂ and HMDS, in DMF at 130 °C for 24 h (Scheme 1.17).⁸¹ The compounds **1.81a-c** were obtained in 54–64% yields as non-separable regioisomeric mixtures. Phthalonitriles **1.80g-i** do not yield PCs using standard methodologies such as heating with Zn(OAc)₂ in DMAE.⁸²

The ¹H NMR spectra of ZnPCs **1.81a-c** (see Section 4.1.20–22, Figures 4.54–56) show that the peaks are broadened due to the presence of regioisomers and the slight aggregation in solution at the concentrations used for the NMR. The structures of ZnPCs **1.81a-c** were confirmed by MALDI-TOF mass spectrometry (see Figures S82–S84 of SI in the article).⁸³ In order to measure the preliminary photophysical properties of these new dyads, aggregation, fluorescence, and photodegradation studies were performed as described below.



Scheme 1.17 – Synthesis of zinc phthalocyanine-quinoline dyads (**1.81a-c**).

1.2.4 Aggregation, photobleaching and photophysical properties of zinc phthalocyanine-quinoline dyads (1.81a-c)

The UV-Vis spectra of dyads **1.81a-c** show intense Q band absorption in THF at 695 nm. Compared with the unsubstituted zinc phthalocyanine (666 nm), the Q bands of ZnPCs **1.81a-c** are red-shifted by 29 nm, showing the effect of the extended π -system (quinoline moieties).

The aggregation behavior of the ZnPCs **1.81a-c** was studied by concentration-dependent UV-Vis spectral measurements in THF at room temperature. As observed for compound **1.81a** (Figure 1.8), the intensity of the Q-band absorption increased with the concentration without producing new bands (normally blue-shifted). The bands perfectly followed Lambert-Beer's law (Figure 1.8 inset plot), suggesting no aggregation in this solvent at the concentrations tested. Similar behavior was found for ZnPCs **1.81b** and **1.81c** (see Section 1.4.8, Figures 1.11 and 1.12).

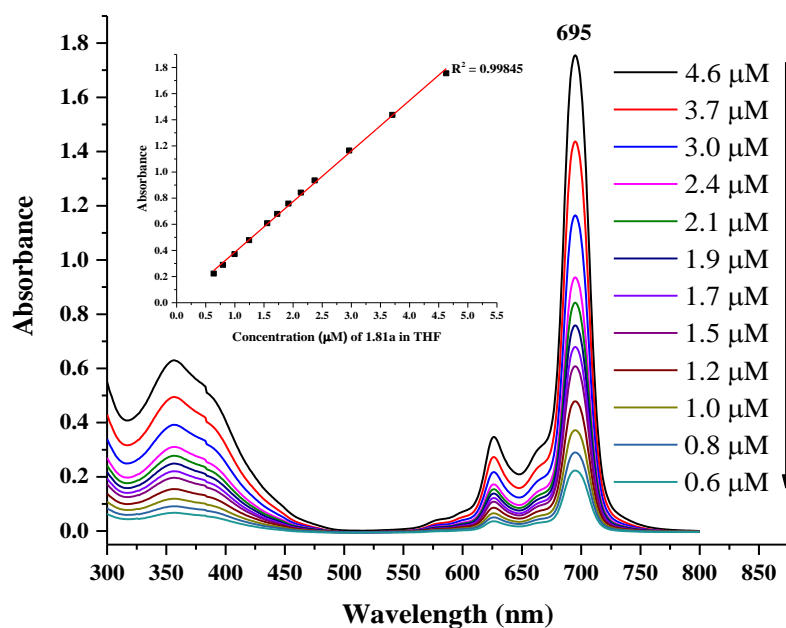


Figure 1.8 – Aggregation behavior of ZnPc **1.81a** in THF at different concentrations. The inset plots the Q band absorption at 695 nm vs. the concentration of **1.81a**.

Fluorescence measurements were studied under identical conditions in degassed THF at r.t. (Figure 1.9). Upon excitation at 630 nm, fluorescence emissions at 705 nm were found for all compounds, with the quantum yields of 0.16 (ZnPc **1.81a**) and 0.15 (ZnPcs **1.81b** and **1.81c**) relative to ZnPC standard ($\Phi_F = 0.25$ in THF),⁸⁴ and Stokes shifts of 10 nm (Table 1.4).

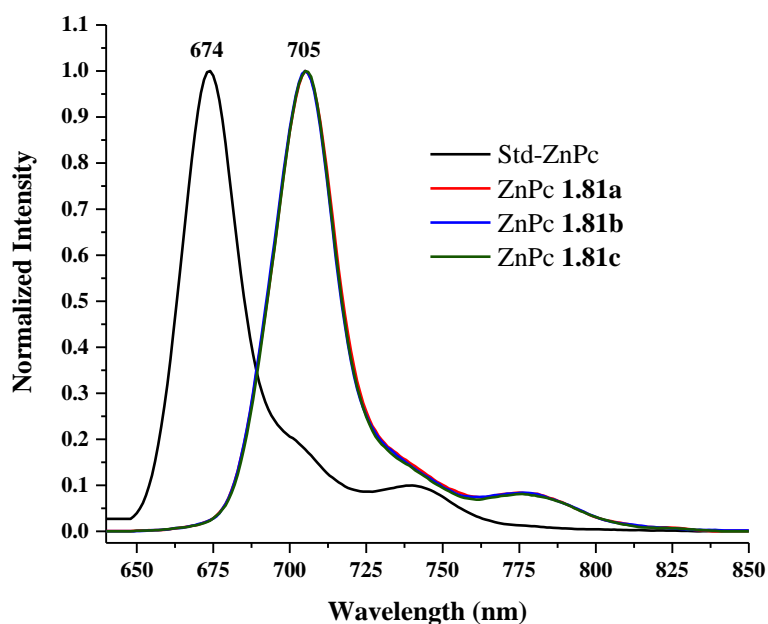


Figure 1.9 – Normalized emission spectra for Std-ZnPc (black line), **1.81a** (red line), **1.81b** (blue line) and **1.81c** (green line).

Table 1.4 – Photophysical parameters of ZnPCs **1.81a-c** in THF.

ZnPc	λ (nm) (log ϵ)	$\lambda_{em}^{[a]}$ (nm)	Stokes (nm)	$\Phi_F^{[b]}$
1.81a	357 (5.14), 626 (4.89), 695 (5.59)	705	10	0.16
1.81b	355 (5.05), 626 (4.77), 695 (5.50)	705	10	0.15
1.81c	355 (5.19), 626 (4.92), 695 (5.63)	705	10	0.15

^[a]Excited at 630 nm. All the emission analyses were carried out in degassed THF at r.t.

^[b]Relative to Std-ZnPc in THF as the reference ($\Phi_F = 0.25$).⁸⁴

The photobleaching studies (example in Figure 1.10 for ZnPC **1.81a**) were also performed in THF, and the ZnPCs **1.81a-c** showed no significant degradation after irradiation for 2 h with a white LED lamp (30 W) (see Section 1.4.11, Figures 1.15 and 1.16).

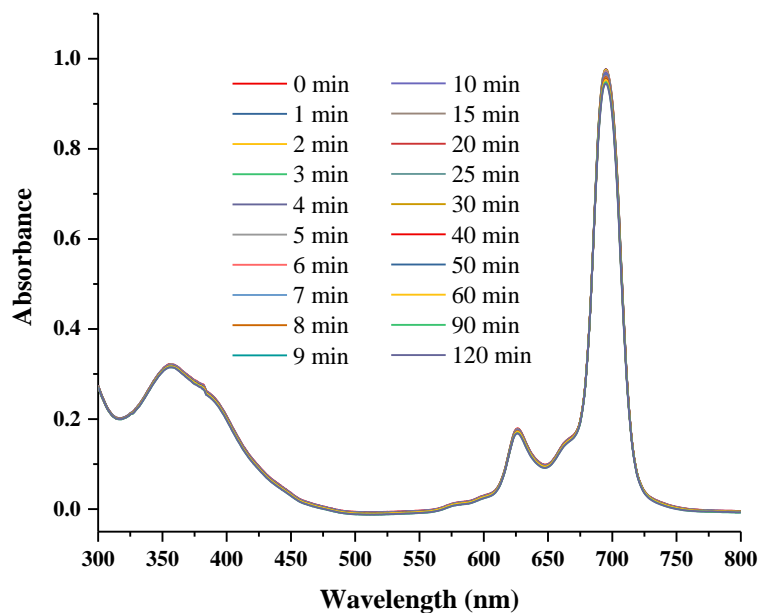


Figure 1.10 – Photobleaching study of ZnPc **1.81a** in THF.

1.3 Conclusion

We have developed a multicomponent approach for the synthesis of phthalonitrile-quinoline dyads by the reaction of 4-formylphthalonitrile, anilines, and phenylacetylenes in acetonitrile at 100 °C for 24 h in the presence of NbCl₅ and *p*-chloranil. The methodology describes the scope (17 examples, 40–81% yield) and scalability for the preparation of the phthalonitrile-quinoline dyad **1.80c** on a 600 mg-scale. Experimental mechanistic insights on the key MCR process are described, using a deuterated reagent, clearly showing the pericyclic nature of a hetero-Diels-Alder reaction between imines (generated *in situ* from anilines and 4-formylphthalonitrile) and phenylacetylenes.

To show the versatility of our phthalonitrile library, we have also synthesized three new zinc phthalocyanine derivatives and measured their photophysical properties including UV-Vis absorption spectra, fluorescence emissions, molar absorption coefficients, Stokes shifts and the relative fluorescence quantum yields in THF solution. The aggregation behavior of the ZnPCs in THF was investigated by concentration-dependent UV-Vis measurements (from 5.4 x 10⁻⁶ M to 0.6 x 10⁻⁶ M) and no aggregation was observed in this concentration range. Finally, photobleaching studies were also performed in THF and no significant degradation of ZnPCs occurred after continuous irradiation with a white LED lamp (30 W) for 2 h, which showed high resistance to photobleaching.

1.4 Experimental

1.4.1 Chemicals and materials

The niobium pentachloride was supplied by Companhia Brasileira de Metalurgia e Mineração (CBMM, Brazil) and used as received. All the other reagents were purchased from Sigma-Aldrich or Synth (Brazil) and used as supplied. Anhydrous potassium carbonate was dried at 110 °C for 12 h before use. Tetrahydrofuran was distilled over sodium/benzophenone before use, degassed by bubbling argon through it and stored over molecular sieves (4 Å). Aniline, acetonitrile, and *N,N*-dimethylformamide were dried with calcium hydride, distilled following standard protocols⁸⁵ and stored over molecular sieves (4 Å) under an argon atmosphere. Bis(trimethylsilyl)amine was distilled and stored over molecular sieves (4 Å) under an argon atmosphere. Analytical thin-layer chromatography (TLC) was performed on Merck aluminum sheets coated with silica gel 60 F₂₅₄ and visualized with ultraviolet light (254 or 366 nm) or heating with TLC stains. Gravity column chromatography was performed on silica gel (70-230 mesh, 63-200 μM, pore size 60 Å, Merck), and flash column chromatography was performed on silica gel (230-400 mesh, 40-63 μM, pore size 60 Å, Merck).

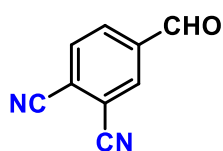
1.4.2 Equipment

¹H NMR, ¹³C NMR, and DEPT-135 spectra were recorded on a Bruker Avance III 400 (operating at 400.15 and 100.62 MHz for ¹H and ¹³C, respectively) or 600 (operating at 600.23 and 150.93 MHz for ¹H and ¹³C, respectively) spectrometers with tetramethylsilane as the internal reference and CDCl₃ or CDCl₃/DMSO-*d*₆ as solvents. All coupling constants (*J* values) are reported in hertz. The following abbreviations were used to describe NMR peak multiplicities: s = singlet, d = doublet, t = triplet, q = quartet, m = multiplet, etc. All NMR data

were processed using the MestReNova 9.0.1 software package. FT-IR spectra were recorded on a Shimadzu IR Prestige-21 spectrophotometer using KBr pellets in the range of 4000-400 cm^{-1} . UV-Vis absorption spectra were recorded on a Perkin Elmer Lambda 25 spectrophotometer using 1 cm optical length quartz cuvettes at 25 °C and tetrahydrofuran (HPLC grade) as the solvent. The fluorescence spectra were recorded on a Shimadzu RF-5301PC spectrofluorophotometer using 1 cm optical length cuvettes at 25 °C and degassed tetrahydrofuran (HPLC grade) as the solvent. EI-MS spectra were acquired at 70 eV on a Shimadzu GCMS-QP5000 mass spectrometer coupled with a Shimadzu GC-17A gas chromatograph. HRMS (ESI-TOF) spectra were registered in a positive ion mode on a Bruker Daltonics (Impact HD) UHR-QqTOF (Ultra-High Resolution Qq-Time-Of-Flight) mass spectrometer. HRMS (MALDI-TOF) spectra were obtained on a Bruker Daltonics Ultraflex extreme MALDI-TOF/TOF mass spectrometer in positive reflector mode using α -cyano-4-hydroxycinnamic acid as the matrix. All melting points were determined on a Microquímica™ MQRPF-301 apparatus. The organic solvents were evaporated using a Büchi Rotavapor R-215 at 40 °C.

1.4.3 Procedure for synthesis of 4-Formylphthalonitrile (**1.77**)

Phthalonitrile **1.77** was prepared in three steps by previously reported procedures.^{68,69} Nitration of commercially available 4-bromobenzaldehyde (**1.74**) with a mixture of H_2SO_4 and NaNO_3 yielded 4-bromo-3-nitrobenzaldehyde (**1.75**) in 92% yield (11.58 g, 50.34 mmol). 3,4-Dibromobenzaldehyde (**1.76**) was then obtained in 83% yield (10.09 g, 38.23 mmol) by the reduction with tin(II) bromide (generated *in situ* from Sn^0 and HBr), followed by diazotization and reaction with CuBr (Sandmeyer reaction). Finally, dibromobenzaldehyde **1.76** was converted into **1.77** by the Rosenmund-von Braun reaction (CuCN) in 60% yield (1.57 g, 10.05 mmol).



Mp: 138–140 °C (Lit.⁸⁶ 138 °C). ¹H NMR (CDCl₃, 400.15 MHz, ppm): δ 10.13 (s, 1H, CHO), 8.34 – 8.29 (m, 1H), 8.24 (dd, *J* = 8.0, 1.6 Hz, 1H), 8.04 (d, *J* = 8.0 Hz, 1H). ¹³C NMR (CDCl₃, 100.62 MHz, ppm): δ 188.3 (CHO), 138.8, 134.5, 133.8, 133.3, 120.3, 117.2, 114.6 (CN), 114.4 (CN). ¹³C NMR (DEPT-135) (CDCl₃, 100.63 MHz, ppm): δ 134.5, 133.8, 133.3. FT-IR (KBr, cm⁻¹): ν = 3105, 3071, 2878 (CHO), 2234 (C≡N), 1709 (C=O), 1597, 1381, 1194, 1096, 945, 851, 752, 530. EI-MS (*m/z* (%)): 156 (54) [M⁺], 155 (100) [M⁺ – H], 127 (38) [M⁺ – CHO], 100 (21), 75 (20), 50 (25).

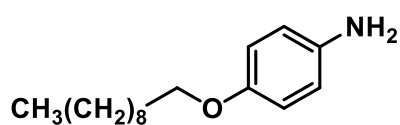
1.4.4 Procedure for synthesis of 4-(Decyloxy)aniline (1.78g)

Aniline **1.78g** was prepared in two steps following reported procedures with some slight modifications.^{87,88}

I. Alkylation of the phenol: A mixture of 4-nitrophenol (3.48 g, 0.025 mol), K₂CO₃ (13.8 g, 0.1 mol) and 1-bromodecane (7.8 mL, 0.0375 mol) in cyclohexanone (50 mL) was stirred under reflux for 3 h. The resultant reaction mixture was filtered to separate the K₂CO₃ and then the cyclohexanone was distilled off under reduced pressure. The residue obtained was purified by silica gel column chromatography (hexane/EtOAc, 9:1 v/v) to afford a yellow oil that was crystallized from ethanol to give 1-(decyloxy)-4-nitrobenzene in 93% yield (6.48 g, 23.2 mmol).

II. Hydrogenation of the aromatic nitro group: 1-(decyloxy)-4-nitrobenzene (1 g, 3.58 mmol) was dissolved in dry THF (5 mL) and 10% Pd/C (0.1 g) was added. The reaction mixture was degassed and stirred under H₂ gas (1 atm) for 12 h at room temperature. The resultant reaction mixture was filtered through a plug of Celite, which was rinsed with CH₂Cl₂. The solvents were removed under vacuum and the remaining residue was purified by flash column

chromatography (silica gel, hexane/EtOAc, 8:2 v/v) to afford the desired aniline **1.78g** in 97% yield (869 mg, 3.48 mmol).



Mp: 40–41 °C. ¹H NMR (CDCl₃, 400.15 MHz, ppm): δ 6.75 (d, *J* = 8.8 Hz, 2H), 6.65 (d, *J* = 8.8 Hz, 2H), 3.88 (t, *J* = 6.6 Hz, 2H), 3.46 (s, 2H), 1.75 (dt, *J* = 14.8, 6.7 Hz, 2H), 1.50 – 1.39 (m, 2H), 1.39 – 1.20 (m, 12H), 0.89 (t, *J* = 6.7 Hz, 3H). ¹³C NMR (CDCl₃, 100.63 MHz, ppm): δ 152.4, 139.8, 116.4, 115.7, 68.7, 31.9, 29.6, 29.5, 29.4, 29.3, 26.1, 22.7, 14.1. ¹³C NMR (DEPT-135) (CDCl₃, 100.63 MHz, ppm): δ 116.4, 115.7, 68.7, 31.9, 29.6, 29.5, 29.4, 29.3, 26.1, 22.7, 14.1. FT-IR (KBr, cm⁻¹): ν = 3385 (NH), 3312 (NH), 2955, 2918, 2849, 1516, 1474, 1246, 1030, 827, 766, 525. EI-MS (*m/z* (%)): 249 (7) [M⁺], 109 (100), 80 (7), 43 (13), 41 (17).

1.4.5 General procedure for the synthesis of phthalonitriles

To a 15-mL glass pressure tube (Ace tube®, back seal, Aldrich Z181064) with magnetic stirring, were added sequentially *p*-chloranil (135.2 mg, 0.55 mmol), NbCl₅ (67.5 mg, 0.25 mmol, 50 mol%) and anhydrous CH₃CN (1 mL) under an argon atmosphere. To this mixture was added a previously prepared solution of 4-formylphthalonitrile (**1.77**) (78.1 mg, 0.5 mmol), anilines (**1.78a-g**) (0.5 mmol) and phenylacetylenes (**1.79a-i**) (0.55 mmol) in 4 mL of anhydrous CH₃CN under argon. Then, the tube was closed and the resulting mixture was stirred at 100 °C in an oil bath for 24 h. After cooling to r.t., the resultant reaction mixture was quenched with H₂O (5 mL) and extracted with CH₂Cl₂ (3 x 20 mL). The combined organic extracts were washed with sat. aqueous NaHCO₃ (3 x 20 mL) and H₂O (3 x 50 mL), dried over Na₂SO₄, filtered, and concentrated under vacuum. Two different methods for purification were used:

Method 1: The residue was chromatographed on silica gel (70-230 mesh) and eluted with CH₂Cl₂/hexane (9:1, v/v). After solvent removal, the product was sonicated with ethanol (10

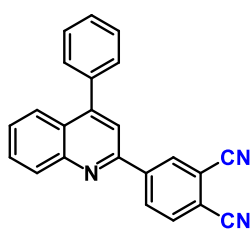
mL) for 20 min, followed by cooling in a refrigerator for 12 h, filtration, and dried under vacuum at room temperature.

Method 2: The residue was sonicated with ethanol (10 mL) for 20 min, followed by cooling in a refrigerator for 12 h, and filtration. This was repeated two more times with ethanol (10 mL) and once with pentane/EtOAc (7:3, v/v; 10 mL). Finally, the product was dried under vacuum at room temperature.

The same procedure was used when the multicomponent reaction was performed in the absence of *p*-chloranil.

1.4.6 Characterization data of phthalonitrile-quinoline dyads

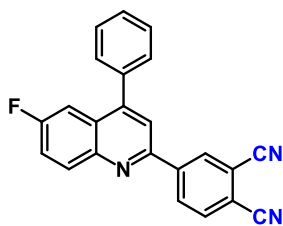
4-(4-Phenylquinolin-2-yl)phthalonitrile (1.80a): The MCR was carried out according to the general procedure with aniline (**1.78a**) (46.6 mg, 0.5 mmol) and phenylacetylene (**1.79a**) (57.3 mg, 0.55 mmol), and purified by method 1 to afford the phthalonitrile **1.80a** in 40% yield (66.9 mg, 0.202 mmol). When the same reaction was carried out in the absence of *p*-chloranil, compound **1.80a** was obtained in 29% yield (48.6 mg, 0.147 mmol). A similar result (43.1 mg, 0.130 mmol, yield 26%) was observed when the MCR was performed in the absence of *p*-chloranil at r.t. for 96 h.



Mp: 240–241 °C. ¹H NMR (CDCl₃, 400.15 MHz, ppm): δ 8.77 (d, *J* = 1.7 Hz, 1H), 8.59 (dd, *J* = 8.3, 1.8 Hz, 1H), 8.26 (d, *J* = 8.6 Hz, 1H), 7.97 (d, *J* = 8.2 Hz, 2H), 7.86 – 7.80 (m, 2H), 7.63 – 7.55 (m, 6H). ¹³C NMR (CDCl₃, 100.62 MHz, ppm): δ 151.8, 150.5, 148.8, 144.3, 137.6, 133.9, 132.5, 131.4, 130.5, 130.4, 129.5, 128.9, 128.8, 127.9, 126.5, 125.9, 118.4, 116.5, 115.6, 115.4. ¹³C NMR (DEPT-135) (CDCl₃, 100.62 MHz, ppm): δ 133.9, 132.5,

131.4, 130.5, 130.4, 129.5, 128.9, 128.8, 127.9, 125.9, 118.4. FT-IR (KBr, cm^{-1}): $\nu = 3115, 3076, 3051, 2234 (\text{C}\equiv\text{N}), 1589, 1489, 1416, 1362, 1217, 924, 887, 854, 766, 698, 579, 528$. HRMS (ESI-TOF): m/z calcd. for $\text{C}_{23}\text{H}_{14}\text{N}_3^+ [\text{M} + \text{H}]^+$: 332.1182; Found: 332.1195.

4-(6-Fluoro-4-phenylquinolin-2-yl)phthalonitrile (1.80b): The MCR was carried out according to the general procedure with 4-fluoroaniline (**1.78b**) (56.1 mg, 0.5 mmol) and phenylacetylene (**1.79a**) (57.3 mg, 0.55 mmol), and purified by method 1 to afford the phthalonitrile **1.80b** in 76% yield (132.5 mg, 0.379 mmol). When the same reaction was carried out in the absence of *p*-chloranil, compound **1.80b** was obtained in 42% yield (74.1 mg, 0.212 mmol).

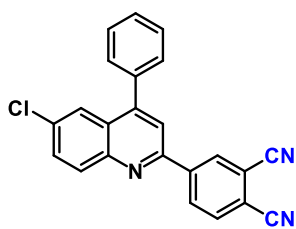


Mp: 238–239 °C. ^1H NMR (CDCl_3 , 400.15 MHz, ppm): δ 8.74 (d, $J = 1.8$ Hz, 1H), 8.56 (dd, $J = 8.3, 1.8$ Hz, 1H), 8.30 – 8.23 (m, 1H), 7.96 (d, $J = 8.2$ Hz, 1H), 7.85 (s, 1H), 7.63 – 7.51 (m, 7H). ^{13}C NMR (CDCl_3 , 100.62 MHz, ppm): δ 161.4 (d, $J = 250.5$ Hz), 151.3 (d, $J = 2.5$ Hz), 150.0 (d, $J = 5.7$ Hz), 146.0, 144.0, 137.2, 134.0, 133.0 (d, $J = 9.2$ Hz), 132.4, 131.3, 129.3, 129.2, 129.0, 127.4 (d, $J = 9.7$ Hz), 120.9 (d, $J = 26.0$ Hz), 118.9, 116.6, 115.7, 115.4, 109.4 (d, $J = 23.2$ Hz). ^{13}C NMR (DEPT-135) (CDCl_3 , 100.62 MHz, ppm): δ 134.0, 133.0 (d, $J = 9.2$ Hz), 132.4, 131.3, 129.3, 129.2, 129.0, 120.9 (d, $J = 26.0$ Hz), 118.9, 109.4 (d, $J = 23.2$ Hz). FT-IR (KBr, cm^{-1}): $\nu = 3115, 3076, 3049, 2234 (\text{C}\equiv\text{N}), 1626, 1591, 1493, 1364, 1234, 1198, 826, 773, 702, 527$. HRMS (ESI-TOF): m/z calcd. for $\text{C}_{23}\text{H}_{13}\text{FN}_3^+ [\text{M} + \text{H}]^+$: 350.1088; Found: 350.1098.

4-(6-Chloro-4-phenylquinolin-2-yl)phthalonitrile (1.80c): The MCR was carried out according to the general procedure with 4-chloroaniline (**1.78c**) (65.1 mg, 0.5 mmol) and phenylacetylene (**1.79a**) (57.3 mg, 0.55 mmol), and purified by method 1 to afford the phthalonitrile **1.80c** in 80% yield (147.4 mg, 0.403 mmol). When the same reaction was carried out in the absence of *p*-chloranil, compound **1.80c** was obtained in 49% yield (90.5 mg, 0.247

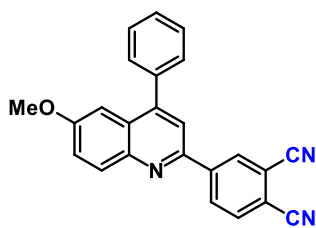
mmol). In the absence of NbCl₅, phthalonitrile **1.80c** was obtained in 6% yield (11.0 mg, 0.03 mmol).

The same procedure was used to scale up this MCR. In this case, a 100-mL glass pressure tube (Ace tube®, back seal, Aldrich Z566241) was used, and the following amounts of reagents were used: 4-chloroaniline (**1.78c**) (325.4 mg, 2.5 mmol), 4-formylphthalonitrile (**1.77**) (390.4 mg, 2.5 mmol), phenylacetylene (**1.79a**) (286.6 mg, 2.75 mmol), *p*-chloranil (676.2 mg, 2.75 mmol), NbCl₅ (337.7 mg, 1.25 mmol), and CH₃CN (25 mL). Yield: 70% (640.2 mg, 1.75 mmol).



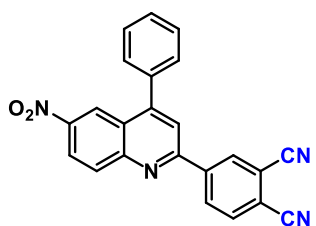
Mp: 261–262 °C. ¹H NMR (CDCl₃, 400.15 MHz, ppm): δ 8.75 (d, *J* = 1.7 Hz, 1H), 8.57 (dd, *J* = 8.2, 1.8 Hz, 1H), 8.20 (d, *J* = 9.0 Hz, 1H), 7.97 (d, *J* = 8.2 Hz, 1H), 7.92 (d, *J* = 2.3 Hz, 1H), 7.86 (s, 1H), 7.76 (dd, *J* = 9.0, 2.3 Hz, 1H), 7.67 – 7.58 (m, 3H), 7.57 – 7.51 (m, 2H). ¹³C NMR (CDCl₃, 100.62 MHz, ppm): δ 152.0, 149.8, 147.2, 143.9, 137.0, 134.0, 132.4, 132.0, 131.5, 131.4, 129.3, 129.2, 129.0, 127.2, 124.7, 119.1, 116.6, 115.8, 115.4, 115.3. ¹³C NMR (DEPT-135) (CDCl₃, 100.62 MHz, ppm): δ 134.0, 132.4, 132.0, 131.5, 131.4, 129.3, 129.2, 129.0, 124.7, 119.1. FT-IR (KBr, cm⁻¹): ν = 3117, 3080, 2235 (C≡N), 1587, 1483, 1362, 1152, 883, 822, 777, 706, 527. HRMS (ESI-TOF): *m/z* calcd. for C₂₃H₁₃ClN₃⁺ [M + H]⁺: 366.0793; Found: 366.0802.

4-(6-Methoxy-4-phenylquinolin-2-yl)phthalonitrile (1.80d): The MCR was carried out according to the general procedure with 4-methoxyaniline (**1.78d**) (61.6 mg, 0.5 mmol) and phenylacetylene (**1.79a**) (57.3 mg, 0.55 mmol), and purified by method 1 to afford the phthalonitrile **1.80d** in 75% yield (135.1 mg, 0.374 mmol). When the same reaction was carried out in the absence of *p*-chloranil, compound **1.80d** was obtained in 52% yield (94.5 mg, 0.261 mmol).



Mp: 197–198 °C. ^1H NMR (CDCl_3 , 600.23 MHz, ppm): δ 8.73 (d, J = 1.8 Hz, 1H), 8.55 (dd, J = 8.2, 1.8 Hz, 1H), 8.15 (d, J = 9.2 Hz, 1H), 7.93 (d, J = 8.2 Hz, 1H), 7.79 (s, 1H), 7.62 – 7.54 (m, 5H), 7.47 (dd, J = 9.2, 2.8 Hz, 1H), 7.21 (d, J = 2.8 Hz, 1H), 3.83 (s, 3H). ^{13}C NMR (CDCl_3 , 150.93 MHz, ppm): δ 159.0, 149.4, 148.8, 145.0, 144.5, 138.0, 133.9, 132.1, 131.9, 131.1, 129.2, 128.9, 128.8, 127.7, 123.1, 118.7, 116.5, 115.6, 115.5, 115.1, 103.6, 55.6. ^{13}C NMR (DEPT-135) (CDCl_3 , 150.93 MHz, ppm): δ 133.9, 132.1, 131.9, 131.1, 129.2, 128.9, 128.8, 123.1, 118.7, 103.6, 55.6. FT-IR (KBr, cm^{-1}): ν = 3113, 3078, 3051, 2949, 2824, 2234 ($\text{C}\equiv\text{N}$), 1626, 1599, 1493, 1368, 1265, 1223, 1042, 854, 826, 700, 528. HRMS (ESI-TOF): m/z calcd. for $\text{C}_{24}\text{H}_{16}\text{N}_3\text{O}^+$ [$\text{M} + \text{H}$] $^+$: 362.1288; Found: 362.1307.

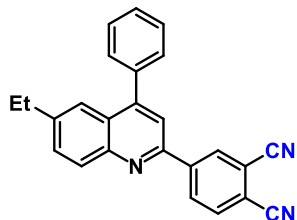
4-(6-Nitro-4-phenylquinolin-2-yl)phthalonitrile (1.80e): The MCR was carried out according to the general procedure with 4-nitroaniline (**1.78e**) (69.1 mg, 0.5 mmol) and phenylacetylene (**1.79a**) (57.3 mg, 0.55 mmol), and purified by method 2 to afford the phthalonitrile **1.80e** in 55% yield (103.6 mg, 0.275 mmol). When the same reaction was carried out in the absence of *p*-chloranil, compound **1.80e** was obtained in 41% yield (77.8 mg, 0.207 mmol).



Mp: > 300 °C. ^1H NMR (CDCl_3 , 400.15 MHz, ppm): δ 8.91 (d, J = 2.5 Hz, 1H), 8.80 (d, J = 1.2 Hz, 1H), 8.63 (dd, J = 8.2, 1.8 Hz, 1H), 8.58 (dd, J = 9.2, 2.5 Hz, 1H), 8.40 (d, J = 9.3 Hz, 1H), 8.06 – 7.97 (m, 2H), 7.72 – 7.62 (m, 3H), 7.62 – 7.52 (m, 2H). ^{13}C NMR (CDCl_3 , 100.62 MHz, ppm): δ 154.9, 152.7, 146.3, 143.0, 136.0, 134.0, 132.6, 132.1, 131.6, 129.8, 129.3, 125.5, 123.8, 122.9, 119.7, 116.7, 116.5, 115.1. ^{13}C NMR (DEPT-135) (CDCl_3 , 100.62 MHz, ppm): δ 134.0, 132.6, 132.1, 131.6, 129.8, 129.3, 123.8, 122.9, 119.7. FT-IR (KBr, cm^{-1}): ν = 3105, 3080, 3051, 2235 ($\text{C}\equiv\text{N}$), 1620, 1591, 1551, 1485, 1410, 1342, 1084, 841, 810, 766, 746, 704, 527. HRMS (ESI-TOF): m/z calcd. for $\text{C}_{23}\text{H}_{13}\text{N}_4\text{O}_2^+$ [$\text{M} + \text{H}$] $^+$: 377.1033; Found: 377.1042.

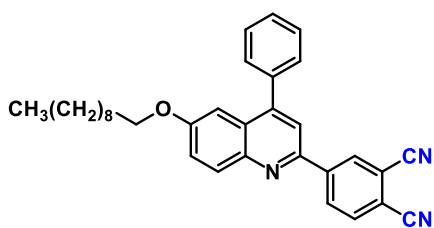
4-(6-Ethyl-4-phenylquinolin-2-yl)phthalonitrile (1.80f): The MCR was carried out according to the general procedure with 4-ethylaniline (**1.78f**) (61.8 mg, 0.5 mmol) and

phenylacetylene (**1.79a**) (57.3 mg, 0.55 mmol), and purified by method 1 to afford the phthalonitrile **1.80f** in 75% yield (135.3 mg, 0.376 mmol).



Mp: 215–216 °C. $^1\text{H NMR}$ (CDCl_3 , 400.15 MHz, ppm): δ 8.75 (d, $J = 1.6$ Hz, 1H), 8.56 (dd, $J = 8.2, 1.8$ Hz, 1H), 8.18 (d, $J = 8.6$ Hz, 1H), 7.94 (d, $J = 8.2$ Hz, 1H), 7.80 (s, 1H), 7.75 – 7.66 (m, 2H), 7.64 – 7.51 (m, 5H), 2.81 (q, $J = 7.6$ Hz, 2H), 1.30 (t, $J = 7.6$ Hz, 3H). $^{13}\text{C NMR}$ (CDCl_3 , 100.63 MHz, ppm): δ 150.9, 149.8, 147.6, 144.5, 144.4, 137.8, 133.9, 132.4, 131.6, 131.3, 130.3, 129.4, 128.8, 126.5, 123.4, 118.4, 116.5, 115.5, 115.4, 115.3, 29.2, 15.4. $^{13}\text{C NMR}$ (DEPT-135) (CDCl_3 , 100.63 MHz, ppm): δ 133.9, 132.4, 131.6, 131.3, 130.3, 129.4, 128.8, 123.4, 118.4, 29.2, 15.4. FT-IR (KBr, cm^{-1}): $\nu = 3074, 2965, 2230$ ($\text{C}\equiv\text{N}$), 1597, 1585, 1489, 1414, 845, 700, 523. HRMS (ESI-TOF): m/z calcd. for $\text{C}_{25}\text{H}_{18}\text{N}_3^+$ [$\text{M} + \text{H}$] $^+$: 360.1495; Found: 360.1498.

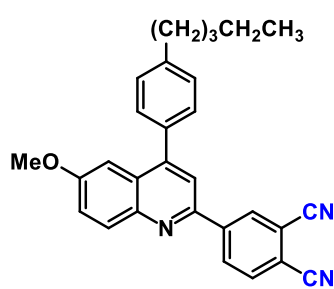
4-(6-(Decyloxy)-4-phenylquinolin-2-yl)phthalonitrile (1.80g): The MCR was carried out according to the general procedure with 4-(decyloxy)aniline (**1.78g**) (124.7 mg, 0.5 mmol) and phenylacetylene (**1.79a**) (57.3 mg, 0.55 mmol), and purified by method 1 to afford the phthalonitrile **1.80g** in 76% yield (185.1 mg, 0.379 mmol).



Mp: 128–130 °C. $^1\text{H NMR}$ (CDCl_3 , 400.15 MHz, ppm): δ 8.73 (d, $J = 1.2$ Hz, 1H), 8.55 (dd, $J = 8.3, 1.5$ Hz, 1H), 8.14 (d, $J = 9.2$ Hz, 1H), 7.93 (d, $J = 8.2$ Hz, 1H), 7.77 (s, 1H), 7.65 – 7.51 (m, 5H), 7.47 (dd, $J = 9.1, 2.7$ Hz, 1H), 7.19 (d, $J = 2.6$ Hz, 1H), 3.96 (t, $J = 6.5$ Hz, 2H), 1.79 (dt, $J = 14.9, 6.4$ Hz, 2H), 1.50 – 1.41 (m, 2H), 1.39 – 1.21 (m, 12H), 0.89 (t, $J = 6.7$ Hz, 3H). $^{13}\text{C NMR}$ (CDCl_3 , 100.63 MHz, ppm): δ 158.5, 149.2, 148.7, 144.8, 144.5, 138.0, 133.9, 132.1, 131.8, 131.0, 129.2, 128.9, 128.8, 127.7, 123.3, 118.6, 116.4, 115.6, 155.5, 115.0, 104.3, 68.4, 31.9, 29.5, 29.4, 29.3, 29.1, 26.0, 22.7, 14.1. $^{13}\text{C NMR}$ (DEPT-135) (CDCl_3 , 100.63 MHz, ppm): δ 133.9, 132.1, 131.8, 131.0, 129.2, 128.9, 128.8, 123.3, 118.6, 104.3, 68.4, 31.9, 29.5, 29.4, 29.3, 29.1, 26.0, 22.7, 14.1. FT-IR (KBr, cm^{-1}): $\nu = 3078, 3049, 2918, 2851, 2234$ ($\text{C}\equiv\text{N}$), 1622, 1599,

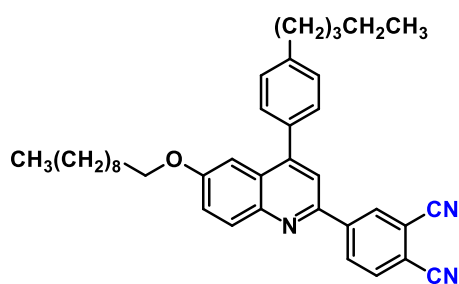
1489, 1470, 1369, 1223, 1036, 860, 825, 702, 527. HRMS (ESI-TOF): m/z calcd. for $C_{33}H_{34}N_3O^+$ [$M + H$] $^+$: 488.2696; Found: 488.2703.

4-(6-Methoxy-4-(4-pentylphenyl)quinolin-2-yl)phthalonitrile (1.80h): The MCR was carried out according to the general procedure with 4-methoxyaniline (**1.78d**) (61.6 mg, 0.5 mmol) and 1-ethynyl-4-pentylbenzene (**1.79b**) (97.7 mg, 0.55 mmol), and purified by method 1 to afford the phthalonitrile **1.80h** in 70% yield (150.9 mg, 0.350 mmol).



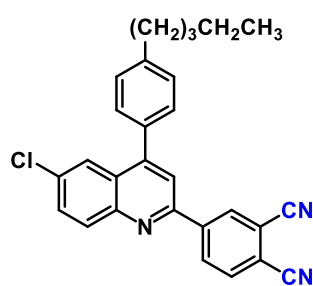
Mp: 177–178 °C. 1H NMR ($CDCl_3$, 400.15 MHz, ppm): δ 8.70 (d, $J = 1.5$ Hz, 1H), 8.52 (dd, $J = 8.3, 1.7$ Hz, 1H), 8.12 (d, $J = 9.2$ Hz, 1H), 7.91 (d, $J = 8.2$ Hz, 1H), 7.76 (s, 1H), 7.51 – 7.43 (m, 3H), 7.42 – 7.36 (m, 2H), 7.28 – 7.23 (m, 1H), 3.83 (s, 3H), 2.74 (t, $J = 7.8$ Hz, 2H), 1.73 (quint, $J = 7.4$ Hz, 2H), 1.46 – 1.34 (m, 4H), 0.95 (t, $J = 7.0$ Hz, 3H). ^{13}C NMR ($CDCl_3$, 100.62 MHz, ppm): δ 158.9, 149.4, 148.9, 145.0, 144.5, 143.9, 135.2, 133.9, 132.1, 131.9, 131.0, 129.1, 128.9, 127.8, 122.9, 118.7, 116.4, 115.6, 115.5, 115.0, 103.8, 55.6, 35.8, 31.6, 31.1, 22.6, 14.1. ^{13}C NMR (DEPT-135) ($CDCl_3$, 100.62 MHz, ppm): δ 133.9, 132.1, 131.9, 131.0, 129.1, 129.0, 122.9, 118.7, 103.8, 55.6, 35.8, 31.6, 31.1, 22.6, 14.1. FT-IR (KBr, cm^{-1}): $\nu = 3084, 3034, 2994, 2951, 2924, 2859, 2239$ ($C\equiv N$), 2230 ($C\equiv N$), 1620, 1595, 1493, 1470, 1225, 1042, 847, 831, 523. HRMS (ESI-TOF): m/z calcd. for $C_{29}H_{26}N_3O^+$ [$M + H$] $^+$: 432.2070; Found: 432.2088.

4-(6-(Decyloxy)-4-(4-pentylphenyl)quinolin-2-yl)phthalonitrile (1.80i): The MCR was carried out according to the general procedure with 4-(decyloxy)aniline (**1.78g**) (124.7 mg, 0.5 mmol) and 1-ethynyl-4-pentylbenzene (**1.79b**) (97.7 mg, 0.55 mmol), and purified by method 1 to afford the phthalonitrile **1.80i** in 81% yield (226.9 mg, 0.407 mmol).



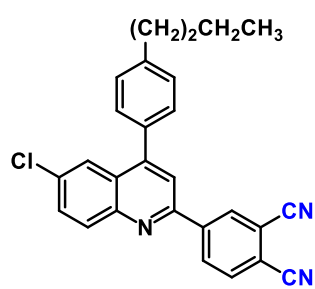
Mp: 145–147 °C. ^1H NMR (CDCl_3 , 400.15 MHz, ppm): δ 8.72 (br s, 1H), 8.54 (dd, $J = 8.2, 1.4$ Hz, 1H), 8.13 (d, $J = 9.2$ Hz, 1H), 7.93 (d, $J = 8.2$ Hz, 1H), 7.77 (s, 1H), 7.53 – 7.35 (m, 5H), 7.25 (d, $J = 2.2$ Hz, 1H), 3.97 (t, $J = 6.5$ Hz, 2H), 2.75 (t, $J = 7.6$ Hz, 2H), 1.87 – 1.69 (m, 4H), 1.51 – 1.23 (m, 18H), 0.95 (t, $J = 6.8$ Hz, 3H), 0.89 (t, $J = 6.6$ Hz, 3H). ^{13}C NMR (CDCl_3 , 100.63 MHz, ppm): δ 158.4, 149.2, 148.8, 144.9, 144.6, 143.8, 135.2, 133.9, 132.1, 131.8, 131.0, 129.1, 128.9, 127.8, 123.2, 118.6, 116.4, 115.6, 115.5, 115.0, 104.5, 68.3, 35.8, 31.9, 31.6, 31.1, 29.6, 29.4, 29.3, 29.1, 26.1, 22.7, 22.6, 14.1, 14.0. ^{13}C NMR (DEPT-135) (CDCl_3 , 100.63 MHz, ppm): δ 133.9, 132.1, 131.8, 131.0, 129.1, 128.9, 123.2, 118.6, 104.5, 68.3, 35.8, 31.9, 31.6, 31.1, 29.6, 29.4, 29.3, 29.1, 26.1, 22.7, 22.6, 14.1, 14.0. FT-IR (KBr, cm^{-1}): $\nu = 3040, 2924, 2853, 2226$ ($\text{C}\equiv\text{N}$), 1618, 1597, 1493, 1261, 1215, 1126, 1032, 825, 525. HRMS (ESI-TOF): m/z calcd. for $\text{C}_{38}\text{H}_{44}\text{N}_3\text{O}^+$ [$\text{M} + \text{H}$] $^+$: 558.3479; Found: 558.3483.

4-(6-Chloro-4-(4-pentylphenyl)quinolin-2-yl)phthalonitrile (1.80j): The MCR was carried out according to the general procedure with 4-chloroaniline (**1.78c**) (65.1 mg, 0.5 mmol) and 1-ethynyl-4-pentylbenzene (**1.79b**) (97.7 mg, 0.55 mmol), and purified by method 1 to afford the phthalonitrile **1.80j** in 80% yield (174.9 mg, 0.401 mmol).



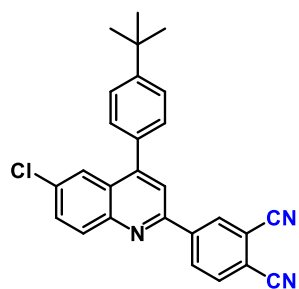
Mp: 224–226 °C. ^1H NMR (CDCl_3 , 400.15 MHz, ppm): δ 8.74 (d, $J = 1.6$ Hz, 1H), 8.56 (dd, $J = 8.2, 1.7$ Hz, 1H), 8.18 (d, $J = 9.0$ Hz, 1H), 8.01 – 7.92 (m, 2H), 7.85 (s, 1H), 7.74 (dd, $J = 9.0, 2.3$ Hz, 1H), 7.51 – 7.36 (m, 4H), 2.76 (t, $J = 7.8$ Hz, 2H), 1.74 (quint, $J = 7.4$ Hz, 2H), 1.48 – 1.34 (m, 4H), 0.96 (t, $J = 7.0$ Hz, 3H). ^{13}C NMR (CDCl_3 , 100.63 MHz, ppm): δ 152.0, 149.9, 147.2, 144.4, 143.9, 134.2, 134.0, 133.8, 132.4, 131.9, 131.4, 129.3, 129.1, 127.2, 124.8, 119.1, 116.6, 115.8, 115.4, 115.3, 35.8, 31.6, 31.1, 22.6, 14.1. ^{13}C NMR (DEPT-135) (CDCl_3 , 100.63 MHz, ppm): δ 134.0, 132.4, 131.9, 131.4, 129.3, 129.1, 124.8, 119.1, 35.8, 31.6, 31.1, 22.6, 14.1. FT-IR (KBr, cm^{-1}): $\nu = 3080, 2924, 2857, 2234$ ($\text{C}\equiv\text{N}$), 1595, 1483, 1362, 1155, 827, 525. HRMS (ESI-TOF): m/z calcd. for $\text{C}_{28}\text{H}_{23}\text{ClN}_3^+$ [$\text{M} + \text{H}$] $^+$: 436.1575; Found: 436.1573.

4-(4-(4-Butylphenyl)-6-chloroquinolin-2-yl)phthalonitrile (1.80k): The MCR was carried out according to the general procedure with 4-chloroaniline (**1.78c**) (65.1 mg, 0.5 mmol) and 1-butyl-4-ethynylbenzene (**1.79c**) (91.6 mg, 0.55 mmol), and purified by method 1 to afford the phthalonitrile **1.80k** in 73% yield (154.3 mg, 0.366 mmol).



Mp: 224–225 °C. ^1H NMR (CDCl_3 , 400.15 MHz, ppm): δ 8.74 (d, $J = 0.9$ Hz, 1H), 8.57 (dd, $J = 8.2, 1.3$ Hz, 1H), 8.18 (d, $J = 9.0$ Hz, 1H), 8.04–7.91 (m, 2H), 7.85 (s, 1H), 7.74 (dd, $J = 9.0, 2.0$ Hz, 1H), 7.52–7.36 (m, 4H), 2.77 (t, $J = 7.7$ Hz, 2H), 1.73 (quint, $J = 7.6$ Hz, 2H), 1.46 (sext, $J = 7.4$ Hz, 2H), 1.01 (t, $J = 7.3$ Hz, 3H). ^{13}C NMR (CDCl_3 , 100.63 MHz, ppm): δ 152.0, 149.9, 147.2, 144.3, 143.9, 134.2, 134.0, 133.8, 132.4, 131.9, 131.4, 129.3, 129.1, 127.3, 124.8, 119.1, 116.6, 115.8, 115.4, 115.3, 35.5, 33.6, 22.4, 14.0. ^{13}C NMR (DEPT-135) (CDCl_3 , 100.63 MHz, ppm): δ 134.0, 132.4, 131.9, 131.4, 129.3, 129.1, 124.8, 119.1, 35.5, 33.6, 22.4, 14.0. FT-IR (KBr, cm^{-1}): $\nu = 3080, 3034, 2957, 2930, 2858, 2232$ ($\text{C}\equiv\text{N}$), 1595, 1483, 1155, 825, 523. HRMS (ESI-TOF): m/z calcd. for $\text{C}_{27}\text{H}_{21}\text{ClN}_3^+$ [$\text{M} + \text{H}$] $^+$: 422.1419; Found: 422.1422.

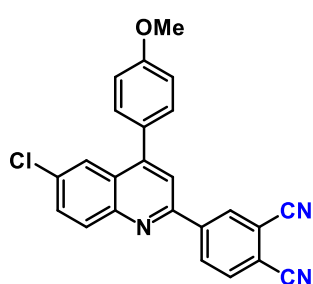
4-(4-(4-(*tert*-Butyl)phenyl)-6-chloroquinolin-2-yl)phthalonitrile (1.80l): The MCR was carried out according to the general procedure with 4-chloroaniline (**1.78c**) (65.1 mg, 0.5 mmol) and 1-(*tert*-butyl)-4-ethynylbenzene (**1.79d**) (90.7 mg, 0.55 mmol), and purified by method 1 to afford the phthalonitrile **1.80l** in 79% yield (166.9 mg, 0.395 mmol).



Mp: 298–300 °C. ^1H NMR (CDCl_3 , 400.15 MHz, ppm): δ 8.74 (d, $J = 1.4$ Hz, 1H), 8.56 (dd, $J = 8.2, 1.6$ Hz, 1H), 8.19 (d, $J = 9.0$ Hz, 1H), 7.99 (d, $J = 2.2$ Hz, 1H), 7.96 (d, $J = 8.2$ Hz, 1H), 7.85 (s, 1H), 7.75 (dd, $J = 9.0, 2.3$ Hz, 1H), 7.63 (d, $J = 8.3$ Hz, 2H), 7.49 (d, $J = 8.3$ Hz, 2H), 1.45 (s, 9H). ^{13}C NMR (CDCl_3 , 100.63 MHz, ppm): δ 152.5, 152.0, 149.8, 147.2, 143.9, 134.0, 133.8, 132.4, 131.9, 131.4, 129.1, 127.2, 126.0, 124.8, 119.1, 116.6, 115.8, 115.4, 115.3, 31.3. ^{13}C NMR (DEPT-135) (CDCl_3 , 100.63 MHz, ppm): δ 134.0, 132.4, 131.9, 131.4, 129.1, 126.0, 124.8, 119.1, 31.3. FT-IR (KBr,

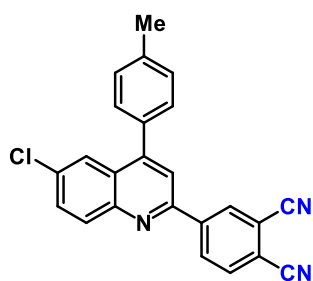
cm⁻¹): $\nu = 3084, 2951, 2904, 2868, 2235$ (C≡N), 1597, 1483, 1362, 1157, 849, 827, 600, 525. HRMS (ESI-TOF): m/z calcd. for C₂₇H₂₁ClN₃⁺ [M + H]⁺: 422.1419; Found: 422.1418.

4-(6-Chloro-4-(4-methoxyphenyl)quinolin-2-yl)phthalonitrile (1.80m): The MCR was carried out according to the general procedure with 4-chloroaniline (**1.78c**) (65.1 mg, 0.5 mmol) and 1-ethynyl-4-methoxybenzene (**1.79e**) (74.9 mg, 0.55 mmol), and purified by method 2 to afford the phthalonitrile **1.80m** in 78% yield (155.3 mg, 0.392 mmol).



Mp: dec. above 280 °C. ¹H NMR (CDCl₃, 400.15 MHz, ppm) δ 8.74 (d, $J = 1.6$ Hz, 1H), 8.57 (dd, $J = 8.2, 1.8$ Hz, 1H), 8.18 (d, $J = 9.0$ Hz, 1H), 7.97 (dd, $J = 5.2, 3.0$ Hz, 2H), 7.83 (s, 1H), 7.75 (dd, $J = 9.0, 2.3$ Hz, 1H), 7.51 – 7.46 (m, 2H), 7.16 – 7.11 (m, 2H), 3.95 (s, 3H). FT-IR (KBr, cm⁻¹): $\nu = 3233, 3078, 2941, 2845, 2237$ (C≡N), 1593, 1514, 1483, 1263, 1180, 1032, 824, 569, 523. HRMS (ESI-TOF): m/z calcd. for C₂₄H₁₅ClN₃O⁺ [M + H]⁺: 396.0898; Found: 396.0905.

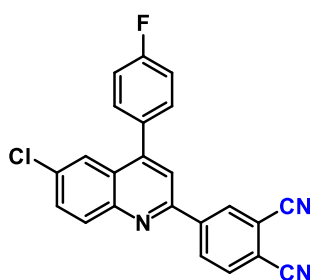
4-(6-Chloro-4-(*p*-tolyl)quinolin-2-yl)phthalonitrile (1.80n): The MCR was carried out according to the general procedure with 4-chloroaniline (**1.78c**) (65.1 mg, 0.5 mmol) and 1-ethynyl-4-methylbenzene (**1.79f**) (65.9 mg, 0.55 mmol), and purified by method 2 to afford the phthalonitrile **1.80n** in 80% yield (152.7 mg, 0.402 mmol).



Mp: 272–274 °C. ¹H NMR (CDCl₃, 400.15 MHz, ppm): δ 8.74 (d, $J = 1.6$ Hz, 1H), 8.56 (dd, $J = 8.3, 1.7$ Hz, 1H), 8.19 (d, $J = 9.0$ Hz, 1H), 7.99 – 7.93 (m, 2H), 7.84 (s, 1H), 7.75 (dd, $J = 9.0, 2.3$ Hz, 1H), 7.46 – 7.39 (m, 4H), 2.51 (s, 3H). ¹³C NMR (CDCl₃, 100.62 MHz, ppm): δ 152.0, 149.8, 147.2, 143.9, 139.4, 134.0, 133.9, 132.4, 131.9, 131.4, 129.7, 129.3, 127.3, 124.8, 119.0, 116.6, 115.8, 115.4, 21.4. ¹³C NMR (DEPT-135) (CDCl₃, 100.62 MHz, ppm): δ 134.0, 132.4, 131.9, 131.4, 129.7, 129.3, 124.8, 119.0, 21.4. FT-IR (KBr, cm⁻¹): $\nu = 3080, 2920, 2232$ (C≡N), 1595, 1483, 1153, 856,

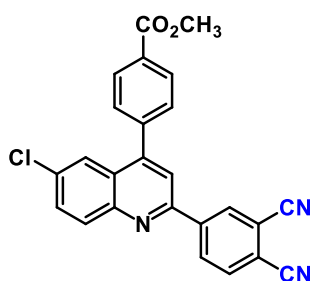
845, 814, 525. HRMS (ESI-TOF): m/z calcd. for $C_{24}H_{15}ClN_3^+$ $[M + H]^+$: 380.0949; Found: 380.0949.

4-(6-Chloro-4-(4-fluorophenyl)quinolin-2-yl)phthalonitrile (1.80o): The MCR was carried out according to the general procedure with 4-chloroaniline (**1.78c**) (65.1 mg, 0.5 mmol) and 1-ethynyl-4-fluorobenzene (**1.79g**) (66.7 mg, 0.55 mmol), and purified by method 2 to afford the phthalonitrile **1.80o** in 79% yield (152.4 mg, 0.397 mmol).



Mp: > 300 °C. 1H NMR ($CDCl_3$, 400.15 MHz, ppm): δ 8.74 (d, $J = 1.5$ Hz, 1H), 8.57 (dd, $J = 8.2, 1.7$ Hz, 1H), 8.21 (d, $J = 9.0$ Hz, 1H), 7.97 (d, $J = 8.2$ Hz, 1H), 7.87 (d, $J = 2.2$ Hz, 1H), 7.83 (s, 1H), 7.77 (dd, $J = 9.0, 2.3$ Hz, 1H), 7.56 – 7.50 (m, 2H), 7.35 – 7.29 (m, 2H). FT-IR (KBr, cm^{-1}): $\nu = 3076, 2234$ ($C\equiv N$), 1597, 1514, 1483, 1364, 1240, 1165, 847, 829, 825, 527. HRMS (ESI-TOF): m/z calcd. for $C_{23}H_{12}ClFN_3^+$ $[M + H]^+$: 384.0698; Found: 384.0703.

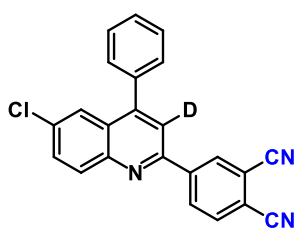
Methyl 4-(6-chloro-2-(3,4-dicyanophenyl)quinolin-4-yl)benzoate (1.80p): The MCR was carried out according to the general procedure with 4-chloroaniline (**1.78c**) (65.1 mg, 0.5 mmol) and methyl 4-ethynylbenzoate (**1.79h**) (97.9 mg, 0.55 mmol), and purified by method 2 to afford the phthalonitrile **1.80p** in 57% yield (120.5 mg, 0.284 mmol).



Mp: 281–283 °C. 1H NMR ($CDCl_3$, 400.15 MHz, ppm): δ 8.76 (d, $J = 1.4$ Hz, 1H), 8.57 (dd, $J = 8.3, 1.8$ Hz, 1H), 8.30 – 8.25 (m, 2H), 8.22 (d, $J = 9.1$ Hz, 1H), 7.98 (d, $J = 8.3$ Hz, 1H), 7.87 (s, 1H), 7.83 (d, $J = 2.2$ Hz, 1H), 7.78 (dd, $J = 9.0, 2.3$ Hz, 1H), 7.65 – 7.60 (m, 2H), 4.02 (s, 3H). ^{13}C NMR ($CDCl_3$, 100.62 MHz, ppm): δ 166.5, 152.0, 148.6, 147.1, 143.6, 141.4, 134.4, 134.0, 132.4, 132.1, 131.7, 131.4, 130.9, 130.2, 129.5, 126.7, 124.3, 118.9, 116.7, 116.0, 115.3, 52.5. ^{13}C NMR (DEPT-135) ($CDCl_3$, 100.62 MHz, ppm): δ 134.0, 132.4, 132.1, 131.7, 131.4, 130.2, 129.5, 124.3, 118.9, 52.5. FT-IR (KBr, cm^{-1}): $\nu = 3078, 2955, 2237$ ($C\equiv N$), 1728 ($C=O$), 1593, 1483, 1288,

1119, 854, 827, 708, 525. HRMS (ESI-TOF): m/z calcd. for $C_{25}H_{15}ClN_3O_2^+$ $[M + H]^+$: 424.0847; Found: 424.0852.

4-(6-Chloro-4-phenylquinolin-2-yl-3-*d*)phthalonitrile (1.80q): The MCR was carried out according to the general procedure with 4-chloroaniline (**1.78c**) (65.1 mg, 0.5 mmol) and phenylacetylene-*d* (**1.79i**) (56.7 mg, 0.55 mmol), and purified by method 1 to afford the phthalonitrile **1.80q** in 74% yield (135.6 mg, 0.369 mmol).



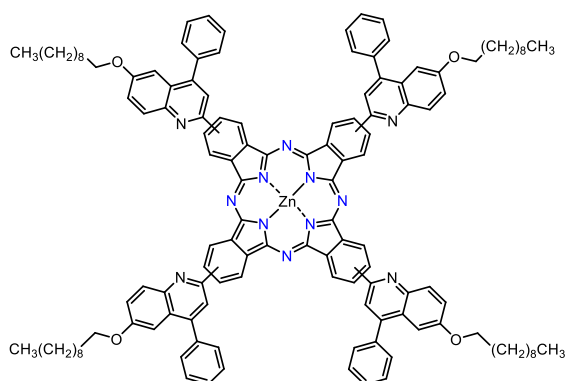
Mp: 260–261 °C. 1H NMR ($CDCl_3$, 600.23 MHz, ppm): δ 8.75 (d, $J = 1.7$ Hz, 1H), 8.57 (dd, $J = 8.2, 1.8$ Hz, 1H), 8.20 (d, $J = 9.0$ Hz, 1H), 7.97 (d, $J = 8.2$ Hz, 1H), 7.92 (d, $J = 2.3$ Hz, 1H), 7.76 (dd, $J = 9.0, 2.3$ Hz, 1H), 7.64 – 7.57 (m, 3H), 7.56 – 7.52 (m, 2H). ^{13}C NMR ($CDCl_3$, 150.93 MHz, ppm): δ 152.0, 149.7, 147.2, 143.8, 136.9, 134.0, 132.4, 132.0, 131.5, 131.4, 129.3, 129.2, 129.1, 127.2, 124.7, 118.8 (t, $J = 25.0$ Hz), 116.6, 115.8, 115.4, 115.3. ^{13}C NMR (DEPT-135) ($CDCl_3$, 150.93 MHz, ppm): δ 134.0, 132.4, 132.0, 131.5, 131.4, 129.3, 129.2, 129.1, 124.7. FT-IR (KBr, cm^{-1}): $\nu = 3115, 3080, 3055, 2234$ ($C\equiv N$), 1599, 1537, 1481, 1358, 1086, 826, 766, 746, 704, 573, 527. HRMS (ESI-TOF): m/z calcd. for $C_{23}H_{12}DCIN_3$ $[M + H]^+$: 367.0855; Found: 367.0865.

1.4.7 General procedure for the synthesis of ZnPCs **1.81a-c**

ZnPCs **1.81a-c** were synthesized following previously reported procedures with minor modifications.⁸¹ To a 15-mL glass pressure tube (Ace pressure tube®, back seal, Aldrich Z181064) equipped with a magnetic stir bar and rubber septum, were added sequentially phthalonitrile derivatives (**1.80g-i**) (0.09 mmol), $Zn(OTf)_2$ (8.3 mg, 22.5 μ mol, 0.25 equiv.), HMDS (76 μ L, 4 equiv.) and DMF (200 μ L) under an argon atmosphere at room temperature. The tube was closed and the resulting mixture was stirred at 130 °C under light protection for 24 h. After cooling to r.t., 5 mL of methanol was added, and the solid was filtered under vacuum and washed with methanol.

1.4.7.1 Zinc phthalocyanine-quinoline 1.81a

The crude solid obtained from phthalonitrile **1.80g** (43.9 mg, 0.09 mmol) was purified by flash column chromatography (silica gel, 230-400 mesh), eluting initially with dichloromethane/toluene/ethyl acetate (4:4:2, v/v/v) to remove fluorescent impurities and then with toluene/ethyl acetate/methanol (6:3:1, v/v/v) to elute the product. Evaporation of the elute gave a solid which was dissolved in a small amount of chloroform, methanol was added, and the solution was stored at r.t. overnight. The green solid obtained was filtered, washed with methanol, and then dried under vacuum to afford the pure ZnPC **1.81a** (24.5 mg, 12.15 μ mol, 54%).

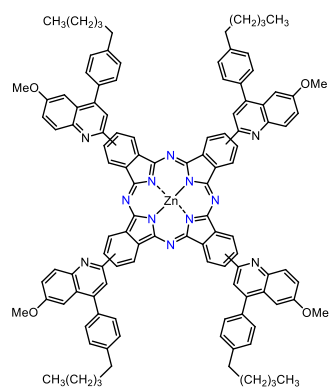


$^1\text{H NMR}$ ($\text{CDCl}_3/\text{DMSO}-d_6 = 2:1$, 400.15 MHz, ppm): δ 9.63 – 9.11 (m, 6H), 8.91 – 8.43 (m, 8H), 8.33 – 7.98 (m, 14H), 7.91 – 7.74 (m, 10H), 7.49 – 6.96 (m, 10H), 4.01 – 3.66 (m, 8H), 1.92 – 1.73 (m, 8H), 1.62 – 1.26 (m, 56H), 1.02 – 0.90 (m, 12H). UV-Vis (THF): $\lambda_{\text{max}}/\text{nm}$ ($\log \epsilon$) = 695 (5.59), 626 (4.89), 357 (5.14). FT-IR (KBr, cm^{-1}): $\nu = 2922, 2853, 1618, 1589, 1545, 1491, 1385, 1356, 1225, 1095, 910, 831, 748, 702$. HRMS (MALDI-TOF): m/z calcd. for $\text{C}_{132}\text{H}_{133}\text{N}_{12}\text{O}_4\text{Zn}^+$ [$\text{M} + \text{H}$] $^+$: 2013.9859; Found: 2013.9837.

1.4.7.2 Zinc phthalocyanine-quinoline 1.81b

The crude solid obtained from phthalonitrile **1.80h** (38.8 mg, 0.09 mmol) was purified by flash column chromatography (silica gel, 230-400 mesh), eluting initially with toluene/ethyl acetate (8:2, v/v) to remove fluorescent impurities and then with toluene/ethyl acetate/methanol (7:2:1, v/v/v) to elute the product. Evaporation of the elute gave a solid which

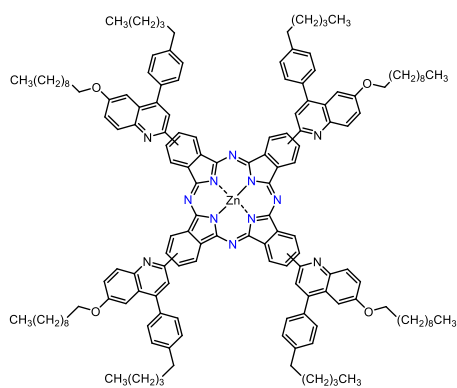
was dissolved in a small amount of chloroform, methanol was added, and the solution was stored at r.t. overnight. The green solid obtained was filtered, washed with methanol, and then dried under vacuum to afford the pure ZnPC **1.81b** (25.9 mg, 14.45 μmol , 64%).



$^1\text{H NMR}$ ($\text{CDCl}_3/\text{DMSO}-d_6 = 2:1$, 400.15 MHz, ppm): δ 9.71 – 9.14 (m, 6H), 8.99 – 8.42 (m, 8H), 8.35 – 8.02 (m, 9H), 7.89 – 7.57 (m, 12H), 7.51 – 6.98 (m, 9H), 4.00 – 3.58 (m, 12H), 3.09 – 2.81 (m, 8H), 2.08 – 1.82 (m, 8H), 1.68 – 1.38 (m, 16H), 1.13 – 0.91 (m, 12H). UV-Vis (THF): $\lambda_{\text{max}}/\text{nm}$ ($\log \epsilon$) = 695 (5.50), 626 (4.77), 355 (5.05). FT-IR (KBr, cm^{-1}): $\nu = 2926, 2853, 1620, 1589, 1545, 1493, 1385, 1356, 1227, 1095, 903, 831, 750$. HRMS (MALDI-TOF): m/z calcd. for $\text{C}_{116}\text{H}_{101}\text{N}_{12}\text{O}_4\text{Zn}^+ [\text{M} + \text{H}]^+$: 1789.7355; Found: 1789.7329.

1.4.7.3 Zinc phthalocyanine-quinoline **1.81c**

The crude solid obtained from phthalonitrile **1.80i** (50.2 mg, 0.09 mmol) was purified by flash column chromatography (silica gel, 230-400 mesh), eluting initially with dichloromethane/toluene/ethyl acetate (6:2:2, v/v/v) to remove fluorescent impurities and then with toluene/ethyl acetate/methanol (7:2:1, v/v/v) to elute the product. Evaporation of the elute gave a solid which was dissolved in a small amount of chloroform, methanol was added, and the solution was stored at r.t. overnight. The green solid obtained was filtered, washed with methanol, and then dried under vacuum to afford the pure ZnPC **1.81c** (30.0 mg, 13.06 μmol , 58%).



^1H NMR ($\text{CDCl}_3/\text{DMSO}-d_6 = 2:1$, 400.15 MHz, ppm): δ 9.77 – 9.10 (m, 6H), 9.05 – 8.42 (m, 8H), 8.39 – 8.01 (m, 9H), 7.97 – 7.75 (m, 7H), 7.67 – 7.53 (m, 5H), 7.51 – 7.02 (m, 9H), 4.10 – 3.68 (m, 8H), 3.02 – 2.82 (m, 8H), 2.13 – 1.75 (m, 16H), 1.68 – 1.24 (m, 72H), 1.15 – 0.90 (m, 24H). UV-Vis (THF): $\lambda_{\text{max}}/\text{nm}$ ($\log \epsilon$) = 695 (5.63), 626 (4.92), 355 (5.19). FT-IR (KBr, cm^{-1}): $\nu = 2924, 2853, 1618, 1589, 1545, 1493, 1385, 1356, 1223, 1095, 910, 829, 748$. HRMS (MALDI-TOF): m/z calcd. for $\text{C}_{152}\text{H}_{173}\text{N}_{12}\text{O}_4\text{Zn}^+ [\text{M} + \text{H}]^+$: 2294.2989; Found: 2294.3037.

1.4.8 Aggregation studies

The aggregation behavior of ZnPCs **1.81a-c** was investigated in THF using UV-Vis spectroscopy (see Figure 1.8, Section 1.2.4, and Figures 1.11 and 1.12 below). Different concentrations of ZnPCs **1.81a-c** were prepared and the absorbances measured.

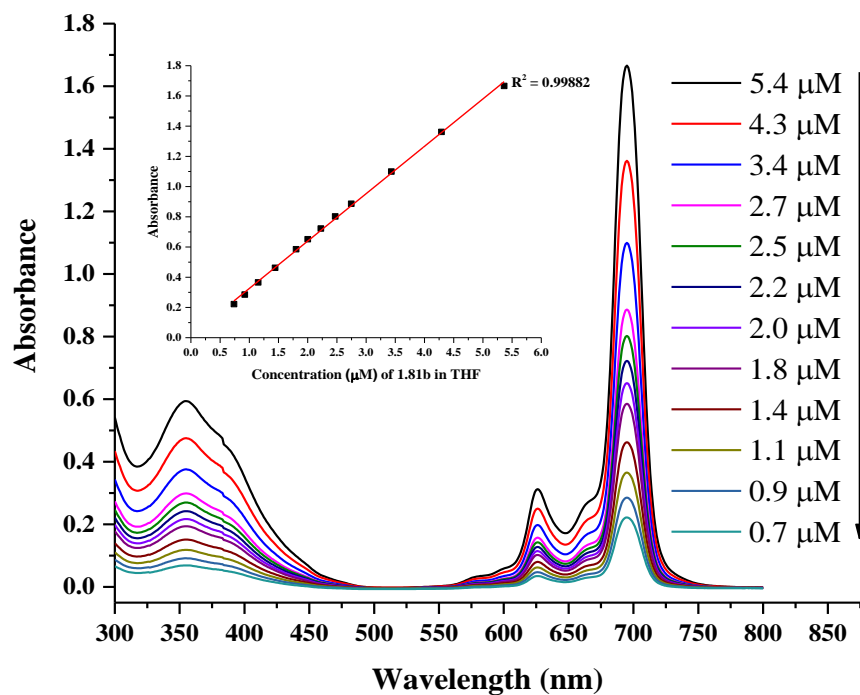


Figure 1.11 – Aggregation behavior of ZnPC **1.81b** in THF at different concentrations. The inset plots the Q band absorption at 695 nm vs. the concentration of **1.81b**.

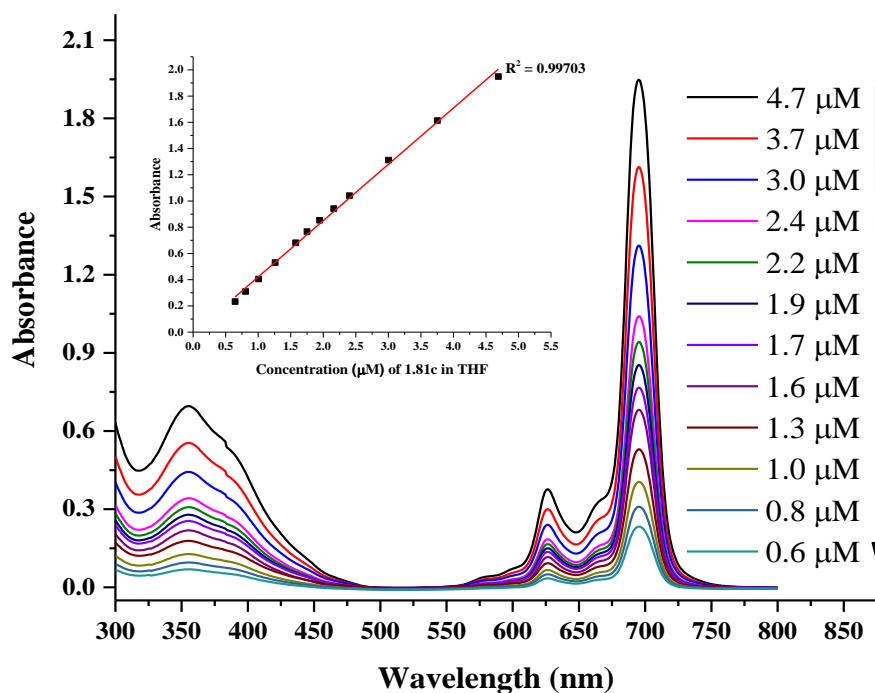


Figure 1.12 – Aggregation behavior of ZnPC **1.81c** in THF at different concentrations. The inset plots the Q band absorption at 695 nm vs. the concentration of **1.81c**.

1.4.9 Fluorescence measurements

The values of Φ_F were obtained by comparing the areas under the fluorescence spectra of the samples (ZnPCs **1.81a-c**) with the area under the fluorescence spectrum of the standard (unsubstituted ZnPC) (see Figure 1.13 and Table 1.5).⁸⁴ A solution of each compound was prepared in THF and the absorbances at the excitation wavelength ($\lambda_{ex} = 630$ nm) were adjusted to be 0.05 for comparison. Dissolved oxygen was removed from the solutions by bubbling argon. The calculation was performed by Eq. (1):

$$\Phi_F = \Phi_F^{Std} \times \frac{F \times A_{Std}}{F_{Std} \times A} \quad (1)$$

In Eq. (1), Φ_F^{Std} is the fluorescence quantum yield of the standard (for unsubstituted ZnPC is 0.25 in THF),⁸⁴ F and F_{Std} are the areas under the fluorescence emission

curves of the sample and standard, respectively. A and A_{Std} are the absorbances of the sample and standard, respectively, at the excitation wavelength ($\lambda_{ex} = 630$ nm).

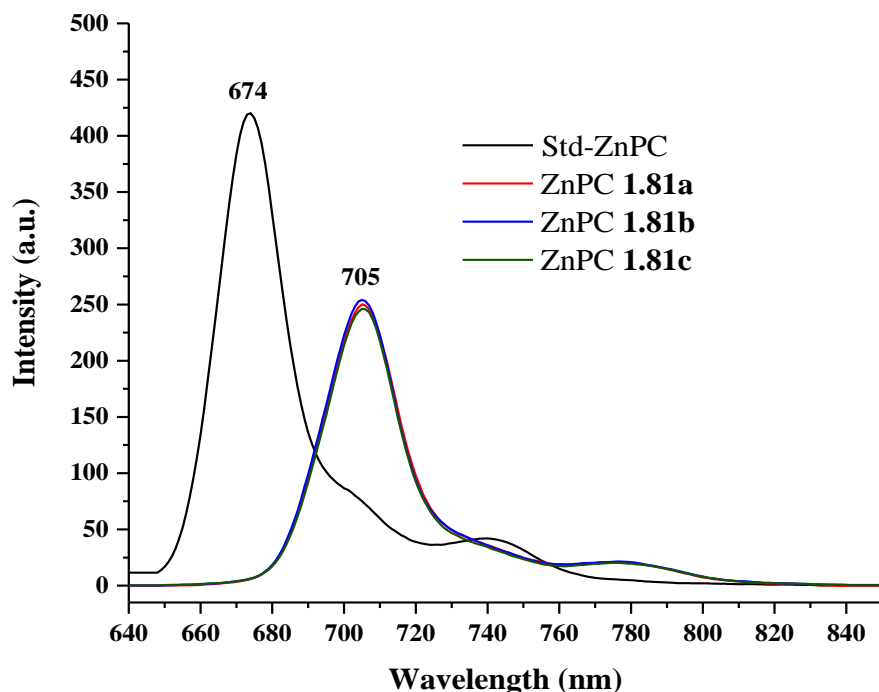


Figure 1.13 – Emission spectra of ZnPCs **1.81a-c** and standard ZnPC.

Table 1.5 – Data for obtainment of Φ_F for ZnPCs **1.81a-c**.

Compound	Absorbance	Area
Std-ZnPC	0.05045	13402.2145
ZnPC 1.81a	0.04913	8513.6715
ZnPC 1.81b	0.05291	8639.6650
ZnPC 1.81c	0.05257	8297.9135

1.4.10 Molar absorption coefficient (ϵ)

The values for ϵ (see Table 1.6–1.8) were obtained from the data of Figures 1.8, 1.11, and 1.12. All the graphs of absorbance against concentration for each band are in agreement with the Lambert-Beer's law, affording straight lines with $R^2 > 0.99$. In each graph,

the slope of this line is the molar absorptivity (ϵ) divided by the optical path length, as described in the Eq. (2):⁸⁹

$$A = \epsilon \times c \times l \quad (2)$$

In Eq. (2), A is the absorbance, c is the concentration and l is the optical path length, respectively.

Table 1.6 – Data for obtainment of ϵ for ZnPC **1.81a**.

Concentration x 10 ⁻⁶ (mol.L ⁻¹)	Absorbance		
	(357 nm)	(626 nm)	(695 nm)
4.629	0.63	0.3471	1.7554
3.704	0.4945	0.2731	1.4375
2.963	0.3921	0.2175	1.1649
2.37	0.3105	0.1726	0.9359
2.133	0.2778	0.1543	0.8426
1.92	0.2489	0.1385	0.759
1.728	0.2203	0.1219	0.6795
1.555	0.1966	0.1085	0.6083
1.244	0.1546	0.0863	0.4788
0.995	0.1191	0.0656	0.3723
0.796	0.0915	0.0507	0.2901
0.637	0.0674	0.0363	0.2233

$$\epsilon_{357} = 139,910 \text{ L.mol}^{-1}.\text{cm}^{-1}; \epsilon_{626} = 77,238 \text{ L.mol}^{-1}.\text{cm}^{-1}; \epsilon_{695} = 386,967 \text{ L.mol}^{-1}.\text{cm}^{-1}$$

Table 1.7 – Data for obtainment of ϵ for ZnPC **1.81b**.

Concentration x 10 ⁻⁶ (mol.L ⁻¹)	Absorbance		
	(355 nm)	(626 nm)	(695 nm)
5.364	0.594	0.3126	1.6659
4.291	0.4754	0.2505	1.3616
3.433	0.3759	0.198	1.0997
2.746	0.299	0.1578	0.8866
2.472	0.2698	0.1428	0.8026
2.225	0.2422	0.1281	0.7226
2.002	0.2171	0.1148	0.6516
1.802	0.194	0.1025	0.5855
1.442	0.1517	0.0801	0.4625
1.153	0.1188	0.0624	0.3659
0.923	0.0918	0.0473	0.2853
0.738	0.069	0.035	0.2223

$$\epsilon_{355} = 113,232 \text{ L.mol}^{-1}.\text{cm}^{-1}; \epsilon_{626} = 59,776 \text{ L.mol}^{-1}.\text{cm}^{-1}; \epsilon_{695} = 313,528 \text{ L.mol}^{-1}.\text{cm}^{-1}$$

Table 1.8 – Data for obtainment of ϵ for ZnPC **1.81c**.

Concentration x 10 ⁻⁶ (mol.L ⁻¹)	Absorbance		
	(355 nm)	(626 nm)	(695 nm)
4.691	0.6958	0.3766	1.9488
3.753	0.5545	0.3002	1.6134
3.002	0.4433	0.2401	1.3119
2.402	0.3419	0.1848	1.0409
2.162	0.308	0.166	0.9422
1.945	0.2789	0.15	0.8532
1.751	0.2548	0.1361	0.7669
1.576	0.219	0.116	0.6816
1.261	0.1787	0.0927	0.53
1.008	0.128	0.0668	0.405
0.807	0.0957	0.05	0.3096
0.645	0.0694	0.0345	0.2332

$$\epsilon_{355} = 154,274 \text{ L.mol}^{-1}.\text{cm}^{-1}; \epsilon_{626} = 84,402 \text{ L.mol}^{-1}.\text{cm}^{-1}; \epsilon_{695} = 429,210 \text{ L.mol}^{-1}.\text{cm}^{-1}$$

1.4.11 Photobleaching studies

A solution of ZnPCs **1.81a-c** in THF with an absorbance near 1 was irradiated in the dark with a white LED lamp (30 W) (Figure 1.14) for intervals of 1 min (10 irradiations), 5 min (4 irradiations), 10 min (3 irradiations), and 30 min (2 irradiations), totaling 2 h. After each irradiation, the UV–Vis spectrum was measured to detect any photobleaching due to reduction of photosensitizer concentration (see Figures 1.10, 1.15, and 1.16).



Figure 1.14 – Experimental setup used in the photobleaching studies.

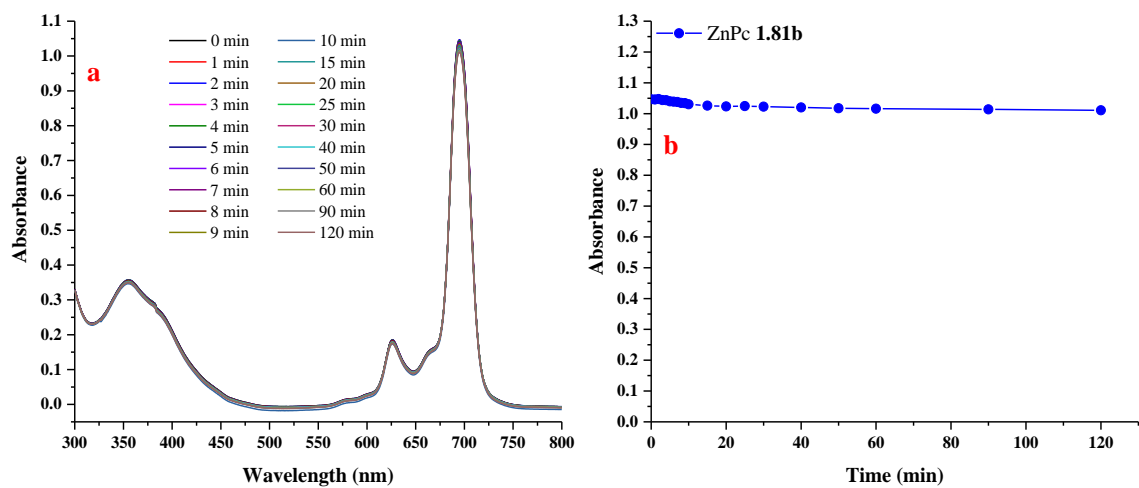


Figure 1.15 – a) Photobleaching study of ZnPc **1.81b** in THF. **b)** Plot of Q band absorbance vs. time.

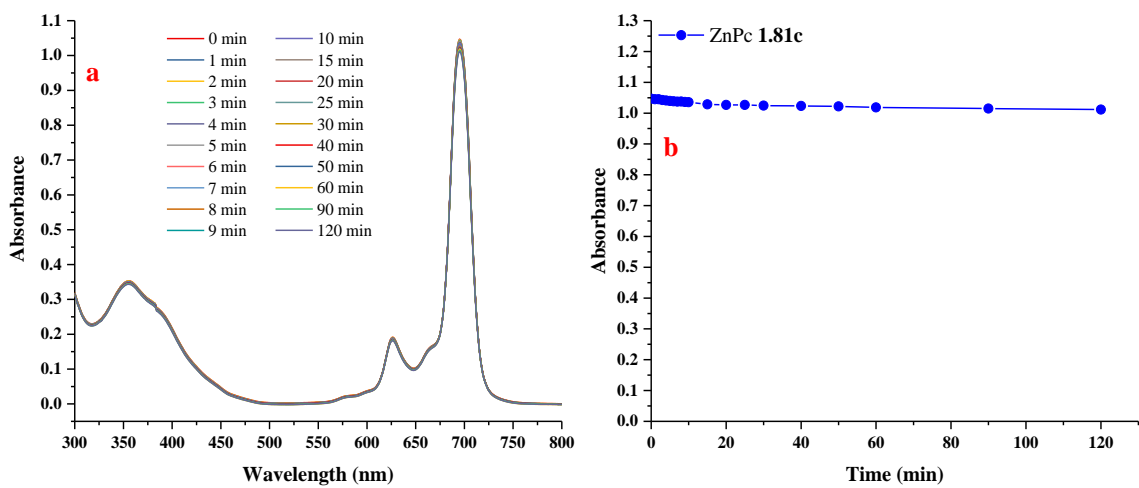


Figure 1.16 – a) Photobleaching study of ZnPc **1.81c** in THF. **b)** Plot of Q band absorbance vs. time.

Reference

- 1 MCKEOWN, N. B. *Phthalocyanines Materials: Synthesis, Structure and Function*. Cambridge: Cambridge University Press, 1998. 211 p.
- 2 DE LA TORRE, G.; NICOLAU, M. & TORRES, T. "Phthalocyanines: synthesis, supramolecular organization, and physical properties". In: NALWA, H. S. (Ed.). *Supramol. Photosensit. Electroact. Mater.* San Diego: Academic Press, 2001, ch. 1, pp. 1-111.
- 3 SHARMAN, W. M. & VAN LIER, J. E. "Synthesis of phthalocyanine precursors". In: KADISH, K. M.; SMITH, K. M. & GUILARD, R. (Ed.). *The Porphyrin Handbook*. Amsterdam: Academic Press, 2003, vol. 15, ch. 97, pp. 1-60.
- 4 RIO, Y.; RODRIGUEZ-MORGADE, M. S. & TORRES, T. "Modulating the electronic properties of porphyrinoids: a voyage from the violet to the infrared regions of the electromagnetic spectrum". *Org. Biomol. Chem.*, 6 (11): 1877, 2008.
- 5 GOBO, N. R. S. *Estratégias Sintéticas para a Preparação de Novos Fotossensibilizadores do Tipo Ftalocianinas*. São Carlos, Programa de Pós-Graduação em Química - UFSCar, 2013. Dissertação de mestrado, p. 173.
- 6 TOPAL, S. Z.; İŞCI, Ü.; KUMRU, U.; ATILLA, D.; GÜREK, A. G.; HIREL, C., et al. "Modulation of the electronic and spectroscopic properties of Zn(II) phthalocyanines by their substitution pattern". *Dalton Trans.*, 43 (18): 6897, 2014.
- 7 FURUYAMA, T.; SATOH, K.; KUSHIYA, T. & KOBAYASHI, N. "Design, synthesis, and properties of phthalocyanine complexes with main-group elements showing main absorption and fluorescence beyond 1000 nm". *J. Am. Chem. Soc.*, 136 (2): 765, 2014.
- 8 MACK, J. & KOBAYASHI, N. "Low symmetry phthalocyanines and their analogues". *Chem. Rev.*, 111 (2): 281, 2011.
- 9 LUKYANETS, E. A. & NEMYKIN, V. N. "The key role of peripheral substituents in the chemistry of phthalocyanines and their analogs". *J. Porphyrins Phthalocyanines*, 14 (1): 1, 2010.
- 10 CHO, K. T.; RAKSTYS, K.; CAVAZZINI, M.; ORLANDI, S.; POZZI, G. & NAZEERUDDIN, M. K. "Perovskite solar cells employing molecularly engineered Zn(II) phthalocyanines as hole-transporting materials". *Nano Energy*, 30: 853, 2016.
- 11 KONG, X.; ZHANG, X.; GAO, D.; QI, D.; CHEN, Y. & JIANG, J. "Air-stable ambipolar field-effect transistor based on a solution-processed octanaphthoxy-substituted tris(phthalocyaninato) europium semiconductor with high and balanced carrier mobilities". *Chem. Sci.*, 6 (3): 1967, 2015.

- 12 LU, G.; KONG, X.; MA, P.; WANG, K.; CHEN, Y. & JIANG, J. "Amphiphilic (phthalocyaninato) (porphyrinato) europium triple-decker nanoribbons with air-stable ambipolar OFET performance". *ACS Appl. Mater. Interfaces*, 8 (9): 6174, 2016.
- 13 URBANI, M.; RAGOUSI, M.-E.; NAZEERUDDIN, M. K. & TORRES, T. "Phthalocyanines for dye-sensitized solar cells". *Coord. Chem. Rev.*, 381: 1, 2019.
- 14 BASOVA, T.; HASSAN, A.; DURMUŞ, M.; GÜREK, A. G. & AHSEN, V. "Liquid crystalline metal phthalocyanines: structural organization on the substrate surface". *Coord. Chem. Rev.*, 310: 131, 2016.
- 15 CHINO, Y.; OHTA, K.; KIMURA, M. & YASUTAKE, M. "Discotic liquid crystals of transition metal complexes, 53†: synthesis and mesomorphism of phthalocyanines substituted by *m*-alkoxyphenylthio groups". *J. Porphyrins Phthalocyanines*, 21 (3): 159, 2017.
- 16 SOROKIN, A. B. "Phthalocyanine metal complexes in catalysis". *Chem. Rev.*, 113 (10): 8152, 2013.
- 17 CASTRO, K. A. D. F.; FIGUEIRA, F.; ALMEIDA PAZ, F. A.; TOMÉ, J. P. C.; DA SILVA, R. S.; NAKAGAKI, S., et al. "Copper-phthalocyanine coordination polymer as a reusable catechol oxidase biomimetic catalyst". *Dalton Trans.*, 48 (23): 8144, 2019.
- 18 KLYAMER, D. D.; SUKHIKH, A. S.; KRASNOV, P. O.; GROMILOV, S. A.; MOROZOVA, N. B. & BASOVA, T. V. "Thin films of tetrafluorosubstituted cobalt phthalocyanine: structure and sensor properties". *Appl. Surf. Sci.*, 372: 79, 2016.
- 19 MANI, V.; DEVAENATHIPATHY, R.; CHEN, S.-M.; GU, J.-A. & HUANG, S.-T. "Synthesis and characterization of graphene-cobalt phthalocyanines and graphene-iron phthalocyanine composites and their enzymatic fuel cell application". *Renewable Energy*, 74: 867, 2015.
- 20 WANG, H.; WANG, B.-W.; BIAN, Y.; GAO, S. & JIANG, J. "Single-molecule magnetism of tetrapyrrole lanthanide compounds with sandwich multiple-decker structures". *Coord. Chem. Rev.*, 306: 195, 2016.
- 21 LI, X.; PENG, X.-H.; ZHENG, B.-D.; TANG, J.; ZHAO, Y.; ZHENG, B.-Y., et al. "New application of phthalocyanine molecules: from photodynamic therapy to photothermal therapy by means of structural regulation rather than formation of aggregates". *Chem. Sci.*, 9 (8): 2098, 2018.
- 22 DE LA TORRE, G.; CLAESSENS, C. G. & TORRES, T. "Phthalocyanines: old dyes, new materials. Putting color in nanotechnology". *Chem. Commun.*, (20): 2000, 2007.
- 23 ZHANG, Y. & LOVELL, J. F. "Recent applications of phthalocyanines and naphthalocyanines for imaging and therapy". *Wiley Interdiscip. Rev.: Nanomed. Nanobiotechnol.*, 9 (1): e1420, 2017.

- 24 LI, X.; ZHENG, B.-D.; PENG, X.-H.; LI, S.-Z.; YING, J.-W.; ZHAO, Y., et al. "Phthalocyanines as medicinal photosensitizers: developments in the last five years". *Coord. Chem. Rev.*, 379: 147, 2019.
- 25 ROGUIN, L. P.; CHIARANTE, N.; GARCÍA VIOR, M. C. & MARINO, J. "Zinc(II) phthalocyanines as photosensitizers for antitumor photodynamic therapy". *Int. J. Biochem. Cell Biol.*, 114: 105575, 2019.
- 26 SNOW, A. W. "Phthalocyanine aggregation". In: KADISH, K. M.; SMITH, K. M. & GUILARD, R. (Ed.). *The Porphyrin Handbook*. Amsterdam: Academic Press, 2003, vol. 17, ch. 109, pp. 129-176.
- 27 GOBO, N. R. S.; BROCKSOM, T. J. & OLIVEIRA, K. T. D. "Soluble and non-aggregated phthalocyanines: synthesis, mechanistic aspects and their main building blocks". *Curr. Org. Synth.*, 14 (8): 1132, 2017.
- 28 CIDLINA, A.; NOVAKOVA, V.; MILETIN, M. & ZIMCIK, P. "Peripheral substitution as a tool for tuning electron-accepting properties of phthalocyanine analogs in intramolecular charge transfer". *Dalton Trans.*, 44 (15): 6961, 2015.
- 29 CLAESSENS, C. G.; HAHN, U. & TORRES, T. "Phthalocyanines: from outstanding electronic properties to emerging applications". *Chem. Rec.*, 8 (2): 75, 2008.
- 30 SHARMAN, W. M. & LIER, J. E. V. "Use of palladium catalysis in the synthesis of novel porphyrins and phthalocyanines". *J. Porphyrins Phthalocyanines*, 4 (5): 441, 2000.
- 31 MARTÍNEZ-DÍAZ, M. V.; QUINTILIANI, M. & TORRES, T. "Functionalisation of phthalocyanines and subphthalocyanines by transition-metal-catalysed reactions". *Synlett*, (1): 1, 2008.
- 32 ALI, H.; AIT-MOHAND, S.; GOSSELIN, S.; VAN LIER, J. E. & GUÉRIN, B. "Phthalocyanine-peptide conjugates via palladium-catalyzed cross-coupling reactions". *J. Org. Chem.*, 76 (6): 1887, 2011.
- 33 YANIK, H.; AL-RAQA, S. Y.; ALJUHANI, A. & DURMUŞ, M. "The synthesis of novel directly conjugated zinc(II) phthalocyanine via palladium-catalyzed Suzuki–Miyaura cross-coupling reaction and its quaternized water-soluble derivative: investigation of photophysical and photochemical properties". *Dyes Pigm.*, 134: 531, 2016.
- 34 MOLEK, C. D.; HALFEN, J. A.; LOE, J. C. & MCGAFF, R. W. "Solventothermal synthesis and X-ray crystal structures of two nickel complexes with novel alkoxy-substituted phthalocyanine ligands". *Chem. Commun.*, (24): 2644, 2001.
- 35 OLIVER, S. W. & SMITH, T. D. "Oligomeric cyclization of dinitriles in the synthesis of phthalocyanines and related compounds: the role of the alkoxide anion". *J. Chem. Soc., Perkin Trans. 2*, (11): 1579, 1987.

- 36 MCKEOWN, N. B. "The synthesis of symmetrical phthalocyanines". In: KADISH, K. M.; SMITH, K. M. & GUILARD, R. (Ed.). *The Porphyrin Handbook*. San Diego: Academic Press, 2003, vol. 15, ch. 98, pp. 61-124.
- 37 BAUMANN, F.; BIENERT, B.; RÖSCH, G.; VOLLMANN, H. & WOLF, W. "Isoindolenine als Zwischenprodukte der Phthalocyanin-Synthese". *Angew. Chem. Int. Ed.*, 68 (4): 133, 1956.
- 38 GASPARD, S. & MAILLARD, P. "Structure des Phthalocyanines tétra tertio-butyles: mécanisme de la synthèse". *Tetrahedron*, 43 (6): 1083, 1987.
- 39 ERK, P. & HENGELSBERG, H. "Phthalocyanine dyes and pigments". In: KADISH, K. M.; SMITH, K. M. & GUILARD, R. (Ed.). *The Porphyrin Handbook*. Amsterdam: Academic Press, 2003, vol. 19, ch. 119, pp. 105-149.
- 40 HARUHIKO, T.; SHOJIRO, S.; SHOJIRO, O. & SHINSAKU, S. "Synthesis of phthalocyanines from phthalonitrile with organic strong bases". *Chem. Lett.*, 9 (10): 1277, 1980.
- 41 HURLEY, T. J.; ROBINSON, M. A. & TROTZ, S. I. "Complexes derived from 1,3-diiminoisoindoline-containing ligands. II. Stepwise formation of nickel phthalocyanine". *Inorg. Chem.*, 6 (2): 389, 1967.
- 42 NOLAN, K. J. M.; HU, M. & LEZNOFF, C. C. "'Adjacent' substituted phthalocyanines". *Synlett*, (5): 593, 1997.
- 43 RAGER, C.; SCHMID, G. & HANACK, M. "Influence of substituents, reaction conditions and central metals on the isomer distributions of 1(4)-tetrasubstituted phthalocyanines". *Chem. Eur. J.*, 5 (1): 280, 1999.
- 44 HAMCIUC, C.; CARJA, I.-D.; HAMCIUC, E.; VLAD-BUBULAC, T. & IGNAT, M. "Phthalonitrile-containing aromatic polyimide thin films with nano-actuation properties". *Polym. Adv. Technol.*, 24 (2): 258, 2013.
- 45 ZONG, L.; LIU, C.; ZHANG, S.; WANG, J. & JIAN, X. "Enhanced thermal properties of phthalonitrile networks by cooperating phenyl-s-triazine moieties in backbones". *Polymer*, 77: 177, 2015.
- 46 KÖYSAL, O.; OKUTAN, M.; SAN, S. E.; DURMUŞ, M.; ECEVIT, F. N. & AHSEN, V. "Diffraction efficiency enhancement caused by employing liquid crystal phthalonitrile derivative in nematic liquid crystals". *Dyes Pigm.*, 73 (1): 98, 2007.
- 47 AUGUSTINE, D.; MATHEW, D. & NAIR, C. P. R. "Phthalonitrile resin bearing cyanate ester groups: synthesis and characterization". *RSC Adv.*, 5 (111): 91254, 2015.
- 48 XU, M.; LUO, Y.; LEI, Y. & LIU, X. "Phthalonitrile-based resin for advanced composite materials: curing behavior studies". *Polym. Test.*, 55: 38, 2016.

- 49 MA, J.; LIU, T.; WANG, W. & YANG, Y. "Preparation and properties of poly(aryl ether ketone)-based phthalonitrile conductive composite film". *High Perform. Polym.*, 31 (1): 3, 2019.
- 50 MANLEY-KING, C. I.; BERGH, J. J. & PETZER, J. P. "Monoamine oxidase inhibition by C4-substituted phthalonitriles". *Bioorg. Chem.*, 40: 114, 2012.
- 51 VAN DER WALT, M. M.; TERRE'BLANCHE, G.; LOURENS, A. C. U.; PETZER, A. & PETZER, J. P. "Sulfanylphthalonitrile analogues as selective and potent inhibitors of monoamine oxidase B". *Bioorg. Med. Chem. Lett.*, 22 (24): 7367, 2012.
- 52 KANTAR, G. K.; BALTAŞ, N.; MENTEŞE, E. & ŞAŞMAZ, S. "Microwave-assisted synthesis and investigation of xanthine oxidase inhibition of new phthalonitrile and phthalocyanines containing morpholino substituted 1,2,4-triazole-3-one". *J. Organomet. Chem.*, 787: 8, 2015.
- 53 GÜZEL, E.; KOÇYIĞIT, Ü. M.; ARSLAN, B. S.; ATAŞ, M.; TASLIMI, P.; GÖKALP, F., et al. "Aminopyrazole-substituted metallophthalocyanines: preparation, aggregation behavior, and investigation of metabolic enzymes inhibition properties". *Arch. Pharm.*, 352 (2): e1800292, 2019.
- 54 MARTYNOV, A. G.; BIRIN, K. P.; GORBUNOVA, Y. G. & TSIVADZEA, A. Y. "Modern synthetic approaches to phthalonitriles with special emphasis on transition-metal catalyzed cyanation reactions". *Macroheterocycles*, 6 (1): 23, 2013.
- 55 WÖHRLE, D.; ESKES, M.; SHIGEHARA, K. & YAMADA, A. "A simple synthesis of 4,5-disubstituted 1,2-dicyanobenzenes and 2,3,9,10,16,17,23,24-octasubstituted phthalocyanines". *Synthesis*, (2): 194, 1993.
- 56 PARDO, C.; YUSTE, M. & ELGUERO, J. "Tetraimidazophthalocyanines". *J. Porphyrins Phthalocyanines*, 4 (5): 505, 2000.
- 57 NEMYKIN, V. N. & LUKYANETS, E. A. "Synthesis of substituted phthalocyanines". *ARKIVOC*, (1): 136, 2010.
- 58 FAUST, R. & MITZEL, F. "NIR chromophores from small acetylenic building blocks: a Diels–Alder approach to octaalkynylphthalocyanines". *J. Chem. Soc., Perkin Trans. 1*, (22): 3746, 2000.
- 59 FAUST, R. "The modular approach to acetylenic phthalocyanines and phthalocyanine analogues". *Eur. J. Org. Chem.*, (15): 2797, 2001.
- 60 DRECHSLER, U.; PFAFF, M. & HANACK, M. "Synthesis of novel functionalised zinc phthalocyanines applicable in photodynamic therapy". *Eur. J. Org. Chem.*, (12): 3441, 1999.
- 61 NG, A. C. H.; LI, X.-Y. & NG, D. K. P. "Synthesis and photophysical properties of nonaggregated phthalocyanines bearing dendritic substituents". *Macromolecules*, 32 (16): 5292, 1999.

- 62 GÖK, A.; ORMAN, E. B.; SALAN, Ü.; ÖZKAYA, A. R. & BULUT, M. "Synthesis, characterization and electrochemical properties of tetra 7-oxy-3-biphenylcoumarin substituted metal-free, zinc(II), cobalt(II) and indium(III) phthalocyanines". *Dyes Pigm.*, 133: 311, 2016.
- 63 ÖZÇEŞMECI, İ.; BURAT, A. K.; İPEK, Y.; KOCA, A. & BAYIR, Z. A. "Synthesis, electrochemical and spectroelectrochemical properties of phthalocyanines having extended π -electrons conjugation". *Electrochim. Acta*, 89: 270, 2013.
- 64 SUGIMORI, T.; TORIKATA, M.; NOJIMA, J.; TOMINAKA, S.; TOBIKAWA, K.; HANDA, M., et al. "Preparation and properties of octa-substituted phthalocyanines peripherally substituted with phenyl derivatives". *Inorg. Chem. Commun.*, 5 (12): 1031, 2002.
- 65 ARANYOS, V.; CASTAÑO, A. M. & GRENNBERG, H. "An application of the Stille coupling for the preparation of arylated phthalonitriles and phthalocyanines". *Acta Chem. Scand.*, 53: 714, 1999.
- 66 TEREKHOV, D. S.; NOLAN, K. J. M.; MCARTHUR, C. R. & LEZNOFF, C. C. "Synthesis of 2,3,9,10,16,17,23,24-octaalkynylphthalocyanines and the effects of concentration and temperature on their ^1H NMR spectra". *J. Org. Chem.*, 61 (9): 3034, 1996.
- 67 SCHWEIKART, K.-H.; HANACK, M.; LÜER, L. & OELKRUG, D. "Synthesis, absorption and luminescence of a new series of soluble distyrylbenzenes featuring cyano substituents at the peripheral rings". *Eur. J. Org. Chem.*, (2): 293, 2001.
- 68 AN, M.; KIM, S. & HONG, J.-D. "Synthesis and characterization of peripherally ferrocene-modified zinc phthalocyanine for dye-sensitized solar cell". *Bull. Korean Chem. Soc.*, 31 (11): 3272, 2010.
- 69 SWOBODA, P.; SAF, R.; HUMMEL, K.; HOFER, F. & CZAPUTA, R. "Synthesis and characterization of a conjugated polymer with stable radicals in the side groups". *Macromolecules*, 28 (12): 4255, 1995.
- 70 LEARDINI, R.; NANNI, D.; TUNDO, A.; ZANARDI, G. & RUGGIERI, F. "Annulation reactions with iron(III) chloride: oxidation of imines". *J. Org. Chem.*, 57 (6): 1842, 1992.
- 71 BORTOLOTTI, B.; LEARDINI, R.; NANNI, D. & ZANARDI, G. "DDQ-mediated formation of carbon-carbon bonds: oxidation of imines". *Tetrahedron*, 49 (44): 10157, 1993.
- 72 CAO, K.; ZHANG, F.-M.; TU, Y.-Q.; ZHUO, X.-T. & FAN, C.-A. "Iron(III)-catalyzed and air-mediated tandem reaction of aldehydes, alkynes and amines: an efficient approach to substituted quinolines". *Chem. Eur. J.*, 15 (26): 6332, 2009.
- 73 KULKARNI, A. & TÖRÖK, B. "Microwave-assisted multicomponent domino cyclization-aromatization: an efficient approach for the synthesis of substituted quinolines". *Green Chem.*, 12 (5): 875, 2010.

- 74 KUMAR, A. & RAO, V. K. "Microwave-assisted and Yb(OTf)₃-promoted one-pot multicomponent synthesis of substituted quinolines in ionic liquid". *Synlett*, (15): 2157, 2011.
- 75 KUMAR, V.; GOHAIN, M.; VAN TONDER, J. H.; PONRA, S.; BEZUINDENHOUDT, B. C. B.; NTWAEABORWA, O. M., et al. "Synthesis of quinoline based heterocyclic compounds for blue lighting application". *Opt. Mater.*, 50: 275, 2015.
- 76 PATIL, S. S.; PATIL, S. V. & BOBADE, V. D. "Synthesis of aminoindolizine and quinoline derivatives via Fe(acac)₃/TBAOH-catalyzed sequential cross-coupling-cycloisomerization reactions". *Synlett*, (16): 2379, 2011.
- 77 TANG, J.; WANG, L.; MAO, D.; WANG, W.; ZHANG, L.; WU, S., et al. "Ytterbium pentafluorobenzoate as a novel fluorous Lewis acid catalyst in the synthesis of 2,4-disubstituted quinolines". *Tetrahedron*, 67 (44): 8465, 2011.
- 78 YAO, C.; QIN, B.; ZHANG, H.; LU, J.; WANG, D. & TU, S. "One-pot solvent-free synthesis of quinolines by C–H activation/C–C bond formation catalyzed by recyclable iron(III) triflate". *RSC Adv.*, 2 (9): 3759, 2012.
- 79 ZHANG, Y.; LI, P. & WANG, L. "Iron-catalyzed tandem reactions of aldehydes, terminal alkynes, and primary amines as a strategy for the synthesis of quinoline derivatives". *J. Heterocycl. Chem.*, 48 (1): 153, 2011.
- 80 LI, X.; MAO, Z.; WANG, Y.; CHEN, W. & LIN, X. "Molecular iodine-catalyzed and air-mediated tandem synthesis of quinolines via three-component reaction of amines, aldehydes, and alkynes". *Tetrahedron*, 67 (21): 3858, 2011.
- 81 UCHIDA, H.; TANAKA, H.; YOSHIYAMA, H.; REDDY, P. Y.; NAKAMURA, S. & TORU, T. "Novel synthesis of phthalocyanines from phthalonitriles under mild conditions". *Synlett*, (10): 1649, 2002.
- 82 DE OLIVEIRA, K. T.; DE ASSIS, F. F.; RIBEIRO, A. O.; NERI, C. R.; FERNANDES, A. U.; BAPTISTA, M. S., et al. "Synthesis of phthalocyanines–ALA conjugates: water-soluble compounds with low aggregation". *J. Org. Chem.*, 74 (20): 7962, 2009.
- 83 BARTOLOMEU, A. A.; BROCKSOM, T. J.; DA SILVA FILHO, L. C. & DE OLIVEIRA, K. T. "Multicomponent reactions mediated by NbCl₅ for the synthesis of phthalonitrile-quinoline dyads: methodology, scope, mechanistic insights and applications in phthalocyanine synthesis". *Dyes Pigm.*, 151: 391, 2018.
- 84 SAKA, E. T.; DURMUŞ, M. & KANTEKIN, H. "Solvent and central metal effects on the photophysical and photochemical properties of 4-benzyloxybenzoxy substituted phthalocyanines". *J. Organomet. Chem.*, 696 (4): 913, 2011.
- 85 ARMAREGO, W. L. F. & CHAI, C. *Purification of Laboratory Chemicals*. 7th ed. Oxford: Butterworth-Heinemann, 2013. 1024 p.

- 86 GOULOUMIS, A.; LIU, S.-G.; SASTRE, Á.; VÁZQUEZ, P.; ECHEGOYEN, L. & TORRES, T. "Synthesis and electrochemical properties of phthalocyanine–fullerene hybrids". *Chem. Eur. J.*, 6 (19): 3600, 2000.
- 87 BYRON, D. J.; KEATING, D. A.; O'NEILL, M. T.; WILSON, R. C.; GOODBY, J. W. & GRAY, G. W. "The effect of the reversal of the central Schiff's base linkage on liquid crystal properties: the 4-phenylbenzylidene-4'-*n*-alkoxyanilines and 4-(4'-*n*-alkoxy-benzylideneamino)-biphenyls". *Mol. Cryst. Liq. Cryst.*, 58 (3-4): 179, 1980.
- 88 VEERABHADRASWAMY, B. N.; RAO, D. S. S. & YELAMAGGAD, C. V. "Stable ferroelectric liquid crystals derived from salicylaldehyde-core". *J. Phys. Chem. B*, 119 (12): 4539, 2015.
- 89 LAKOWICZ, J. R. *Principles of Fluorescence Spectroscopy*. 3rd ed. New York: Springer US, 2006. 954 p.

Chapter 2: Photoarylation of pyridines using aryldiazonium salts and visible light: an EDA approach

Reproduced with permission from **BARTOLOMEU, A. A.**; SILVA, R. C.; BROCKSON, T. J.; NOËL, T. & DE OLIVEIRA, K. T. "Photoarylation of pyridines using aryldiazonium salts and visible light: an EDA approach". *J. Org. Chem.*, 84 (16): 10459, 2019. Copyright 2019 American Chemical Society.

2 Chapter 2

Chapter 2 is based on our paper published in the Journal of Organic Chemistry in 2019, and it presents the results obtained in the development of a metal-free methodology for the photoarylation of pyridines and other heterocycles (such as quinoline and quinoxaline). This part of the research was developed entirely at UFSCar-Brazil under the guidance of Prof. Dr. Kleber T. de Oliveira, with the contributions of Prof. Dr. Timothy Noël (TU/e, The Netherlands), and in collaboration with a Ph.D. student from our team, Rodrigo Costa e Silva, who synthesized compounds **2.22s-u**, performed the scale-up experiment, carried out the UV-Vis and aggregation studies, and helped write the manuscript and supporting information.

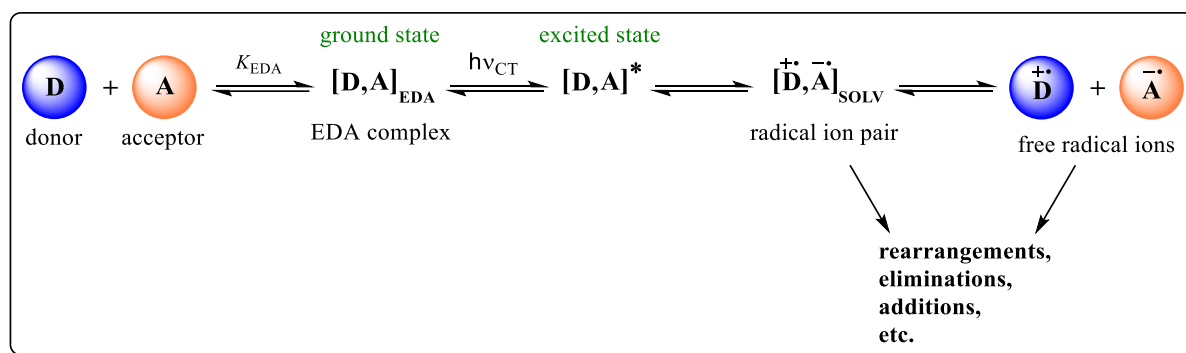
2.1 Introduction

2.1.1 Electron donor-acceptor complex

In 1952, Robert Sanderson Mulliken formulated a theory, known as the “Mulliken's Theory of Charge-Transfer Complexes”, to rationalize the appearance of color when mixing two colorless or nearly colorless organic molecules.^{1,2} Since the pioneering work of Mulliken, the electron-transfer theory has been extensively studied. Important contributions were made by Marcus, Taube, Hush, Kochi, and others.³ According to Mulliken's theory, an electron-rich molecule of low ionization potential (a donor D) may interact with an electron-poor molecule of high electron-affinity (an acceptor A) to produce an encounter complex (D,A), which is commonly called an electron donor-acceptor complex.³ This weak, reversible, ground-state association in solution (or in the gas phase) possesses physical properties different from those of the individual components. For example, the formation of such complexes is often accompanied by the appearance of a new absorption band (sometimes

in the visible region), the charge-transfer band, which is associated with an intracomplex SET from the donor to acceptor.

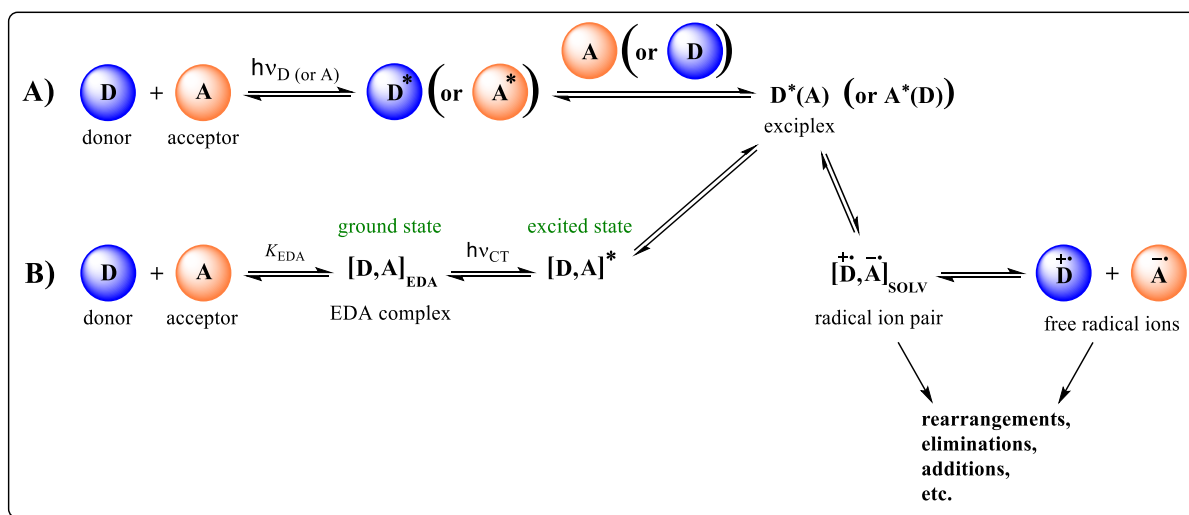
Upon light irradiation, the electrically neutral EDA complex ($[D,A]$) changes from its ground to excited state ($[D,A]^*$). This excited complex can produce an electron transfer event, thus generating a radical ion pair trapped in the solvent cage ($[D^{\bullet+},A^{\bullet-}]_{SOLV}$). Once formed, this radical species may undergo different reaction pathways, suffer back-electron transfer or even escape from the solvent cage to yield free radical ions (Scheme 2.1).³



Scheme 2.1 – EDA complex formation and its synthetic use enabled by light. Adapted from Lima et al. (2016).³

Concurrently to the process described above, excitation of the individual components D (or A) can lead to excited forms D^* (or A^*), which can react with non-excited counterparts A (or D) to provide the exciplexes $D^*(A)$ (or $A^*(D)$), respectively. Such exciplexes can produce electron transfer events, leading to the same above-mentioned ion-radical pair ($[D^{\bullet+},A^{\bullet-}]_{SOLV}$) (see Scheme 2.2A).³

It is noteworthy that the exciplex originated from charge-transfer band irradiation (see Scheme 2.2B) requires only minor changes in the solvent reorganization, since the dyad was previously assembled in the ground state. On the other hand, the exciplex produced from local band irradiation (see Scheme 2.2A) is dynamically assembled in the excited state and for this reason requires a high level of solvent reorganization.³



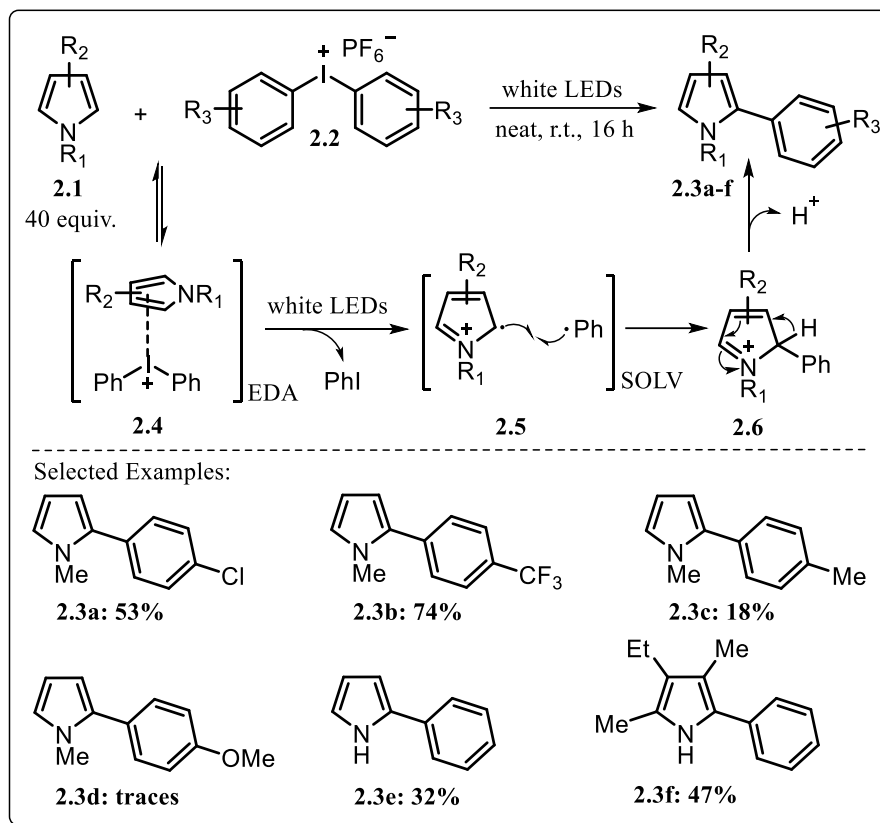
Scheme 2.2 – Exciplex complex formation and its synthetic use enabled by light. Adapted from Lima et al. (2016).³

Further theoretical details about Mulliken’s charge transfer theory, Marcus’s electron transfer theory, and other important contributions can be found elsewhere.³⁻⁸

Although the physicochemical properties of EDA complexes have been studied since the 1950s, their synthetic applications were investigated more intensively 20-30 years later (e.g., in studies involving $S_{RN}1$ substitutions and the nitration of aromatic compounds).³ Notable modern achievements include biaryl coupling (as shown in detail below),⁹⁻¹¹ asymmetric alkylation,^{12,13} radical cyclization,^{14,15} radical fluoroalkylation,¹⁶⁻¹⁸ oxidative annulation,¹⁹ radical acylation,²⁰ and others.²¹⁻²⁹

In 2013, Chatani and co-workers¹¹ showed that the arylation of some pyrroles (**2.1**) with diaryliodonium salts (**2.2**) using white LEDs could be achieved at room temperature even in the absence of a photocatalyst (Scheme 2.3). The UV-Vis analysis of the reaction mixture revealed a new absorption band in a visible region, the CT band, due to the formation of an EDA complex (**2.4**) between the pyrrole and the diaryliodonium salt. It is worth mentioning that the arylation of pyrroles and other *N*-heterocycles (such as pyridine, quinoxaline, and indole) with diaryliodonium salts have also been reported under thermal

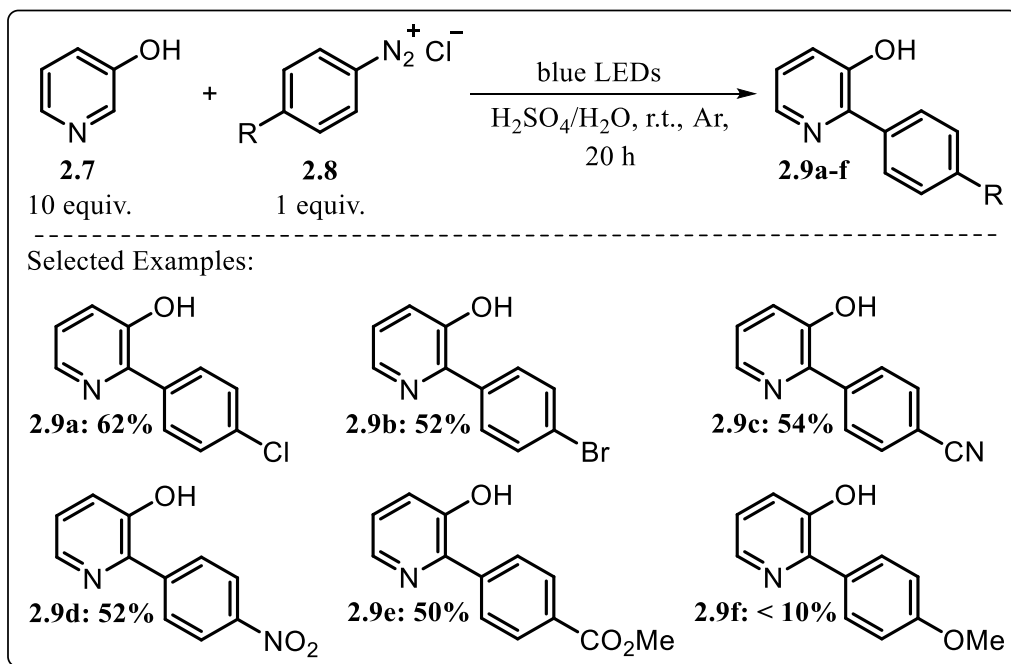
conditions,^{30,31} since diaryliodonium salts are known to transform into aryl radicals via decomposition (thermal or photochemical).³²⁻³⁴



Scheme 2.3 – EDA complex-photoinduced arylation of pyrroles with diaryliodonium salts.

In 2017, Heinrich and co-workers⁹ reported that the arylation of some arenes and heteroarenes with *para*-substituted aryldiazonium salts does not require the use of an additional photocatalyst and other additives, and can be conducted under simple UV-photocatalysis (250 W, iron lamp, black glass filter), UV-Vis (250 W, iron lamp, no filter) or visible-light (10 W, blue LED lamp) irradiation using argon or air atmosphere. They postulated that these photoinduced transformations may occur independently of the formation of a strong CT complex between the diazonium salt and the aromatic substrate. They also have shown the direct C–H arylation of 3-hydroxypyridine (**2.7**) with some aryldiazonium salts (**2.8**), in 50-62% yields (**2.9a-e**) using visible-light irradiation (Scheme 2.4). However, this methodology

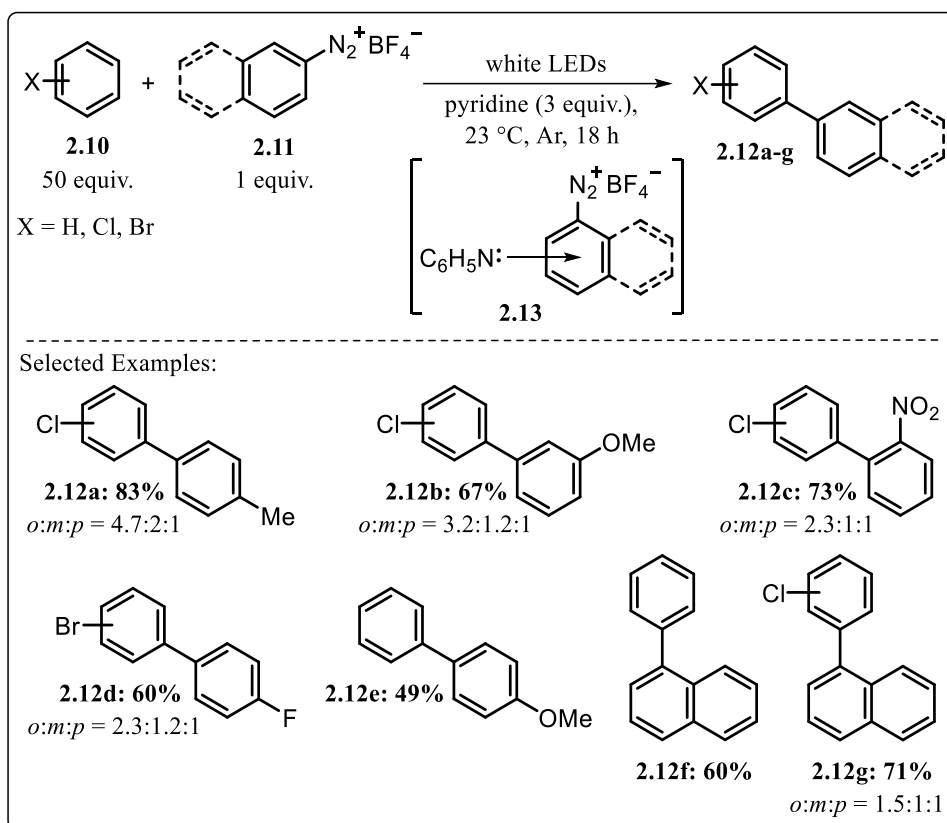
does not work well for the aryldiazonium salt bearing a *para*-methoxy group (see product **2.9f**) even when electron-rich (hetero)arenes (hydroquinone, 1,4-dimethoxybenzene, and furfurylamine) were employed as substrates (<10% isolated yields).⁹



Scheme 2.4 – Photoarylation of 3-hydroxypyridine with aryldiazonium salts.

The results obtained by Chatani's group and Heinrich's group left some questions to be answered and motivated us to study the direct arylation of pyridines and other *N*-heterocycles (such as quinoline and quinoxaline) with aryldiazonium tetrafluoroborates using blue light in the absence of a photocatalyst (see Section 2.2.1).

While we were reviewing our manuscript, Lee and co-workers¹⁰ reported a similar protocol involving the Gomberg-Bachmann reaction (Scheme 2.5). In this study, the authors propose the formation of an EDA complex **2.13** between the diazonium salts **2.11** and pyridine for the aryl radical generation and posterior arylation of (halo)benzenes **2.10** (not pyridines or heterocycles).



Scheme 2.5 – Photoarylation of (halo)benzenes with aryldiazonium salts.

Recently, Lee and co-workers³⁵ employed our previously used strategy to generate aryl radical and applied it to the direct C3-arylation of 2*H*-indazoles, further supporting our proposed mechanism (see Section 2.2.2).

2.1.2 Pyridines

Pyridine moieties are common in natural products,³⁶⁻⁴¹ agrochemicals,⁴²⁻⁴⁴ and drugs approved by the FDA.^{45,46} Moreover, relevant clinical drugs such as crizotinib (**2.14**), enasidenib (**2.15**), vismodegib (**2.16**), nilotinib (**2.17**), etoricoxib (**2.18**), and atazanavir (**2.19**) contain the pyridine nucleus directly linked to aryl or heteroaryl units (Figure 2.1).⁴⁵⁻⁴⁸ Therefore, the development of new and efficient methodologies for the direct C–H arylation or heteroarylation of this electron-deficient heterocycle is of great interest.

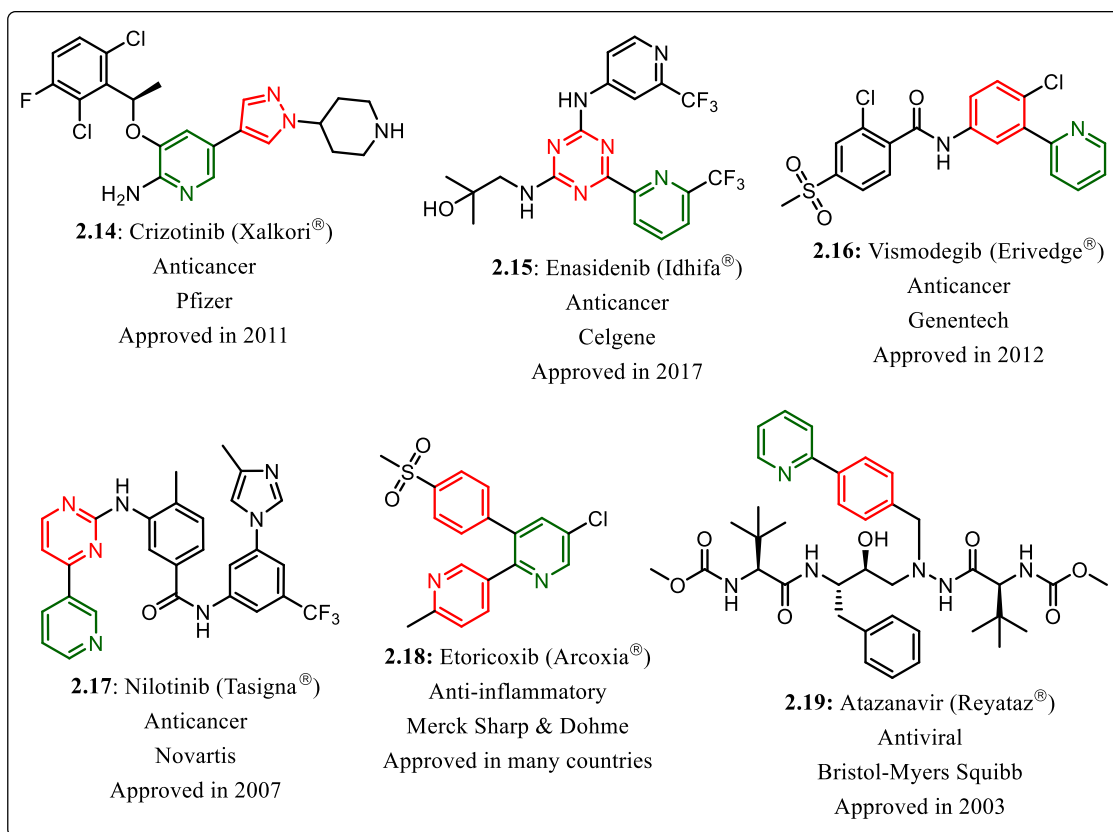
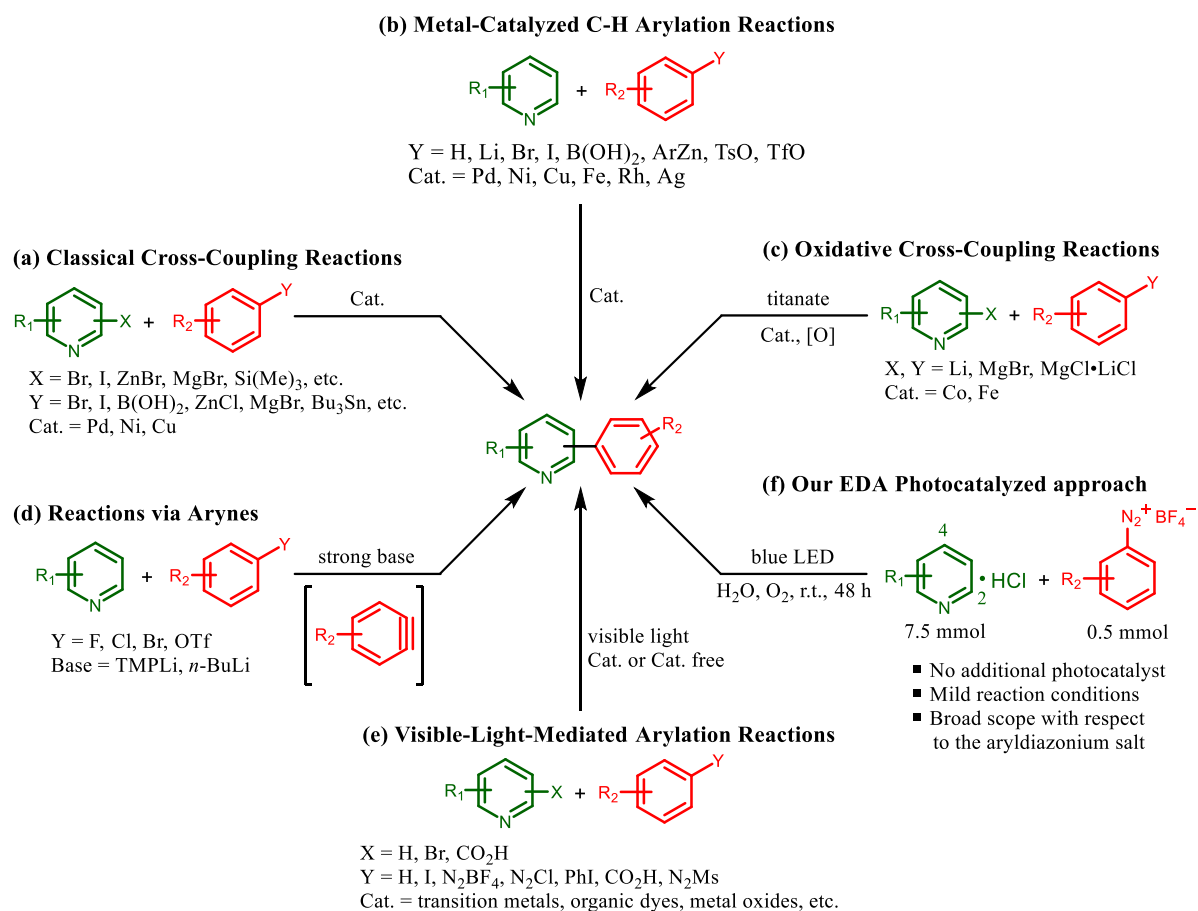


Figure 2.1 – Structures of drugs that contain the pyridine nucleus (in green) directly linked to aryl or heteroaryl units (in red).

The synthesis of biaryls containing a pyridine motif has been traditionally carried out by classical cross-coupling reactions such as Suzuki-Miyaura,⁴⁹⁻⁵² Negishi,⁵³⁻⁵⁵ Stille,^{51,56,57} Hiyama,^{58,59} and Kumada^{60,61} couplings (Scheme 2.6, eq. a). These structures can also be synthesized by C–H activation reactions (Scheme 2.6, eq. b),⁶²⁻⁶⁵ oxidative cross-coupling reactions (Scheme 2.6, eq. c),⁶⁶⁻⁶⁸ reactions via arynes (Scheme 2.6, eq. d),⁶⁹⁻⁷¹ and alternatively by radical-based methodologies,^{72,73} which have received much attention recently in studies involving photocatalysis.⁷⁴⁻⁸⁰ Such photocatalyzed reactions have been performed with various aryl radical precursors such as aryldiazonium^{9,81-87} and diaryliodonium salts,^{11,88} aryl boronic⁶⁵ and carboxylic acids,⁶² benzenesulfonyl chlorides (not tested with a pyridine nucleus),⁸⁹ arylazosulfones (tested with the pyrazolopyridine nucleus),^{90,91} diazoanhydrides (with pyridine *N*-oxide),⁹² and halo(hetero)arenes⁹³⁻⁹⁵ in the presence of ruthenium complexes,^{82,85} iridium

complexes,^{11,62,93} organic dyes,^{83,84,94-96} metal oxides,^{81,86,97} and other (photo)catalysts (Scheme 2.6, eq. e).^{98,99} However, the radical arylation of arenes and heteroarenes has been achieved with only a few aryl radical precursors, even in the absence of a photocatalyst.^{11,90,92,100}



Scheme 2.6 – Approaches for the synthesis of biaryls containing the pyridine nucleus.

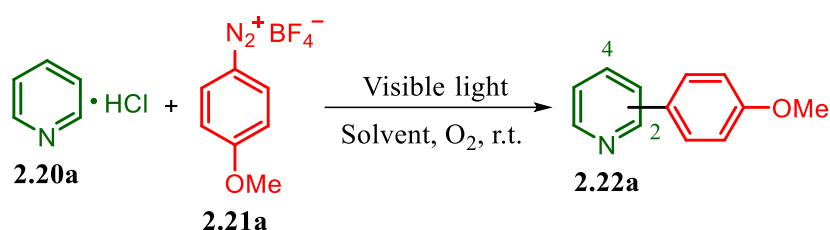
We now report a protocol for the direct C–H arylation of pyridines and other *N*-heterocycles (such as quinoline and quinoxaline), in water, with several aryldiazonium tetrafluoroborates substituted by electron-donor, -neutral and -acceptor groups, and with no base or additives, at room temperature, and using visible-light irradiation (blue LED) in the absence of photocatalysts (Scheme 2.6, eq. f). We postulate the occurrence of a visible-light photoactive EDA complex for the aryl radical generation which is supported by UV-Vis and ¹H and ¹H-¹⁵N NMR (correlation spectroscopy).

2.2 Results and discussion

2.2.1 Photoarylation of *N*-heterocycles

We started our investigation with pyridine hydrochloride (**2.20a**) and 4-methoxybenzenediazonium tetrafluoroborate (**2.21a**) as the model substrates using a homemade batch photoreactor with blue or white 30 W LEDs (see details of the photoreactor setup in the section 2.4.2). First, the reaction between **2.20a** (7.5 mmol) and **2.21a** (0.5 mmol) in MeOH (1.5 mL) was tested at r.t., under an O₂ atmosphere and in the dark, but only traces of the 2-aryl-regioisomer **2.22a** could be detected by gas chromatography-mass spectrometry (GC-MS) after 48 h (Table 2.1, entry 1). Subsequently, we performed the reaction under the same conditions but in the presence of blue LED light, obtaining a mixture of 2-aryl/4-aryl substituted pyridines (**2.22a**) in 84% yield (entry 2).

We also evaluated whether the activation of the pyridine moiety as the hydrochloride is needed, and carried out the same reaction with 7.5 mmol of free base pyridine and irradiation by blue LED. The result was a mixture of the 2- and 4-aryl-regioisomers **2.22a** in 20% yield (Table 2.1, entry 3). This experiment led us to the conclusion that pyridinium salts are essential for this protocol. Changing the amount of pyridine hydrochloride (**2.20a**) relative to the diazonium salt **2.21a** resulted in 41 to 90% yields of **2.22a** (entries 2, 4, and 5). Keeping 7.5 mmol of **2.20a** and increasing **2.21a** to 1 mmol also resulted in a lower yield (55%) (entry 6) showing that high excesses of **2.20a** relative to **2.21a** are important for the efficiency of the protocol. Although the reaction with 10 mmol of **2.20a** significantly improved the yield of **2.22a** (entry 5), we decided to continue screening the conditions using 7.5 mmol of this substrate. This excess of pyridinium salt is imperative and will be clarified below in the section of mechanistic studies (see Section 2.2.2).

Table 2.1 – Screening of the reaction conditions.^[a]

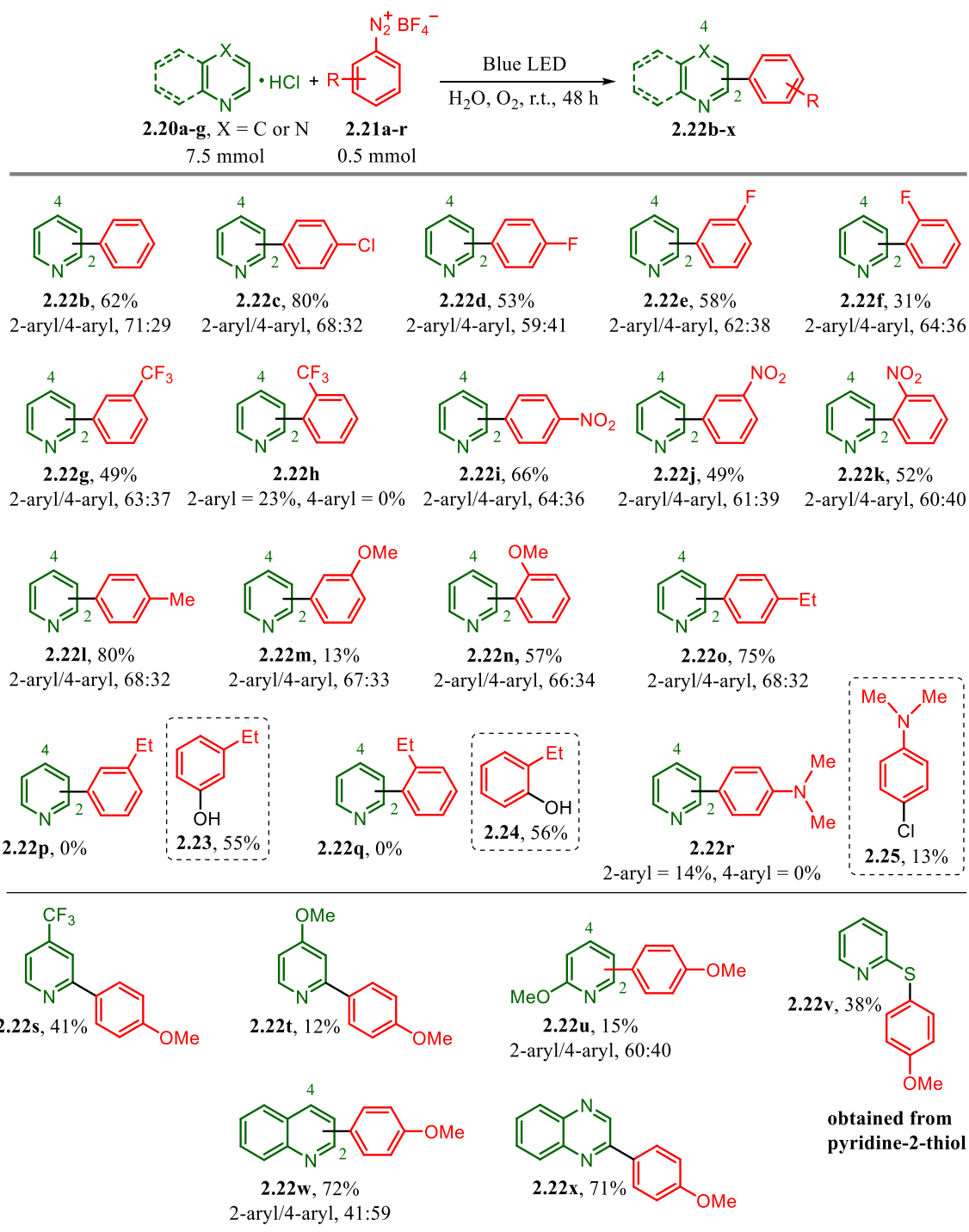
Entry	2.20a (mmol)	2.21a (mmol)	Light source (30 W)	Solvent	Time (h)	2-aryl/4-aryl ^[e]	Yield 2.22a ^[f]
1	7.5	0.5	None	MeOH	48	-	Traces
2	7.5	0.5	Blue LED	MeOH	48	71:29	84
3	7.5 ^[b]	0.5	Blue LED	MeOH	48	68:32	20
4	5	0.5	Blue LED	MeOH	48	67:33	41
5	10	0.5	Blue LED	MeOH	48	67:33	90
6	7.5	1	Blue LED	MeOH	48	68:32	55
7 ^[c]	7.5	0.5	Blue LED	MeOH	48	71:29	75
8	7.5	0.5	Blue LED	MeOH	24	72:28	72
9	7.5	0.5	White LED	MeOH	48	73:27	59
10	7.5	0.5	Blue LED	EtOH	48	67:33	69
11	7.5	0.5	Blue LED	DMF	48	77:23	64
12	7.5	0.5	Blue LED	DMF/MeOH (1:1)	48	71:29	63
13	7.5	0.5	Blue LED	DMF/MeOH (1:2)	48	69:31	71
14	7.5	0.5	Blue LED	DMSO	48	73:27	82
15	7.5	0.5	Blue LED	H₂O	48	71:29	96
16 ^[d]	30	2	Blue LED	H ₂ O	48	67:33	79
17	7.5	0.5	none	H ₂ O	48	-	Traces

^[a]Reaction conditions: pyridine hydrochloride (**2.20a**) (5, 7.5 and 10 mmol), 4-methoxybenzenediazonium tetrafluoroborate (**2.21a**) (0.5 and 1 mmol) in solvent (1.5 mL) at r.t. under an O₂ atmosphere for 24 or 48 h. ^[b]With 7.5 mmol of free base pyridine. ^[c]Previously deoxygenated and maintained under argon atmosphere. ^[d]Scale-up reaction performed under the same reaction conditions of entry 15, but in 6 mL of H₂O with **2.22a** obtained in 0.3 g-scale. ^[e]Determined after isolation. ^[f]Isolated yields.

The influence of the atmosphere, reaction time, and LED light source was also evaluated (Table 2.1, entries 7–9, respectively). It was observed that the yield of **2.22a** decreased when the reaction was performed under an argon atmosphere (75% yield, entry 7 vs 2) or when a shorter reaction time (24 h) was considered (72% yield, entry 8). Additionally, when white LEDs were employed under the same reaction conditions (entry 9) a lower yield (59%) was obtained.

We also investigated the effect of other solvents [EtOH, dimethylformamide (DMF), dimethylsulfoxide (DMSO) and H₂O] or mixtures of solvents (DMF/MeOH, 1:1 or 1:2, v/v) on the yield of **2.22a** (Table 2.1, entries 10–15). To our delight, when H₂O was used as the solvent, the desired product **2.22a** was obtained in 96% yield under identical conditions (entry 15). It is worth noting that the yield of the arylated product **2.22a** is positively correlated with increases in the solvent polarity used in the reaction (entries 11, 10, 2, and 15, respectively). The only exception was the reaction carried out in DMSO (entry 14). The robustness of the protocol (entry 16) was also tested reacting 2 mmols of **2.21a** in the same optimized conditions (entry 15), giving the product **2.22a** in 79% yield (0.3 g-scale). Finally, we checked the optimized reaction condition for the pyridine arylation (entry 15) in the absence of light, and again only traces of the 2-aryl-regioisomer **2.22a** could be detected by GC-MS after 48 h (entry 17). These results show that the arylation reaction is promoted by visible-light irradiation and does not require a photocatalyst to occur under mild and environmentally friendly conditions.

With the optimized reaction conditions in hands (Table 2.1, entry 15), we proceeded to evaluate the diazonium salt scope. As shown in Scheme 2.7, several aryldiazonium salts with different substitution patterns, substituted pyridines, quinoline, and quinoxaline are compatible with our arylation protocol.



Scheme 2.7 – Evaluation of the reaction scope. All reactions were carried out on a scale of 7.5 mmol of **2.20a-g** and 0.5 mmol of **2.21a-r** in H₂O (1.5 mL). Isolated yields and product ratios were determined after column chromatography.

Among the aryldiazonium tetrafluoroborate salts tested for the direct arylation of the pyridine moiety, electron-donor (Scheme 2.7, **2.22l** and **2.22o**) and -neutral 4-substituted

aryldiazonium salts (Scheme 2.7, **2.22b** and **2.22c**) were more efficient than electron-acceptor 4-substituted ones (Scheme 2.7, **2.22d** and **2.22i**). However, the reaction with the aryldiazonium salt **2.21r** containing the π -donor group 4-N(Me)₂ provided the 2-arylated pyridine (**2.22r**) in only 14% yield, and the diazo-substituted product **2.25** in 13% yield.

In the work reported by Heinrich and co-workers (2016),¹⁰¹ an aryldiazonium chloride salt containing the same 4-dimethylamino group was unsuccessful in the radical arylation of 3-hydroxypyridine mediated by TiCl₃, which suggests incompatibility of this type of substrate with radical C–H arylation protocols.

Intriguingly, the aryldiazonium salts **2.21p** (R = 3-Ethyl) and **2.21q** (R = 2-Ethyl) also underwent substitution reactions by hydroxyl groups (from the solvent water) to give the phenols **2.23** and **2.24** in yields of 55% and 56%, respectively. The use of π -acceptor (NO₂) or donor (OMe) substituents at the 2 and 3 positions of the aryldiazonium ring decreased product yields compared with the same substituents at the 4-position of the diazonium salts. However, this effect was more pronounced for the methoxy donor substituent (Scheme 2.7, **2.22m** and **2.22n**) than for the nitro acceptor (Scheme 2.7, **2.22i-k**). Furthermore, lower yields were observed when σ -acceptor (F and CF₃) groups were present at the 2- and 3-positions of the aryldiazonium rings (see Scheme 2.7, **2.22e** vs **2.22f** and **2.22g** vs **2.22h**).

Maas et al. (2001) reported that some diazonium salts such as 3-methoxybenzenediazonium (**2.21m**) and certain heteroarenediazonium tetrafluoroborates are known to decompose when dried,¹⁰² which may explain the low yield obtained for biaryl **2.22m** (13%). Indeed, Heinrich and co-workers (2016) also reported problems with the use of an aryldiazonium chloride containing the *meta*-methoxy group, which partially decomposed before the addition to the reaction mixture.¹⁰¹ In the case of compounds **2.22e-h** bearing σ -acceptor (F and CF₃) groups, the difference in yields between the *ortho* and *meta* derivatives can be due to steric and/or electronic factors. However, we do not rule out the possibility that the yields of these and other reactions (such as Scheme 2.7, **2.22p**, **2.22q**) are correlated with

the (photo)stability of the corresponding aryldiazonium salts. In addition to the nature of the counter-ion, it is known that the substituent nature and position on the cation are of the greatest importance for the stability of the aryldiazonium salt.^{103,104}

We also included additional *N*-heterocycles (Scheme 2.7) to scope with the 4-(trifluoromethyl)pyridine (giving **2.22s** in 41% yield), 4-methoxypyridine (giving **2.22t** in 12% yield), 2-methoxypyridine (giving **2.22u** in 15% yield), pyridine-2-thiol (giving **2.22v** in 38% yield), quinoline (giving **2.22w** in 72% yield), and quinoxaline (giving **2.22x** in 71% yield). Overall, the substituted pyridines with electron-withdrawing and -donating groups yielded products from low to acceptable yields (12-41%). The pyridine-2-thiol yielded the product **2.22v** (38%) with the arylation in the thiol position and not in the aromatic ring. Both quinoline and quinoxaline provided arylated products in good yields (71-72%), demonstrating additional possibilities to apply this methodology.

To extend the scope of our photochemical protocol, other substituted pyridines (as hydrochloride) were examined as substrates with 4-methoxybenzenediazonium tetrafluoroborate (**2.21a**). We found that 2-methylpyridine (**2.20h**), 3-hydroxypyridine (**2.20i**), 2-(trifluoromethyl)pyridine (**2.20j**), 2-nitropyridine (**2.20k**), and 4-(dimethylamino)pyridine (**2.20l**) were not compatible with this reaction protocol under optimized conditions (Figure 2.2).

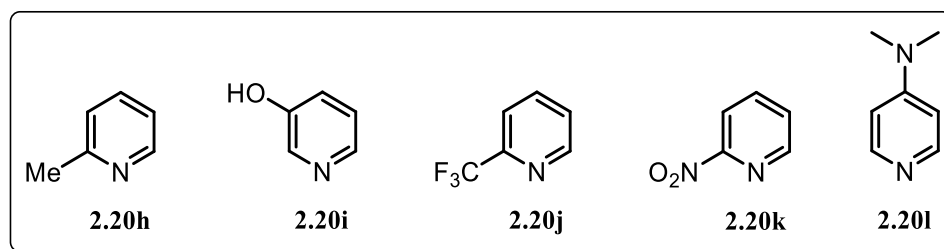


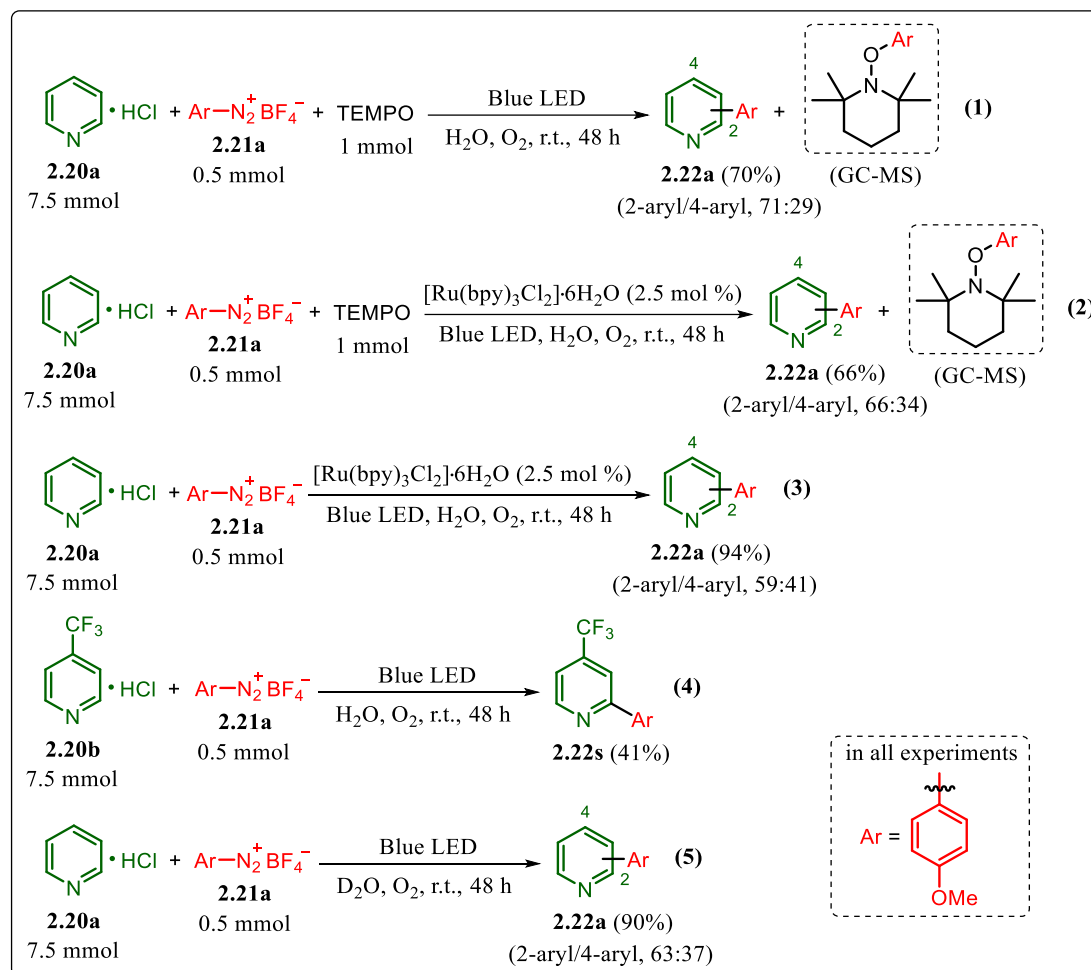
Figure 2.2 – Unsuccessful substrates in our photochemical approach.

2.2.2 Mechanistic insights and counterpoints with Ru-photocatalyzed reactions

To gain some insight into the mechanism of this metal-free C–H photoarylation reaction, we conducted several controlled experiments with substrates **2.20a** and **2.21a** and compared our results with the literature using Ru photocatalysts (see Scheme 2.8). As observed in our experiments performed in the dark (Table 2.1, entries 1 and 17) only traces of the 2-aryl-regioisomer **2.22a** could be detected by GC-MS after 48 h, showing that the reaction is being promoted by blue LED visible-light. We also performed a reaction in the presence of 2 equiv. of the radical scavenger TEMPO and only partial inhibition of the reaction was observed (Scheme 2.8, eq. 1). The aryl radical was trapped with TEMPO and was detected by GC-MS (see Section 2.4.7, Figure 2.9) and **2.22a** obtained in 70% yield (as against 96% yield, Table 2.1, entry 15, in the absence of TEMPO). This suggests that the reaction involves radical intermediates, but complete radical trapping with full inhibition was not observed, probably because of the low solubility of TEMPO in water (~0.03 M at 25 °C).¹⁰⁵

Subsequently, we tried to reproduce in our setup and optimized substrate proportions, the reaction between **2.20a** and **2.21a** reported by Xue et al. (2014) using Ru(bpy)₃Cl₂ (2.5 mol%) in the presence of 2 equiv. of TEMPO.⁸⁵ However, in our hands, the compound **2.22a** was obtained in 66% yield and only traces of the radical trapped with TEMPO could be detected by CG-MS, against the 0% described by the aforementioned authors (Scheme 2.8, eq. 2 and Figure 2.10, Section 2.4.7). Furthermore, we tried to reproduce the same previous reaction without TEMPO (Scheme 2.8, eq. 3) and obtained the compound **2.22a** in 94% yield. This result is statistically the same as compared to that reported in the mentioned literature (93%) with the Ru photocatalyst. However, this is also consistent with the yield we obtained without a photocatalyst (96%, Table 2.1, entry 15), proving that these photoarylation reactions work in 48 h (against the 60-80 h reported) without the Ru catalysts. It is important to highlight that the literature background reaction⁸⁵ uses *p*-CF₃-pyridine (**2.20b**) with **2.21a** (Scheme 2.8,

eq. 4) and mentions that only traces of the product **2.22s** were formed. We obtained the product **2.22s** in 41% yield after 48 h, as opposed to the reported traces obtained by Xue et al. (2014) after 60 h.⁸⁵



Scheme 2.8 – Mechanistic investigations.

These results show an inconsistency between our data and the above-mentioned report, but these differences may be due to the different reagent proportions, as well as their use of 45 W white CFL lamps or 3 W blue LEDs against the 30 W blue LEDs used in this study.

An additional control experiment was performed with deuterated water as solvent (Scheme 2.8, eq. 5), obtaining **2.22a** in a comparable 90% yield and with no incorporation of deuterium, showing no hydrogen transfer.

In order to understand which intermediate is photoactive in this reaction (a photochemical intermediate such as a diazopyridinium salt or an EDA complex) we carried out several UV-Vis, ^1H and ^1H - ^{15}N HMBC NMR studies. The literature indicates that the formation of colored CT complexes between the electron-poor aryldiazonium salts and aromatic hydrocarbons occurs spontaneously, presenting a progressive bathochromic (red) shift with the decrease of the ionization potential of these aromatic substrates.^{106,107} We have successfully detected a new UV-Vis band by mixing **2.20a** and **2.21a** as demonstrated in Figure 2.3A, and confirmed a very close match between the CT band (black line) and the blue LED emission (blue line) (Figure 2.3A, inset).

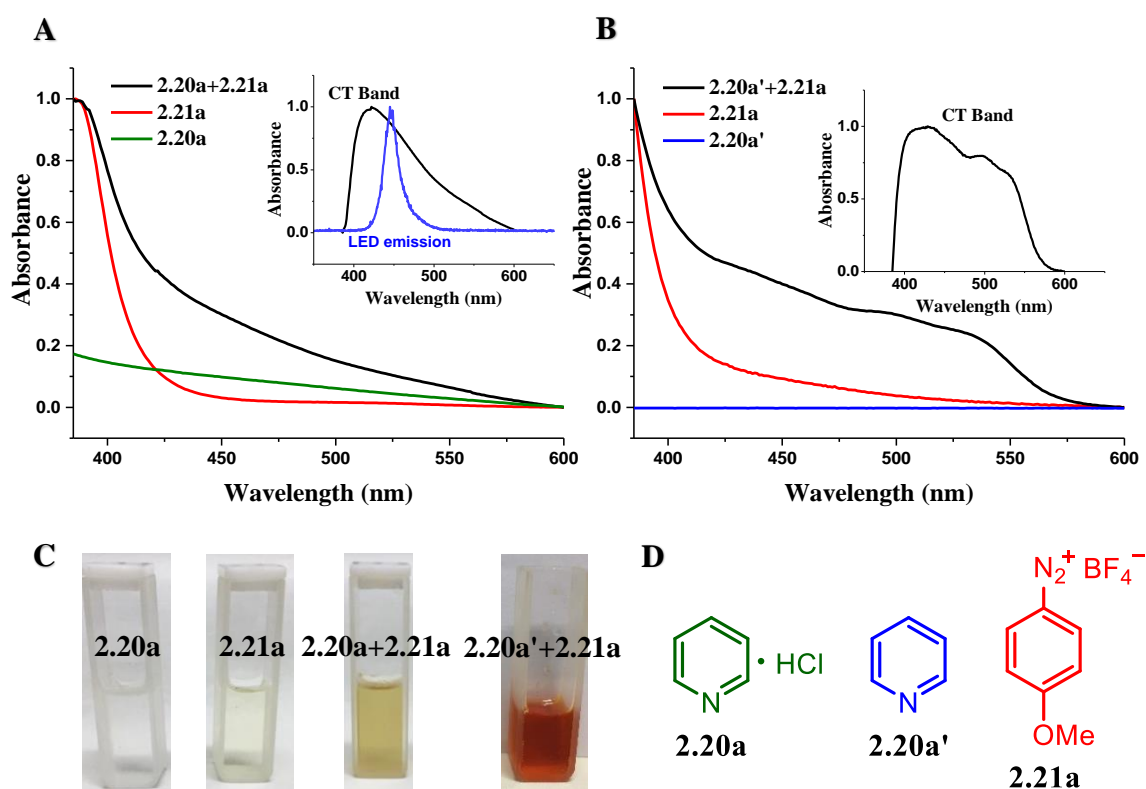


Figure 2.3 – (A) UV-Vis absorption spectra of **2.20a** (3 mmol), **2.21a** (0.2 mmol), and the mixture of **2.20a** and **2.21a** at 2 and 0.13 M in H_2O , respectively. Inset: CT band of (**2.20a** + **2.21a**) EDA complex. (B) UV-Vis absorption spectra in NaCl solution (1 M) for **2.20a'** (3 mmol), **2.21a** (0.2 mmol) and the mixture of **2.20a'** and **2.21a** at 2 and 0.13 M in H_2O , respectively. Inset: CT band of (**2.20a'** + **2.21a**) EDA complex. (C) Images of the solutions **2.20a**, **2.21a**, **2.20a** + **2.21a** and **2.20a'** + **2.21a**. (D) Molecular structure of the species.

These first studies by UV-Vis (Figure 2.3A) are consistent with the occurrence of an EDA complex. However, it is well-known in the literature that EDA complexes are supramolecular structures.³ In the case of diazonium salt and pyridine mixtures, the literature describes the occurrence of diazopyridinium salts at low temperatures,¹⁰⁸ which are discrete structures and that cannot be considered EDA complexes. In an effort to gather more data and confirm the real photochemical intermediate of this study, we performed an experiment with the diazonium salt **2.21a** in the presence of NaCl instead of pyridinium chloride, obtaining exactly the same UV-Vis band of the diazonium salt **2.21a** and showing that the chloride ion is not able to form an EDA with **2.21a**. In addition, a UV-Vis experiment with the diazonium salt **2.21a** and free pyridine (**2.20a'**) revealed a very similar new UV-Vis band with a more noticeably colored solution (see Figure 2.3B and 2.3C). We concluded that there is an evident interaction between pyridine and the diazonium salt moieties, which is present when mixing py·HCl (**2.20a**) and the diazonium salt **2.21a**. Because of the acid-base equilibrium, the concentration of free pyridine is low, and the EDA formed is more discrete (low concentration). However, in the presence of high concentrations of free pyridine **2.20a'** the occurrence of the EDA complex is more evident (Figure 2.3B). It is important to highlight that our methodology deals with the formation of an EDA but also with a relative concentration of protonated pyridine or heterocycle in order to have the radical acceptor activated.

We also performed ¹H NMR experiments in D₂O analyzing **2.20a** and **2.21a** individually and mixtures of both in different proportions.¹⁰⁹ First, aggregation studies at high concentrations of **2.20a** (from 70 to 280 mM) and **2.21a** (from 35 to 140 mM) were carried out by ¹H NMR (see Figure 2.8, Section 2.4.6), and no aggregation in solution was detected even at high concentrations (140 or 280 mM); it is well-known that aggregation on aromatic compounds in solutions can cause dramatic chemical shifts.¹¹⁰

In the ¹H NMR analysis of the mixture of both **2.20a** and **2.21a** (1:1 equiv.) in D₂O, we observed a slight protection (upfield shift) for the signal of the hydrogens adjacent to

the methoxy group (at 7.4 ppm) of diazonium salt **2.21a** and a slight deprotection (downfield shift) of the ^1H signals in **2.20a** (Figure 2.4). Similarly, the mixture of the diazonium salt **2.21a** and free pyridine (**2.20a'**) yielded ^1H NMR analyses with protected signals for the diazonium salt **2.21** in both 1:1 and 1:5 molar ratios (especially at 1:5 molar ratio) and deprotected signals for the free pyridine (**2.20a'**) at 1:1 molar ratio (Figure 2.5). This indicates an electron-donor effect from the pyridine nucleus and an electron-acceptor effect from the diazonium salt moiety. It is important to highlight that the more relevant deprotection effect in the 1:5 molar ratio experiment is in agreement with the supramolecular properties of the EDA complexes. Additional experiments of ^1H - ^{15}N HMBC were performed in D_2O (see Figure 2.11, Section 2.4.8). Only ^1H - ^{15}N correlations of individual **2.20a'** and **2.21a** were observed in the mixture solution, with no photochemically active intermediate such as a diazopyridinium salt detected.

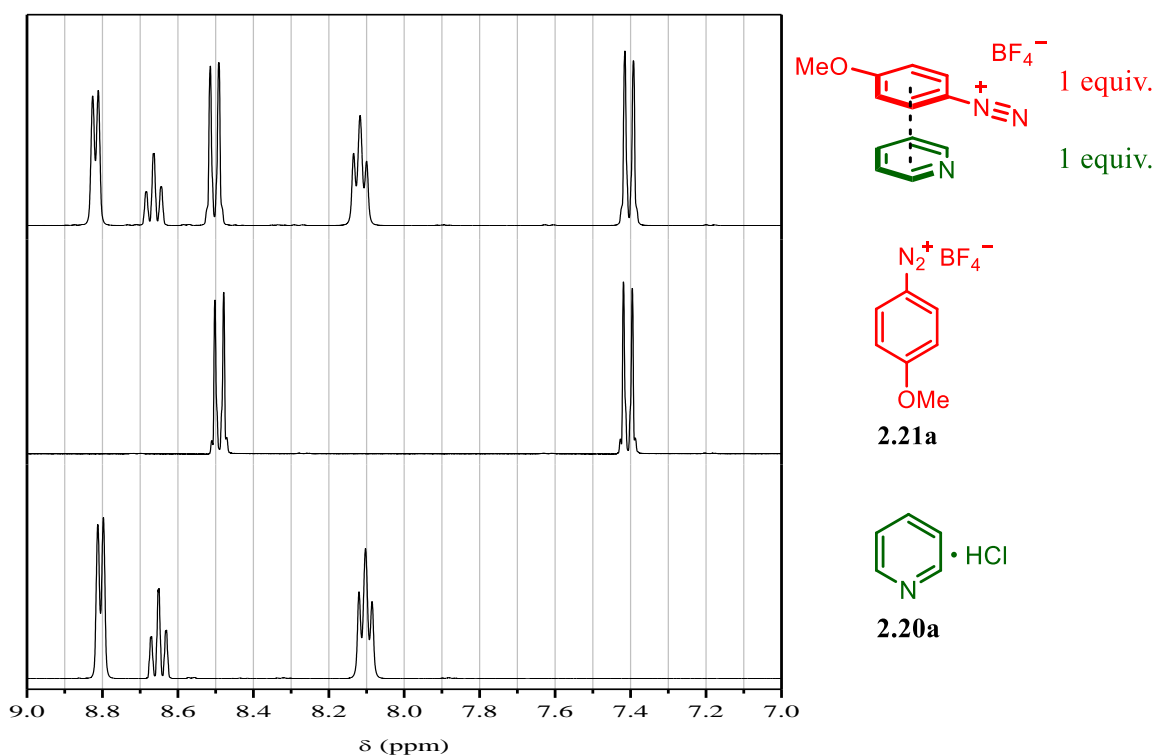


Figure 2.4 – ^1H NMR spectrum for **2.20a** (at 35 mM), **2.21a** (at 35 mM), and their mixture at 35 mM (1:1 equiv.) in D_2O .

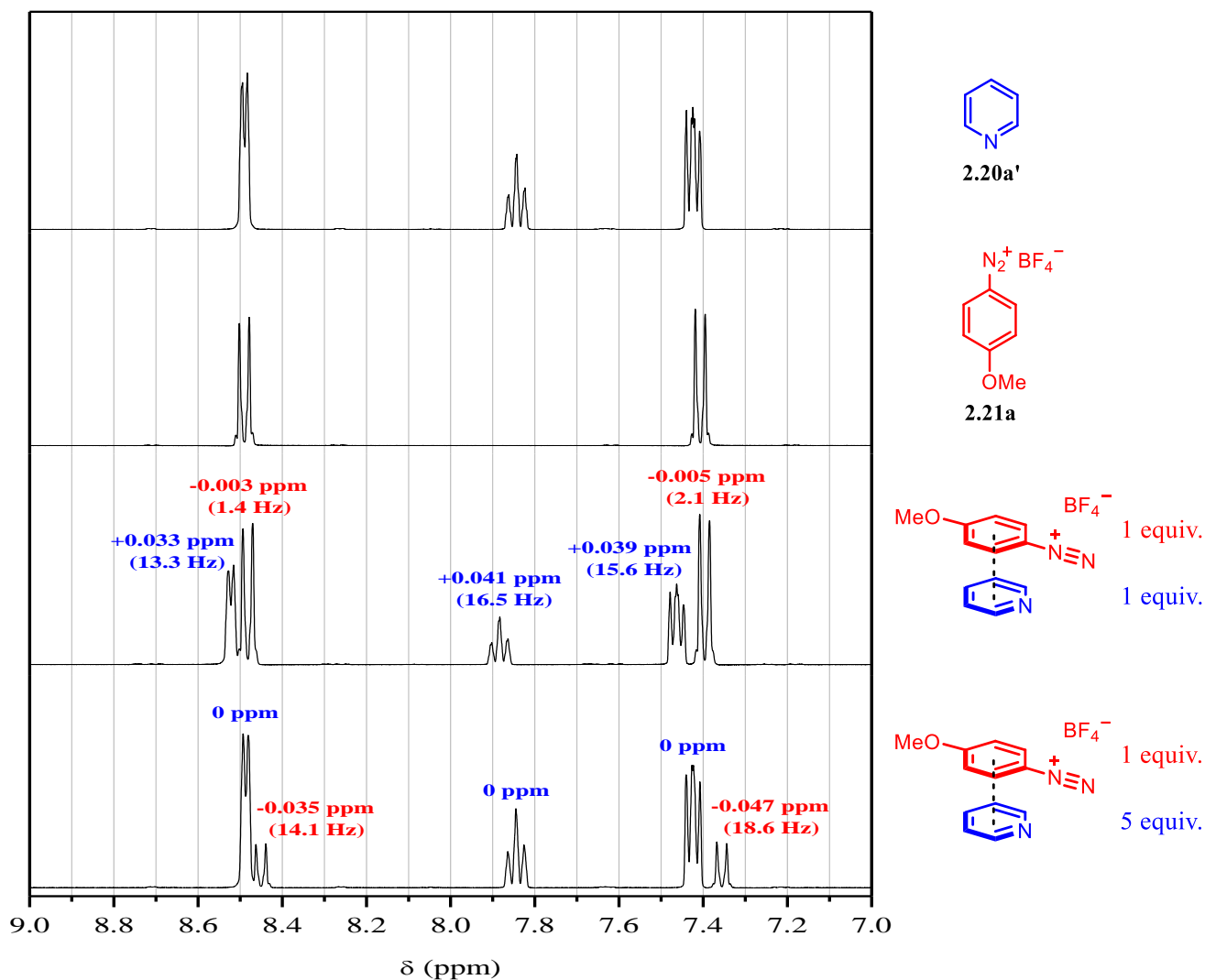
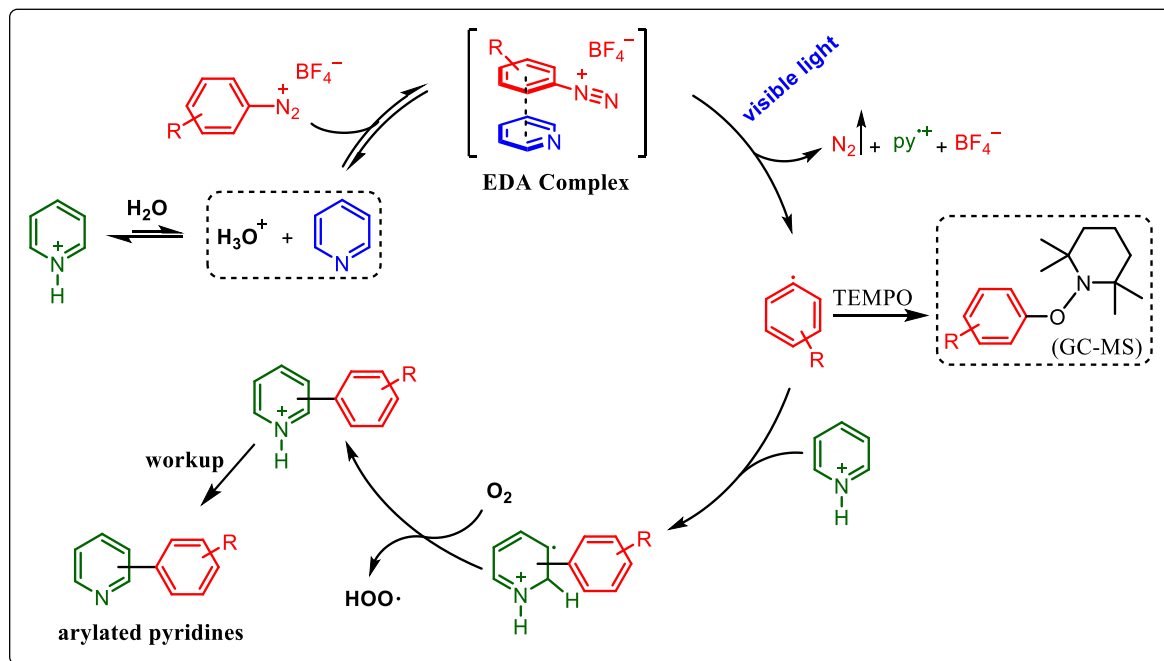


Figure 2.5 – ^1H NMR spectrum for **2.20a'** (at 35 mM), **2.21a** (at 35 mM), and their mixture (1:1 equiv. at 35 mM and 1:5 equiv., 35:175 mM) in D_2O .

Based on these results, we propose a plausible mechanism for the visible light-induced direct C–H arylation of *N*-heterocycles (exemplified for pyridines) (Scheme 2.9). Initially, the aryldiazonium salt reversibly combines with free pyridine/heterocycle generating the EDA complex, which absorbs blue light, and then it dissociates in the excited state to produce the aryl radical.^{10,111} Next, the aryl radical reacts with the pyridinium salt (or *N*-heterocycle salt) to form a new radical intermediate. The latter is subsequently re-aromatized by reaction with oxygen gas. It is relevant to highlight that we have confirmed that the oxygen

atmosphere has an important role in improving the yields.⁹ Finally, aqueous workup liberates the desired arylated *N*-heterocycles.



Scheme 2.9 – Proposed mechanism for the visible-light-induced direct C–H arylation of *N*-heterocycles, as exemplified for pyridines.

2.3 Conclusion

A metal-free methodology for the photoarylation of pyridines and other heterocycles, in water, is described giving 2- and 4-arylated-products in yields up to 96% (22 examples). The scope of the diazonium salt (16 examples) is presented showing the relative strength of this methodology when both electron-withdrawing (F and NO₂) and -donating (OMe) groups are attached to the diazonium salts (*ortho*, *meta*, and *para* positions). The substrate scope of the reaction was further extended to include additional *N*-heterocycles like 4-(trifluoromethyl)pyridine, 4-methoxypyridine, 2-methoxypyridine, pyridine-2-thiol, quinoline, and quinoxaline. Among them, the last two yielded arylated products in good yields (71-72%) and offer additional opportunities to apply this methodology. Other substituted pyridines (as hydrochloride) including 2-methylpyridine, 3-hydroxypyridine, 2-(trifluoromethyl)pyridine, 2-nitropyridine, and 4-(dimethylamino)pyridine were examined as substrates with 4-methoxybenzenediazonium tetrafluoroborate; however, no product was observed under the optimized reaction conditions.

The robustness of the protocol was also demonstrated by a scale-up experiment (2 mmol) which provided product **2.22a** in a consistent yield of 79% (0.3 g-scale). Mechanistic investigations were carried out through control experiments (dark control reactions, radical trapping reactions with TEMPO, reaction with deuterated solvent (D₂O), and reactions using a Ru(bpy)₃Cl₂ photocatalyst) and other additional studies (UV-Vis, ¹H and ¹H-¹⁵N HMBC NMR), supporting the proposed mechanism and the occurrence of an EDA complex between free pyridine/heterocycle (donor) and diazonium salt (acceptor).

2.4 Experimental

2.4.1 General information

All commercial reagents were used without further purification. Aryldiazonium salts were prepared according to the literature procedure.¹¹² All reactions were carried out under an oxygen atmosphere. Reactions were monitored by thin-layer chromatography carried out on 0.25 mm silica plates, using shortwave UV light (254 or 365 nm) for visualization. Flash column chromatography was performed on silica gel (70–230 mesh). NMR spectra were recorded on a Bruker Avance 400 MHz instrument, and chemical shifts for ¹H and ¹³C NMR are reported in ppm relative to tetramethylsilane as internal reference. All coupling constants (*J* values) are reported in hertz. The following abbreviations were used to describe NMR peak multiplicities: s = singlet, d = doublet, t = triplet, q = quartet, m = multiplet, etc. All NMR data were processed using the MestReNova 9.0.1 software package. High-resolution mass spectra (HRMS) were performed on Agilent LC-6545, Q-TOF MS with Jet Stream ESI ionization. UV–vis absorption spectra were recorded on a PerkinElmer Lambda 25 UV–visible absorption spectrophotometer.

2.4.2 Photochemical reactor

These studies were carried out in a home-made photoreactor.^{113,114} The reactor was made from a commercial plastic recipient for silica gel storage (Figure 2.6A). The materials utilized for assembling the photoreactor were electric connections, AC adapter, fan, and LED strips (Figure 2.6B).



Figure 2.6 – (A) Commercial plastic recipient. (B) Materials used in the assembly: 1) electric connections (speaker wire cable, plastic strip connector, and DC male/female connectors), 2) AC adapter, 3) fan, and 4) LED strips.

First, the recipient was cleaned and cut as shown in Figures 2.7A and B. Then, the blue LED strips were fastened to the container's inner walls. Next, the LEDs and fan were plugged into the AC adapter through DC male/female connectors (Figure 2.7C). The reaction tube was then connected to the reactor center (Figure 2.7D and E). Finally, the irradiation was started with the fan blowing from the top (Figure 2.7F and G).

The photoreactor emission range is 400 to 500 nm (blue LED) with a maximum of 455 nm and a total power of 28 W (in series mode).

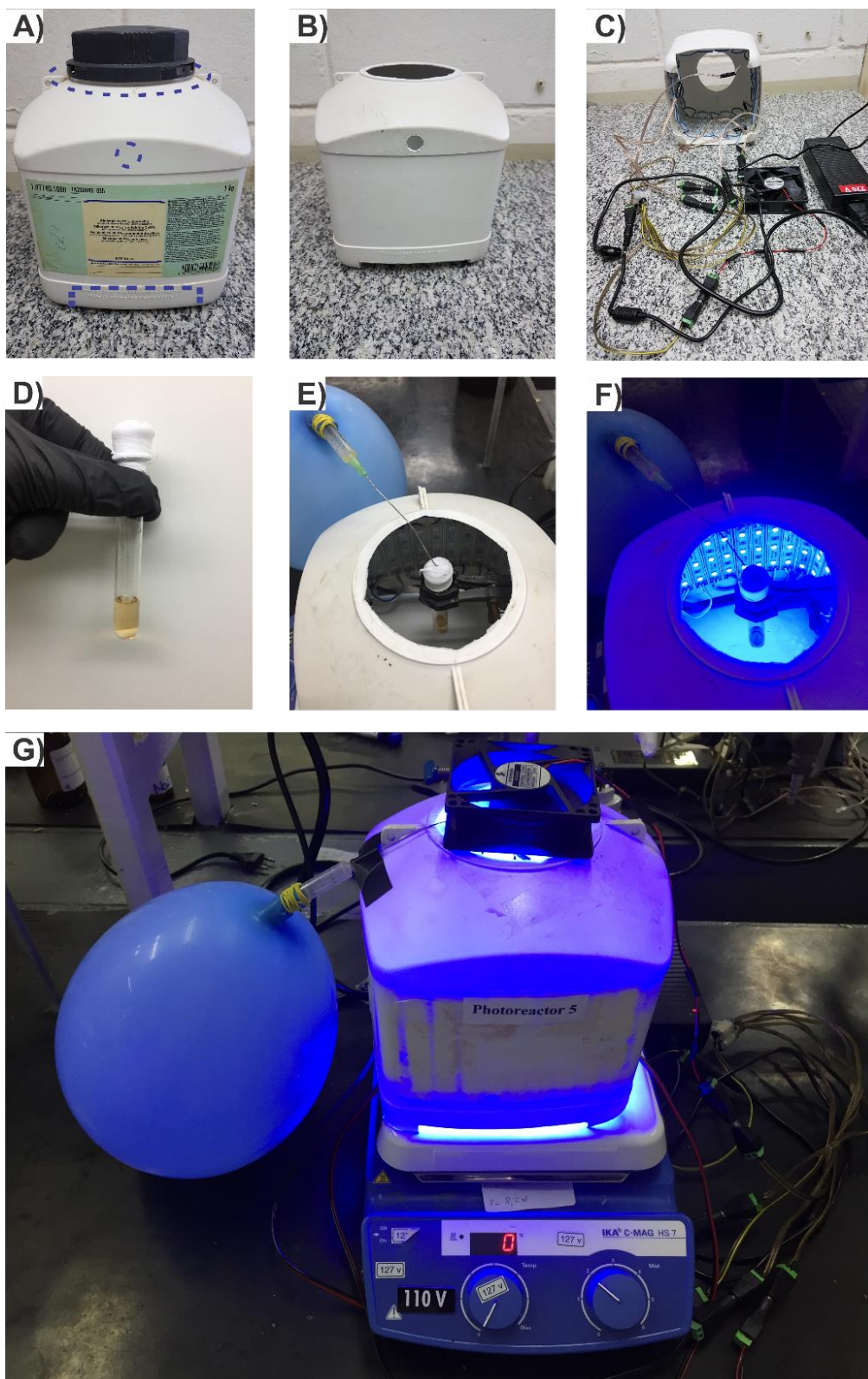


Figure 2.7 – Step-by-step photoreactor assembly: (A) Location of container cut, (B) Container cut open, (C) LED strips and fan installed and plugged into the AC adapter, (D) Reaction tube, (E) Reaction tube connected to the reactor center, (F) Irradiation started, and (G) Photoreactor assembled with irradiation of the reaction tube.

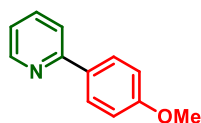
2.4.3 General procedure for the synthesis of aryldiazonium salts

To a solution of aniline (10 mmol) in distilled H₂O (4 mL), aq. HBF₄ 50 wt% was added (3.4 mL) and the mixture was stirred while cooled to 0 °C. Subsequently, a solution of NaNO₂ (10 mmol, 690 mg) in H₂O (2 mL) was added dropwise. After addition, the reaction mixture was stirred for 45 min and then the solid filtered off under vacuum. The precipitate was redissolved in a minimum amount of acetone (ca. 5–8 mL). Diethyl ether was added until precipitation of the diazonium tetrafluoroborate. The solid was filtered off and washed with diethyl ether and dried under vacuum. The NMR data were consistent with those previously reported.¹¹³

2.4.4 General procedure for the photoarylation of *N*-heterocycles

To a test tube (borosilicate, 10 mm internal diameter and 1 mm thick walls) *N*-heterocycle hydrochloride salt (**2.20a-g**) (7.5 mmol, 15 equiv.) was added to 1.5 mL of H₂O. The test tube was then sonicated to remove the solubilized air and saturated with pure O₂ by bubbling this gas for 10 min. The aryldiazonium salt (**2.21a-r**) (0.5 mmol, 1 equiv.) was quickly added; the tube was closed and sealed with a Teflon tape. The reaction mixture was stirred and irradiated using a homemade batch photoreactor (30 W blue LEDs) under an oxygen atmosphere (balloon) at r.t. for 48 h. The reaction mixture was quenched with saturated aqueous NaHCO₃ (10 mL) and extracted with EtOAc (3 × 20 mL). The organic extracts were washed with brine (1 × 10 mL), dried over MgSO₄, filtered, and the solution was concentrated under vacuum. The crude reaction product was chromatographed on silica gel (70–230 mesh) using EtOAc/hexane mixtures of increasing polarity to afford 2-aryl/4-aryl-substituted pyridines (**2.22a-o** and **2.22r-u**), 2-((4-methoxyphenyl)thio)pyridine (**2.22v**), 2-aryl/4-arylquinoline (**2.22w**), and 2-aryl-quinoxaline (**2.22x**) in yields ranging from 12 to 96%.

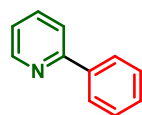
2.4.5 Characterization data of arylated *N*-heterocycles



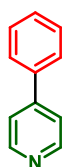
2-(4-Methoxyphenyl)pyridine – 2-Aryl (2.22a): The compound 2-aryl (2.22a) (known compound)⁶⁰ was synthesized following the general procedure. It was obtained in 68% yield (0.341 mmol, 63.2 mg) as a yellow solid after purification on silica gel column chromatography (hexane/EtOAc = from 9/1 (v/v) to 7/3 (v/v)). Mp: 51–53 °C (lit.⁶⁰ mp: 53–55 °C). ¹H NMR (400 MHz, CDCl₃): δ 8.65 (ddd, *J* = 4.9, 1.9, 1.0 Hz, 1H), 7.95 (d, *J* = 9.0 Hz, 2H), 7.75 – 7.64 (m, 2H), 7.17 (ddd, *J* = 7.2, 4.8, 1.4 Hz, 1H), 7.00 (d, *J* = 9.0 Hz, 2H), 3.86 (s, 3H). ¹³C NMR (100 MHz, CDCl₃): δ 160.5, 157.1, 149.5, 136.7, 132.0, 128.2, 121.4, 119.8, 114.1, 55.4.



4-(4-Methoxyphenyl)pyridine – 4-Aryl (2.22a): The compound 4-aryl (2.22a) (known compound)¹¹⁵ was synthesized following the general procedure. It was obtained in 28% yield (0.138 mmol, 25.5 mg) as a yellow solid after purification over silica gel column chromatography (hexane/EtOAc = from 9/1 (v/v) to 7/3 (v/v)). Mp: 91–94 °C (lit.¹¹⁵ mp: 94–96 °C). ¹H NMR (400 MHz, CDCl₃): δ 8.62 (d, *J* = 6.3 Hz, 2H), 7.61 (d, *J* = 8.9 Hz, 2H), 7.49 – 7.45 (m, 2H), 7.01 (d, *J* = 8.9 Hz, 2H), 3.87 (s, 3H). ¹³C NMR (100 MHz, CDCl₃): δ 160.5, 150.2, 147.8, 130.3, 128.2, 121.1, 114.6, 55.4.

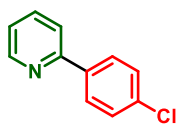


2-Phenylpyridine – 2-Aryl (2.22b): The compound 2-aryl (2.22b) (known compound)^{116,117} was synthesized following the general procedure. It was obtained in 44% yield (0.219 mmol, 34.0 mg) as a yellow oil after purification over silica gel column chromatography (hexane/EtOAc = from 9.5/0.5 (v/v) to 8/2 (v/v)). ¹H NMR (400 MHz, CDCl₃): δ 8.74 – 8.65 (m, 1H), 8.02 – 7.94 (m, 2H), 7.79 – 7.70 (m, 2H), 7.52 – 7.45 (m, 2H), 7.44 – 7.38 (m, 1H), 7.23 (ddd, *J* = 6.7, 4.8, 2.1 Hz, 1H). ¹³C NMR (100 MHz, CDCl₃): δ 157.5, 149.7, 139.4, 136.8, 129.0, 128.8, 126.9, 122.1, 120.6.

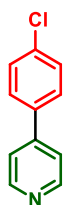


4-Phenylpyridine – 4-Aryl (2.22b): The compound 4-aryl (2.22b) (known compound)¹¹⁷ was synthesized following the general procedure. It was obtained in 18% yield (0.090 mmol, 13.9 mg) as a yellow solid after purification over silica gel column chromatography (hexane/EtOAc = from 9.5/0.5 (v/v) to 8/2 (v/v)). Mp: 62–64 °C (lit.¹¹⁷ mp: 67–68 °C). ¹H NMR (400 MHz, CDCl₃): δ 8.66 (d, *J* = 5.6 Hz, 2H), 7.69 – 7.59 (m, 2H),

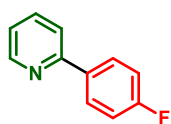
7.55 – 7.37 (m, 5H). ^{13}C NMR (100 MHz, CDCl_3): δ 150.3, 148.4, 138.1, 129.1, 129.0, 127.0, 121.7.



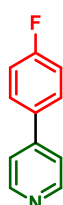
2-(4-Chlorophenyl)pyridine – 2-Aryl (2.22c): The compound 2-aryl (**2.22c**) (known compound)¹¹⁷ was synthesized following the general procedure. It was obtained in 54% yield (0.272 mmol, 51.6 mg) as a yellow solid after purification over silica gel column chromatography (hexane/EtOAc = from 9/1 (v/v) to 7/3 (v/v)). Mp: 46–48 °C (lit.¹¹⁷ mp: 44–45 °C). ^1H NMR (400 MHz, CDCl_3): δ 8.69 (ddd, $J = 4.8, 1.8, 1.0$ Hz, 1H), 7.94 (d, $J = 8.8$ Hz, 2H), 7.76 (ddd, $J = 8.0, 7.3, 1.8$ Hz, 1H), 7.70 (dt, $J = 8.0, 1.2$ Hz, 1H), 7.45 (d, $J = 8.8$ Hz, 2H), 7.27 – 7.22 (m, 1H). ^{13}C NMR (100 MHz, CDCl_3): δ 156.2, 149.8, 137.8, 136.9, 135.1, 128.9, 128.2, 122.4, 120.4.



4-(4-Chlorophenyl)pyridine – 4-Aryl (2.22c): The compound 4-aryl (**2.22c**) (known compound)¹¹⁷ was synthesized following the general procedure. It was obtained in 26% yield (0.128 mmol, 24.3 mg) as a yellow solid after purification over silica gel column chromatography (hexane/EtOAc = from 9/1 (v/v) to 7/3 (v/v)). Mp: 70–71 °C (lit.¹¹⁷ mp: 70–71 °C). ^1H NMR (400 MHz, CDCl_3): δ 8.68 (s, 2H), 7.58 (d, $J = 8.8$ Hz, 2H), 7.52 – 7.41 (m, 4H). ^{13}C NMR (100 MHz, CDCl_3): δ 150.4, 147.1, 136.6, 135.3, 129.4, 128.3, 121.5.

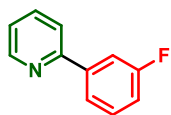


2-(4-Fluorophenyl)pyridine – 2-Aryl (2.22d): The compound 2-aryl (**2.22d**) (known compound)⁶⁰ was synthesized following the general procedure. It was obtained in 31% yield (0.156 mmol, 27.1 mg) as a white solid after purification over silica gel column chromatography (dichloromethane/EtOAc = 9.5/0.5 (v/v)). Mp: 35–37 °C (lit.⁶⁰ mp: 39–41 °C). ^1H NMR (400 MHz, CDCl_3): δ 8.68 (ddd, $J = 4.9, 1.9, 1.0$ Hz, 1H), 8.02 – 7.93 (m, 2H), 7.75 (ddd, $J = 8.0, 7.3, 1.8$ Hz, 1H), 7.68 (dt, $J = 8.0, 1.1$ Hz, 1H), 7.23 (ddd, $J = 7.3, 4.8, 1.2$ Hz, 1H), 7.19 – 7.12 (m, 2H). ^{13}C NMR (100 MHz, CDCl_3): δ 163.5 (d, $J = 248.3$ Hz), 156.5, 149.7, 136.8, 135.5, 128.7 (d, $J = 8.3$ Hz), 122.1, 120.2, 115.7 (d, $J = 21.4$ Hz).



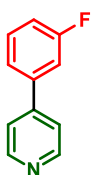
4-(4-Fluorophenyl)pyridine – 4-Aryl (2.22d): The compound 4-aryl (**2.22d**) (known compound)¹¹⁸ was synthesized following the general procedure. It was obtained in 22% yield (0.109 mmol, 19.0 mg) as a white solid after purification over silica gel column chromatography (hexane/EtOAc = from 9/1 (v/v) to 7/3 (v/v)). Mp: 112–114 °C (lit.¹¹⁸

mp: 116–118 °C). ¹H NMR (400 MHz, CDCl₃): δ 8.66 (d, *J* = 5.2 Hz, 2H), 7.66 – 7.59 (m, 2H), 7.51 – 7.43 (m, 2H), 7.23 – 7.14 (m, 2H). ¹³C NMR (100 MHz, CDCl₃): δ 163.5 (d, *J* = 249.3 Hz), 150.2, 147.4, 134.2, 134.1, 128.8 (d, *J* = 8.3 Hz), 121.5, 116.2 (d, *J* = 22.0 Hz).



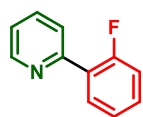
2-(3-Fluorophenyl)pyridine – 2-Aryl (2.22e): The compound 2-aryl (2.22e) (known compound)¹¹⁹ was synthesized following the general procedure. It was obtained in 36% yield (0.178 mmol, 30.8 mg) as a yellow oil after purification

over silica gel column chromatography (hexane/EtOAc = from 9/1 (v/v) to 7/3 (v/v)). ¹H NMR (400 MHz, acetone-*d*₆): δ 8.70 (ddd, *J* = 4.8, 1.8, 1.0 Hz, 1H), 8.04 – 7.95 (m, 2H), 7.95 – 7.87 (m, 2H), 7.58 – 7.50 (m, 1H), 7.38 (ddd, *J* = 7.5, 4.8, 1.1 Hz, 1H), 7.21 (dddd, *J* = 8.2, 2.7, 0.9 Hz, 1H). ¹³C NMR (100 MHz, acetone-*d*₆): δ 164.2 (d, *J* = 243.1 Hz), 156.1, 150.6, 142.7 (d, *J* = 7.5 Hz), 138.0, 131.4 (d, *J* = 8.5 Hz), 123.9, 123.3 (d, *J* = 1.8 Hz), 121.2, 116.4 (d, *J* = 21.4 Hz), 114.1 (d, *J* = 23.2 Hz).



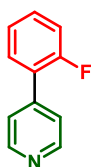
4-(3-Fluorophenyl)pyridine – 4-Aryl (2.22e): The compound 4-aryl (2.22e) (known compound)¹²⁰ was synthesized following the general procedure. It was obtained in 22% yield (0.109 mmol, 18.9 mg) as a yellow oil after purification over silica gel column chromatography (hexane/EtOAc = from 9/1 (v/v) to 7/3 (v/v)). ¹H NMR (400

MHz, CDCl₃): δ 8.68 (d, *J* = 6.2 Hz, 2H), 7.51 – 7.40 (m, 4H), 7.37 – 7.30 (m, 1H), 7.18 – 7.11 (m, 1H). ¹³C NMR (100 MHz, CDCl₃): δ 163.2 (d, *J* = 246.9 Hz), 150.4, 147.1, 140.4 (d, *J* = 7.9 Hz), 130.7 (d, *J* = 8.2 Hz), 122.7 (d, *J* = 2.1 Hz), 121.6, 116.0 (d, *J* = 20.9 Hz), 114.0 (d, *J* = 22.4 Hz).

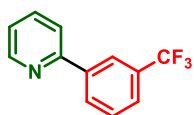


2-(2-Fluorophenyl)pyridine – 2-Aryl (2.22f): The compound 2-aryl (2.22f) (known compound)¹²¹ was synthesized following the general procedure. It was obtained in 20% yield (0.098 mmol, 16.9 mg) as a yellow oil after purification

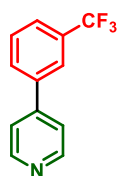
over silica gel column chromatography (hexane/EtOAc = from 9/1 (v/v) to 7/3 (v/v)). ¹H NMR (400 MHz, CDCl₃): δ 8.59 (ddd, *J* = 4.8, 1.9, 1.1 Hz, 1H), 7.92 (td, *J* = 7.9, 1.9 Hz, 1H), 7.78 – 7.68 (m, 2H), 7.34 (dddd, *J* = 8.2, 7.4, 5.0, 1.9, 1H), 7.26 – 7.17 (m, 2H), 7.12 (dddd, *J* = 11.8, 8.2, 1.2, 0.4 Hz, 1H). ¹³C NMR (100 MHz, acetone-*d*₆): δ 161.4 (d, *J* = 248.3 Hz), 153.9, 150.7, 137.4, 132.0, 131.5 (d, *J* = 8.7 Hz), 128.3 (d, *J* = 11.3 Hz), 125.4, 125.1 (d, *J* = 9.8 Hz), 123.5, 116.9 (d, *J* = 23.2 Hz).



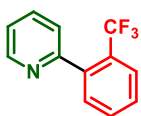
4-(2-Fluorophenyl)pyridine – 4-Aryl (2.22f): The compound 4-aryl (**2.22f**) (new compound) was obtained synthesized the general procedure. It was obtained in 11% yield (0.054 mmol, 9.4 mg) as a yellow solid after purification over silica gel column chromatography (hexane/EtOAc = from 9/1 (v/v) to 7/3 (v/v)). Mp: 62–64 °C. ¹H NMR (400 MHz, acetone-*d*₆): δ 8.55 (d, *J* = 5.9 Hz, 2H), 7.53 – 7.48 (m, 1H), 7.44 (dt, *J* = 4.5, 1.6 Hz, 2H), 7.39 (dddd, *J* = 8.3, 7.5, 5.1, 1.8, 1H), 7.23 (td, *J* = 7.6, 1.2 Hz, 1H), 7.17 (dddd, *J* = 11.2, 8.3, 1.2, 0.4 Hz, 1H). ¹³C NMR (100 MHz, acetone-*d*₆): δ 160.6 (d, *J* = 248.3 Hz), 150.9, 143.9, 131.9 (d, *J* = 8.4 Hz), 131.5 (d, *J* = 2.2 Hz), 127.0 (d, *J* = 12.8 Hz), 126.0 (d, *J* = 3.2 Hz), 124.4, 117.1 (d, *J* = 22.6 Hz). HRMS–ESI–TOF: *m/z* calcd for C₁₁H₉FN [M + H]⁺, 174.0714; Found, 174.0712.



2-(3-(Trifluoromethyl)phenyl)pyridine – 2-Aryl (2.22g): The compound 2-aryl (**2.22g**) (known compound)¹²² was synthesized following the general procedure. It was obtained in 31% yield (0.154 mmol, 34.5 mg) as a yellow oil after purification over silica gel column chromatography (hexane/EtOAc = from 9/1 (v/v) to 7/3 (v/v)). ¹H NMR (400 MHz, CDCl₃): δ 8.73 (ddd, *J* = 4.8, 1.8, 1.1 Hz, 1H), 8.32 – 8.26 (m, 1H), 8.21 – 8.16 (m, 1H), 7.83 – 7.75 (m, 2H), 7.70 – 7.65 (m, 1H), 7.63 – 7.57 (m, 1H), 7.29 (ddd, *J* = 7.0, 4.8, 1.7 Hz, 1H). ¹³C NMR (100 MHz, CDCl₃): δ 155.9, 149.9, 140.1, 137.0, 131.2 (q, *J* = 32.3 Hz), 130.1, 129.2, 125.5 (q, *J* = 4.0 Hz), 123.8 (q, *J* = 4.0 Hz), 122.8, 120.6.

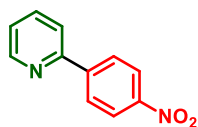


4-(3-(Trifluoromethyl)phenyl)pyridine – 4-Aryl (2.22g): The compound 4-aryl (**2.22g**) (known compound)¹²³ was synthesized following the general procedure. It was obtained in 18% yield (0.093 mmol, 20.7 mg) as a yellow oil after purification over silica gel column chromatography (hexane/EtOAc = from 9/1 (v/v) to 7/3 (v/v)). ¹H NMR (400 MHz, CDCl₃): δ 8.71 (d, *J* = 5.9 Hz, 2H), 7.89 – 7.85 (m 1H), 7.84 – 7.79 (m, 1H), 7.74 – 7.69 (m, 1H), 7.66 – 7.60 (m 1H), 7.55 – 7.50 (m, 2H). ¹³C NMR (100 MHz, CDCl₃): δ 150.4, 147.0, 139.0, 131.6 (q, *J* = 32.5 Hz), 130.3, 129.7, 125.7 (q, *J* = 3.7 Hz), 123.9 (q, *J* = 3.7 Hz), 121.7.

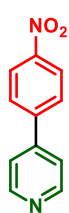


2-(2-(Trifluoromethyl)phenyl)pyridine – 2-Aryl (2.22h): The compound 2-aryl (**2.22h**) (known compound)¹²⁴ was synthesized following the general procedure. It was obtained in 23% yield (0.113 mmol, 25.4 mg) as a yellow oil after purification over silica gel column chromatography (toluene/EtOAc = from 9.5/0.5 (v/v) to 9/1

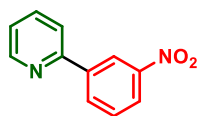
(v/v). ^1H NMR (400 MHz, CDCl_3): δ 8.69 (ddd, $J = 4.9, 1.8, 0.9$ Hz, 1H), 7.80 – 7.72 (m, 2H), 7.66 – 7.58 (m, 1H), 7.56 – 7.48 (m, 2H), 7.43 (d, $J = 7.8$ Hz, 1H), 7.31 (ddd, $J = 7.6, 4.9, 1.2$, 1H). ^{13}C NMR (100 MHz, CDCl_3): δ 157.8, 149.2, 140.0, 136.0, 131.6, 131.5, 128.3, 126.3 (q, $J = 5.3$ Hz), 125.4, 124.0, 122.7, 122.5.



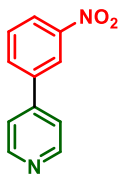
2-(4-Nitrophenyl)pyridine – 2-Aryl (2.22i): The compound 2-aryl (**2.22i**) (known compound)¹²⁵ was synthesized following the general procedure. It was obtained in 42% yield (0.210 mmol, 42.0 mg) as a white solid after purification over silica gel column chromatography (hexane/EtOAc = from 9/1 (v/v) to 7/3 (v/v)). Mp: 132–133 °C (lit.¹²⁵ mp: 130–131 °C). ^1H NMR (400 MHz, CDCl_3): δ 8.80 – 8.71 (m, 1H), 8.34 (d, $J = 9.1$ Hz, 2H), 8.19 (d, $J = 9.1$ Hz, 2H), 7.88 – 7.78 (m, 2H), 7.35 (ddd, $J = 6.3, 4.8, 2.2$, 1H). ^{13}C NMR (100 MHz, CDCl_3): δ 154.9, 150.1, 148.1, 145.3, 137.2, 127.7, 124.0, 123.5, 121.2.



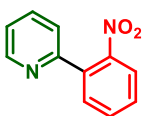
4-(4-Nitrophenyl)pyridine – 2-Aryl (2.22i): The compound 4-aryl (**2.22i**) (known compound)¹²⁵ was synthesized following the general procedure. It was obtained in 24% yield (0.120 mmol, 24.0 mg) as a white solid after purification over silica gel column chromatography (hexane/EtOAc = from 9/1 (v/v) to 7/3 (v/v)). Mp: 120–123 °C (lit.¹²⁵ mp: 122–124 °C). ^1H NMR (400 MHz, CDCl_3): δ 8.76 (d, $J = 4.1$ Hz, 2H), 8.36 (d, $J = 8.9$ Hz, 2H), 7.80 (d, $J = 8.9$ Hz, 2H), 7.58 – 7.50 (m, 2H). ^{13}C NMR (100 MHz, CDCl_3): δ 150.7, 148.2, 146.0, 144.5, 128.0, 124.4, 121.8.



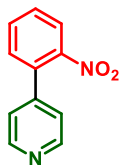
2-(3-Nitrophenyl)pyridine – 2-Aryl (2.22j): The compound 2-aryl (**2.22j**) (known compound)¹²⁶ was synthesized following the general procedure. It was obtained in 30% yield (0.15 mmol, 29.9 mg) as a yellow solid after purification over silica gel column chromatography (hexane/EtOAc = from 9.5/0.5 (v/v) to 7/3 (v/v)). Mp: 72–73 °C (lit.¹²⁶ mp: 72–73 °C). ^1H NMR (400 MHz, CDCl_3): δ 8.87 (t, $J = 2.0$ Hz, 1H), 8.77 – 8.71 (m, 1H), 8.37 (ddd, $J = 7.8, 1.7, 1.1$ Hz, 1H), 8.27 (ddd, $J = 8.2, 2.3, 1.0$ Hz, 1H), 7.88 – 7.79 (m, 2H), 7.65 (t, $J = 8.0$ Hz, 1H), 7.33 (ddd, $J = 6.2, 4.8, 2.4$, 1H). ^{13}C NMR (100 MHz, CDCl_3): δ 154.8, 150.0, 148.8, 141.0, 137.2, 132.7, 129.7, 123.6, 123.3, 121.8, 120.6.



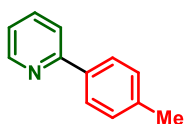
4-(3-Nitrophenyl)pyridine – 4-Aryl (2.22j): The compound 4-aryl (**2.22j**) (known compound)¹²⁶ was synthesized following the general procedure. It was obtained in 19% yield (0.096 mmol, 19.2 mg) as an orange solid after purification over silica gel column chromatography (hexane/EtOAc = from 9.5/0.5 (v/v) to 7/3 (v/v)). Mp: 103–105 °C (lit.¹²⁶ mp: 109–110 °C). ¹H NMR (400 MHz, CDCl₃): δ 8.76 (d, *J* = 5.3 Hz, 2H), 8.51 (t, *J* = 1.9 Hz, 1H), 8.32 (ddd, *J* = 8.2, 2.3, 1.0 Hz, 1H), 7.98 (ddd, *J* = 7.8, 1.8, 1.0 Hz, 1H), 7.70 (t, *J* = 8.0 Hz, 1H), 7.60 – 7.54 (m, 2H). ¹³C NMR (100 MHz, CDCl₃): δ 150.6, 148.9, 145.9, 139.9, 132.9, 130.3, 123.8, 122.0, 121.6.



2-(2-Nitrophenyl)pyridine – 2-Aryl (2.22k): The compound 2-aryl (**2.22k**) (known compound)¹²⁷ was synthesized following the general procedure. It was obtained in 31% yield (0.153 mmol, 30.6 mg) as a yellow solid after purification over silica gel column chromatography (hexane/EtOAc = from 9.5/0.5 (v/v) to 7/3 (v/v)). Mp: 71–72 °C. ¹H NMR (400 MHz, CDCl₃): δ 8.89 – 8.84 (m, 1H), 8.77 – 8.72 (m, 1H), 8.38 (ddd, *J* = 7.8, 1.7, 1.1 Hz, 1H), 8.27 (ddd, *J* = 8.2, 2.3, 1.1 Hz, 1H), 7.87 – 7.79 (m, 2H), 7.70 – 7.62 (m, 1H), 7.34 (ddd, *J* = 6.1, 4.8, 2.4 Hz, 1H). ¹³C NMR (100 MHz, CDCl₃): δ 154.8, 150.0, 148.8, 141.0, 137.2, 132.7, 129.7, 123.6, 123.3, 121.8, 120.6.



4-(2-Nitrophenyl)pyridine – 4-Aryl (2.22k): The compound 4-aryl (**2.22k**) (known compound)¹²⁸ was synthesized following the general procedure. It was obtained in 21% yield (0.103 mmol, 20.7 mg) as a yellow solid after purification over silica gel column chromatography (hexane/EtOAc = from 9.5/0.5 (v/v) to 7/3 (v/v)). Mp: 51–52 °C (lit.¹²⁸ mp: 49–50 °C). ¹H NMR (400 MHz, CDCl₃): δ 8.76 (d, *J* = 5.8 Hz, 2H), 8.54 – 8.49 (m, 1H), 8.32 (ddd, *J* = 8.2, 2.3, 1.0 Hz, 1H), 7.98 (ddd, *J* = 7.8, 1.8, 1.0 Hz, 1H), 7.74 – 7.67 (m, 1H), 7.61 – 7.53 (m, 2H). ¹³C NMR (100 MHz, CDCl₃): δ 150.6, 148.9, 146.0, 139.9, 132.9, 130.3, 123.8, 122.0, 121.6.

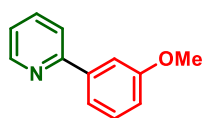


2-(*p*-Tolyl)pyridine – 2-Aryl (2.22l): The compound 2-aryl (**2.22l**) (known compound)¹¹⁷ was synthesized following the general procedure. It was obtained in 54% yield (0.270 mmol, 45.8 mg) as a yellow oil after purification over silica gel column chromatography (hexane/EtOAc = from 9.5/0.5 (v/v) to 8/2 (v/v)). ¹H NMR (400 MHz, CDCl₃): δ 8.71 – 8.65 (m, 1H), 7.89 (d, *J* = 8.2 Hz, 2H), 7.76 – 7.67 (m, 2H),

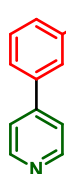
7.31 – 7.26 (m, 2H), 7.20 (ddd, $J = 6.7, 4.8, 2.0$ Hz, 1H), 2.41 (s, 3H). ^{13}C NMR (100 MHz, CDCl_3): δ 157.5, 149.6, 139.0, 136.7, 136.6, 129.5, 126.8, 121.8, 120.3, 21.3.



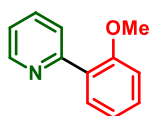
4-(*p*-Tolyl)pyridine – 4-Aryl (2.22l): The compound 4-aryl (**2.22l**) (known compound)¹¹⁷ was synthesized following the general procedure. It was obtained in 26% yield (0.130 mmol, 22.0 mg) as a yellow solid after purification over silica gel column chromatography (hexane/EtOAc = from 9.5/0.5 (v/v) to 8/2 (v/v)). Mp: 86–88 °C (lit.¹¹⁷ mp: 89–90 °C). ^1H NMR (400 MHz, CDCl_3): δ 8.64 (d, $J = 4.9$ Hz, 2H), 7.55 (d, $J = 8.2$ Hz, 2H), 7.52 – 7.46 (m, 2H), 7.30 (d, $J = 7.8$ Hz, 2H), 2.42 (s, 3H). ^{13}C NMR (100 MHz, CDCl_3): δ 150.2, 148.2, 139.2, 135.2, 129.9, 126.8, 121.4, 21.2.



2-(3-Methoxyphenyl)pyridine – 2-Aryl (2.22m): The compound 2-aryl (**2.22m**) (known compound)¹¹⁵ was synthesized following the general procedure. It was obtained in 9% yield (0.043 mmol, 8.00 mg) as an oil after purification over silica gel column chromatography (hexane/2-propanol = from 9.5/0.5 (v/v)). ^1H NMR (400 MHz, CDCl_3): δ 8.70 (ddd, $J = 4.8, 1.7, 1.0$ Hz, 1H), 7.80 – 7.70 (m, 2H), 7.61 – 7.57 (m, 1H), 7.54 (ddd, $J = 7.7, 1.6, 1.0$ Hz, 1H), 7.39 (t, $J = 7.9$ Hz, 1H), 7.26 – 7.22 (m, 1H), 6.97 (ddd, $J = 8.2, 2.6, 1.0$ Hz, 1H), 3.90 (s, 3H). ^{13}C NMR (100 MHz, CDCl_3): δ 160.1, 157.2, 149.5, 140.8, 136.8, 129.7, 122.3, 120.8, 119.3, 115.2, 112.0, 55.4.

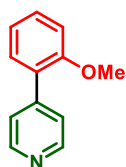


4-(3-Methoxyphenyl)pyridine – 4-Aryl (2.22n): The compound 4-aryl (**2.22n**) (known compound)¹²⁹ was synthesized following the general procedure. It was obtained in 4% yield (0.022 mmol, 4.00 mg) as an oil after purification over silica gel column chromatography (hexane/EtOAc = from 9/1 (v/v) to 7/3 (v/v)). ^1H NMR (400 MHz, CDCl_3): δ 8.66 (d, $J = 4.2$ Hz, 2H), 7.54 – 7.47 (m, 2H), 7.41 (t, $J = 7.9$ Hz, 1H), 7.22 (ddd, $J = 7.7, 1.7, 1.0$ Hz, 1H), 7.18 – 7.14 (m, 1H), 6.99 (ddd, $J = 8.3, 2.6, 1.0$ Hz, 1H), 3.88 (s, 3H). ^{13}C NMR (100 MHz, CDCl_3): δ 160.2, 150.1, 148.4, 139.6, 130.2, 121.8, 119.4, 114.4, 112.8, 55.4.

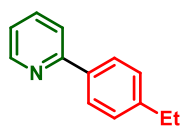


2-(2-Methoxyphenyl)pyridine – 2-Aryl (2.22o): The compound 2-aryl (**2.22o**) (known compound)¹¹⁹ was synthesized following the general procedure. It was obtained in 38% yield (0.192 mmol, 35.5 mg) as a yellow oil after purification over silica gel column chromatography (hexane/EtOAc = from 9.5/0.5 (v/v) to 7/3 (v/v)). ^1H

NMR (400 MHz, CDCl₃): δ 8.70 (ddd, $J = 4.9, 1.9, 1.0$ Hz, 1H), 7.81 (dt, $J = 8.0, 1.1$ Hz, 1H), 7.76 (dd, $J = 7.6, 1.8$ Hz, 1H), 7.72 – 7.67 (m, 1H), 7.38 (ddd, $J = 8.3, 7.4, 1.8$ Hz, 1H), 7.20 (ddd, $J = 7.5, 4.9, 1.2$ Hz, 1H), 7.08 (td, $J = 7.5, 1.1$ Hz, 1H), 7.01 (dd, $J = 8.3, 1.0$ Hz, 1H), 3.86 (s, 3H). ¹³C NMR (100 MHz, CDCl₃): δ 156.9, 156.1, 149.4, 135.6, 131.2, 129.9, 129.1, 125.1, 121.7, 121.0, 111.3, 55.6.



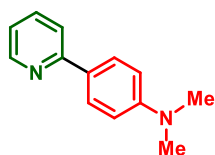
4-(2-Methoxyphenyl)pyridine – 4-Aryl (2.22n): The compound 4-aryl (**2.22n**) (known compound)¹¹⁵ was synthesized following the general procedure. It was obtained in 19% yield (0.098 mmol, 18.1 mg) as a yellow solid after purification over silica gel column chromatography (hexane/EtOAc = from 9.5/0.5 (v/v) to 7/3 (v/v)). Mp: 56–59 °C (lit.¹¹⁵ mp: 63–64 °C). ¹H NMR (400 MHz, CDCl₃): δ 8.63 (d, $J = 5.9$ Hz, 2H), 7.54 – 7.48 (m, 2H), 7.41 (ddd, $J = 8.3, 7.4, 1.8$ Hz, 1H), 7.35 (dd, $J = 7.6, 1.8$ Hz, 1H), 7.07 (td, $J = 7.5, 1.1$ Hz, 1H), 7.02 (dd, $J = 8.4, 1.0$ Hz, 1H), 3.85 (s, 3H). ¹³C NMR (100 MHz, CDCl₃): δ 156.5, 149.1, 146.3, 130.4, 130.2, 127.7, 121.1, 111.4, 55.6.



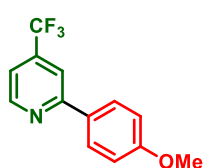
2-(4-Ethylphenyl)pyridine – 2-Aryl (2.22o): The compound 2-aryl (**2.22o**) (known compound)¹³⁰ was synthesized following the general procedure. It was obtained in 51% yield (0.253 mmol, 46.4 mg) as a yellow oil after purification over silica gel column chromatography (hexane/EtOAc = from 9.5/0.5 (v/v) to 8/2 (v/v)). ¹H NMR (400 MHz, CDCl₃): δ 8.68 (ddd, $J = 4.8, 1.7, 1.1$ Hz, 1H), 7.91 (d, $J = 8.4$ Hz, 2H), 7.76 – 7.68 (m, 2H), 7.34 – 7.28 (m, 2H), 7.20 (ddd, $J = 6.3, 4.8, 2.1$ Hz, 1H), 2.71 (q, $J = 7.6$ Hz, 2H), 1.27 (t, $J = 7.6$ Hz, 3H). ¹³C NMR (100 MHz, CDCl₃): δ 157.5, 149.6, 145.3, 136.9, 136.7, 128.3, 126.9, 121.8, 120.3, 28.7, 15.5.



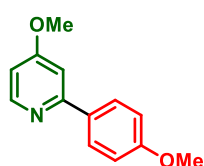
4-(4-Ethylphenyl)pyridine – 4-Aryl (2.22o): The compound 4-aryl (**2.22o**) (new compound) was synthesized following the general procedure. It was obtained in 24% yield (0.120 mmol, 22.0 mg) as a white solid after purification over silica gel column chromatography (hexane/EtOAc = from 9.5/0.5 (v/v) to 8/2 (v/v)). Mp: 49–50 °C. ¹H NMR (400 MHz, CDCl₃): δ 8.68 – 8.57 (m, 2H), 7.58 (d, $J = 8.3$ Hz, 2H), 7.53 – 7.48 (m, 2H), 7.36 – 7.30 (m, 2H), 2.72 (q, $J = 7.6$ Hz, 2H), 1.29 (t, $J = 7.6$ Hz, 3H). ¹³C NMR (100 MHz, CDCl₃): δ 150.1, 148.3, 145.5, 135.4, 128.7, 126.9, 121.5, 28.6, 15.5. HRMS–ESITOF: m/z calcd for C₁₃H₁₄N [M + H]⁺, 184.1121; Found, 184.1119.



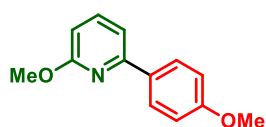
***N,N*-Dimethyl-4-(pyridin-2-yl)aniline – 2-Aryl (2.22r):** The compound 2-aryl (**2.22r**) (known compound)¹³¹ was synthesized following the general procedure. It was obtained in 14% yield (0.068 mmol, 13.6 mg) as a yellow solid after purification over silica gel column chromatography (hexane/EtOAc = from 9/1 (v/v) to 7/3 (v/v)). Mp: 90–91 °C (lit.¹³¹ mp: 91–92 °C). ¹H NMR (400 MHz, CDCl₃): δ 8.66 – 8.59 (m, 1H), 7.92 (d, *J* = 9.1 Hz, 2H), 7.71 – 7.62 (m, 2H), 7.11 (ddd, *J* = 6.6, 4.9, 1.8 Hz, 1H), 6.80 (d, *J* = 9.0 Hz, 2H), 3.02 (s, 6H). ¹³C NMR (100 MHz, CDCl₃): δ 157.5, 151.1, 149.2, 136.7, 127.8, 127.0, 120.6, 119.2, 112.2, 40.4.



2-(4-Methoxyphenyl)-4-(trifluoromethyl)pyridine – 2-Aryl (2.22s): The compound 2-aryl (**2.22s**) (known compound)⁸⁵ was synthesized following the general procedure. It was obtained in 41% yield (0.204 mmol, 51.6 mg) as a yellow solid after purification over silica gel column chromatography (hexane/EtOAc = 9/1 (v/v)). Mp: 45–46 °C (lit.⁸⁵ mp: 43–44 °C). ¹H NMR (400 MHz, CDCl₃): δ 8.81 (d, *J* = 5.1 Hz, 1H), 7.99 (d, *J* = 8.9 Hz, 2H), 7.88 – 7.84 (m, 1H), 7.38 (ddd, *J* = 5.1, 1.6, 0.7 Hz, 1H), 7.02 (d, *J* = 9.0 Hz, 2H), 3.88 (s, 3H). ¹³C NMR (100 MHz, CDCl₃): δ 161.1, 158.4, 150.5, 139.0 (q, *J* = 33.7 Hz), 130.6, 128.4, 123.0, (q, *J* = 273.2 Hz), 116.7 (q, *J* = 3.0 Hz), 115.2 (q, *J* = 3.7 Hz), 114.3, 55.4.

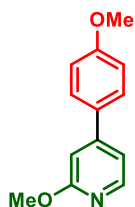


4-Methoxy-2-(4-methoxyphenyl)pyridine – 2-Aryl (2.22t): The compound 2-aryl (**2.22t**) (known compound)¹³² was synthesized following the general procedure. It was obtained in 12% yield (0.061 mmol, 13.2 mg) as a yellow solid after purification over silica gel column chromatography (hexane/EtOAc = 7/3 (v/v)). mp 62–64 °C. ¹H NMR (400 MHz, CDCl₃): δ 8.48 (d, *J* = 5.7 Hz, 1H), 7.92 (d, *J* = 8.6 Hz, 2H), 7.17 (d, *J* = 2.3 Hz, 1H), 6.98 (d, *J* = 8.6 Hz, 2H), 6.72 (dd, *J* = 5.7, 2.3 Hz, 1H), 3.89 (s, 3H), 3.86 (s, 3H). ¹³C NMR (100 MHz, CDCl₃): δ 166.4, 160.5, 158.9, 150.8, 132.0, 128.2, 114.0, 107.6, 106.0, 55.4, 55.1.

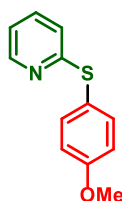


2-Methoxy-6-(4-methoxyphenyl)pyridine – 2-Aryl (2.22u): The compound 2-aryl (**2.22u**) (known compound)¹²² was synthesized following the general procedure. It was obtained in 9% yield (0.047 mmol, 10.2 mg) as a yellow solid after purification over silica gel column chromatography (hexane/EtOAc = from 8/2 (v/v) to 6/4 (v/v)). Mp: 122–124 °C (lit.¹²² mp: 120–121 °C). ¹H

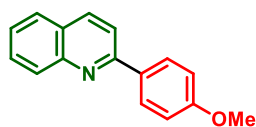
NMR (400 MHz, CDCl₃): δ 8.00 (d, J = 9.0 Hz, 2H), 7.59 (dd, J = 8.2, 7.5 Hz, 1H), 7.27 (dd, J = 7.5, 0.7 Hz, 1H), 6.98 (d, J = 8.9 Hz, 2H), 6.63 (dd, J = 8.2, 0.7 Hz, 1H), 4.03 (s, 3H), 3.86 (s, 3H). ¹³C NMR (100 MHz, CDCl₃): δ 163.7, 160.3, 154.4, 139.1, 131.8, 128.0, 114.0, 111.9, 108.3, 55.4, 53.2.



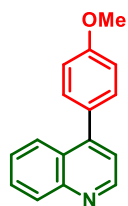
2-Methoxy-4-(4-methoxyphenyl)pyridine – 4-Aryl (2.22u): The compound 4-aryl (**2.22u**) (new compound) was synthesized following the general procedure. It was obtained in 6% yield (0.03 mmol, 6.5 mg) as a yellow solid after purification over silica gel column chromatography (hexane/EtOAc = from 8/2 (v/v) to 6/4 (v/v)). Mp: 61–65 °C. ¹H NMR (400 MHz, CDCl₃): δ 8.18 (dd, J = 5.4, 0.7 Hz, 1H), 7.58 (d, J = 8.9 Hz, 2H), 7.08 (dd, J = 5.4, 1.6 Hz, 1H), 6.99 (d, J = 8.9 Hz, 2H), 6.92 (dd, J = 1.6, 0.7 Hz, 1H), 3.98 (s, 3H), 3.86 (s, 3H). ¹³C NMR (100 MHz, CDCl₃): δ 164.9, 160.4, 150.7, 147.1, 130.5, 128.1, 115.0, 114.4, 107.7, 55.4, 53.5. HRMS–ESI–TOF: m/z calcd for C₁₃H₁₄NO₂ [M + H]⁺, 216.1024; Found, 216.1016.



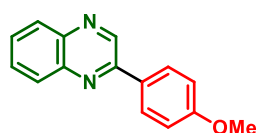
2-((4-Methoxyphenyl)thio)pyridine (2.22v): The compound **2.22v** (known compound)¹³³ was synthesized following the general procedure. It was obtained in 38% yield (0.189 mmol, 41.0 mg) as a yellow solid after purification over silica gel column chromatography (hexane/EtOAc = from 9/1 (v/v) to 7/3 (v/v)). Mp: 44–46 °C. ¹H NMR (400 MHz, CDCl₃): δ 8.41 (ddd, J = 4.9, 1.9, 0.9 Hz, 1H), 7.54 (d, J = 8.9 Hz, 2H), 7.43 (ddd, J = 8.1, 7.4, 1.9 Hz, 1H), 7.00 – 6.93 (m, 3H), 6.80 – 6.77 (m, 1H), 3.85 (s, 3H). ¹³C NMR (100 MHz, CDCl₃): δ 161.8, 159.7, 148.4, 136.2, 135.6, 120.1, 119.4, 118.4, 114.3, 54.4.



2-(4-Methoxyphenyl)quinoline – 2-Aryl (2.22w): The compound 2-aryl (**2.22w**) (known compound)^{134,135} was synthesized following the general procedure. It was obtained in 30% yield (0.150 mmol, 35.4 mg) as a yellow solid after purification over silica gel column chromatography (hexane/EtOAc = from 9.5/0.5 (v/v) to 7/3 (v/v)). Mp: 122–123 °C (lit.¹³⁴ mp: 118–119 °C). ¹H NMR (400 MHz, CDCl₃): δ 8.22 – 8.08 (m, 4H), 7.83 (d, J = 8.7 Hz, 1H), 7.80 (dd, J = 8.0, 1.4 Hz, 1H), 7.71 (ddd, J = 8.5, 6.9, 1.5 Hz, 1H), 7.49 (ddd, J = 8.1, 6.9, 1.2 Hz, 1H), 7.05 (d, J = 8.9 Hz, 2H), 3.88 (s, 3H). ¹³C NMR (100 MHz, CDCl₃): δ 160.8, 156.9, 148.3, 136.7, 132.3, 129.6, 129.5, 128.9, 127.4, 126.9, 125.9, 118.6, 114.2, 55.4.



4-(4-Methoxyphenyl)quinoline – 4-Aryl (2.22w): The compound 4-aryl (**2.22w**) (known compound)¹³⁵ was synthesized following the general procedure. It was obtained in 42% yield (0.212 mmol, 50.0 mg) as a yellow solid after purification over silica gel column chromatography (hexane/EtOAc = from 9.5/0.5 (v/v) to 7/3 (v/v)). Mp: 75–80 °C. ¹H NMR (400 MHz, CDCl₃): δ 8.92 (d, *J* = 4.4 Hz, 1H), 8.20 – 8.14 (m, 1H), 8.00 – 7.94 (m, 1H), 7.72 (ddd, *J* = 8.4, 6.8, 1.4 Hz, 1H), 7.50 (ddd, *J* = 8.3, 6.8, 1.3 Hz, 1H), 7.46 (d, *J* = 8.8 Hz, 2H), 7.32 (d, *J* = 4.4 Hz, 1H), 7.06 (d, *J* = 8.8 Hz, 2H), 3.90 (s, 3H). ¹³C NMR (100 MHz, CDCl₃): δ 159.9, 150.0, 148.7, 148.2, 130.8, 130.3, 129.8, 129.3, 127.0, 126.5, 125.9, 121.3, 114.1, 55.4.



2-(4-Methoxyphenyl)quinoxaline – 2-Aryl (2.22x): The compound 2-aryl (**2.22x**) (known compound)¹³⁶ was synthesized following the general procedure. It was obtained in 71% yield (0.356 mmol, 84.0 mg) as an orange solid after purification over silica gel column chromatography (toluene/EtOAc = from 9/1 (v/v)). Mp: 98–100 °C (lit.¹³⁶ mp: 100–102 °C). ¹H NMR (400 MHz, CDCl₃): δ 9.31 (s, 1H), 8.20 (d, *J* = 8.9 Hz, 2H), 8.16 – 8.08 (m, 2H), 7.82 – 7.69 (m, 2H), 7.10 (d, *J* = 8.9 Hz, 2H), 3.92 (s, 3H). ¹³C NMR (100 MHz, CDCl₃): δ 161.5, 151.4, 143.1, 142.3, 141.2, 130.2, 129.4, 129.3, 129.1, 129.0, 114.6, 55.4.

2.4.6 NMR spectra for checking aggregation at high concentration

The aggregation studies were carried out using ^1H NMR spectroscopy (Figure 2.8). The spectra were acquired for a solution of **2.20a** in 70, 140, 210 and 280 mM, and **2.21a** in 35, 70, 105 and 140 mM in D_2O (500 μL). These solutions were prepared from a stock solution of **2.20a** and **2.21a**.

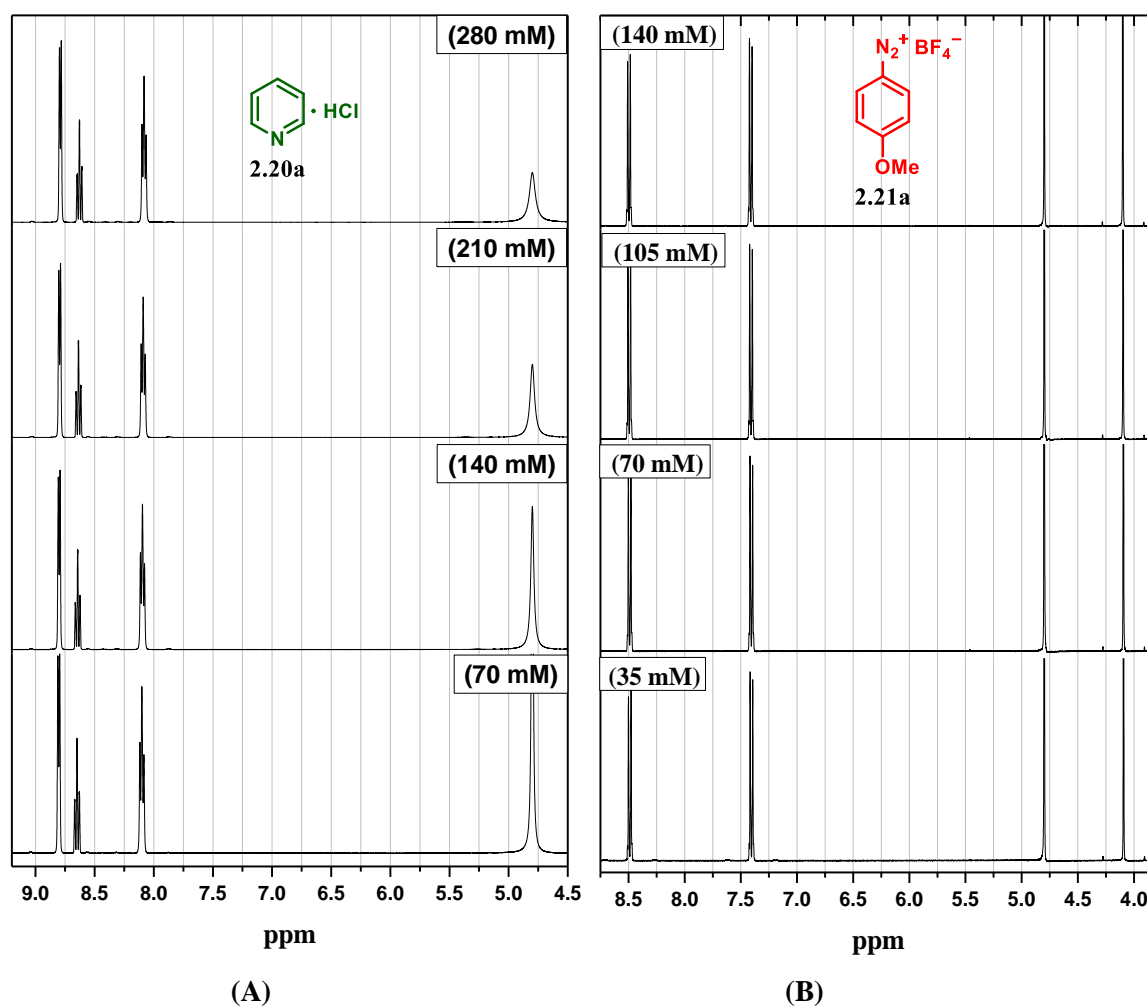


Figure 2.8 – ^1H NMR spectrum in D_2O (500 μL). (A) **2.20a** in 70, 140, 210 and 280 mM. (B) **2.21a** in 35, 70, 105 and 140 mM.

2.4.7 Radical quenching experiments

In order to elucidate the mechanism, radical quenching experiments with TEMPO were carried out (Figures 2.9 and 2.10).

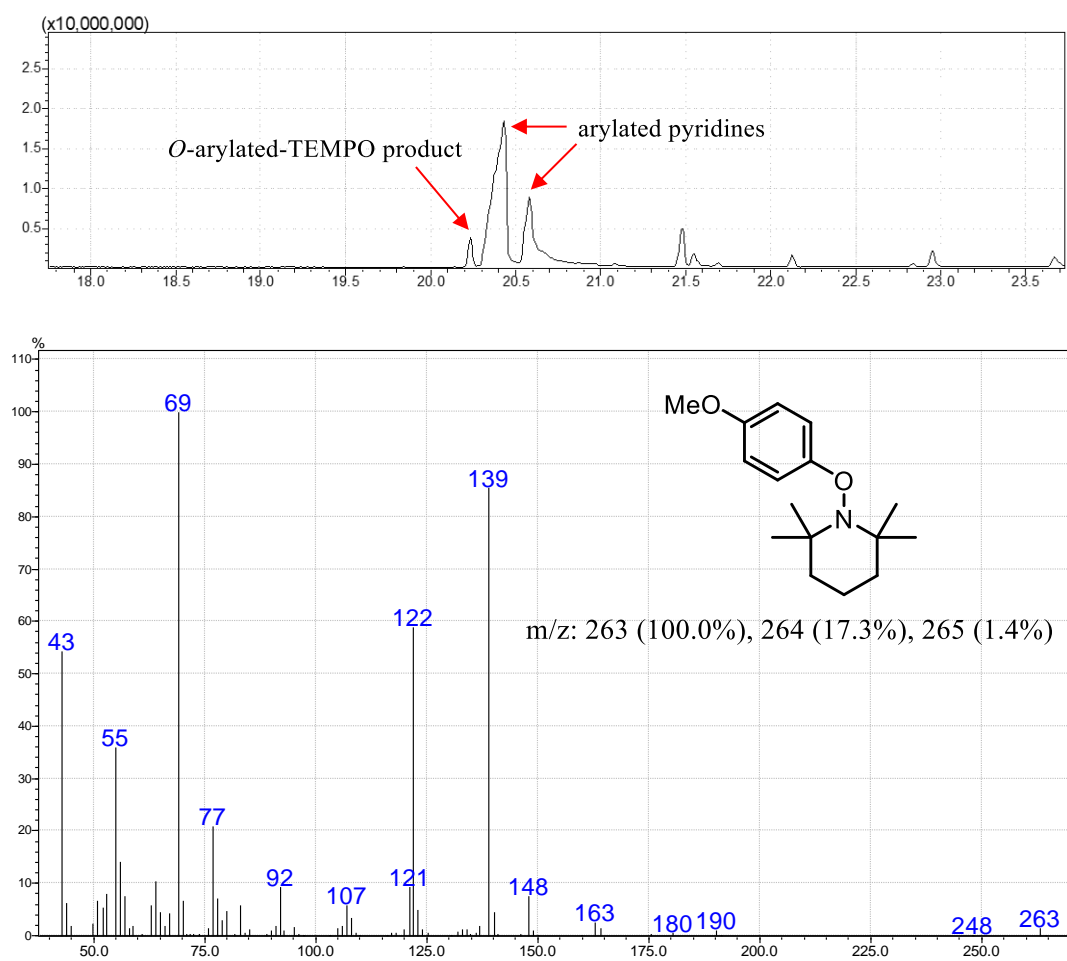


Figure 2.9 – (a) Chromatogram of the crude reaction mixture in the absence of $\text{Ru}(\text{bpy})_3\text{Cl}_2$.
(b) GC-MS spectrum of *O*-arylated-TEMPO product.

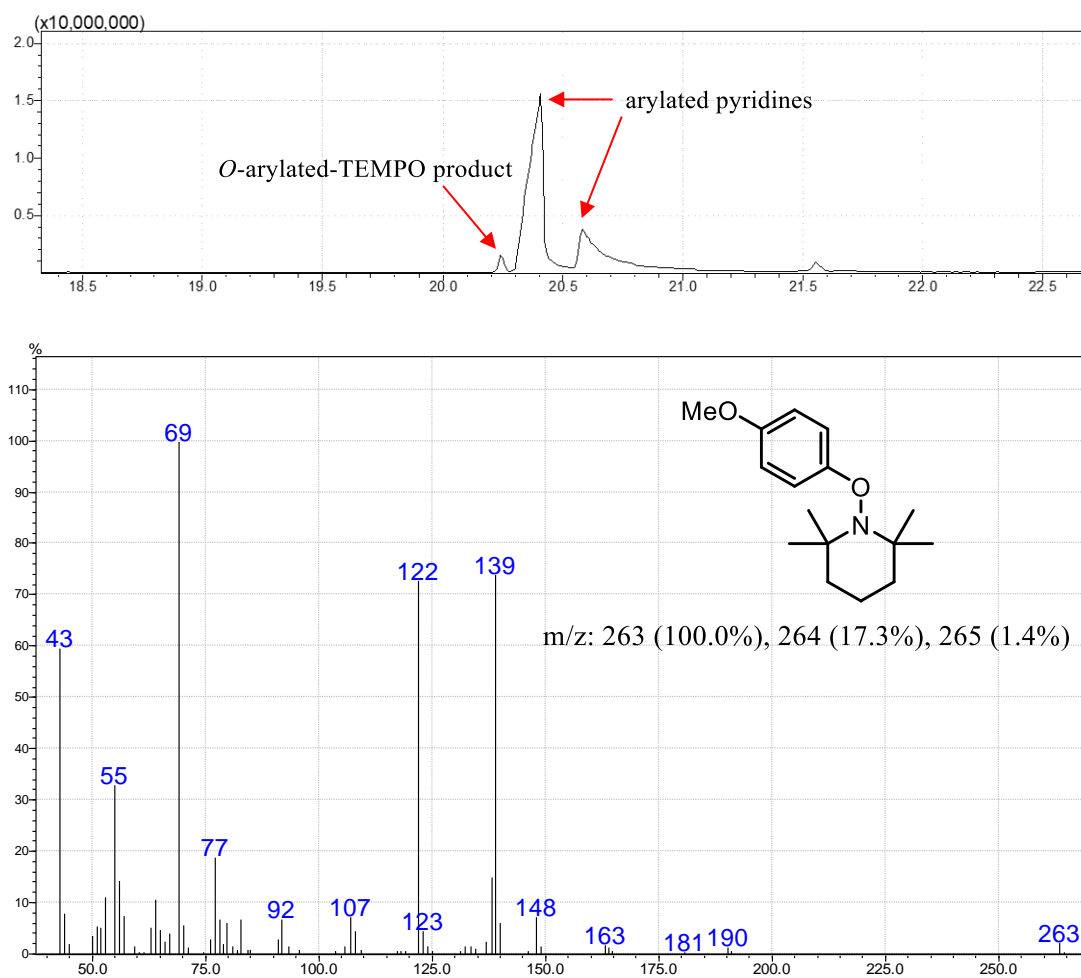
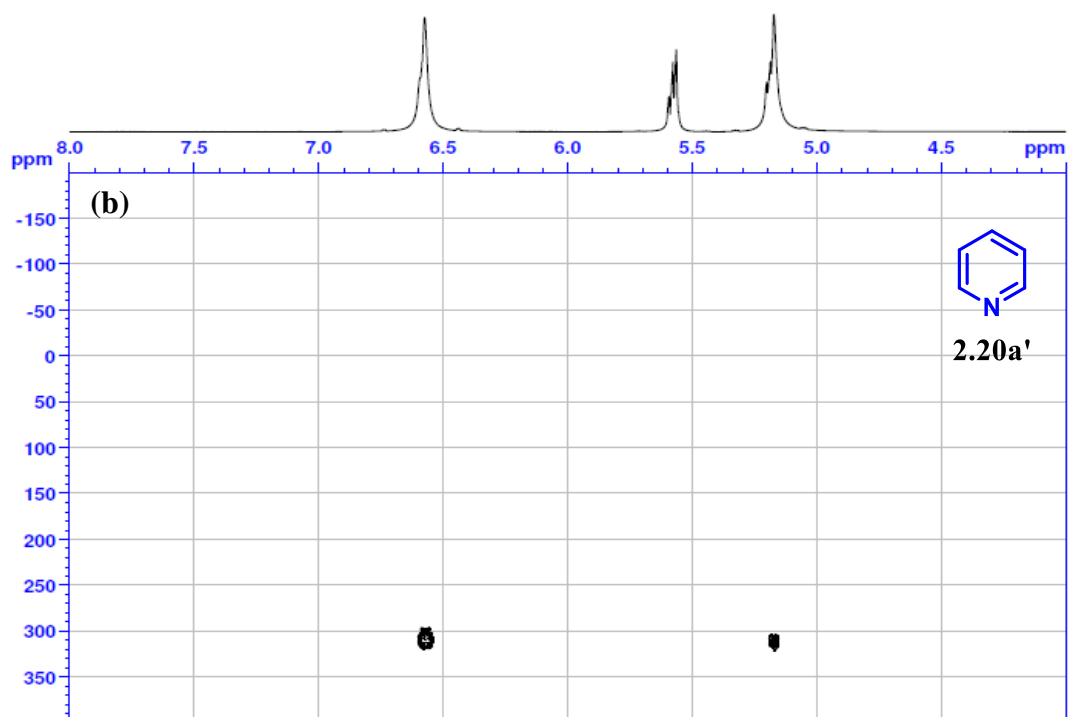
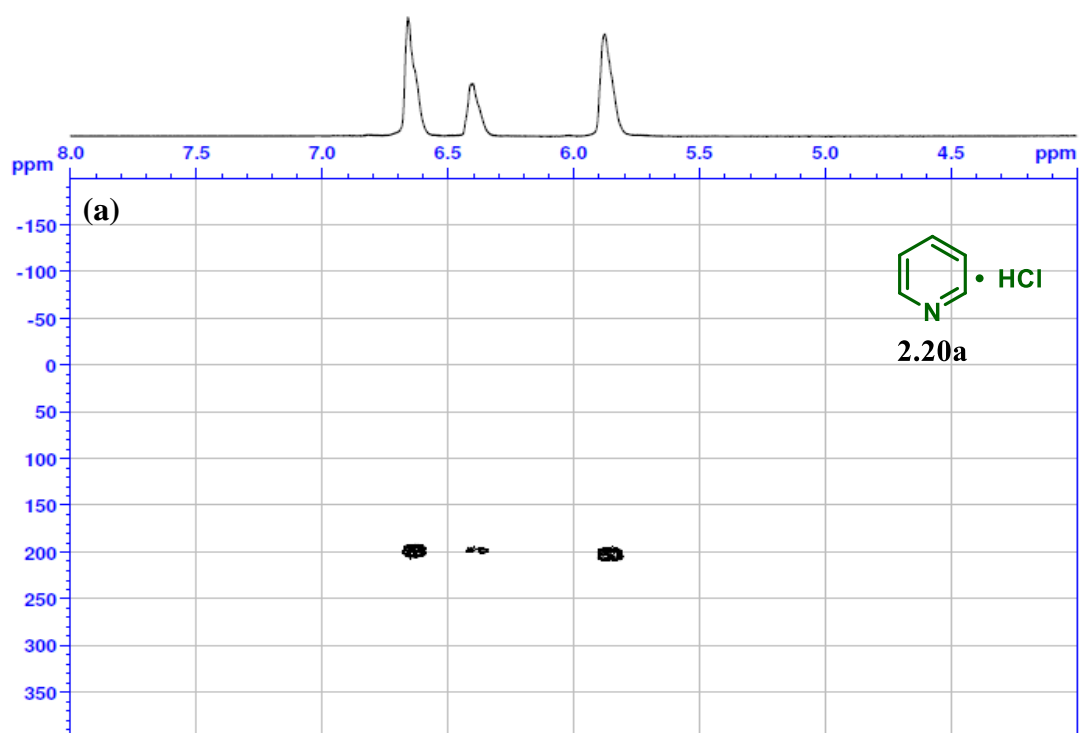
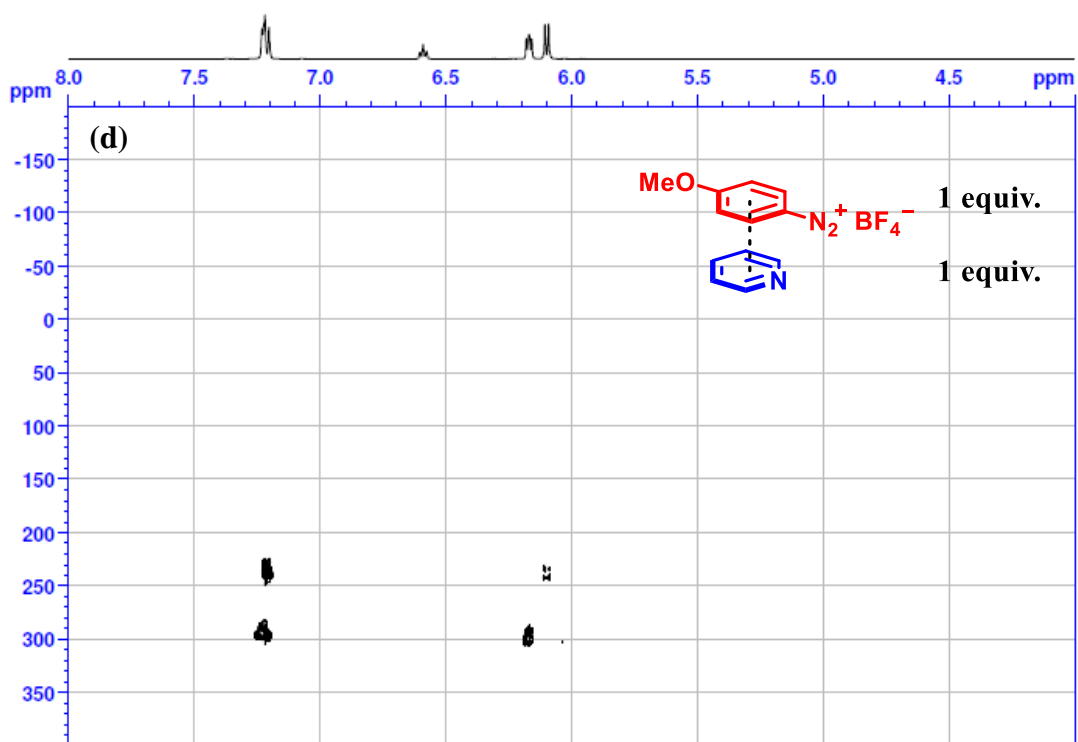
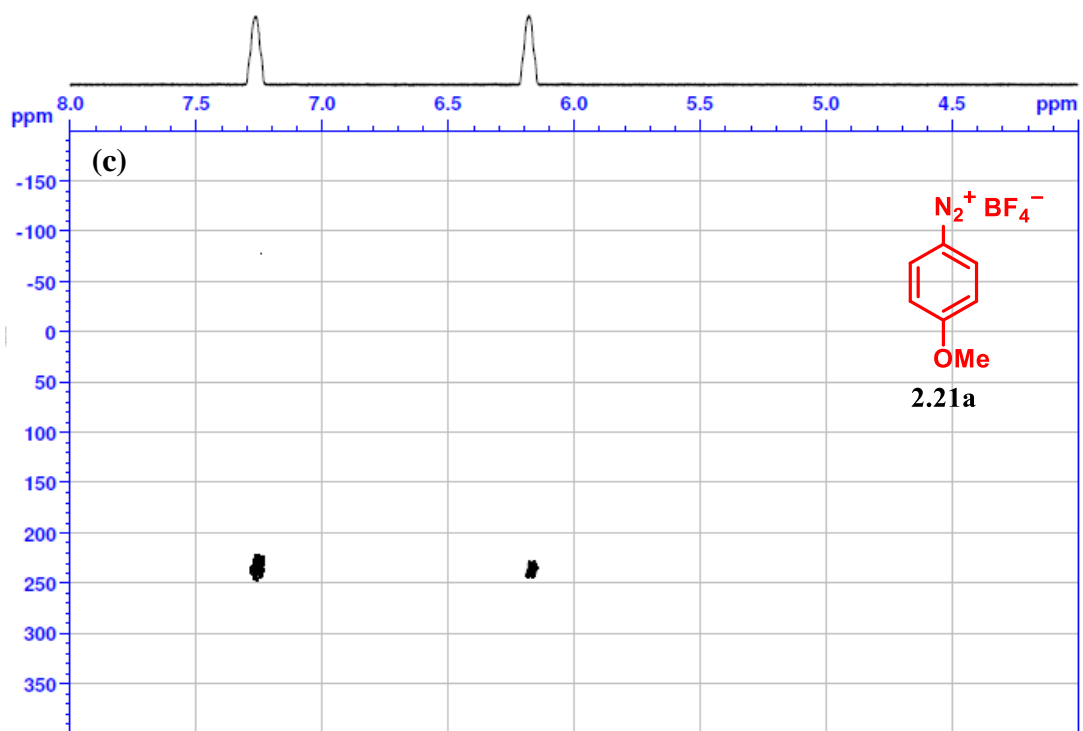


Figure 2.10 – (a) Chromatogram of the crude reaction mixture in the presence of $\text{Ru}(\text{bpy})_3\text{Cl}_2$. (b) GC-MS spectrum of *O*-arylated-TEMPO product.

2.4.8 ^1H - ^{15}N HMBC analyses





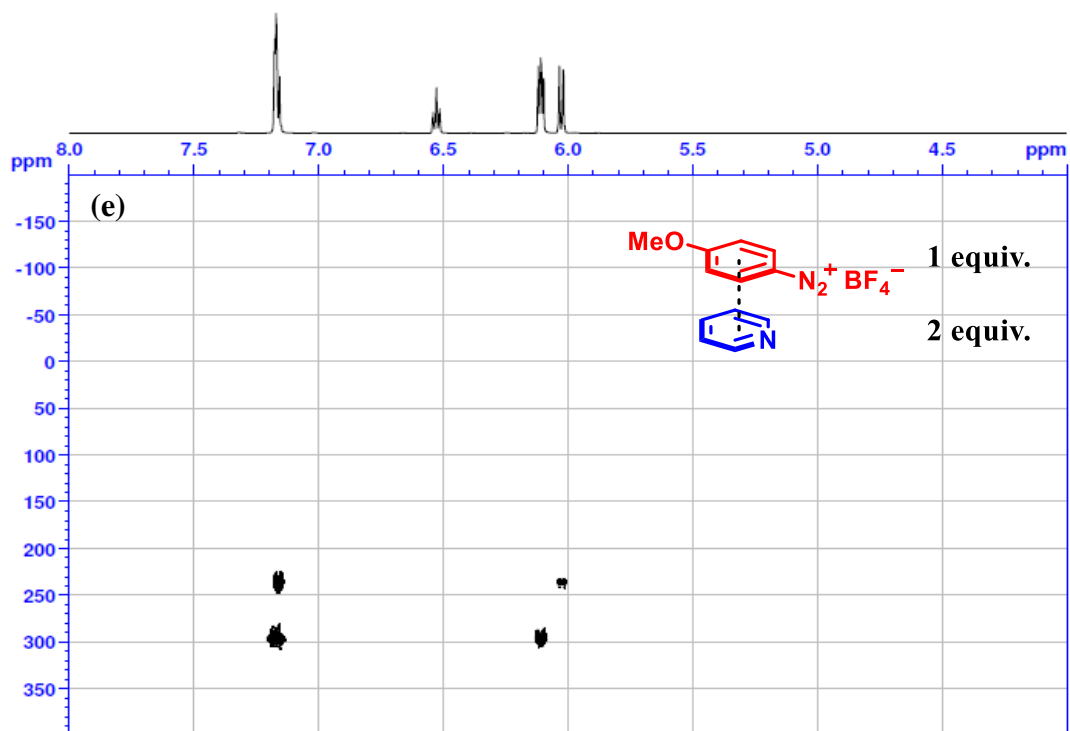


Figure 2.11 – Correlation map ^1H - ^{15}N HMBC: (a) **2.20a**, (b) **2.20a'**, (c) **2.21a**, (d) **2.20a'** + **2.21a** (1:1 equiv.), and (e) **2.20a'** + **2.21a** (1:2 equiv.).

Reference

- 1 MULLIKEN, R. S. "Molecular compounds and their spectra. II". *J. Am. Chem. Soc.*, 74 (3): 811, 1952.
- 2 MULLIKEN, R. S. "Molecular compounds and their spectra. III. The interaction of electron donors and acceptors". *J. Phys. Chem.*, 56 (7): 801, 1952.
- 3 LIMA, C. G. S.; DE M. LIMA, T.; DUARTE, M.; JURBERG, I. D. & PAIXÃO, M. W. "Organic synthesis enabled by light-irradiation of EDA complexes: theoretical background and synthetic applications". *ACS Catal.*, 6 (3): 1389, 2016.
- 4 MARCUS, R. A. "Electron transfer reactions in chemistry: theory and experiment (Nobel lecture)". *Angew. Chem. Int. Ed. Engl.*, 32 (8): 1111, 1993.
- 5 HUSH, N. S. "Adiabatic theory of outer sphere electron-transfer reactions in solution". *Trans. Faraday Soc.*, 57: 557, 1961.
- 6 HUSH, N. S. "Intervalence-transfer absorption. Part 2. Theoretical considerations and spectroscopic data". In: COTTON, F. A. (Ed.). *Prog. Inorg. Chem.* New York: John Wiley & Sons, Inc., 1967, vol. 8, pp. 391-444.
- 7 HUBIG, S. M.; BOCKMAN, T. M. & KOCHI, J. K. "Optimized electron transfer in charge-transfer ion pairs. Pronounced inner-sphere behavior of olefin donors". *J. Am. Chem. Soc.*, 118 (16): 3842, 1996.
- 8 KOCHI, J. K. "Charge-transfer excitation of molecular complexes in organic and organometallic chemistry". *Pure Appl. Chem.*, 63 (2): 255, 1991.
- 9 FÜRST, M. C. D.; GANS, E.; BÖCK, M. J. & HEINRICH, M. R. "Visible-light-induced, catalyst-free radical arylations of arenes and heteroarenes with aryldiazonium salts". *Chem. Eur. J.*, 23 (61): 15312, 2017.
- 10 LEE, J.; HONG, B. & LEE, A. "Visible-light-promoted, catalyst-free Gomberg–Bachmann reaction: synthesis of biaryls". *J. Org. Chem.*, 84 (14): 9297, 2019.
- 11 TOBISU, M.; FURUKAWA, T. & CHATANI, N. "Visible light-mediated direct arylation of arenes and heteroarenes using diaryliodonium salts in the presence and absence of a photocatalyst". *Chem. Lett.*, 42 (10): 1203, 2013.
- 12 ARCEO, E.; JURBERG, I. D.; ÁLVAREZ-FERNÁNDEZ, A. & MELCHIORRE, P. "Photochemical activity of a key donor–acceptor complex can drive stereoselective catalytic α -alkylation of aldehydes". *Nat. Chem.*, 5: 750, 2013.
- 13 BAHAMONDE, A. & MELCHIORRE, P. "Mechanism of the stereoselective α -alkylation of aldehydes driven by the photochemical activity of enamines". *J. Am. Chem. Soc.*, 138 (25): 8019, 2016.

- 14 DAVIES, J.; BOOTH, S. G.; ESSAFI, S.; DRYFE, R. A. W. & LEONORI, D. "Visible-light-mediated generation of nitrogen-centered radicals: metal-free hydroimination and iminohydroxylation cyclization reactions". *Angew. Chem. Int. Ed.*, 54 (47): 14017, 2015.
- 15 SUN, J.; HE, Y.; AN, X.-D.; ZHANG, X.; YU, L. & YU, S. "Visible-light-induced iminyl radical formation via electron-donor–acceptor complexes: a photocatalyst-free approach to phenanthridines and quinolines". *Org. Chem. Front.*, 5 (6): 977, 2018.
- 16 CHENG, Y. & YU, S. "Hydrotrifluoromethylation of unactivated alkenes and alkynes enabled by an electron-donor–acceptor complex of Togni's reagent with a tertiary amine". *Org. Lett.*, 18 (12): 2962, 2016.
- 17 JIANG, H.; HE, Y.; CHENG, Y. & YU, S. "Radical alkynyltrifluoromethylation of alkenes initiated by an electron donor–acceptor complex". *Org. Lett.*, 19 (5): 1240, 2017.
- 18 TU, H.-Y.; ZHU, S.; QING, F.-L. & CHU, L. "A four-component radical cascade trifluoromethylation reaction of alkenes enabled by an electron-donor–acceptor complex". *Chem. Commun.*, 54 (90): 12710, 2018.
- 19 HSU, C.-W. & SUNDÉN, H. " α -Aminoalkyl radical addition to maleimides via electron donor–acceptor complexes". *Org. Lett.*, 20 (7): 2051, 2018.
- 20 ZHANG, H.-H. & YU, S. "Visible-light-induced radical acylation of imines with α -ketoacids enabled by electron-donor–acceptor complexes". *Org. Lett.*, 21 (10): 3711, 2019.
- 21 LIU, B.; LIM, C.-H. & MIYAKE, G. M. "Visible-light-promoted C–S cross-coupling via intermolecular charge transfer". *J. Am. Chem. Soc.*, 139 (39): 13616, 2017.
- 22 LIU, B.; LIM, C.-H. & MIYAKE, G. M. "Light-driven intermolecular charge transfer induced reactivity of ethynylbenziodoxol(on)e and phenols". *J. Am. Chem. Soc.*, 140 (40): 12829, 2018.
- 23 CHEN, L.; LIANG, J.; CHEN, Z.-Y.; CHEN, J.; YAN, M. & ZHANG, X.-J. "A convenient synthesis of sulfones via light promoted coupling of sodium sulfinates and aryl halides". *Adv. Synth. Catal.*, 361 (5): 956, 2019.
- 24 JAMES, M. J.; STRIETH-KALTHOFF, F.; SANDFORT, F.; KLAUCK, F. J. R.; WAGENER, F. & GLORIUS, F. "Visible-light-mediated charge transfer enables C–C bond formation with traceless acceptor groups". *Chem. Eur. J.*, 25 (35): 8240, 2019.
- 25 LIANG, K.; LI, N.; ZHANG, Y.; LI, T. & XIA, C. "Transition-metal-free α -arylation of oxindoles via visible-light-promoted electron transfer". *Chem. Sci.*, 10 (10): 3049, 2019.
- 26 CAIUBY, C. A. D.; ALI, A.; SANTANA, V. T.; LUCAS, F. W. S.; SANTOS, M. S.; CORRÊA, A. G., et al. "Intramolecular radical cyclization approach to access highly substituted indolines and 2,3-dihydrobenzofurans under visible-light". *RSC Adv.*, 8 (23): 12879, 2018.

- 27 YANG, M.; CAO, T.; XU, T. & LIAO, S. "Visible-light-induced deaminative thioesterification of amino acid derived Katritzky salts via electron donor–acceptor complex formation". *Org. Lett.*, 21 (21): 8673, 2019.
- 28 GE, Q.-Q.; QIAN, J.-S. & XUAN, J. "Electron donor–acceptor complex enabled decarboxylative sulfonylation of cinnamic acids under visible-light irradiation". *J. Org. Chem.*, 84 (13): 8691, 2019.
- 29 WU, J.; HE, L.; NOBLE, A. & AGGARWAL, V. K. "Photoinduced deaminative borylation of alkylamines". *J. Am. Chem. Soc.*, 140 (34): 10700, 2018.
- 30 ACKERMANN, L.; DELL'ACQUA, M.; FENNER, S.; VICENTE, R. & SANDMANN, R. "Metal-free direct arylations of indoles and pyrroles with diaryliodonium salts". *Org. Lett.*, 13 (9): 2358, 2011.
- 31 WEN, J.; ZHANG, R.-Y.; CHEN, S.-Y.; ZHANG, J. & YU, X.-Q. "Direct arylation of arene and *N*-heteroarenes with diaryliodonium salts without the use of transition metal catalyst". *J. Org. Chem.*, 77 (1): 766, 2012.
- 32 DEKTAR, J. L. & HACKER, N. P. "Photochemistry of diaryliodonium salts". *J. Org. Chem.*, 55 (2): 639, 1990.
- 33 LUBINKOWSKI, J. J.; GIMENEZ ARRIECHE, C. & MCEWEN, W. E. "Aryl radical departure aptitudes in reactions of diaryliodonium fluoroborates with sodium ethoxide". *J. Org. Chem.*, 45 (11): 2076, 1980.
- 34 WANG, X. & STUDER, A. "Iodine(III) reagents in radical chemistry". *Acc. Chem. Res.*, 50 (7): 1712, 2017.
- 35 AGANDA, K. C. C.; KIM, J. & LEE, A. "Visible-light-mediated direct C3-arylation of 2*H*-indazoles enabled by an electron-donor–acceptor complex". *Org. Biomol. Chem.*, 17 (45): 9698, 2019.
- 36 ANTIPOVA, T. V.; ZAITSEV, K. V.; ZHEREBKER, A. Y.; TAFEENKO, V. A.; BASKUNOV, B. P.; ZHELIFONOVA, V. P., et al. "Monasnicotinic acid, a novel pyridine alkaloid of the fungus *Aspergillus cavernicola*: isolation and structure elucidation". *Mendeleev Commun.*, 28 (1): 55, 2018.
- 37 FAN, D.; LI, T.; ZHENG, Z.; ZHU, G.-Y.; YAO, X.; JIANG, Z.-H., et al. "Macrolide sesquiterpene pyridine alkaloids from the stems of *Tripterygium regelii*". *J. Nat. Med.*, 73: 23, 2019.
- 38 FRANCISCO, W.; PIVATTO, M.; DANUELLO, A.; REGASINI, L. O.; BACCINI, L. R.; YOUNG, M. C. M., et al. "Pyridine alkaloids from *Senna multijuga* as acetylcholinesterase inhibitors". *J. Nat. Prod.*, 75 (3): 408, 2012.
- 39 GAO, C.; HUANG, X.-X.; BAI, M.; WU, J.; LI, J.-Y.; LIU, Q.-B., et al. "Anti-inflammatory sesquiterpene pyridine alkaloids from *Tripterygium wilfordii*". *Fitoterapia*, 105: 49, 2015.

- 40 SANTOS, V. A. F. F. M.; REGASINI, L. O.; NOGUEIRA, C. R.; PASSERINI, G. D.; MARTINEZ, I.; BOLZANI, V. S., et al. "Antiprotozoal sesquiterpene pyridine alkaloids from *Maytenus ilicifolia*". *J. Nat. Prod.*, 75 (5): 991, 2012.
- 41 SHUBINA, L. K.; MAKARIEVA, T. N.; YASHUNSKY, D. V.; NIFANTIEV, N. E.; DENISENKO, V. A.; DMITRENOK, P. S., et al. "Pyridine nucleosides neopetrosides A and B from a marine *Neopetrosia* sp. sponge. Synthesis of neopetroside A and its β -riboside analogue". *J. Nat. Prod.*, 78 (6): 1383, 2015.
- 42 EPP, J. B.; ALEXANDER, A. L.; BALKO, T. W.; BUYSSE, A. M.; BREWSTER, W. K.; BRYAN, K., et al. "The discovery of Arylex™ active and Rinskor™ active: two novel auxin herbicides". *Bioorg. Med. Chem.*, 24 (3): 362, 2016.
- 43 FUJIWARA, T. & O'HAGAN, D. "Successful fluorine-containing herbicide agrochemicals". *J. Fluorine Chem.*, 167: 16, 2014.
- 44 GUAN, A.-Y.; LIU, C.-L.; SUN, X.-F.; XIE, Y. & WANG, M.-A. "Discovery of pyridine-based agrochemicals by using intermediate derivatization methods". *Bioorg. Med. Chem.*, 24 (3): 342, 2016.
- 45 VITAKU, E.; SMITH, D. T. & NJARDARSON, J. T. "Analysis of the structural diversity, substitution patterns, and frequency of nitrogen heterocycles among U.S. FDA approved pharmaceuticals". *J. Med. Chem.*, 57 (24): 10257, 2014.
- 46 WU, Y.-J. "Heterocycles and medicine: a survey of the heterocyclic drugs approved by the U.S. FDA from 2000 to present". In: GRIBBLE, G. W. & JOULE, J. A. (Ed.). *Prog. Heterocycl. Chem.* Amsterdam: Elsevier, 2012, vol. 24, ch. 1, pp. 1-53.
- 47 LIU, R.; XU, K.-P. & TAN, G.-S. "Cyclooxygenase-2 inhibitors in lung cancer treatment: bench to bed". *Eur. J. Pharmacol.*, 769: 127, 2015.
- 48 TALATI, C. & SWEET, K. "Recently approved therapies in acute myeloid leukemia: a complex treatment landscape". *Leuk. Res.*, 73: 58, 2018.
- 49 ICHIKAWA, T.; NETSU, M.; MIZUNO, M.; MIZUSAKI, T.; TAKAGI, Y.; SAWAMA, Y., et al. "Development of a unique heterogeneous palladium catalyst for the Suzuki–Miyaura reaction using (hetero)aryl chlorides and chemoselective hydrogenation". *Adv. Synth. Catal.*, 359 (13): 2269, 2017.
- 50 ILIE, A.; ROIBAN, G.-D. & REETZ, M. T. "Di-*tert*-butyl *N,N*-diethylphosphoramidite as an air stable ligand for Suzuki–Miyaura and Buchwald–Hartwig reactions". *ChemistrySelect*, 2 (4): 1392, 2017.
- 51 LEE, D.-H.; JUNG, J.-Y. & JIN, M.-J. "Highly active and recyclable silica gel-supported palladium catalyst for mild cross-coupling reactions of unactivated heteroaryl chlorides". *Green Chem.*, 12 (11): 2024, 2010.
- 52 OUYANG, J.-S.; LI, Y.-F.; HUANG, F.-D.; LU, D.-D. & LIU, F.-S. "The highly efficient Suzuki–Miyaura cross-coupling of (hetero)aryl chlorides and (hetero)arylboronic acids catalyzed by "bulky-yet-flexible" palladium–PEPSSI complexes in air". *ChemCatChem*, 10 (2): 371, 2018.

- 53 LUZUNG, M. R.; PATEL, J. S. & YIN, J. "A mild Negishi cross-coupling of 2-heterocyclic organozinc reagents and aryl chlorides". *J. Org. Chem.*, 75 (23): 8330, 2010.
- 54 ROESNER, S. & BUCHWALD, S. L. "Continuous-flow synthesis of biaryls by Negishi cross-coupling of fluoro- and trifluoromethyl-substituted (hetero)arenes". *Angew. Chem. Int. Ed.*, 55 (35): 10463, 2016.
- 55 YAMAMOTO, K.; OTSUKA, S.; NOGI, K. & YORIMITSU, H. "Nickel-catalyzed cross-coupling reaction of aryl sulfoxides with arylzinc reagents: when the leaving group is an oxidant". *ACS Catal.*, 7 (11): 7623, 2017.
- 56 LEE, D.-H.; QIAN, Y.; PARK, J.-H.; LEE, J.-S.; SHIM, S.-E. & JIN, M.-J. "A highly active and general catalyst for the Stille coupling reaction of unreactive aryl, heteroaryl, and vinyl chlorides under mild conditions". *Adv. Synth. Catal.*, 355 (9): 1729, 2013.
- 57 LEE, D.-H.; TAHER, A.; AHN, W.-S. & JIN, M.-J. "Room temperature Stille cross-coupling reaction of unreactive aryl chlorides and heteroaryl chlorides". *Chem. Commun.*, 46 (3): 478, 2010.
- 58 BLAKEMORE, D. C. & MARPLES, L. A. "Palladium(0)-catalysed cross-coupling of 2-trimethylsilylpyridine with aryl halides". *Tetrahedron Lett.*, 52 (32): 4192, 2011.
- 59 GURUNG, S. K.; THAPA, S.; VANGALA, A. S. & GIRI, R. "Copper-catalyzed Hiyama coupling of (hetero)aryltrioxy silanes with (hetero)aryl iodides". *Org. Lett.*, 15 (20): 5378, 2013.
- 60 ACKERMANN, L.; POTUKUCHI, H. K.; KAPDI, A. R. & SCHULZKE, C. "Kumada–Corriu cross-couplings with 2-pyridyl Grignard reagents". *Chem. Eur. J.*, 16 (11): 3300, 2010.
- 61 LIU, N. & WANG, Z.-X. "Kumada coupling of aryl, heteroaryl, and vinyl chlorides catalyzed by amido pincer nickel complexes". *J. Org. Chem.*, 76 (24): 10031, 2011.
- 62 CANDISH, L.; FREITAG, M.; GENSCHE, T. & GLORIUS, F. "Mild, visible light-mediated decarboxylation of aryl carboxylic acids to access aryl radicals". *Chem. Sci.*, 8 (5): 3618, 2017.
- 63 HUSSAIN, I. & SINGH, T. "Synthesis of biaryls through aromatic C–H bond activation: a review of recent developments". *Adv. Synth. Catal.*, 356 (8): 1661, 2014.
- 64 MURAKAMI, K.; YAMADA, S.; KANEDA, T. & ITAMI, K. "C–H functionalization of azines". *Chem. Rev.*, 117 (13): 9302, 2017.
- 65 SEIPLE, I. B.; SU, S.; RODRIGUEZ, R. A.; GIANATASSIO, R.; FUJIWARA, Y.; SOBEL, A. L., et al. "Direct C–H arylation of electron-deficient heterocycles with arylboronic acids". *J. Am. Chem. Soc.*, 132 (38): 13194, 2010.

- 66 LIAO, L.-Y.; LIU, K.-M. & DUAN, X.-F. "Unified protocol for cobalt-catalyzed oxidative assembly of two aryl metal reagents using oxygen as an oxidant". *J. Org. Chem.*, 80 (20): 9856, 2015.
- 67 LIU, K. M.; LIAO, L. Y. & DUAN, X. F. "Iron catalyzed oxidative assembly of *N*-heteroaryl and aryl metal reagents using oxygen as an oxidant". *Chem. Commun.*, 51 (6): 1124, 2015.
- 68 LIU, K.-M.; ZHANG, R. & DUAN, X.-F. "Room-temperature cobalt-catalyzed arylation of aromatic acids: overriding the *ortho*-selectivity via the oxidative assembly of carboxylate and aryl titanate reagents using oxygen". *Org. Biomol. Chem.*, 14 (5): 1593, 2016.
- 69 GARCÍA-LÓPEZ, J.-A. & GREANEY, M. F. "Synthesis of biaryls using aryne intermediates". *Chem. Soc. Rev.*, 45 (24): 6766, 2016.
- 70 TRUONG, T. & DAUGULIS, O. "Base-mediated intermolecular sp² C–H bond arylation via benzyne intermediates". *J. Am. Chem. Soc.*, 133 (12): 4243, 2011.
- 71 TRUONG, T.; MESGAR, M.; LE, K. K. A. & DAUGULIS, O. "General method for functionalized polyaryl synthesis via aryne intermediates". *J. Am. Chem. Soc.*, 136 (24): 8568, 2014.
- 72 BONIN, H.; SAUTHIER, M. & FELPIN, F.-X. "Transition metal-mediated direct C–H arylation of heteroarenes involving aryl radicals". *Adv. Synth. Catal.*, 356 (4): 645, 2014.
- 73 ROSSI, R.; LESSI, M.; MANZINI, C.; MARIANETTI, G. & BELLINA, F. "Transition metal-free direct C–H (hetero)arylation of heteroarenes: a sustainable methodology to access (hetero)aryl-substituted heteroarenes". *Adv. Synth. Catal.*, 357 (18): 3777, 2015.
- 74 GHOSH, I.; MARZO, L.; DAS, A.; SHAIKH, R. & KÖNIG, B. "Visible light mediated photoredox catalytic arylation reactions". *Acc. Chem. Res.*, 49 (8): 1566, 2016.
- 75 MAJEK, M. & JACOBI VON WANGELIN, A. "Mechanistic perspectives on organic photoredox catalysis for aromatic substitutions". *Acc. Chem. Res.*, 49 (10): 2316, 2016.
- 76 MATSUI, J. K.; LANG, S. B.; HEITZ, D. R. & MOLANDER, G. A. "Photoredox-mediated routes to radicals: the value of catalytic radical generation in synthetic methods development". *ACS Catal.*, 7 (4): 2563, 2017.
- 77 RAVELLI, D.; FAGNONI, M. & ALBINI, A. "Photoorganocatalysis. What for?". *Chem. Soc. Rev.*, 42 (1): 97, 2013.
- 78 RAVELLI, D.; PROTTI, S. & FAGNONI, M. "Carbon–carbon bond forming reactions via photogenerated intermediates". *Chem. Rev.*, 116 (17): 9850, 2016.

- 79 ROMERO, N. A. & NICEWICZ, D. A. "Organic photoredox catalysis". *Chem. Rev.*, 116 (17): 10075, 2016.
- 80 WANG, C.-S.; DIXNEUF, P. H. & SOULÉ, J.-F. "Photoredox catalysis for building C–C bonds from C(sp²)–H bonds". *Chem. Rev.*, 118 (16): 7532, 2018.
- 81 FABRY, D. C.; HO, Y. A.; ZAPF, R.; TREMEL, W.; PANTHÖFER, M.; RUEPING, M., et al. "Blue light mediated C–H arylation of heteroarenes using TiO₂ as an immobilized photocatalyst in a continuous-flow microreactor". *Green Chem.*, 19 (8): 1911, 2017.
- 82 GOMES, F.; NARBONNE, V.; BLANCHARD, F.; MAESTRI, G. & MALACRIA, M. "Formal base-free homolytic aromatic substitutions via photoredox catalysis". *Org. Chem. Front.*, 2 (5): 464, 2015.
- 83 HUANG, L. & ZHAO, J. "Iodo-bodipys as visible-light-absorbing dual-functional photoredox catalysts for preparation of highly functionalized organic compounds by formation of C–C bonds via reductive and oxidative quenching catalytic mechanisms". *RSC Adv.*, 3 (45): 23377, 2013.
- 84 RYBICKA-JASIŃSKA, K.; KÖNIG, B. & GRYKO, D. "Porphyrin-catalyzed photochemical C–H arylation of heteroarenes". *Eur. J. Org. Chem.*, (15): 2104, 2017.
- 85 XUE, D.; JIA, Z. H.; ZHAO, C. J.; ZHANG, Y. Y.; WANG, C. & XIAO, J. "Direct arylation of *N*-heteroarenes with aryldiazonium salts by photoredox catalysis in water". *Chem. Eur. J.*, 20 (10): 2960, 2014.
- 86 ZOLLER, J.; FABRY, D. C. & RUEPING, M. "Unexpected dual role of titanium dioxide in the visible light heterogeneous catalyzed C–H arylation of heteroarenes". *ACS Catal.*, 5 (6): 3900, 2015.
- 87 ZUO, X.; WU, W. & SU, W. "Visible-light photoredox catalysis: direct arylation of electron-deficient heterocycles and arenes with aryl diazonium salts". *Acta Chim. Sinica*, 73 (12): 1298, 2015.
- 88 LIU, Y.-X.; XUE, D.; WANG, J.-D.; ZHAO, C.-J.; ZOU, Q.-Z.; WANG, C., et al. "Room-temperature arylation of arenes and heteroarenes with diaryl-iodonium salts by photoredox catalysis". *Synlett*, 24 (4): 507, 2013.
- 89 CHAUDHARY, R. & NATARAJAN, P. "Visible light photoredox activation of sulfonyl chlorides: applications in organic synthesis". *ChemistrySelect*, 2 (22): 6458, 2017.
- 90 CRESPI, S.; PROTTI, S. & FAGNONI, M. "Wavelength selective generation of aryl radicals and aryl cations for metal-free photoarylations". *J. Org. Chem.*, 81 (20): 9612, 2016.
- 91 DA SILVA JÚNIOR, P. E.; AMIN, H. I. M.; NAUTH, A. M.; DA SILVA EMERY, F.; PROTTI, S. & OPATZ, T. "Flow photochemistry of azosulfones: application of "sunflow" reactors". *ChemPhotoChem*, 2 (10): 878, 2018.

- 92 CANTILLO, D.; MATEOS, C.; RINCON, J. A.; DE FRUTOS, O. & KAPPE, C. O. "Light-induced C–H arylation of (hetero)arenes by in situ generated diazo anhydrides". *Chem. Eur. J.*, 21 (37): 12894, 2015.
- 93 CHENG, Y.; GU, X. & LI, P. "Visible-light photoredox in homolytic aromatic substitution: direct arylation of arenes with aryl halides". *Org. Lett.*, 15 (11): 2664, 2013.
- 94 GHOSH, I. & KÖNIG, B. "Chromoselective photocatalysis: controlled bond activation through light-color regulation of redox potentials". *Angew. Chem. Int. Ed.*, 55 (27): 7676, 2016.
- 95 MEYER, A. U.; SLANINA, T.; YAO, C.-J. & KÖNIG, B. "Metal-free perfluoroarylation by visible light photoredox catalysis". *ACS Catal.*, 6 (1): 369, 2016.
- 96 FENG, Y.-S.; BU, X.-S.; HUANG, B.; RONG, C.; DAI, J.-J.; XU, J., et al. "NADH coenzyme model compound as photocatalyst for the direct arylation of (hetero)arenes". *Tetrahedron Lett.*, 58 (20): 1939, 2017.
- 97 BUGLIONI, L.; RIENTE, P.; PALOMARES, E. & PERICÀS, M. A. "Visible-light-promoted arylation reactions photocatalyzed by bismuth(III) oxide". *Eur. J. Org. Chem.*, (46): 6986, 2017.
- 98 AHMED, J.; P, S.; VIJAYKUMAR, G.; JOSE, A.; RAJ, M. & MANDAL, S. K. "A new face of phenalenyl-based radicals in the transition metal-free C–H arylation of heteroarenes at room temperature: trapping the radical initiator via C–C σ -bond formation". *Chem. Sci.*, 8 (11): 7798, 2017.
- 99 XU, Z.; GAO, L.; WANG, L.; GONG, M.; WANG, W. & YUAN, R. "Visible light photoredox catalyzed biaryl synthesis using nitrogen heterocycles as promoter". *ACS Catal.*, 5 (1): 45, 2015.
- 100 MARZO, L.; WANG, S. & KÖNIG, B. "Visible-light-mediated radical arylation of anilines with acceptor-substituted (hetero)aryl halides". *Org. Lett.*, 19 (21): 5976, 2017.
- 101 FÜRST, M. C. D.; BOCK, L. R. & HEINRICH, M. R. "Regioselective radical arylation of 3-hydroxypyridines". *J. Org. Chem.*, 81 (13): 5752, 2016.
- 102 MAAS, G.; TANAKA, M. & SAKAKURA, T. "Benzenediazonium tetrafluoroborate". In: PAQUETTE, L. A. (Ed.). *Encyclopedia of Reagents for Organic Synthesis*. New York: John Wiley & Sons, 2001.
- 103 OGER, N.; D'HALLUIN, M.; LE GROGNEC, E. & FELPIN, F.-X. "Using aryl diazonium salts in palladium-catalyzed reactions under safer conditions". *Org. Process Res. Dev.*, 18 (12): 1786, 2014.
- 104 ULLRICH, R. & GREWER, T. "Decomposition of aromatic diazonium compounds". *Thermochim. Acta*, 225 (2): 201, 1993.

- 105 JOLICOEUR, C. & FRIEDMAN, H. L. "Hydrophobic nitroxide radicals as probes to investigate the hydrophobic interaction". *J. Solution Chem.*, 3 (1): 15, 1974.
- 106 BOCKMAN, T. M.; KOSYNKIN, D. & KOCHI, J. K. "Isolation and structure elucidation of transient (colored) complexes of arenediazonium with aromatic hydrocarbons as intermediates in arylations and azo couplings". *J. Org. Chem.*, 62 (17): 5811, 1997.
- 107 KOSYNKIN, D.; BOCKMAN, T. M. & KOCHI, J. K. "Thermal (iodide) and photoinduced electron-transfer catalysis in biaryl synthesis via aromatic arylations with diazonium salts". *J. Am. Chem. Soc.*, 119 (21): 4846, 1997.
- 108 LOEWENSCHUSS, H.; WAHL JR., G. H. & ZOLLINGER, H. "Dediazoniating of arenediazonium ions in homogeneous solution. Part IX. Spectral evidence for a homolytic mechanism involving pyridine complexes". *Helv. Chim. Acta*, 59 (5): 1438, 1976.
- 109 FOSTER, R. & FYFE, C. A. "Electron-donor-acceptor complex formation by compounds of biological interest. Part III. Indole complexes". *J. Chem. Soc. B*, (0): 926, 1966.
- 110 UCHOA, A. F.; DE OLIVEIRA, K. T.; BAPTISTA, M. S.; BORTOLUZZI, A. J.; IAMAMOTO, Y. & SERRA, O. A. "Chlorin photosensitizers sterically designed to prevent self-aggregation". *J. Org. Chem.*, 76 (21): 8824, 2011.
- 111 ZOLLINGER, H. "Nitrogen as leaving group: dediazoniating of aromatic diazonium ions". *Angew. Chem. Int. Ed.*, 17 (3): 141, 1978.
- 112 HANSEN, M. J.; LERCH, M. M.; SZYMANSKI, W. & FERINGA, B. L. "Direct and versatile synthesis of red-shifted azobenzenes". *Angew. Chem. Int. Ed.*, 55 (43): 13514, 2016.
- 113 DE SOUZA, A. A. N.; SILVA, N. S.; MÜLLER, A. V.; POLO, A. S.; BROCKSOM, T. J. & DE OLIVEIRA, K. T. "Porphyrins as photoredox catalysts in Csp²-H arylations: batch and continuous flow approaches". *J. Org. Chem.*, 83 (24): 15077, 2018.
- 114 DE SOUZA, J. M.; BROCKSOM, T. J.; MCQUADE, D. T. & DE OLIVEIRA, K. T. "Continuous endoperoxidation of conjugated dienes and subsequent rearrangements leading to C-H oxidized synthons". *J. Org. Chem.*, 83 (15): 7574, 2018.
- 115 PARMENTIER, M.; GROS, P. & FORT, Y. "Pyridino-directed lithiation of anisylpyridines: new access to functional pyridylphenols". *Tetrahedron*, 61 (13): 3261, 2005.
- 116 HU, H.; GE, C.; ZHANG, A. & DING, L. "Synthesis of novel 3,5-dichloro-2-arylpyridines by palladium acetate-catalyzed ligand-free suzuki reactions in aqueous media". *Molecules*, 14 (9): 3153, 2009.
- 117 LI, M. & HUA, R. "Gold(I)-catalyzed direct C-H arylation of pyrazine and pyridine with aryl bromides". *Tetrahedron Lett.*, 50 (13): 1478, 2009.

- 118 PANDA, S.; COFFIN, A.; NGUYEN, Q. N.; TANTILLO, D. J. & READY, J. M. "Synthesis and utility of dihydropyridine boronic esters". *Angew. Chem. Int. Ed.*, 55 (6): 2205, 2016.
- 119 LI, Y.; LIU, W. & KUANG, C. "Direct arylation of pyridines without the use of a transition metal catalyst". *Chem. Commun.*, 50 (54): 7124, 2014.
- 120 JOHNSTON, A. J. S.; LING, K. B.; SALE, D.; LEBRASSEUR, N. & LARROSA, I. "Direct *ortho*-arylation of pyridinecarboxylic acids: overcoming the deactivating effect of sp²-nitrogen". *Org. Lett.*, 18 (23): 6094, 2016.
- 121 RASHKIN, M. J. & WATERS, M. L. "Unexpected substituent effects in offset π - π stacked interactions in water". *J. Am. Chem. Soc.*, 124 (9): 1860, 2002.
- 122 BILLINGSLEY, K. L. & BUCHWALD, S. L. "A general and efficient method for the Suzuki-Miyaura coupling of 2-pyridyl nucleophiles". *Angew. Chem. Int. Ed.*, 47 (25): 4695, 2008.
- 123 PAVLOVIC, V.; PETKOVIC, M.; POPOVIC, S. & SAVIC, V. "Synthesis of 4-aryl-2-aminopyridine derivatives and related compounds". *Synth. Commun.*, 39 (23): 4249, 2009.
- 124 GOSMINI, C.; BASSENE-ERNST, C. & DURANDETTI, M. "Synthesis of functionalized 2-arylpyridines from 2-halopyridines and various aryl halides via a nickel catalysis". *Tetrahedron*, 65 (31): 6141, 2009.
- 125 WILEY, R. H.; CALLAHAN, P. X.; JARBOE, C. H.; NIELSEN, J. T. & WAKEFIELD, B. J. "Pyridine analogs of *p*-terphenyl and *p*-quaterphenyl". *J. Org. Chem.*, 25 (3): 366, 1960.
- 126 KATRITZKY, A. R. & SIMMONS, P. "Interaction at a distance in conjugated systems. Part I. The basicities of (amino- and nitro-phenyl)-pyridines and -pyridine 1-oxides". *J. Chem. Soc.*, (0): 1511, 1960.
- 127 LIU, Y.-K.; LOU, S.-J.; XU, D.-Q. & XU, Z.-Y. "Regiospecific synthesis of nitroarenes by palladium-catalyzed nitrogen-donor-directed aromatic C-H nitration". *Chem. Eur. J.*, 16 (46): 13590, 2010.
- 128 ISHIKURA, M.; OHTA, T. & TERASHIMA, M. "A novel synthesis of 4-aryl- and 4-heteroarylpyridines via diethyl(4-pyridyl)borane". *Chem. Pharm. Bull.*, 33 (11): 4755, 1985.
- 129 HE, R.-T.; WANG, J.-F.; WANG, H.-F.; REN, Z.-G. & LANG, J.-P. "Palladium dichloride adduct of *N,N*-bis-(diphenylphosphanylmethyl)-2-aminopyridine: synthesis, structure and catalytic performance in the decarboxylative cross-coupling of 4-picolinic acid with aryl bromide". *Dalton Trans.*, 43 (25): 9786, 2014.
- 130 LI, X.; TENG, Y.; FENG, F.; HU, Q. & YUAN, Z. "Aqueous Suzuki-Miyaura reaction with 0.6 equiv. of base: green and efficient access to biaryls and unsymmetrical terphenyls". *ChemistrySelect*, 3 (21): 6022, 2018.

- 131 XIE, L.-G. & WANG, Z.-X. "Cross-coupling of aryl/alkenyl ethers with aryl grignard reagents through nickel-catalyzed C–O activation". *Chem. Eur. J.*, 17 (18): 4972, 2011.
- 132 BHAKUNI, B. S.; YADAV, A.; KUMAR, S. & KUMAR, S. "AMVN-initiated expedient synthesis of biaryls by the coupling reaction of unactivated arenes and heteroarenes with aryl iodides". *New J. Chem.*, 38 (2): 827, 2014.
- 133 GARCÍA-RUBIA, A.; FERNÁNDEZ-IBÁÑEZ, M. Á.; GÓMEZ ARRAYÁS, R. & CARRETERO, J. C. "2-Pyridyl sulfoxide: a versatile and removable directing group for the Pd^{II}-catalyzed direct C–H olefination of arenes". *Chem. Eur. J.*, 17 (13): 3567, 2011.
- 134 HU, B.; LI, Y.; DONG, W.; XIE, X.; WAN, J. & ZHANG, Z. "Visible light-induced aerobic C–N bond activation: a photocatalytic strategy for the preparation of 2-arylpyridines and 2-arylquinolines". *RSC Adv.*, 6 (54): 48315, 2016.
- 135 YUAN, J.-W.; YANG, L.-R.; MAO, P. & QU, L.-B. "AgNO₃-catalyzed direct C–H arylation of quinolines by oxidative decarboxylation of aromatic carboxylic acids". *Org. Chem. Front.*, 4 (4): 545, 2017.
- 136 WUNDERLICH, S. H.; ROHBOGNER, C. J.; UNSINN, A. & KNOCHER, P. "Scaleable preparation of functionalized organometallics via directed ortho metalation using Mg- and Zn-amide bases". *Org. Process Res. Dev.*, 14 (2): 339, 2010.

Chapter 3: Sulfonyl fluoride synthesis through electrochemical oxidative coupling of thiols and potassium fluoride

Reproduced with permission from [#]LAUDADIO, G.; [#]BARTOLOMEU, A. A.; VERWIJLEN, L. M. H. M.; CAO, Y.; DE OLIVEIRA, K. T. & NOËL, T. “Sulfonyl fluoride synthesis through electrochemical oxidative coupling of thiols and potassium fluoride”. *J. Am. Chem. Soc.*, 141 (30): 11832, 2019. Copyright 2019 American Chemical Society.

[#]These authors contributed equally to this work.

3 Chapter 3

Chapter 3 is based on our paper published in the Journal of the American Chemical Society in 2019, and it presents the results obtained in the development of an electrochemical approach for the synthesis of sulfonyl fluorides through oxidative coupling of thiols and potassium fluoride. This study was developed entirely in the Netherlands under the guidance of Prof. Dr. Timothy Noël (TU/e, The Netherlands), with the contributions of Prof. Dr. Kleber T. de Oliveira (UFSCar, Brazil), and in collaboration with Ph.D. student Gabriele Laudadio, who wrote the published version of the supporting information (which is slightly different from that described in Section 3.4), performed the cyclic voltammetry analyses, helped in the kinetic experiments under batch conditions, and contributed to the purification of some compounds. The principal investigator Dr. Timothy Noël wrote the paper with input from Gabriele Laudadio and Aloisio de A. Bartolomeu. Lucas M. H. M. Verwijlen carried out some scope reactions and contributed to the purification of some compounds. Yran Cao performed the kinetic experiment under continuous flow conditions.

3.1 Introduction

3.1.1 Basic concepts in organic electrochemistry

Electrolysis is a process that uses electrical energy to drive a non-spontaneous chemical reaction. It is carried out in an electrochemical cell, an apparatus composed of an electroactive species/substrate, electrolyte, solvent, and at least two electrodes (a cathode and an anode). The cathode is the electrode connected to the negative terminal of the power source (e.g., galvanostat, potentiostat or DC power supply) and is reductive. The anode is the electrode connected to the positive terminal and is oxidative. There are two basic options to manufacture

the electrochemical cell: a divided or undivided cell (Figure 3.1). In an undivided cell the electrodes are in the same chamber, whereas in a divided cell, the electrodes are kept in different chambers, separated by a small porous frit (or an ion-exchange membrane) that only permits charge to pass through it and, therefore, enables the two half-reactions to occur separately from each other. Although an undivided cell is preferred because of its simplicity to manufacture and low cost, sometimes the redox reaction intermediates are incompatible or unstable towards the other electrode and must be separated.^{1,2}

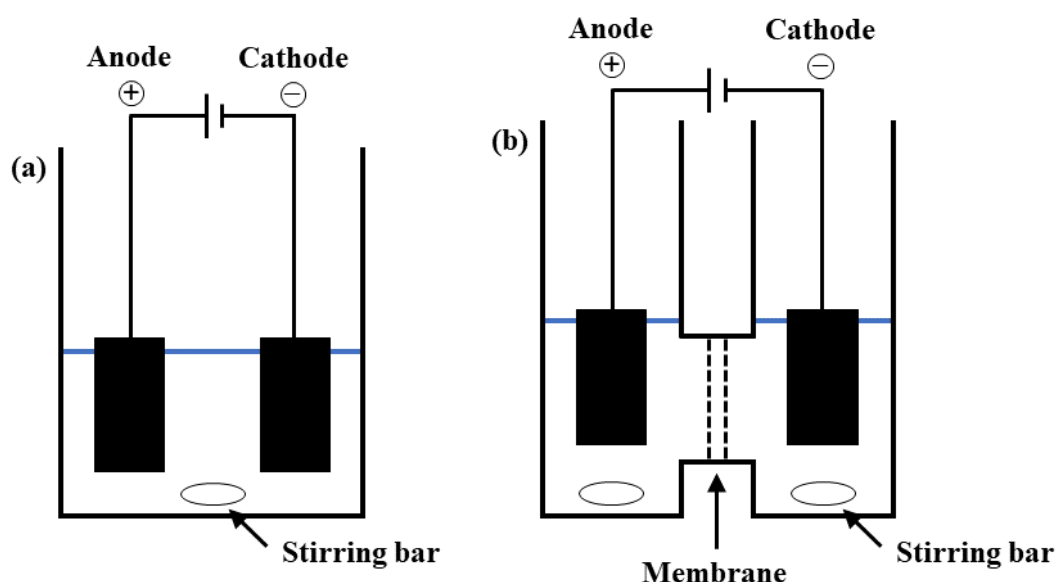


Figure 3.1 – Typical glass cells used for electrosynthesis. (a) undivided beaker-type cell and (b) H-type cell with membrane.²

The redox reactions that occur on the electrode surface can be explained by the molecular orbital theory (Figure 3.2).³

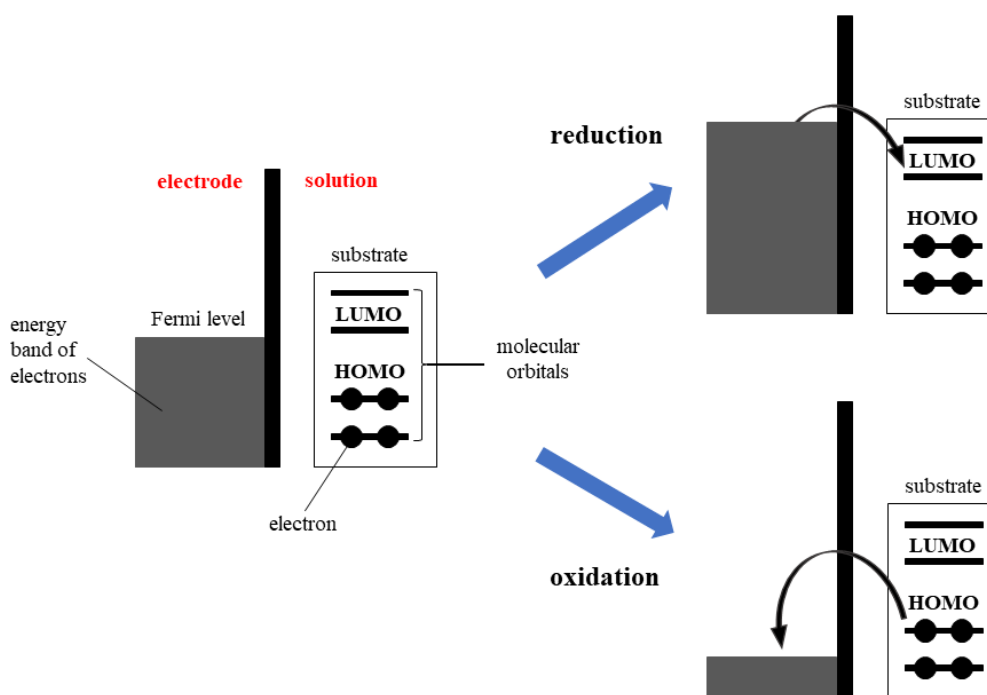


Figure 3.2 – Schematic diagram of the electron transfer on the surface of the electrode.

Adapted from Yoshida and Nishiwaki (1998).³

In the oxidation process, an electron from the HOMO of the organic molecule is transferred to the electrode surface (anode) to generate a cation radical species, while in the reduction process, an electron is removed from the electrode surface (cathode) and subsequently transferred to the LUMO of the organic molecule to generate an anion radical species. After that, these radical species (intermediates) may undergo subsequent reactions to yield final products.

The electrodes may be manufactured from a wide variety of inert conducting materials, including carbon-based materials (graphite, glassy carbon, reticulated vitreous carbon), platinum, magnesium, copper, nickel, stainless steel, etc. In this operation mode of electrodes, the electroconversion occurs on its surface and the selectivity can be obtained by adjusting the applied potential (Figure 3.3a). Although this strategy is useful for simple molecules, an electrocatalytic approach is required to obtain selectivity in more complex molecules (e.g., compounds containing several different moieties such as double bonds, triple

bonds, alcohols, etc.). This can be achieved either by an active electrode (i.e., an electrode that has electrocatalytically active species on its surface) or by using a redox mediator soluble in the electrolyte. In the former case (Figure 3.3b), the electroconversion is less dominated by the applied potential since the redox-active layer acts as a redox filter. Besides providing a unique reactivity, these electrodes are not consumed due to the low solubility of the redox-active component. In the other case (Figure 3.3c), the problems associated with heterogeneous electron transfer (e.g., overpotentials) can generally be avoided during the electrolysis, affording higher selectivities and shorter reaction times.¹ Therefore, the electroconversion can be performed at milder potentials compared to reactions without the addition of a mediator. The disadvantages of this strategy may include higher costs and additional waste generation.⁴

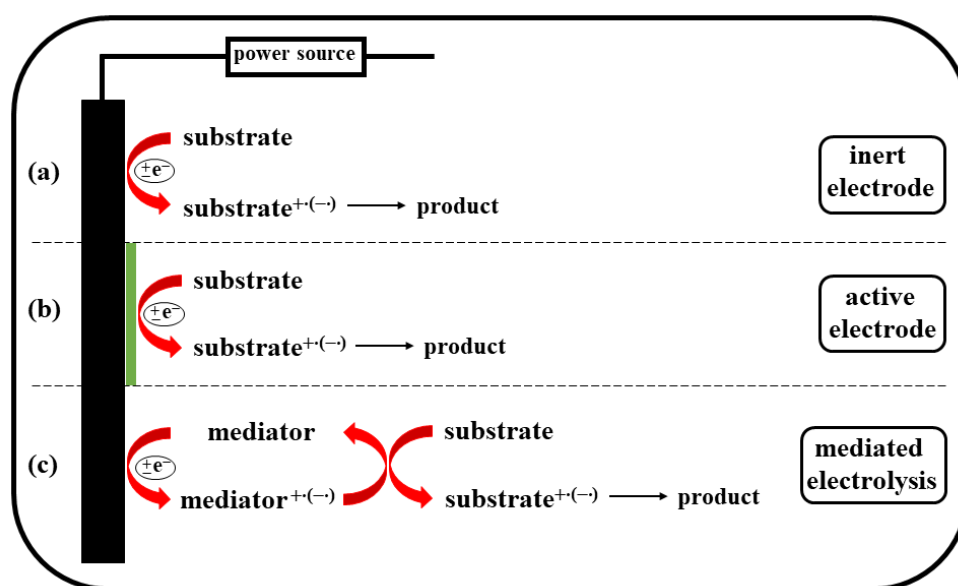


Figure 3.3 – Different operation modes of electrodes in electrochemical processes. Adapted from Möhle et al. (2018).⁴

Suitable organic solvents that can be used in electrochemical processes are, for example, methanol, acetone, acetonitrile, dimethyl sulfoxide, *N,N*-dimethylformamide, as well as nonconventional organic solvents like trifluoroacetic acid, trifluoroethanol, ionic liquids, and

supercritical fluids.^{1,2} Common supporting electrolytes are the alkali metal perchlorates (e.g., NaClO₄, LiClO₄) and tetraalkylammonium salts [e.g., (Me)₄NBF₄, (*n*-Bu)₄NClO₄]. In addition, acids (e.g., H₂SO₄, HCl), bases (e.g., NaOH, LiOH) and buffer solutions are also used.⁵

Electrochemical reactions can be conducted in a constant-potential (potentiostatic) or constant-current (galvanostatic) modes.²

In a constant-potential experiment, a three-electrode system consisting of a working electrode, a counter electrode, and a reference electrode [such as the aqueous saturated calomel electrode or the silver-silver chloride electrode (Ag/AgCl)] is used. In this setup, the potential of the working electrode is held constant with respect to a reference electrode using a potentiostat.² This method provides improvements in selectivity with precise control of the applied potential, yet suffers inherent disadvantages. First, the redox potential of each different substrate must be known or measured in advance. Second, the electrical resistance of the cell under potentiostatic conditions increases during the reaction as the substrate is consumed and the current drops, resulting in a longer reaction time.⁶ This is shown in Equation 3.1, where V is the potential difference, i is the current intensity and R is the resistance of the electrochemical cell (1st Ohm's law).

$$V = i \cdot R \quad (3.1)$$

In a constant-current experiment, a simpler two-electrode system is utilized with only a working electrode and a counter electrode.² In this setup, the current is held constant while the potential of the working electrode increases until it matches the oxidation potential of the substrate molecule in solution with the lowest oxidation potential. This potential remains constant until the substrate is consumed and then begins to increase again until it matches that of the substrate in solution with the next highest oxidation potential.⁷ However, especially at

low current densities, the potential begins to increase only when the substrate has been almost completely consumed and this effect becomes negligible.⁶

Finally, it is noteworthy that the selectivity of electrochemical reactions is quite complicated since it is controlled by many factors, including electrode materials, solvents, supporting electrolytes, current density, applied potential, stirring, etc.²

Further information about organic electrochemistry can be found elsewhere.^{2,8}

3.1.2 Organic electrosynthesis

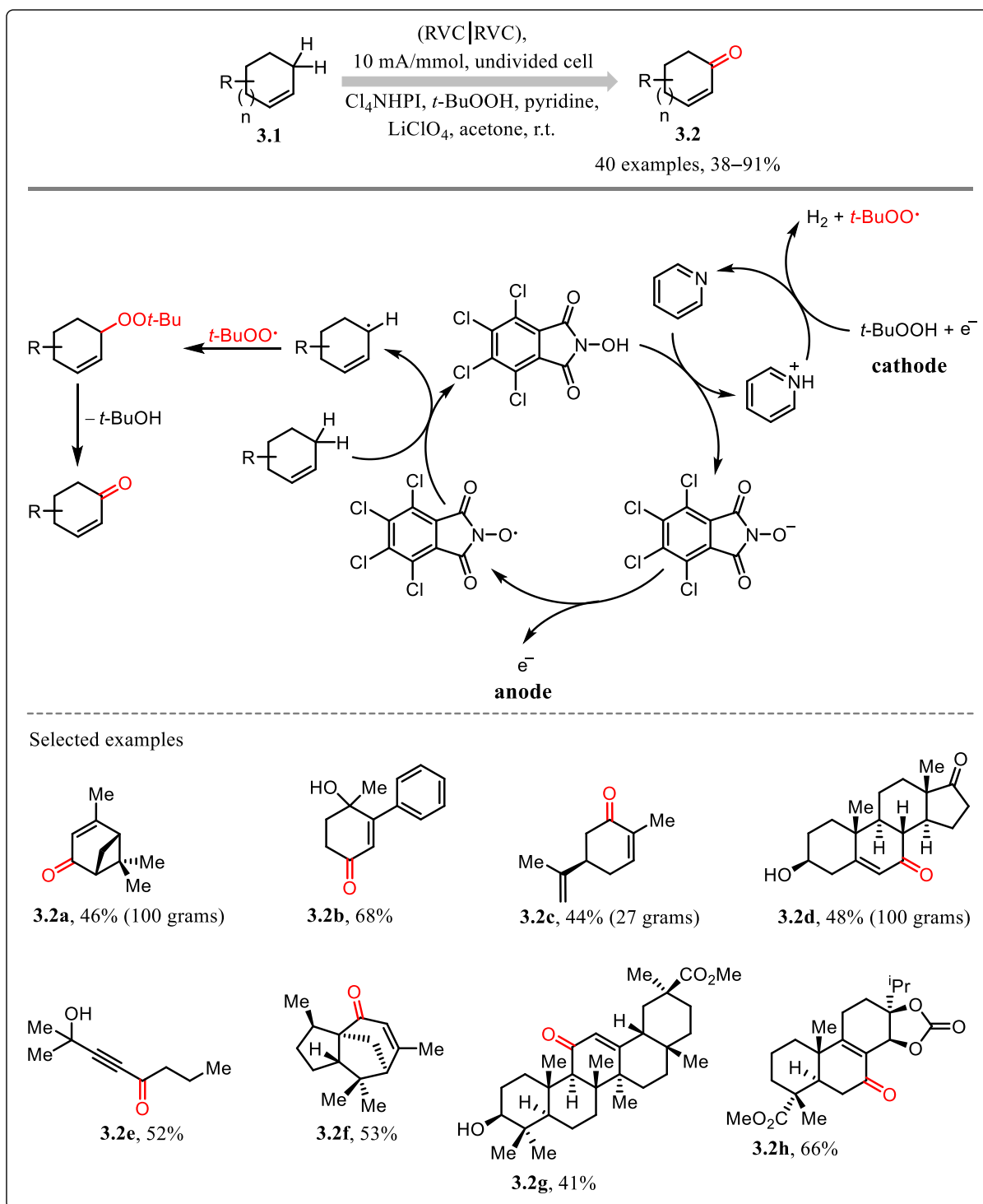
Organic electrosynthesis is considered to be a versatile and environmentally friendly method.^{9,10} In this process, costly, toxic, and hazardous redox chemicals can be substituted by electric current (the so-called “direct” electrolysis) or generated (and/or regenerated) *in situ* (the so-called “indirect” electrolysis) in the course of electrolysis.¹⁰ Another interesting feature is that electrosyntheses can occur under mild conditions; since the reaction rate can be controlled by adjusting the current density or applied potential,¹⁰ even reactions with high activation energies can be carried out at or near r.t. and atmospheric pressure.

Michael Faraday was probably the first who electrolyzed an acetate solution to produce gaseous hydrocarbons.^{1,11} However, it was Adolph W. H. Kolbe who studied the electrolysis (anodic oxidation) of aqueous solutions of organic salts (acetate, valerate) in detail, and therefore he is considered by some as the “father” of organic electrochemistry.¹¹ Christian F. Schönbein reported what appears to be the first example of electrochemical reduction (cathodic reduction) of an organic compound in the reductive dehalogenation of trichloromethanesulfonic acid to methanesulfonic acid at a zinc electrode.¹²

Although organic electrochemistry has been used in the chemical industry for decades,¹³⁻¹⁵ it historically has been viewed as a niche technology by the synthetic community.¹⁶

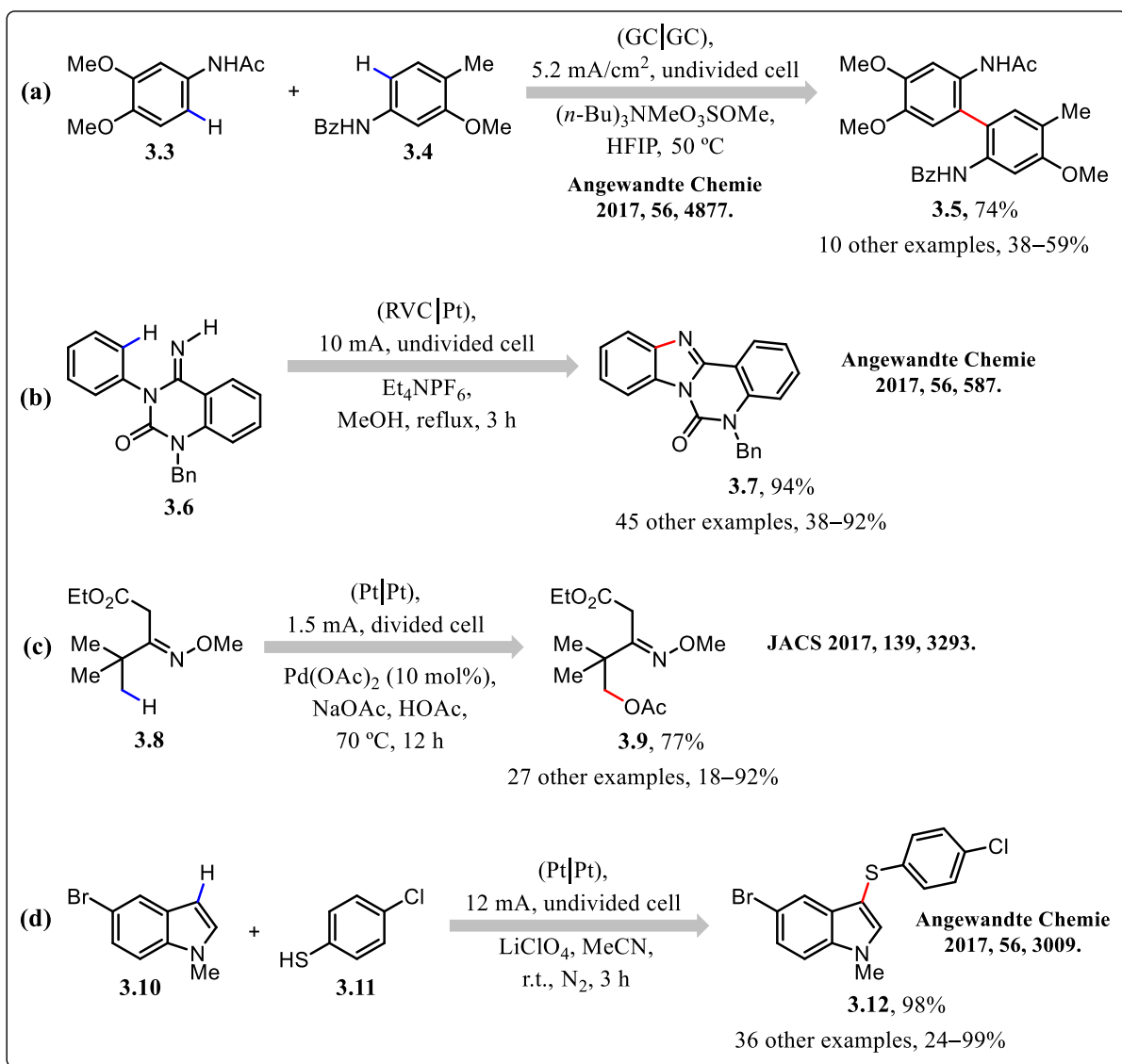
One reason for this is that electrosynthesis requires sophisticated technical infrastructure, which has discouraged many organic chemists from using it. More recently, however, organic electrochemistry has undergone a renaissance,^{17,18} and many research groups worldwide are currently working on the development of new electrochemical synthetic methodologies.^{4,17-26}

In 2016, Baran and co-workers reported an electrochemical oxidation of allylic methylene groups to give unsaturated ketones (Scheme 3.1).²⁷ Using this sustainable protocol, a wide variety of substrates (40 examples, 38–91% yield) were selectively oxidized, including fifteen natural product scaffolds such as α -pinene (oxidized to verbenone on a 100-g scale), limonene (oxidized to carvone on a 27-g scale), valencene (oxidized to nootkatone), dehydroepiandrosterone (oxidized to respective enone on a 100-g scale), etc. According to the authors, deprotonation of the *N*-hydroxyphthalimide catalyst (Cl₄NHPI) by pyridine, followed by anodic oxidation, leads to the tetra-chlorophthalimido *N*-oxyl radical species. Then, upon abstraction of a hydrogen atom from the olefinic substrate, the catalyst is regenerated and the resulting allylic radical reacts with a *tert*-butyl peroxy radical (electrochemically generated) to give the enone after elimination of *t*-BuOH.



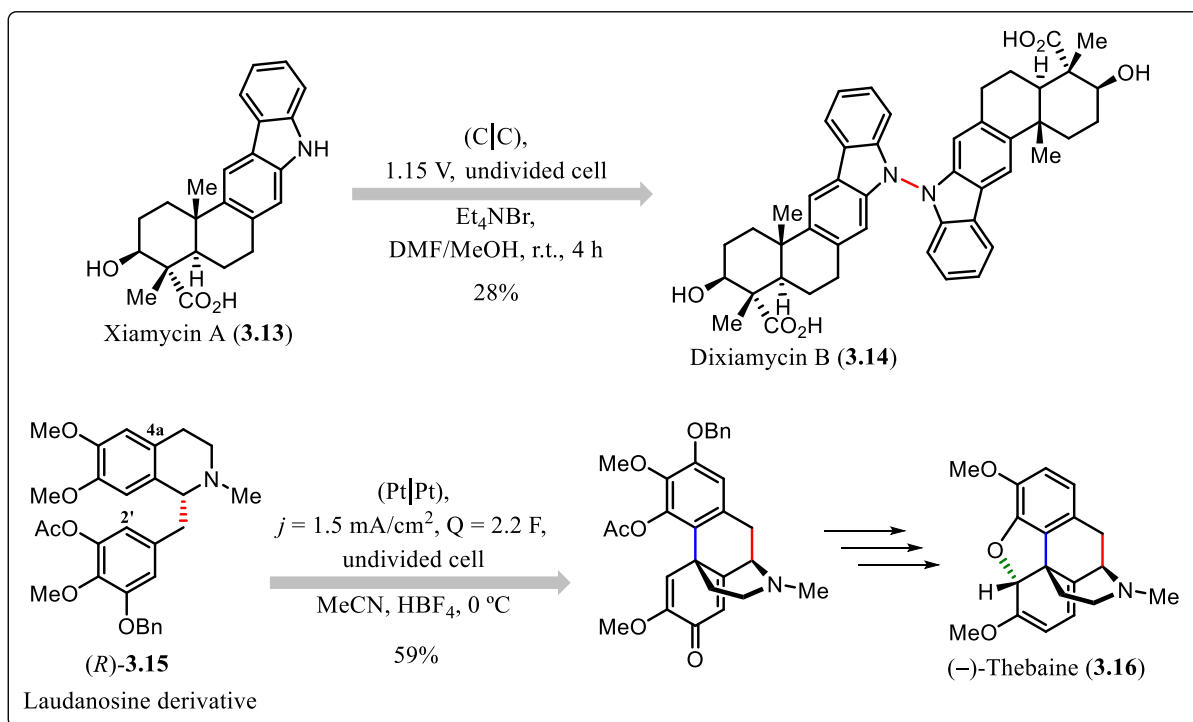
Scheme 3.1 – Indirect electrochemical allylic C–H oxidation.

One of the strengths of organic electrochemistry is the possibility of forming C–C, C–N, C–O, and C–S bonds from C–H bonds as exemplified in Scheme 3.2.^{28–31}



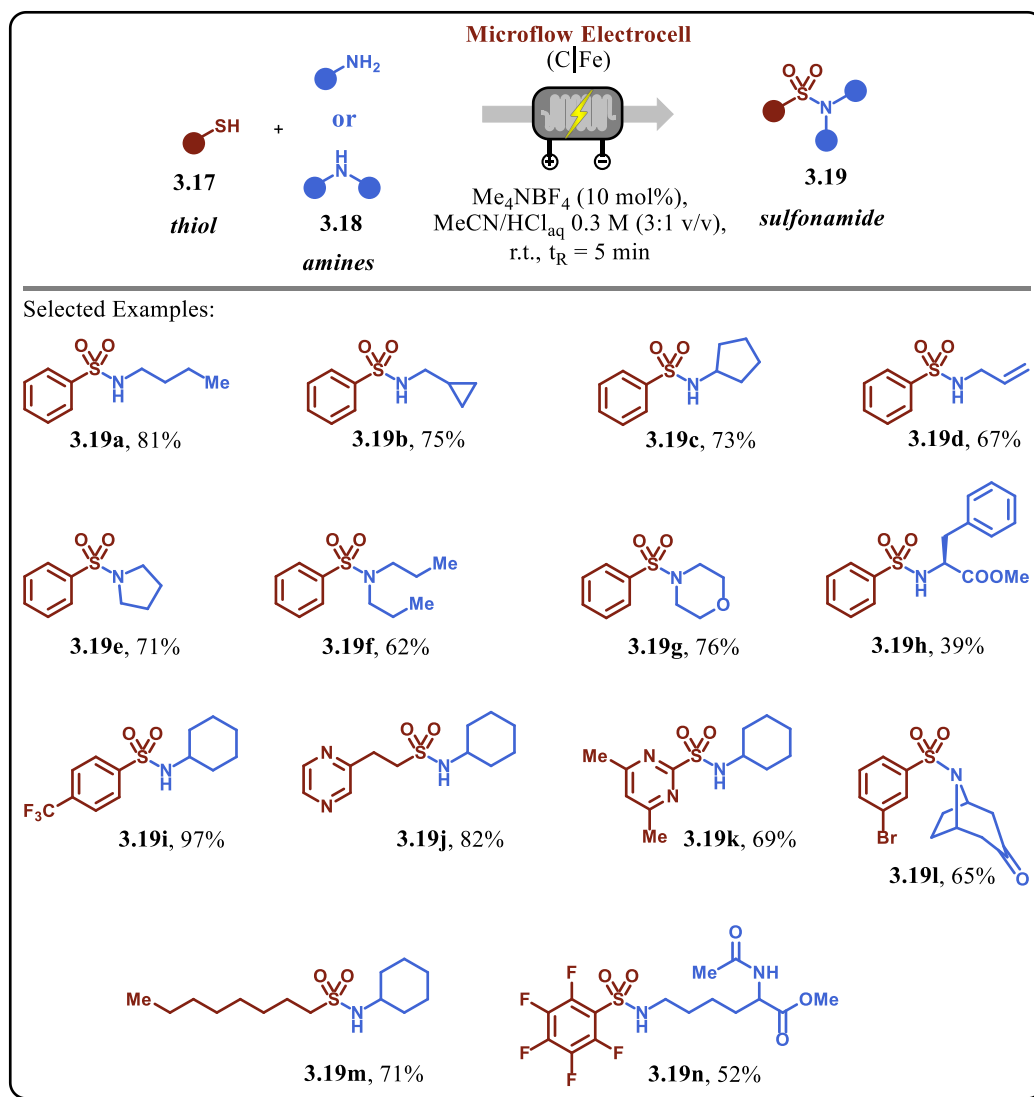
Scheme 3.2 – Electrochemically induced C–C (a), C–N (b), C–O (c), and C–S (d) bonds formation from C–H bonds.

Electrochemical methods have also been applied in the synthesis of natural products such as dixiamycin B (**3.14**) (a rare N–N linked dimeric indole alkaloid) and (–)-thebaine (**3.16**) (a minor opium alkaloid) (Scheme 3.3), and various complex scaffolds.^{18,23,32,33}



Scheme 3.3 – Electrochemical synthesis of natural products.

Just recently, Noël and co-workers (2019) developed an electrochemical approach for the synthesis of sulfonamides from thiols and amines (two readily available and inexpensive feedstocks) under continuous flow conditions (Scheme 3.4).³⁴ This novel reaction protocol requires no additional catalysts or sacrificial reagents and can be performed in only 5 min of residence time at room temperature. It also displays a broad substrate scope with respect to both coupling partners and functional group compatibility, and only H₂ is formed as a by-product at the counter electrode.



Scheme 3.4 – Electrochemical sulfonamide synthesis by direct anodic coupling of thiols and amines.

Other relevant examples of electrochemical transformations can be found in several recent reviews.^{1,4,17,18,20,26,35,36}

3.1.3 Sulfonyl fluorides

Sulfonyl fluorides are considered a privileged moiety in chemistry due to their unique balance between reactivity and stability, which is in sharp contrast with analogous sulfonyl chlorides.³⁷ In these compounds, the sulfur-fluorine bond is not very reactive. For

example, sulfonyl fluorides are resistant to reduction, hydrolytically stable, and resistant to bond cleavage in metal catalysis.³⁷⁻³⁹ In particular, sulfonyl fluorides have been successfully used in chemical biology as covalent protein modifiers, strong protease inhibitors, and activity-based probes (Figure 3.4).³⁹⁻⁴⁴ In addition, aromatic sulfonyl fluorides have been used as fluorinating reagents,⁴⁵ ¹⁸F-radiolabeling agents^{46,47} and have found applications in other useful transformations,³⁸ including polymerizations.⁴⁸⁻⁵⁰ However, the breakthrough application for sulfonyl fluorides is their utility as stable and robust sulfonyl precursors for the SuFEx click chemistry.^{37,51}

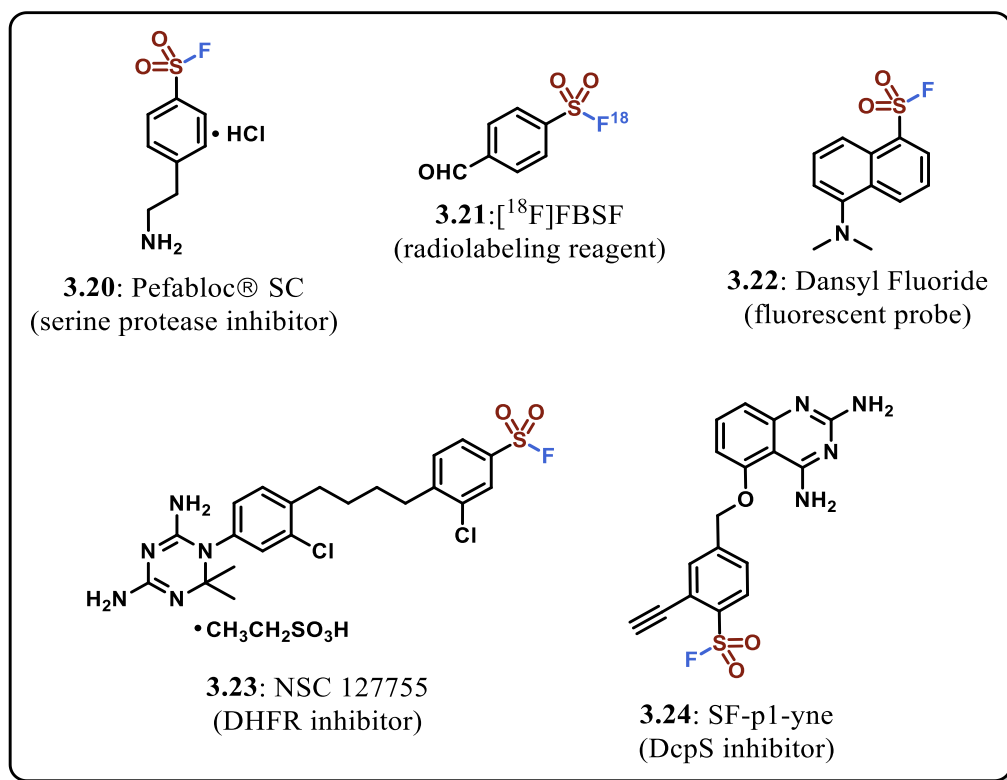


Figure 3.4 – Representative sulfonyl fluorides and their function.

Due to their evident value, efficient syntheses of sulfonyl fluorides starting from readily available and cheap starting materials are highly desired. The classical strategy to access these functional groups involves a chloride/fluoride exchange of sulfonyl chlorides using fluoride sources such as KF, KHF₂, and TBAF (Scheme 3.5, eq. a).^{37,52-54} However, sulfonyl

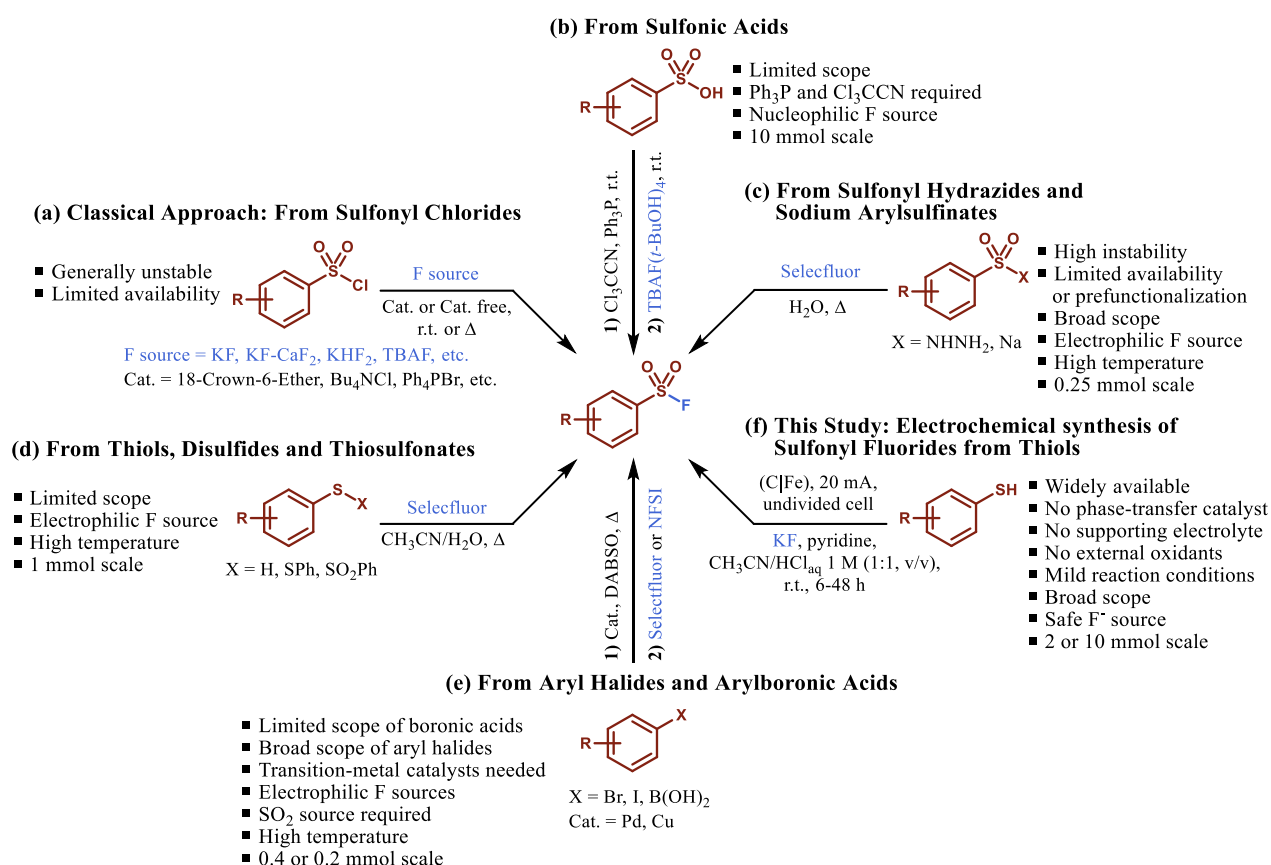
chlorides are not widely available and must be prepared from the corresponding thiols using a combination of oxidizing and chlorinating reagents.⁵⁵ In order to avoid toxic and unstable sulfonyl chlorides, new synthetic methods have been developed using alternative starting materials, including sulfonic acids (Scheme 3.5, eq. b),⁵⁶ sulfonyl hydrazides or sodium arylsulfonates (Scheme 3.5, eq. c),⁵⁷ and other starting material.⁵⁸⁻⁶⁶ Kirihara and co-workers (2011, 2014) reported a method to transform thiols, disulfides, and thiosulfonates into sulfonyl fluorides using Selectfluor and refluxing conditions (Scheme 3.5, eq. d).^{67,68} Also, transition metal-based cross-coupling strategies have been developed which utilize aryl halides and arylboronic acids in combination with DABSO and electrophilic fluorinating reagents, such as Selectfluor and NFSI (Scheme 3.5, eq. e).^{39,69,70} Despite the synthetic value of these approaches, the use of costly and atom-inefficient fluoride sources limits their feasibility for small scale applications.

It is evident that the development of a new synthetic method that directly uses commodity chemicals, such as thiols and alkaline fluoride salts, would be particularly useful given the wide availability and the low cost of these starting materials.

Even so, it is immediately clear that a number of challenges must be overcome to develop such a hitherto elusive transformation. First, fluoride is poorly soluble in organic solvents (even in highly polar aprotic solvents like DMSO)⁷¹ and is hardly reactive in its solvated form in aqueous media. Second, combining nucleophilic fluorine reagents with thiols to establish a single S–F bond appears unlikely.⁷²⁻⁷⁴

Nevertheless, based on the observation found by Noël and co-workers in the electrochemical synthesis of sulfonamides (see Scheme 3.4),³⁴ that the use of an electrolyte with BF_4^- counterion gave traces of sulfonyl fluoride under an unoptimized condition,⁷⁵ we speculated that the union of these stubborn starting materials would not only be plausible using electrochemical activation but would also facilitate the oxidation to sulfonyl fluoride via anodic oxidation.

We report herein the discovery and optimization of an electrochemical method that meets these design criteria. The method utilizes KF as a readily available, safe and cost-efficient fluoride source. Moreover, anodic oxidation allows us to avoid stoichiometric amounts of oxidants and enables the direct use of thiols or disulfides as convenient and widely available starting materials (Scheme 3.5, eq. f).



Scheme 3.5 – Established synthetic routes to prepare sulfonyl fluorides.

3.2 Results and discussion

We started our investigation by screening different solvent combinations using thiophenol (**3.25a**) with KF (5 equiv.) serving as the fluorine source, and employing graphite as anode and stainless-steel as cathode. As shown in Table 3.1, MeOH/H₂O (entry 1) and DMF (entry 2) were not effective (only disulfide was formed), while pure CH₃CN gave a

heterogeneous mixture (KF is poorly soluble in CH₃CN). Adding the minimum amount of water to get everything into solution proved to be the most effective (Table 3.1, entry 3, 65% of desired product **3.26a**). Without pyridine, only a small amount of **3.26a** was observed (entry 4). The addition of acid seemed to affect the reaction (entry 5). Employing stainless-steel as the anode, no reaction occurred and the electrode was damaged due to corrosion (Table 3.1, entry 6). Finally, we checked the unoptimized reaction condition (entry 3) in the absence of electricity, and no traces of sulfonyl fluoride **3.26a** could be detected by GC-MS after 24 h (entry 7), which shows that the reaction is electrochemically driven.

Table 3.1 – Preliminary experiments.^[a]

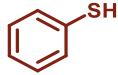
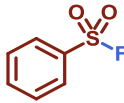
Batch Electrocell
3.2 V, undivided cell
KF (5 equiv.),
Pyridine (0 or 1 equiv.),
Solvent,
r.t., 24 h

Entry	Solvent	Electrodes	Pyridine (equiv.)	Yield (%) ^[c]
1	MeOH/H ₂ O (1:1)	C Fe	1	Traces
2	DMF	C Fe	1	0
3	CH₃CN/H₂O (1:1)	C Fe	1	65
4	CH ₃ CN/H ₂ O (1:1)	C Fe	0	7
5	CH ₃ CN/H ₂ SO ₄ 0.3 M (1:1)	C Fe	1	21
6	CH ₃ CN/H ₂ O (1:1)	Fe Fe	1	0
7 ^[b]	CH ₃ CN/H ₂ O (1:1)	C Fe	1	0

^[a]Thiophenol (2 mmol, 1 equiv.), KF (5 equiv.), pyridine (0 or 1 equiv.), solvent (20 mL), r.t., 24 h, and a constant voltage of 3.2 V. ^[b]No electricity. ^[c]GC yields were calculated using biphenyl as an internal standard.

Next, we investigated the effect of the amount of pyridine on the yield of sulfonyl fluoride **3.26a** (Table 3.2). From Table 3.2, we can see that 4 equiv. of pyridine gave a quantitative GC yield (entry 5).

Table 3.2 – Amount of pyridine.^[a]

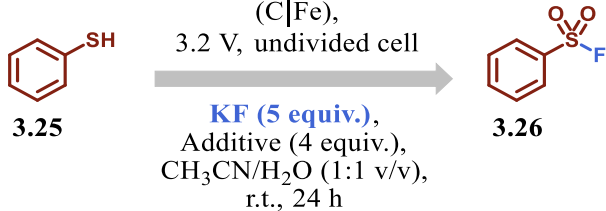
Batch Electrocell (C Fe), 3.2 V, undivided cell		
 3.25a	→	 3.26a
KF (5 equiv.), Pyridine (0 – 5 equiv.), CH ₃ CN/H ₂ O (1:1 v/v), r.t., 24 h		
Entry	Pyridine (equiv.)	Yield (%) ^[b]
1	0	7
2	1	65
3	2	75
4	3	87 (68)
5	4	98 (78)
6	5	98

^[a]Thiophenol (2 mmol, 1 equiv.), KF (5 equiv.), pyridine (0 – 5 equiv.), CH₃CN/H₂O (1:1 v/v, 20 mL), r.t., 24 h, and a constant voltage of 3.2 V. ^[b]GC yields were calculated using biphenyl as an internal standard. Isolated yields in brackets.

In addition to pyridine, other additives were also screened (Table 3.3). We believe that the additive is important for two reasons: as a phase transfer catalyst to leverage fluoride to the organic phase and as an electron mediator.^{76,77} From Table 3.3, it can be observed that only pyridine was effective in our transformation (entry 1).

Table 3.3 – Additive screening.^[a]

Batch Electrocell
(C|Fe),
3.2 V, undivided cell



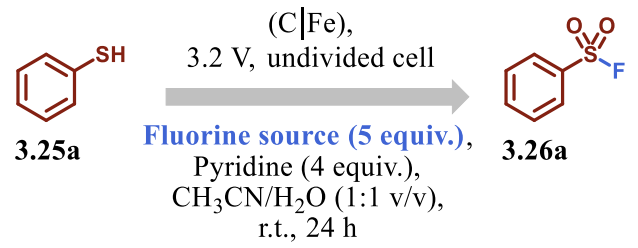
Entry	Additive (4 equiv.)	Yield (%) ^[c]
1^[b]	Pyridine	98 (78)
2	DMAP	0
3	Et ₃ N	0
4	Quinoline	4

^[a]Thiophenol (2 mmol, 1 equiv.), KF (5 equiv.), additive (4 equiv.), CH₃CN/H₂O (1:1 v/v, 20 mL), r.t., 24 h, and a constant voltage of 3.2 V. ^[b]Entry 1 depicts the result shown previously in entry 5 of Table 3.2. ^[c]GC yields were calculated using biphenyl as an internal standard. Isolated yield in brackets.

A screening of different fluorine sources was also carried out (Table 3.4). Sodium fluoride showed poor yields after 24 h, probably because of its poor solubility (entry 2). TBAF showed low conversion as well (Table 3.4, entry 4), while the more expensive and highly soluble CsF (72 \$/mol)⁷⁸ proved to be effective (entry 3). With Selectfluor, an electrophilic fluorine source, full conversion was observed as well (entry 5). However, in comparison to KF, the use of Selectfluor is not preferred due to the high cost of this reagent (KF 8 \$/mol vs Selectfluor 407 \$/mol).⁷⁸

Table 3.4 – Fluorine sources.^[a]

Batch Electrocell
(C|Fe),
3.2 V, undivided cell



Entry	Fluorine source (5 equiv.)	Yield (%) ^[d]
1 ^[b]	KF	98 (78)
2	NaF	23
3	CsF	75
4	TBAF	18
5 ^[c]	Selectfluor	99

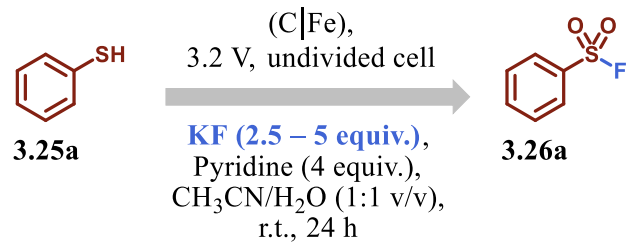
^[a]Thiophenol (2 mmol, 1 equiv.), fluorine source (5 equiv.), pyridine (4 equiv.), CH₃CN/H₂O (1:1 v/v, 20 mL), r.t., 24 h, and a constant voltage of 3.2 V. ^[b]Entry 1 depicts the result shown previously in entry 5 of Table 3.2. ^[c]With 1.5 equiv. of Selectfluor. ^[d]GC yields were calculated using biphenyl as an internal standard. Isolated yield in brackets.

We also evaluated the total amount of KF required for this electrochemical transformation (Table 3.5). From Table 3.5, we can see that 5 equiv. of KF was optimal (entry 1). With lower amounts, a decrease in yield was observed (entries 2 and 3). This result might indicate that KF also acts as a supporting electrolyte.

In order to verify our hypothesis, the reaction was carried out in the presence of supporting electrolytes (Table 3.6). From Table 3.6, we can see that by adding electrolyte, the total amount of KF could be reduced. Bu₄NClO₄ worked particularly well (entry 2), while LiClO₄ did not show any improvement (entries 3 and 4). However, since KF is considerably cheaper than any supportive electrolyte, we decided to keep a higher amount of this fluoride source.

Table 3.5 – Evaluation of the total amount of KF.^[a]

Batch Electrocell
(C|Fe),
3.2 V, undivided cell

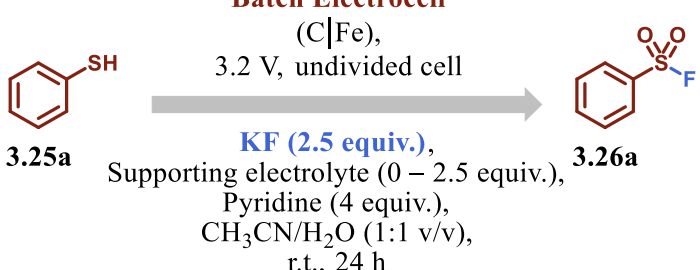


Entry	KF (equiv.)	Yield (%) ^[c]
1 ^[b]	5	98 (78)
2	4	84
3	2.5	40

^[a]Thiophenol (2 mmol, 1 equiv.), KF (2.5 – 5 equiv.), pyridine (4 equiv.), CH₃CN/H₂O (1:1 v/v, 20 mL), r.t., 24 h, and a constant voltage of 3.2 V. ^[b]Entry 1 depicts the result shown previously in entry 5 of Table 3.2. ^[c]GC yields were calculated using biphenyl as an internal standard. Isolated yield in brackets.

Table 3.6 – Influence of supporting electrolyte.^[a]

Batch Electrocell
(C|Fe),
3.2 V, undivided cell



Entry	Supporting electrolyte (equiv.)	Yield (%) ^[b]
1	No electrolyte	40
2	Bu ₄ NClO ₄ (1)	74
3	LiClO ₄ (1)	39
4	LiClO ₄ (2.5)	22

^[a]Thiophenol (2 mmol, 1 equiv.), KF (2.5 equiv.), supporting electrolyte (0 – 2.5 equiv.), pyridine (4 equiv.), CH₃CN/H₂O (1:1 v/v, 20 mL), r.t., 24 h, and a constant voltage of 3.2 V. ^[b]GC yields were calculated using biphenyl as an internal standard.

Similar results were obtained in 24 h when the current was varied from 20 to 40 mA (Table 3.7, entries 1–3). Nevertheless, we also observed that the rate of decomposition of the product increased at higher current density, especially at reaction times longer than 24 h.

Therefore, we decided to go for a milder reaction using a lower current density (4.2 mA/cm²) (Table 3.7, entry 1, galvanostatic conditions).

Table 3.7 – Constant current screening.^[a]

Batch Electrocell
(C|Fe),
20 – 40 mA, undivided cell
KF (5 equiv.),
Pyridine (4 equiv.),
CH₃CN/H₂O (1:1 v/v),
r.t., 24 h

Entry	Current applied (mA)	Current density (mA/cm ²) ^[b]	Yield (%) ^[c]
1	20	4.2	80
2	30	6.2	81
3	40	8.3	81

^[a]Thiophenol (2 mmol, 1 equiv.), KF (5 equiv.), pyridine (4 equiv.), CH₃CN/H₂O (1:1 v/v, 20 mL), r.t., 24 h, and a constant current of 20 to 40 mA. ^[b]Total active area 4.8 cm². ^[c]GC yields were calculated using biphenyl as an internal standard.

When the most optimal conditions (Tables 3.2 and 3.7; entries 5 and 1, respectively) were tested for various substrates (e.g., 4-chlorothiophenol, 4-bromothiophenol, 4-methylthiophenol, 2-mercaptopyridine, and others), we found out that some of those were not working. In order to establish more general reaction conditions, we carried out a small re-optimization (under galvanostatic conditions) which would be compatible with most substrates. At this point, 4,6-dimethylpyrimidine-2-thiol (**3.25b**) was used as a benchmark molecule to optimize the new conditions (see Table 3.8).

Table 3.8 – Further optimization screening.^[a]

Batch Electrocell
(C|Fe),
20 mA, undivided cell

KF (5 equiv.),
Pyridine (0 – 4 equiv.),
Additive (0 – 1 equiv.),
Solvent,
r.t., 12–48 h

Entry	Solvent	Additive (equiv.)	Pyridine (equiv.)	Time (h)	Yield (%) ^[b]
1	CH ₃ CN/H ₂ O (1:1)	None	4	24	Traces
2	CH ₃ CN/H ₂ O (1:1)	18-crown-6 (0.1)	4	24	Traces
3	CH ₃ CN/H ₂ O (1:1)	18-crown-6 (0.5)	4	24	Traces
4	CH ₃ CN/H ₂ O (1:1)	Bu ₄ NClO ₄ (1)	4	24	10
5	CH ₃ CN/H ₂ O (1:1)	Bu ₄ NCl (1)	4	24	11
6	CH ₃ CN/HCl 0.1 M (1:1)	None	4	24	Traces
7	CH ₃ CN/HCl 0.1 M (1:1)	Bu ₄ NCl (0.05)	4	24	14
8	CH ₃ CN/HCl 0.3 M (1:1)	None	4	24	35
9	CH ₃ CN/HCl 0.3 M (1:1)	None	4	48	9
10	CH ₃ CN/HCl 0.5 M (1:1)	None	4	18	31
11	CH ₃ CN/HCl 0.5 M (1:1)	None	4	24	25
12	CH ₃ CN/HCl 1 M (1:1)	None	4	12	45
13	CH₃CN/HCl 1 M (1:1)	None	1	12	77 (74)
14	CH ₃ CN/HCl 1 M (1:1)	None	1.5	12	56
15	CH ₃ CN/HCl 1 M (1:1)	None	2	12	51
16	CH ₃ CN/HCl 1 M (1:1)	None	3	12	50
17	CH ₃ CN/HCl 1 M (1:1)	None	0	12	54
18	CH ₃ CN/ <i>p</i> -TsOH 1 M (1:1)	None	1	12	25

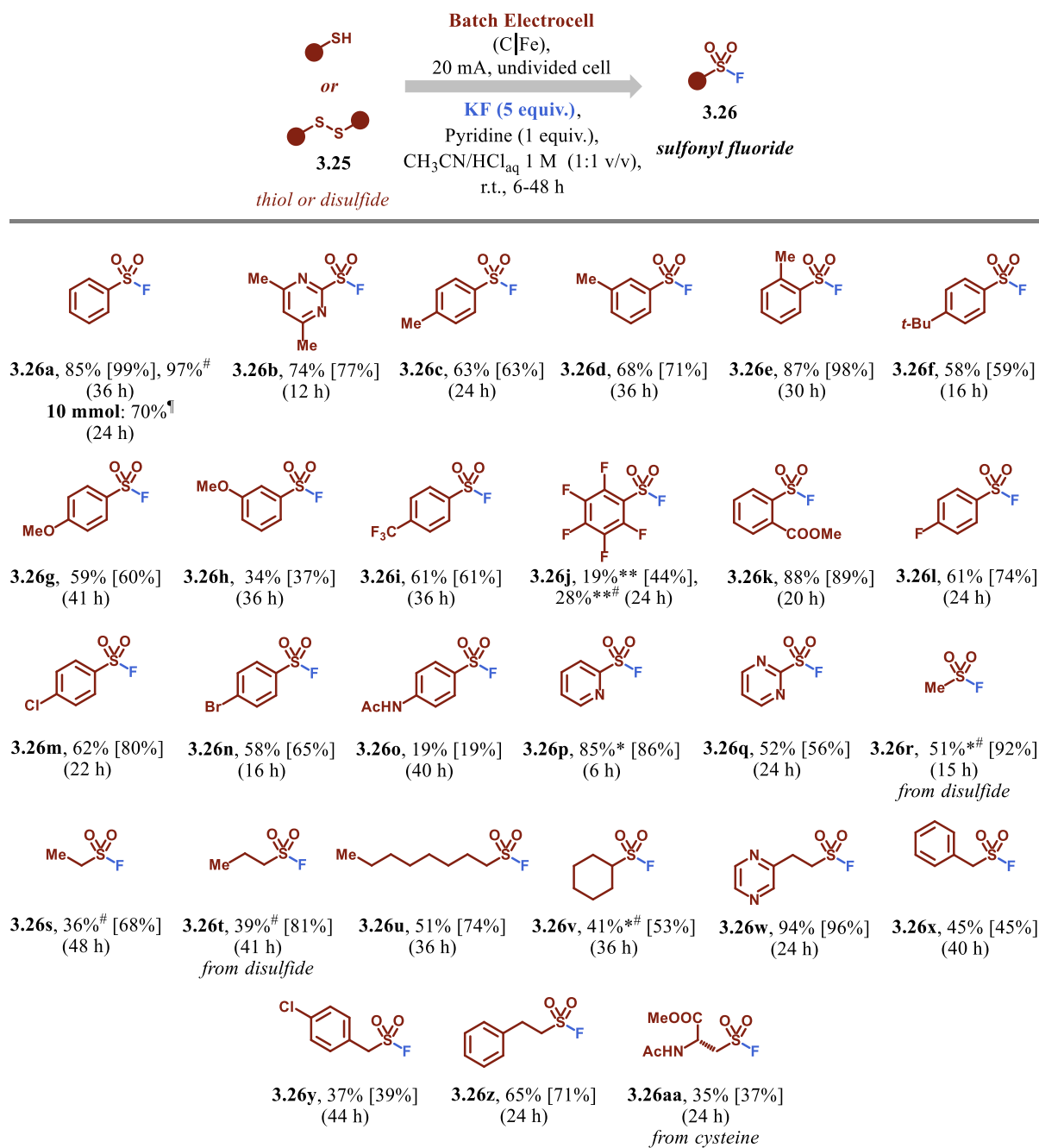
^[a]4,6-Dimethylpyrimidine-2-thiol (2 mmol, 1 equiv.), KF (5 equiv.), pyridine (0 – 4 equiv.), additive (0 – 1 equiv.), solvent (20 mL), r.t., 12–48 h, and a constant current of 20 mA (4.2 mA/cm²). ^[b]Yields were calculated by ¹⁹F NMR using trifluorotoluene as an internal standard. Isolated yield in brackets.

Only traces of sulfonyl fluoride **3.26b** were observed using the standard conditions (Table 3.8, entry 1). Taking into account the biphasic nature of our reaction mixture, we evaluated the need for an additional phase transfer catalyst, as reported in literature.⁵⁴ To our surprise, 18-crown-6 did not increase conversion whatsoever (entries 2 and 3), while with Bu₄NClO₄ and Bu₄NCl only around 10% of the fluorinated product **3.26b** was obtained (entries

4 and 5). Next, the addition of an acid was investigated (Table 3.8, entries 6–18). A low concentration of acid showed only traces of **3.26b** (entry 6), while the addition of a catalytic amount of Bu₄NCl led to 14% of NMR yield (entry 7). Increasing the concentration of acid resulted in higher yields (entries 8–12) and with 1 M HCl good NMR yield was observed (45%, entry 12). Notably, prolonged reaction times led to consistent decreases in yield due to degradation (compare entries 8 and 9, 10 and 11). Next, the amount of pyridine was investigated (Table 3.8, entries 13–17). A stoichiometric amount of pyridine resulted in the highest yield (77%, entry 13). Further increments were detrimental under these new conditions (entries 14–16). Notably, the reaction occurred even without pyridine (entry 17), but a lower yield (54%) was observed in this case. Finally, PTSA was tested instead of HCl (entry 18). As a result, the sulfonyl fluoride **3.26b** was obtained in only 25% NMR yield.

With the optimal conditions in hands (Table 3.8, entry 13), we next turned our attention to examine the generality of this electrochemical transformation (Scheme 3.6).

As shown in Scheme 3.6, a wide variety of structurally and electronically distinct thiols can be transformed into the corresponding sulfonyl fluorides. First, with a diverse set of thiophenols, it was determined that substrates bearing electron-neutral (**3.26a**, **3.26c–f**), -donating (**3.26g,h**) and -withdrawing substituents (**3.26i–k**) were all compatible with the reaction conditions; the NMR yields ranged from 37 to 99%. Due to the volatility of some products, isolated yields were in some cases lower than observed with ¹⁹F NMR. This could be partially avoided by converting the obtained volatile sulfonyl fluoride *in situ* to the corresponding sulfonate through reaction with phenol (e.g., **3.26a**). The electrochemical reaction is not particularly sensitive to steric hindrance, as *ortho*-substituted thiophenols displayed similar yields to unsubstituted variants (**3.26a** versus **3.26e**). Also, halogenated thiophenols (**3.26l–n**) were suitable reaction partners (NMR yields 65–80%), providing opportunities to further functionalize the formed sulfonyl fluorides using cross-coupling chemistry.



Scheme 3.6 – Substrate scope for the electrochemical sulfonyl fluoride synthesis. Reported yields are isolated and reproduced at least two times. Yields between [brackets] are those referring to ¹⁹F NMR yields calculated with PhCF₃ as an internal standard. Reaction conditions: thiol (2 mmol) or disulfide (1 mmol), KF (5 equiv.), pyridine (1 equiv.), CH₃CN/HCl_{aq} 1 M (20 mL, 1:1 v/v), C anode/Fe cathode, 20 mA (4.2 mA/cm²). *3.2 V applied potential. **4.0 V applied potential. [#]Isolated as a phenyl sulfonate derivative through reaction with phenol. [¶]Scale-up reaction conditions: thiophenol (10 mmol), KF (5 equiv.), pyridine (1 equiv.), CH₃CN/HCl_{aq} 1 M (40 mL, 1:1 v/v), C anode/Fe cathode, 3.2 V applied potential.

Protected amines (**3.26o**), previously unreactive substrates in the electrochemical sulfonamide chemistry,³⁴ were tolerated under the current reaction conditions, albeit with a lower NMR yield of 19%. Heterocyclic thiols (**3.26b,p,q**), which are among the most widely used moieties in pharmaceutical and agrochemical syntheses,^{79,80} were also effective for this transformation (NMR yields 56–86%). Notably, compound **3.26q** is also known as PyFluor, an effective deoxyfluorination reagent reported by Doyle and co-workers (2015).⁴⁵

We next examined a variety of different primary and secondary aliphatic thiols, including methanethiol (**3.26r**), ethanethiol (**3.26s**), propanethiol (**3.26t**), *n*-octanethiol (**3.26u**), cyclohexylthiol (**3.26v**), pyrazineethanethiol (**3.26w**), benzylthiol (**3.26x**), *p*-chlorobenzylthiol (**3.26y**), 2-phenylethanethiol (**3.26z**) and cysteine (**3.26aa**). All proved to be competent reaction partners yielding the corresponding sulfonyl fluorides in synthetically useful NMR yields (37–96%). By using corresponding disulfides, the most volatile and odorous thiols can be avoided (**3.26r,t**). Interestingly, we were able to engage cysteine (**3.26aa**) in our electrochemical sulfonyl fluoride protocol, providing opportunities to prepare new nonproteinogenic amino acid building blocks.

A list of unsuccessful substrates is given in Figure 3.5. Regarding thiols, reactions with tertiary thiols (**3.30–3.33**) and most heterocyclic thiols (e.g., **3.42–3.45**) showed decomposition, due to the cleavage of C–S bond. Steric hindrance can compromise the formation of the disulfide. 2-Naphthalenethiol (**3.41**) showed low solubility in the reaction medium and only traces of product could be observed. With allyl mercaptan (**3.28**), cyclopentanethiol (**3.29**), and 1-thio- β -D-glucose tetraacetate (**3.46**) only poor conversions were observed. Surprisingly, with 2-furanmethanethiol (**3.27**) only traces of product were detected via GC-MS. Unfortunately, this method seemed to be incompatible with thiols containing nitro (**3.37**), amino (**3.39**) or hydroxyl (**3.38, 3.40**) groups.

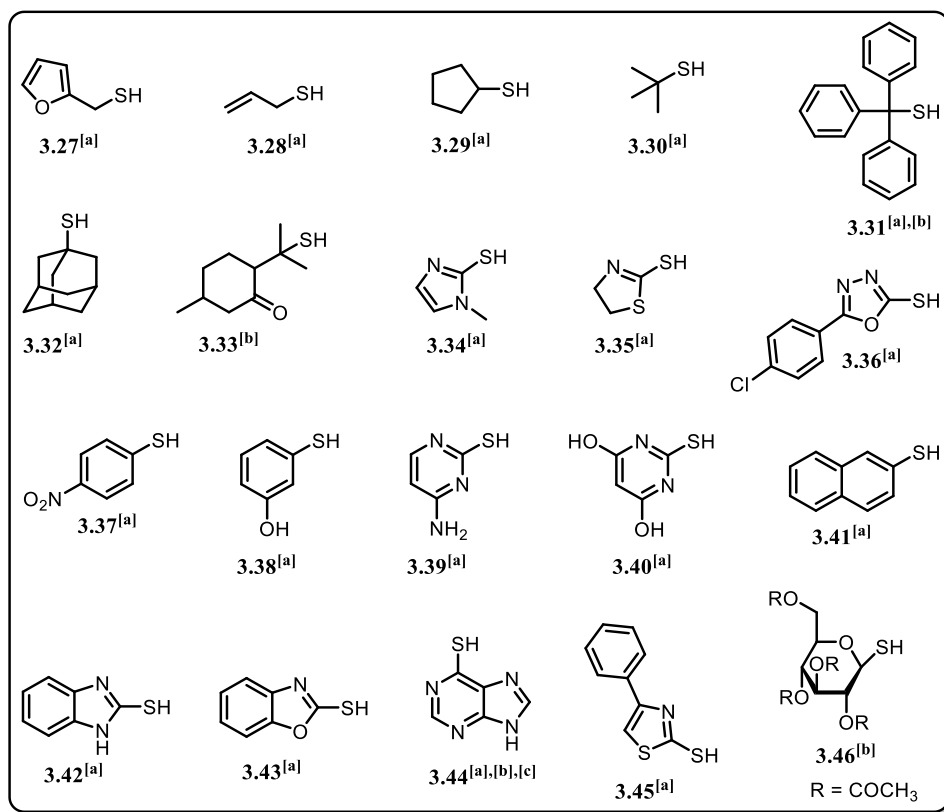


Figure 3.5 – List of unsuccessful substrates in our electrochemical approach. ^[a]Reaction conditions: thiol (2 mmol), KF (5 equiv.), pyridine (1 equiv.), CH₃CN/HCl_{aq} 1 M (20 mL, 1:1 v/v), C anode/Fe cathode, 20 mA (4.2 mA/cm²). ^[b]3.2 V applied potential. ^[c]4.0 V applied potential.

To obtain insights into the underlying mechanism, several additional experiments were carried out (see Figure 3.6 below and Sections 3.5 and 3.6).

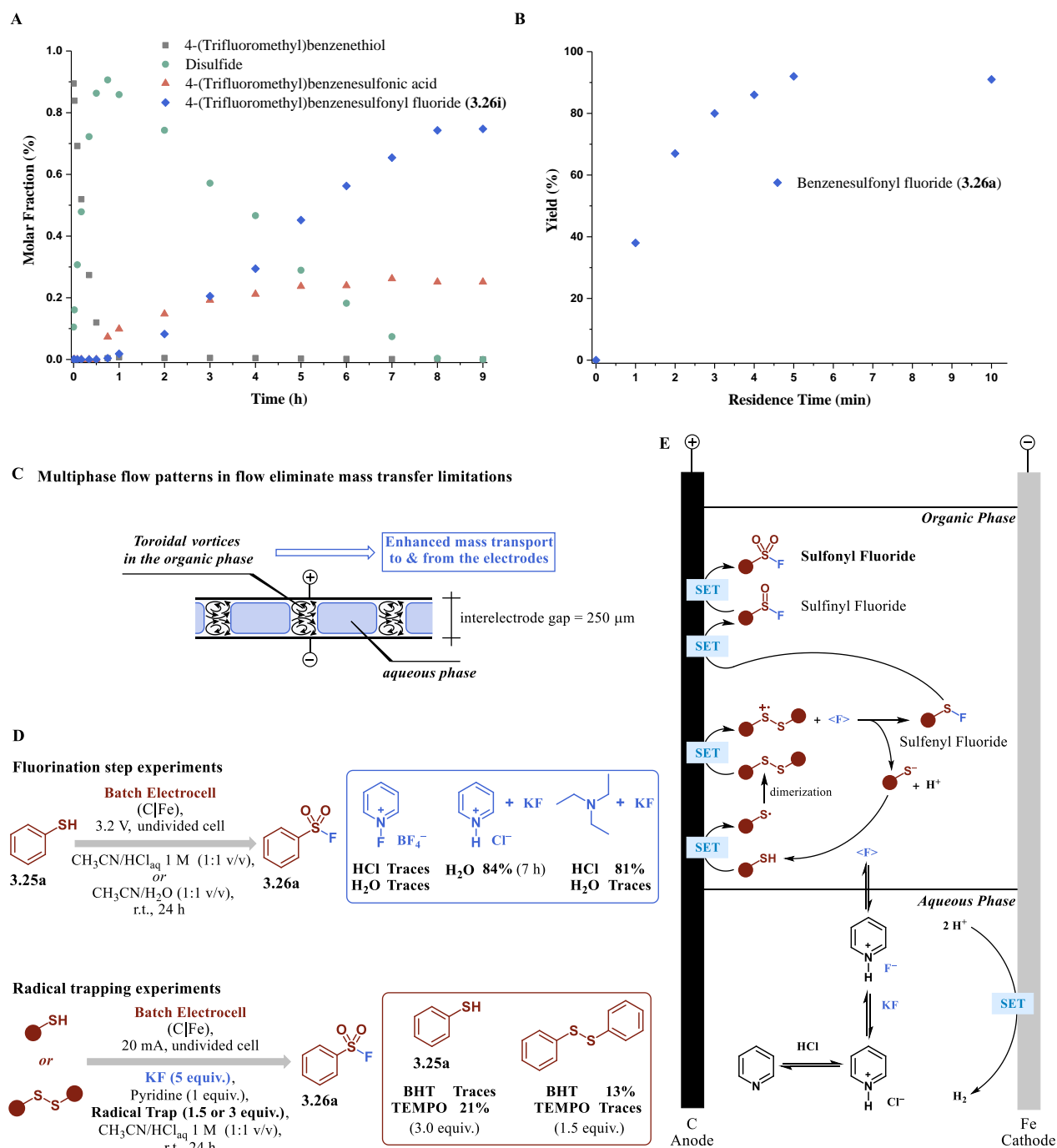


Figure 3.6 – Mechanistic investigation of the electrochemical sulfonyl fluoride synthesis. **(A)** ^{19}F NMR kinetic batch experiment (see Section 3.4.4.5). **(B)** Kinetic experiment carried out in an electrochemical microreactor (GC-FID, see Section 3.4.4.6). **(C)** Toroidal vortices in segmented flow result in enhanced mass transport to and from the electrodes. **(D)** Fluorination step experiments and radical trapping experiments. GC yield (biphenyl as an internal standard). **(E)** Proposed mechanism 1.

Kinetic experiments revealed a rapid conversion of 4-(trifluoromethyl)thiophenol via anodic oxidation to the corresponding disulfide within 45 min (Figure 3.6A). Next, the disulfide intermediate is consumed and the corresponding sulfonyl fluoride (**3.26i**) is formed. The pseudo-zero-order behavior suggests that mass transfer limitations from the bulk to the electrode surface occur during the batch electrochemical transformation.

Indeed, when the reaction is carried out in an electrochemical microflow reactor with a small interelectrode gap (250 μm),⁸¹ full conversion of thiol **3.25a** is observed in only 5 min reaction time (Figure 3.6B). The reduced reaction times observed in flow can be attributed to (i) the increased electrode surface-to-volume ratio, (ii) a high interfacial area between the organic and the aqueous phase and (iii) an intensified mass transport to and from the electrodes due to multiphase fluid patterns (Figure 3.6C).^{21,82-84}

Oxidation of the disulfide results in the formation of a radical cation⁸⁵ which can react further with nucleophilic fluoride to yield the corresponding sulfonyl fluoride, with the release of thiolate anion (by getting a hydrogen, thiolate anion becomes thiol) (Figure 3.6E). At this point, we still wondered whether a nucleophilic or electrophilic fluorination, with an *in situ* generated 1-fluoropyridinium reagent, was operative under these reaction conditions. Hence, we carried out the reaction in the presence of 1-fluoropyridinium tetrafluoroborate and observed only traces of product **3.26a** (Figure 3.6D). In contrast, using either HCl-pyridine or HCl-Et₃N in combination with KF allowed us to obtain **3.26a** in high NMR yields (Figure 3.6D), indicating the presence of a nucleophilic fluorination. Adding TEMPO or BHT as radical scavengers reduced the efficacy of the electrochemical process (Figure 3.6D), validating the presence of radical intermediates.

Next, two consecutive oxidation steps resulted in the formation of the targeted sulfonyl fluoride (**3.26i**). Unfortunately, attempts to detect and/or isolate key intermediates

(sulfenyl fluoride and sulfinyl fluoride) have been unsuccessful, as they are generally perceived as unstable.^{86,87}

The main by-product formed in the electrochemical sulfonyl fluoride synthesis is probably sulfonic acid (see Figure 3.6A and Figure 3.10 in Section 3.5, respectively), which originates from anodic oxidation of disulfides or through hydrolysis of sulfonyl fluorides.⁸⁸

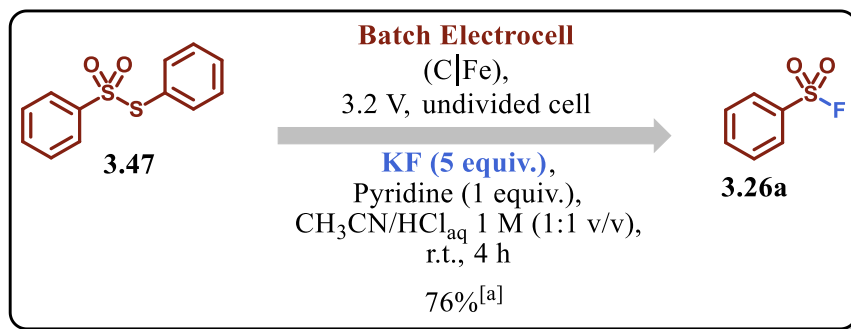
3.2.1 Additional studies after the publication

Formally, we were not able to rule out a nucleophilic attack of fluoride to the disulfide radical (Figure 3.6E) nor characterize the sulfinyl fluoride, leaving some doubts about the last steps of our mechanistic proposal. As it is obvious, there was an urgency to communicate these results in the literature due to the significance of this discovery, and we decided to publish even in the absence of a fully elucidated mechanism. Fortunately, the editor and referee's from JACS assured us that, at that moment, there was no need for a fully elucidated mechanism. However, we decided to invest some time to elucidate it more after the publication (Schemes 3.7 and 3.8 and Figure 3.7).

Basically, additional experiments using adequate GC-MS conditions allowed us to promptly detect the disulfide, and after some hours the intermediate *S*-phenyl benzenethiosulfonate **3.47** (see Figure 3.7H)⁸⁹ was completely consumed giving the sulfonyl fluoride **3.26a**. Moreover, when the reaction was performed starting with thiosulfonate **3.47**, under the same reaction conditions, the corresponding sulfonyl fluoride **3.26a** was obtained in 76% GC yield after 4 h (see Scheme 3.7 and Figure 3.7E–G).

Later, in our laboratory in São Carlos/Brazil, we continued to investigate the mechanism of this electrochemical reaction. Unsurprisingly, in the absence of electricity, the same reaction from *S*-phenyl benzenethiosulfonate **3.47** (1 mmol scale) provided no traces of the expected sulfonyl fluoride **3.26a** after 12 h (monitored by TLC). However, when the

electrochemical cell was put into operation, full conversion of thiosulfonate **3.47** to sulfonyl fluoride **3.26a** was accomplished within 4 h in excellent isolated yield (93%), which shows that the last step of the mechanism (see Scheme 3.8) is also electrochemically driven.



Scheme 3.7 – Electrochemical synthesis of sulfonyl fluoride from thiosulfonate. ^[a]GC yield.

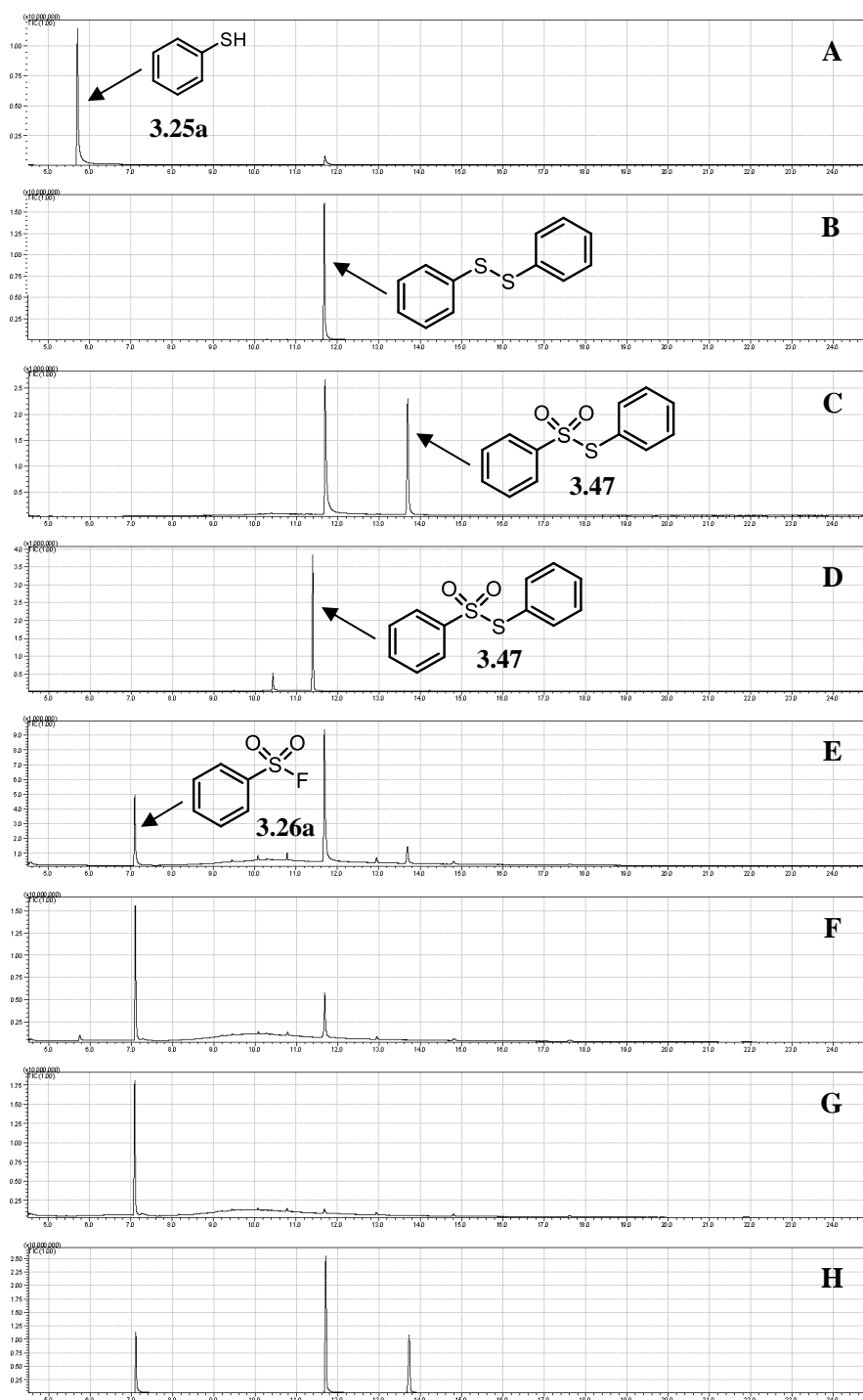
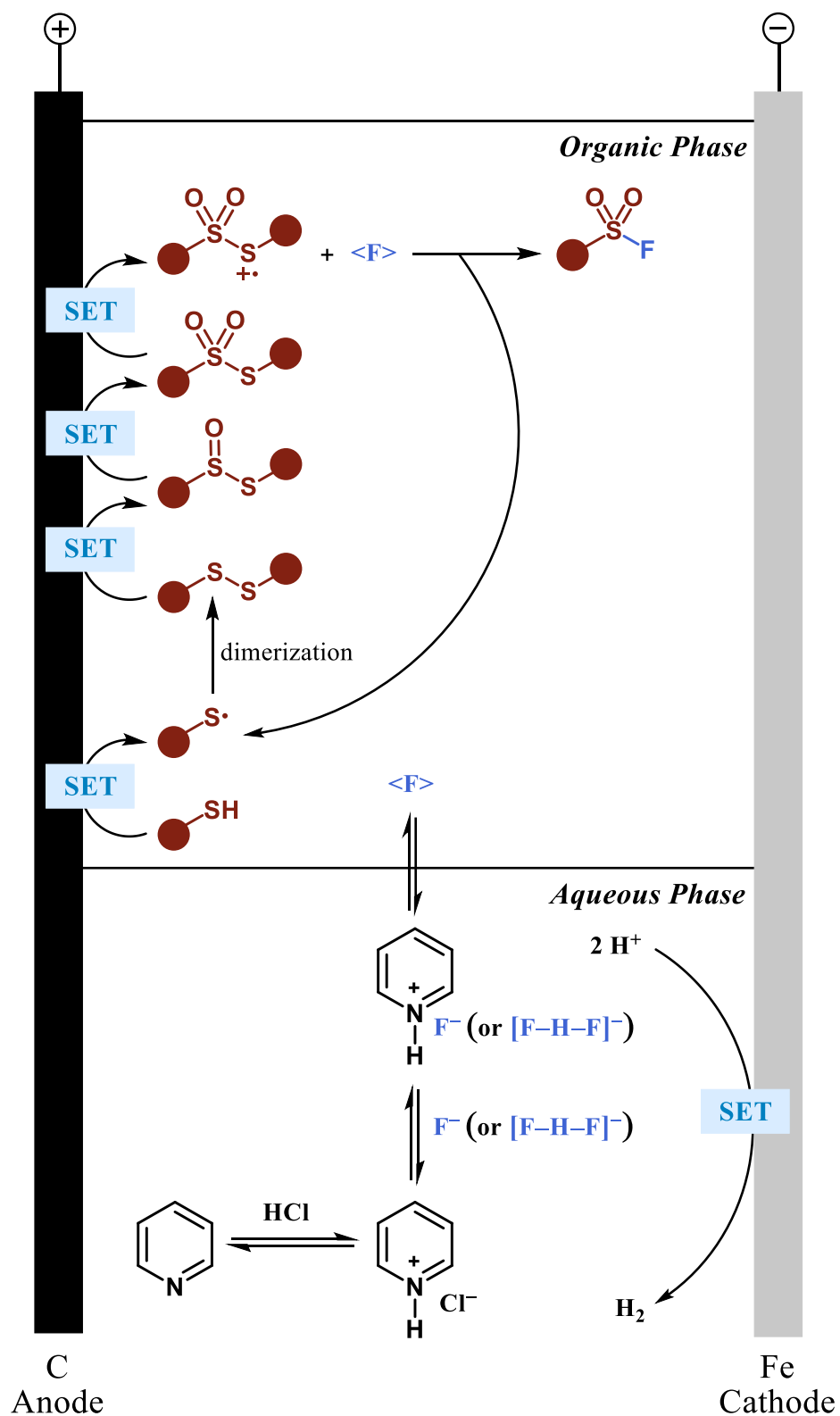


Figure 3.7 – (A) *GC-MS chromatogram of PhSH. (B) *GC-MS chromatogram of PhSSPh. (C) *GC-MS chromatogram of PhSO₂SPh. (D) **GC-MS chromatogram of PhSO₂SPh. (E) *GC-MS chromatogram for the synthesis of PhSO₂F from PhSO₂SPh after 1 h. (F) *GC-MS chromatogram for the synthesis of PhSO₂F from PhSO₂SPh after 2 h. (G) *GC-MS chromatogram for the synthesis of PhSO₂F from PhSO₂SPh after 4 h. (H) *GC-MS chromatogram for the synthesis of PhSO₂F from PhSH after 6 h (Scale-up experiment).

*DB-5ms column. **Rxi-1ms column.



Scheme 3.8 – Proposed mechanism 2.

3.3 Conclusion

The electrochemical approach described herein demonstrates the ability to directly convert thiols or disulfides into sulfonyl fluorides using KF as an ideal fluoride source in terms of cost, safety, and availability. No additional oxidants nor additional catalysts are required and, due to mild reaction conditions, the reaction displays a broad substrate scope (27 examples, 19–97% isolated yield), including a variety of alkyl, benzyl, aryl, and heteroaryl thiols or disulfides.

Kinetic and other additional studies (such as radical trapping and fluorination step experiments) were performed in an attempt to clarify the reaction mechanism. The kinetic experiments revealed a rapid conversion of thiol to disulfide and the formation of traces of other fluorinated species such as *S*-phenyl benzenethiosulfonate, which was also detected using adequate GC-MS conditions. The radical trapping experiments with different radical scavengers (TEMPO, BHT, and benzoquinone) did not afford any radical trapped species, but the efficacy of the electrochemical process was reduced under such conditions, indicating the presence of radical intermediates. The fluorination step experiments suggested the formation in equilibrium of $\text{py}\cdot\text{HCl}$ and then via anion exchange leads to a highly reactive anionic species ($\text{py}\cdot\text{HF}$ or $[\text{pyH}]^+[\text{F}-\text{H}-\text{F}]^-$ adduct). However, we also cannot rule out the possibility that a bifluoride $[\text{F}-\text{H}-\text{F}]^-$ anion is acting as a nucleophilic fluorination agent.

Furthermore, through additional experiments, we were able to show that *S*-phenyl benzenethiosulfonate is the likely precursor of the sulfonyl fluoride and its conversion is also electrochemically driven; however, the proof of the final nucleophilic attack remained to be elucidated. It is important to mention that electrochemical mechanisms are still quite challenging since many reactions and setups are under development as a new hot topic in organic chemistry.

3.4 Experimental

3.4.1 General information

All reagents and solvents were used as received without further purification. Reagents and solvents were bought from Sigma Aldrich, TCI, and Fluorochem. Technical solvents were bought from VWR International and Biosolve and used as received. All capillary tubing and microfluidic fittings were purchased from IDEX Health & Science. Disposable syringes were from BD Discardit II[®] or NORM-JECT[®], purchased from VWR Scientific. Syringe pumps were purchased from Chemix Inc. model Fusion 200 Touch. Product isolation was performed manually using silica (60, F254, Merck[™]) or automatically by a Biotage[®] Isolera[™] Spektra Four, with Biotage[®] SNAP KP-Sil 25 or 50 g flash chromatography cartridges. TLC analysis was performed using silica on aluminum foils TLC plates (F254, Supelco Sigma-Aldrich[™]) with visualization under ultraviolet light (254 nm and 365 nm) or appropriate TLC staining. The cyclic voltammetry analyses were performed with an IVIUM CompactStat. ¹H (400MHz), ¹⁹F (400MHz) and ¹³C (100MHz) spectra were recorded at r.t. using a Bruker-Avance 400. ¹H NMR spectra are reported in parts per million (ppm) downfield relative to CDCl₃ (7.26 ppm) and all ¹³C NMR spectra are reported in ppm relative to CDCl₃ (77.2 ppm) unless stated otherwise.

NMR spectra uses the following abbreviations to describe the multiplicity: s = singlet, d = doublet, t = triplet, q = quartet, p = pentet, h = hextet, hept = heptet, m = multiplet, dd = double doublet, td = triple doublet, etc. All NMR data were processed using the MestReNova 9.0.1 software package. Known products were characterized by comparing to the corresponding ¹H NMR, ¹⁹F NMR, and ¹³C NMR from literature. GC analyses were performed on a GC-MS combination (Shimadzu GC-2010 Plus coupled to a Mass Spectrometer; Shimadzu GCMS-QP 2010 Ultra) with an auto sampler unit (AOC-20i, Shimadzu). Melting points were

determined with a Buchi B-560 capillary melting point apparatus in open capillaries and are uncorrected. The names of all products were generated using the PerkinElmer ChemDraw Ultra v.12.0.2 software package.

3.4.2 Electrochemical reactor

For the electrochemical continuous-flow reaction, a homemade flow cell was used together with a Velleman LABPS3005D power supply (Figure 3.8). The cell consists of a working electrode and a counter electrode, with a PTFE gasket containing micro-channels in between. The material used for the electrodes were stainless-steel electrode (316L) and graphite AC-K800 premium grade (purchased by AgieCharmilles). The active reactor volume is 700 μL . This results in an undivided electrochemical cell. In the cell, direct contact between the electrode surface and the reaction mixture is established. The reaction mixture is pumped through the system via a syringe pump and is collected in a glass vial. All the technical data of the electrochemical microreactor are reported elsewhere.⁸¹

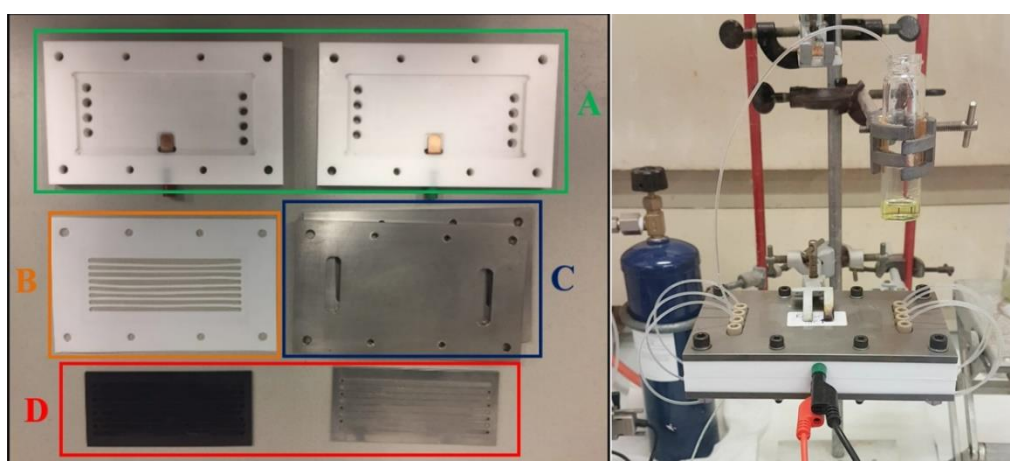


Figure 3.8 – **Right:** Assembled electrochemical flow reactor. **Left:** Components of the flow reactor. **A:** PTFE electrode holders. **B:** PTFE gasket (8 channel configuration). **C:** Outer stainless-steel plates. **D:** Electrodes (Left graphite, Right stainless-steel).

For the batch electrochemical reactions, a glassy vessel was used, equipped with electrodes connected to a Velleman LABPS3005D power supply with crocodile clamps (Figure 3.9).³⁴

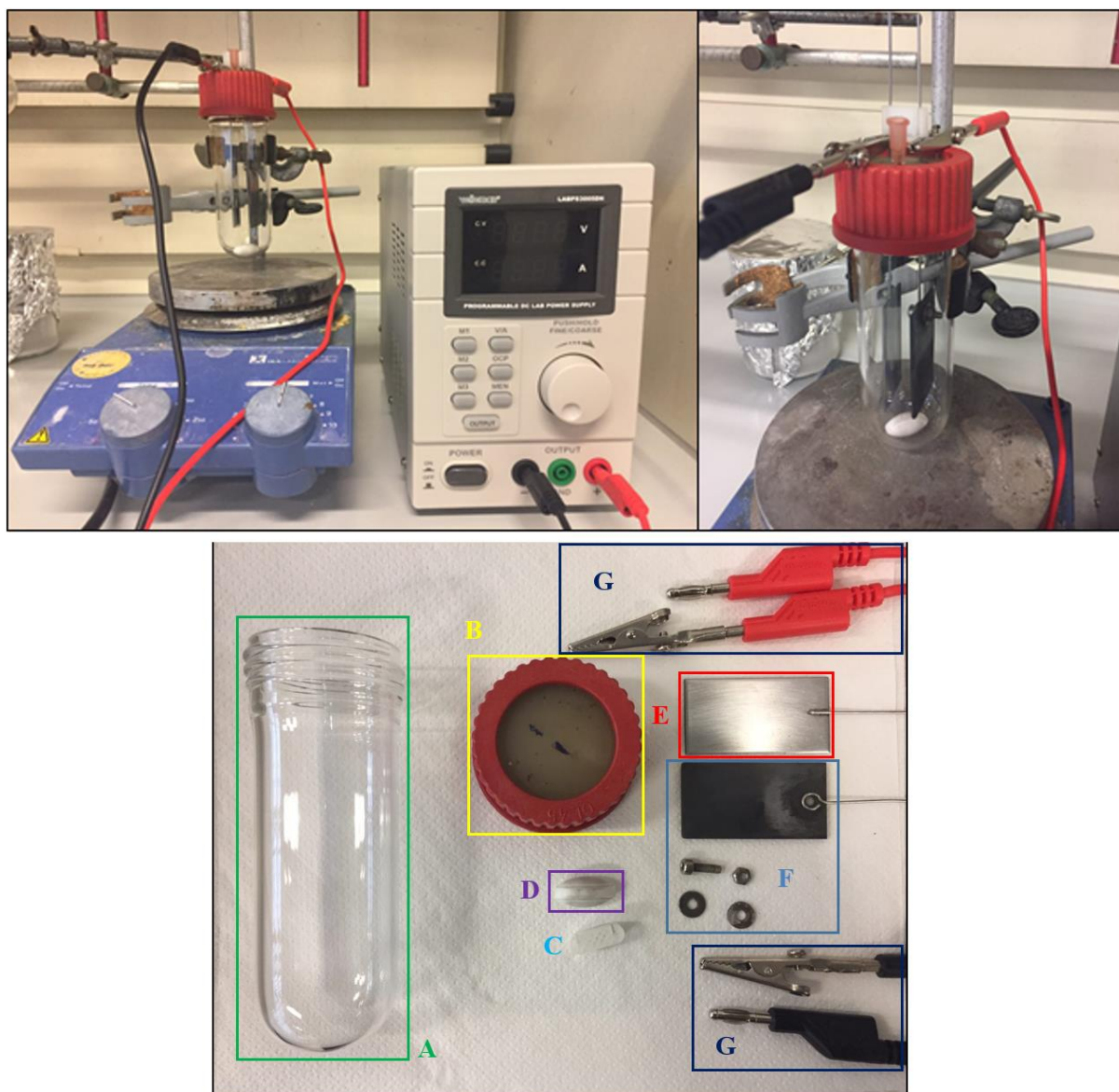


Figure 3.9 – Top: Assembled electrochemical batch reactor. **Bottom:** Components of the batch reactor. **A:** Boiling tube with screw cap. **B:** Screw cap with septum. **C:** 3D printed PLA spacer, 0.7 cm. **D:** Magnetic stirring bar. **E:** Steel cathode, dimensions 4.5 cm x 2.5 cm. **F:** Graphite anode (4.5 cm x 2.5 cm) with screws. **G:** Cables used to connect the power supply to the reactor. The septum is pierced with a needle to allow the hydrogen gas formed during the cathodic reduction to escape.

3.4.3 Reaction optimization

During the screening, the solution was charged into an electrocell and the electrodes are submerged in the reaction mixture. The current (20 mA, 4.2 mA/cm², max voltage 5 V) or constant voltage (3.2 or 4 V) was set. The reaction was followed by GC-MS, GC-FID, and/or TLC. GC yields were calculated using an internal standard method (biphenyl was used as an internal standard).

3.4.4 General procedures

3.4.4.1 Cleaning procedures

In this paragraph, the cleaning procedure for both the batch and the microflow setups will be described. It is important to mention that proper cleaning of the electrodes is crucial to guarantee the success of the reaction.

3.4.4.1.1 Batch reactor

The vial, magnetic stir bar, and cap are washed first with water, then with acetone and dried. The stainless-steel electrode is first washed with 1 M HCl and scrubbed with a sponge twice, then the electrode is submerged in acetone and sonicated for 15 min. The graphite electrode is first wiped with paper and washed with CH₃CN five times. It is important to keep the electrodes dry after use (e.g., do not submerge them in any solvent for storage). Otherwise, the reaction does not proceed anymore, probably because of passivation of the electrode surface. The graphite electrodes are replaced every 15 reactions.

3.4.4.1.2 Flow reactor

When the reaction is completed, the power supply and the pump feeding the reaction mixture are turned off. The reactor is cleaned with CH₃CN (10 mL, 0.5 mL/min). After this, the reactor is disassembled removing all the loops first, then all the screws. Subsequently, the gasket is cleaned with acetone on both sides. The stainless-steel electrode is first washed with HCl 1 M and scrubbed with a sponge twice, then rinsed with acetone. Next, the gasket, loops, and stainless-steel electrode are submerged in a beaker full of acetone and sonicated for 15 min. The graphite electrode is wiped with paper and washed with CH₃CN five times. The electrode holders are washed with acetone and dried with paper. The copper contacts are first washed with HCl 1 M, scrubbed with fine sandpaper, and finally rinsed with acetone. After these processes, all the components are dried with paper and the reactor is reassembled.

3.4.4.2 General procedure for electrochemical synthesis of sulfonyl fluorides

Potassium fluoride (10 mmol) was dissolved in the appropriate amount of stock solution (20 mL, 1:1 v/v CH₃CN/HCl_{aq} 1 M). Next, pyridine (2 mmol) was added via syringe. The solution was stirred until complete dissolution of the solids, after which the thiol, disulfide or thiosulfonate substrate (2 mmol, 1 mmol or 1 mmol, respectively) were added. The septum is pierced with a needle and the electrodes (graphite anode and stainless-steel cathode, approximate distance 1 cm) are positioned in the liquid reaction mixture. The electrodes are connected to a power supply set to 20 mA. A constant current was applied for 12–48 h (until full conversion of the substrate is achieved as judged by GC-MS or TLC). In some cases, constant potential was found beneficial to obtain optimal results (the applied potential was set to 3.2 V or 4 V). After the reaction was complete, the power supply was turned off and, after addition of water, the crude mixture was extracted three times with EtOAc (3 x 20 mL), dried

with MgSO₄ and concentrated under reduced pressure. The resulting crude mixture was purified using silica gel column chromatography and analyzed by TLC, GC-MS, ¹H NMR, ¹⁹F NMR, and ¹³C NMR spectroscopy.

3.4.4.3 General procedure for derivatization of volatile sulfonyl fluorides

For some compounds of the scope, derivatization was required due to their volatility. After the electrochemical reaction was complete (see general procedure 3.4.4.2), the power supply was turned off and the electrodes were removed. Next, the reaction mixture was neutralized with sodium bicarbonate (5 mL of saturated aqueous solution). Phenol (3 equiv.) and cesium carbonate (3 equiv.) were added subsequently. For the aromatic sulfonyl fluorides, the reaction was carried out at r.t., while for the aliphatic the reaction mixture was heated to 60 °C. The derivatization was followed by TLC and GC-MS and when full conversion was achieved a ¹⁹F NMR spectrum was recorded to ensure complete conversion of the sulfonyl fluoride. Subsequently, the reaction was extracted with ethyl acetate (3 x 20 mL) and the organic phase was washed with 1 M NaOH solution (3 x 20 mL) to remove the excess of phenol. The resulted organic phase was dried with MgSO₄, concentrated under reduced pressure, and purified using silica gel column chromatography. The purified material was next analyzed by TLC, GC-MS, ¹H NMR, ¹⁹F NMR, and ¹³C NMR spectroscopy.

3.4.4.4 Procedure for the scale-up experiment

Potassium fluoride (50 mmol) was dissolved in the required amount of stock solution (40 mL, 1:1 v/v CH₃CN/HCl_{aq} 1 M) and followed by the addition of pyridine (10 mmol). The solution was stirred until complete dissolution of the solids (biphasic mixture). Next, thiophenol (10 mmol) was added. The septum is pierced with a needle and the electrodes

(graphite anode and stainless-steel cathode, approximate distance 1 cm) are positioned in the reactor solution. The electrodes are connected to the power supply, which is set to 3.2 V (applied potential) and the solution is kept at a constant voltage for 24 h under continuous stirring. After the reaction was complete, the power supply was turned off and, after addition of water, the crude mixture was extracted three times with EtOAc (3 x 30 mL), dried with MgSO₄ and concentrated under reduced pressure. The resulting crude mixture was purified using silica gel column chromatography (10:1 v/v Cy:EtOAc) to give a colorless oil (1128 mg, 70%).

3.4.4.5 Procedure for the kinetic experiment in batch conditions

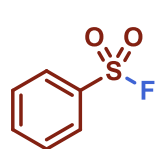
Potassium fluoride (10 mmol) was dissolved in the required amount of stock solution (20 mL, 1:1 v/v CH₃CN/HCl_{aq} 1 M) and followed by the addition of pyridine (2 mmol). The solution was stirred until complete dissolution of the solids. Next, 4-(trifluoromethyl)thiophenol (2 mmol) was added. The septum is pierced with a needle and the electrodes (graphite anode and stainless-steel cathode, approximate distance 1 cm) are positioned in the reactor solution. Next, a sample was taken before starting the reaction. The electrodes are connected to the power supply, which is set to 3.2 V for the potentiostatic experiment (applied potential) and 20 mA for the galvanostatic experiment, and the solution is kept at a constant voltage for 9–24 h under continuous stirring. During the reaction, samples were taken (0.2 mL) and complemented with DMSO (0.5 mL). The resulting samples were analyzed by ¹⁹F NMR.

3.4.4.6 Procedure for the kinetic experiment in flow conditions

Thiophenol (2 mmol) together with pyridine (10 mmol) were dissolved in acetonitrile (20 mL), while potassium fluoride (10 mmol) was dissolved in HCl_{aq} 1 M (20 mL).

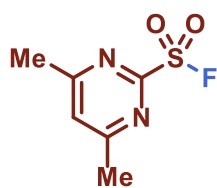
The two different mixtures were swirled until homogeneous before being taken up in a 20 ml disposable syringe. The solutions were pumped with the same flowrate (in order to obtain a 1:1 organic/aqueous mixture) through a T-mixer and then into the electrochemical setup equipped with a graphite anode and stainless-steel cathode at 0.25 mm thick gasket using PFA tubing ($\phi = 750 \mu\text{m}$). The potential was set to 3.3 V. Different residence times were scanned during the experiment (from 1 to 10 min). For every data point, after the reaction had reached steady state (12 min at 0.15 mL/min), the corresponding current was noted and a sample (0.2 mL) was collected in a vial and complemented with CH_3CN before analyzing the samples using GC-MS (biphenyl as standard).

3.4.5 Characterization data of sulfonyl fluorides

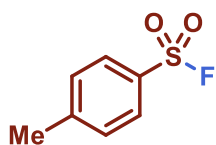


Benzenesulfonyl fluoride (3.26a):^{47,57,70} Following the general procedure (3.4.4.2), obtained at 20 mA for 36 h. Purified by flash chromatography on silica (cyclohexane/ethyl acetate 99:1) to give a colorless oil (272 mg, 85%). ^1H NMR (399 MHz, CDCl_3): δ 8.00 (d, $J = 7.9$ Hz, 2H), 7.78 (t, $J = 7.5$ Hz, 1H), 7.63 (t, $J = 7.7$ Hz, 2H). ^{13}C NMR (100 MHz, CDCl_3): δ 135.7, 133.1 (d, $J = 24.3$ Hz), 129.8, 128.4. ^{19}F NMR (376 MHz, CDCl_3): δ 65.9 (s, 1F).

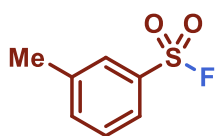
Following the general procedure (3.4.4.3), obtained at 20 mA for 36 h. When full conversion was achieved (followed by GC-MS), *in situ* derivatization was performed (See characterization **3.26a-der**).



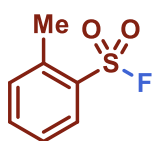
4,6-Dimethylpyrimidine-2-sulfonyl fluoride (3.26b):⁶¹ Following the general procedure (3.4.4.2), obtained at 20 mA for 12 h. Purified by flash chromatography on silica (cyclohexane/ethyl acetate 4:1) to give a white solid (281 mg, 74%). Mp: 60–61 °C (Lit.⁶¹ mp: 57–58 °C). ^1H NMR (399 MHz, CDCl_3): δ 7.36 (s, 1H), 2.64 (s, 6H). ^{13}C NMR (100 MHz, CDCl_3): δ 170.3, 170.2, 160.1 (d, $J = 36.7$ Hz), 124.6, 24.0. ^{19}F NMR (376 MHz, CDCl_3): δ 48.7 (s, 1F).



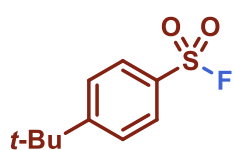
4-Methylbenzenesulfonyl fluoride (3.26c):^{57,70,90} Following the general procedure (3.4.4.2), obtained at 20 mA for 24 h. Purified by flash chromatography on silica (cyclohexane/ethyl acetate 99:1) to give a white solid (220 mg, 63%). Mp: 40–42 °C (Lit.⁹⁰ mp: 40.5–42 °C). ¹H NMR (399 MHz, CDCl₃): δ 7.87 (d, *J* = 8.4 Hz, 2H), 7.41 (d, *J* = 8.1 Hz, 2H), 2.48 (s, 3H). ¹³C NMR (100 MHz, CDCl₃): δ 147.3, 130.4, 130.1 (d, *J* = 24.2 Hz), 128.5, 21.9. ¹⁹F NMR (376 MHz, CDCl₃): δ 66.2 (s, 1F).



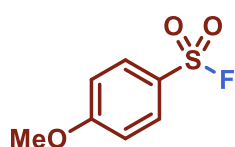
3-Methylbenzenesulfonyl fluoride (3.26d):⁷⁰ Following the general procedure (3.4.4.2), obtained at 20 mA for 36 h. Purified by flash chromatography on silica (cyclohexane/ethyl acetate 99:1) to give a colorless oil (237 mg, 68%). HRMS (ESI): *m/z* calcd. for C₇H₇O₂SFNa [M + Na]⁺: 197.0043; found: 197.0043. ¹H NMR (399 MHz, CDCl₃): δ 7.85 – 7.76 (m, 2H), 7.61 – 7.54 (m, 1H), 7.54 – 7.47 (m, 1H), 2.47 (s, 3H). ¹³C NMR (100 MHz, CDCl₃): δ 140.3, 136.5, 133.0 (d, *J* = 23.6 Hz), 129.6, 128.7, 125.6, 21.3. ¹⁹F NMR (376 MHz, CDCl₃): δ 65.8 (s, 1F).



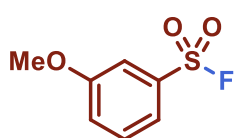
2-Methylbenzenesulfonyl fluoride (3.26e):³⁷ Following the general procedure (3.4.4.2), obtained at 20 mA for 30 h. Purified by flash chromatography on silica (cyclohexane/ethyl acetate 99:1) to give a colorless oil (303 mg, 87%). ¹H NMR (399 MHz, CDCl₃): δ 8.02 (d, *J* = 7.9 Hz, 1H), 7.68 – 7.58 (m, 1H), 7.47 – 7.36 (m, 2H), 2.69 (s, 3H). ¹³C NMR (100 MHz, CDCl₃): δ 139.1, 135.4, 133.0, 132.4 (d, *J* = 22.1 Hz), 130.1 (d, *J* = 1.7 Hz), 126.8, 20.3 (d, *J* = 1.3 Hz). ¹⁹F NMR (376 MHz, CDCl₃): δ 60.3 (s, 1F).



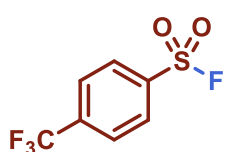
4-(*tert*-Butyl)benzenesulfonyl fluoride (3.26f):^{57,69,91} Following the general procedure (3.4.4.2), obtained at 20 mA for 16 h. Purified by flash chromatography on silica (cyclohexane/ethyl acetate 99:1) to give a white solid (251 mg, 58%). Mp: 62–64 °C (Lit.⁹¹ mp: 64–64.5 °C). ¹H NMR (399 MHz, CDCl₃): δ 7.93 (d, *J* = 8.3 Hz, 2H), 7.64 (d, *J* = 8.3 Hz, 2H), 1.36 (s, 9H). ¹³C NMR (100 MHz, CDCl₃): δ 160.1, 130.0 (d, *J* = 24.2 Hz), 128.4, 126.8, 35.6, 31.0. ¹⁹F NMR (376 MHz, CDCl₃): δ 66.2 (s, 1F).



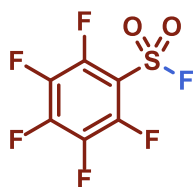
4-Methoxybenzenesulfonyl fluoride (3.26g):^{47,57,70} Following the general procedure (3.4.4.2), obtained at 20 mA for 41 h. Purified by flash chromatography on silica (cyclohexane/ethyl acetate 10:1) to give a yellow oil (224 mg, 59%). ¹H NMR (399 MHz, CDCl₃): δ 7.92 (d, J = 9.0 Hz, 2H), 7.05 (d, J = 8.9 Hz, 2H), 3.91 (s, 3H). ¹³C NMR (100 MHz, CDCl₃): δ 165.4, 130.9, 124.1 (d, J = 24.6 Hz), 115.0, 56.0. ¹⁹F NMR (376 MHz, CDCl₃): δ 67.3 (s, 1F).



3-Methoxybenzenesulfonyl fluoride (3.26h):⁷⁰ Following the general procedure (3.4.4.2), obtained at 20 mA for 36 h. Purified by flash chromatography on silica (cyclohexane/ethyl acetate 10:1) to give a pale yellow oil (129 mg, 34%). ¹H NMR (399 MHz, CDCl₃): δ 7.60 (dt, J = 7.8, 0.9 Hz, 1H), 7.52 (td, J = 8.0, 1.1 Hz, 1H), 7.47 (t, J = 2.2 Hz, 1H), 7.28 (dd, J = 8.3, 2.3 Hz, 1H), 3.89 (s, 3H). ¹³C NMR (100 MHz, CDCl₃): δ 160.3, 134.1 (d, J = 24.2 Hz), 130.8, 122.3, 120.7, 112.8, 56.0. ¹⁹F NMR (376 MHz, CDCl₃): δ 65.6 (s, 1F).

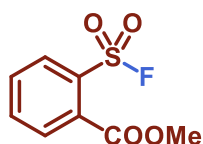


4-(Trifluoromethyl)benzenesulfonyl fluoride (3.26i):^{57,92} Following the general procedure (3.4.4.2), obtained at 20 mA for 36 h. Purified by flash chromatography on silica (cyclohexane/ethyl acetate 99:1) to give a white solid (278 mg, 61%). Mp: 67–69 °C (Lit.⁹² mp: 68–69 °C). ¹H NMR (399 MHz, CDCl₃): δ 8.17 (d, J = 8.2 Hz, 2H), 7.92 (d, J = 8.1 Hz, 2H). ¹³C NMR (100 MHz, CDCl₃): δ 137.3 (q, J = 33.4 Hz), 136.6 (d, J = 27.2 Hz), 129.3, 127.1 (q, J = 3.7 Hz), 122.9 (q, J = 273.3 Hz). ¹⁹F NMR (376 MHz, CDCl₃): δ 65.8 (s, 1F), -63.6 (s, 3F).

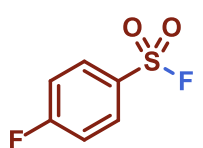


2,3,4,5,6-Pentafluorobenzenesulfonyl fluoride (3.26j):⁴⁵ Following the general procedure (3.4.4.2), obtained at 4.0 V for 24 h. Purified by flash chromatography on silica (cyclohexane/ethyl acetate 99:1) to give a colorless oil (95 mg, 19%). ¹³C NMR (100 MHz, CDCl₃): δ 148.8 – 144.9 (m), 147.2 – 143.4 (m), 140.7 – 136.2 (m), 111.2 – 109.1 (m). ¹⁹F NMR (376 MHz, CDCl₃): δ 74.3 (t, J = 14.6 Hz, 1F), -130.8 – -133.8 (m, 2F), -136.9 – -140.9 (m, 1F), -153.4 – -160.8 (m, 2F).

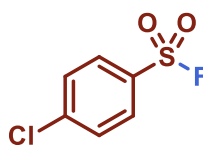
Following the general procedure (3.4.4.3), obtained at 4.0 V for 24 h. When full conversion was achieved (followed by GC-MS), *in situ* derivatization was performed (See characterization **3.26j-der**).



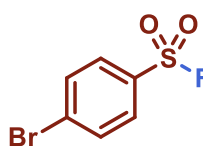
Methyl 2-(fluorosulfonyl)benzoate (3.26k):⁹³ Following the general procedure (3.4.4.2), obtained at 20 mA for 20 h. Purified by flash chromatography on silica (cyclohexane/ethyl acetate 10:1) to give a colorless oil (384 mg, 88%). HRMS (ESI): m/z calcd. for $C_8H_7O_4SFNa$ $[M + Na]^+$: 240.9941; found: 240.9941. 1H NMR (399 MHz, $CDCl_3$): δ 8.15 (dd, $J = 7.9, 1.3$ Hz, 1H), 7.87 (dd, $J = 7.8, 1.6$ Hz, 1H), 7.82 (td, $J = 7.6, 1.3$ Hz, 1H), 7.73 (m, 1H), 3.98 (s, 3H). ^{13}C NMR (100 MHz, $CDCl_3$): δ 165.9, 135.4, 133.2, 132.0 (d, $J = 26.3$ Hz), 131.8, 130.9, 130.6 (d, $J = 1.6$ Hz), 53.6. ^{19}F NMR (376 MHz, $CDCl_3$): δ 64.5 (s, 1F).



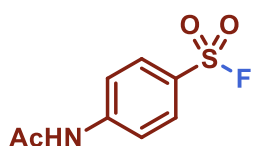
4-Fluorobenzenesulfonyl fluoride (3.26l):^{47,57,70} Following the general procedure (3.4.4.2), obtained at 20 mA for 24 h. Purified by flash chromatography on silica (cyclohexane/ethyl acetate 99:1) to give a colorless oil (217 mg, 61%). 1H NMR (399 MHz, $CDCl_3$): δ 8.12 – 8.01 (m, 2H), 7.32 (t, $J = 8.4$ Hz, 2H). ^{13}C NMR (100 MHz, $CDCl_3$): δ 167.0 (d, $J = 259.8$ Hz), 131.7 (d, $J = 10.1$ Hz), 129.1 (dd, $J = 25.9, 3.4$ Hz), 117.4 (d, $J = 23.1$ Hz). ^{19}F NMR (376 MHz, $CDCl_3$): δ 66.7 (s, 1F), -99.26–-99.44 (m, 1F).



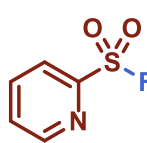
4-Chlorobenzenesulfonyl fluoride (3.26m):^{39,47,57,70} Following the general procedure (3.4.4.2), obtained at 20 mA for 22 h. Purified by flash chromatography on silica (cyclohexane/ethyl acetate 10:1) to give a white solid (241 mg, 62%). Mp: 48–50 °C (Lit.³⁹ mp: 49–53 °C). 1H NMR (399 MHz, $CDCl_3$): δ 7.95 (d, $J = 8.6$ Hz, 2H), 7.61 (d, $J = 8.5$ Hz, 2H). ^{13}C NMR (100 MHz, $CDCl_3$): δ 142.8, 131.5 (d, $J = 25.7$ Hz), 130.2, 130.0. ^{19}F NMR (376 MHz, $CDCl_3$): δ 66.4 (s, 1F).



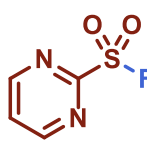
4-Bromobenzenesulfonyl fluoride (3.26n):^{47,94} Following the general procedure (3.4.4.2), obtained at 20 mA for 16 h. Purified by flash chromatography on silica (cyclohexane/ethyl acetate 10:1) to give a white solid (277 mg, 58%). Mp: 64–65 °C (Lit.⁹⁴ mp: 58.1–59.8 °C). 1H NMR (399 MHz, $CDCl_3$): δ 7.87 (d, $J = 8.7$ Hz, 2H), 7.78 (d, $J = 8.4$ Hz, 2H). ^{13}C NMR (100 MHz, $CDCl_3$): δ 133.2, 132.0 (d, $J = 25.7$ Hz), 131.4, 129.9. ^{19}F NMR (376 MHz, $CDCl_3$): δ 66.4 (s, 1F).



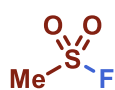
4-Acetamidobenzenesulfonyl fluoride (3.26o):^{47,57} Following the general procedure (3.4.4.2), obtained at 20 mA for 40 h. Purified by flash chromatography on silica (cyclohexane/ethyl acetate 4:1) to give a white solid (82 mg, 19%). Mp: 174–175 °C (Lit.⁴⁷ mp: 175–176 °C). ¹H NMR (399 MHz, CDCl₃): δ 7.96 (d, *J* = 8.6 Hz, 2H), 7.79 (d, *J* = 8.6 Hz, 2H), 7.55 (s, 1H), 2.25 (s, 3H). ¹³C NMR (100 MHz, CDCl₃): δ 168.8, 144.6, 130.2, 127.3 (d, *J* = 25.1 Hz), 119.5, 25.0. ¹⁹F NMR (376 MHz, CDCl₃): δ 66.8 (s, 1F).



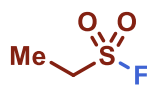
Pyridine-2-sulfonyl fluoride (3.26p):⁴⁵ Following the general procedure (3.4.4.2), obtained at 3.2 V for 6 h. Purified by flash chromatography on silica (cyclohexane/ethyl acetate 4:1) to give a yellow oil (274 mg, 85%). ¹H NMR (399 MHz, CDCl₃): δ 8.83 (d, *J* = 4.3 Hz, 1H), 8.13 (d, *J* = 7.8 Hz, 1H), 8.06 (tt, *J* = 7.7, 1.5 Hz, 1H), 7.72 (ddd, *J* = 7.6, 4.7, 1.2 Hz, 1H). ¹³C NMR (100 MHz, CDCl₃): δ 151.4 (d, *J* = 30.4 Hz), 151.1 (d, *J* = 1.2 Hz), 138.9, 129.4, 124.2 (d, *J* = 2.2 Hz). ¹⁹F NMR (376 MHz, CDCl₃): δ 55.8 (s, 1F).



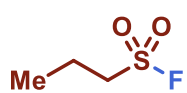
Pyrimidine-2-sulfonyl fluoride (3.26q):^{45,61} Following the general procedure (3.4.4.2), obtained at 20 mA for 24 h. Purified by flash chromatography on silica (cyclohexane/ethyl acetate 4:1) to give a white solid (169 mg, 52%). Mp: 56–58 °C (Lit.⁶¹ mp: 58–60 °C). ¹H NMR (399 MHz, CDCl₃): δ 9.04 (d, *J* = 4.9 Hz, 2H), 7.73 (t, *J* = 4.9 Hz, 1H). ¹³C NMR (100 MHz, CDCl₃): δ 160.8 (d, *J* = 38.8 Hz), 159.4 (d, *J* = 1.6 Hz), 125.5. ¹⁹F NMR (376 MHz, CDCl₃): δ 49.5 (s, 1F).



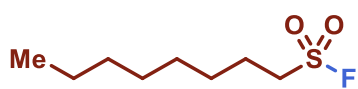
Methanesulfonyl fluoride (3.26r): Following the general procedure (3.4.4.3), obtained at 3.2 V for 15 h starting by dimethyl disulfide. When full conversion was achieved (followed by GC-MS), *in situ* derivatization was performed (See characterization **3.26r-der**).



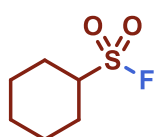
Ethanesulfonyl fluoride (3.26s): Following the general procedure (3.4.4.3), obtained at 20 mA for 48 h. When full conversion was achieved (followed by GC-MS), *in situ* derivatization was performed (See characterization **3.26s-der**).



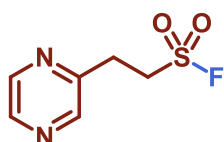
Propane-1-sulfonyl fluoride (3.26t): Following the general procedure (3.4.4.3), obtained at 20 mA for 41 h starting by dipropyl disulfide. When full conversion was achieved (followed by GC-MS), *in situ* derivatization was performed (See characterization **3.26t-der**).



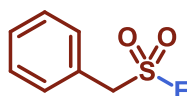
Octane-1-sulfonyl fluoride (3.26u):⁵⁷ Following the general procedure (3.4.4.2), obtained at 20 mA for 36 h. Purified by flash chromatography on silica (cyclohexane/ethyl acetate 99:1) to give a colorless oil (200 mg, 51%). ¹H NMR (399 MHz, CDCl₃): δ 3.42 – 3.29 (m, 2H), 1.94 (p, J = 7.7 Hz, 2H), 1.48 (p, J = 7.4 Hz, 2H), 1.39 – 1.22 (m, 8H), 0.88 (t, J = 6.9 Hz, 3H). ¹³C NMR (100 MHz, CDCl₃): δ 51.0 (d, J = 15.9 Hz), 31.8, 29.0, 28.9, 28.0, 23.5, 22.7, 14.2. ¹⁹F NMR (376 MHz, CDCl₃): δ 53.2 (t, J = 4.2 Hz, 1F).



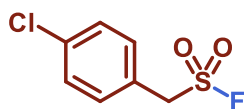
Cyclohexane-1-sulfonyl fluoride (3.26v):⁷⁰ Following the general procedure (3.4.4.3), obtained at 3.2 V for 36 h. When full conversion was achieved (followed by GC-MS), *in situ* derivatization was performed (See characterization **3.26v-der**).



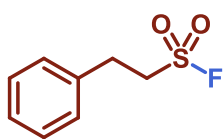
2-(Pyrazin-2-yl)ethane-1-sulfonyl fluoride (3.26w): Following the general procedure (3.4.4.2), obtained at 20 mA for 24 h. Purified by flash chromatography on silica (cyclohexane/ethyl acetate 4:1) to give a white off solid (357 mg, 94%). HRMS (ESI): m/z calcd. for C₆H₇N₂O₂SFNa [M + Na]⁺: 213.0104; found: 213.0104. Mp: 220 °C (degr.). ¹H NMR (399 MHz, CDCl₃): δ 8.61 – 8.39 (m, 3H), 4.01 – 3.83 (m, 2H), 3.43 (t, J = 7.6 Hz, 2H). ¹³C NMR (100 MHz, CDCl₃): δ 151.4, 144.7, 144.3, 143.8, 49.0 (d, J = 17.6 Hz), 28.6. ¹⁹F NMR (376 MHz, CDCl₃): δ 53.9 (t, J = 4.8 Hz, 1F).



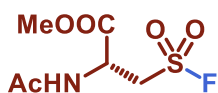
Phenylmethanesulfonyl fluoride (3.26x):^{57,70,92} Following the general procedure (3.4.4.2), obtained at 20 mA for 40 h. Purified by flash chromatography on silica (cyclohexane/ethyl acetate 99:1) to give a colorless oil (157 mg, 45%). Mp: 92–93 °C (Lit.⁹² mp: 93–94 °C). ¹H NMR (399 MHz, CDCl₃): δ 7.55 – 7.34 (m, 5H), 4.60 (d, J = 3.2 Hz, 2H). ¹³C NMR (100 MHz, CDCl₃): δ 130.8, 130.0, 129.4, 125.6, 57.0 (d, J = 17.7 Hz). ¹⁹F NMR (376 MHz, CDCl₃): δ 51.4 (t, J = 3.4 Hz, 1F).



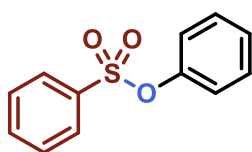
(4-Chloro-phenyl)methanesulfonyl fluoride (3.26y):⁹⁵ Following the general procedure (3.4.4.2), obtained at 20 mA for 44 h. Purified by flash chromatography on silica (cyclohexane/ethyl acetate 99:1) to give a white off solid (154 mg, 37%). HRMS (ESI): m/z calcd. for $C_7H_6O_2SClFNa$ $[M + Na]^+$: 230.9653; found: 230.9653. Mp: 149–150 °C (Lit.⁹⁵ mp: 143–145 °C). 1H NMR (399 MHz, $CDCl_3$): δ 7.43 (d, $J = 8.5$ Hz, 2H), 7.37 (d, $J = 8.6$ Hz, 2H), 4.57 (d, $J = 3.1$ Hz, 2H). ^{13}C NMR (100 MHz, $CDCl_3$): δ 136.5, 132.1, 129.8, 124.1, 56.3 (d, $J = 18.4$ Hz). ^{19}F NMR (376 MHz, $CDCl_3$): δ 51.6 (t, $J = 3.2$ Hz, 1F).



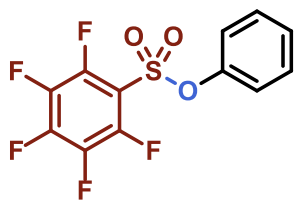
2-Phenylethane-1-sulfonyl fluoride (3.26z): Following the general procedure (3.4.4.2), obtained at 20 mA for 24 h. Purified by flash chromatography on silica (cyclohexane/ethyl acetate 99:1) to give a colorless oil (244 mg, 65%). HRMS (ESI): m/z calcd. for $C_8H_9O_2SFNa$ $[M + Na]^+$: 211.0199; found: 211.0199. 1H NMR (399 MHz, $CDCl_3$): δ 7.41 – 7.34 (m, 2H), 7.32 (tt, $J = 7.3, 1.5$ Hz, 1H), 7.27 – 7.21 (m, 2H), 3.68 – 3.58 (m, 2H), 3.29 – 3.21 (m, 2H). ^{13}C NMR (100 MHz, $CDCl_3$): δ 136.1, 129.2, 128.5, 127.7, 52.2 (d, $J = 15.6$ Hz), 29.7. ^{19}F NMR (376 MHz, $CDCl_3$): δ 53.2 (t, $J = 4.2$ Hz, 1F).



Methyl acetyl(fluorosulfonyl)-D-alaninate (3.26aa): Following the general procedure (3.4.4.2), obtained at 20 mA for 24 h. Purified by flash chromatography on silica (cyclohexane/ethyl acetate 4:1) to give a white solid (159 mg, 35%). HRMS (ESI): m/z calcd. for $C_6H_{10}NO_5SFNa$ $[M + Na]^+$: 250.0156; found: 250.0156. Mp: 159–160 °C. 1H NMR (399 MHz, $CDCl_3$): δ 6.48 (brs, 1H), 4.91 (dq, $J = 6.3, 4.3$ Hz, 1H), 4.22 (ddd, $J = 15.2, 4.6, 2.5$ Hz, 1H), 4.07 (ddd, $J = 15.2, 6.0, 4.6$ Hz, 1H), 3.86 (s, 3H), 2.09 (s, 3H). ^{13}C NMR (100 MHz, $CDCl_3$): δ 170.5, 168.2, 53.9, 51.6 (d, $J = 14.9$ Hz), 48.8, 23.0. ^{19}F NMR (376 MHz, $CDCl_3$): δ 63.3 (dt, $J = 6.0, 2.9$ Hz, 1F).



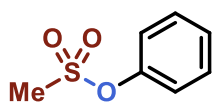
Phenyl phenylsulfonate (3.26a-der):⁹⁶ Following the general procedure (3.4.4.3), obtained at r.t. in 2 h. Purified by flash chromatography on silica (cyclohexane/ethyl acetate 99:1) to give a colorless oil (454 mg, 97%) (mp: Lit.⁹⁶ mp: 34–35 °C). 1H NMR (399 MHz, $CDCl_3$): δ 7.96 – 7.83 (m, 2H), 7.69 (tt, $J = 7.5, 1.3$ Hz, 1H), 7.60 – 7.51 (m, 2H), 7.37 – 7.24 (m, 3H), 7.12 – 6.98 (m, 2H). ^{13}C NMR (100 MHz, $CDCl_3$): δ 149.4, 135.1, 134.2, 129.6, 129.1, 128.2, 127.1, 122.1.



Phenyl 2,3,4,5,6-pentafluorobenzenesulfonate (3.26j-der):⁹⁷

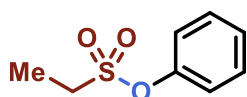
Following the general procedure (3.4.4.3), obtained at room temperature in 2 h. Purified by flash chromatography on silica (cyclohexane/ethyl acetate 99:1) to give a white solid (181 mg, 28%).

HRMS (ESI): m/z calcd. for $C_{12}H_5O_3SF_5Na$ $[M + Na]^+$: 346.9772; found: 346.9772. Mp: 72–74 °C. 1H NMR (399 MHz, $CDCl_3$): δ 7.44 – 7.31 (m, 3H), 7.23 – 7.14 (m, 2H). ^{13}C NMR (100 MHz, $CDCl_3$): δ 149.0, 146.9 – 146.4 (m), 144.2 – 143.8 (m), 139.6 – 139.1 (m), 137.0 – 136.5 (m), 130.4, 128.3, 121.6, 112.2 – 111.7 (m). ^{19}F NMR (376 MHz, $CDCl_3$): δ -132.56 – -133.20 (m, 2F), -141.74 (tt, $J = 21.1, 8.1$ Hz, 1F), -157.19 – -157.89 (m, 2F).



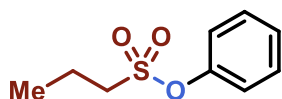
Phenyl methanesulfonate (3.26r-der):⁹⁸

Following the general procedure (3.4.4.3), obtained at 60 °C in 12 h. Purified by flash chromatography on silica (cyclohexane/ethyl acetate 99:1) to give a white off solid (176 mg, 51%). Mp: 62–63 °C (Lit.⁹⁸ mp: 60–62 °C). 1H NMR (399 MHz, $CDCl_3$): δ 7.38 (t, $J = 7.9$ Hz, 2H), 7.33 – 7.20 (m, 3H), 3.09 (s, 3H). ^{13}C NMR (100 MHz, $CDCl_3$): δ 149.4, 130.1, 127.5, 122.1, 37.4.



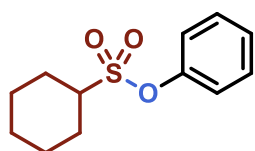
Phenyl ethanesulfonate (3.26s-der):⁹⁹

Following the general procedure (3.4.4.3), obtained at 60 °C in 12 h. Purified by flash chromatography on silica (cyclohexane/ethyl acetate 99:1) to give a colorless oil (134 mg, 36%). 1H NMR (399 MHz, $CDCl_3$): δ 7.46 – 7.36 (m, 2H), 7.34 – 7.25 (m, 3H), 3.28 (q, $J = 7.4$ Hz, 2H), 1.54 (t, $J = 7.4$ Hz, 3H). ^{13}C NMR (100 MHz, $CDCl_3$): δ 149.3, 130.1, 127.3, 122.1, 45.1, 8.4.



Phenyl propane-1-sulfonate (3.26t-der): Following the general procedure (3.4.4.3), obtained at 60 °C in 24 h. Purified by flash chromatography on silica (cyclohexane/ethyl acetate 99:1) to give a colorless oil (156 mg, 39%).

HRMS (ESI): m/z calcd. for $C_9H_{12}O_3SNa$ $[M + Na]^+$: 223.0399; found: 223.0399. 1H NMR (399 MHz, $CDCl_3$): δ 7.44 – 7.36 (m, 2H), 7.33 – 7.24 (m, 3H), 3.24 – 3.18 (m, 2H), 2.07 – 1.95 (m, 2H), 1.11 (t, $J = 7.5$ Hz, 3H). ^{13}C NMR (100 MHz, $CDCl_3$): δ 149.3, 130.0, 127.2, 122.1, 52.1, 17.4, 12.9.

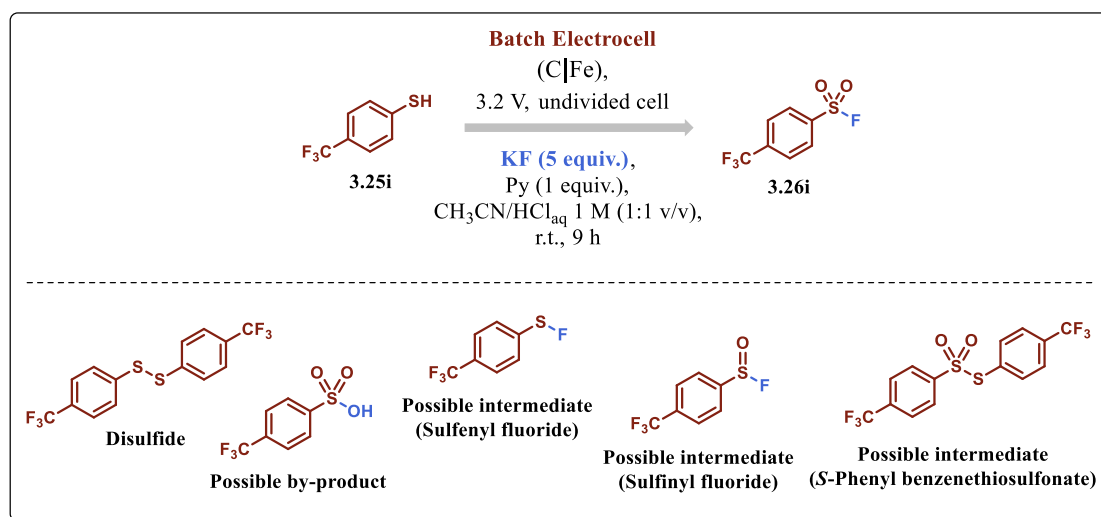


Phenyl cyclohexanesulfonate (3.26v-der): Following the general procedure (3.4.4.3), obtained at 60 °C in 24 h. Purified by flash chromatography on silica (cyclohexane/ethyl acetate 99:1) to give a colorless oil (197 mg, 41%). HRMS (ESI): m/z calcd. for $C_{12}H_{16}O_3SNa$ $[M + Na]^+$: 263.0712; found: 263.0712. 1H NMR (399 MHz, $CDCl_3$): δ 7.40 – 7.31 (m, 2H), 7.27 – 7.18 (m, 3H), 3.14 (tt, $J = 12.1, 3.5$ Hz, 1H), 2.30 (dd, $J = 13.3, 3.6$ Hz, 2H), 1.96 – 1.84 (m, 2H), 1.76 – 1.61 (m, 3H), 1.35 – 1.18 (m, 3H). ^{13}C NMR (100 MHz, $CDCl_3$): δ 149.2, 130.0, 127.0, 122.2, 60.2, 26.7, 25.1, 25.0.

3.5 Mechanistic studies

3.5.1 Kinetic experiments

First, a kinetic experiment at constant potential conditions was carried out (see Scheme 3.9 and Figures 3.10 and 3.11).



Scheme 3.9 – Kinetic experiment at constant potential conditions.

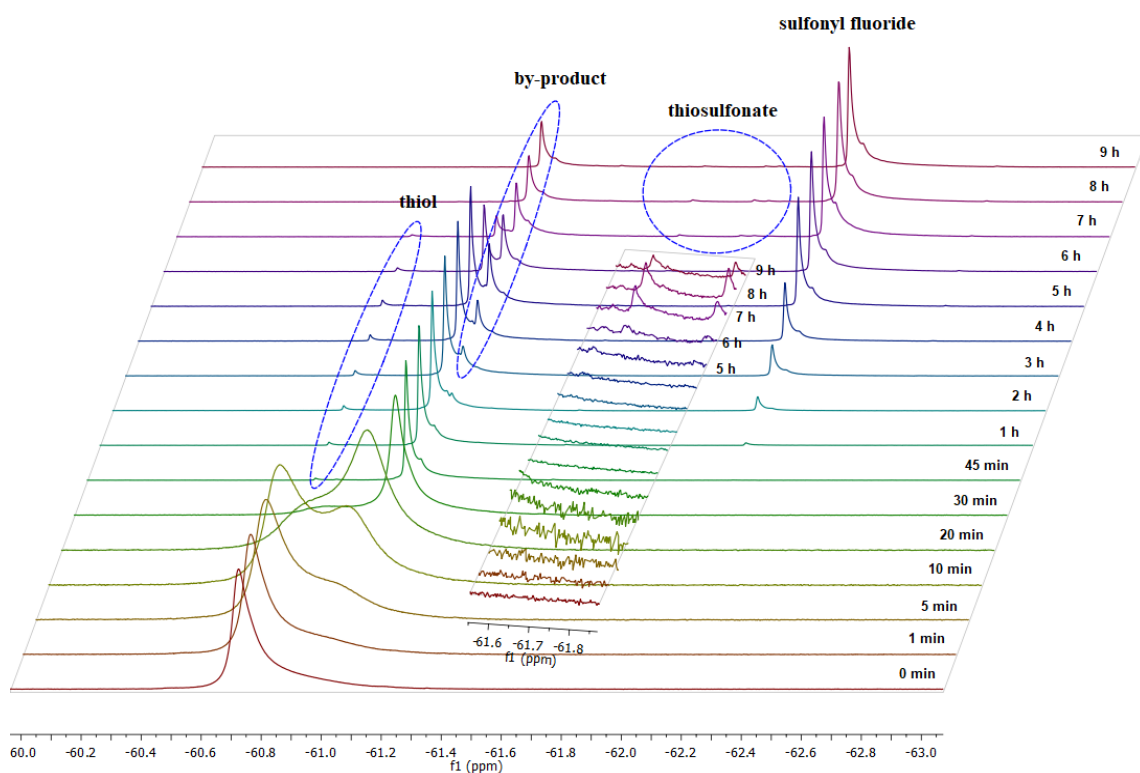
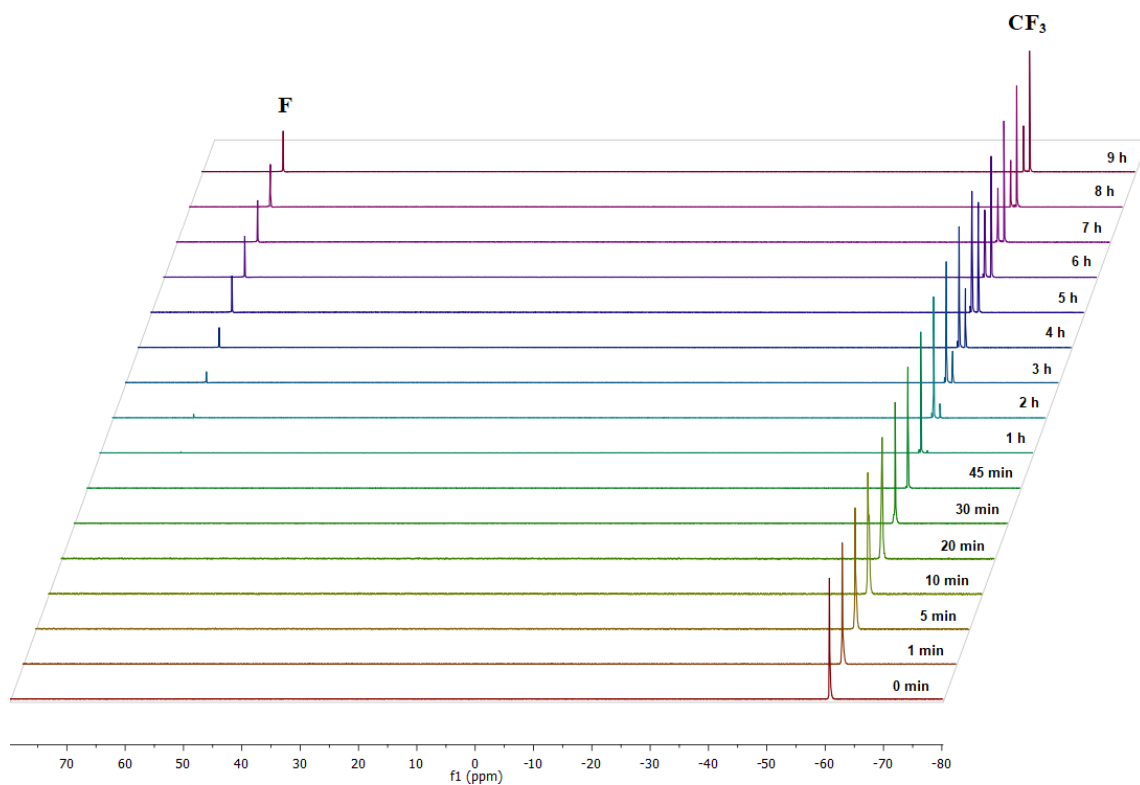


Figure 3.10 – Kinetic experiment at constant potential conditions. 1D ^{19}F NMR stacked spectra for the time course array of the reaction from 0 to 9 h reaction time (samples taken at the reaction time mentioned on each spectrum). **Top:** Full range stacked spectra. **Bottom:** Zoom from -63.0 to -60.0 ppm.

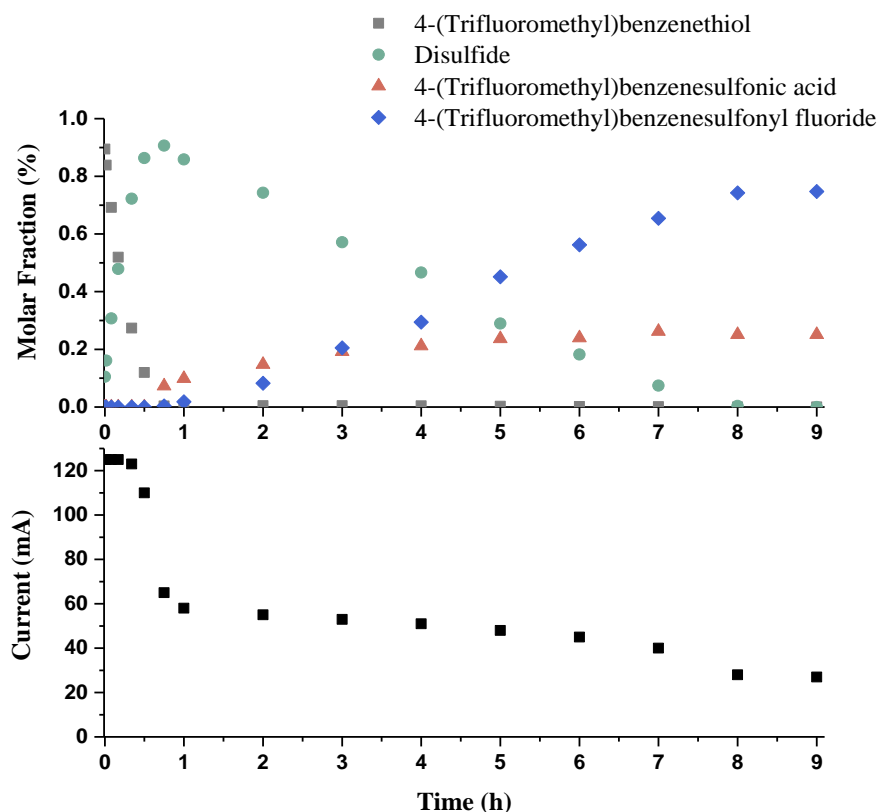
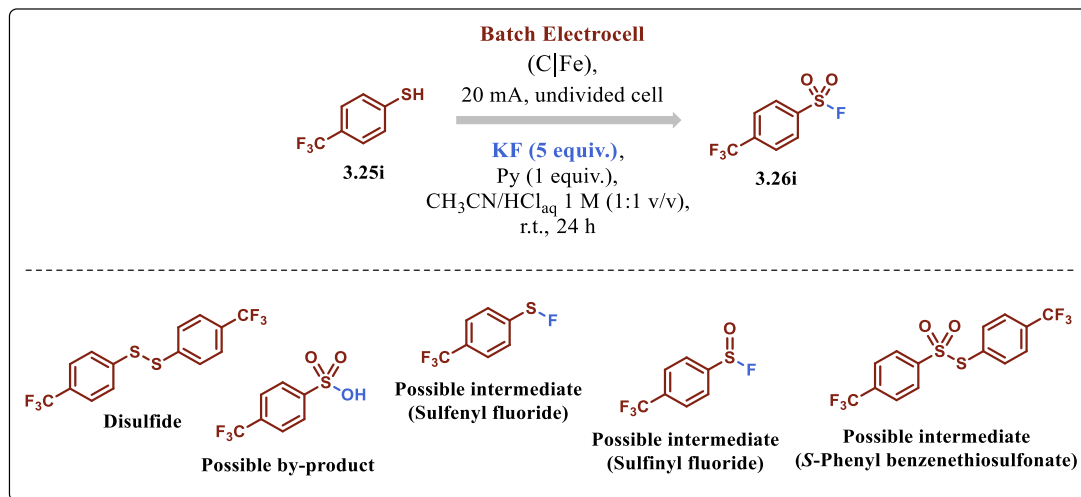


Figure 3.11 – Kinetic experiment at constant potential conditions. **Top:** Integration of peaks of the ^{19}F NMR plot. **Bottom:** Current intensity over time.

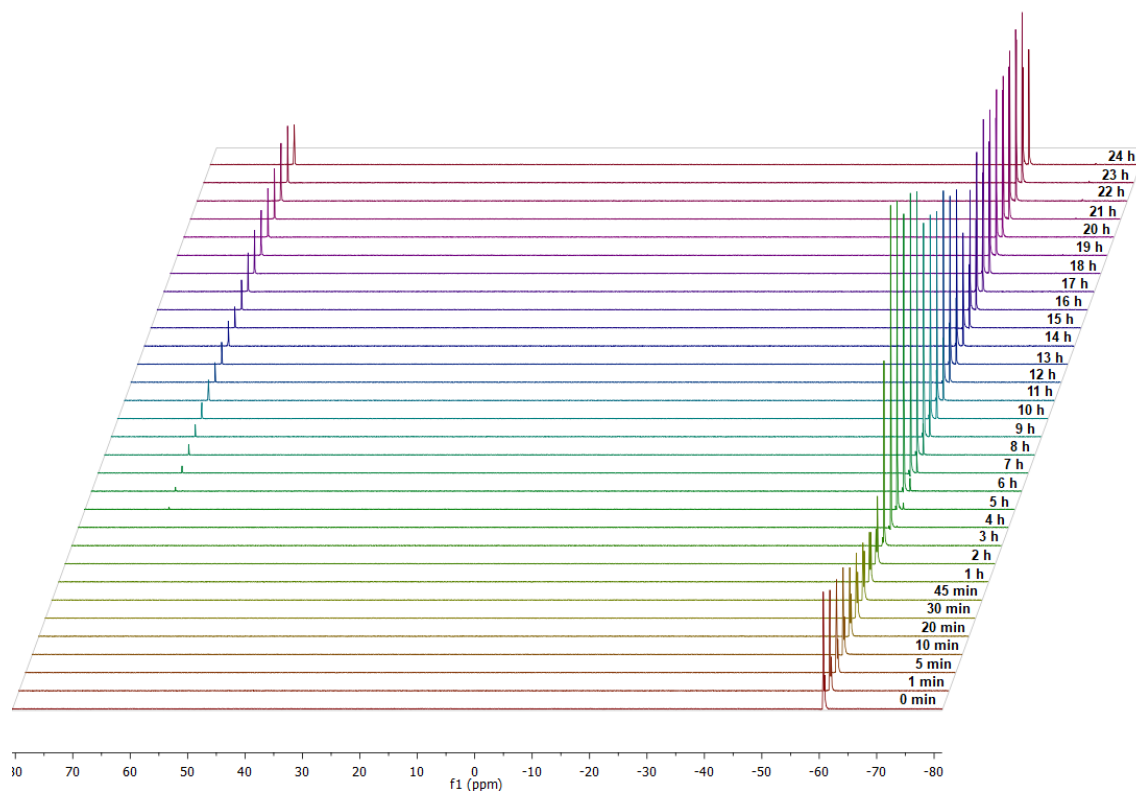
The experiment showed a rapid conversion of thiol **3.25i** to disulfide (within 45 minutes). After this event, the formation of the product **3.26i** is observed. Interestingly, a by-product (-61.1 ppm) formation was detected, which is attributed to overoxidation products (sulfonic acid). With the formation of **3.26i**, traces of the released thiol **3.25i** could be detected at -60.7 ppm (CF_3 group). It was also possible to observe the formation of traces of other fluorinated species in the region between -62.0 and -61.3 ppm. In particular, the signals at approximately -61.8 and -61.6 ppm can be attributed to the CF_3 groups of the *S*-phenyl benzenethiosulfonate.¹⁰⁰

During the kinetic experiment, a current drop was observed in the first hour, which is in correspondence with the formation of disulfide. Subsequently, the current stabilized around 50 mA until full conversion of the disulfide was observed (see Figure 3.11, bottom).

Next, a kinetic experiment at constant current conditions was carried out (Scheme 3.10 and Figures 3.12 and 3.13).



Scheme 3.10 – Kinetic experiment at constant current conditions.



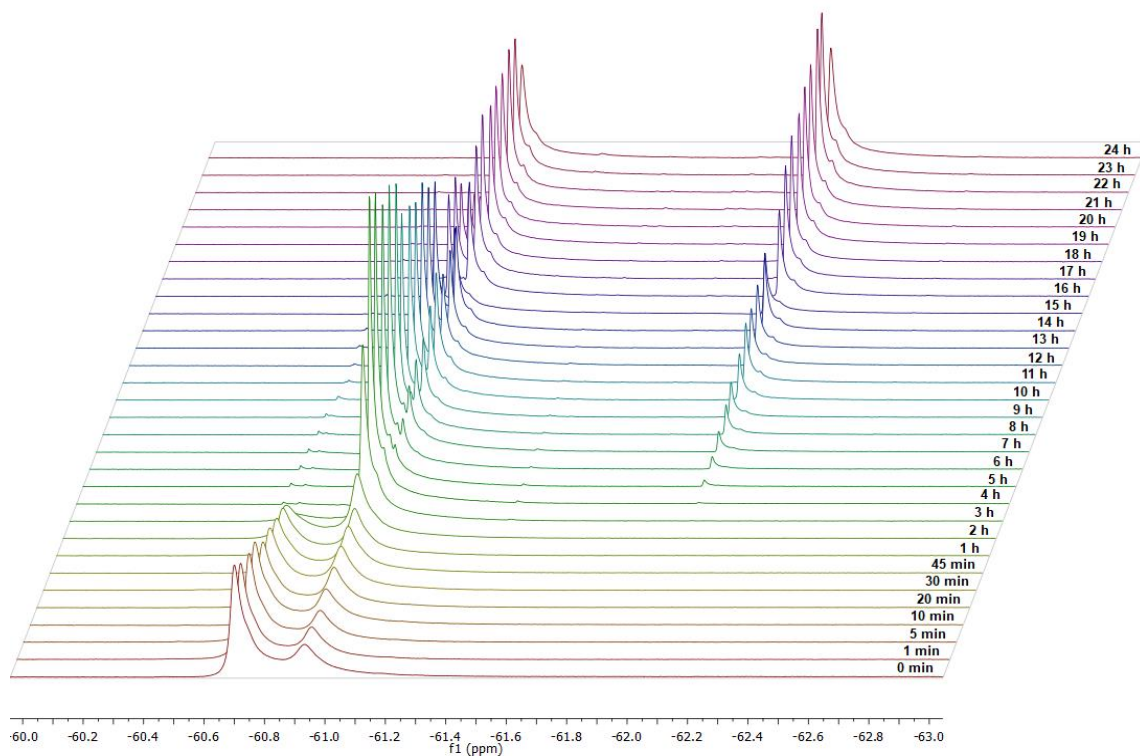


Figure 3.12 – Kinetic experiment at constant current conditions. 1D ^{19}F NMR stacked spectra for the time course array of the reaction from 0 to 24 h reaction time. **Top:** Full range stacked spectra. **Bottom:** Zoom from -63.0 to -60.0 ppm.

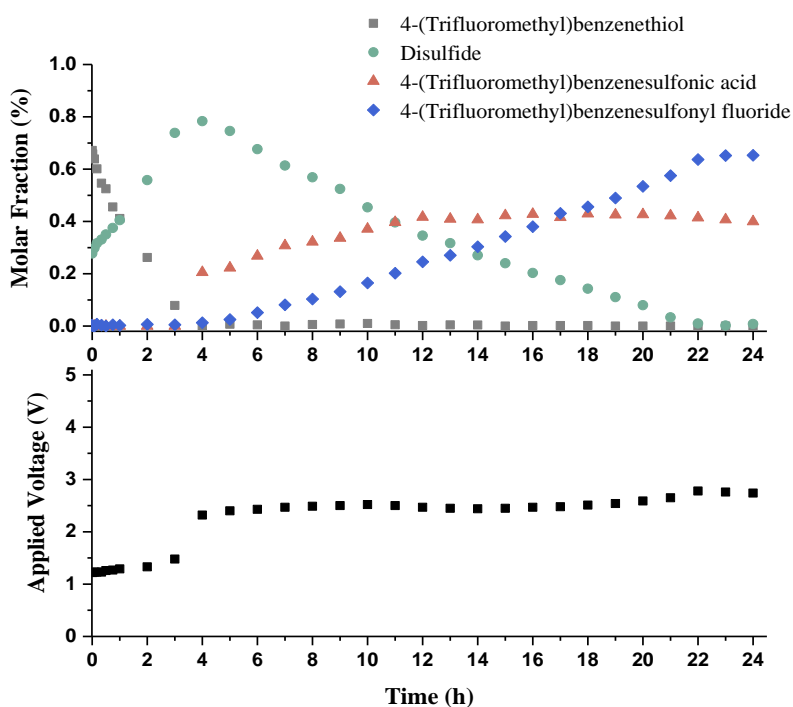
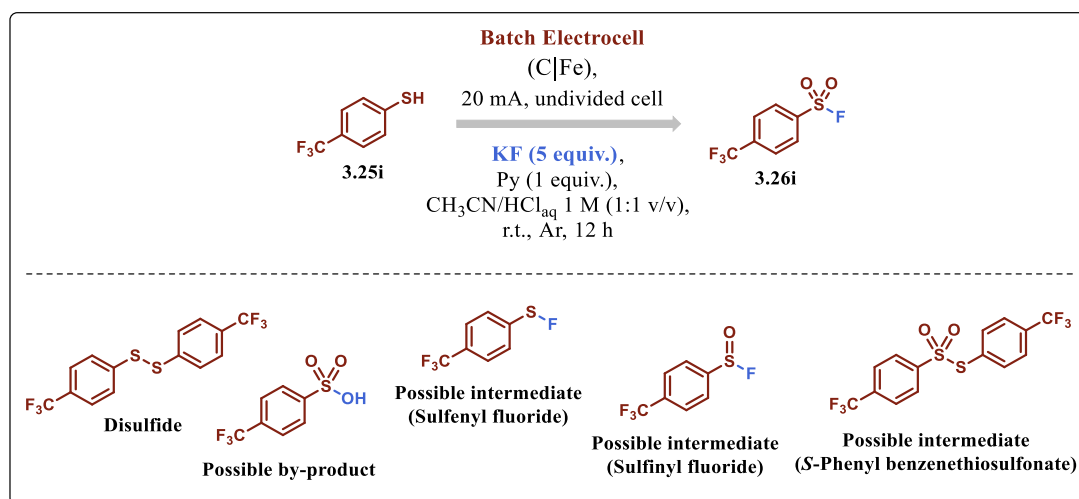


Figure 3.13 – Kinetic experiment at constant current conditions. **Top:** Integration of peaks of the ^{19}F NMR plot. **Bottom:** Applied voltage over time.

The experiment showed a similar outcome to that observed previously (Figures 3.10 and 3.11). At the beginning, conversion to disulfide is observed (within 4 h). During this first step, the potential remains constant at 1.2–1.3 V (Figure 3.13, bottom). When full conversion of disulfide is achieved, the potential rises to 2.4–2.5 V (Figure 3.13, bottom), and the product **3.26i** appears together with the peaks observed in the potentiostatic experiment. Full conversion is reached in 22 h (see Figure 3.13, top).

Finally, a kinetic experiment at constant current under an inert atmosphere was carried out (Scheme 3.11 and Figures 3.14 and 3.15).



Scheme 3.11 – Kinetic experiment at constant current under an inert atmosphere.

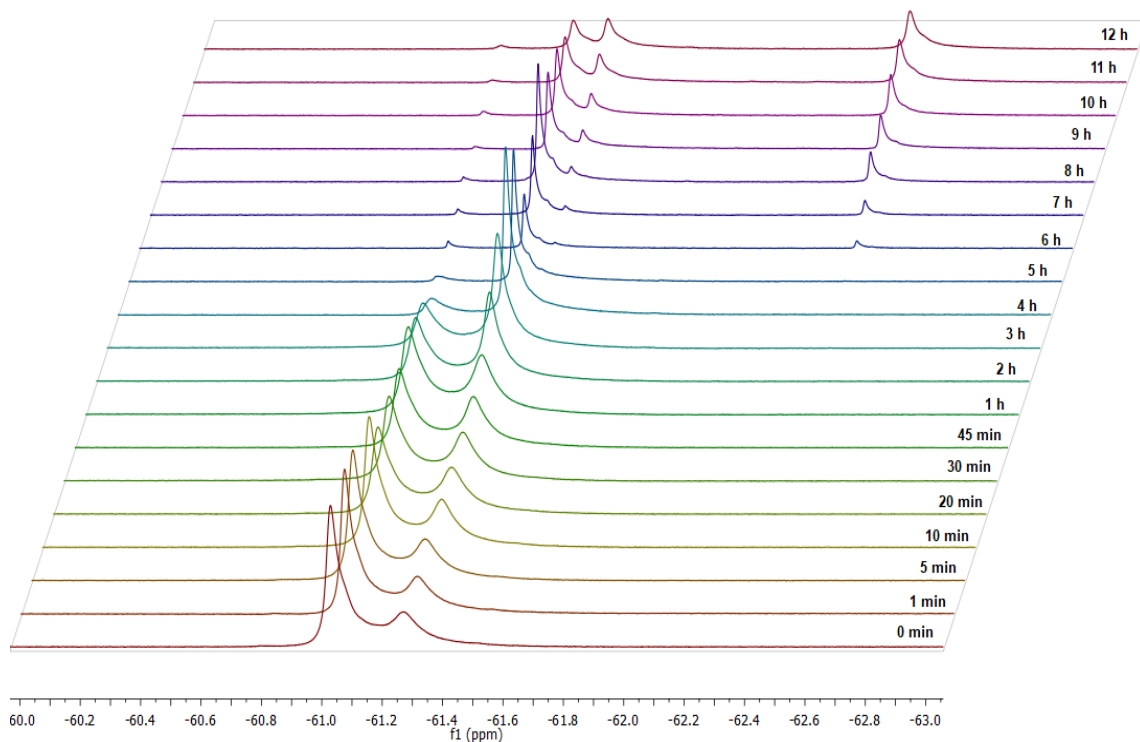
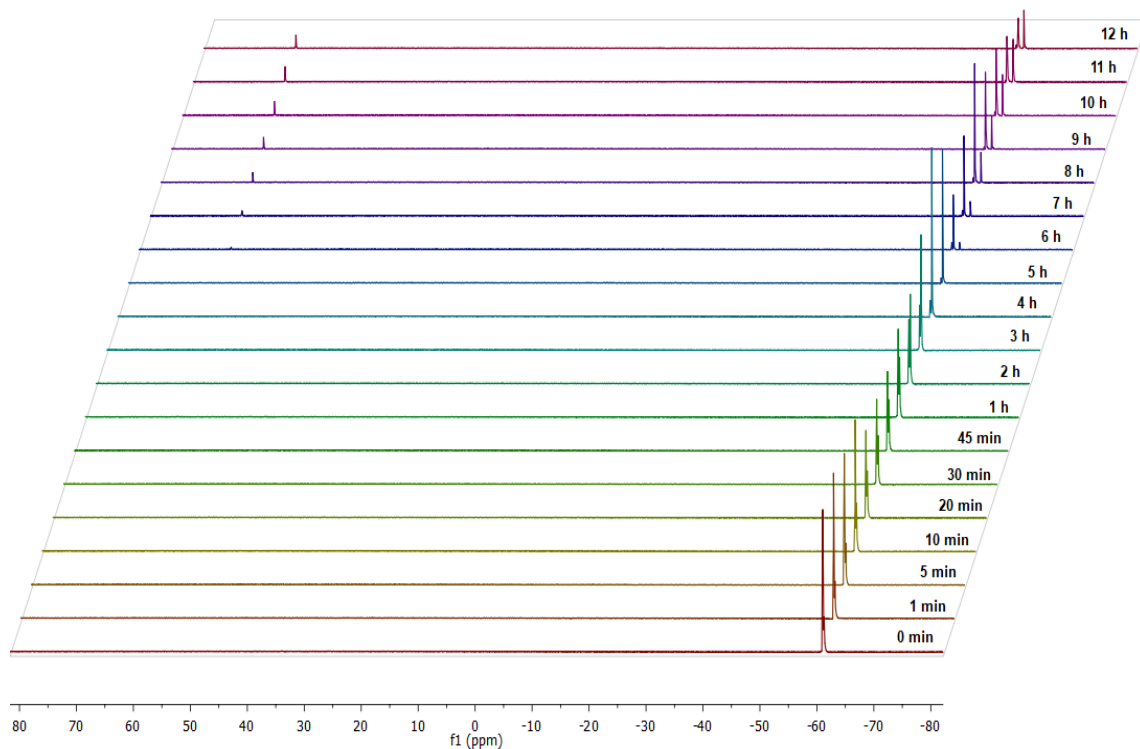


Figure 3.14 – Kinetic experiment at constant current under an inert atmosphere. 1D ^{19}F NMR stacked spectra for the time course array of the reaction from 0 to 12 h reaction time. **Top:** Full range stacked spectra. **Bottom:** Zoom from -63.0 to -60.0 ppm.

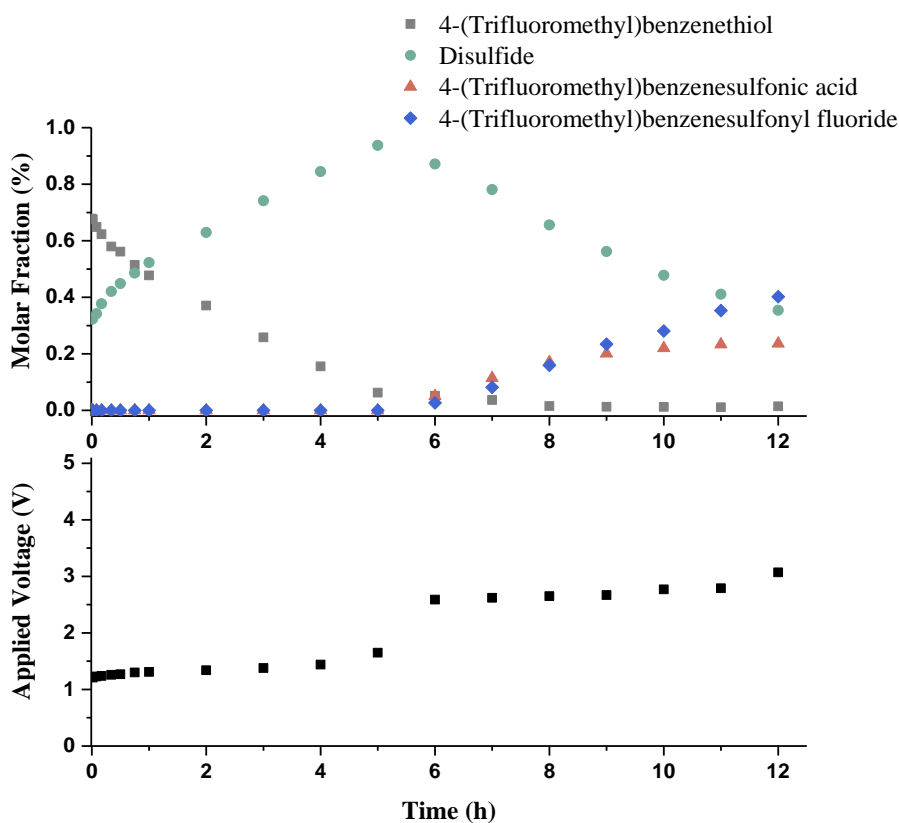


Figure 3.15 – Kinetic experiment at constant current under an inert atmosphere. **Top:** Integration of peaks of the ^{19}F NMR plot. **Bottom:** Applied voltage over time.

The experiment under inert conditions showed a similar reaction pattern to the reaction carried out in air (Figures 3.12 and 3.13). However, at the beginning of the reaction, slower formation of disulfide was observed in comparison to the previous reaction. Also, the byproduct formation rate (sulfonic acid) in air was higher than in argon at the same reaction time (compare Figure 3.13 (top) with Figure 3.15 (top)).

3.5.2 Radical quenching experiments

In order to elucidate the mechanism, radical quenching experiments with TEMPO, BHT, and benzoquinone were carried out (Tables 3.9 and 3.10).

We commenced our investigation using an excess of radical scavengers (1.5–3 equiv.) with thiophenol (**3.25a**) (Table 3.9).

Table 3.9 – Thiophenol quenching experiment^[a]

Electrocell
(C|Fe),
20 mA, undivided cell

3.25a $\xrightarrow{\text{KF (5 equiv.), Py (1 equiv.), Radical scavenger (1.5 or 3 equiv.), CH}_3\text{CN/HCl}_{\text{aq}} \text{ 1 M (1:1 v/v), r.t., 24 h}}$ **3.26a**

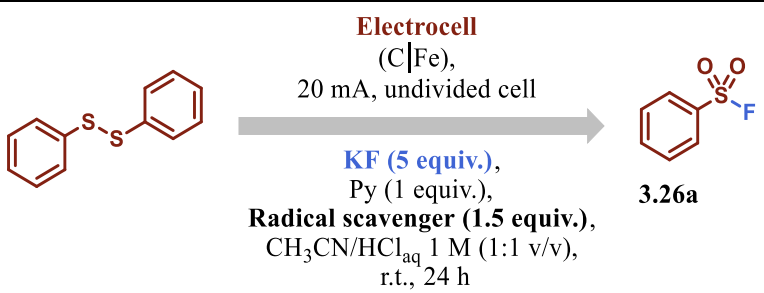
Entry	Radical Scavenger	Product ^[b]
1	BHT (1.5 equiv.)	36%
2	TEMPO (1.5 equiv.)	82%
3	Benzoquinone (1.5 equiv.)	21%
4	BHT (3 equiv.)	Traces
5	TEMPO (3 equiv.)	21%

^[a]Thiophenol (2 mmol), radical scavenger (1.5 or 3 equiv.), KF (5 equiv.), pyridine (1 equiv.), CH₃CN/HCl_{aq} 1 M (1:1 v/v, 20 mL), r.t., 24 h, and a constant current of 20 mA. ^[b]GC yields were calculated with an internal standard (biphenyl).

Generally, the reaction proceeded with lower yields than the standard in all cases. A larger excess of BHT and TEMPO inhibited the reaction completely (or almost completely). No quenched intermediates were detected via GC-MS.

Next, we decided to carry out the same experiment with diphenyl disulfide, in order to avoid any quenching of the radical traps by the thiol **3.25a** (Table 3.10). As a result, only traces or low amounts of product **3.26a** were observed after 24 h. No quenched intermediates were also detected via GC-MS.

Table 3.10 – Diphenyl disulfide quenching experiment^[a]



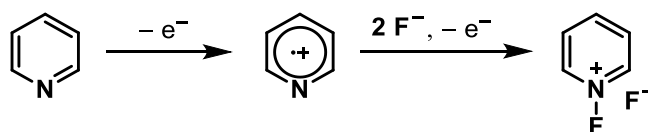
Entry	Radical Scavenger	Product ^[b]
1	BHT	13%
2	TEMPO	Traces
3	Benzoquinone	Traces

^[a]Diphenyl disulfide (1 mmol), radical scavenger (1.5 equiv.), KF (5 equiv.), pyridine (1 equiv.), CH₃CN/HCl_{aq} 1 M (1:1 v/v, 20 mL), r.t., 24 h, and a constant current of 20 mA. ^[b]GC yields were calculated with an internal standard (biphenyl).

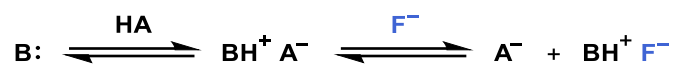
3.6 Fluorination step

Based on the experimental data obtained, we envisioned two different possibilities for the fluorination step:

1. *In situ* formation of an electrophilic fluorinating species via anodic oxidation.



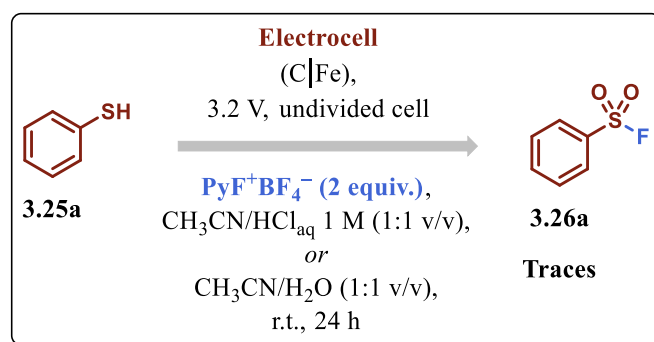
2. *In situ* formation of an amine·HF adduct in acidic conditions, similar to that previously reported in the literature employing alkali-metal fluorides and solid-supported acids in the presence of 2,6-lutidine in dehydrated acetonitrile under electrochemical conditions.⁷⁷



For this reason, we carried out some preliminary reactions, to understand better the fluorination step of our mechanism.

3.6.1 1-Fluoropyridinium

The formation of sulfonyl fluoride employing 1-fluoropyridinium tetrafluoroborate (a common, mild electrophilic fluorinating reagent) was investigated (Scheme 3.12).^{101,102} Hereto, the reaction was performed with 2 equiv. of 1-fluoropyridinium tetrafluoroborate with and without acid. Interestingly, both reactions led to only traces of the product after 24 h.



Scheme 3.12 – 1-Fluoropyridinium tetrafluoroborate experiment.

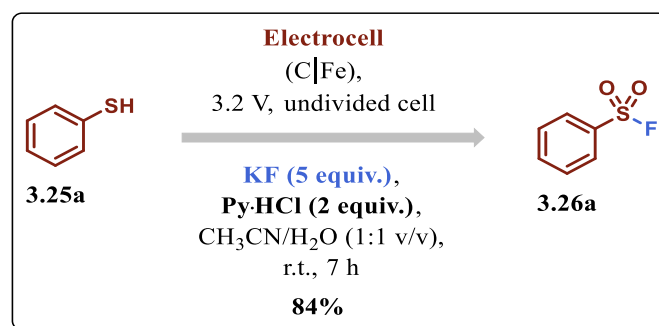
These results might indicate that a mild electrophilic fluorinating reagent is not necessary for the reaction.

We previously carried out an electrochemical reaction with Selectfluor (see Table 3.4, entry 5), which led to almost quantitative GC yield towards the desired product. However, reaction with this strong fluorinating reagent was already proven to occur without

electricity at high temperatures or with prefunctionalized reagents.^{57,67,68} We think that in this case the fluorination step is promoted by Selectfluor, while the electrochemical reaction is needed to accelerate the oxidation step.

3.6.2 Pyridinium chloride

Based on the previous results, we decided to investigate the effect of an amine·HCl salt. Hence, an experiment was carried out with pyridinium chloride and the desired product **3.26a** was obtained in 84% GC yield (Scheme 3.13).



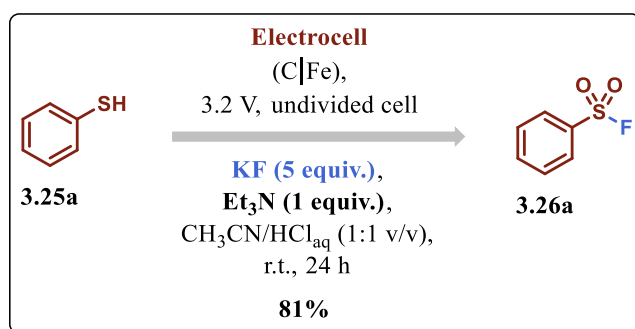
Scheme 3.13 – Pyridinium chloride experiment (GC-FID yield, biphenyl as an internal standard).

This result indicates that the preformed py·HCl followed by anion exchange behaves similarly compared to the standard reaction conditions.

3.6.3 Triethylamine

In order to further prove that our fluorination step happens via an amine·HF adduct, a different amine was tested (Scheme 3.14). During our optimization, we showed that triethylamine in neutral conditions was ineffective (see Table 3.3, entry 3). We tested it again

in the presence of HCl with thiophenol (**3.25a**). As a result, the reaction product **3.26a** was formed after 24 h in good GC yield (81%). However, we also cannot rule out the possibility that a bifluoride $[F-H-F]^-$ anion is acting as a nucleophilic fluorination agent,³⁷ especially in the reactions performed under acidic conditions in the absence of a base (see Table 3.8, entry 17). Another possibility is the formation of an adduct between amine and bifluoride anion in acidic conditions ($[pyH]^+-[F-H-F]^-$ adduct), which is an even more nucleophilic species.



Scheme 3.14 – Triethylamine experiment (GC-FID yield, biphenyl as an internal standard).

3.7 Cyclic voltammetry analyses

Cyclic voltammetry analyses were carried out at room temperature with an IVIUM CompactStat potentiostat (Ivium Technologies B.V., Eindhoven, The Netherlands) using a standard three-electrode cell equipped with a platinum working electrode, a nickel counter electrode, and an SCE reference electrode. The experiments were performed at a concentration of 0.1 M in CH₃CN (30 mL) with an electrolyte (Me₄NBF₄, 0.01 M); however, in some measurements, a small amount of water was added to get everything into solution. Unless specified, a scan rate of 200 mV/s was used.

First, a “blank” voltammogram (i.e. one run for electrolyte solutions only, without a sample) was recorded (Figure 3.16).

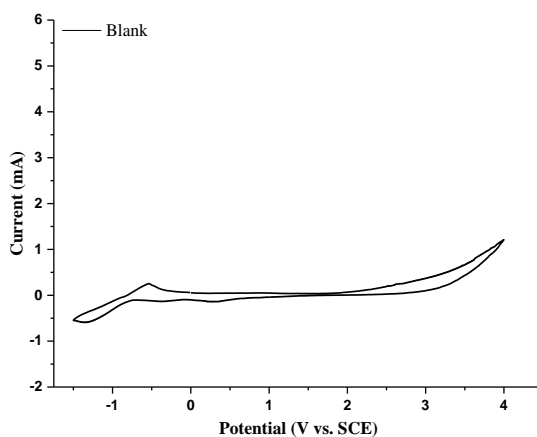


Figure 3.16 – Cyclic voltammogram of blank solution ($\text{CH}_3\text{CN}/0.01 \text{ M Me}_4\text{NBF}_4$).

3.7.1 Starting materials

Thiophenol:

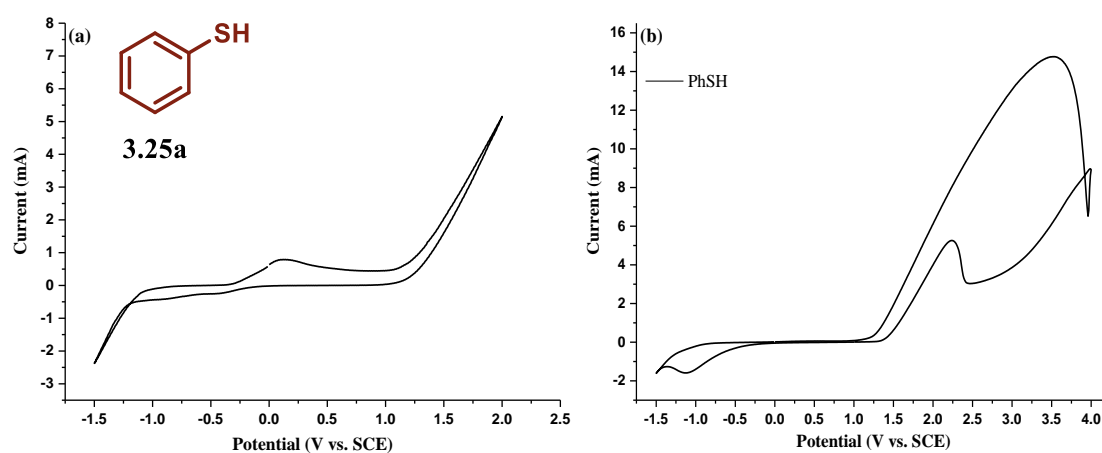


Figure 3.17 – Cyclic voltammograms of thiophenol in CH_3CN ($0.01 \text{ M Me}_4\text{NBF}_4$), measured between (a) -1.5 and 2 V and (b) -1.5 and 4 V .

As shown in Figure 3.17a, the cyclic voltammogram of **3.25a** exhibited an oxidation peak at ca. $+0.1 \text{ V}$ (vs. SCE) related to the oxidation of thiolate anion ($\text{C}_6\text{H}_5\text{S}^-$).¹⁰³ However, the other peak expected at $+1.5 \text{ V}$ (vs. SCE in CH_3CN),¹⁰⁴ corresponding to the oxidation of thiophenol to diphenyl disulfide,^{103,105} was not well-resolved in the voltammogram of Figure 3.17b.

KF:

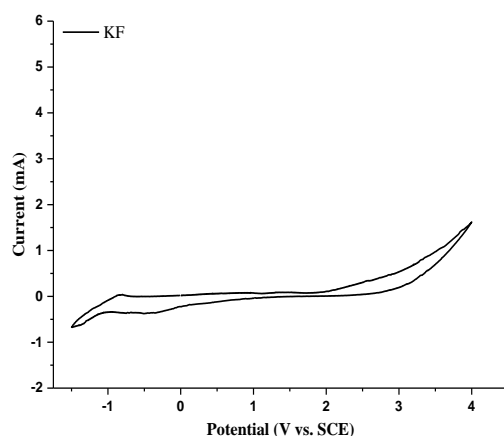


Figure 3.18 – Cyclic voltammogram of KF in CH₃CN/H₂O (0.01 M Me₄NBF₄).

Cyclic voltammogram of KF is shown in Figure 3.18. This alkali fluoride did not lead to a substantial increment in current compared to the electrolyte (Figure 3.16 vs. 3.18).

Diphenyl disulfide:

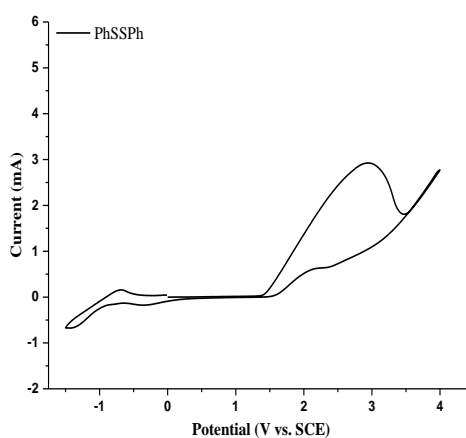
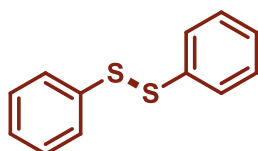


Figure 3.19 – Cyclic voltammogram of diphenyl disulfide in CH₃CN/0.01 M Me₄NBF₄.

The cyclic voltammogram of diphenyl disulfide is shown in Figure 3.19. The oxidation peak expected between +1.6 and +1.8 V (vs. SCE in CH₃CN),^{2,106} corresponding to the oxidation of disulfide to its cation radical,¹⁰⁵ was not well-resolved in this voltammogram.

Pyridine:

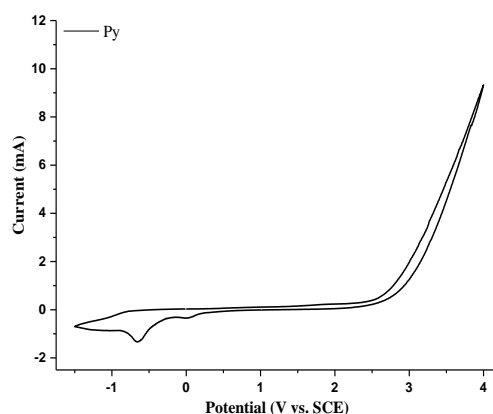


Figure 3.20 – Cyclic voltammogram of pyridine in $\text{CH}_3\text{CN}/0.01 \text{ M Me}_4\text{NBF}_4$.

The cyclic voltammogram of pyridine (Figure 3.20) exhibited a reduction peak at ca. -0.6 V (vs. SCE), but its oxidation peak was not particularly well-resolved.^{2,107}

3.7.2 Reaction mixture

Py + KF

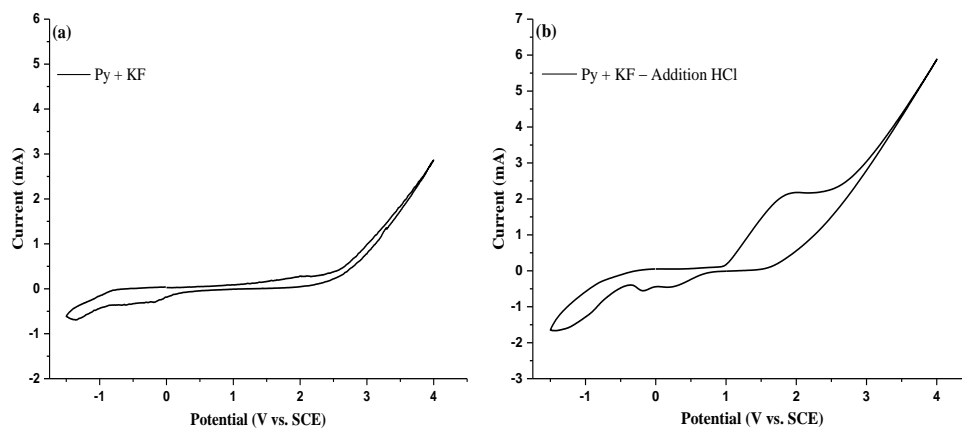


Figure 3.21 – Cyclic voltammograms of mixture of pyridine with KF in $\text{CH}_3\text{CN}/\text{H}_2\text{O}$ ($0.01 \text{ M Me}_4\text{NBF}_4$): (a) without an acid and (b) in the presence one drop of HCl.

A voltammogram of pyridine with KF in acetonitrile/water was recorded. As a result, no significant difference was observed compared to the voltammogram recorded for pyridine alone (see Figure 3.20 vs. 3.21a). The addition of one drop of HCl resulted in the

formation of a broad oxidation wave starting at approximately +0.95 V (vs. SCE) (Figure 3.21b).

Py + KF + PhSH

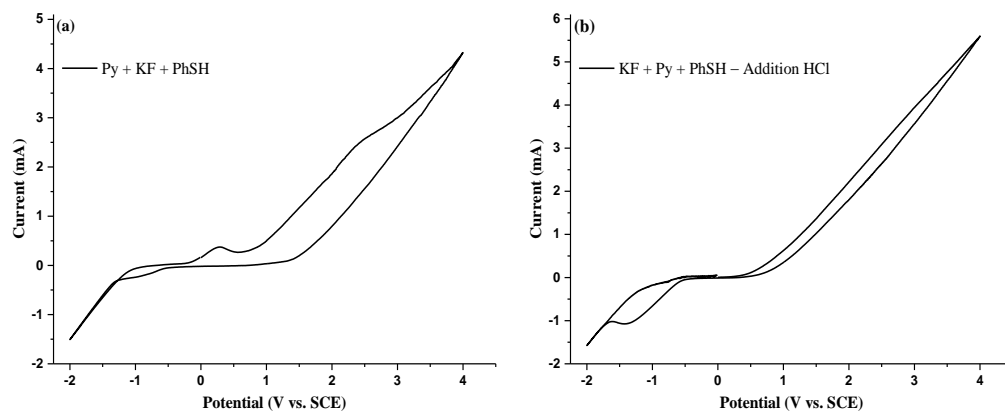


Figure 3.22 – Cyclic voltammograms of reaction mixture (Py + KF + PhSH) in CH₃CN/H₂O (0.01 M Me₄NBF₄): (a) without an acid and (b) in the presence one drop of HCl.

A voltammogram of the reaction mixture (Py + KF + PhSH) in acetonitrile/water was recorded. When thiophenol was added to the mixture of pyridine and KF, a new peak appeared at around +2.3 V (vs. SCE), possibly related to the formation of a fluorinated species of thiol (Figure 3.22a). The addition of acid did not lead to any conclusive result (Figure 3.22b).

Py + KF + PhSSPh

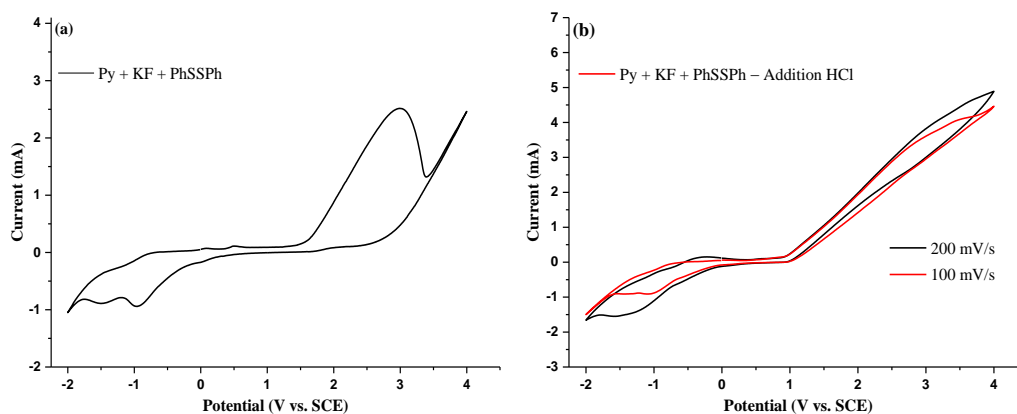


Figure 3.23 – Cyclic voltammograms of reaction mixture (Py + KF + PhSSPh) in CH₃CN/H₂O (0.01 M Me₄NBF₄): (a) without an acid and (b) in the presence one drop of HCl.

A voltammogram with diphenyl disulfide was also recorded. Consequently, no significant change in the benchmark profiles was observed when the reactants were dissolved in acetonitrile/water mixture (see Figures 3.19 and 3.20 vs. 3.23a). Upon adding one drop of hydrochloric acid, the peak of the oxidation of disulfide disappeared, an indication that the disulfide radical might react with another species (Figure 3.23b).

3.7.3 Experiment with Et₃N

To further investigate the effect of the additive on the fluorination, a different base was tested (Figures 3.24 and 3.25).

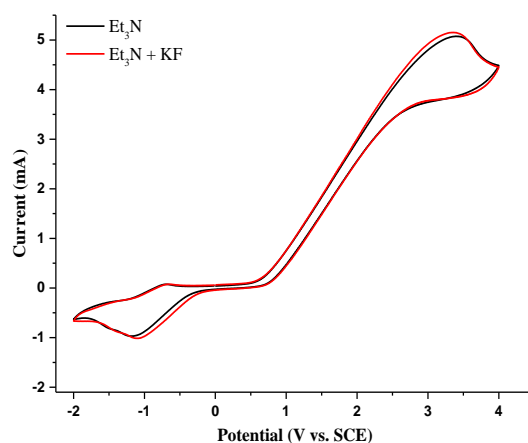


Figure 3.24 – Cyclic voltammograms of Et₃N in CH₃CN/H₂O (0.01 M Me₄NBF₄) with (red line) or without KF (black line).

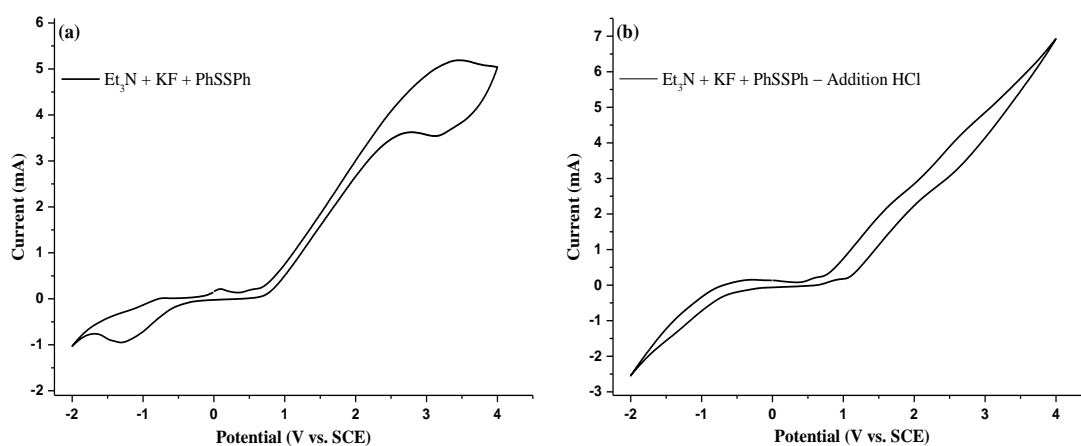


Figure 3.25 – Cyclic voltammograms of reaction mixture ($\text{Et}_3\text{N} + \text{KF} + \text{PhSSPh}$) in $\text{CH}_3\text{CN}/\text{H}_2\text{O}$ (0.01 M Me_4NBF_4): (a) without an acid and (b) in the presence one drop of HCl.

The cyclic voltammogram of triethylamine in $\text{CH}_3\text{CN}/\text{H}_2\text{O}$ containing 0.01 M Me_4NBF_4 is shown in Figure 3.24 (black line). The oxidation peak expected at approximately +0.75 V (vs. SCE),⁷⁷ corresponding to the oxidation of Et_3N to its cation radical, was not well-resolved in this voltammogram. Potassium fluoride was then added and the cyclic voltammogram was recorded again (Figure 3.24, red line), but no difference was observed compared to the previous one. Further addition of diphenyl disulfide did not show substantial changes in the voltammogram, except for the addition of the disulfide profile (Figure 3.25a). The addition of acid did not lead to any conclusive result (Figure 3.25b).

Based on results shown in Sections 3.6 and 3.7, we can speculate that the amine is protonated in acidic media and then via anion exchange¹⁰⁸ generates the actual fluorinating species (amine $\cdot\text{HF}$ or $[\text{amineH}]^+ - [\text{F}-\text{H}-\text{F}]^-$ adduct) (Figure 3.26).

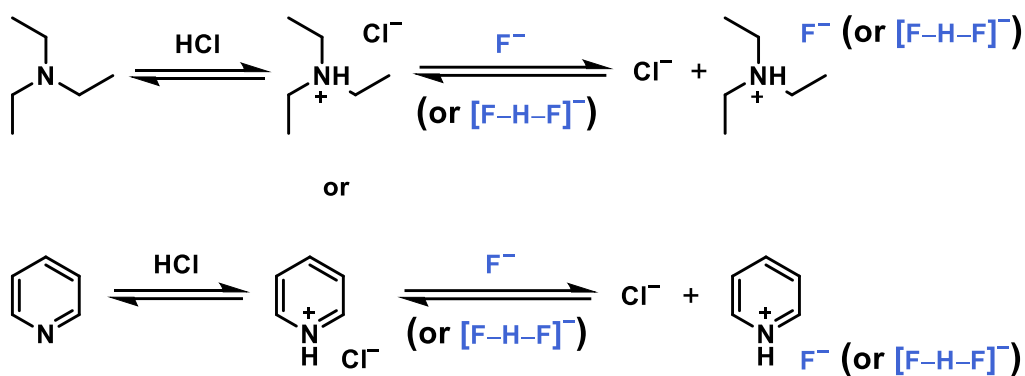
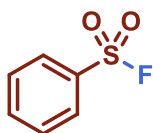


Figure 3.26 – Proposal for the formation of fluorinating species via anion exchange process.

3.8 Faraday efficiency

Assuming complete anodic oxidation for the product (6 e⁻ per mole of substrate).

Average current for the oxidation to sulfoxide



$$\begin{aligned}
 I &= 20 \text{ mA} \\
 r_t &= 36 \text{ h} = 1.30 \times 10^5 \text{ s} \\
 \text{Yield} &= 99\% \\
 Q &= I * r_t = 2.59 \times 10^3 \text{ C}
 \end{aligned}$$

Experimental electron amount

$$n_{e_{\text{expe}}} = \frac{Q}{F} = \frac{2.59 \times 10^3 \text{ C}}{96,485 \text{ C} * \text{mol}^{-1}} = 26.8 \text{ mmol}$$

Theoretical electron amount

$$\begin{aligned}
 V_{\text{reactor}} &= 20 \text{ mL} \\
 C_{\text{substrate}} &= 0.1 \text{ M} & n_{\text{substrate}} &= 12 \text{ mmol} \\
 n_{e_{\text{theo}}} &= 2.0 \text{ mmol} & & \text{(assuming 6 electrons needed)}
 \end{aligned}$$

Faraday Efficiency

$$F_{\text{efficiency}} \% = \frac{n_{e_{\text{theo}}}}{n_{e_{\text{expe}}}} * 100 = \frac{12 \text{ mmol}}{26.8 \text{ mmol}} * 100 = 45\%$$

Reference

- 1 KÄRKÄS, M. D. "Electrochemical strategies for C–H functionalization and C–N bond formation". *Chem. Soc. Rev.*, 47 (15): 5786, 2018.
- 2 FUCHIGAMI, T.; ATOBE, M. & INAGI, S. *Fundamentals and Applications of Organic Electrochemistry*. New York: Wiley, 2014. 240 p.
- 3 YOSHIDA, J.-I. & NISHIWAKI, K. "Redox selective reactions of organo-silicon and -tin compounds". *J. Chem. Soc., Dalton Trans.*, (16): 2589, 1998.
- 4 MÖHLE, S.; ZIRBES, M.; RODRIGO, E.; GIESHOFF, T.; WIEBE, A. & WALDVOGEL, S. R. "Modern electrochemical aspects for the synthesis of value-added organic products". *Angew. Chem. Int. Ed.*, 57 (21): 6018, 2018.
- 5 STANG, C. & HARNISCH, F. "The dilemma of supporting electrolytes for electroorganic synthesis: a case study on Kolbe electrolysis". *ChemSusChem*, 9 (1): 50, 2016.
- 6 PERKINS, R. J. *Anodic Electrochemistry: Controlling the Reactivity of Radical Cation Intermediates*. Department of Chemistry - Washington University in St. Louis, 2016. Doctor of Philosophy, p. 250.
- 7 RENSING, D. T.; NGUYEN, B. H. & MOELLER, K. D. "Considering organic mechanisms and the optimization of current flow in an electrochemical oxidative condensation reaction". *Org. Chem. Front.*, 3 (10): 1236, 2016.
- 8 HAMMERICH, O. & SPEISER, B. *Organic Electrochemistry: Revised and Expanded*. 5th ed. Boca Raton: CRC Press, 2015. 1736 p.
- 9 BLANCO, D. E. & MODESTINO, M. A. "Organic electrosynthesis for sustainable chemical manufacturing". *Trends Chem.*, 1 (1): 8, 2019.
- 10 FRONTANA-URIBE, B. A.; LITTLE, R. D.; IBANEZ, J. G.; PALMA, A. & VASQUEZ-MEDRANO, R. "Organic electrosynthesis: a promising green methodology in organic chemistry". *Green Chem.*, 12 (12): 2099, 2010.
- 11 BARD, A. J.; INZELT, G. & SCHOLZ, F. *Electrochemical Dictionary*. 2nd ed. Berlin: Springer-Verlag, 2012. 991 p.
- 12 LUND, H. "A century of organic electrochemistry". *J. Electrochem. Soc.*, 149 (4): S21, 2002.
- 13 CARDOSO, D. S. P.; ŠLJUKIĆ, B.; SANTOS, D. M. F. & SEQUEIRA, C. A. C. "Organic electrosynthesis: from laboratorial practice to industrial applications". *Org. Process Res. Dev.*, 21 (9): 1213, 2017.
- 14 PLETCHER, D. "Recent developments in organic electrosynthesis". *Rev. Port. Quím.*, 27: 449, 1985.

- 15 SEQUEIRA, C. A. C. & SANTOS, D. M. F. "Electrochemical routes for industrial synthesis". *J. Braz. Chem. Soc.*, 20: 387, 2009.
- 16 WALDVOGEL, S. R. "Electrosynthesis and electrochemistry". *Beilstein J. Org. Chem.*, 11: 949, 2015.
- 17 ECHEVERRIA, P. G.; DELBRAYELLE, D.; LETORT, A.; NOMERTIN, F.; PEREZ, M. & PETIT, L. "The spectacular resurgence of electrochemical redox reactions in organic synthesis". *Aldrichimica Acta*, 51: 3, 2018.
- 18 YAN, M.; KAWAMATA, Y. & BARAN, P. S. "Synthetic organic electrochemical methods since 2000: on the verge of a renaissance". *Chem. Rev.*, 117 (21): 13230, 2017.
- 19 FRANKOWSKI, K. J.; LIU, R.; MILLIGAN, G. L.; MOELLER, K. D. & AUBÉ, J. "Practical electrochemical anodic oxidation of polycyclic lactams for late stage functionalization". *Angew. Chem. Int. Ed.*, 54 (36): 10555, 2015.
- 20 JIANG, Y.; XU, K. & ZENG, C. "Use of electrochemistry in the synthesis of heterocyclic structures". *Chem. Rev.*, 118 (9): 4485, 2018.
- 21 MITSUDO, K.; KURIMOTO, Y.; YOSHIOKA, K. & SUGA, S. "Miniaturization and combinatorial approach in organic electrochemistry". *Chem. Rev.*, 118 (12): 5985, 2018.
- 22 PETERS, B. K.; RODRIGUEZ, K. X.; REISBERG, S. H.; BEIL, S. B.; HICKEY, D. P.; KAWAMATA, Y., et al. "Scalable and safe synthetic organic electroreduction inspired by Li-ion battery chemistry". *Science*, 363 (6429): 838, 2019.
- 23 SHATSKIY, A.; LUNDBERG, H. & KÄRKÄS, M. D. "Organic electrosynthesis: applications in complex molecule synthesis". *ChemElectroChem*, 6 (16): 4067, 2019.
- 24 WIEBE, A.; GIESHOFF, T.; MÖHLE, S.; RODRIGO, E.; ZIRBES, M. & WALDVOGEL, S. R. "Electrifying organic synthesis". *Angew. Chem. Int. Ed.*, 57 (20): 5594, 2018.
- 25 NOËL, T.; CAO, Y. & LAUDADIO, G. "The fundamentals behind the use of flow reactors in electrochemistry". *Acc. Chem. Res.*, 52 (10): 2858, 2019.
- 26 GHOSH, M.; SHINDE, V. S. & RUEPING, M. "A review of asymmetric synthetic organic electrochemistry and electrocatalysis: concepts, applications, recent developments and future directions". *Beilstein J. Org. Chem.*, 15: 2710, 2019.
- 27 HORN, E. J.; ROSEN, B. R.; CHEN, Y.; TANG, J.; CHEN, K.; EASTGATE, M. D., et al. "Scalable and sustainable electrochemical allylic C–H oxidation". *Nature*, 533 (7601): 77, 2016.
- 28 SCHULZ, L.; ENDERS, M.; ELSLER, B.; SCHOLLMAYER, D.; DYBALLA, K. M.; FRANKE, R., et al. "Reagent- and metal-free anodic C–C cross-coupling of aniline derivatives". *Angew. Chem. Int. Ed.*, 56 (17): 4877, 2017.

- 29 WANG, P.; TANG, S.; HUANG, P. & LEI, A. "Electrocatalytic oxidant-free dehydrogenative C–H/S–H cross-coupling". *Angew. Chem. Int. Ed.*, 56 (11): 3009, 2017.
- 30 YANG, Q.-L.; LI, Y.-Q.; MA, C.; FANG, P.; ZHANG, X.-J. & MEI, T.-S. "Palladium-catalyzed C(sp³)–H oxygenation via electrochemical oxidation". *J. Am. Chem. Soc.*, 139 (8): 3293, 2017.
- 31 ZHAO, H.-B.; HOU, Z.-W.; LIU, Z.-J.; ZHOU, Z.-F.; SONG, J. & XU, H.-C. "Amidinyl radical formation through anodic N–H bond cleavage and its application in aromatic C–H bond functionalization". *Angew. Chem. Int. Ed.*, 56 (2): 587, 2017.
- 32 HORN, E. J.; ROSEN, B. R. & BARAN, P. S. "Synthetic organic electrochemistry: an enabling and innately sustainable method". *ACS Cent. Sci.*, 2 (5): 302, 2016.
- 33 LIPP, A.; FERENC, D.; GÜTZ, C.; GEFFE, M.; VIERENGEL, N.; SCHOLLMEYER, D., et al. "A regio- and diastereoselective anodic aryl–aryl coupling in the biomimetic total synthesis of (–)-Thebaine". *Angew. Chem. Int. Ed.*, 57 (34): 11055, 2018.
- 34 LAUDADIO, G.; BARMPOUTSIS, E.; SCHOTTEN, C.; STRUIK, L.; GOVAERTS, S.; BROWNE, D. L., et al. "Sulfonamide synthesis through electrochemical oxidative coupling of amines and thiols". *J. Am. Chem. Soc.*, 141 (14): 5664, 2019.
- 35 WALDVOGEL, S. R.; LIPS, S.; SELT, M.; RIEHL, B. & KAMPF, C. J. "Electrochemical arylation reaction". *Chem. Rev.*, 118 (14): 6706, 2018.
- 36 KINGSTON, C.; PALKOWITZ, M. D.; TAKAHIRA, Y.; VANTOUROUT, J. C.; PETERS, B. K.; KAWAMATA, Y., et al. "A survival guide for the “electro-curious”". *Acc. Chem. Res.*, 53 (1): 72, 2019.
- 37 DONG, J.; KRASNOVA, L.; FINN, M. G. & SHARPLESS, K. B. "Sulfur(VI) fluoride exchange (SuFEx): another good reaction for click chemistry". *Angew. Chem. Int. Ed.*, 53 (36): 9430, 2014.
- 38 CHINTHAKINDI, P. K. & ARVIDSSON, P. I. "Sulfonyl fluorides (SFs): more than click reagents?". *Eur. J. Org. Chem.*, (27-28): 3648, 2018.
- 39 TRIBBY, A. L.; RODRÍGUEZ, I.; SHARIFFUDIN, S. & BALL, N. D. "Pd-catalyzed conversion of aryl iodides to sulfonyl fluorides using SO₂ surrogate DABSO and selectfluor". *J. Org. Chem.*, 82 (4): 2294, 2017.
- 40 AGUILAR, B.; AMISSAH, F.; DUVERNA, R. & LAMANGO, N. S. "Polyisoprenylation potentiates the inhibition of polyisoprenylated methylated protein methyl esterase and the cell degenerative effects of sulfonyl fluorides". *Curr. Cancer Drug Targets*, 11 (6): 752, 2011.
- 41 GRIMSTER, N. P.; CONNELLY, S.; BARANCZAK, A.; DONG, J.; KRASNOVA, L. B.; SHARPLESS, K. B., et al. "Aromatic sulfonyl fluorides covalently kinetically stabilize transthyretin to prevent amyloidogenesis while affording a fluorescent conjugate". *J. Am. Chem. Soc.*, 135 (15): 5656, 2013.

- 42 HETT, E. C.; XU, H.; GEOGHEGAN, K. F.; GOPALSAMY, A.; KYNE, R. E.; MENARD, C. A., et al. "Rational targeting of active-site tyrosine residues using sulfonyl fluoride probes". *ACS Chem. Biol.*, 10 (4): 1094, 2015.
- 43 NARAYANAN, A. & JONES, L. H. "Sulfonyl fluorides as privileged warheads in chemical biology". *Chem. Sci.*, 6 (5): 2650, 2015.
- 44 SHANNON, D. A.; GU, C.; MCLAUGHLIN, C. J.; KAISER, M.; VAN DER HOORN, R. A. L. & WEERAPANA, E. "Sulfonyl fluoride analogues as activity-based probes for serine proteases". *ChemBioChem*, 13 (16): 2327, 2012.
- 45 NIELSEN, M. K.; UGAZ, C. R.; LI, W. & DOYLE, A. G. "PyFluor: a low-cost, stable, and selective deoxyfluorination reagent". *J. Am. Chem. Soc.*, 137 (30): 9571, 2015.
- 46 INKSTER, J. A. H.; LIU, K.; AIT-MOHAND, S.; SCHAFFER, P.; GUÉRIN, B.; RUTH, T. J., et al. "Sulfonyl fluoride-based prosthetic compounds as potential ^{18}F labelling agents". *Chem. Eur. J.*, 18 (35): 11079, 2012.
- 47 MATESIC, L.; WYATT, N. A.; FRASER, B. H.; ROBERTS, M. P.; PHAM, T. Q. & GREGURIC, I. "Ascertaining the suitability of aryl sulfonyl fluorides for [^{18}F]radiochemistry applications: a systematic investigation using microfluidics". *J. Org. Chem.*, 78 (22): 11262, 2013.
- 48 WANG, H.; ZHOU, F.; REN, G.; ZHENG, Q.; CHEN, H.; GAO, B., et al. "SuFEx-based polysulfonate formation from ethenesulfonyl fluoride–amine adducts". *Angew. Chem. Int. Ed.*, 56 (37): 11203, 2017.
- 49 XIAO, X.; ZHOU, F.; JIANG, J.; CHEN, H.; WANG, L.; CHEN, D., et al. "Highly efficient polymerization via sulfur(VI)-fluoride exchange (SuFEx): novel polysulfates bearing a pyrazoline–naphthylamide conjugated moiety and their electrical memory performance". *Polym. Chem.*, 9 (8): 1040, 2018.
- 50 YANG, C.; FLYNN, J. P. & NIU, J. "Facile synthesis of sequence-regulated synthetic polymers using orthogonal SuFEx and CuAAC click reactions". *Angew. Chem. Int. Ed.*, 57 (49): 16194, 2018.
- 51 FATTAH, T. A.; SAEED, A. & ALBERICIO, F. "Recent advances towards sulfur(VI) fluoride exchange (SuFEx) click chemistry". *J. Fluorine Chem.*, 213: 87, 2018.
- 52 BIANCHI, T. A. & CATE, L. A. "Phase transfer catalysis. Preparation of aliphatic and aromatic sulfonyl fluorides". *J. Org. Chem.*, 42 (11): 2031, 1977.
- 53 DAVIES, W. & DICK, J. H. "CCLXXXVI.—Aromatic sulphonyl fluorides. A convenient method of preparation". *J. Chem. Soc.*, (0): 2104, 1931.
- 54 TALKO, A. & BARBASIEWICZ, M. "Nucleophilic fluorination with aqueous bifluoride solution: effect of the phase-transfer catalyst". *ACS Sustainable Chem. Eng.*, 6 (5): 6693, 2018.

- 55 SCHMITT, A.-M. D. & SCHMITT, D. C. "Synthesis of sulfonamides". In: BLAKEMORE, D.; DOYLE, P. & FOBIAN, Y. (Ed.). *Synthetic methods in drug discovery*. The Royal Society of Chemistry, 2016, vol. 2, ch. 13, pp. 123-138.
- 56 KIM, J.-G. & JANG, D. O. "A convenient, one-pot procedure for the preparation of acyl and sulfonyl fluorides using Cl_3CCN , Ph_3P , and $\text{TBAF}(t\text{-BuOH})_4$ ". *Synlett*, (20): 3049, 2010.
- 57 TANG, L.; YANG, Y.; WEN, L.; YANG, X. & WANG, Z. "Catalyst-free radical fluorination of sulfonyl hydrazides in water". *Green Chem.*, 18 (5): 1224, 2016.
- 58 BROUWER, A. J.; CEYLAN, T.; LINDEN, T. V. D. & LISKAMP, R. M. J. "Synthesis of β -aminoethanesulfonyl fluorides or 2-substituted taurine sulfonyl fluorides as potential protease inhibitors". *Tetrahedron Lett.*, 50 (26): 3391, 2009.
- 59 TOULGOAT, F.; LANGLOIS, B. R.; MÉDEBIELLE, M. & SANCHEZ, J.-Y. "An efficient preparation of new sulfonyl fluorides and lithium sulfonates". *J. Org. Chem.*, 72 (24): 9046, 2007.
- 60 TUCKER, J. W.; CHENARD, L. & YOUNG, J. M. "Selective access to heterocyclic sulfonamides and sulfonyl fluorides via a parallel medicinal chemistry enabled method". *ACS Comb. Sci.*, 17 (11): 653, 2015.
- 61 WRIGHT, S. W. & HALLSTROM, K. N. "A convenient preparation of heteroaryl sulfonamides and sulfonyl fluorides from heteroaryl thiols". *J. Org. Chem.*, 71 (3): 1080, 2006.
- 62 LEE, C.; BALL, N. D. & SAMMIS, G. M. "One-pot fluorosulfonylation of Grignard reagents using sulfuryl fluoride". *Chem. Commun.*, 55 (98): 14753, 2019.
- 63 KWON, J. & KIM, B. M. "Synthesis of arenesulfonyl fluorides via sulfuryl fluoride incorporation from arynes". *Org. Lett.*, 21 (2): 428, 2019.
- 64 LIU, Y.; YU, D.; GUO, Y.; XIAO, J.-C.; CHEN, Q.-Y. & LIU, C. "Arenesulfonyl fluoride synthesis via copper-catalyzed fluorosulfonylation of arenediazonium salts". *Org. Lett.*, 22 (6): 2281, 2020.
- 65 PÉREZ-PALAU, M. & CORNELLA, J. "Synthesis of sulfonyl fluorides from sulfonamides". *Eur. J. Org. Chem.*, (17): 2497, 2020.
- 66 ZHONG, T.; PANG, M.-K.; CHEN, Z.-D.; ZHANG, B.; WENG, J. & LU, G. "Copper-free Sandmeyer-type reaction for the synthesis of sulfonyl fluorides". *Org. Lett.*, 22 (8): 3072, 2020.
- 67 KIRIHARA, M.; NAITO, S.; ISHIZUKA, Y.; HANAI, H. & NOGUCHI, T. "Oxidation of disulfides with SelectfluorTM: concise syntheses of thiosulfonates and sulfonyl fluorides". *Tetrahedron Lett.*, 52 (24): 3086, 2011.

- 68 KIRIHARA, M.; NAITO, S.; NISHIMURA, Y.; ISHIZUKA, Y.; IWAI, T.; TAKEUCHI, H., et al. "Oxidation of disulfides with electrophilic halogenating reagents: concise methods for preparation of thiosulfonates and sulfonyl halides". *Tetrahedron*, 70 (14): 2464, 2014.
- 69 CHEN, Y. & WILLIS, M. C. "Copper(I)-catalyzed sulfonylative Suzuki–Miyaura cross-coupling". *Chem. Sci.*, 8 (4): 3249, 2017.
- 70 DAVIES, A. T.; CURTO, J. M.; BAGLEY, S. W. & WILLIS, M. C. "One-pot palladium-catalyzed synthesis of sulfonyl fluorides from aryl bromides". *Chem. Sci.*, 8 (2): 1233, 2017.
- 71 PLIEGO, J. R. & PILÓ-VELOSO, D. "Chemoselective nucleophilic fluorination induced by selective solvation of the S_N2 transition state". *J. Phys. Chem. B*, 111 (7): 1752, 2007.
- 72 PITTS, C. R.; BORNEMANN, D.; LIEBING, P.; SANTSCHI, N. & TOGNI, A. "Making the SF₅ group more accessible: a gas-reagent-free approach to aryl tetrafluoro-λ⁶-sulfanyl chlorides". *Angew. Chem. Int. Ed.*, 58 (7): 1950, 2019.
- 73 UMEMOTO, T.; GARRICK, L. M. & SAITO, N. "Discovery of practical production processes for arylsulfur pentafluorides and their higher homologues, bis- and tris(sulfur pentafluorides): beginning of a new era of "super-trifluoromethyl" arene chemistry and its industry". *Beilstein J. Org. Chem.*, 8: 461, 2012.
- 74 UMEMOTO, T.; SINGH, R. P.; XU, Y. & SAITO, N. "Discovery of 4-*tert*-butyl-2,6-dimethylphenylsulfur trifluoride as a deoxofluorinating agent with high thermal stability as well as unusual resistance to aqueous hydrolysis, and its diverse fluorination capabilities including deoxofluoro-arylsulfonylation with high stereoselectivity". *J. Am. Chem. Soc.*, 132 (51): 18199, 2010.
- 75 ZANDA, M. "Synform issue 2019/11". *Synthesis*, 51 (21): A162, 2019.
- 76 FRANCKE, R. & LITTLE, R. D. "Redox catalysis in organic electrosynthesis: basic principles and recent developments". *Chem. Soc. Rev.*, 43 (8): 2492, 2014.
- 77 TAJIMA, T.; NAKAJIMA, A.; DOI, Y. & FUCHIGAMI, T. "Anodic fluorination based on cation exchange between alkali-metal fluorides and solid-supported acids". *Angew. Chem. Int. Ed.*, 46 (19): 3550, 2007.
- 78 PUPO, G.; VICINI, A. C.; ASCOUGH, D. M. H.; IBBA, F.; CHRISTENSEN, K. E.; THOMPSON, A. L., et al. "Hydrogen bonding phase-transfer catalysis with potassium fluoride: enantioselective synthesis of β-fluoroamines". *J. Am. Chem. Soc.*, 141 (7): 2878, 2019.
- 79 VITAKU, E.; SMITH, D. T. & NJARDARSON, J. T. "Analysis of the structural diversity, substitution patterns, and frequency of nitrogen heterocycles among U.S. FDA approved pharmaceuticals". *J. Med. Chem.*, 57 (24): 10257, 2014.

- 80 WU, Y.-J. "Heterocycles and medicine: a survey of the heterocyclic drugs approved by the U.S. FDA from 2000 to present". In: GRIBBLE, G. W. & JOULE, J. A. (Ed.). Prog. Heterocycl. Chem. Amsterdam: Elsevier, 2012, vol. 24, ch. 1, pp. 1-53.
- 81 LAUDADIO, G.; DE SMET, W.; STRUIK, L.; CAO, Y. & NOËL, T. "Design and application of a modular and scalable electrochemical flow microreactor". J. Flow Chem., 8 (3): 157, 2018.
- 82 ATOBE, M.; TATENO, H. & MATSUMURA, Y. "Applications of flow microreactors in electrosynthetic processes". Chem. Rev., 118 (9): 4541, 2018.
- 83 FOLGUEIRAS-AMADOR, A. A. & WIRTH, T. "Perspectives in flow electrochemistry". J. Flow Chem., 7 (3): 94, 2017.
- 84 PLETCHER, D.; GREEN, R. A. & BROWN, R. C. D. "Flow electrolysis cells for the synthetic organic chemistry laboratory". Chem. Rev., 118 (9): 4573, 2018.
- 85 LAM, K. & GEIGER, W. E. "Anodic oxidation of disulfides: detection and reactions of disulfide radical cations". J. Org. Chem., 78 (16): 8020, 2013.
- 86 SPITZ, C.; LOHIER, J.-F.; SANTOS, J. S.-D. O.; REBOUL, V. & METZNER, P. "Fluoride ion and phosphines as nucleophilic catalysts: synthesis of 1,4-benzothiazepines from cyclic sulfenamides". J. Org. Chem., 74 (10): 3936, 2009.
- 87 SHEPPARD, W. A. "Alkyl- and arylsulfur trifluorides". J. Am. Chem. Soc., 84 (16): 3058, 1962.
- 88 SHAFER, G. J.; FOROHAR, F. & DESMARTEAU, D. D. "Synthesis of potassium 3,6-dioxa- Δ^7 -4-trifluoromethyl perfluorooctyl sulfonate from hydrolysis of 3,6-dioxa- Δ^7 -4-trifluoromethyl perfluorooctyl sulfonyl fluoride. A simple high yield conversion catalyzed by KF". J. Fluorine Chem., 101 (1): 27, 2000.
- 89 YANG, Z.; SHI, Y.; ZHAN, Z.; ZHANG, H.; XING, H.; LU, R., et al. "Sustainable electrocatalytic oxidant-free syntheses of thiosulfonates from thiols". ChemElectroChem, 5 (23): 3619, 2018.
- 90 TRUCE, W. E.; HILL, H. E. & BOUDAKIAN, M. M. "Acetylenic sulfur compounds. I. Preparation and characterization of p-tolymercaptoacetylene and 1-phenyl-2-phenylmercaptoacetylene". J. Am. Chem. Soc., 78 (12): 2760, 1956.
- 91 TALKO, A.; ANTONIAK, D. & BARBASIEWICZ, M. "Directed *ortho*-metalation of arenesulfonyl fluorides and aryl fluorosulfates". Synthesis, 51 (11): 2278, 2019.
- 92 DONG, J. & SHARPLESS, K. B. Sulfur(VI) fluoride compounds and methods for the preparation thereof. Int. Pat. WO 2015/188120 A1, December 10, 2015.
- 93 GAKH, A. A.; ROMANIKO, S. V.; UGRAK, B. I. & FAINZILBERG, A. A. "N-fluorination with cesium fluoroxysulfate". Tetrahedron, 47 (35): 7447, 1991.

- 94 CHEN, G.; CHEN, F.; ZHANG, Y.; YANG, X.; YUAN, X.; WU, F., et al. "The investigation of fluorination reaction of *p*-substituted benzenesulfonimides with fluorine–nitrogen mixed gas to synthesize NFSI analogues". *J. Fluorine Chem.*, 133: 155, 2012.
- 95 LEE, I.; KANG, H. K. & LEE, H. W. "Nucleophilic displacement at sulfur center. 22. Nucleophilic substitution reaction of phenylmethanesulfonyl halides with anilines". *J. Am. Chem. Soc.*, 109 (24): 7472, 1987.
- 96 EROĞLU, F.; KÂHYA, D. & ERDIK, E. "Sulfonyl transfer mechanism in C–S coupling of phenylmagnesium bromide with phenyl arenesulfonates". *J. Organomet. Chem.*, 695 (2): 267, 2010.
- 97 CLARK, D.; FLYGARE, J.; MEDINA, J.; ROSEN, T. & SHAN, B. Pentafluorobenzenesulfonamides and analogs. *Eur. Pat. EP 1 334 719 A2*, August 13, 2003.
- 98 LEI, X.; JALLA, A.; ABOU SHAMA, M. A.; STAFFORD, J. M. & CAO, B. "Chromatography-free and eco-friendly synthesis of aryl tosylates and mesylates". *Synthesis*, 47 (17): 2578, 2015.
- 99 SAKURAI, N. & MUKAIYAMA, T. "A new preparative method of aryl sulfonate esters by using cyclic organobismuth reagents". *Heterocycles*, 74 (1): 771, 2007.
- 100 ZHENG, Y.; QING, F.-L.; HUANG, Y. & XU, X.-H. "Tunable and practical synthesis of thiosulfonates and disulfides from sulfonyl chlorides in the presence of tetrabutylammonium iodide". *Adv. Synth. Catal.*, 358 (21): 3477, 2016.
- 101 ROZATIAN, N.; ASHWORTH, I. W.; SANDFORD, G. & HODGSON, D. R. W. "A quantitative reactivity scale for electrophilic fluorinating reagents". *Chem. Sci.*, 9 (46): 8692, 2018.
- 102 TIMOFEEVA, D. S.; OFIAL, A. R. & MAYR, H. "Kinetics of electrophilic fluorinations of enamines and carbanions: comparison of the fluorinating power of N–F reagents". *J. Am. Chem. Soc.*, 140 (36): 11474, 2018.
- 103 SHONO, T. *Electroorganic Chemistry as a New Tool in Organic Synthesis*. 1st ed. Berlin: Springer-Verlag, 1984. 172 p.
- 104 ROTH, H. G.; ROMERO, N. A. & NICEWICZ, D. A. "Experimental and calculated electrochemical potentials of common organic molecules for applications to single-electron redox chemistry". *Synlett*, 27 (5): 714, 2016.
- 105 TSUCHIDA, E.; NISHIDE, H.; YAMAMOTO, K. & YOSHIDA, S. "Electrooxidative polymerization of thiophenol to yield poly(*p*-phenylene sulfide)". *Macromolecules*, 20 (9): 2315, 1987.

- 106 BANDYOPADHYAY, K.; VIJAYAMOHANAN, K.; VENKATARAMANAN, M. & PRADEEP, T. "Self-assembled monolayers of small aromatic disulfide and diselenide molecules on polycrystalline gold films: a comparative study of the geometrical constraint using temperature-dependent surface-enhanced raman spectroscopy, X-ray photoelectron spectroscopy, and electrochemistry". *Langmuir*, 15 (16): 5314, 1999.
- 107 YAN, Y.; ZEITLER, E. L.; GU, J.; HU, Y. & BOCARSLY, A. B. "Electrochemistry of aqueous pyridinium: exploration of a key aspect of electrocatalytic reduction of CO₂ to methanol". *J. Am. Chem. Soc.*, 135 (38): 14020, 2013.
- 108 GAIS, H. J. "Stoichiometric asymmetric synthesis: section 1.3". In: ENDERS, D. & JAEGER, K. E. (Ed.). *Asymmetric Synthesis with Chemical and Biological Methods*. Weinheim: WILEY-VCH, 2007, ch. 1, pp. 75-115.

NMR Data

4 NMR Data

4.1 Spectra of Chapter 1

4.1.1 ^1H , ^{13}C and DEPT-135 NMR spectra of compound 1.77

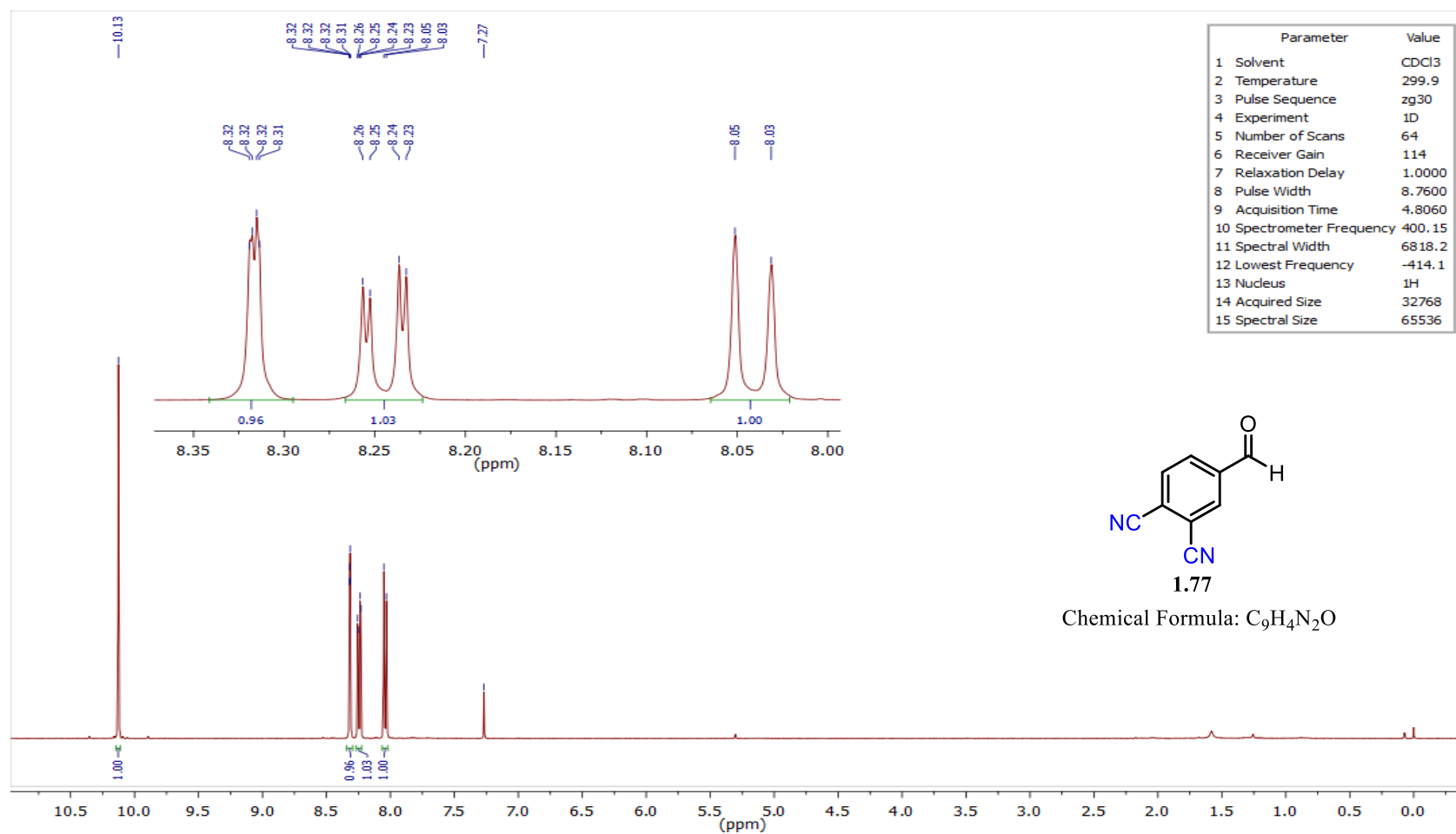


Figure 4.1 – ^1H NMR spectrum of compound 1.77 in CDCl_3 .

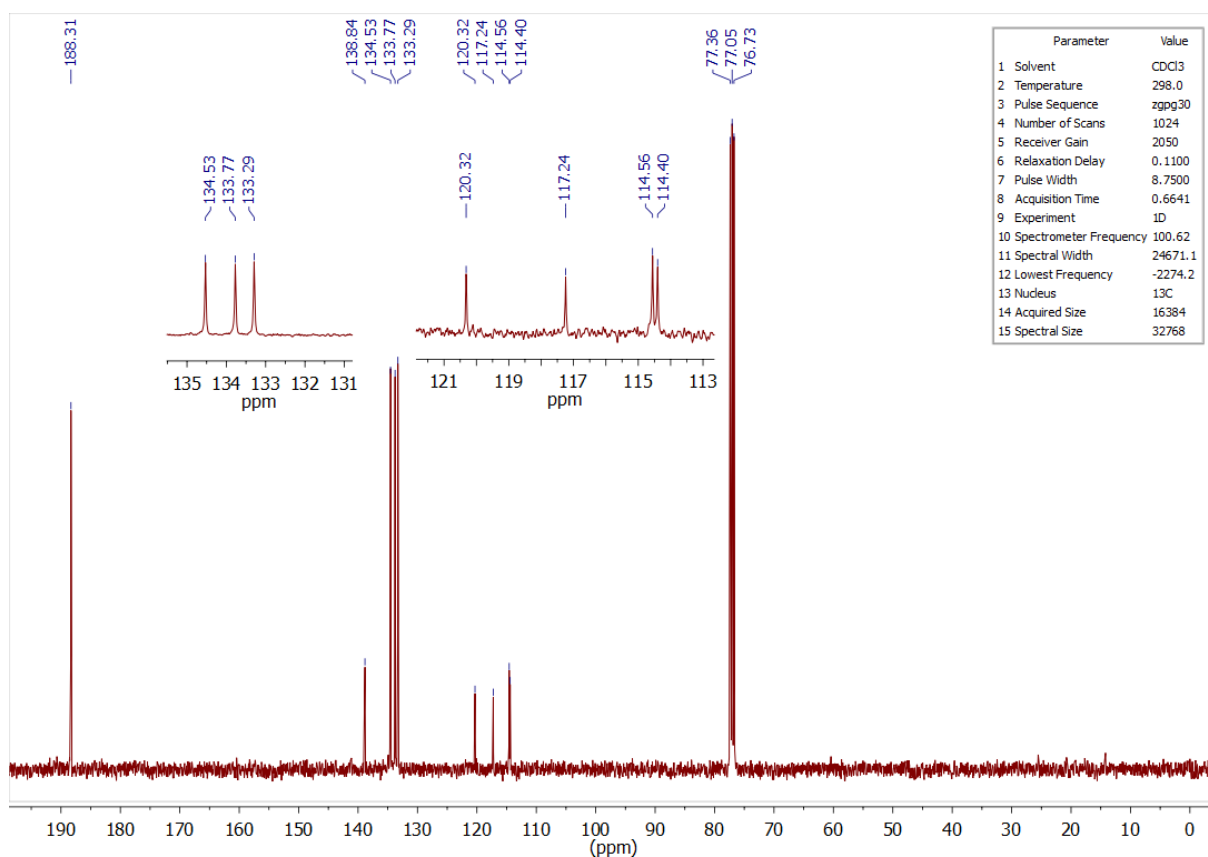


Figure 4.2 – ^{13}C NMR spectrum of compound **1.77** in CDCl_3 .

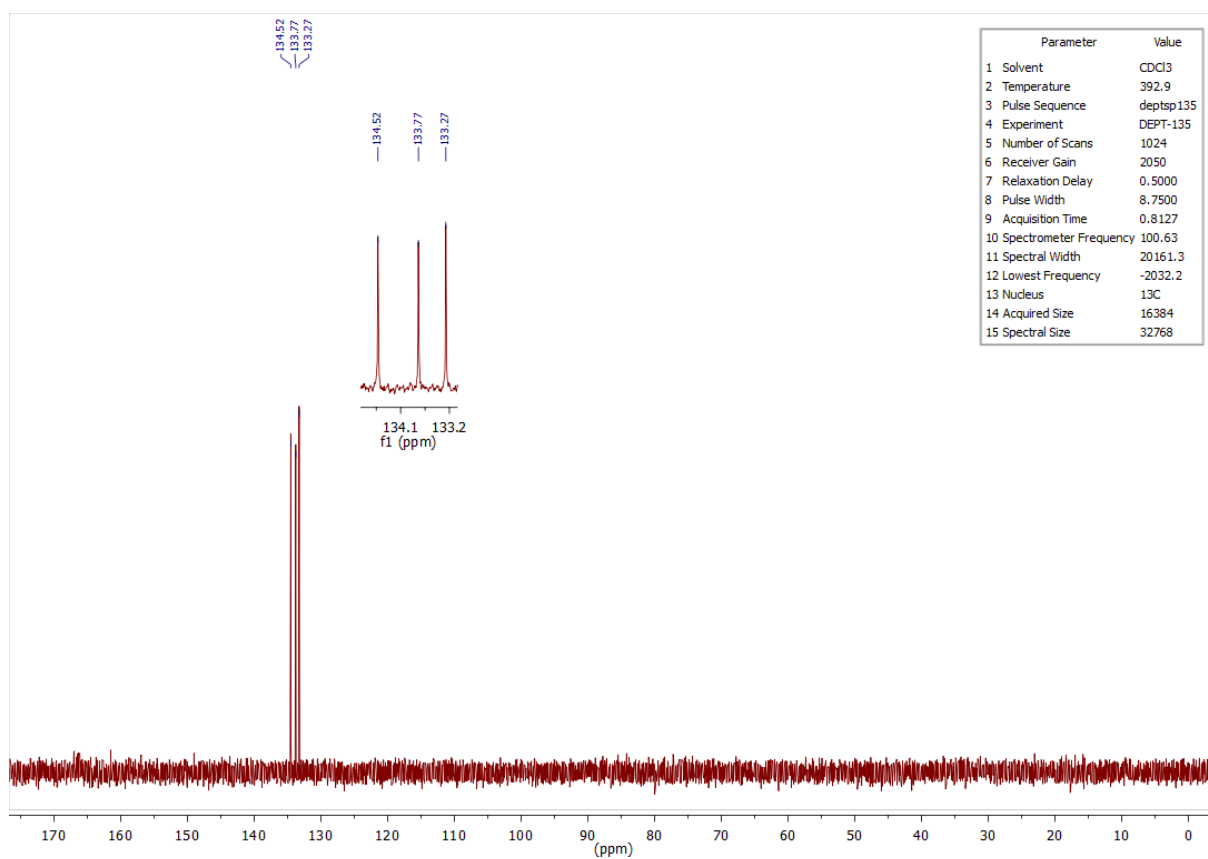


Figure 4.3 – ^{13}C DEPT-135 NMR spectrum of compound **1.77** in CDCl_3 .

4.1.2 ^1H , ^{13}C and DEPT-135 NMR spectra of compound **1.78g**

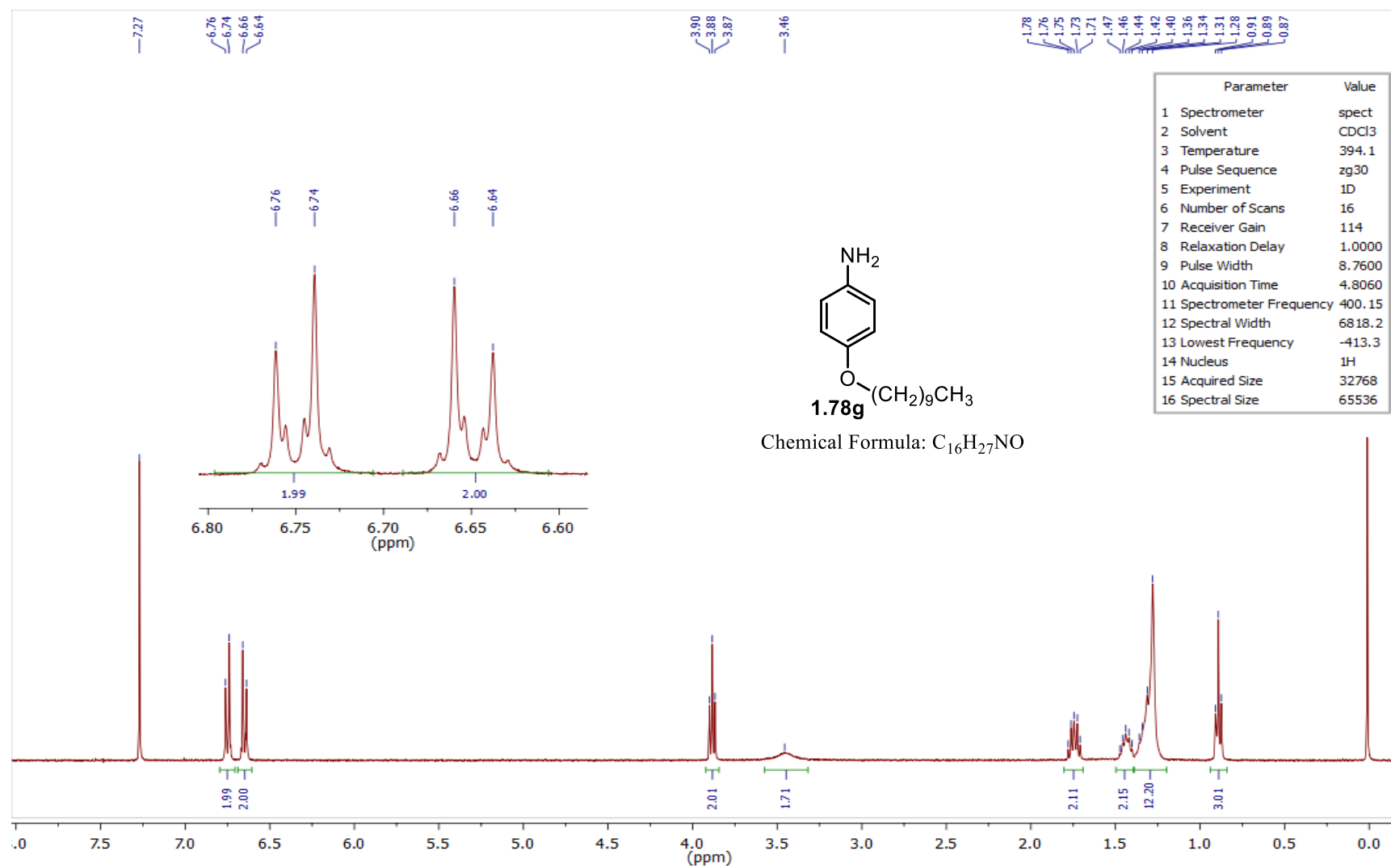


Figure 4.4 – ^1H NMR spectrum of compound **1.78g** in CDCl_3 .

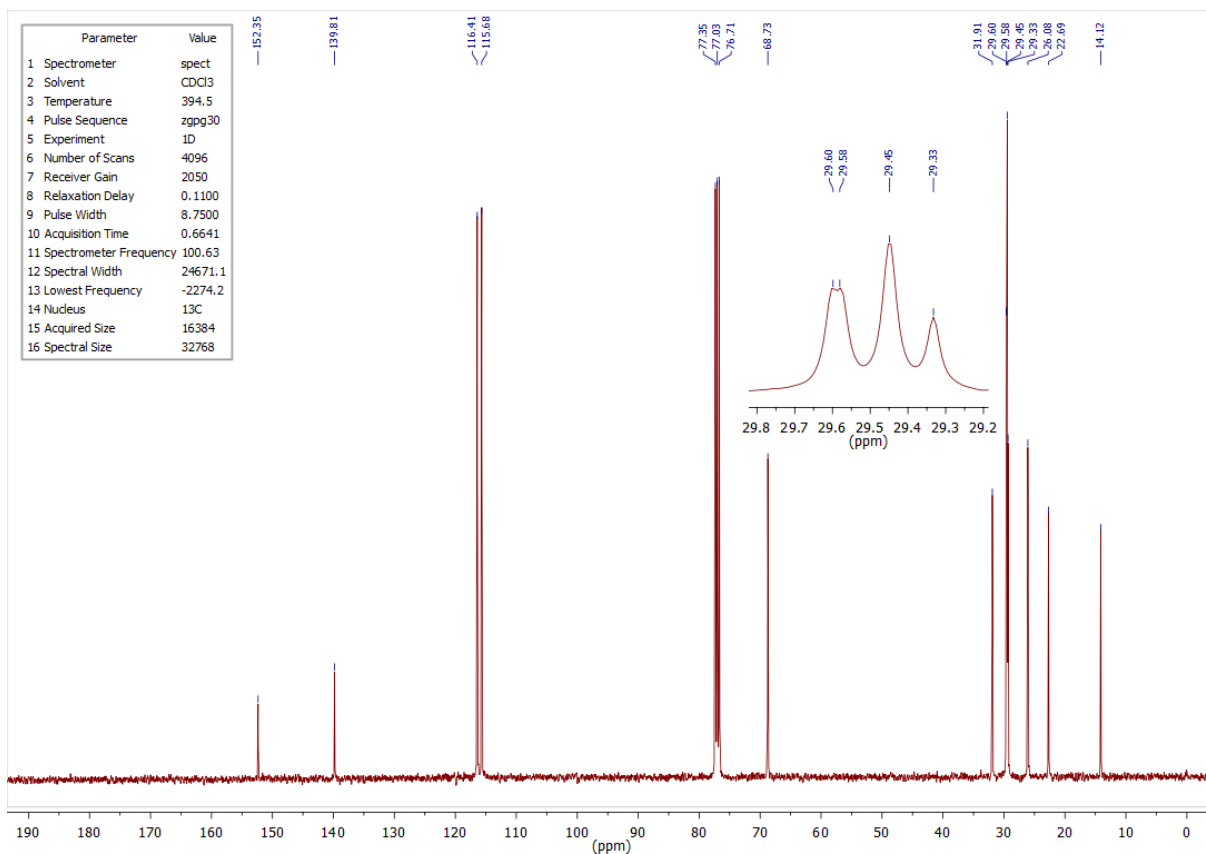


Figure 4.5 – ^{13}C NMR spectrum of compound **1.78g** in CDCl_3 .

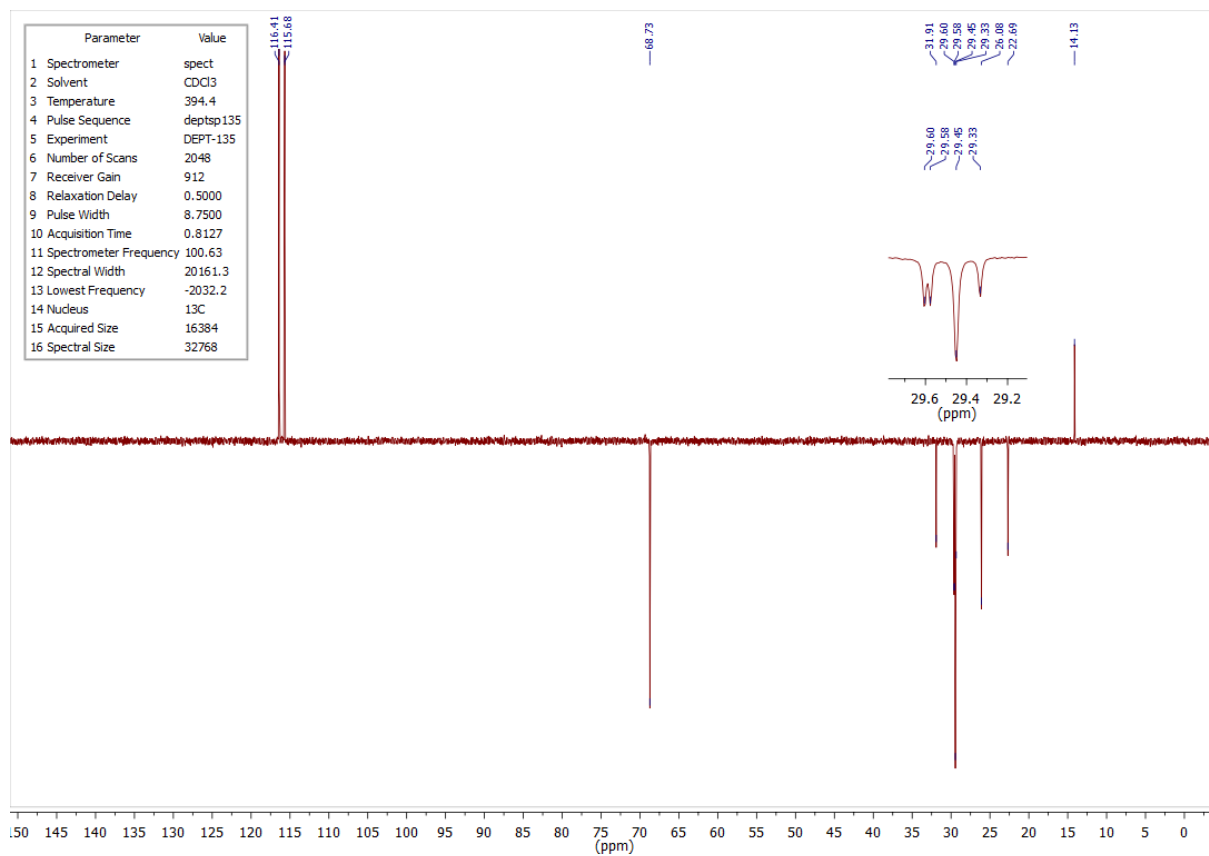


Figure 4.6 – ^{13}C DEPT-135 NMR spectrum of compound **1.78g** in CDCl_3 .

4.1.3 ^1H , ^{13}C and DEPT-135 NMR spectra of compound **1.80a**

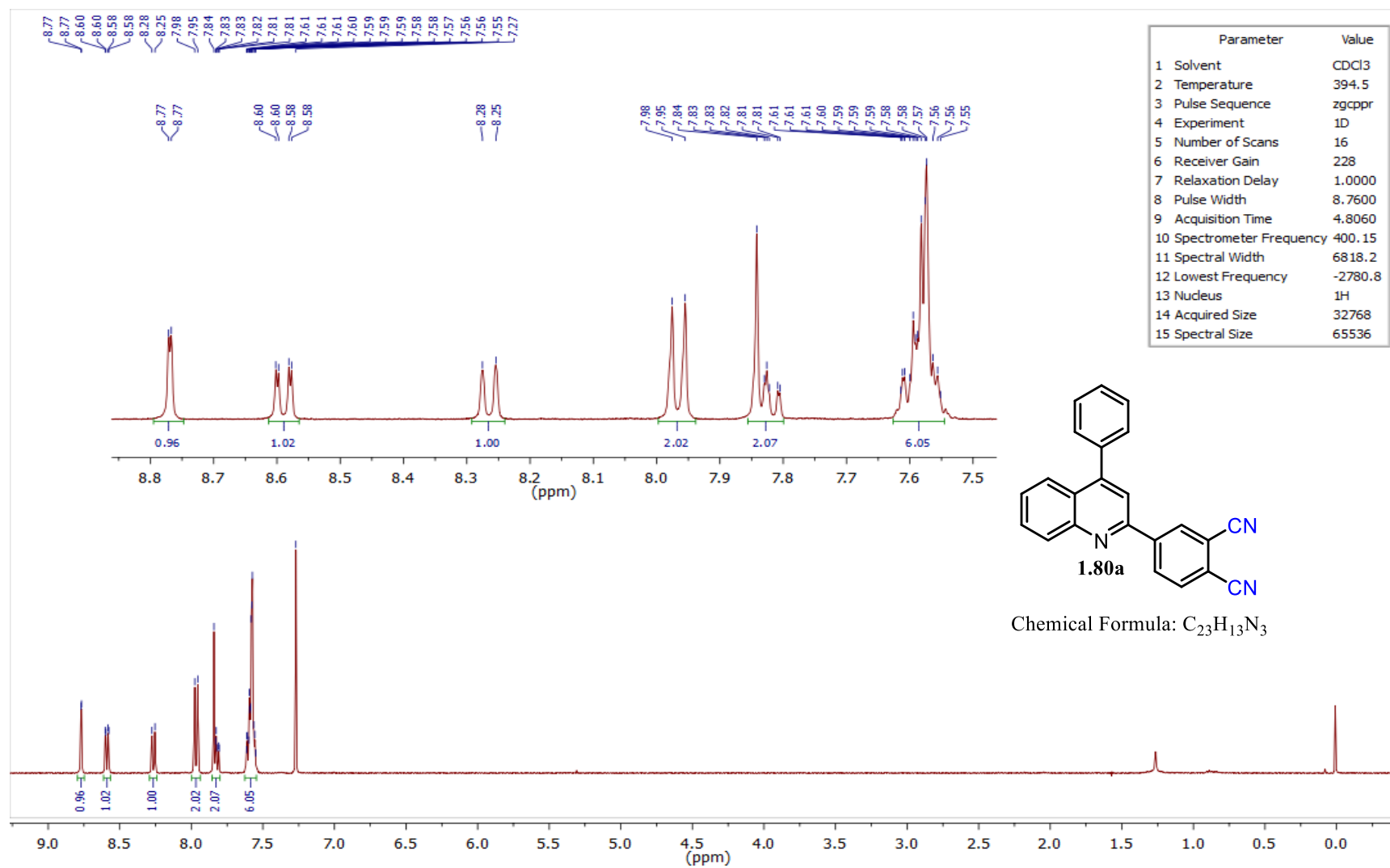


Figure 4.7 – ^1H NMR spectrum of compound **1.80a** in CDCl_3 .

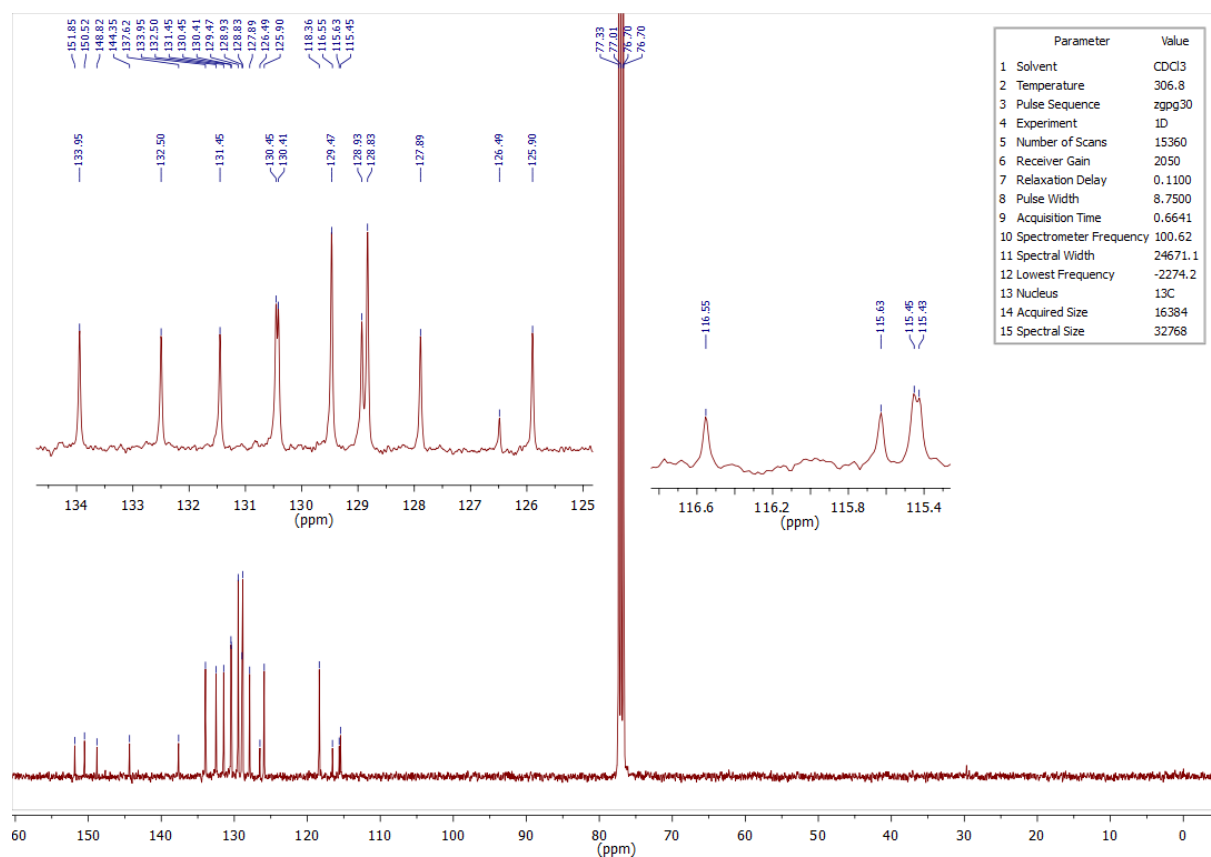


Figure 4.8 – ^{13}C NMR spectrum of compound **1.80a** in CDCl_3 .

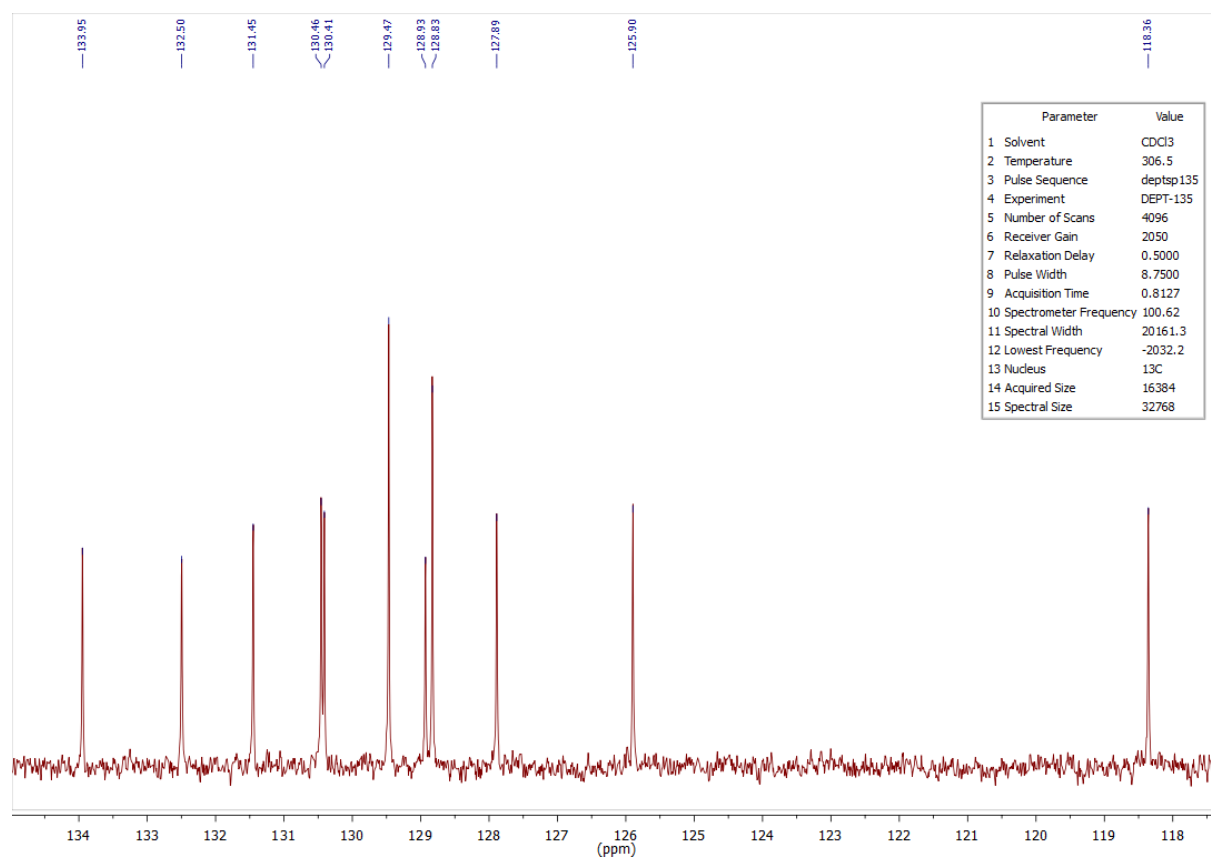


Figure 4.9 – ^{13}C DEPT-135 NMR spectrum of compound **1.80a** in CDCl_3 .

4.1.4 ^1H , ^{13}C and DEPT-135 NMR spectra of compound **1.80b**

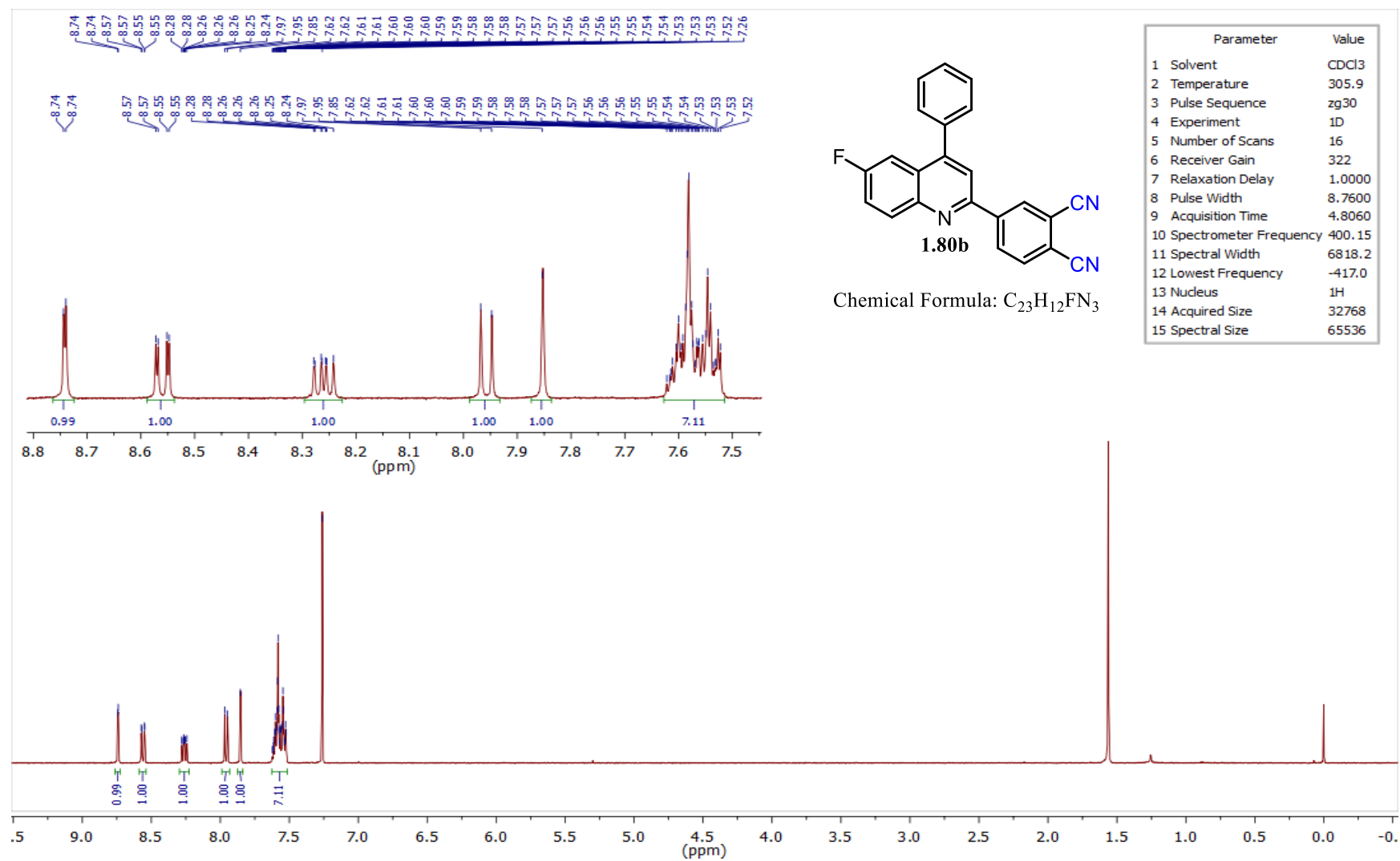


Figure 4.10 – ^1H NMR spectrum of compound **1.80b** in CDCl_3 .

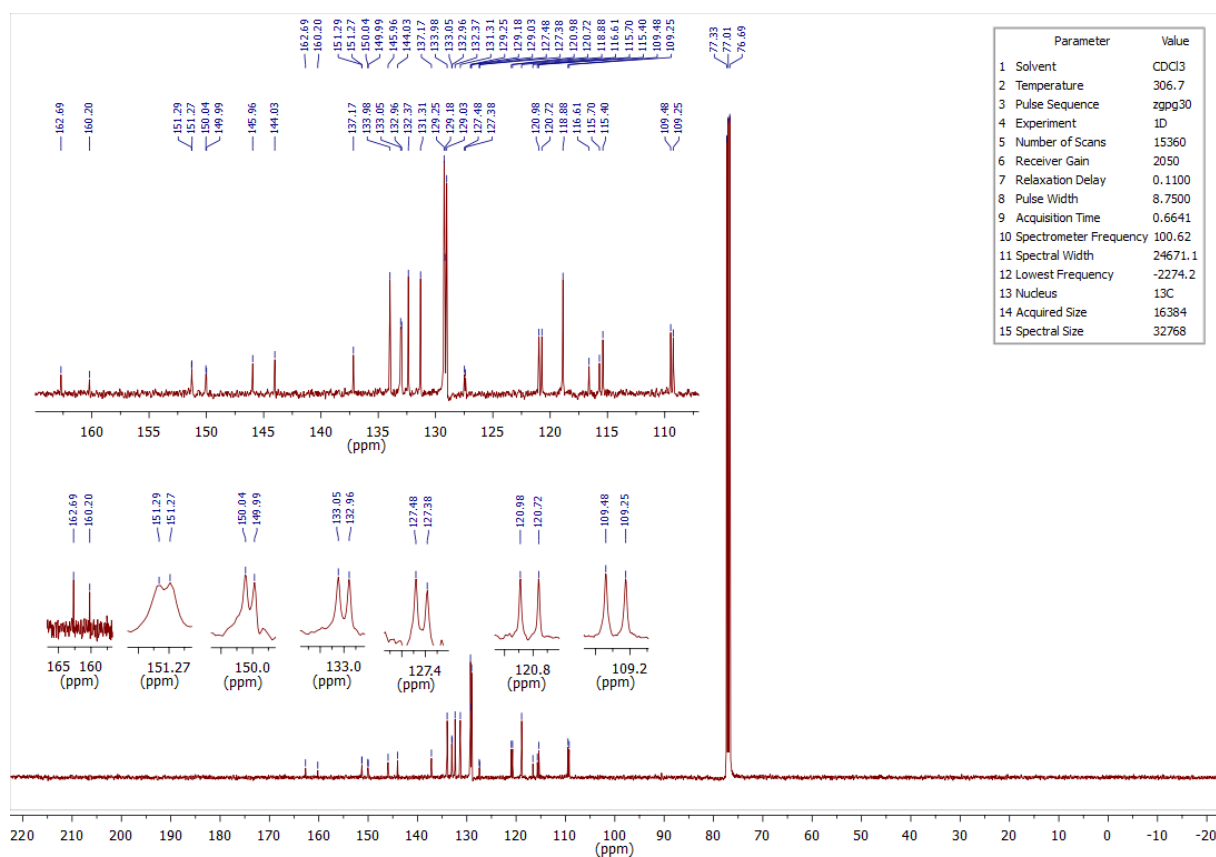


Figure 4.11 – ^{13}C NMR spectrum of compound **1.80b** in CDCl_3 .

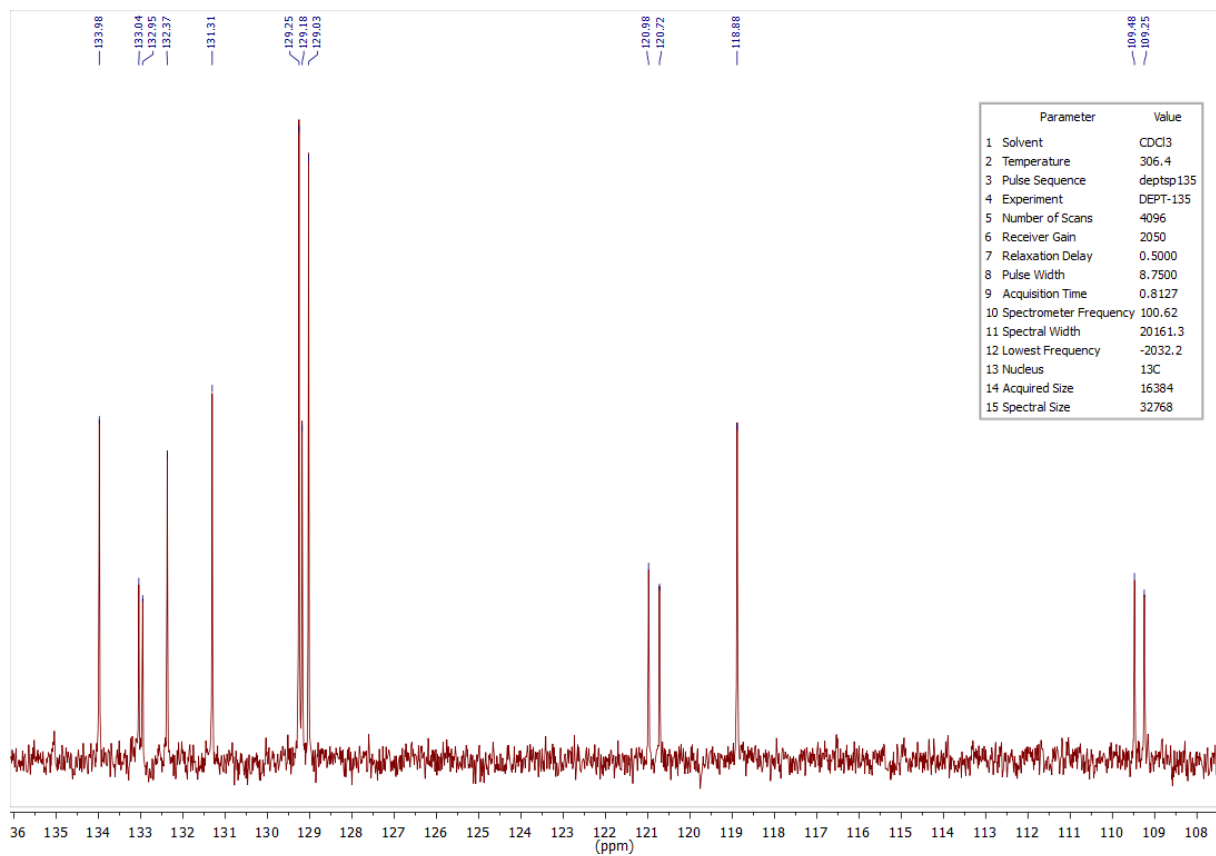


Figure 4.12 – ^{13}C DEPT-135 NMR spectrum of compound **1.80b** in CDCl_3 .

4.1.5 ^1H , ^{13}C and DEPT-135 NMR spectra of compound **1.80c**

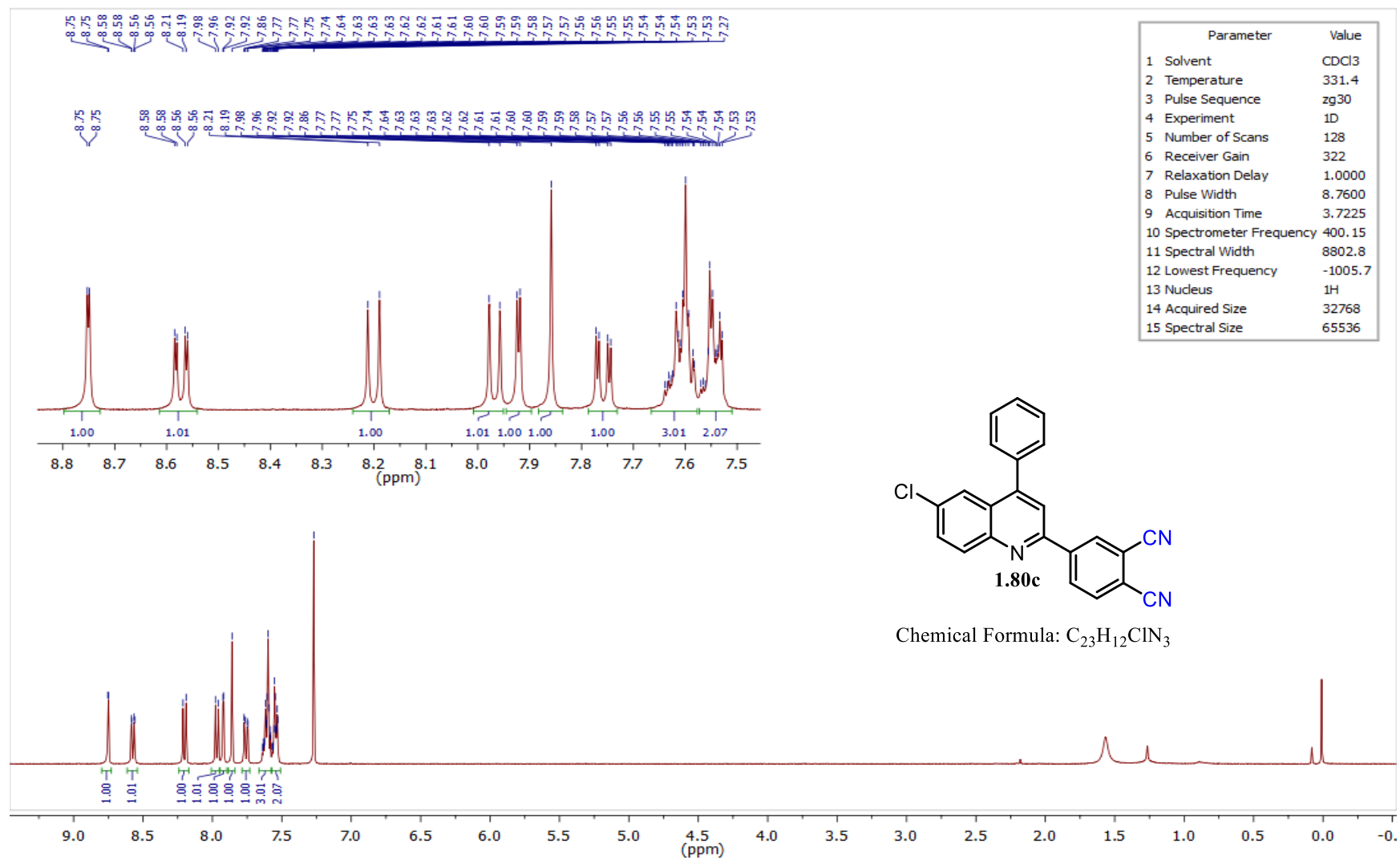


Figure 4.13 – ^1H NMR spectrum of compound **1.80c** in CDCl_3 .

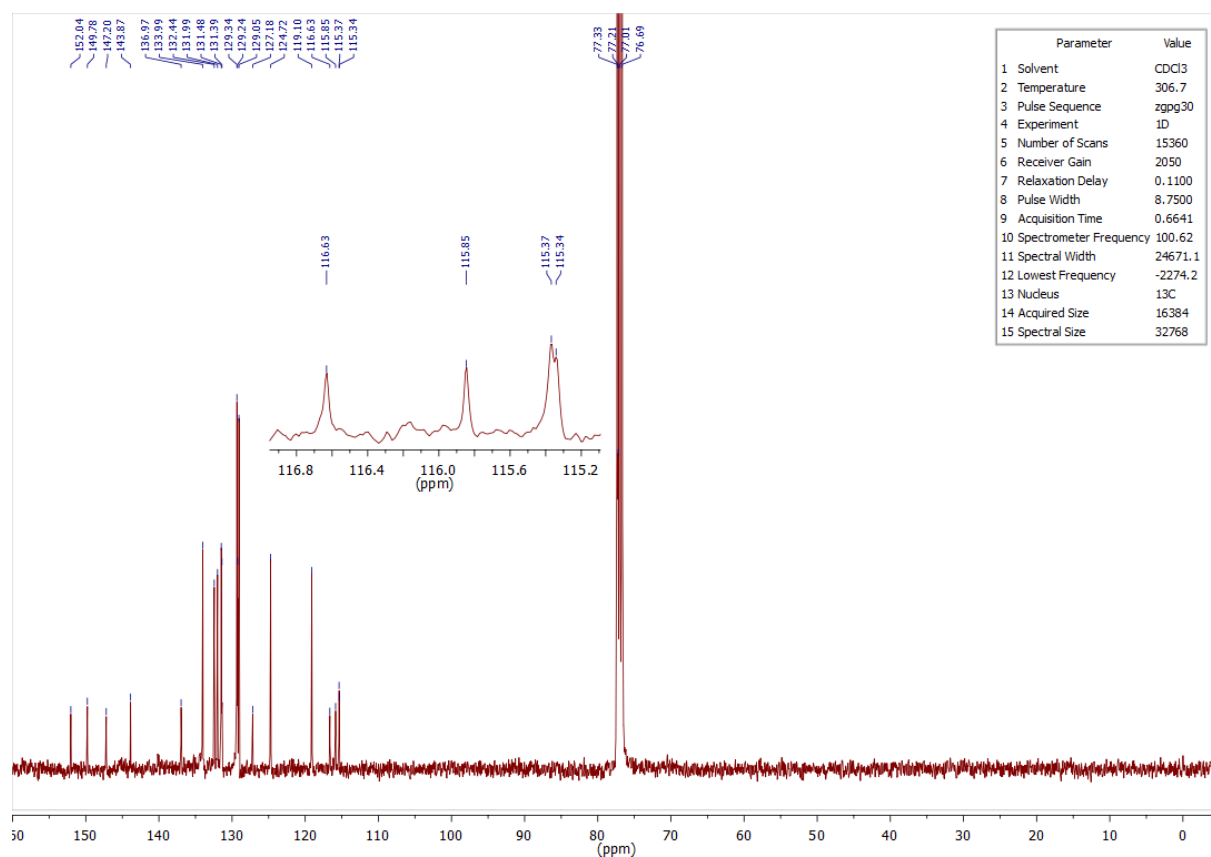


Figure 4.14 – ¹³C NMR spectrum of compound **1.80c** in CDCl₃.

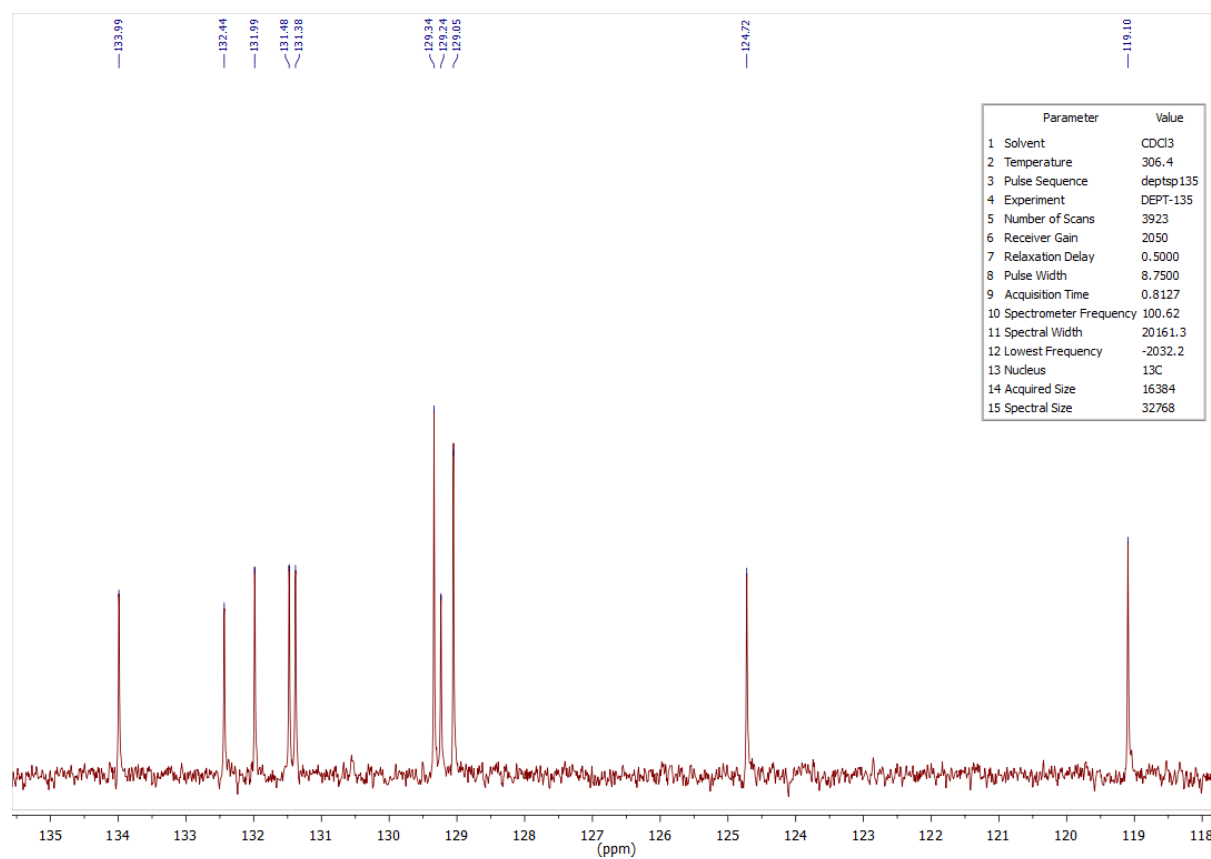


Figure 4.15 – ¹³C DEPT-135 NMR spectrum of compound **1.80c** in CDCl₃.

4.1.6 ^1H , ^{13}C and DEPT-135 NMR spectra of compound **1.80d**

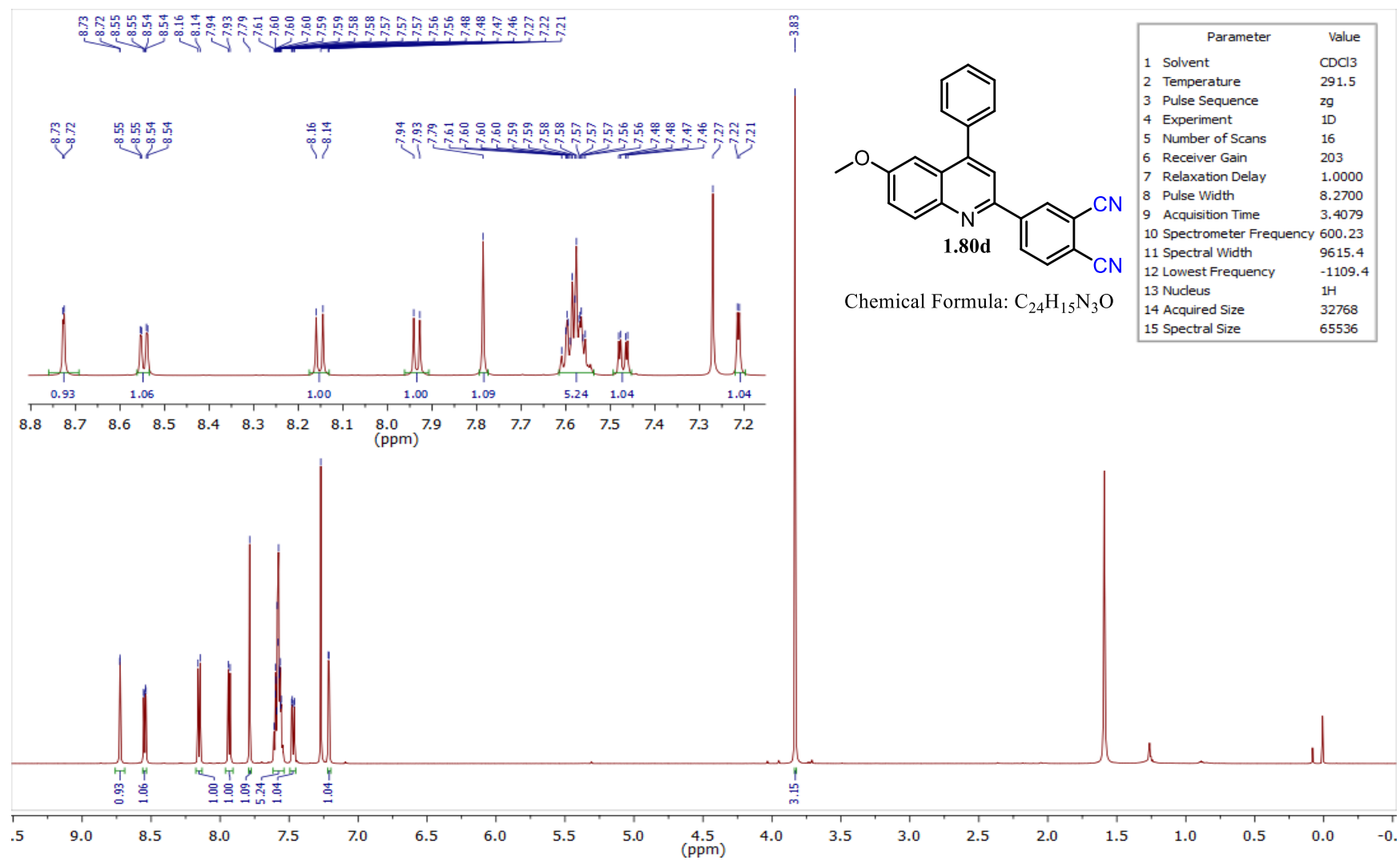


Figure 4.16 – ^1H NMR spectrum of compound **1.80d** in CDCl_3 .

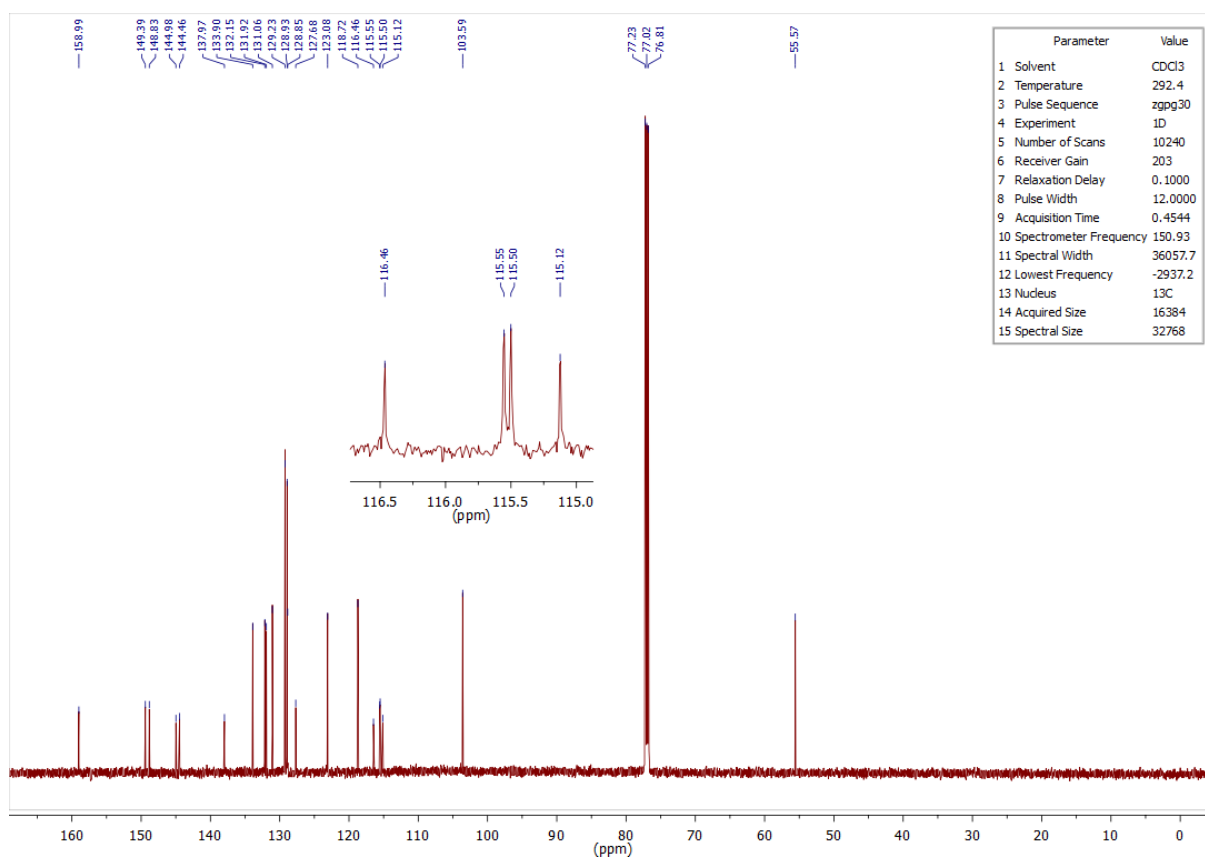


Figure 4.17 – ^{13}C NMR spectrum of compound **1.80d** in CDCl_3 .

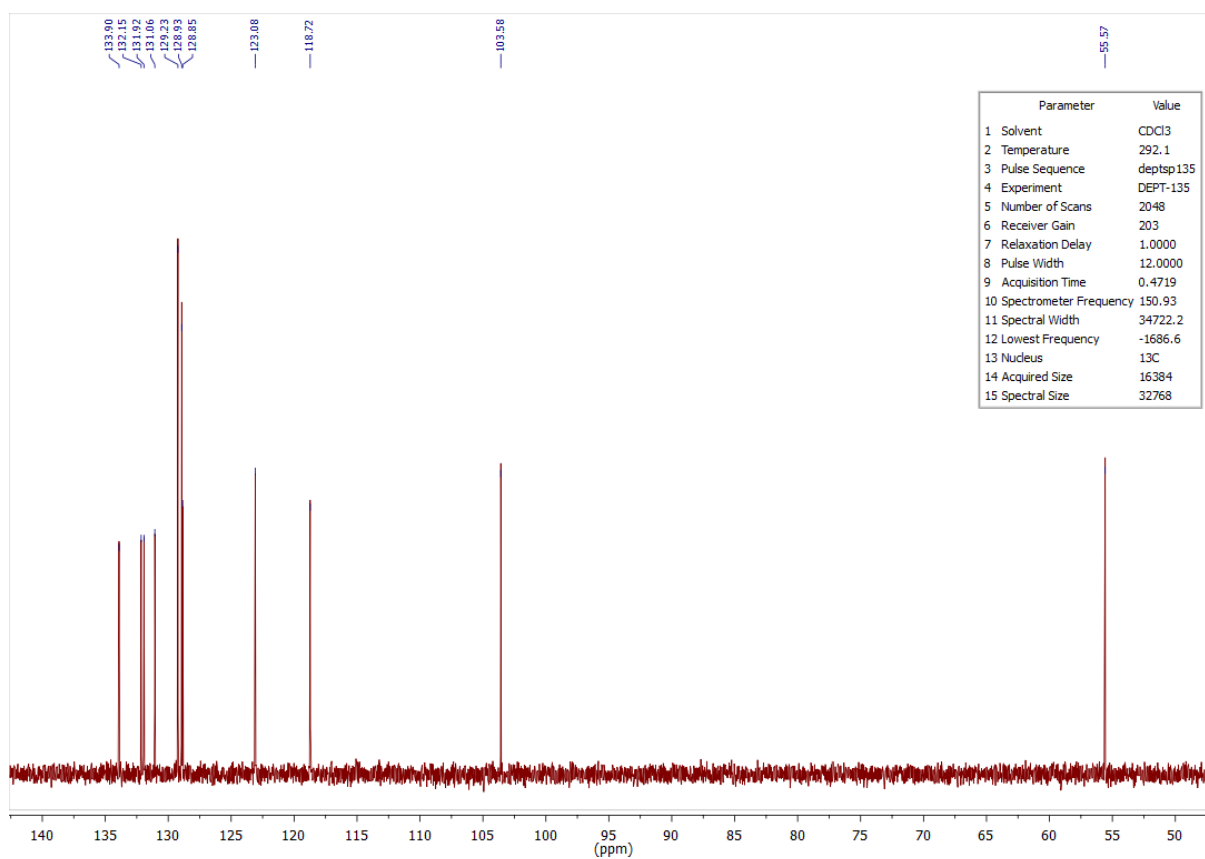


Figure 4.18 – ^{13}C DEPT-135 NMR spectrum of compound **1.80d** in CDCl_3 .

4.1.7 ^1H , ^{13}C and DEPT-135 NMR spectra of compound **1.80e**

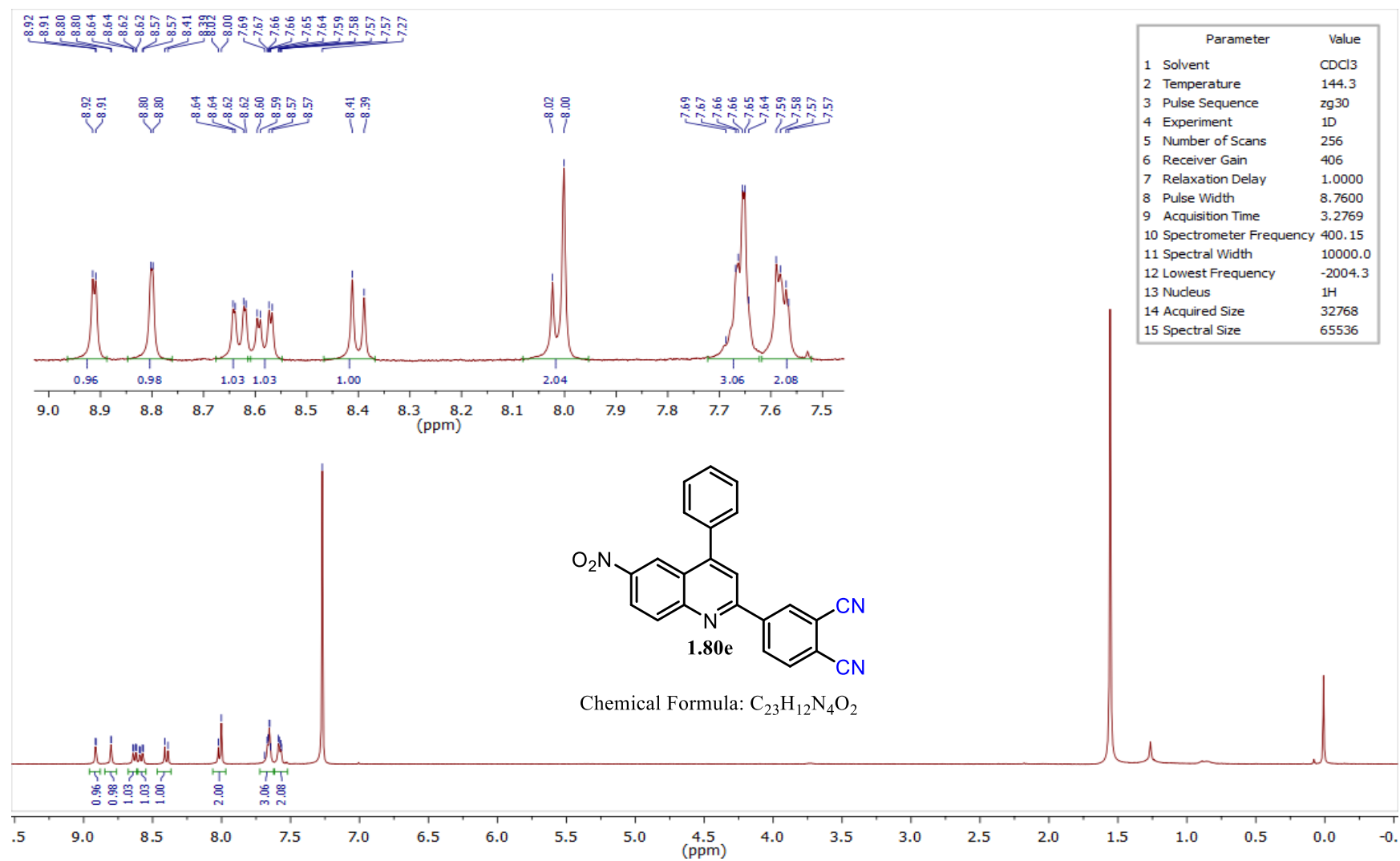


Figure 4.19 – ^1H NMR spectrum of compound **1.80e** in CDCl_3 .

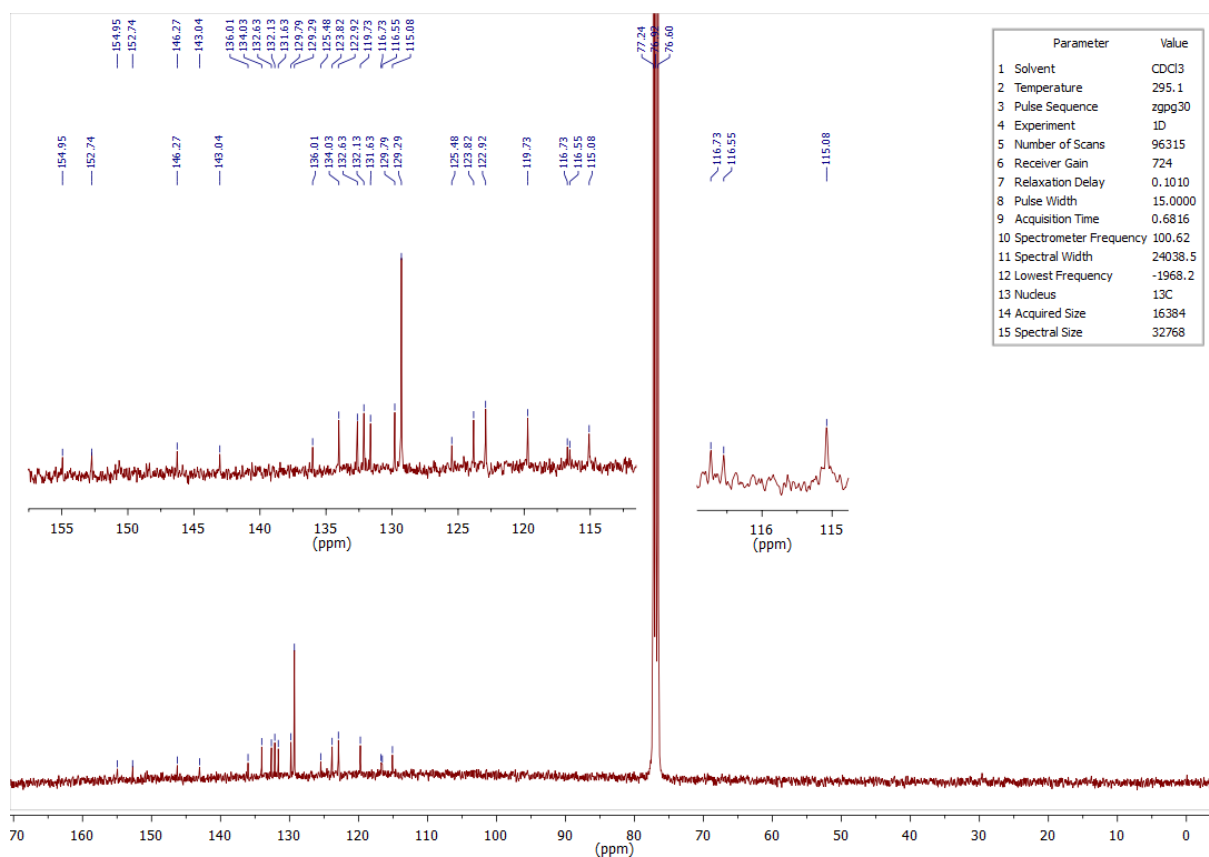


Figure 4.20 – ^{13}C NMR spectrum of compound **1.80e** in CDCl_3 .

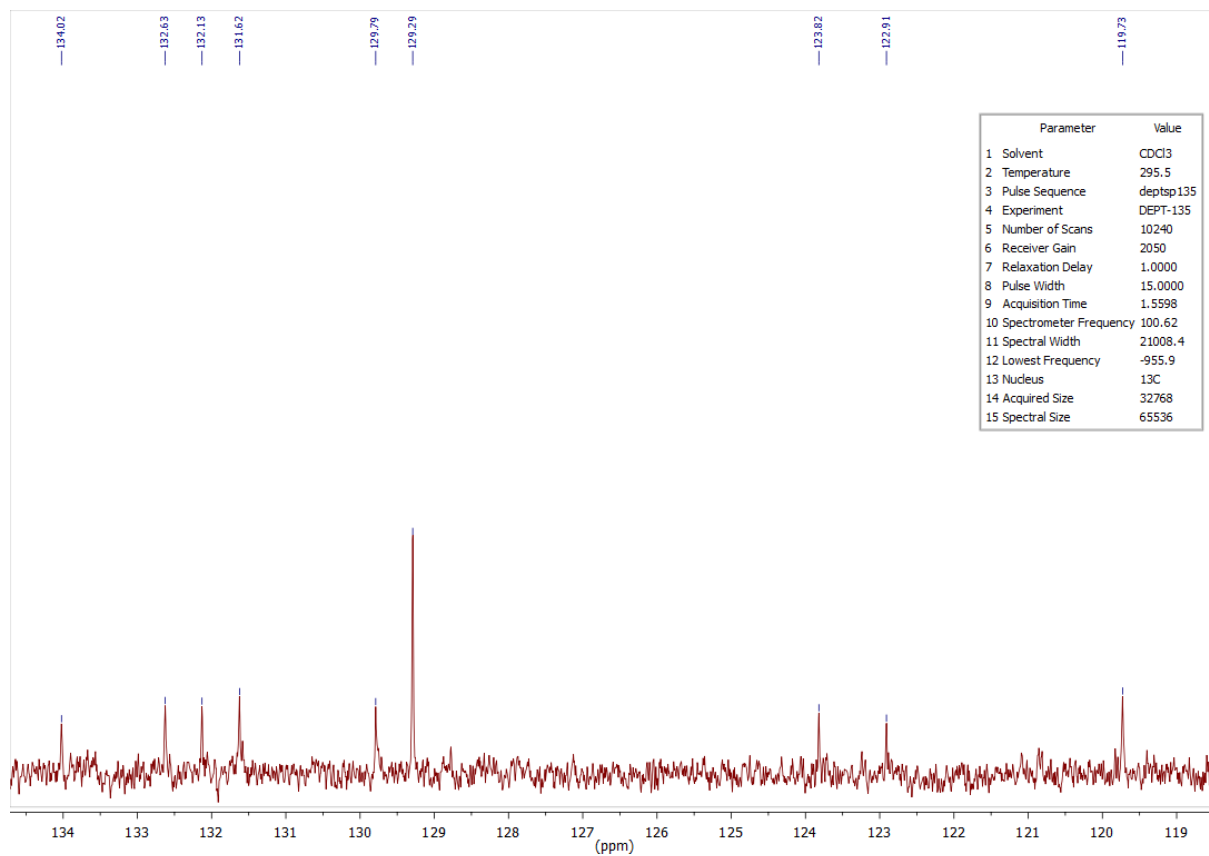


Figure 4.21 – ^{13}C DEPT-135 NMR spectrum of compound **1.80e** in CDCl_3 .

4.1.8 ^1H , ^{13}C and DEPT-135 NMR spectra of compound **1.80f**

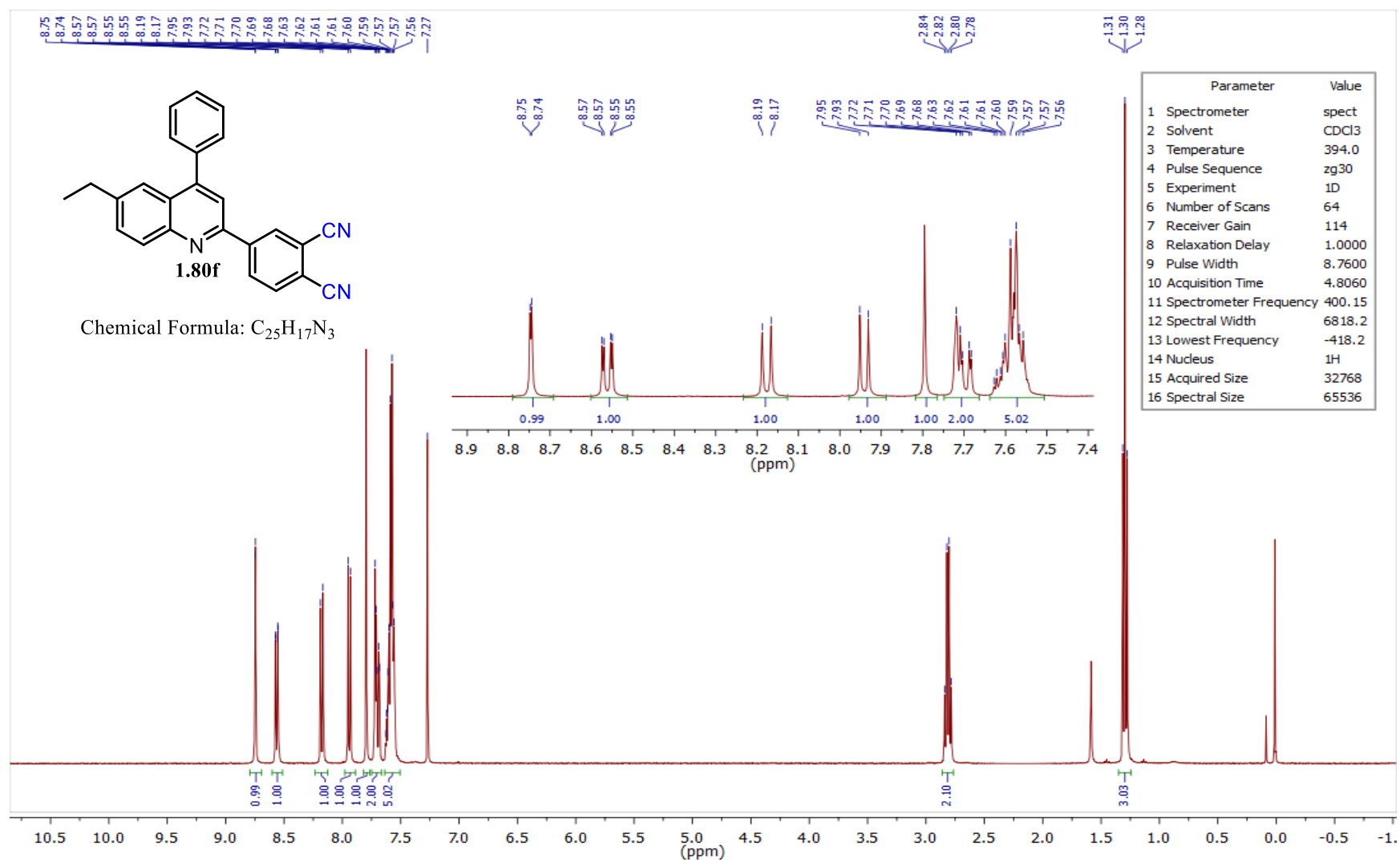


Figure 4.22 – ^1H NMR spectrum of compound **1.80f** in CDCl_3 .

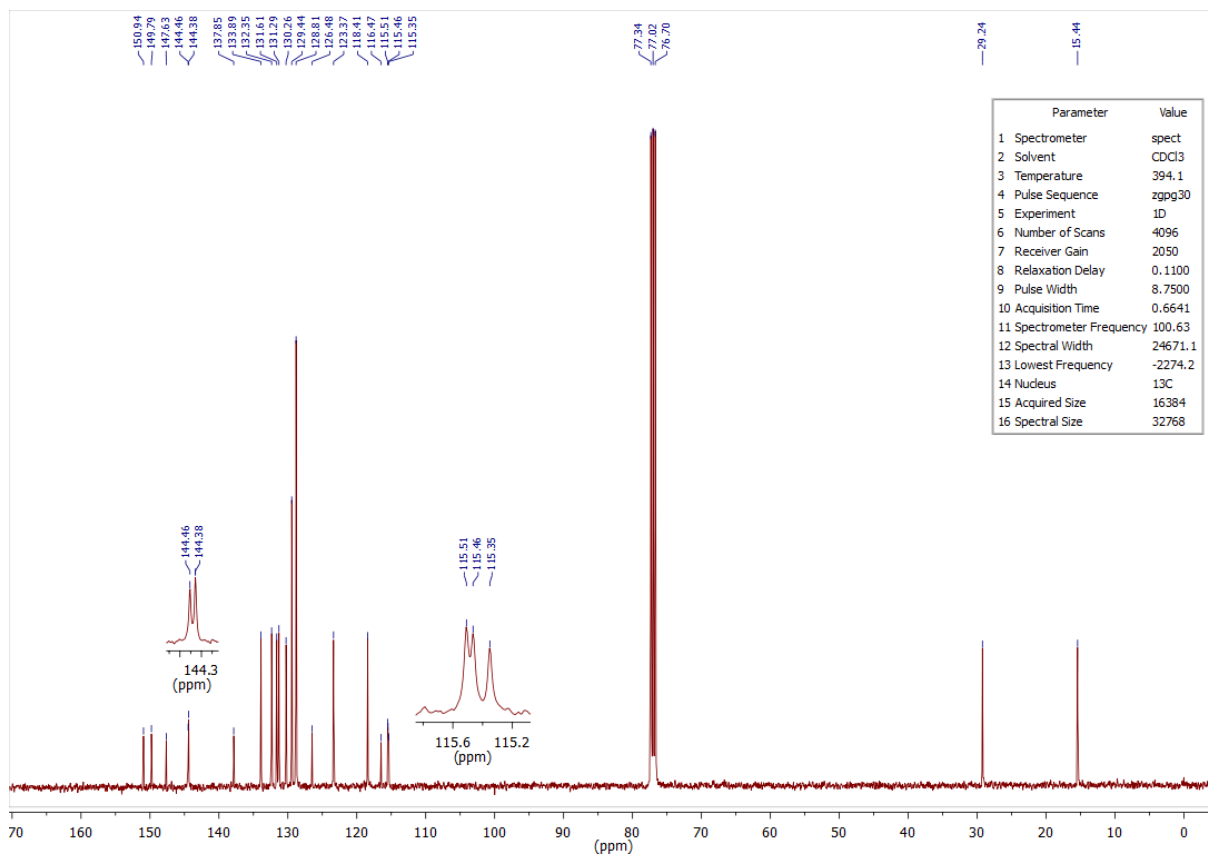


Figure 4.23 – ^{13}C NMR spectrum of compound **1.80f** in CDCl_3 .

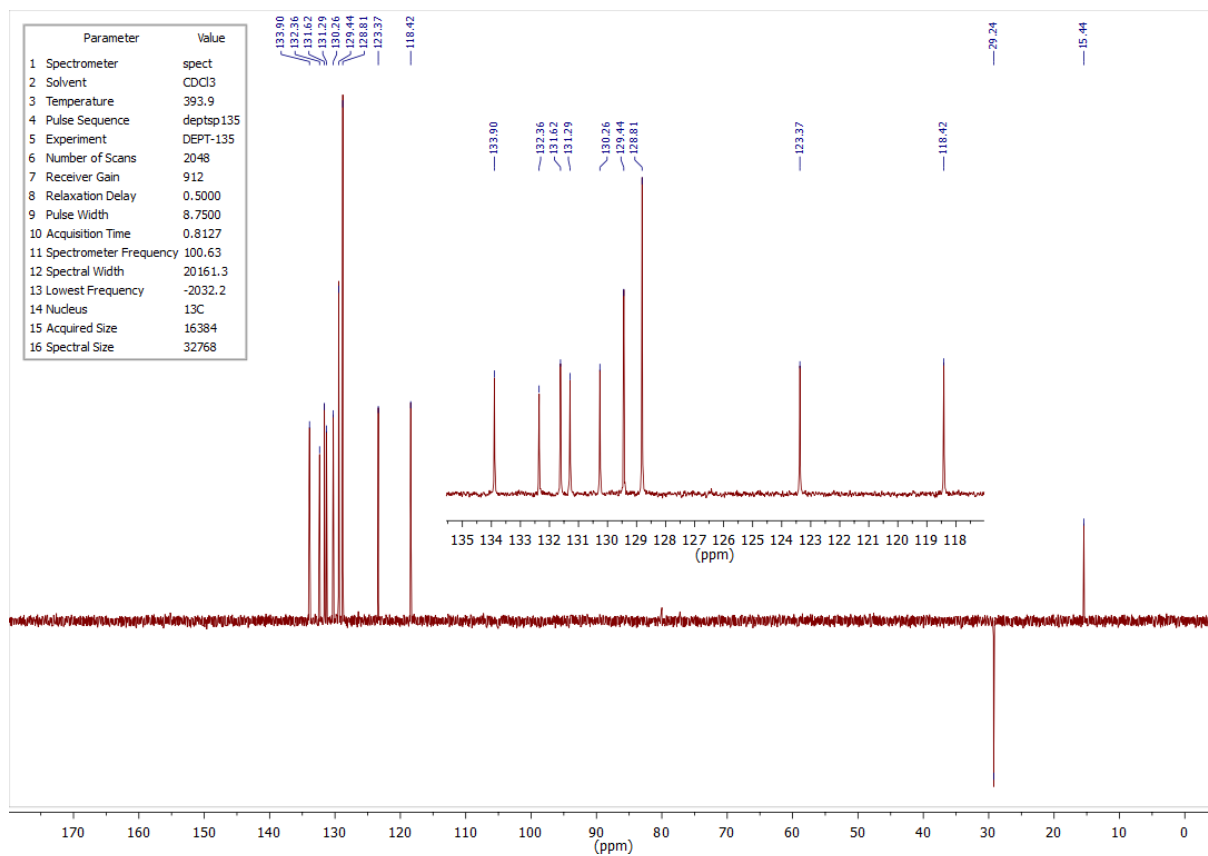


Figure 4.24 – ^{13}C DEPT-135 NMR spectrum of compound **1.80f** in CDCl_3 .

4.1.9 ^1H , ^{13}C and DEPT-135 NMR spectra of compound **1.80g**

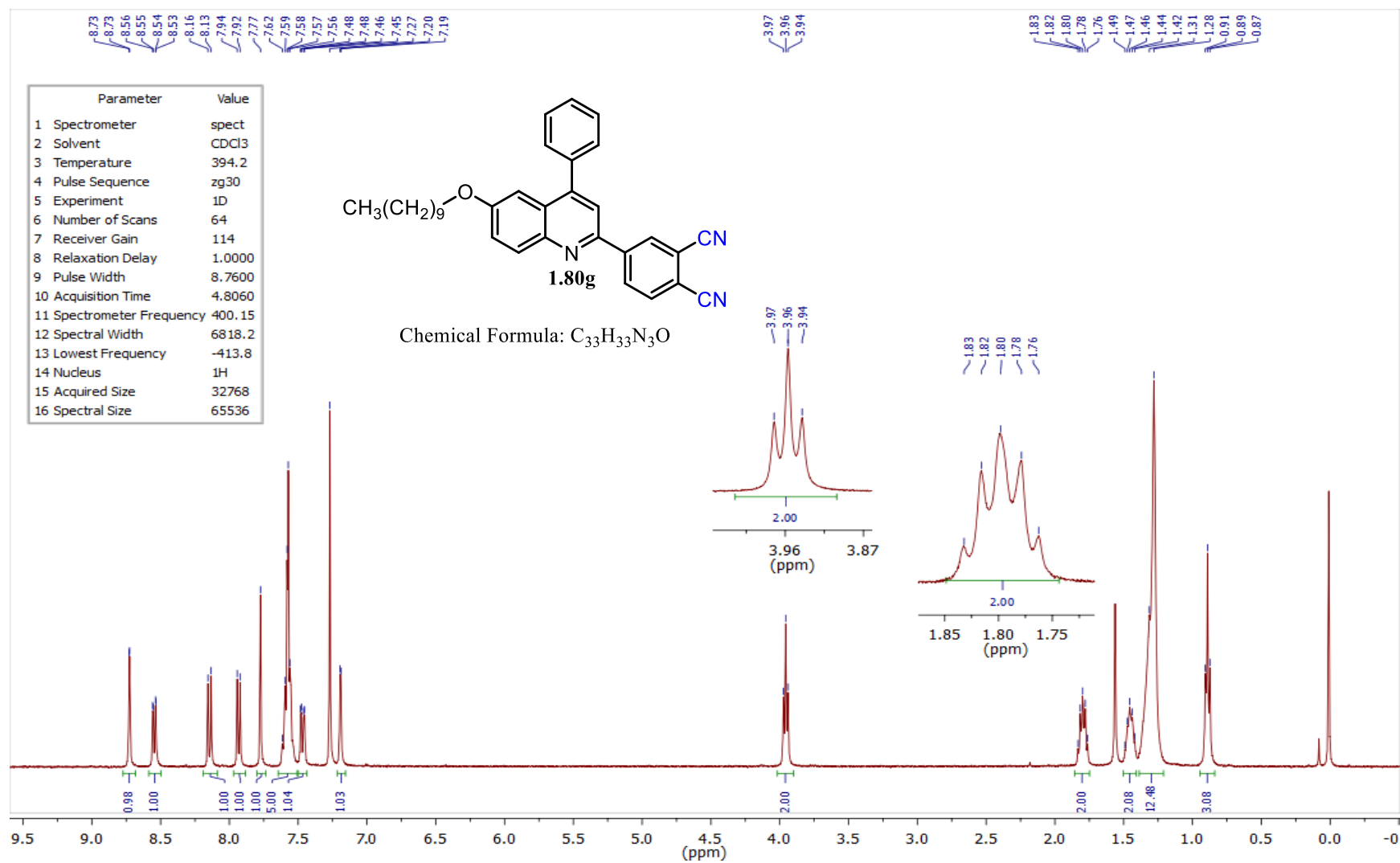


Figure 4.25 – ^1H NMR spectrum of compound **1.80g** in CDCl_3 .

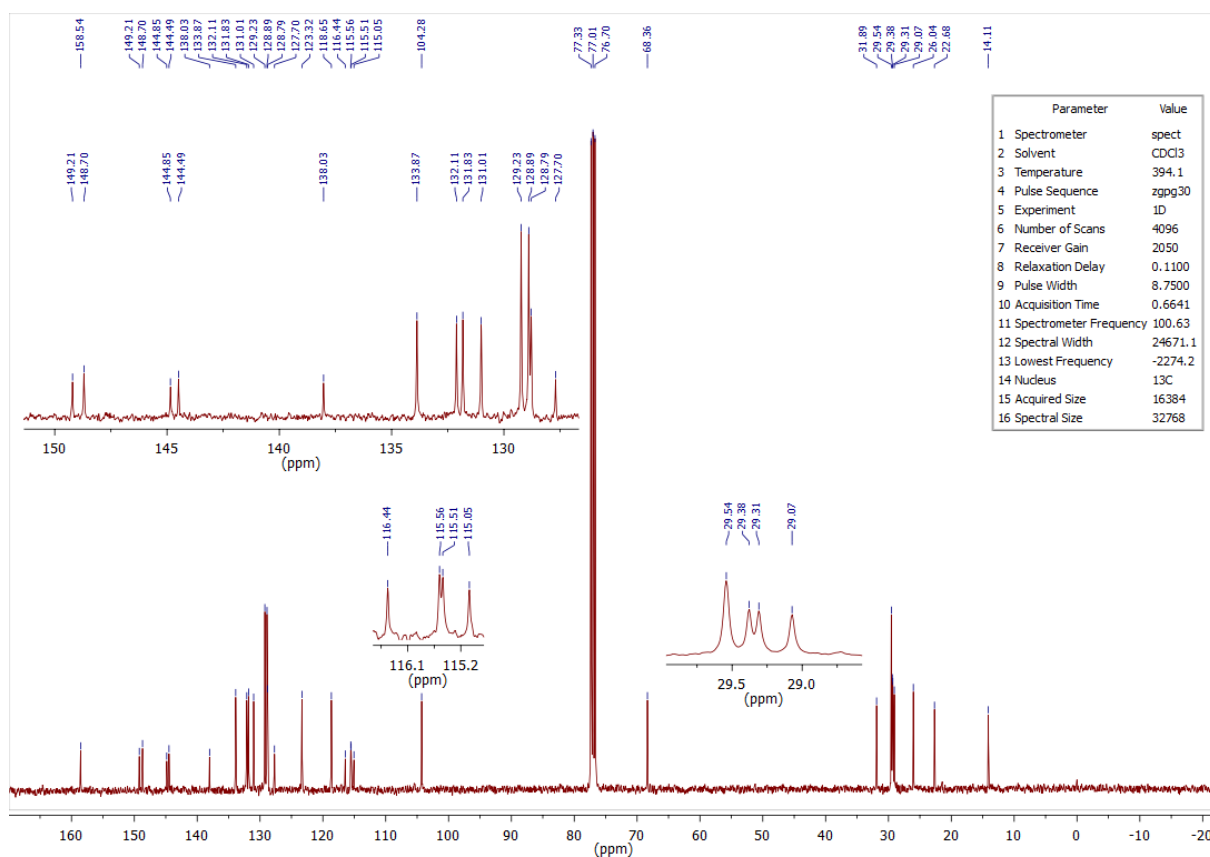


Figure 4.26 – ^{13}C NMR spectrum of compound **1.80g** in CDCl_3 .

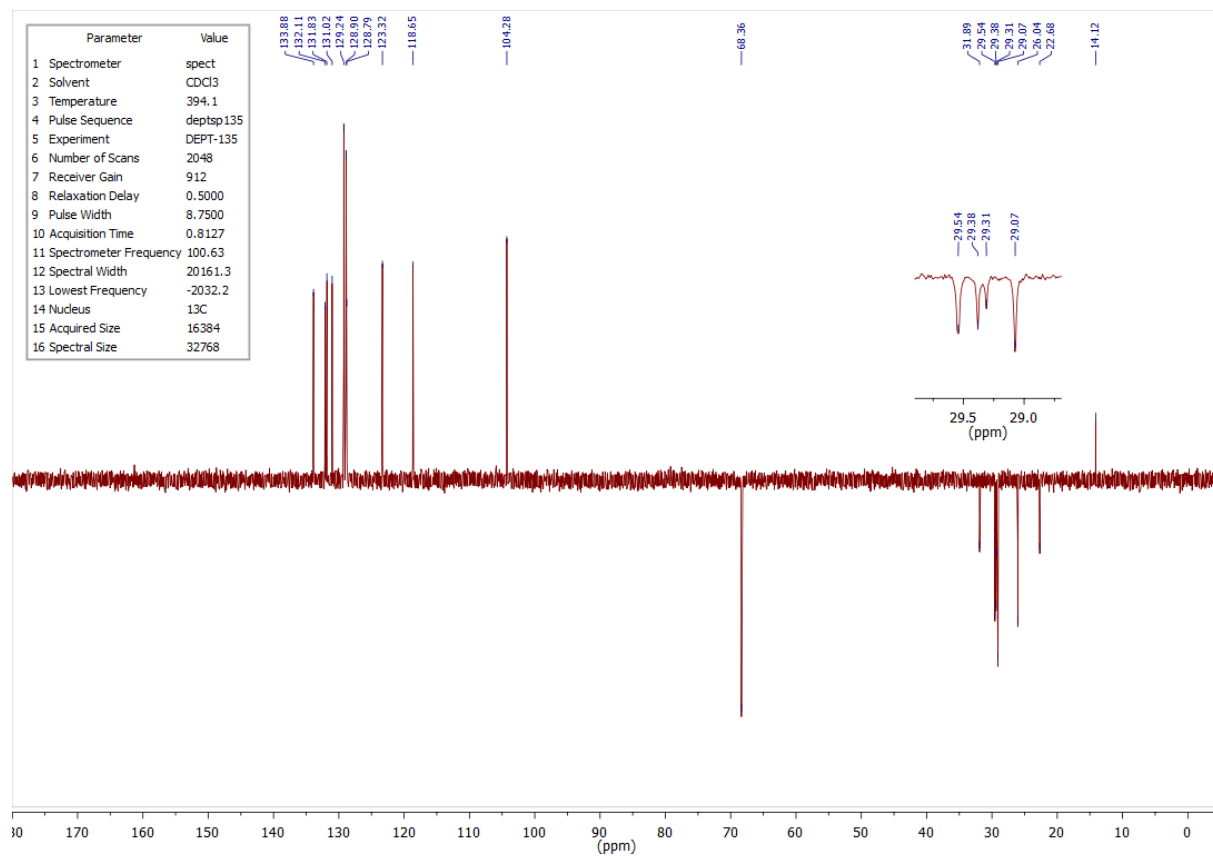


Figure 4.27 – ^{13}C DEPT-135 NMR spectrum of compound **1.80g** in CDCl_3 .

4.1.10 ^1H , ^{13}C and DEPT-135 NMR spectra of compound **1.80h**

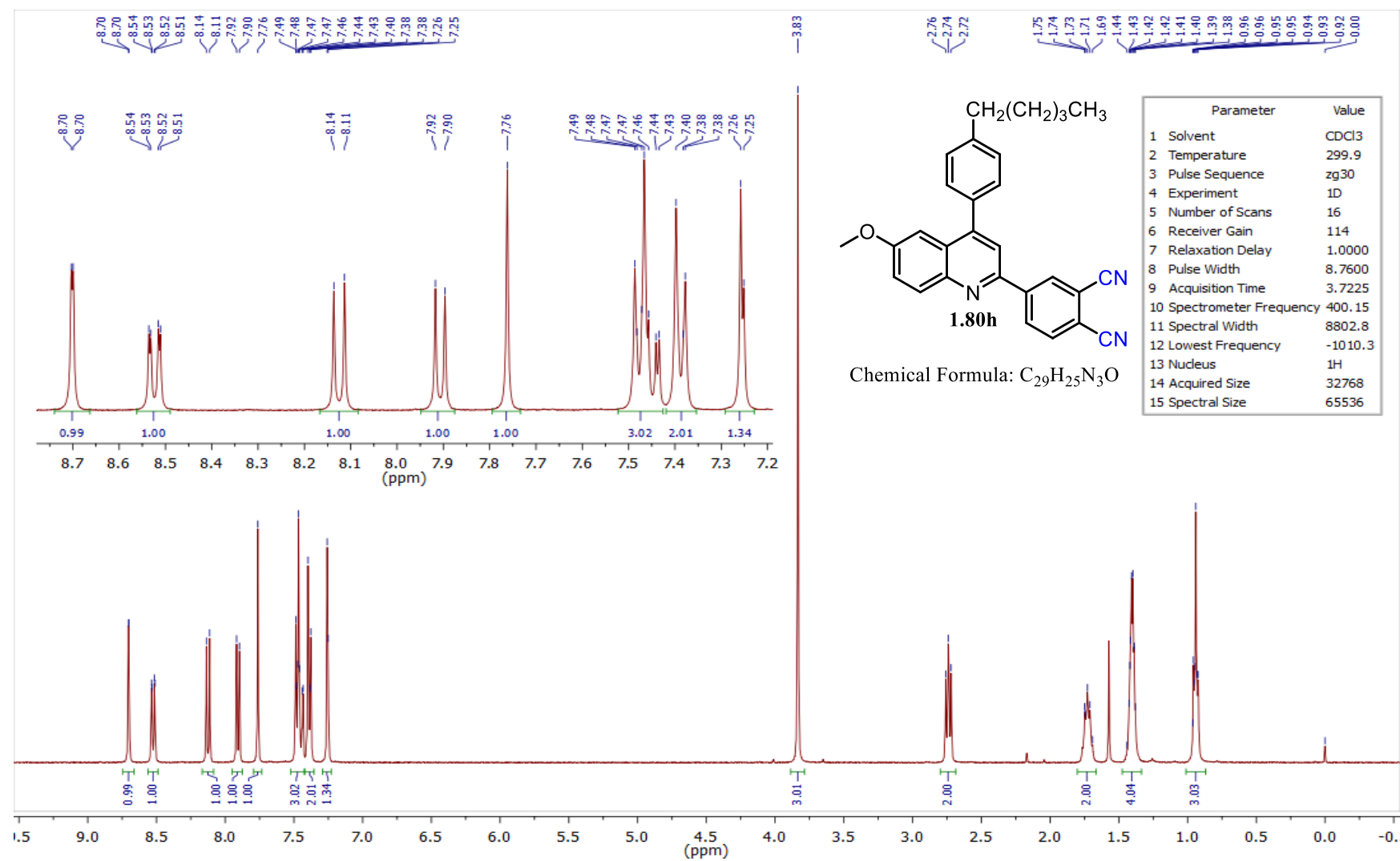


Figure 4.28 – ^1H NMR spectrum of compound **1.80h** in CDCl_3 .

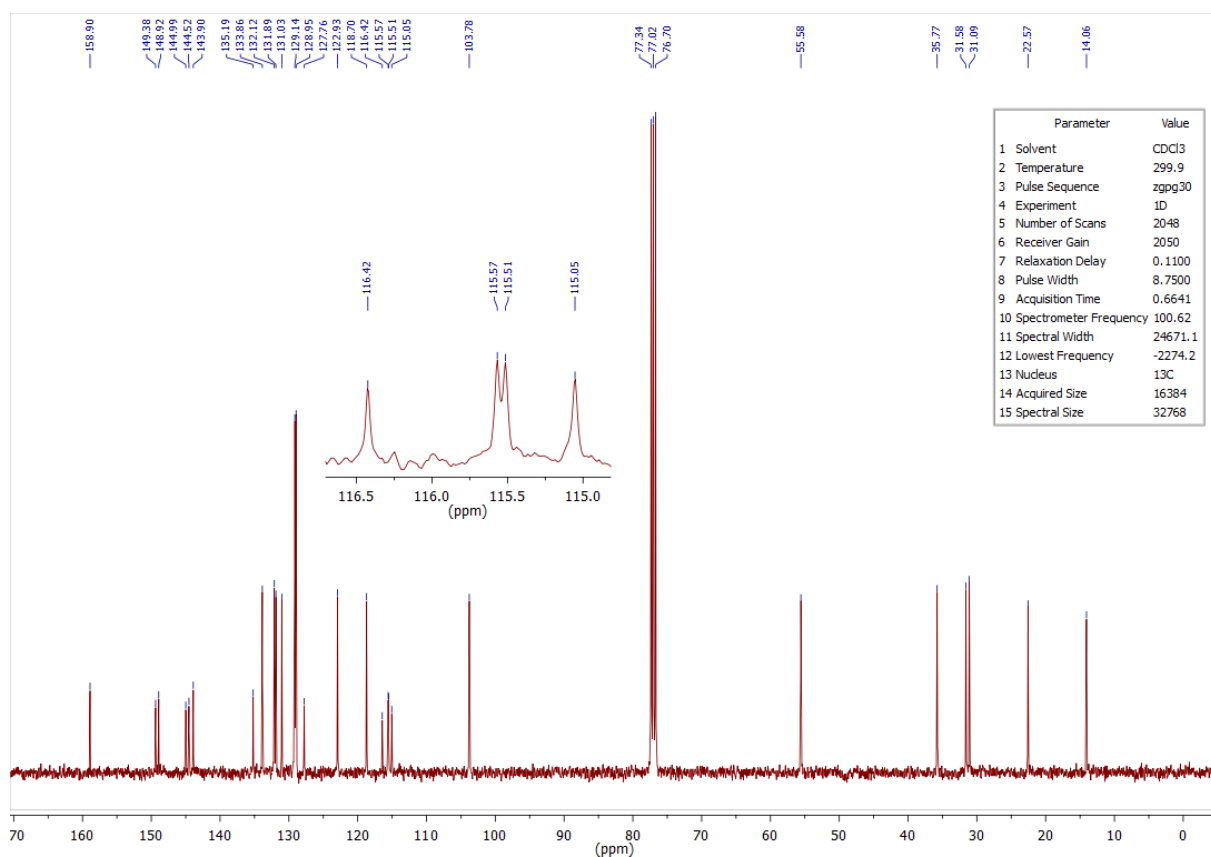


Figure 4.29 – ^{13}C NMR spectrum of compound **1.80h** in CDCl_3 .

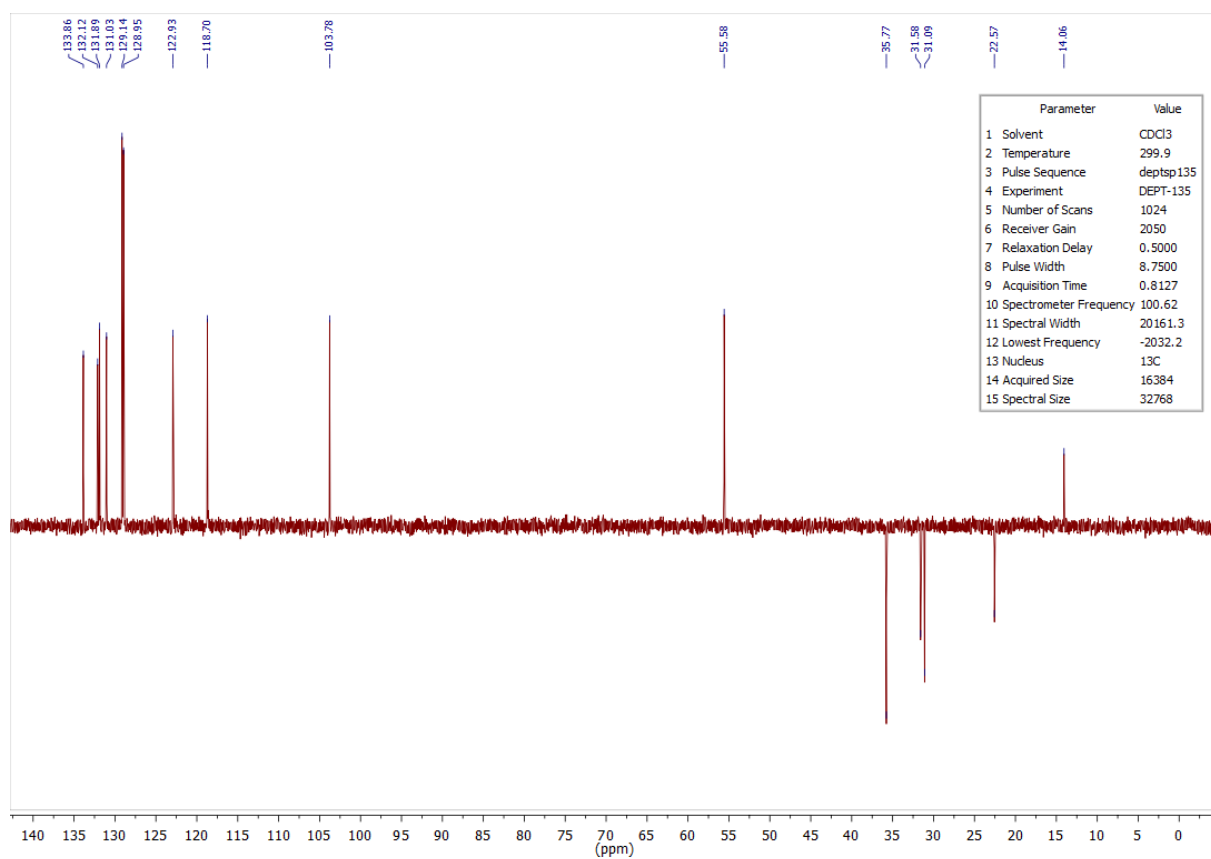


Figure 4.30 – ^{13}C DEPT-135 NMR spectrum of compound **1.80h** in CDCl_3 .

4.1.11 ^1H , ^{13}C and DEPT-135 NMR spectra of compound **1.80i**

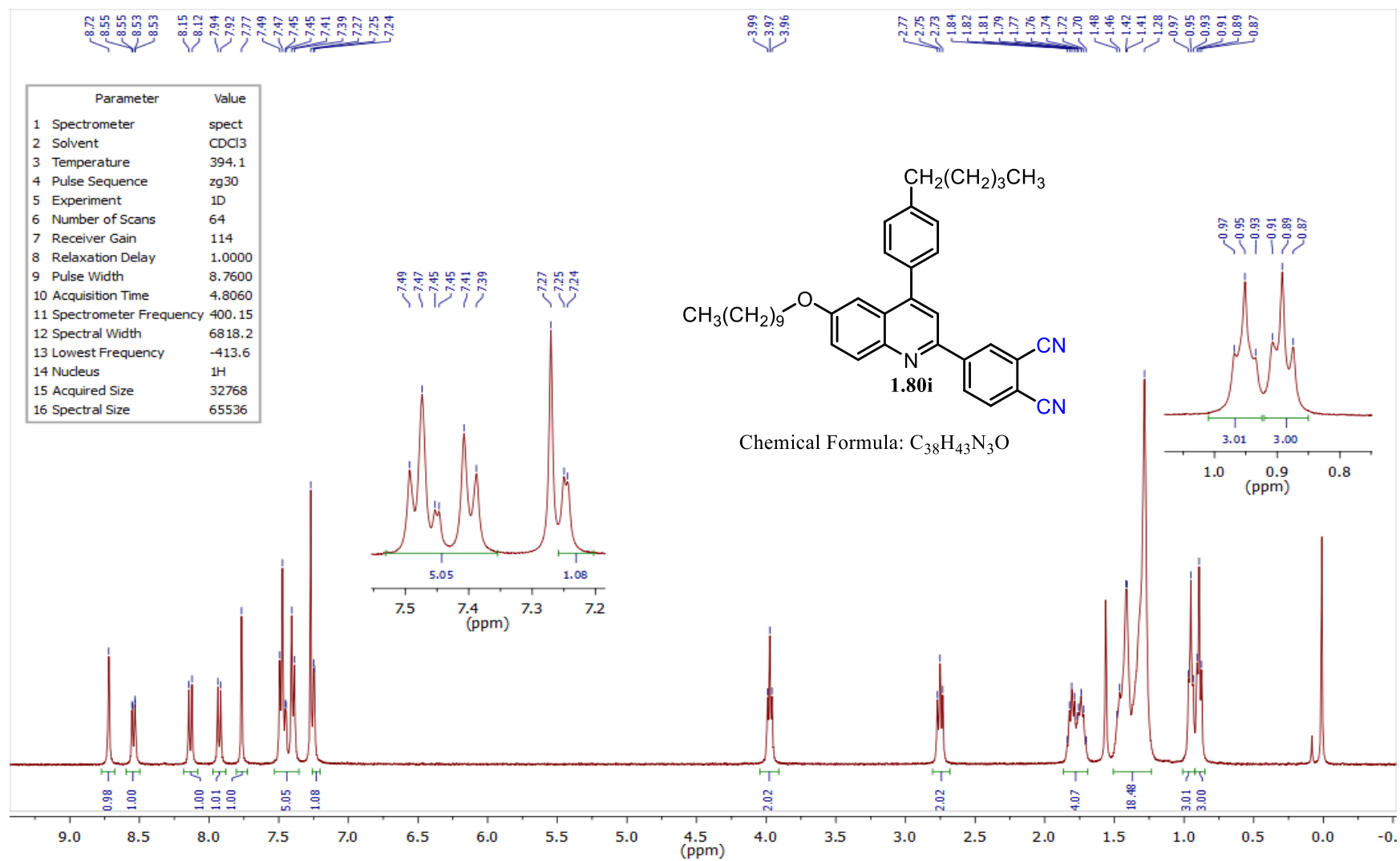


Figure 4.31 – ^1H NMR spectrum of compound **1.80i** in CDCl_3 .

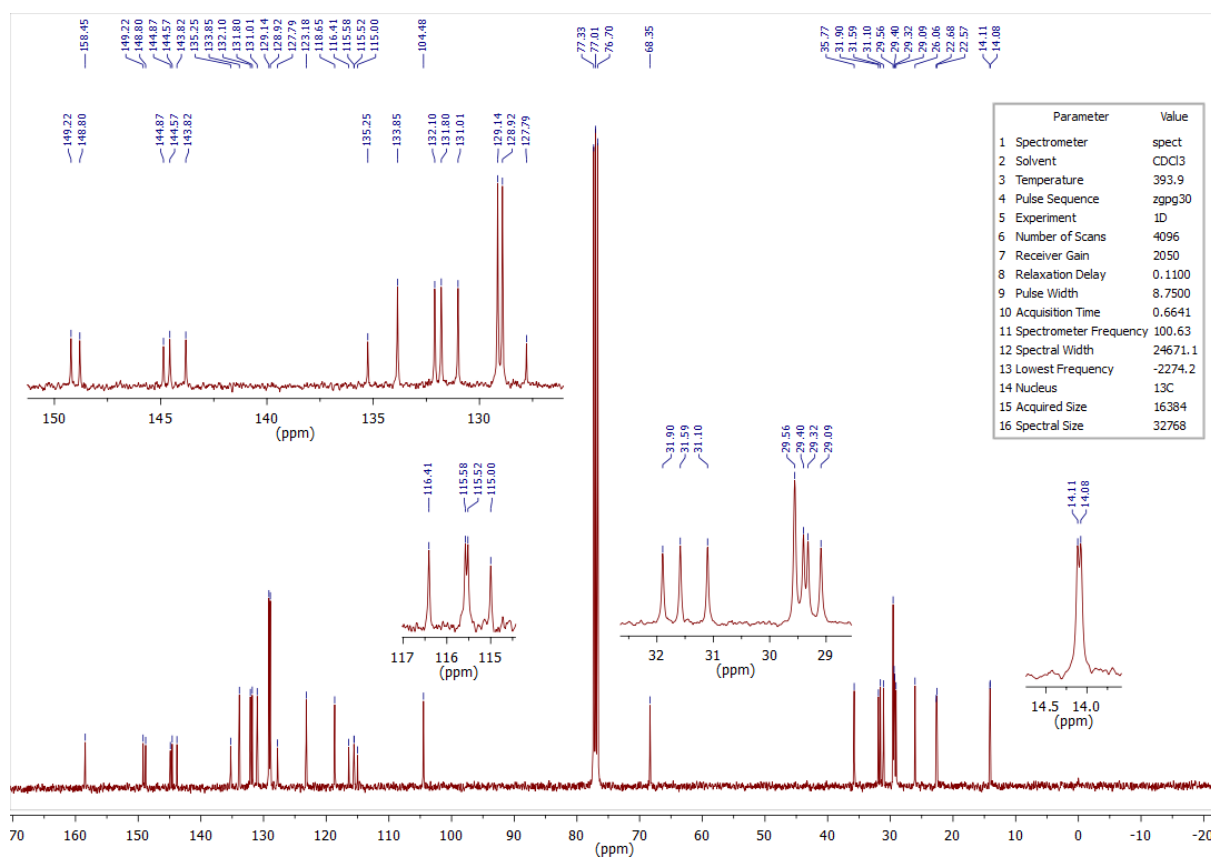


Figure 4.32 – ^{13}C NMR spectrum of compound **1.80i** in CDCl_3 .

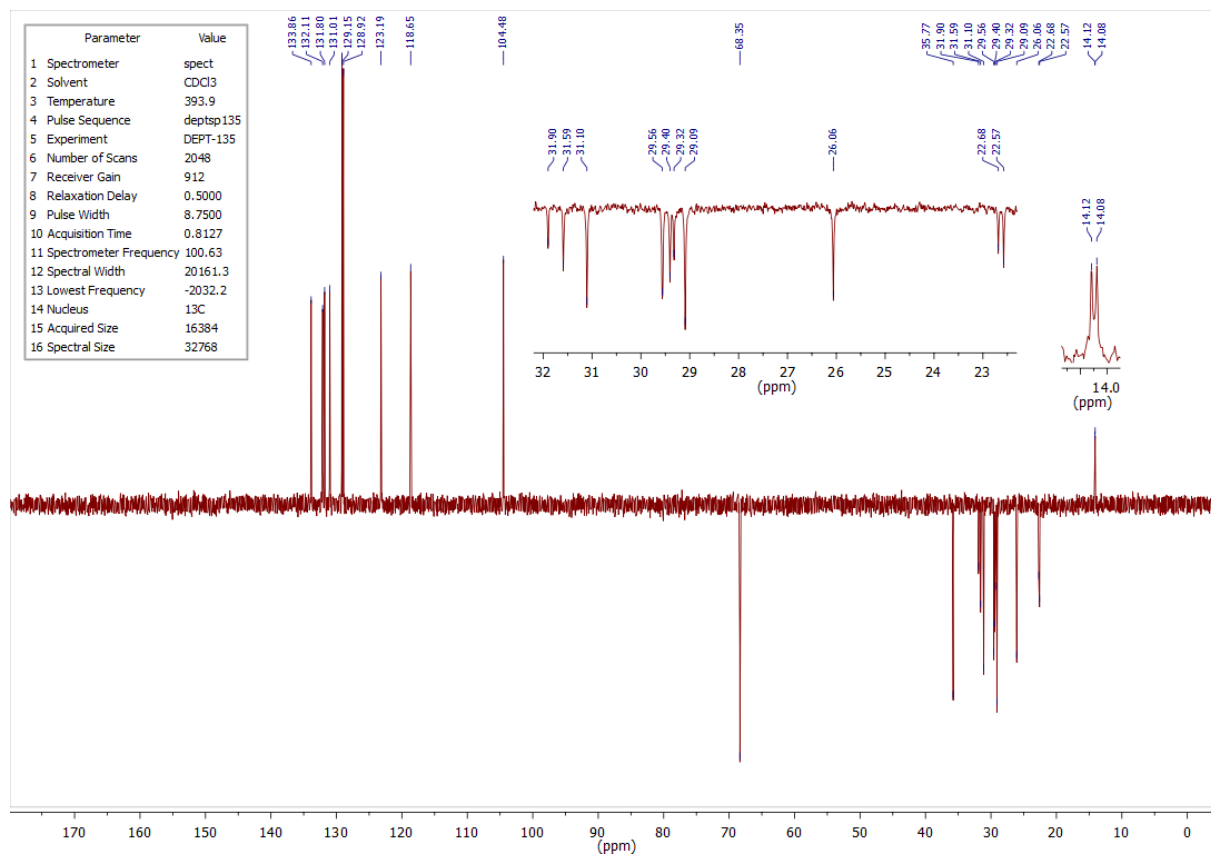


Figure 4.33 – ^{13}C DEPT-135 NMR spectrum of compound **1.80i** in CDCl_3 .

4.1.12 ^1H , ^{13}C and DEPT-135 NMR spectra of compound **1.80j**

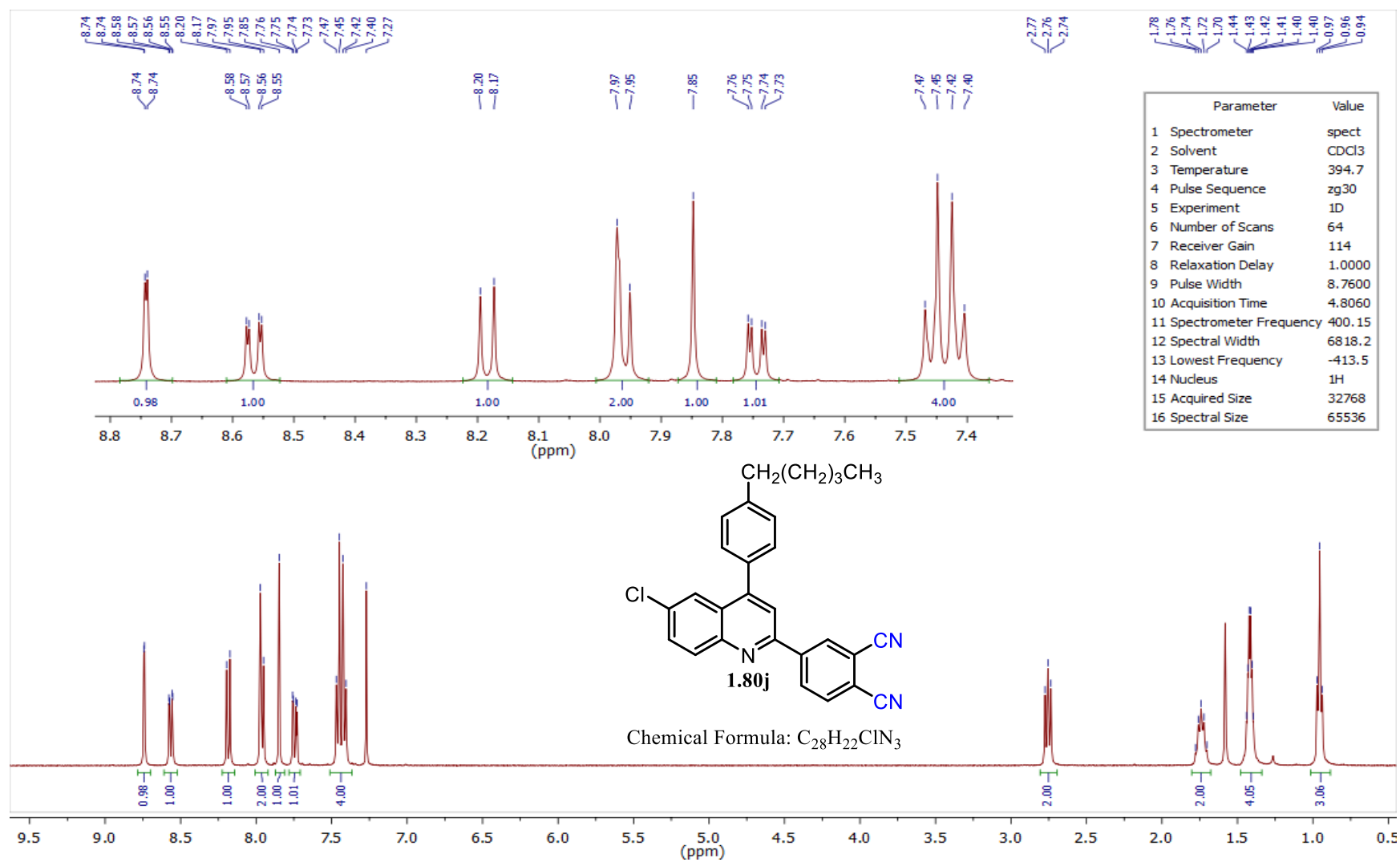


Figure 4.34 – ^1H NMR spectrum of compound **1.80j** in CDCl_3 .

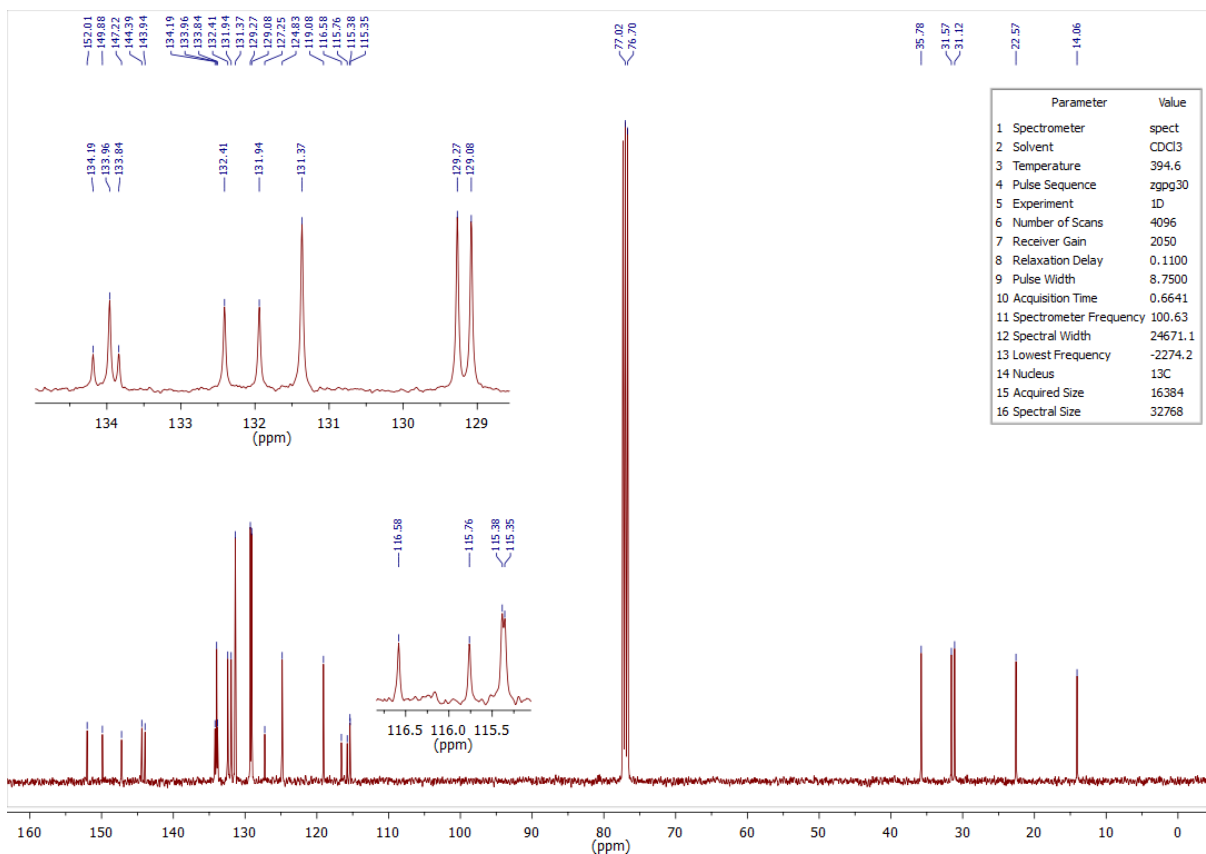


Figure 4.35 – ^{13}C NMR spectrum of compound **1.80j** in CDCl_3 .

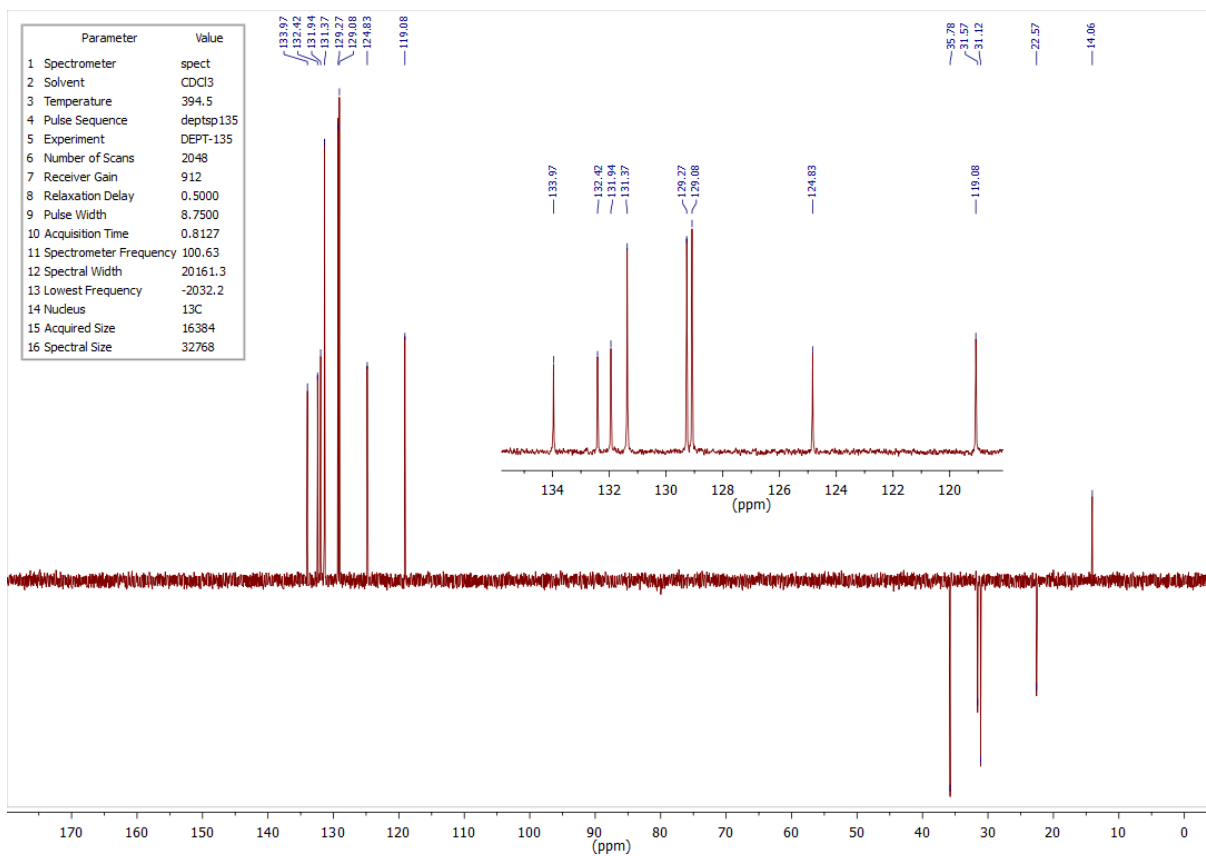


Figure 4.36 – ^{13}C DEPT-135 NMR spectrum of compound **1.80j** in CDCl_3 .

4.1.13 ^1H , ^{13}C and DEPT-135 NMR spectra of compound **1.80k**

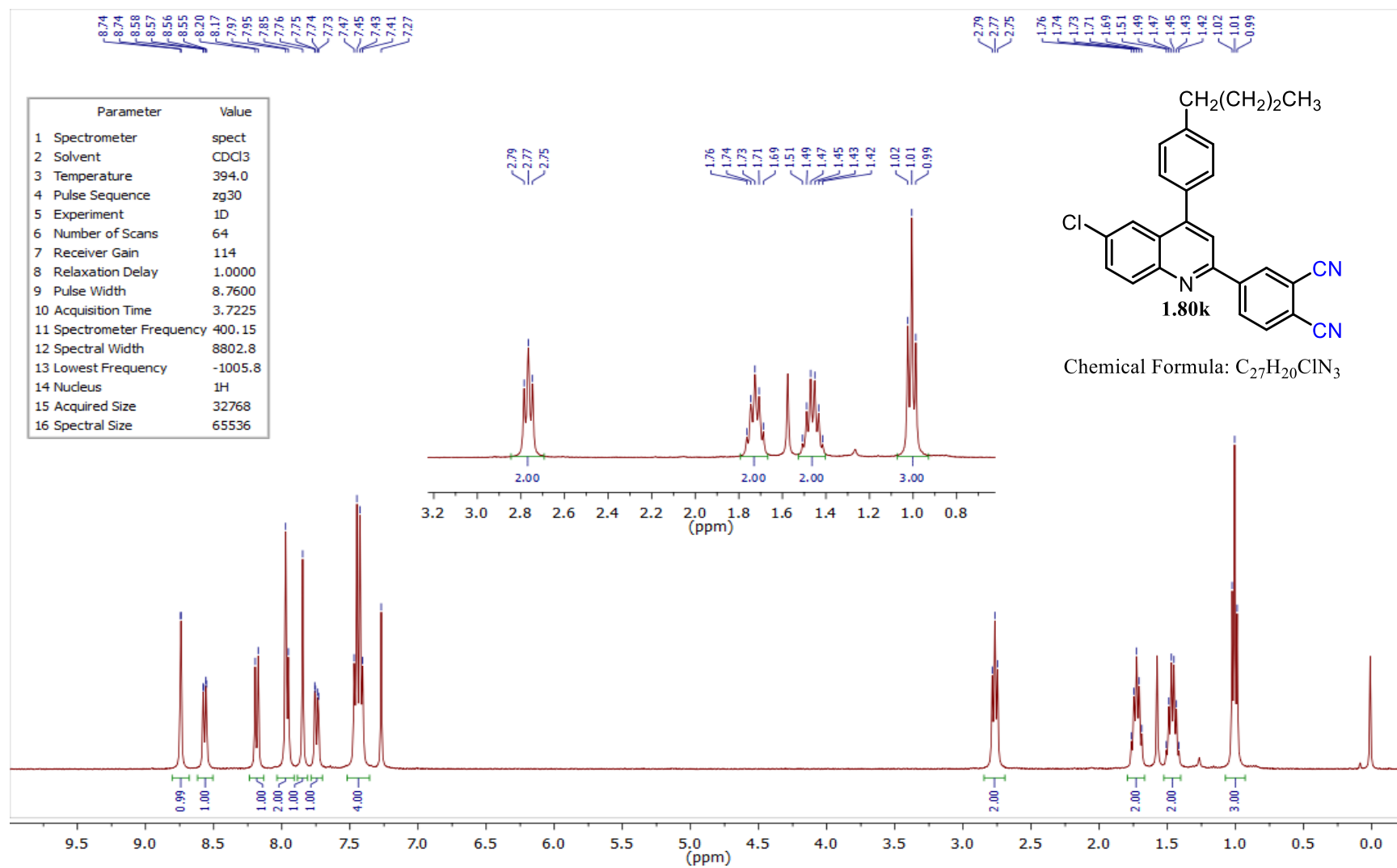


Figure 4.37 – ^1H NMR spectrum of compound **1.80k** in CDCl_3 .

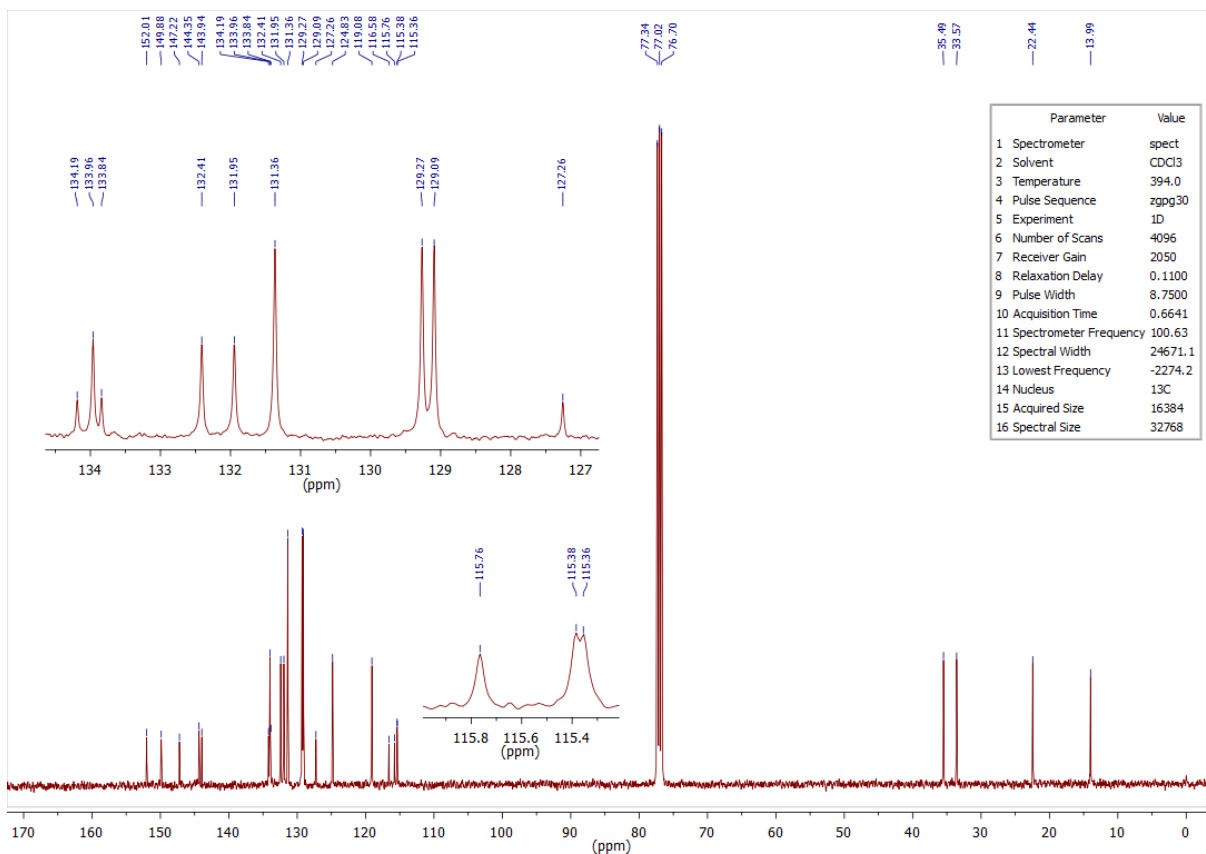


Figure 4.38 – ^{13}C NMR spectrum of compound **1.80k** in CDCl_3 .

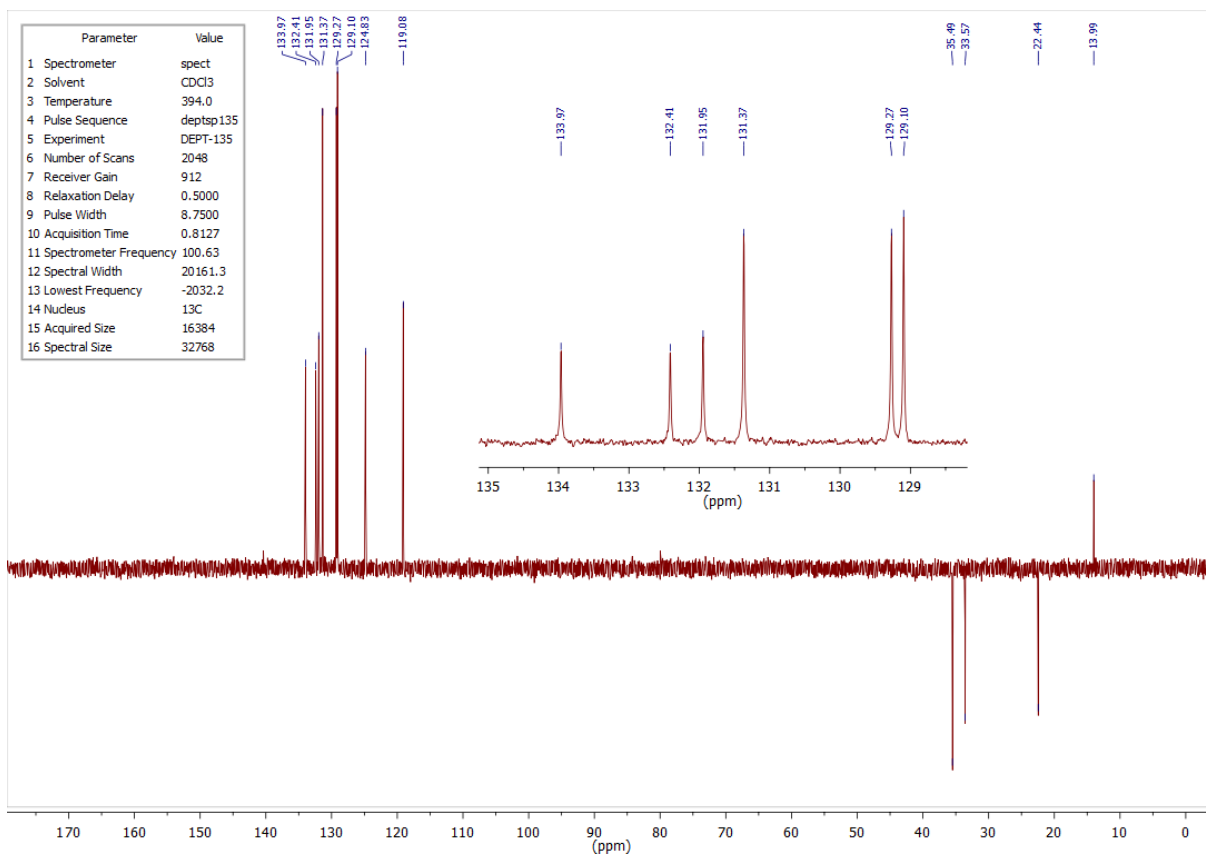


Figure 4.39 – ^{13}C DEPT-135 NMR spectrum of compound **1.80k** in CDCl_3 .

4.1.14 ^1H , ^{13}C and DEPT-135 NMR spectra of compound **1.801**

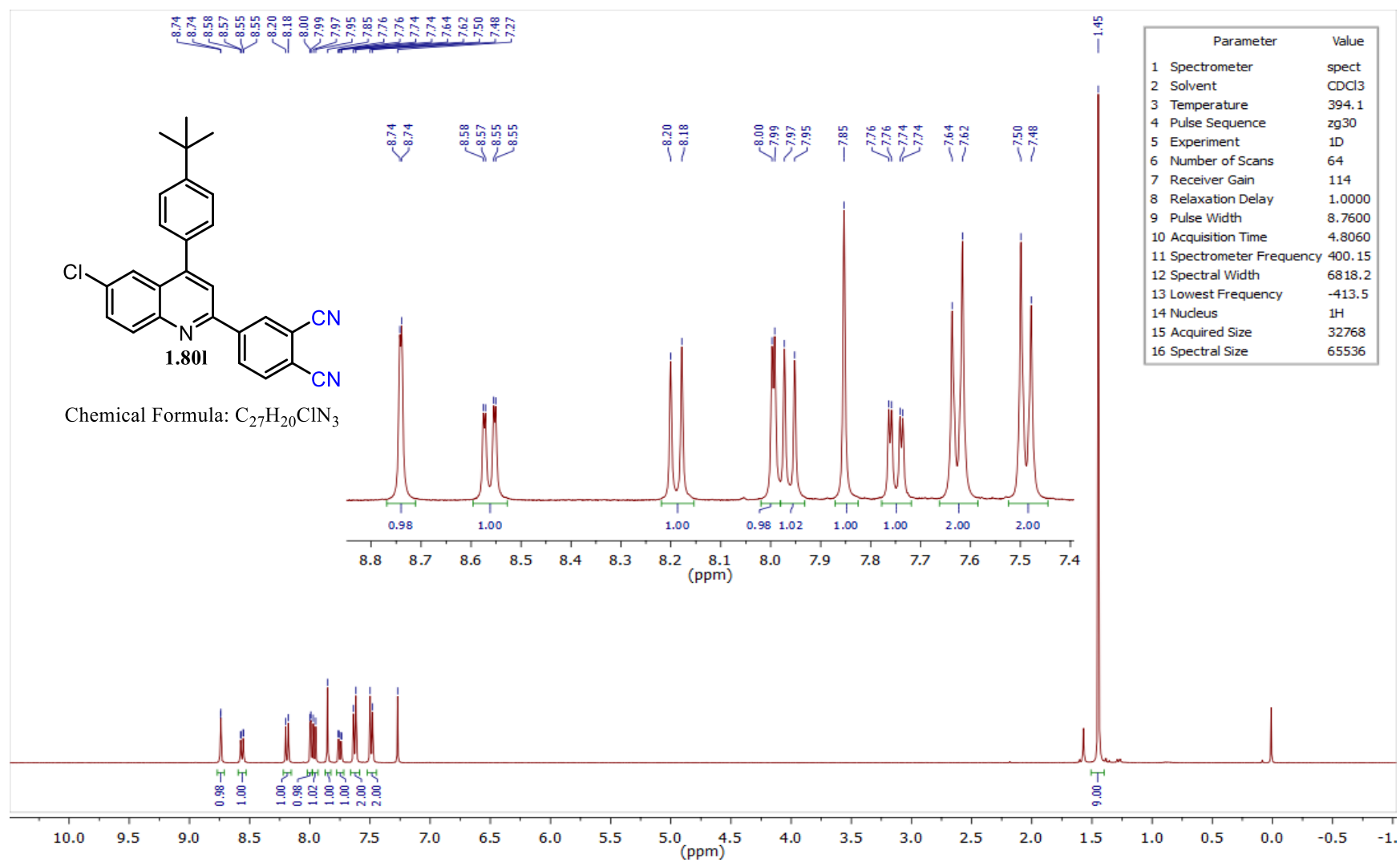


Figure 4.40 – ^1H NMR spectrum of compound **1.801** in CDCl_3 .

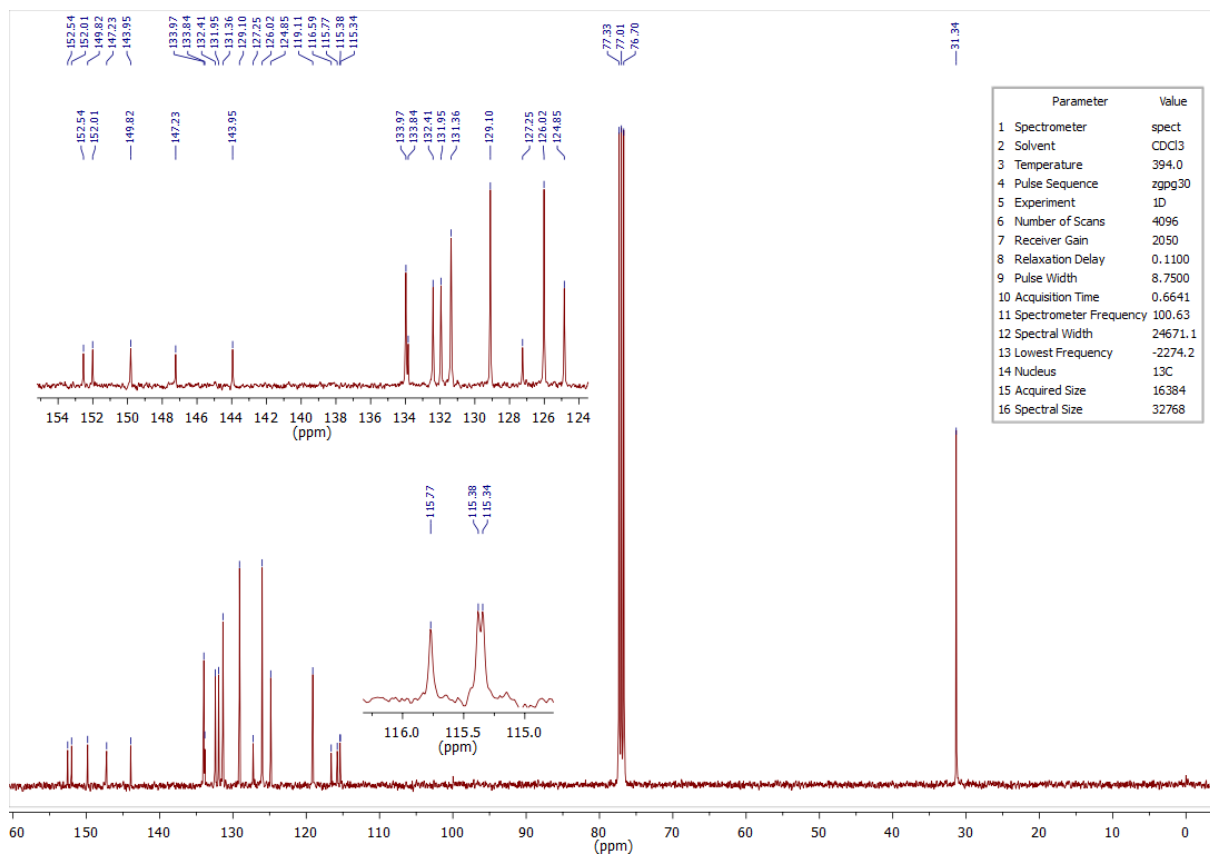


Figure 4.41 – ^{13}C NMR spectrum of compound **1.801** in CDCl_3 .

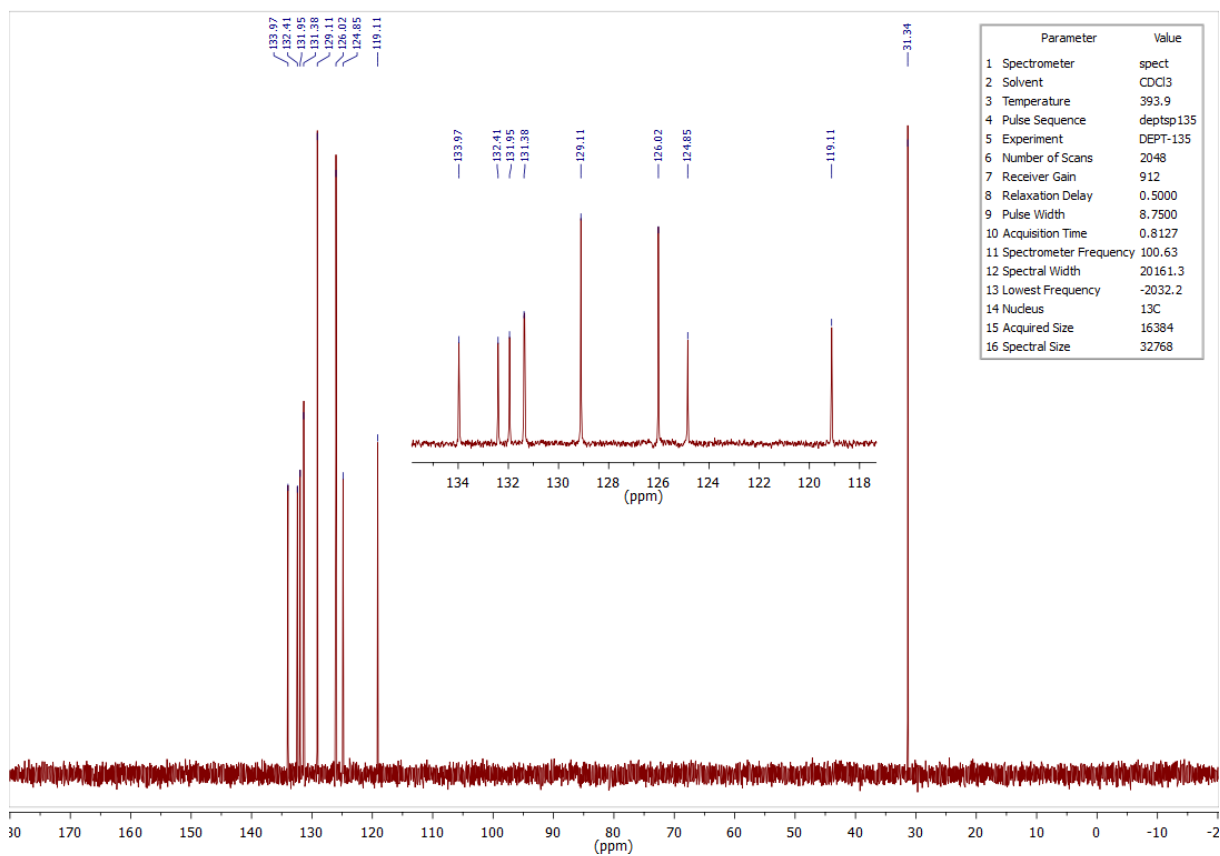


Figure 4.42 – ^{13}C DEPT-135 NMR spectrum of compound **1.801** in CDCl_3 .

4.1.15 ¹H NMR spectrum of compound **1.80m**

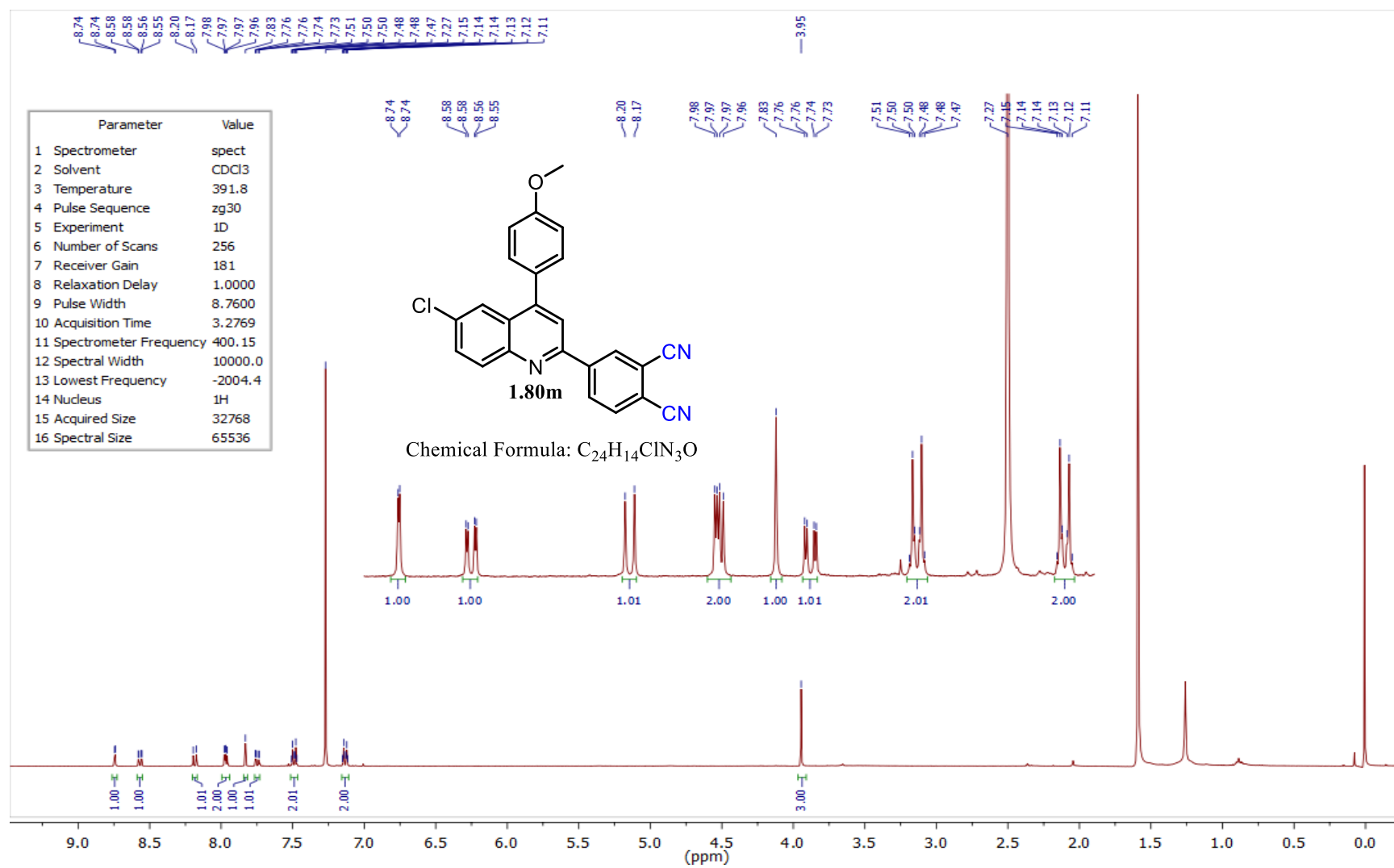


Figure 4.43 – ¹H NMR spectrum of compound **1.80m** in CDCl₃.

4.1.16 ^1H , ^{13}C and DEPT-135 NMR spectra of compound **1.80n**

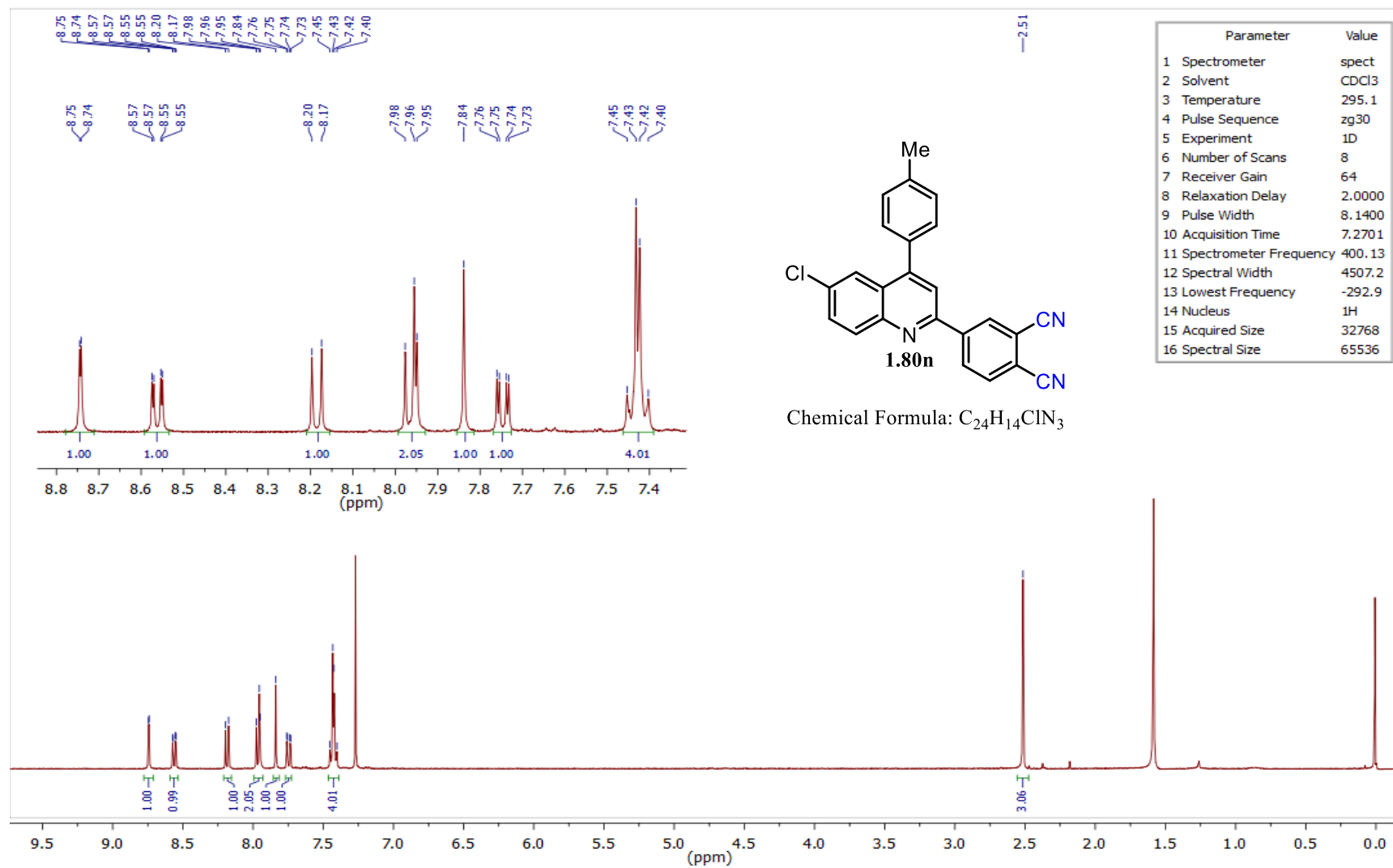


Figure 4.44 – ^1H NMR spectrum of compound **1.80n** in CDCl_3 .

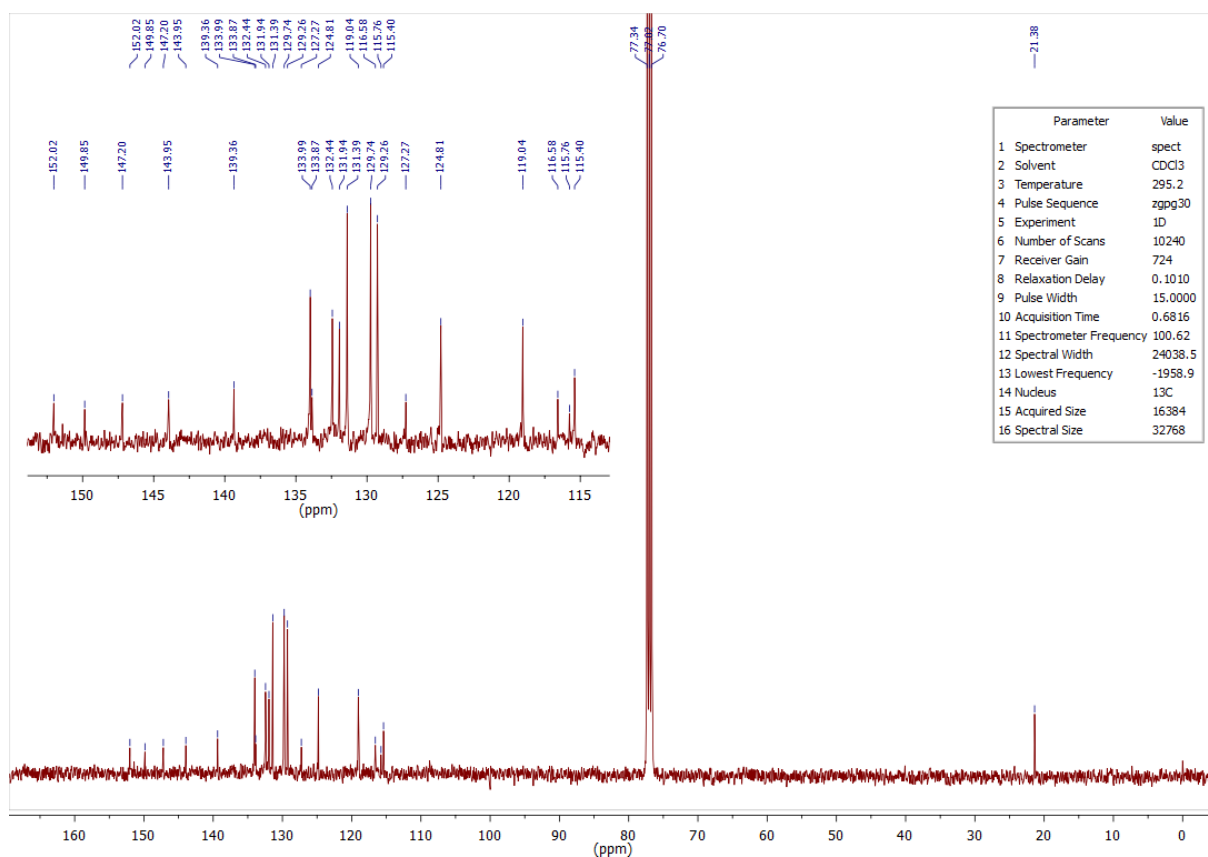


Figure 4.45 – ^{13}C NMR spectrum of compound **1.80n** in CDCl_3 .

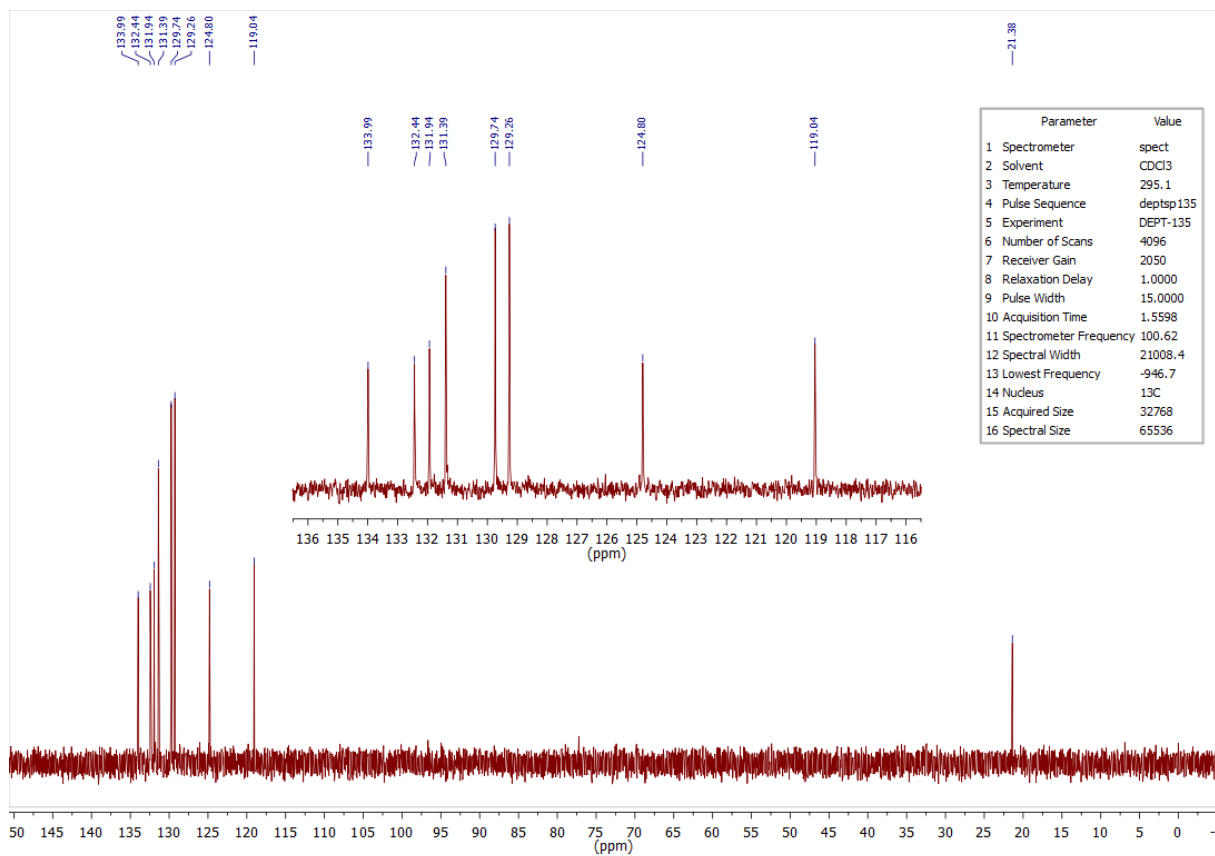


Figure 4.46 – ^{13}C DEPT-135 NMR spectrum of compound **1.80n** in CDCl_3 .

4.1.17 ¹H NMR spectrum of compound 1.80o

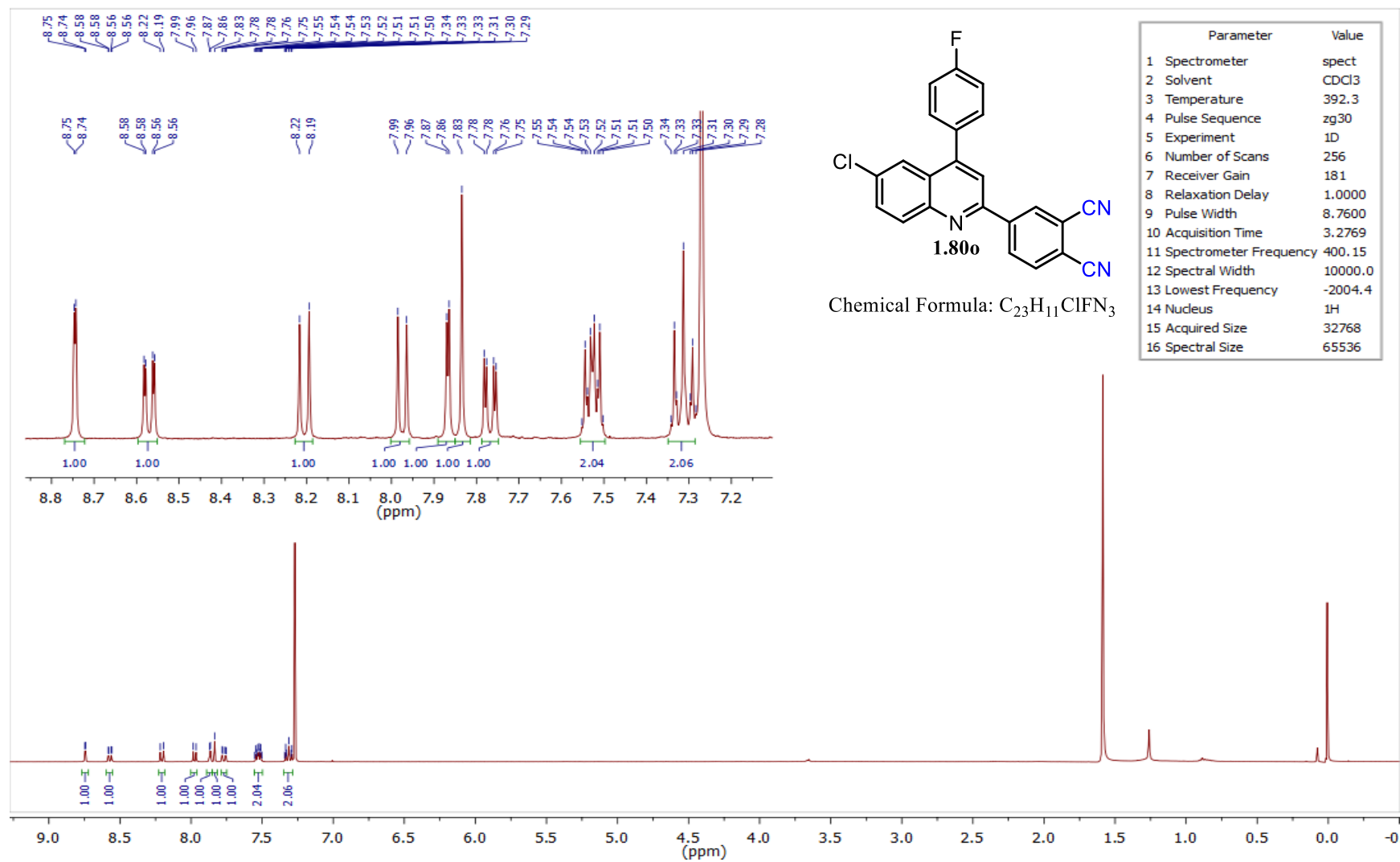


Figure 4.47 – ¹H NMR spectrum of compound 1.80o in CDCl₃.

4.1.18 ^1H , ^{13}C and DEPT-135 NMR spectra of compound **1.80p**

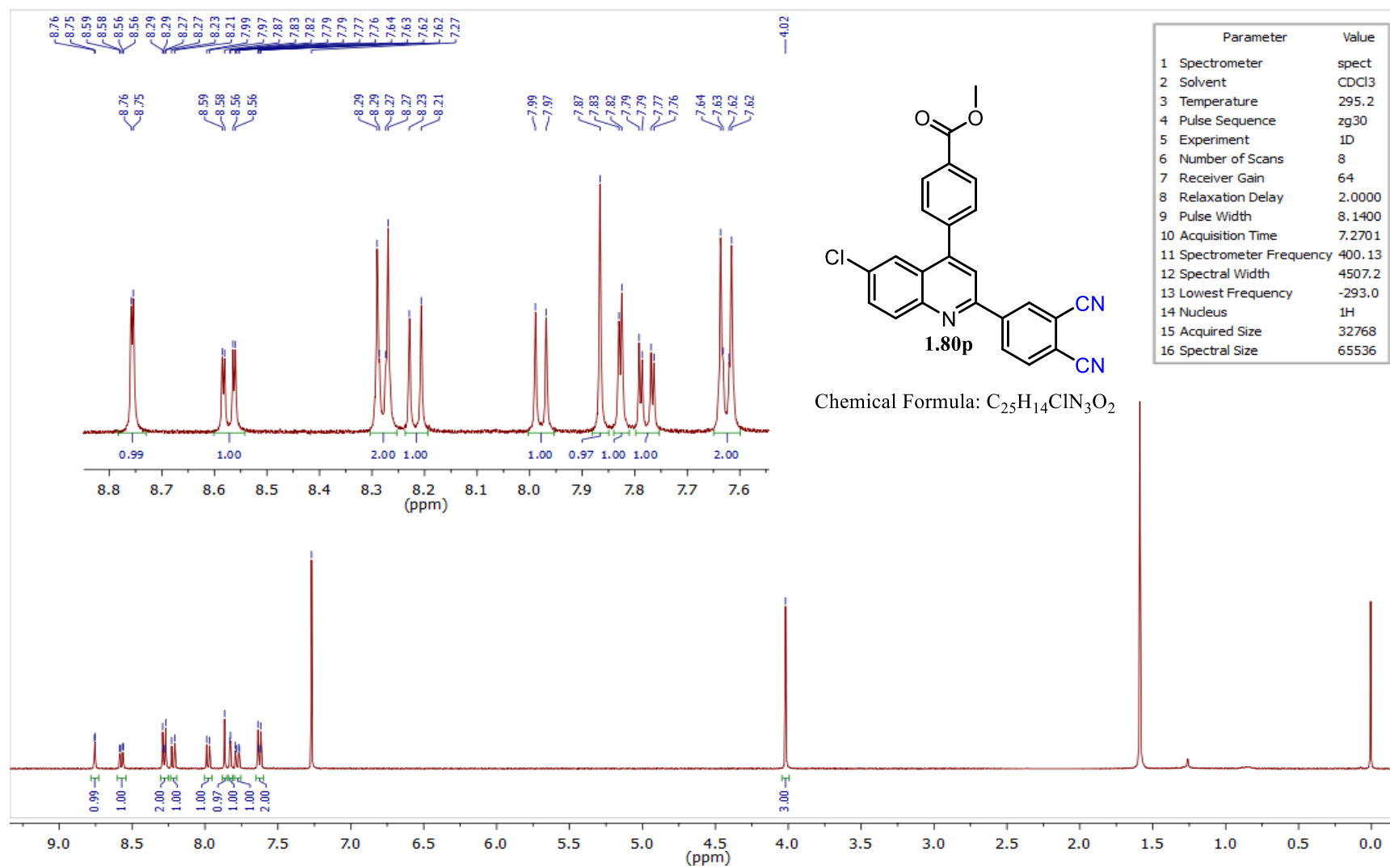


Figure 4.48 – ^1H NMR spectrum of compound **1.80p** in CDCl_3 .

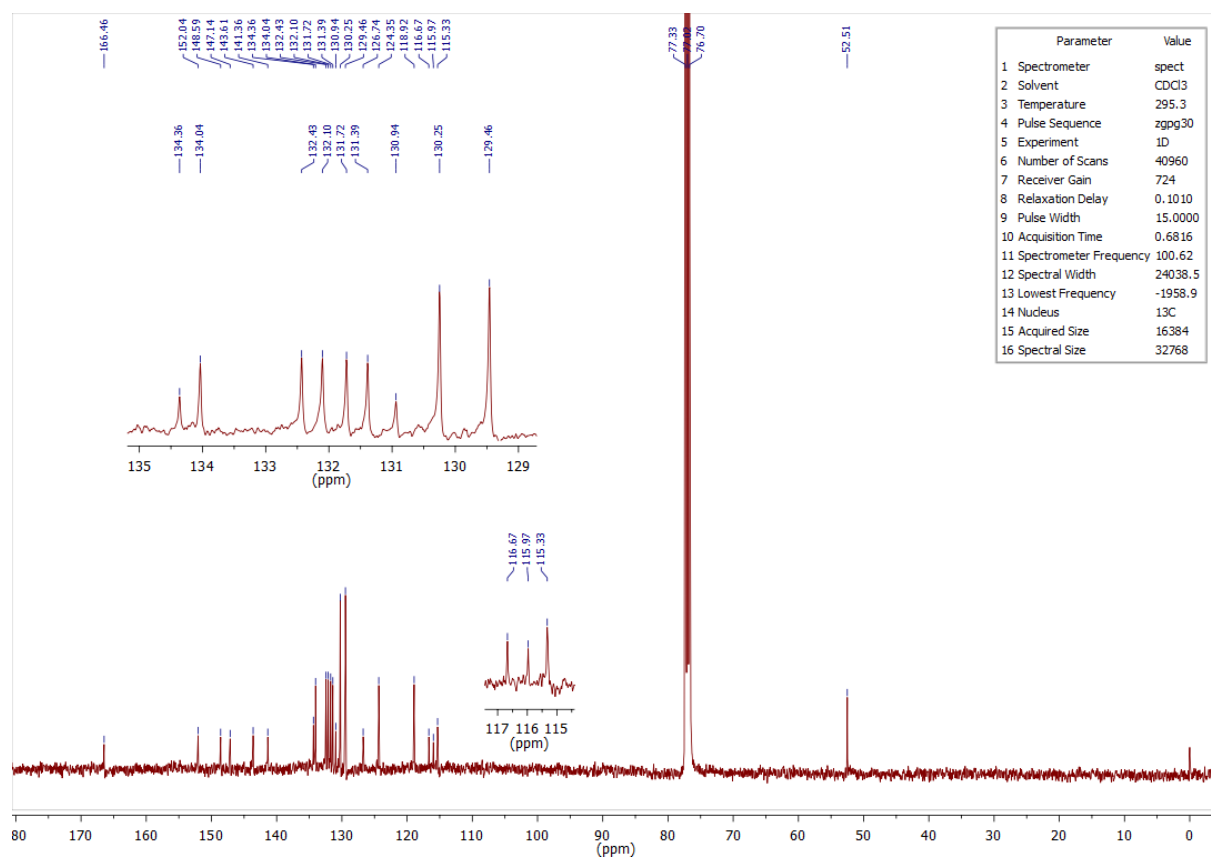


Figure 4.49 – ^{13}C NMR spectrum of compound **1.80p** in CDCl_3 .

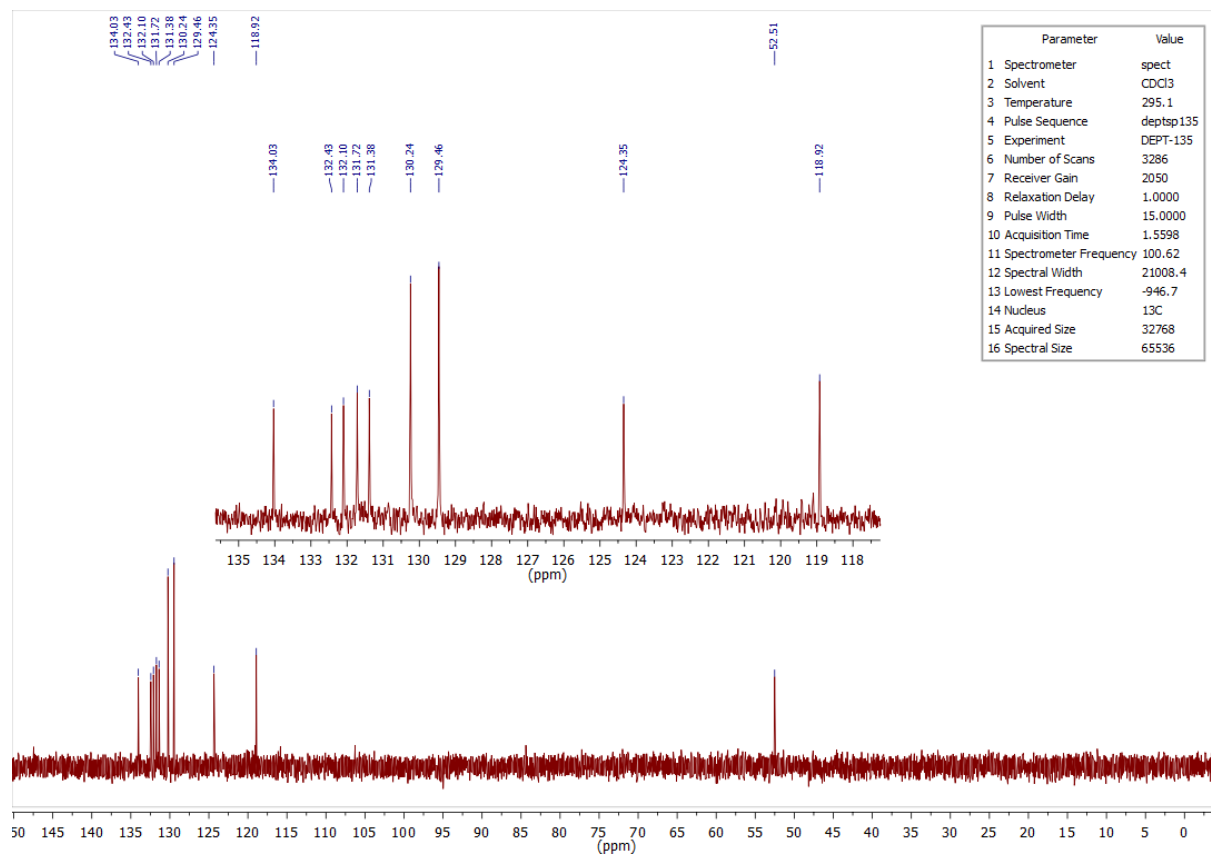


Figure 4.50 – ^{13}C DEPT-135 NMR spectrum of compound **1.80p** in CDCl_3 .

4.1.19 ^1H , ^{13}C and DEPT-135 NMR spectra of compound **1.80q**

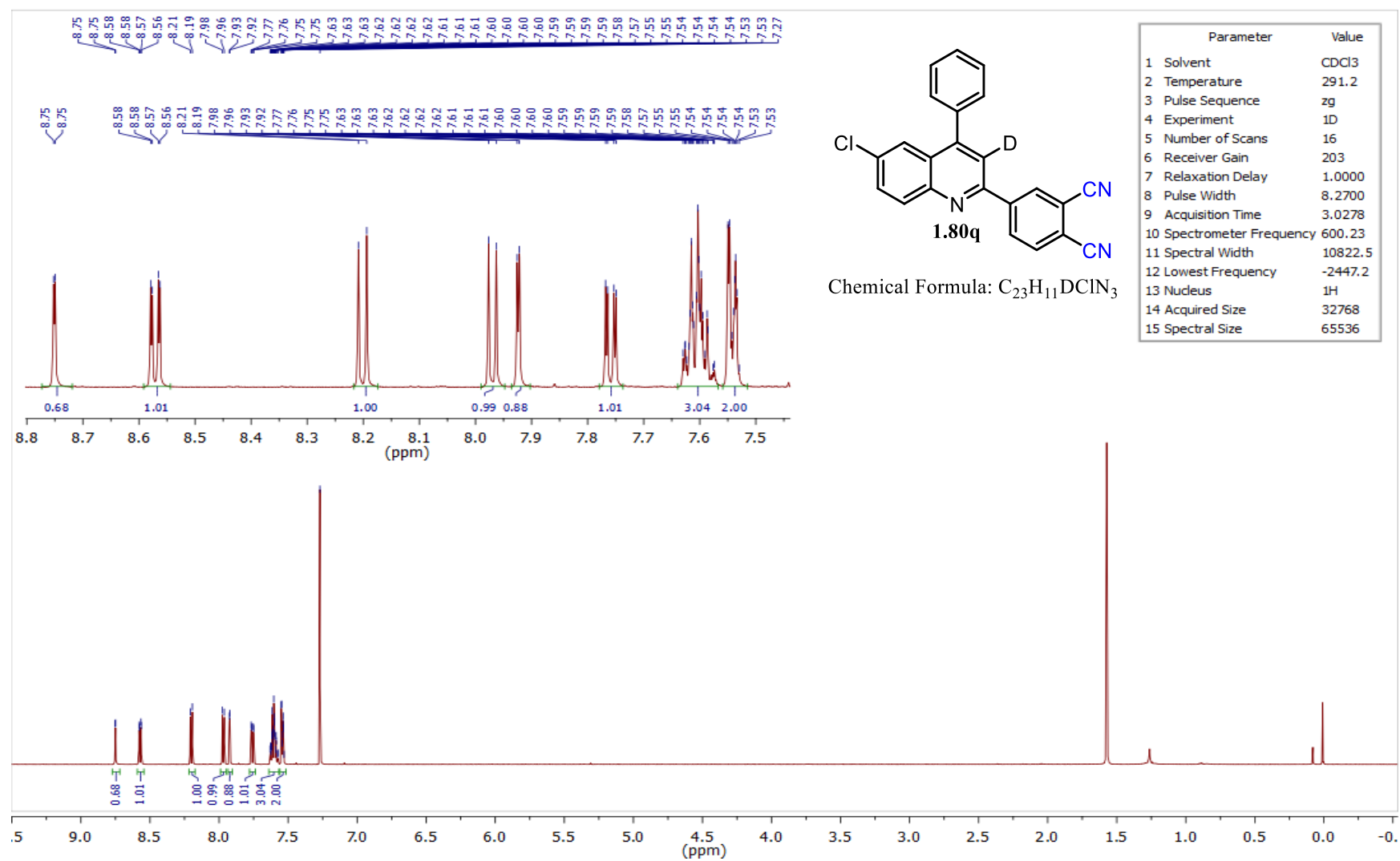


Figure 4.51 – ^1H NMR spectrum of compound **1.80q** in CDCl_3 .

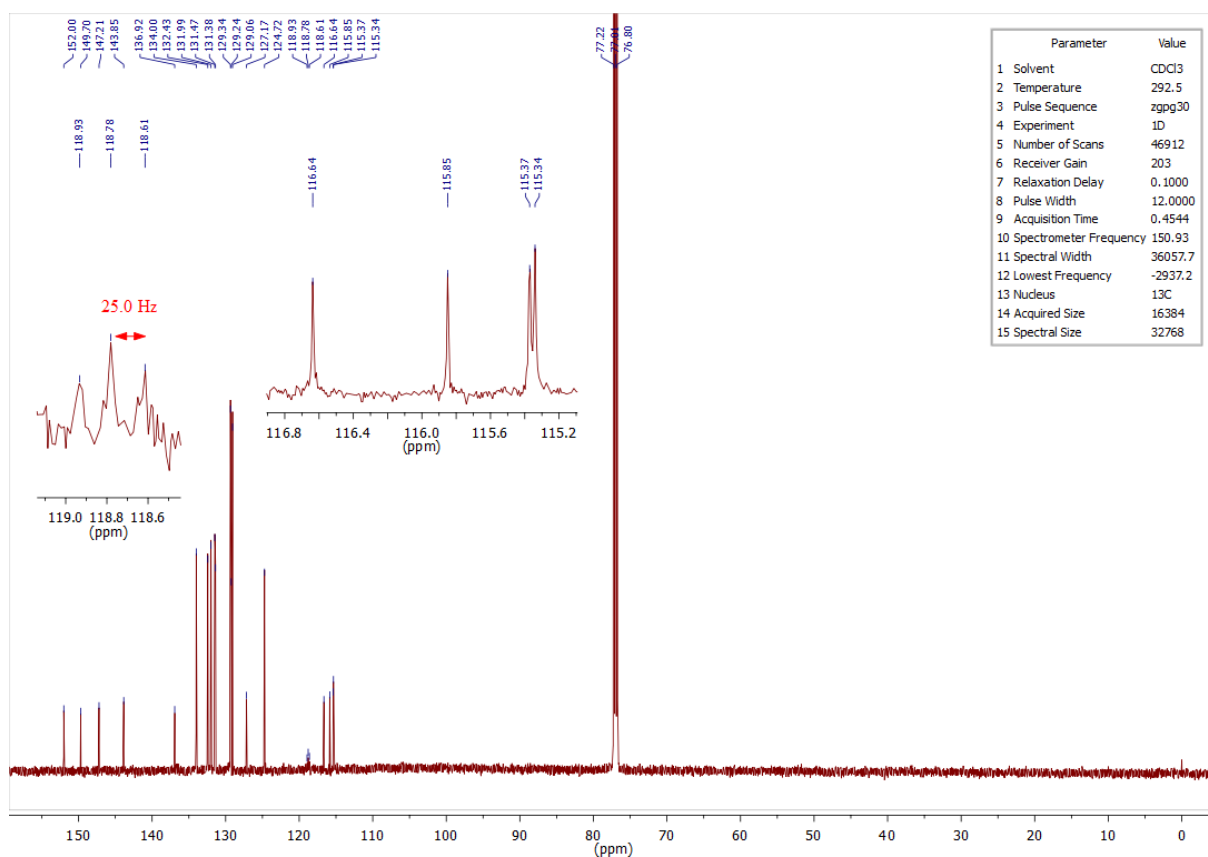


Figure 4.52 – ^{13}C NMR spectrum of compound **1.80q** in CDCl_3 .

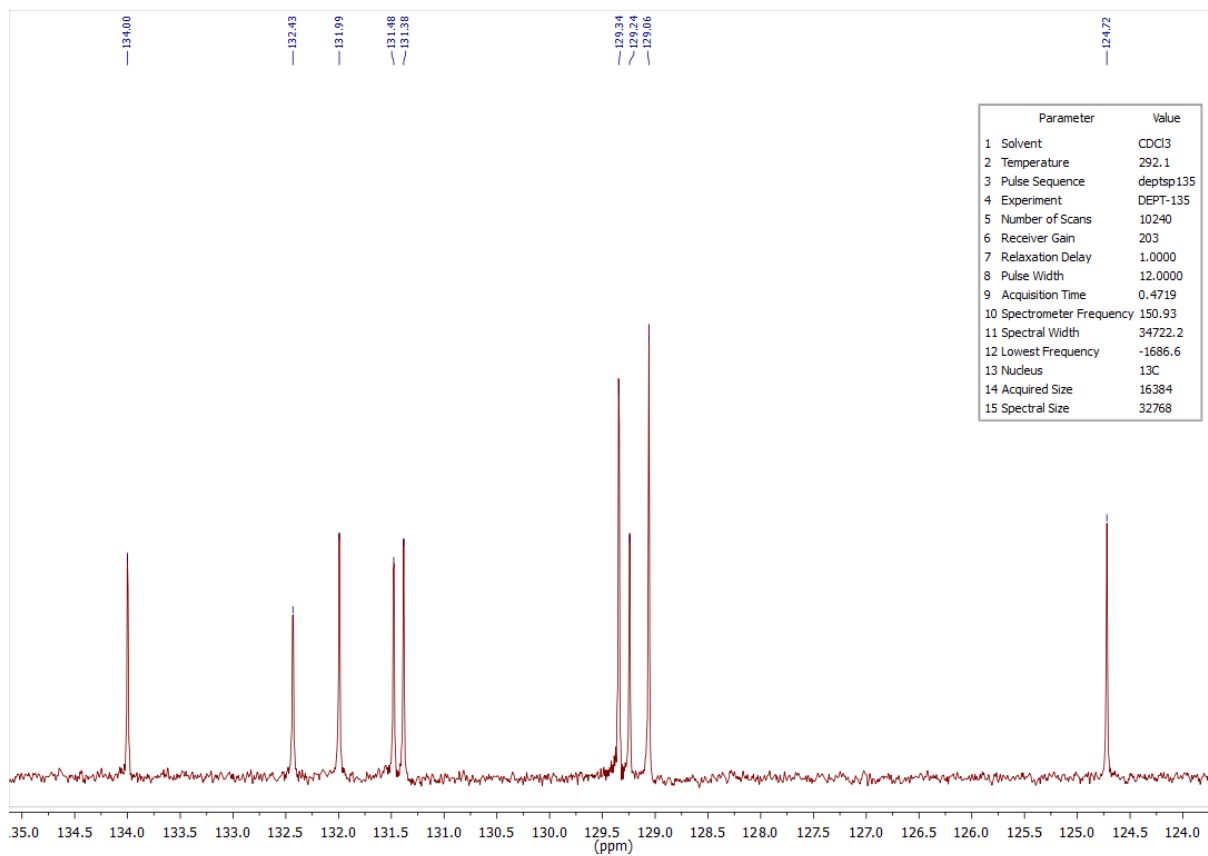


Figure 4.53 – ^{13}C DEPT-135 NMR spectrum of compound **1.80q** in CDCl_3 .

4.1.20 ^1H NMR spectrum of compound 1.81a

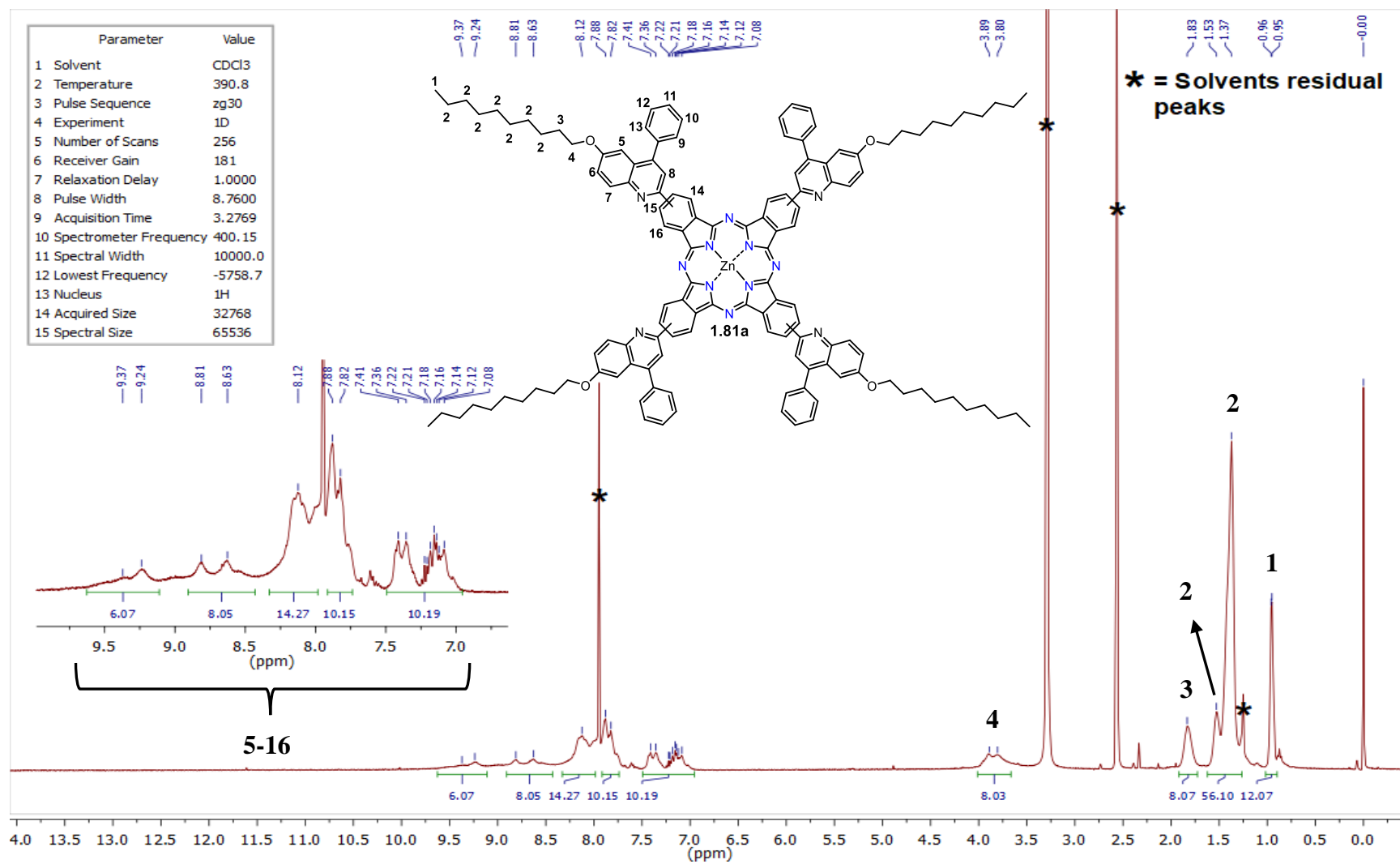


Figure 4.54 – ^1H NMR spectrum of compound 1.81a in $\text{CDCl}_3/\text{DMSO}-d_6$ (2:1).

4.1.21 ¹H NMR spectrum of compound 1.81b

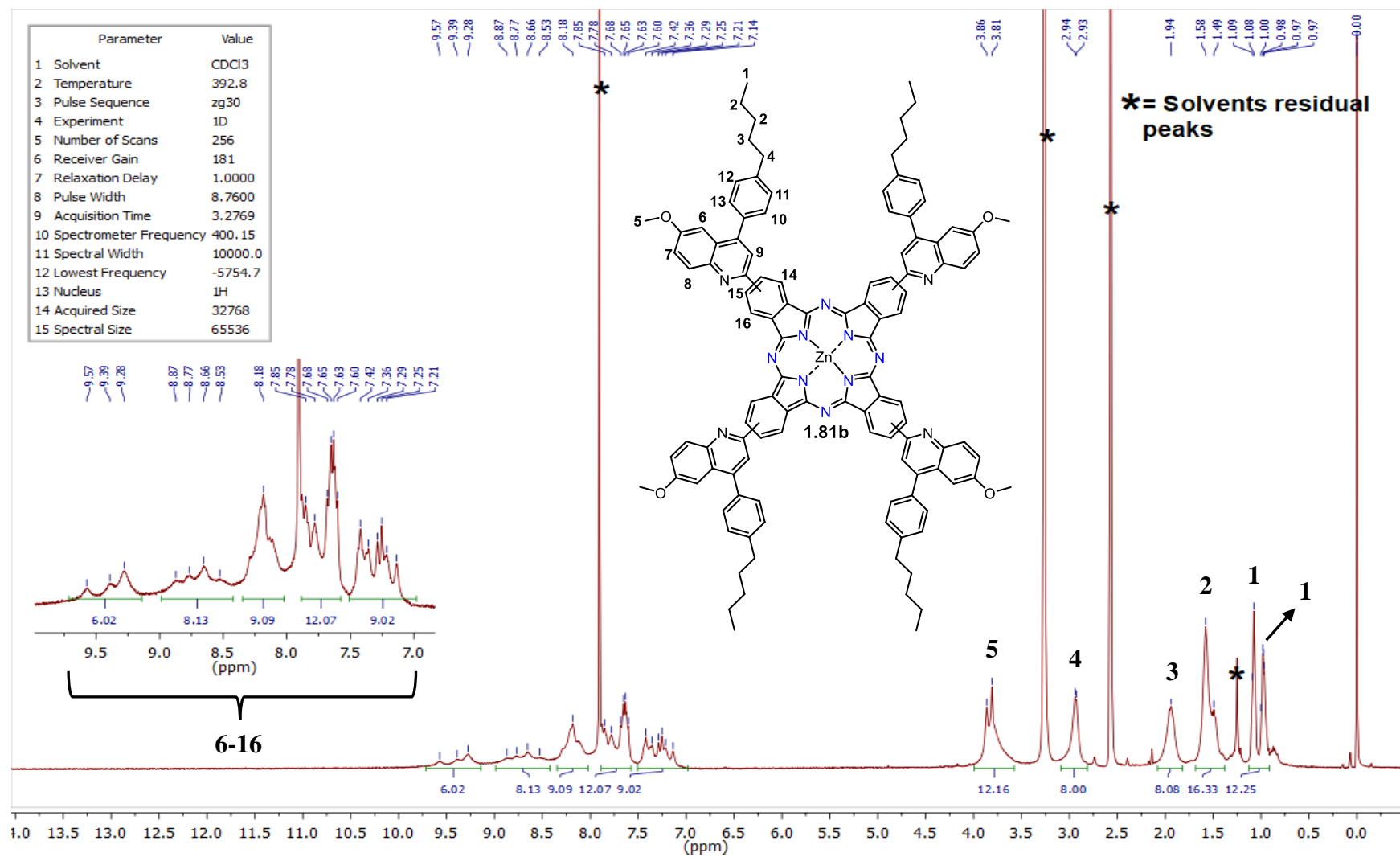


Figure 4.55 – ¹H NMR spectrum of compound **1.81b** in CDCl₃/DMSO-*d*₆ (2:1).

4.1.22 ^1H NMR spectrum of compound **1.81c**

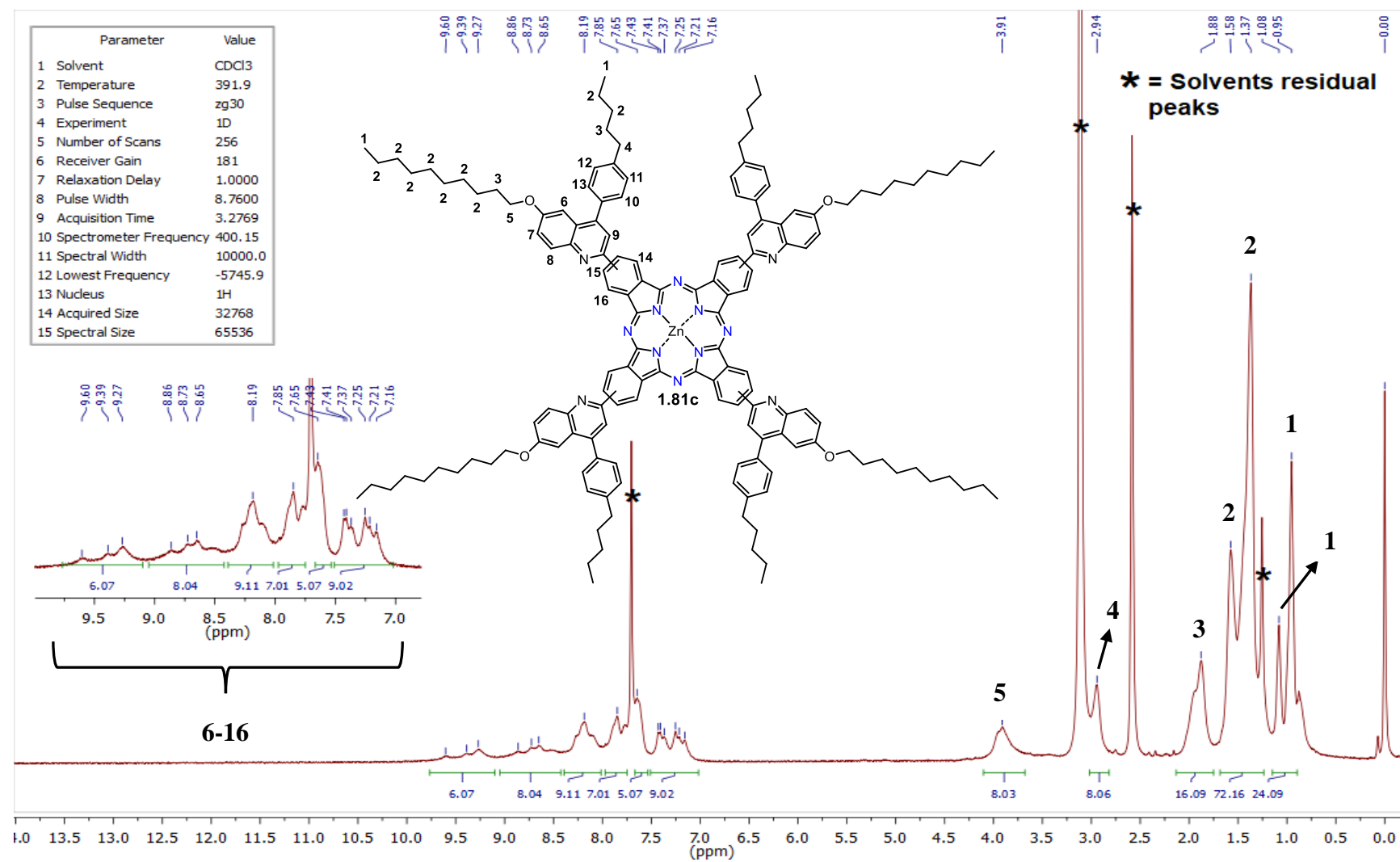


Figure 4.56 – ^1H NMR spectrum of compound **1.81c** in $\text{CDCl}_3/\text{DMSO}-d_6$ (2:1).

4.2 Spectra of Chapter 2

4.2.1 ^1H and ^{13}C NMR spectra of compound 2.22a – 2 aryl

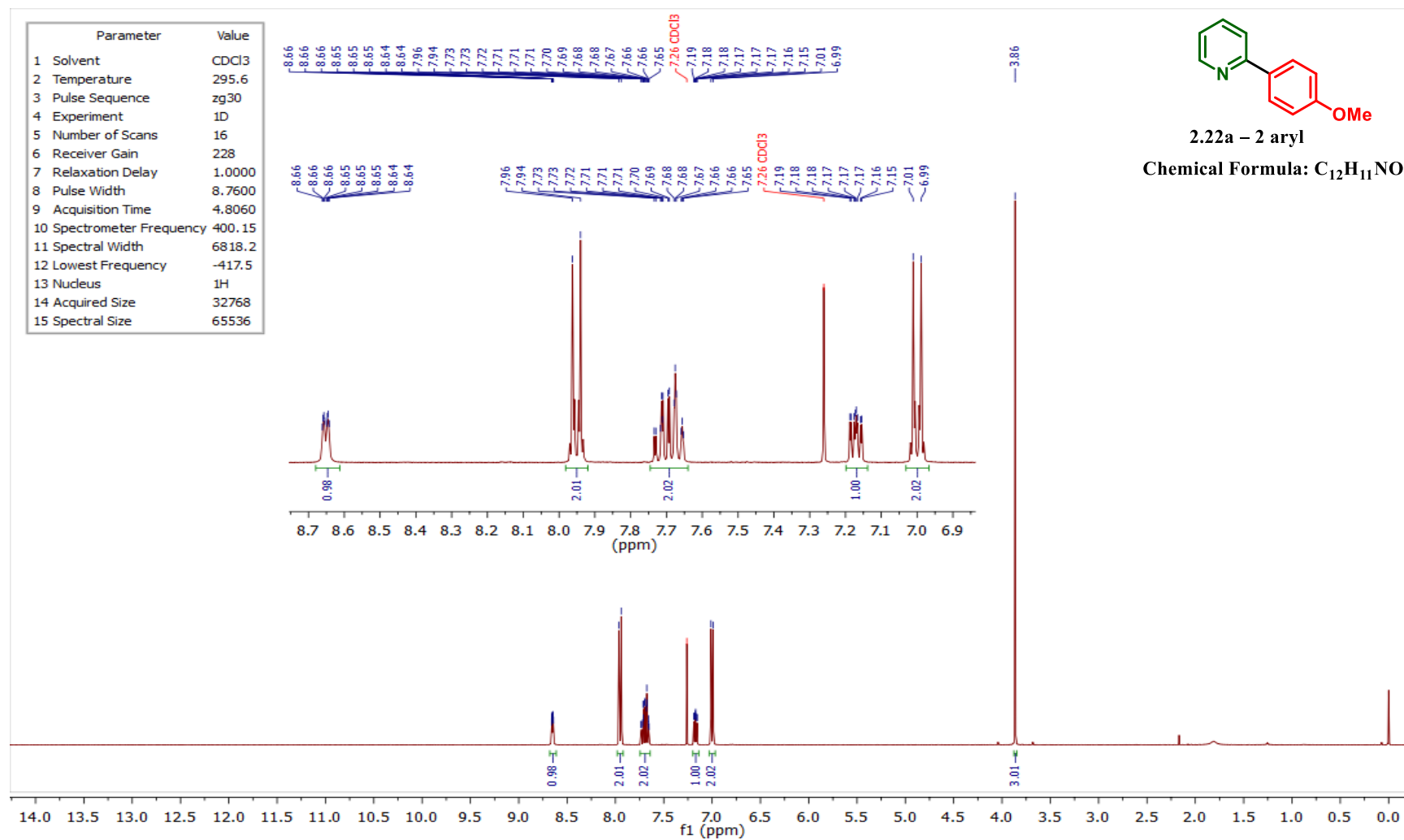


Figure 4.57 – ^1H NMR spectrum of compound 2.22a – 2 aryl in CDCl_3 .

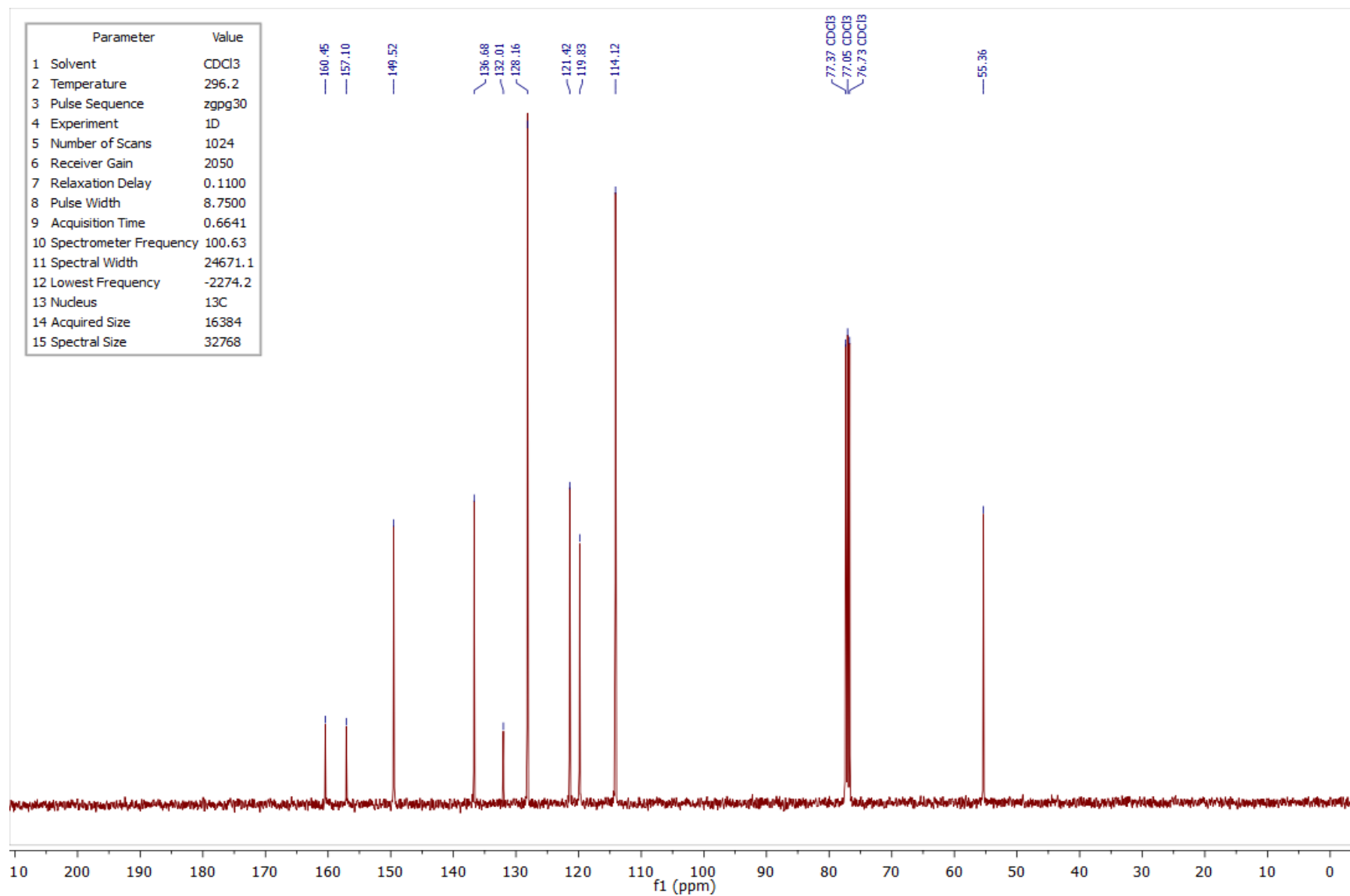


Figure 4.58 – ¹³C NMR spectrum of compound **2.22a – 2 aryl** in CDCl₃.

4.2.2 ^1H and ^{13}C NMR spectra of compound 2.22a – 4 aryl

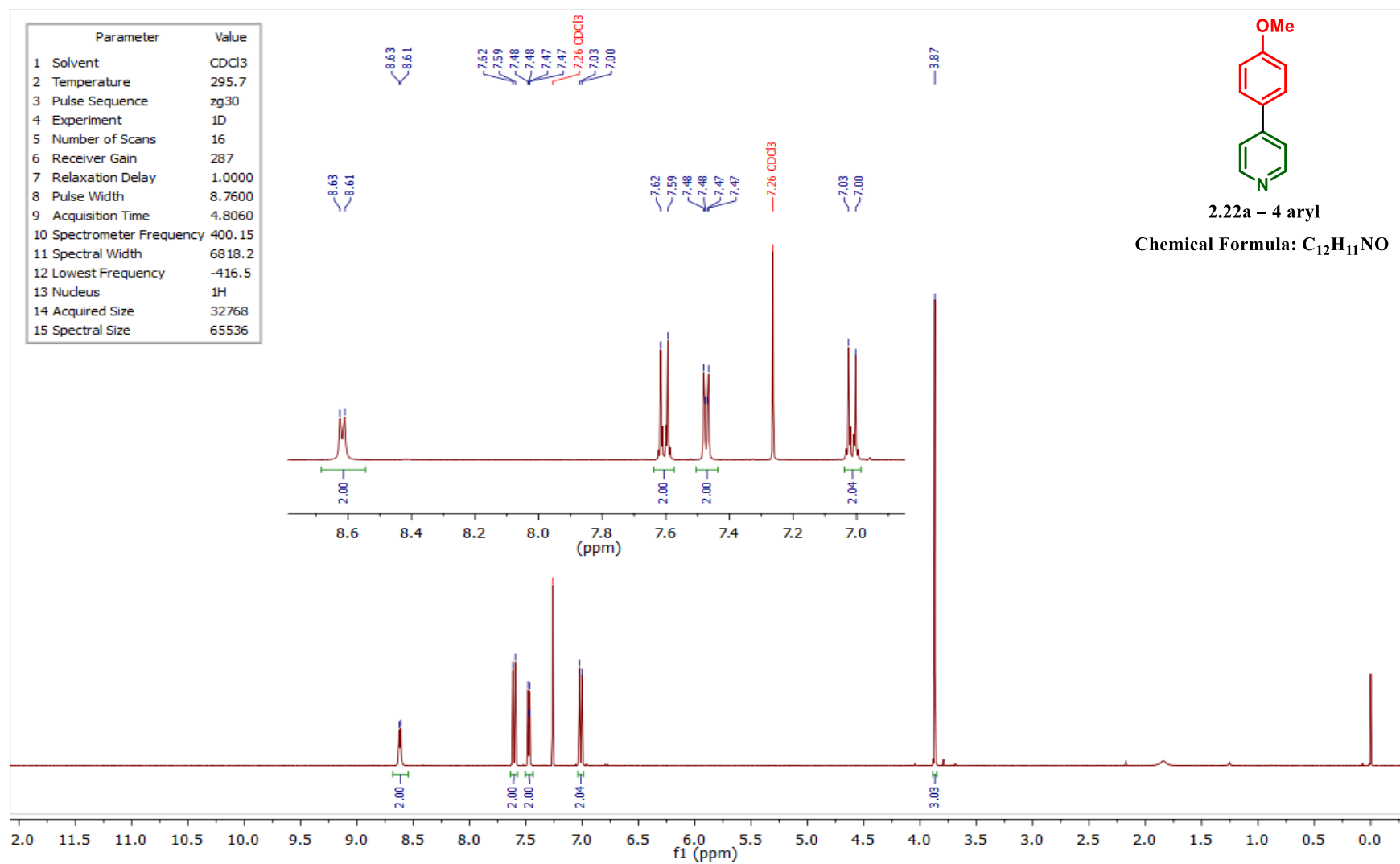


Figure 4.59 – ^1H NMR spectrum of compound 2.22a – 4 aryl in CDCl_3 .

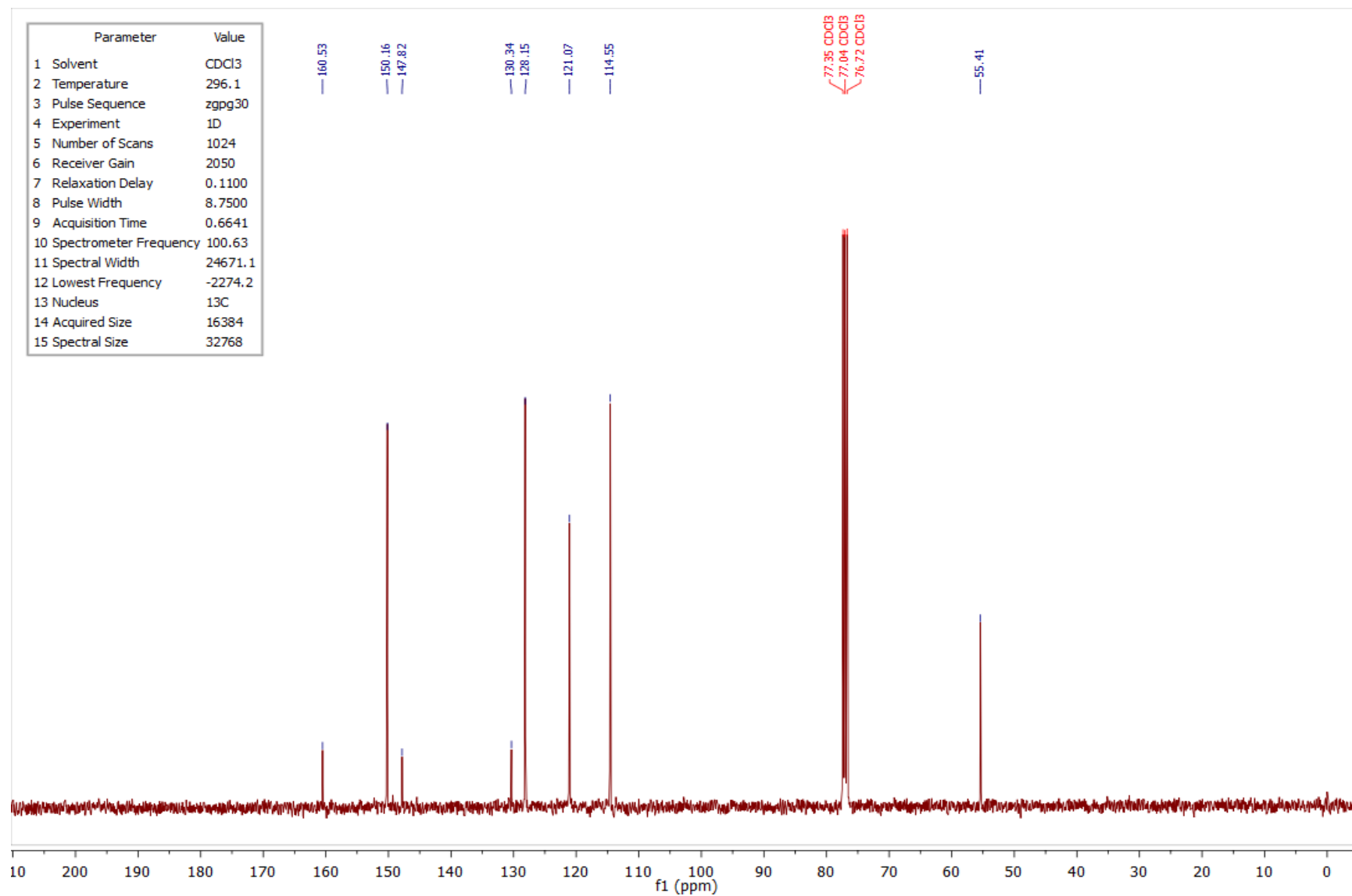


Figure 4.60 – ¹³C NMR spectrum of compound **2.22a** – 4 aryl in CDCl₃.

4.2.3 ^1H and ^{13}C NMR spectra of compound 2.22b – 2 aryl

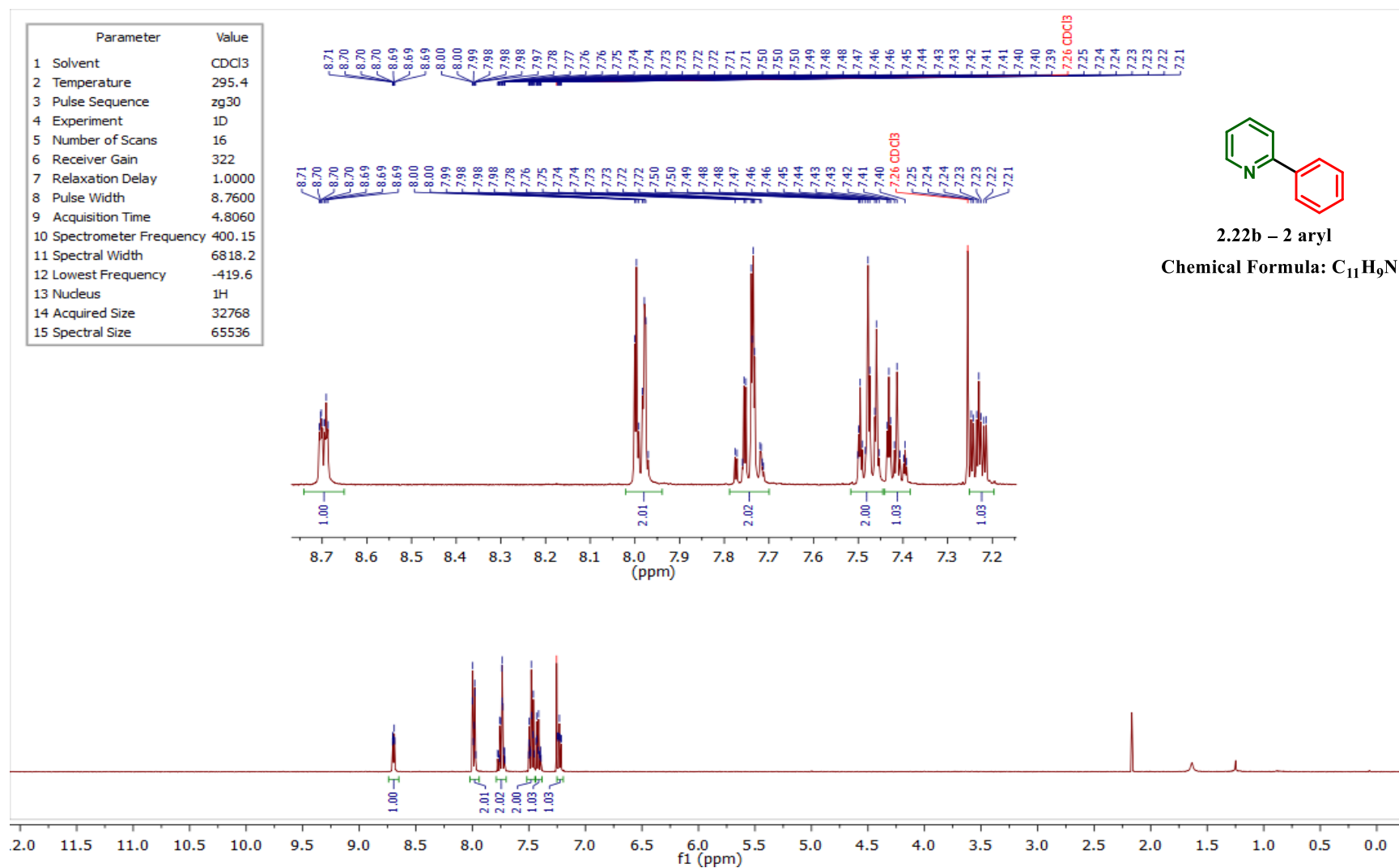


Figure 4.61 – ^1H NMR spectrum of compound 2.22b – 2 aryl in CDCl_3 .

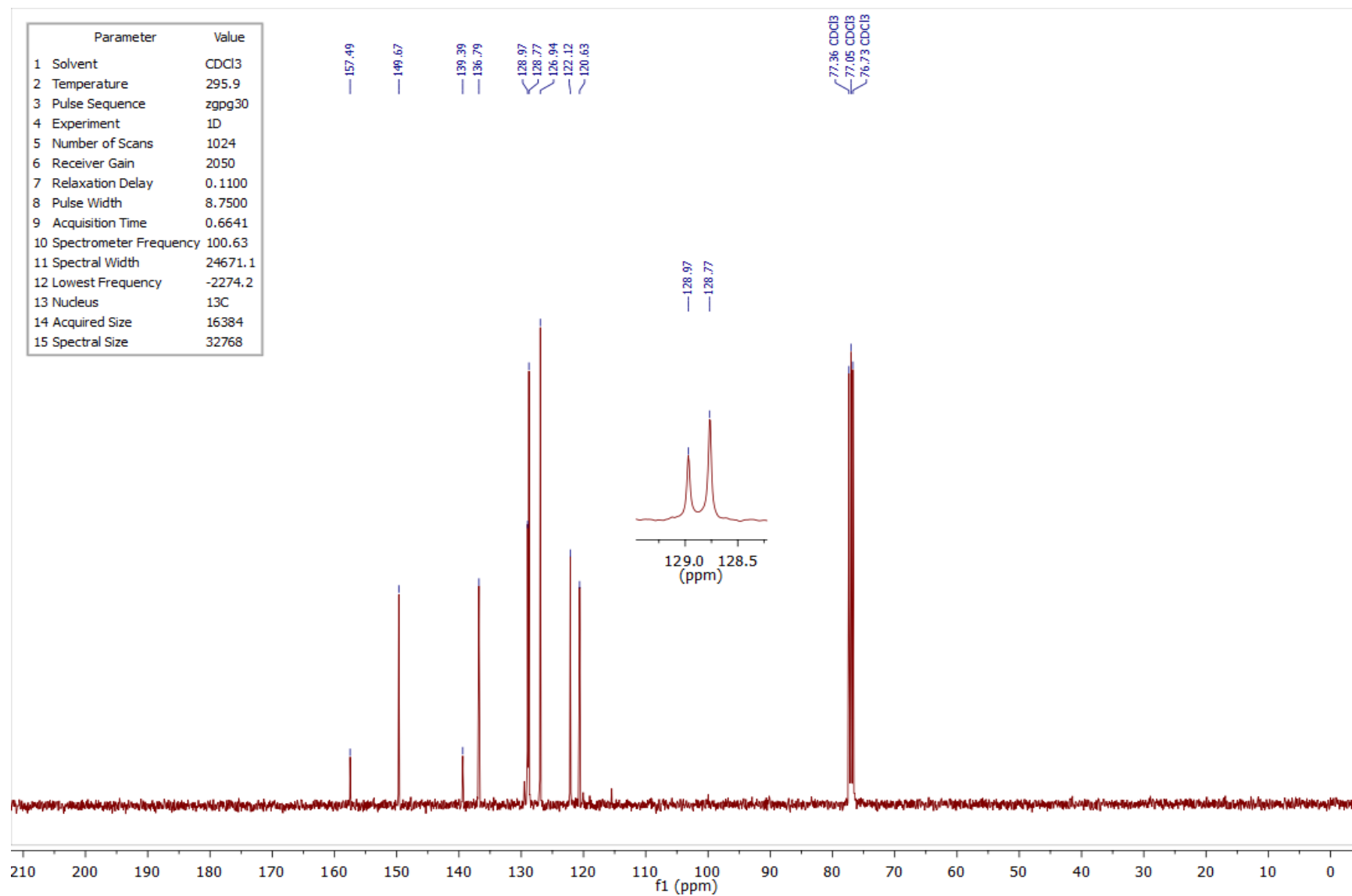


Figure 4.62 – ¹³C NMR spectrum of compound **2.22b – 2 aryl** in CDCl₃.

4.2.4 ^1H and ^{13}C NMR spectra of compound 2.22b – 4 aryl

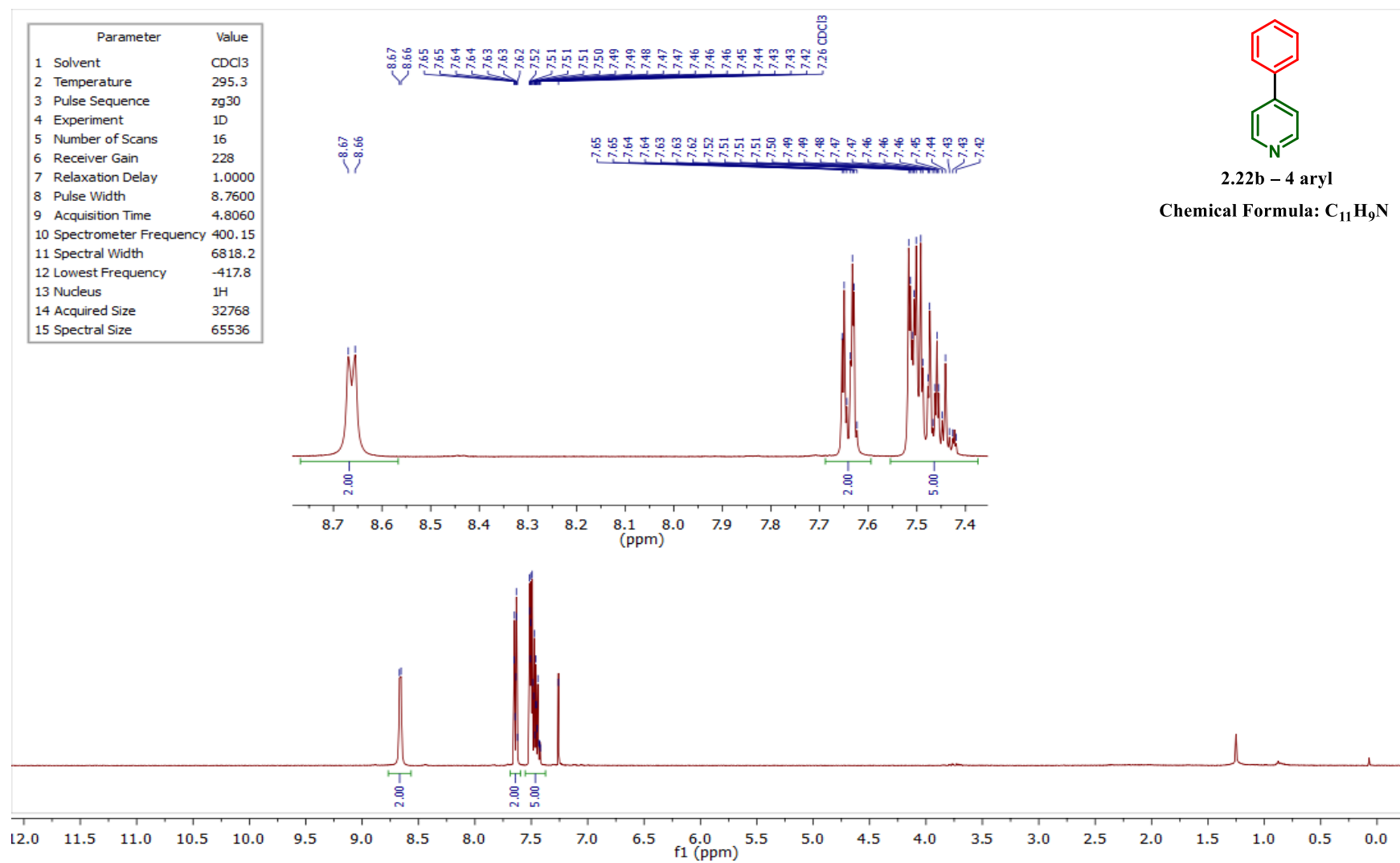


Figure 4.63 – ^1H NMR spectrum of compound 2.22b – 4 aryl in CDCl_3 .

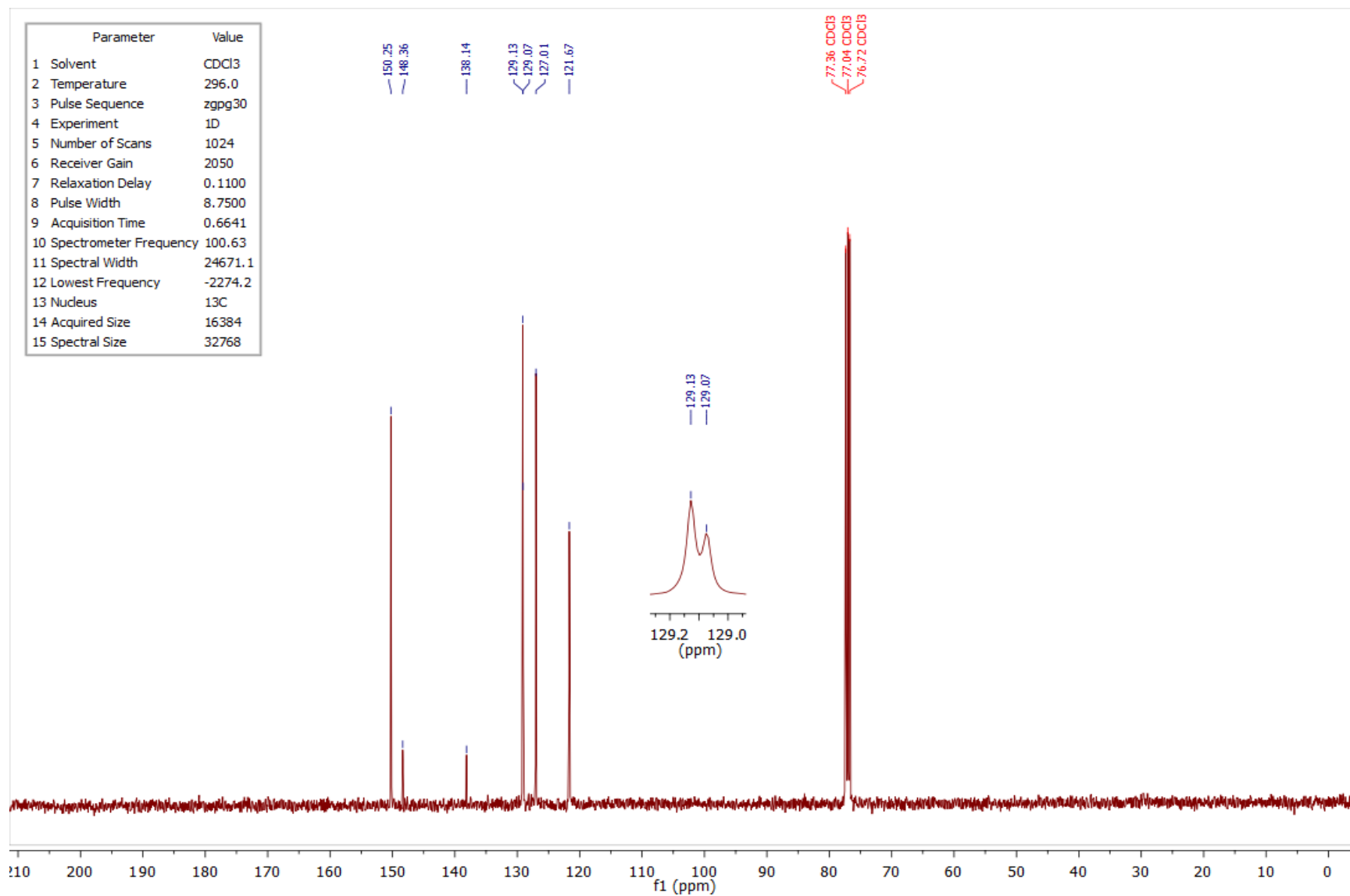


Figure 4.64 – ¹³C NMR spectrum of compound **2.22b – 4 aryl** in CDCl₃.

4.2.5 ¹H and ¹³C NMR spectra of compound 2.22c – 2 aryl

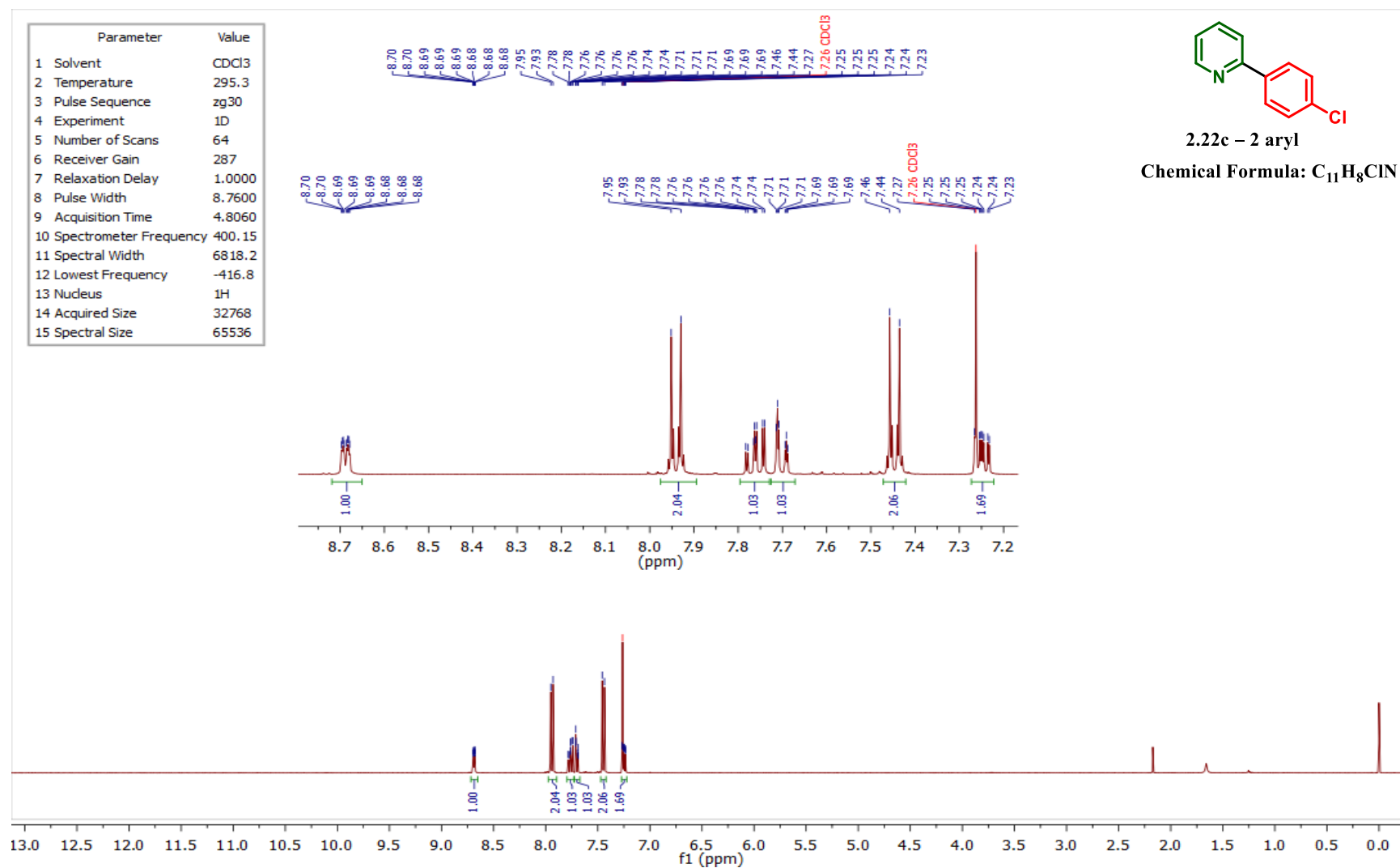


Figure 4.65 – ¹H NMR spectrum of compound 2.22c – 2 aryl in CDCl₃.

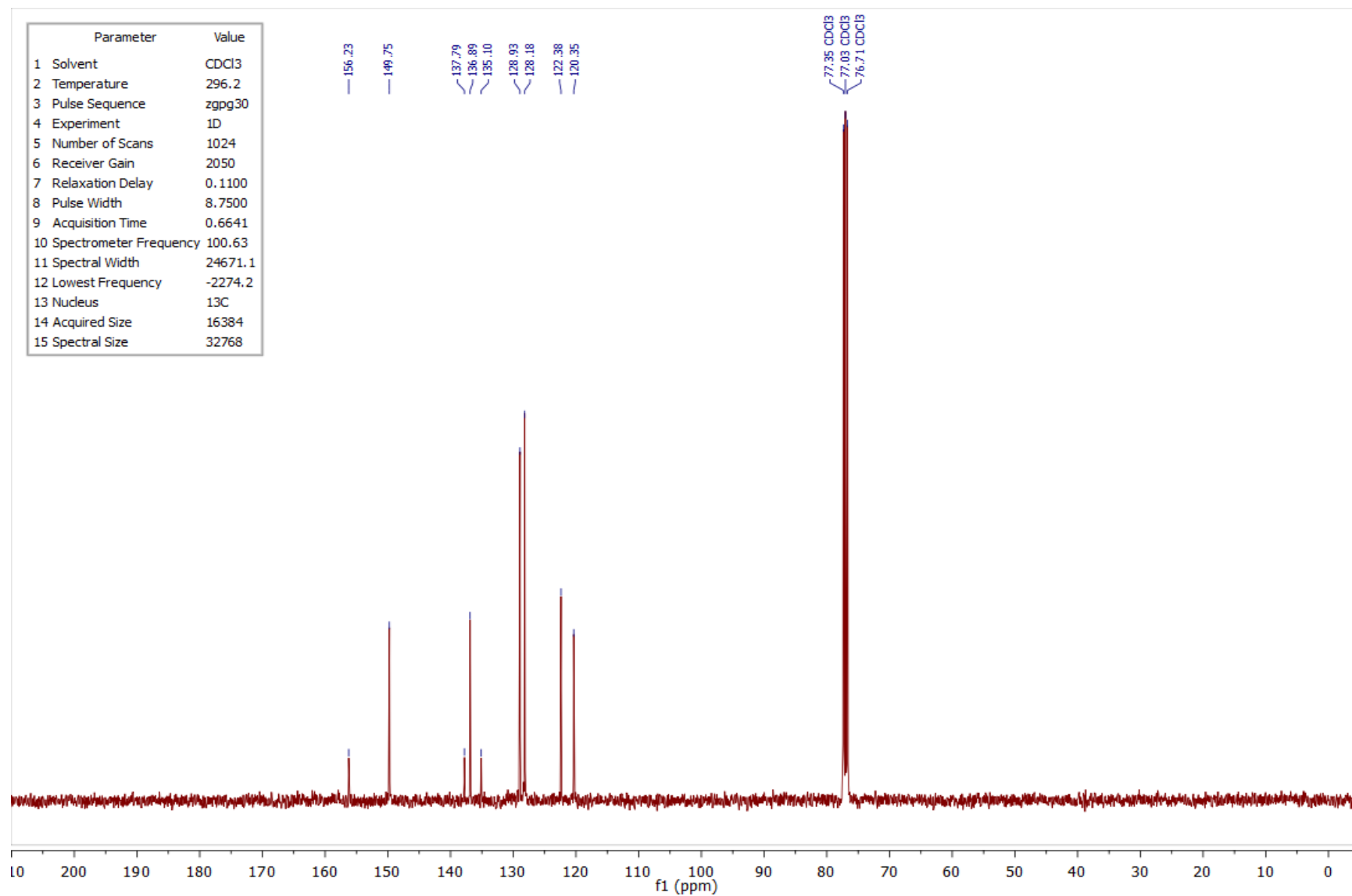


Figure 4.66 – ¹³C NMR spectrum of compound 2.22c – 2 aryl in CDCl₃.

4.2.6 ^1H and ^{13}C NMR spectra of compound 2.22c – 4 aryl

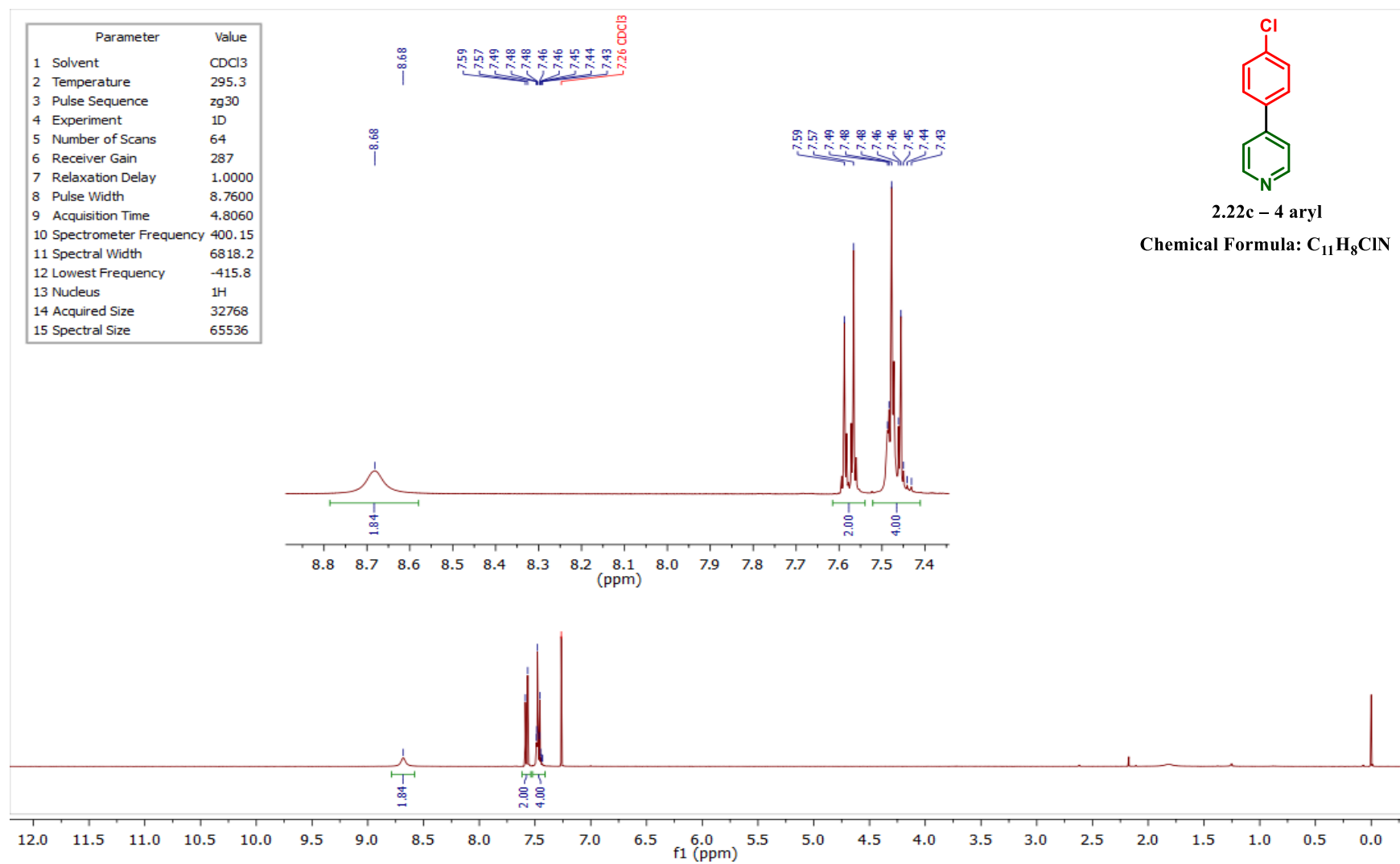


Figure 4.67 – ^1H NMR spectrum of compound 2.22c – 4 aryl in CDCl_3 .

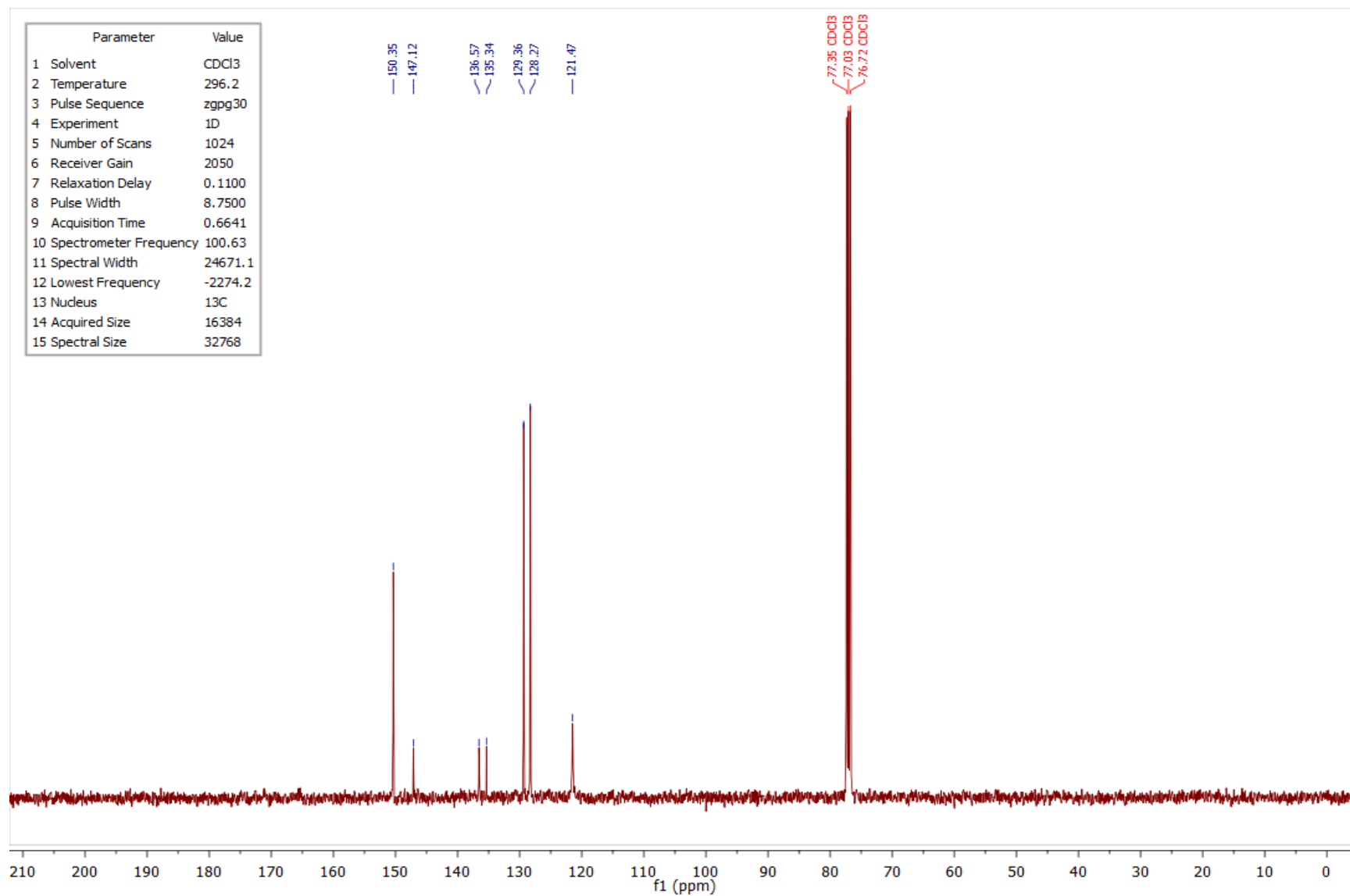


Figure 4.68 – ¹³C NMR spectrum of compound **2.22c – 4 aryl** in CDCl₃.

4.2.7 ^1H and ^{13}C NMR spectra of compound 2.22d – 2 aryl

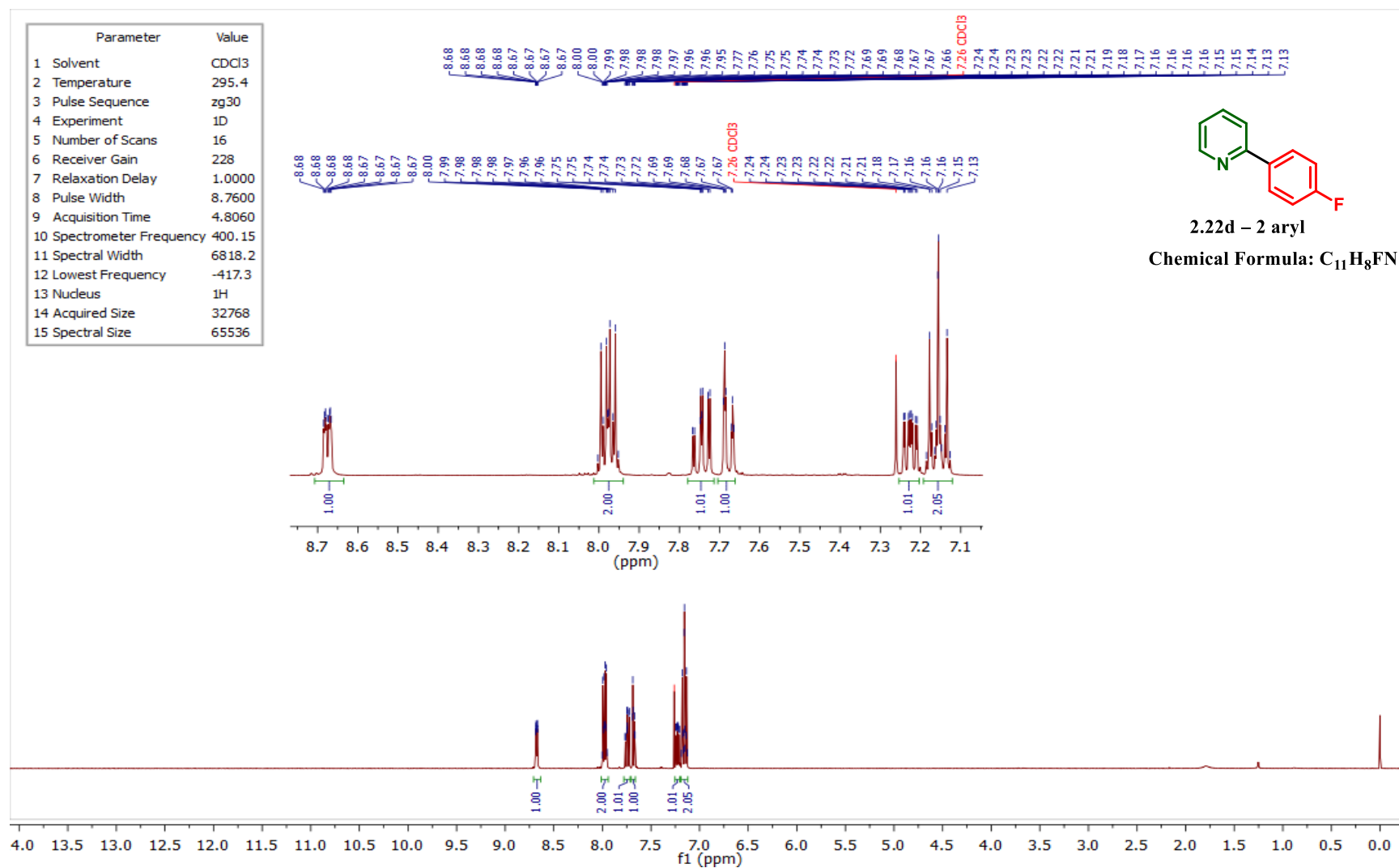


Figure 4.69 – ^1H NMR spectrum of compound 2.22d – 2 aryl in CDCl_3 .

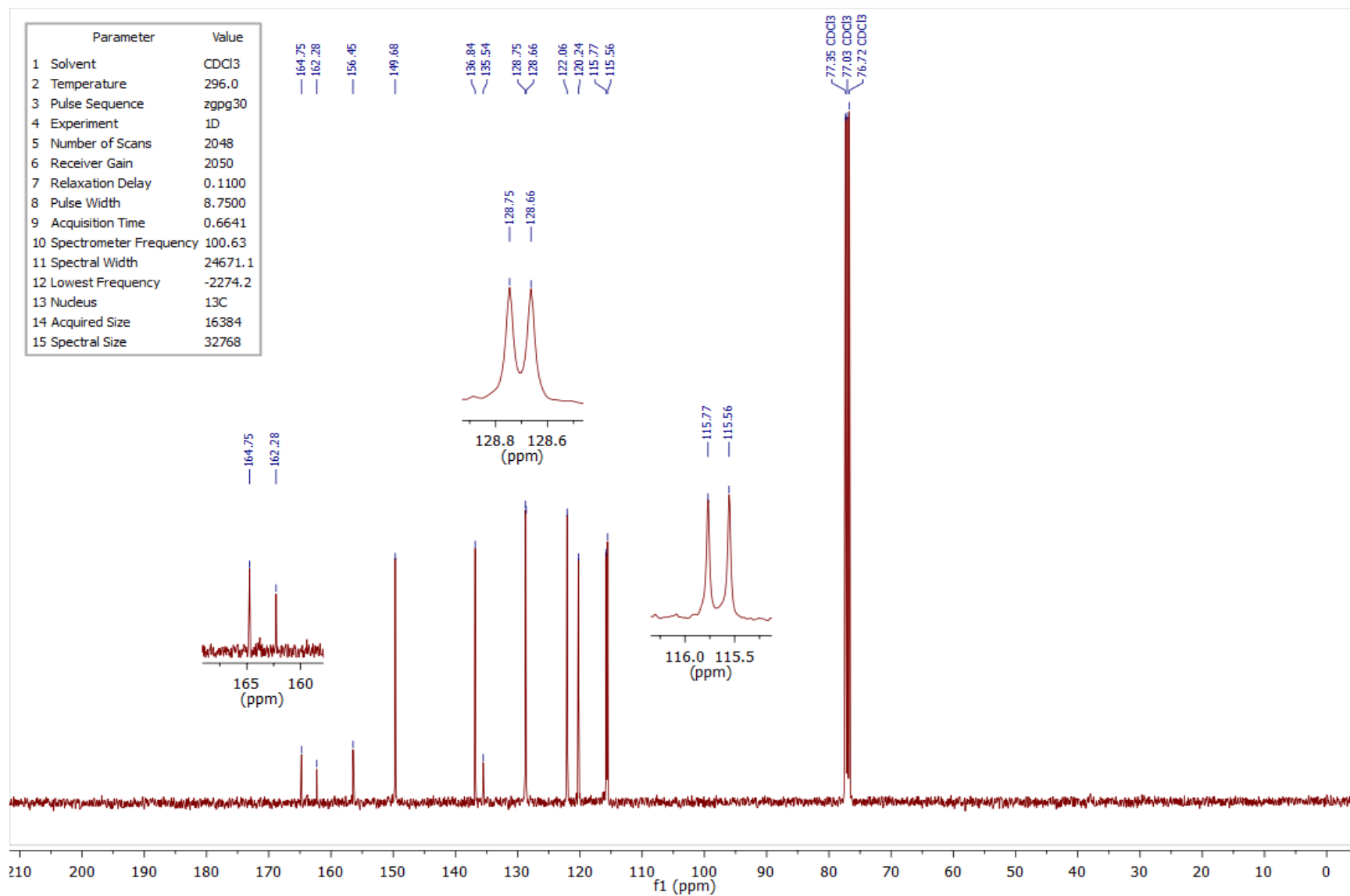


Figure 4.70 – ¹³C NMR spectrum of compound **2.22d – 2 aryl** in CDCl₃.

4.2.8 ^1H and ^{13}C NMR spectra of compound 2.22d – 4 aryl

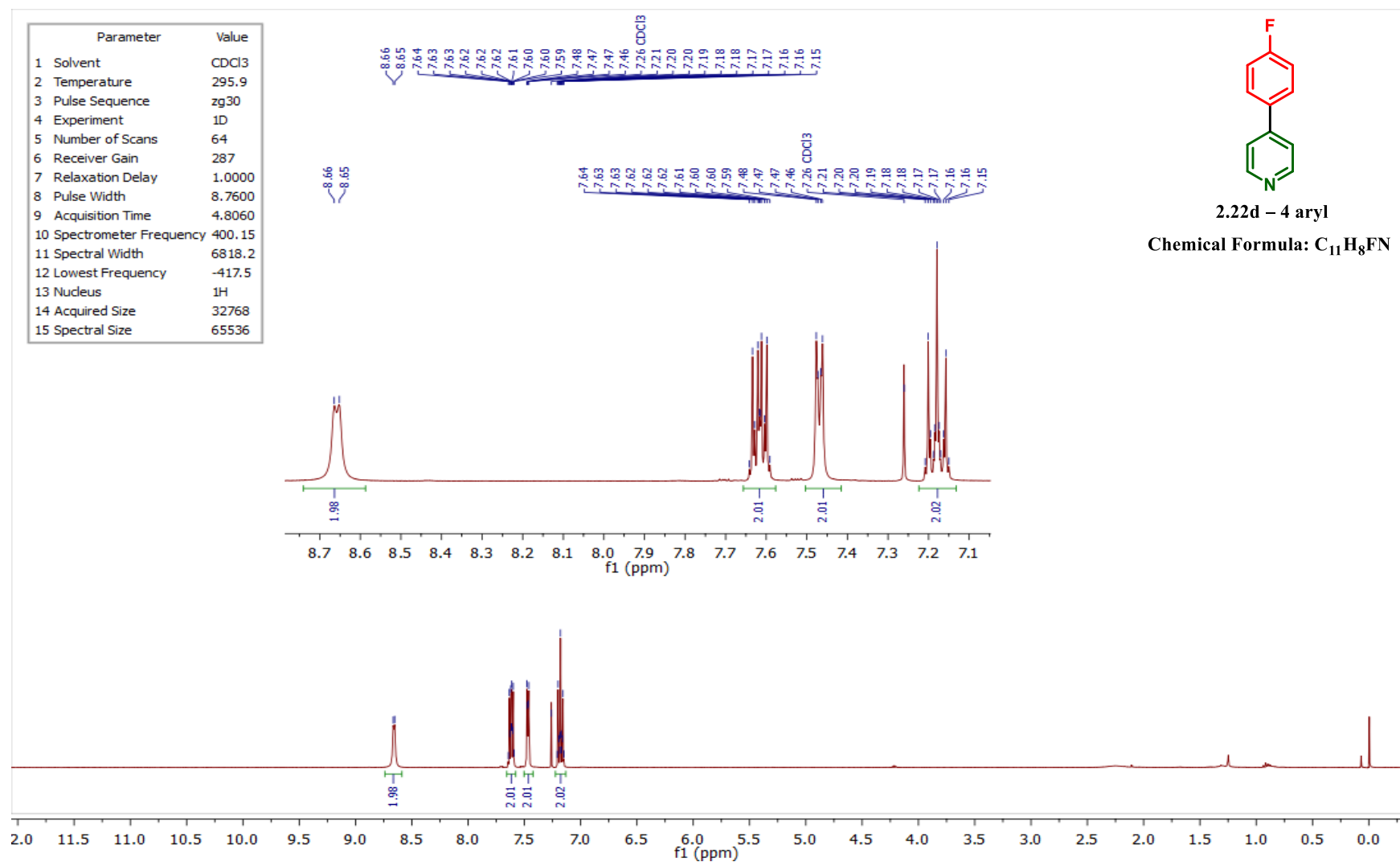


Figure 4.71 – ^1H NMR spectrum of compound 2.22d – 4 aryl in CDCl_3 .

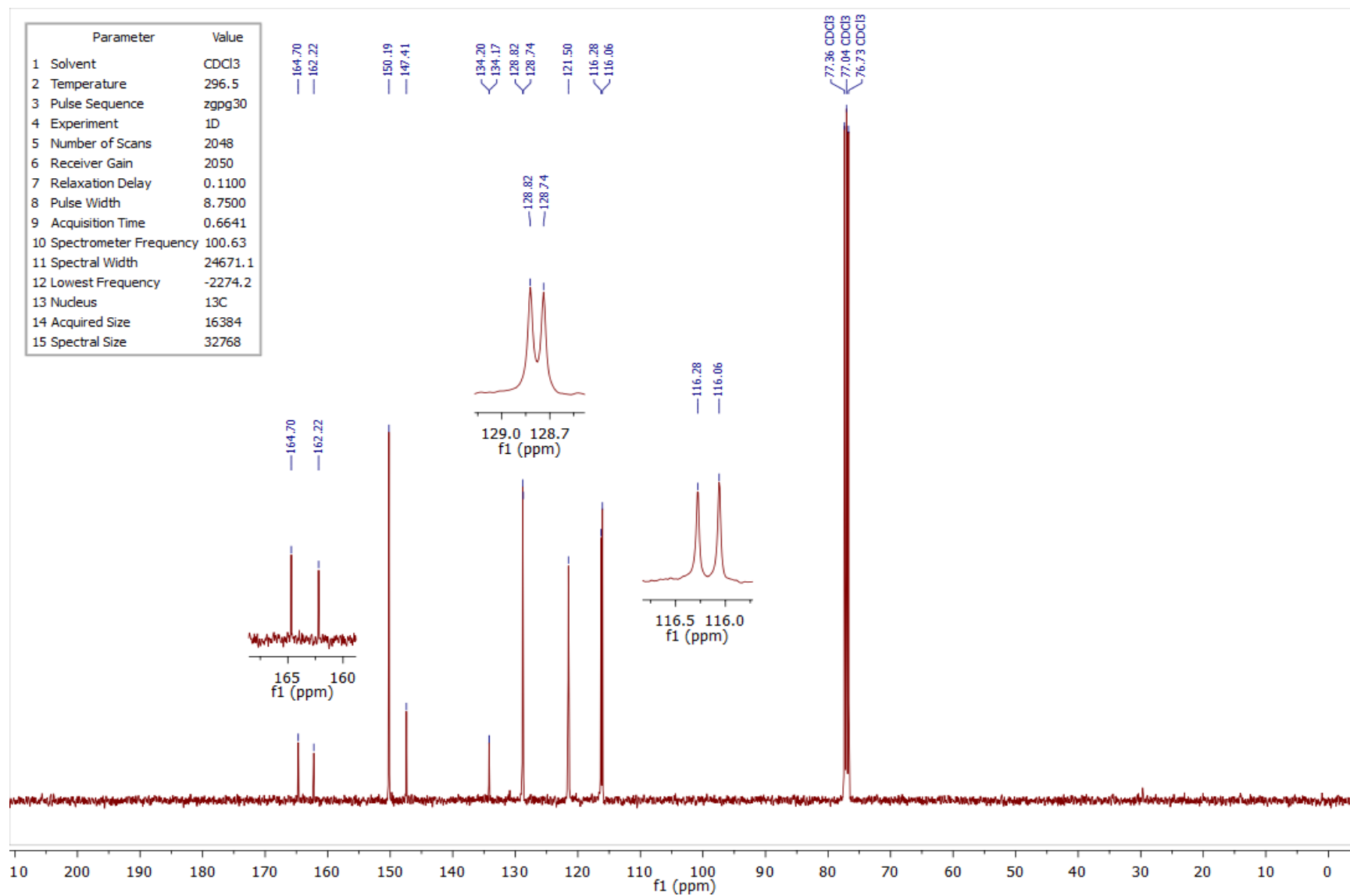


Figure 4.72 – ^{13}C NMR spectrum of compound **2.22d** – **4 aryl** in CDCl_3 .

4.2.9 ^1H and ^{13}C NMR spectra of compound 2.22e – 2 aryl

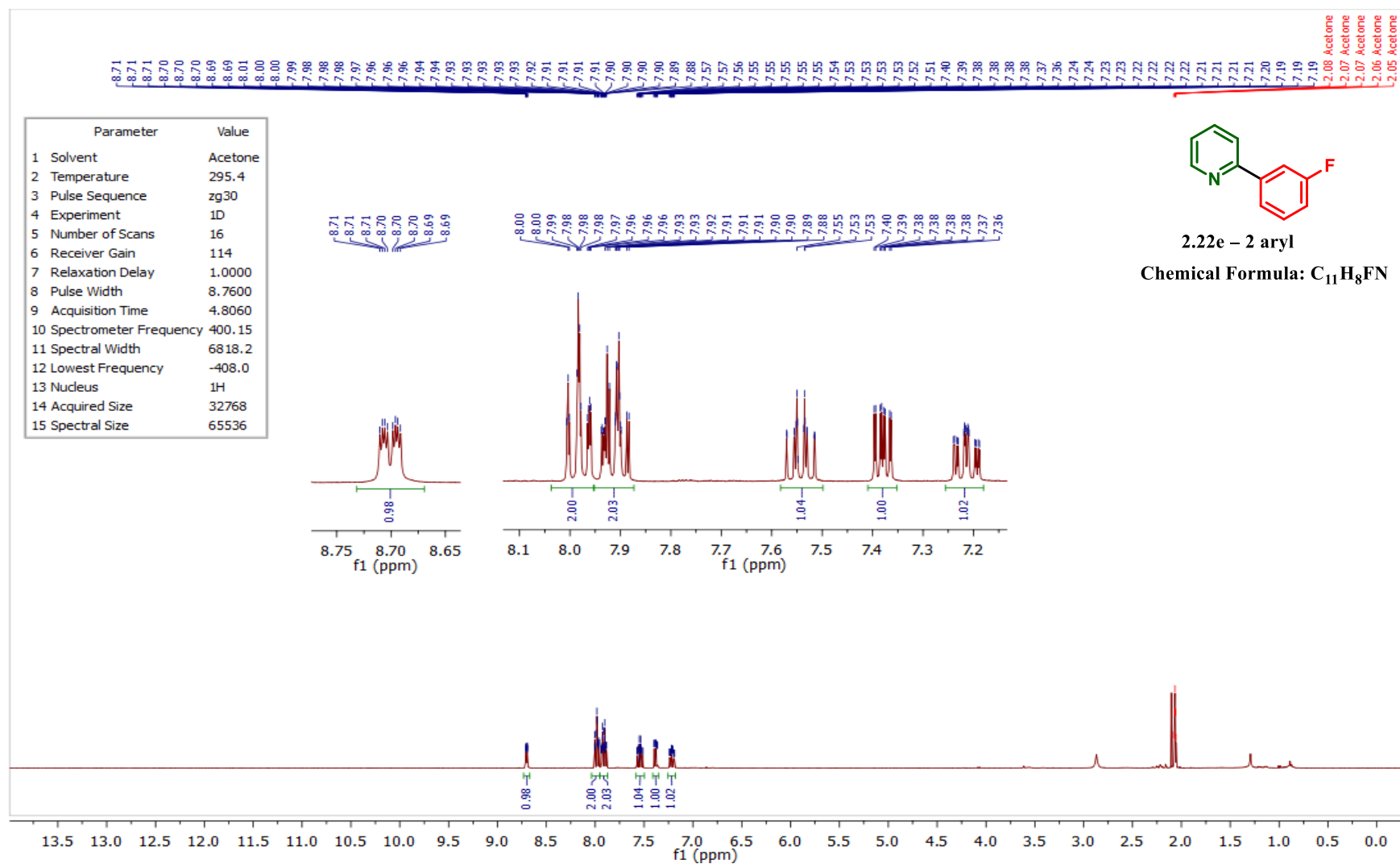


Figure 4.73 – ^1H NMR spectrum of compound 2.22e – 2 aryl in $(\text{CD}_3)_2\text{CO}$.

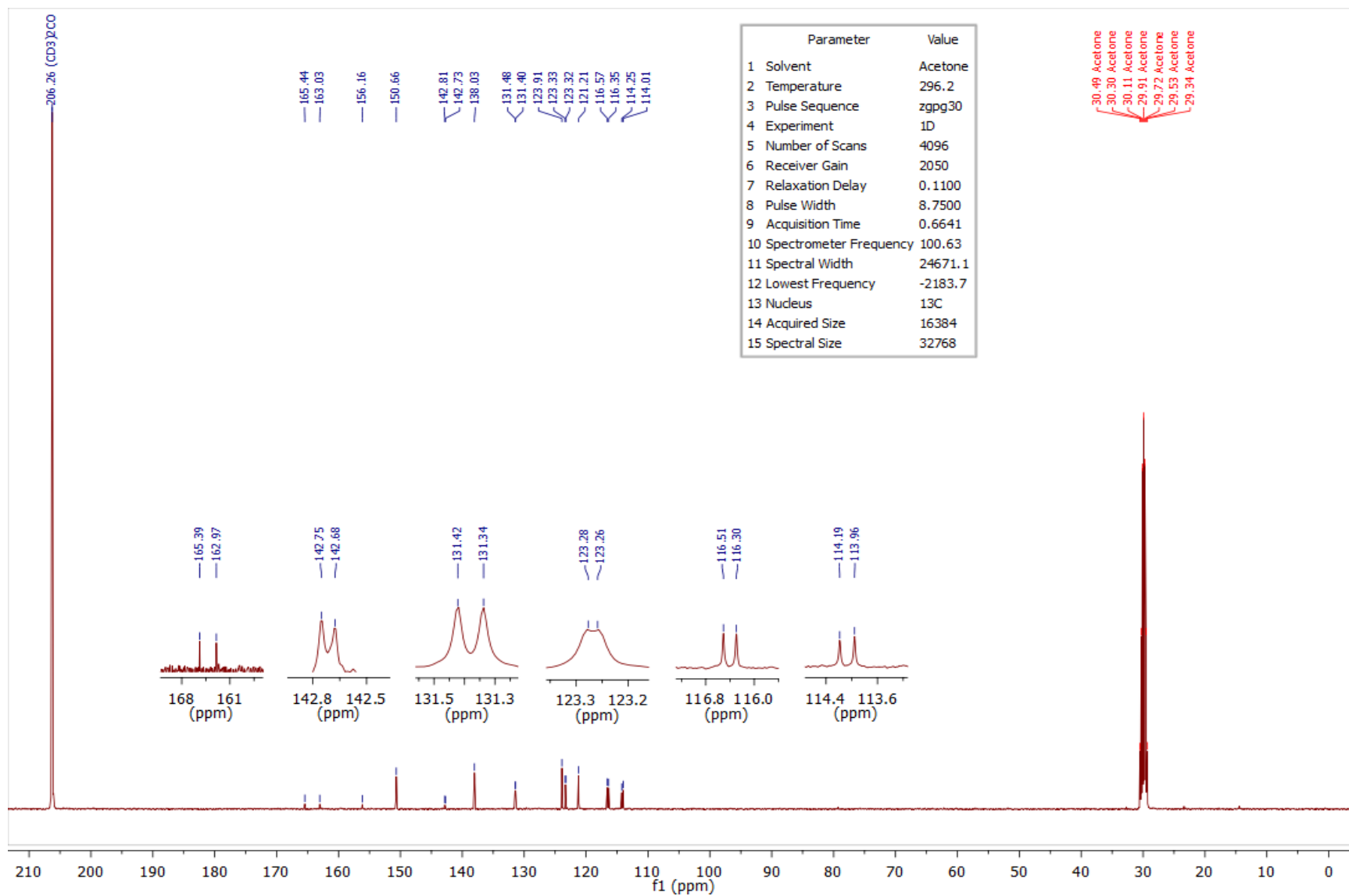


Figure 4.74 – ¹³C NMR spectrum of compound **2.22e – 2 aryl** in (CD₃)₂CO.

4.2.10 ^1H and ^{13}C NMR spectra of compound 2.22e – 4 aryl

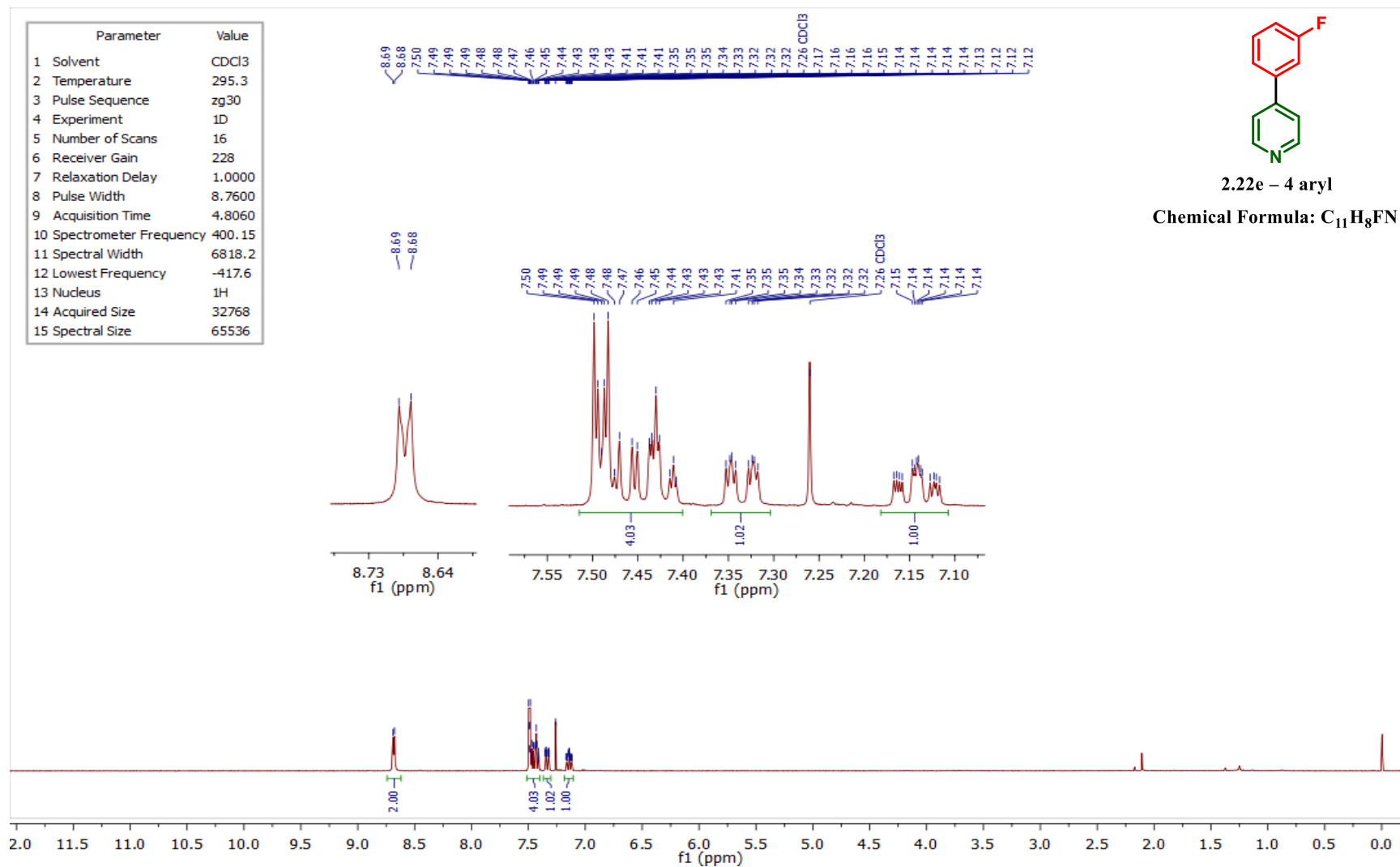


Figure 4.75 – ^1H NMR spectrum of compound 2.22e – 4 aryl in CDCl_3 .

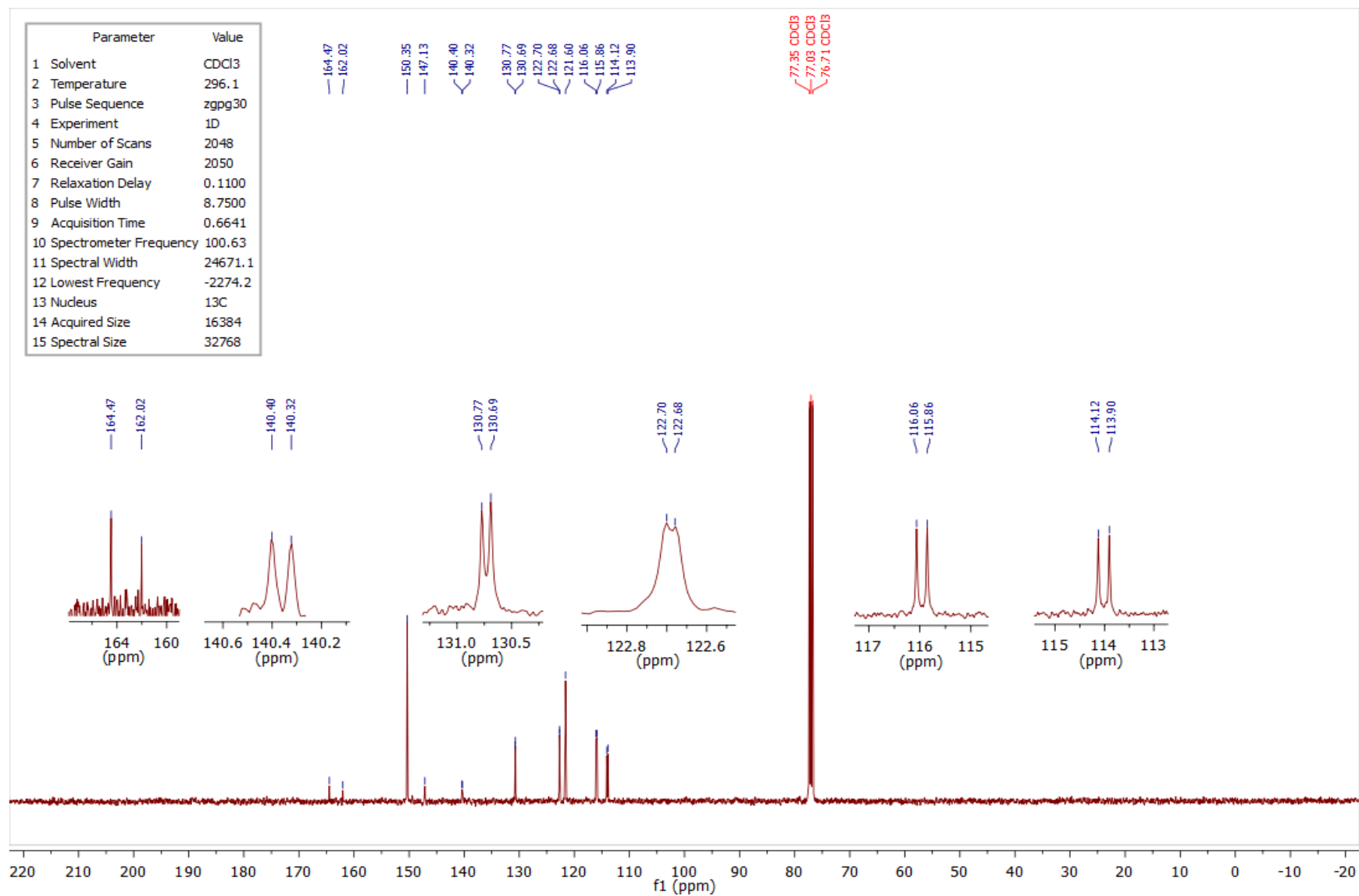


Figure 4.76 – ¹³C NMR spectrum of compound 2.22e – 4 aryl in CDCl₃.

4.2.11 ¹H and ¹³C NMR spectra of compound 2.22f – 2 aryl

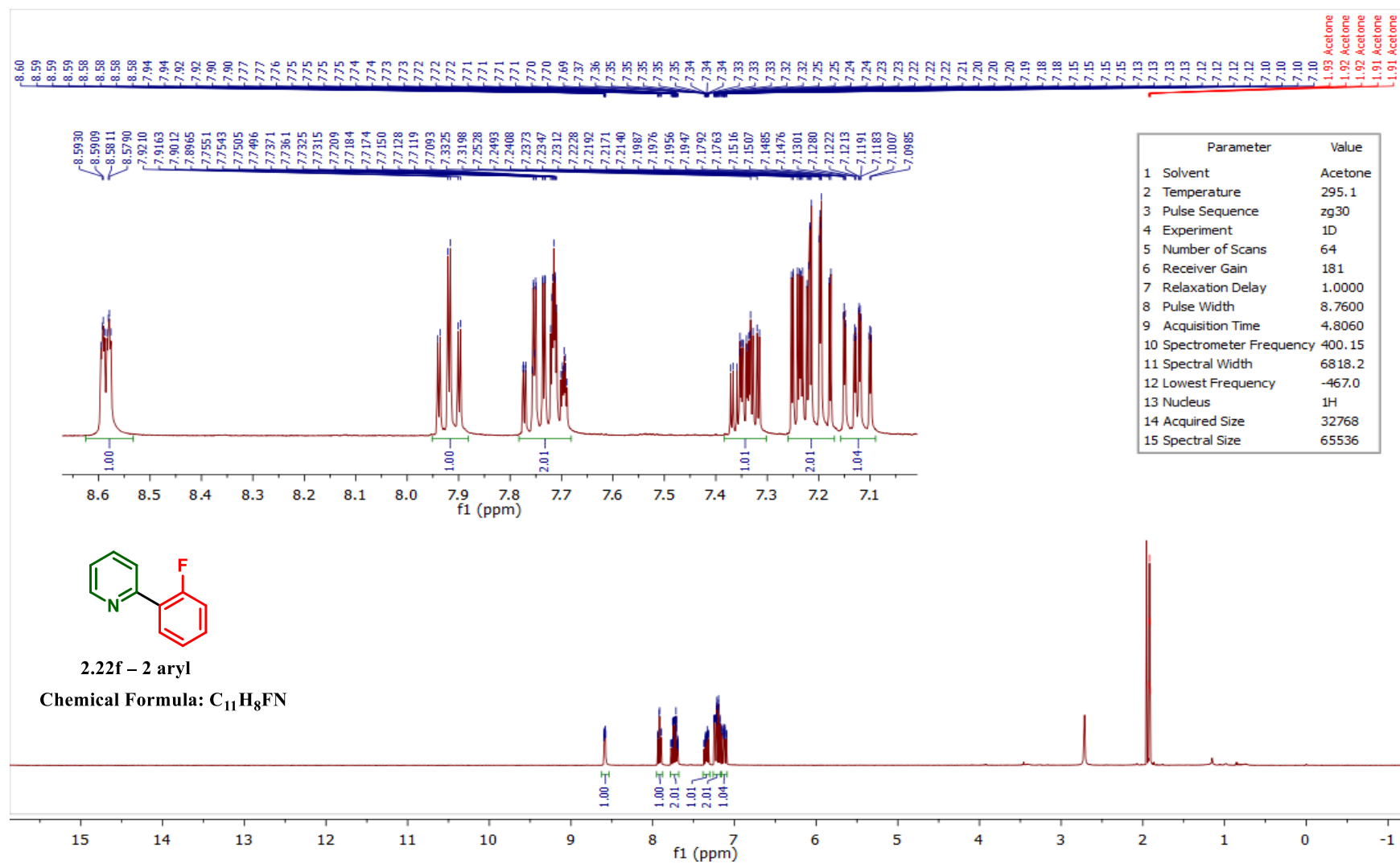


Figure 4.77 – ¹H NMR spectrum of compound 2.22f – 2 aryl in (CD₃)₂CO.

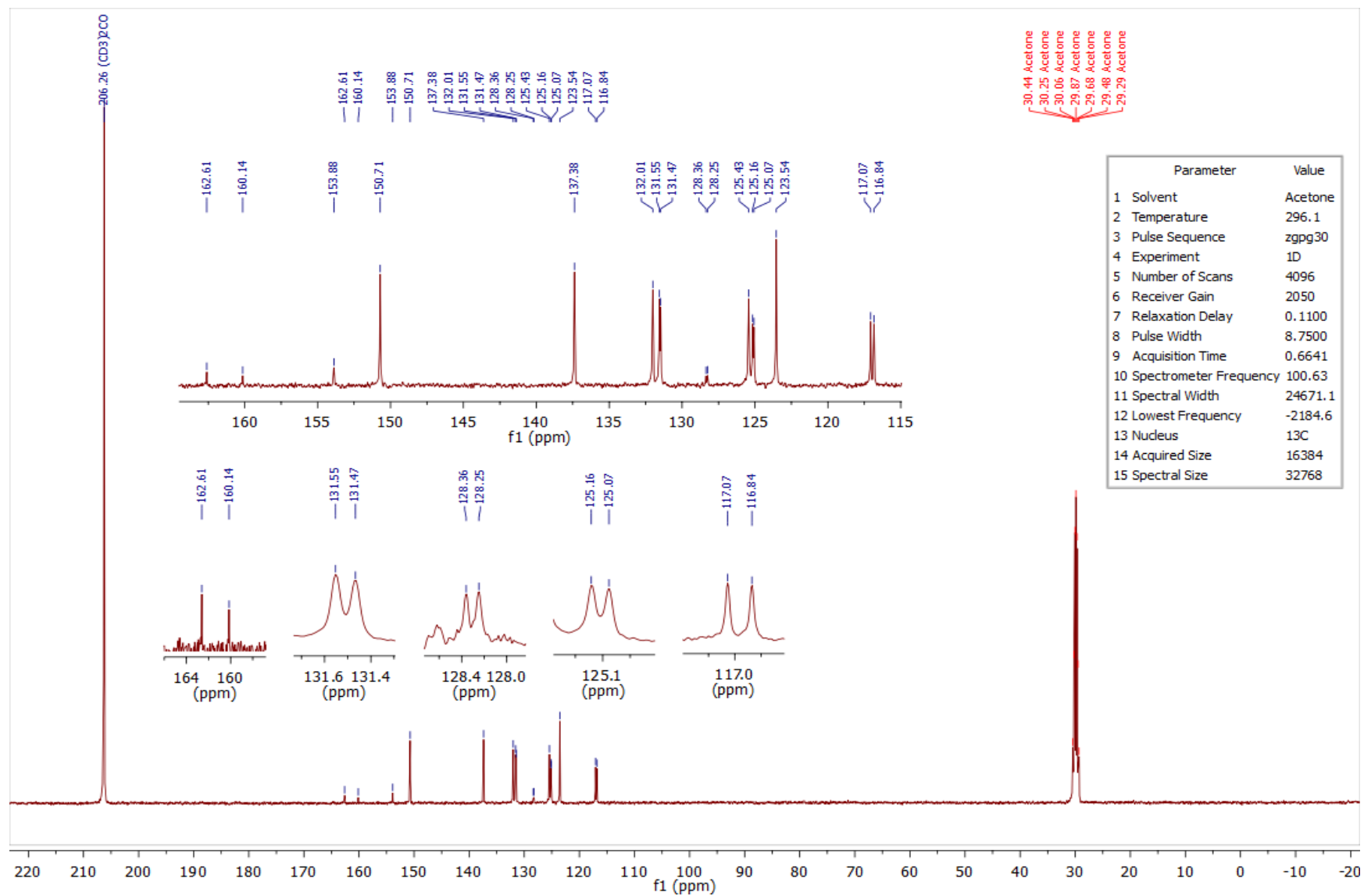


Figure 4.78 – ^{13}C NMR spectrum of compound **2.22f** – **2 aryl** in $(\text{CD}_3)_2\text{CO}$.

4.2.12 ¹H and ¹³C NMR spectra of compound 2.22f – 4 aryl

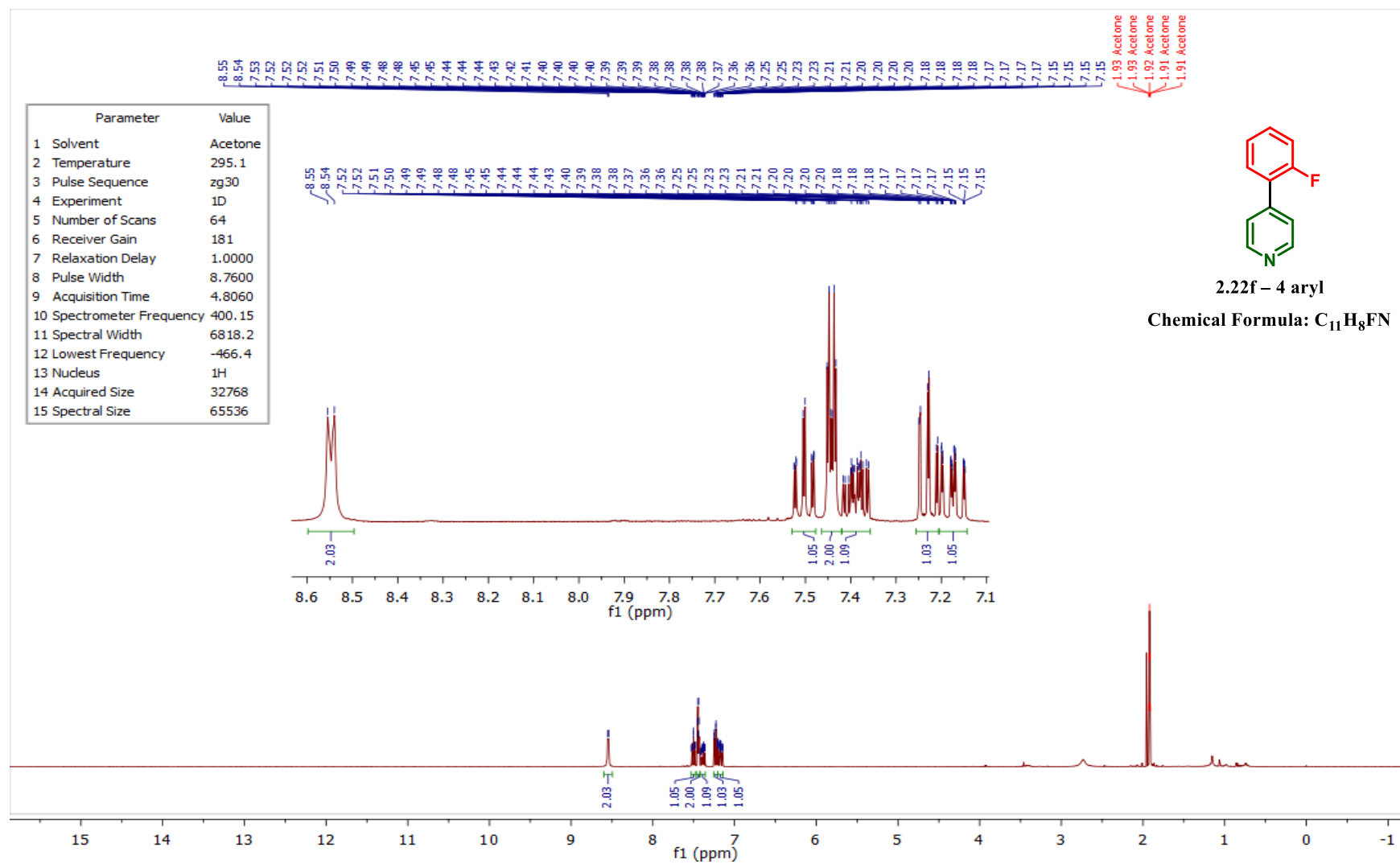


Figure 4.79 – ¹H NMR spectrum of compound 2.22f – 4 aryl in (CD₃)₂CO.

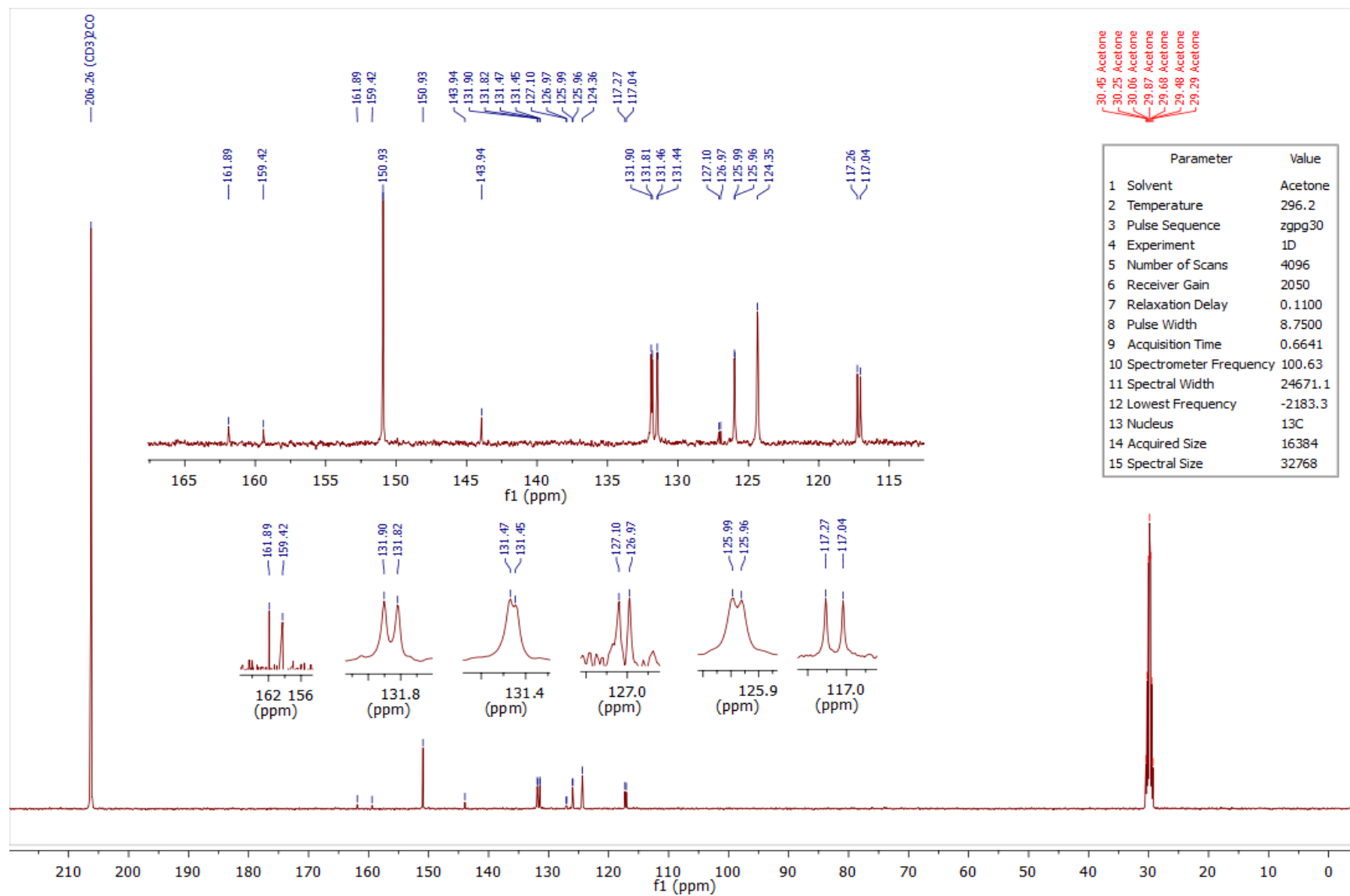


Figure 4.80 – ^{13}C NMR spectrum of compound **2.22f** – **4 aryl** in $(\text{CD}_3)_2\text{CO}$.

4.2.13 ^1H and ^{13}C NMR spectra of compound 2.22g – 2 aryl

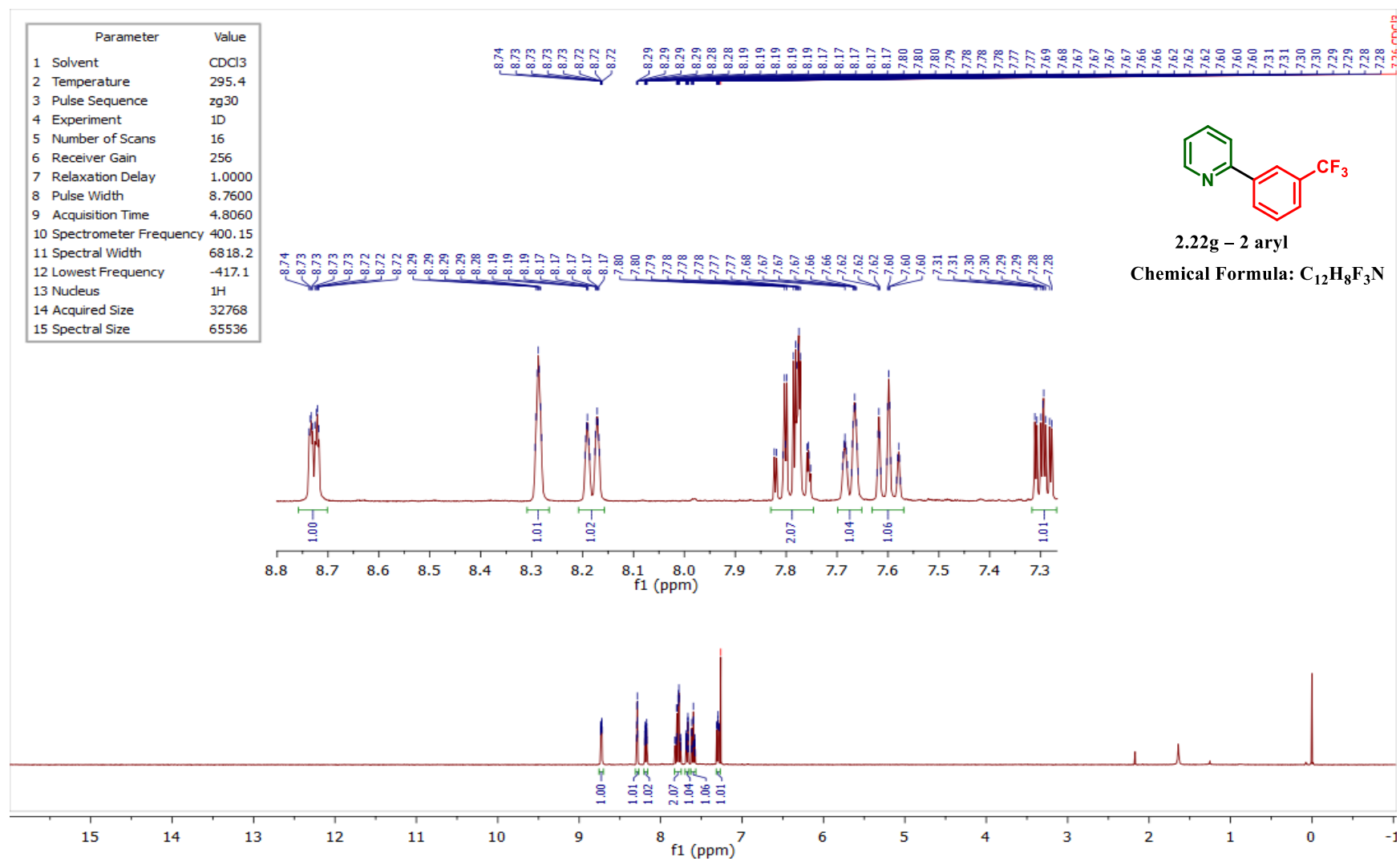


Figure 4.81 – ^1H NMR spectrum of compound 2.22g – 2 aryl in CDCl_3 .

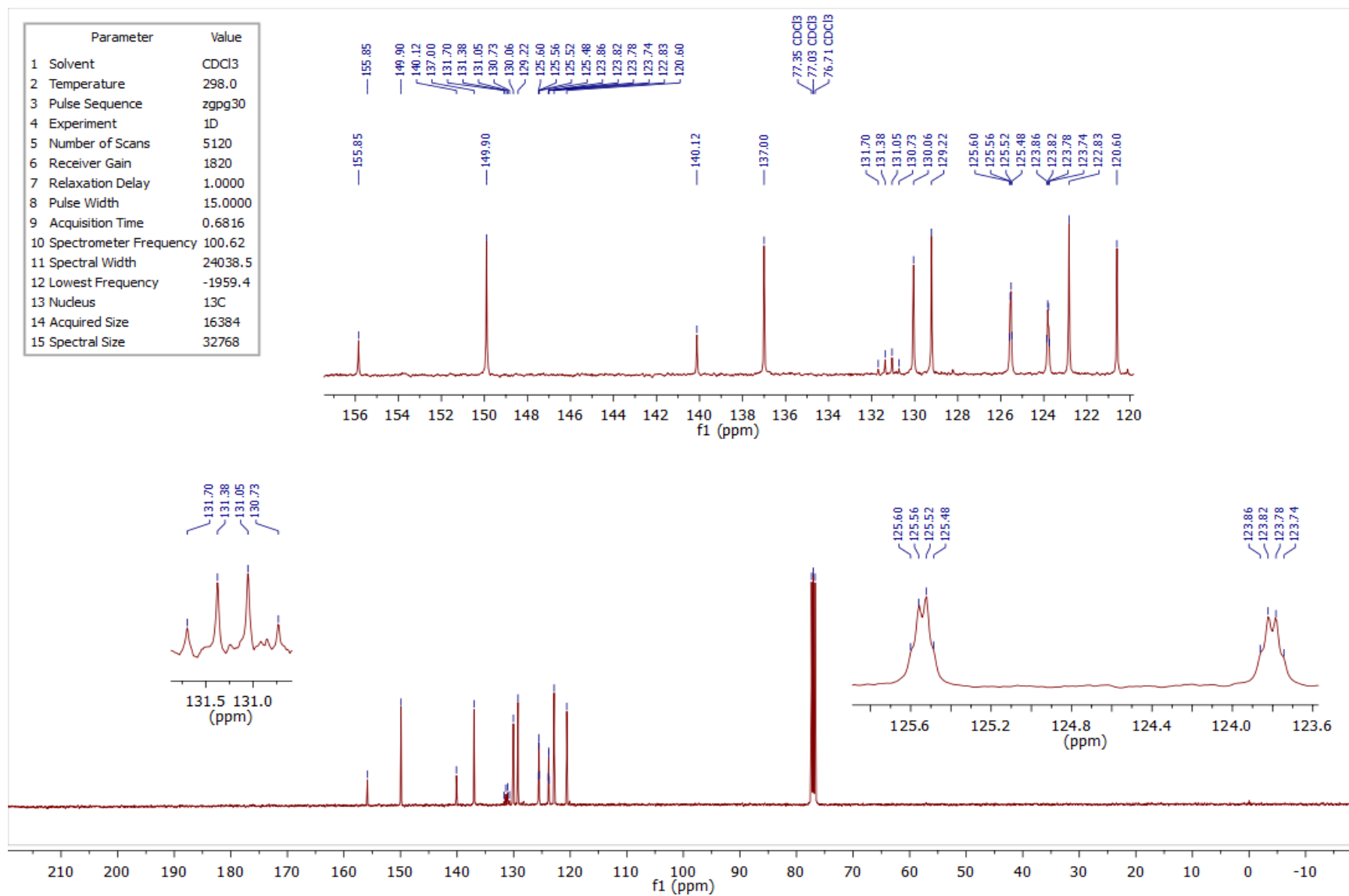


Figure 4.82 – ¹³C NMR spectrum of compound 2.22g – 2 aryl in CDCl₃.

4.2.14 ^1H and ^{13}C NMR spectra of compound 2.22g – 4 aryl

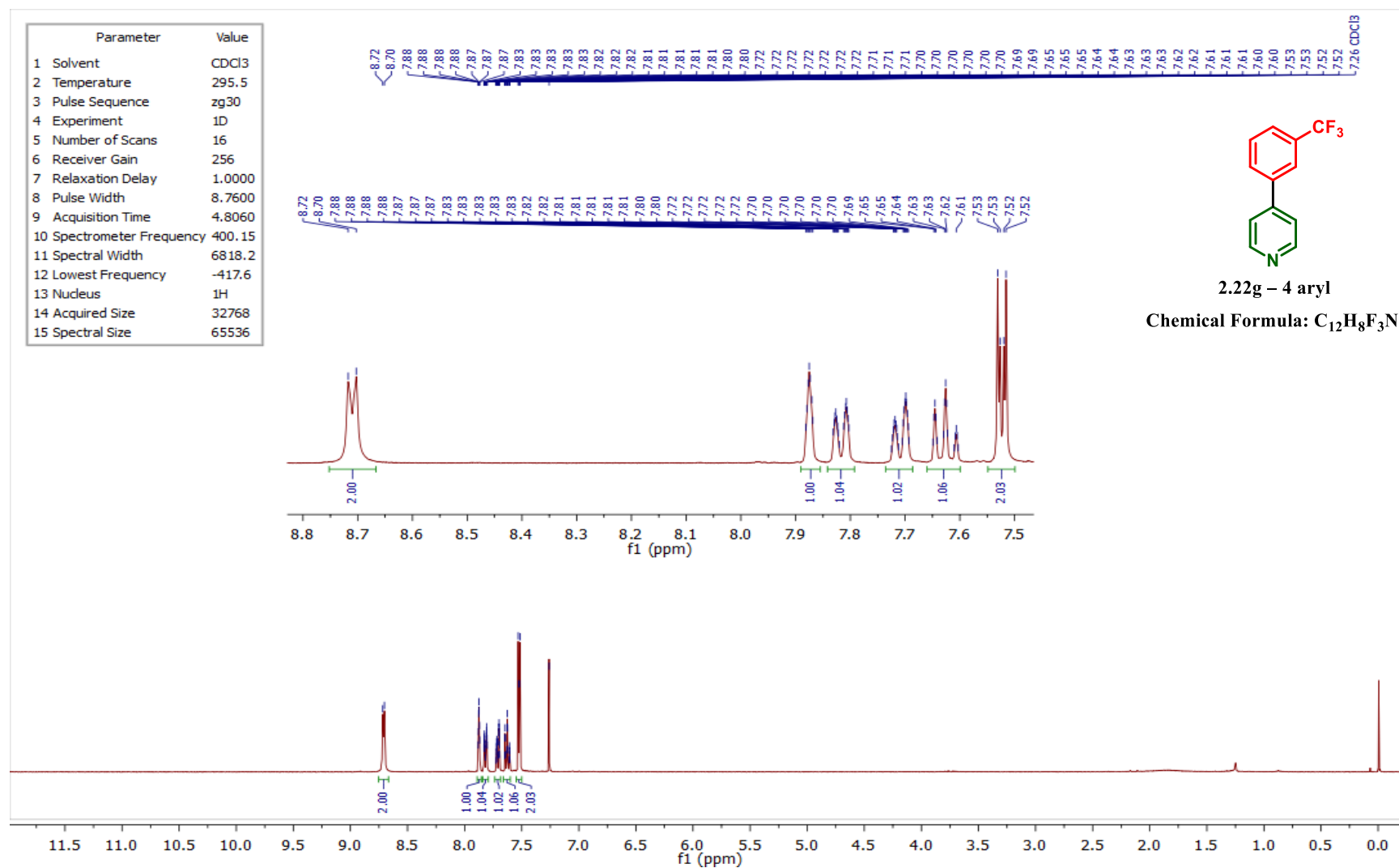


Figure 4.83 – ^1H NMR spectrum of compound 2.22g – 4 aryl in CDCl₃.

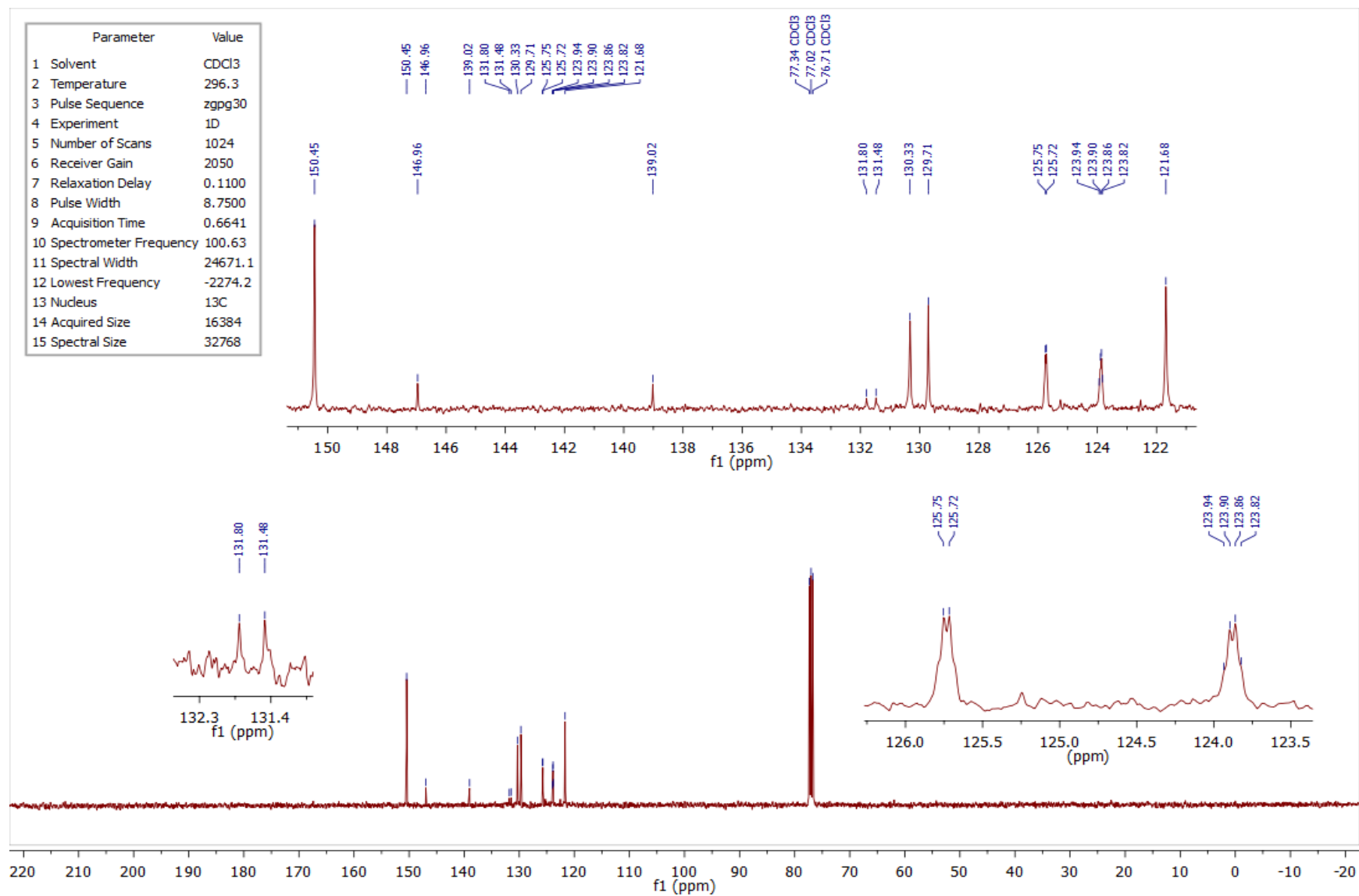


Figure 4.84 – ¹³C NMR spectrum of compound 2.22g – 4 aryl in CDCl₃.

4.2.15 ¹H and ¹³C NMR spectra of compound 2.22h – 2 aryl

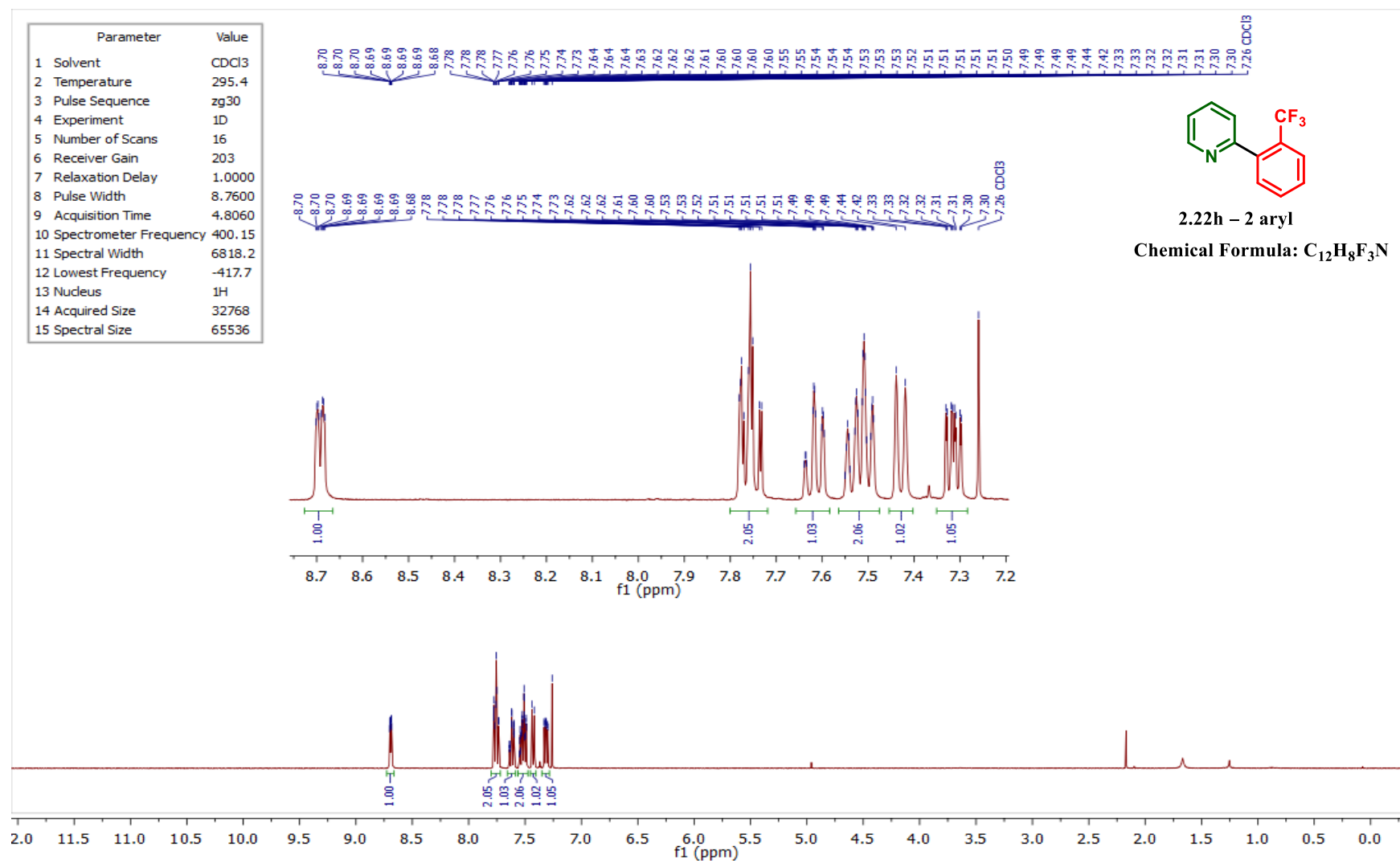


Figure 4.85 – ¹H NMR spectrum of compound 2.22h – 2 aryl in CDCl₃.

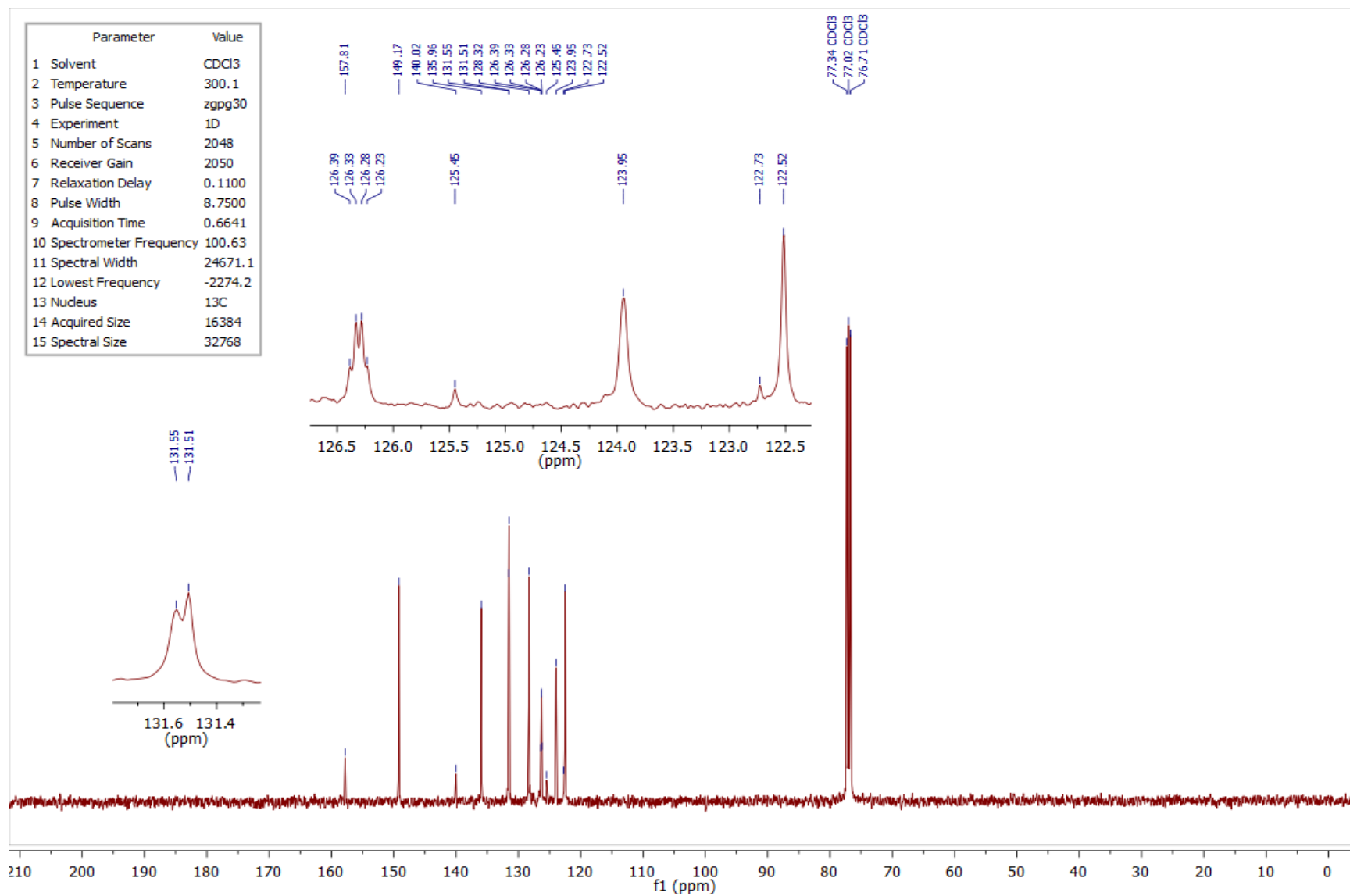


Figure 4.86 – ¹³C NMR spectrum of compound **2.22h – 2 aryl** in CDCl₃.

4.2.16 ^1H and ^{13}C NMR spectra of compound 2.22i – 2 aryl

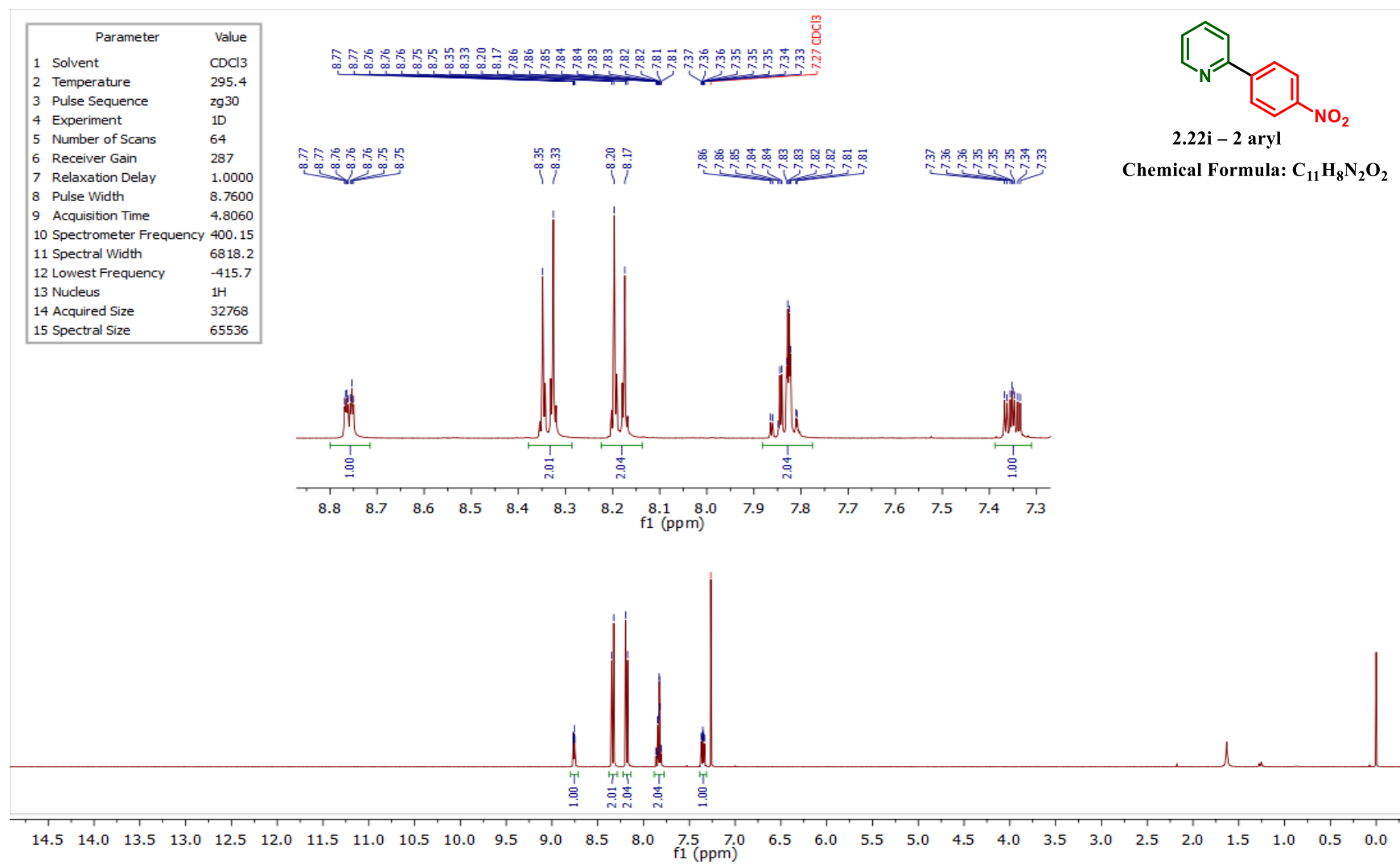


Figure 4.87 – ^1H NMR spectrum of compound 2.22i – 2 aryl in CDCl₃.

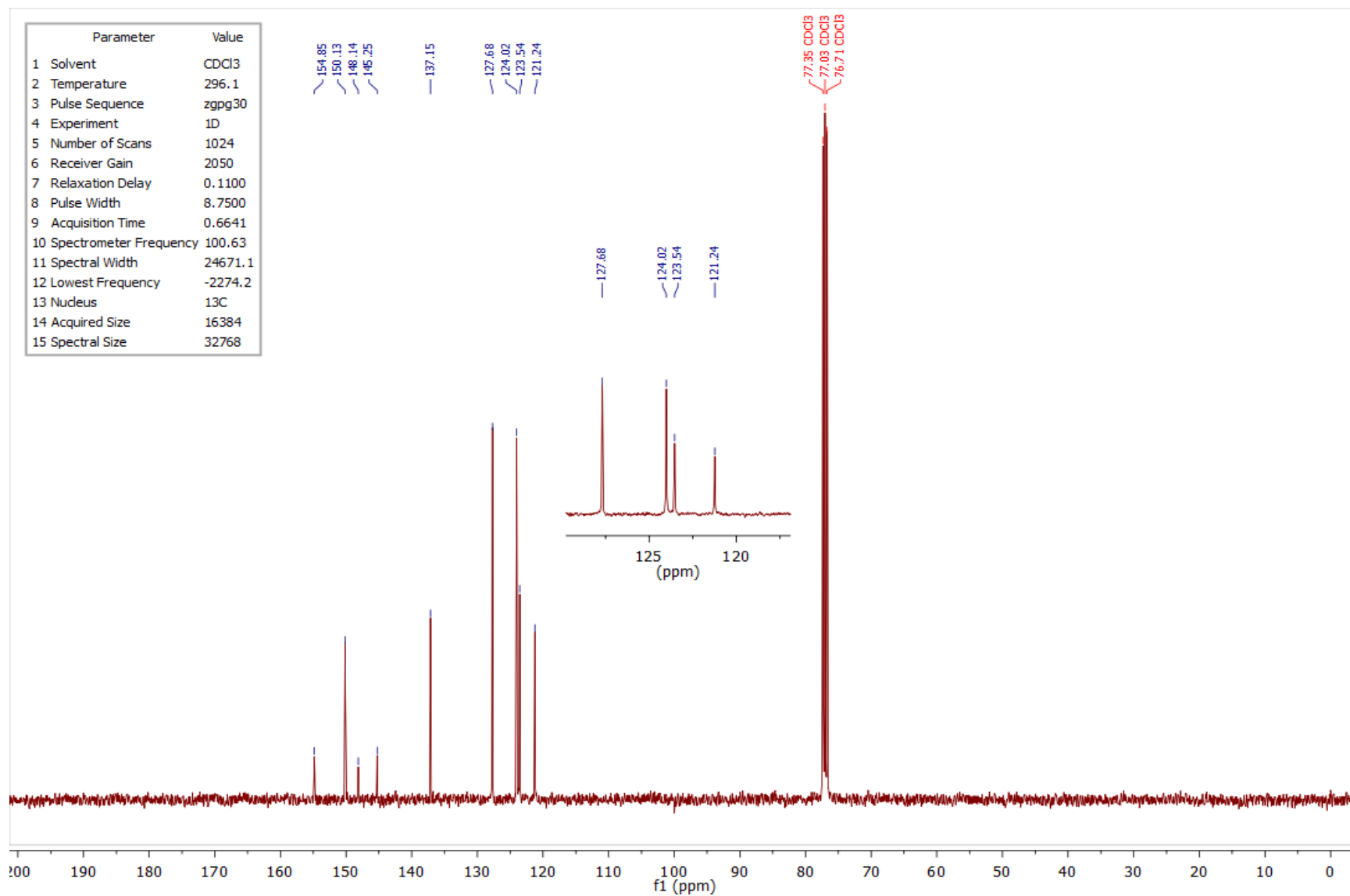


Figure 4.88 – ¹³C NMR spectrum of compound **2.22i** – **2 aryl** in CDCl₃.

4.2.17 ^1H and ^{13}C NMR spectra of compound 2.22i – 4 aryl

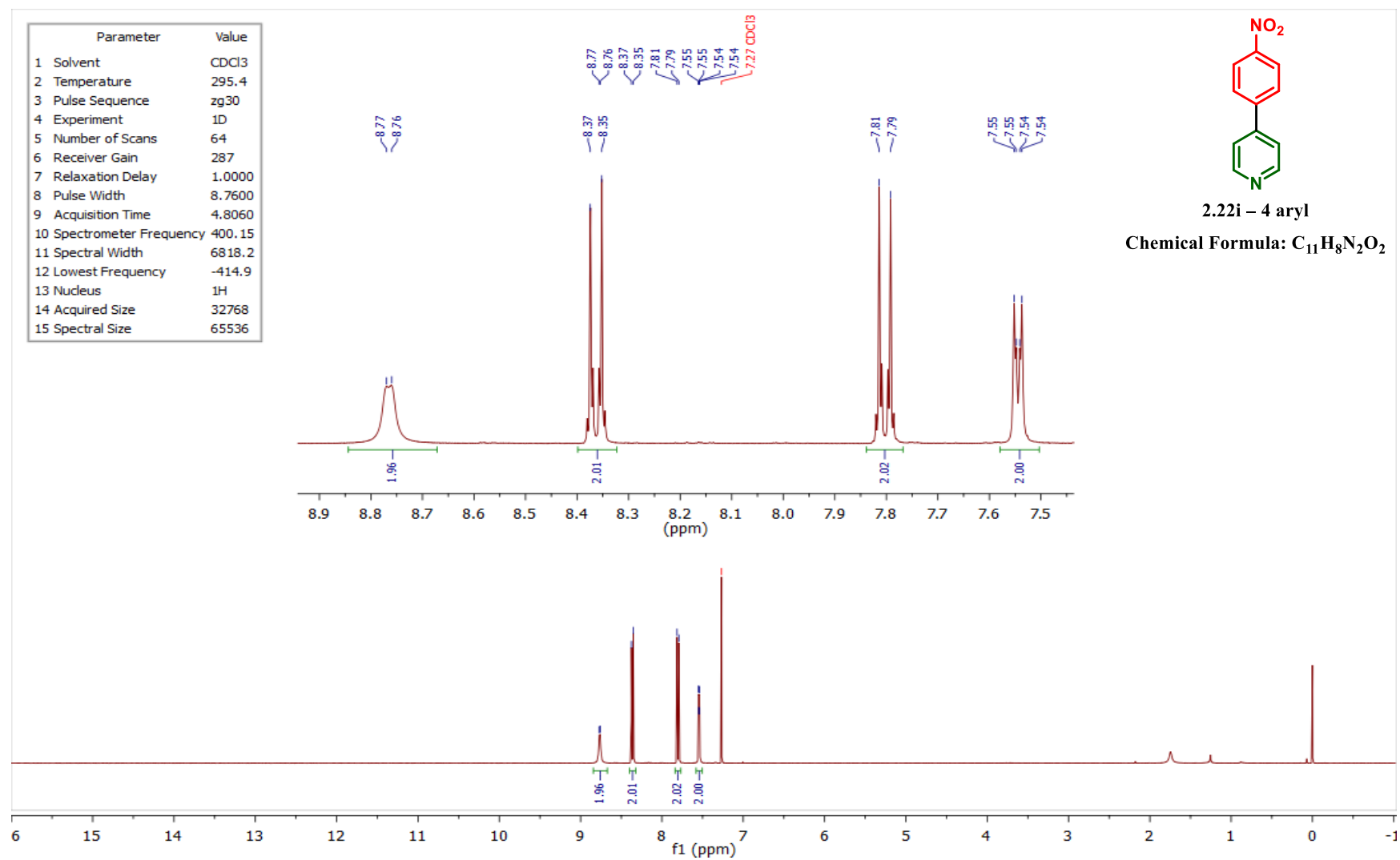


Figure 4.89 – ^1H NMR spectrum of compound 2.22i – 4 aryl in CDCl_3 .

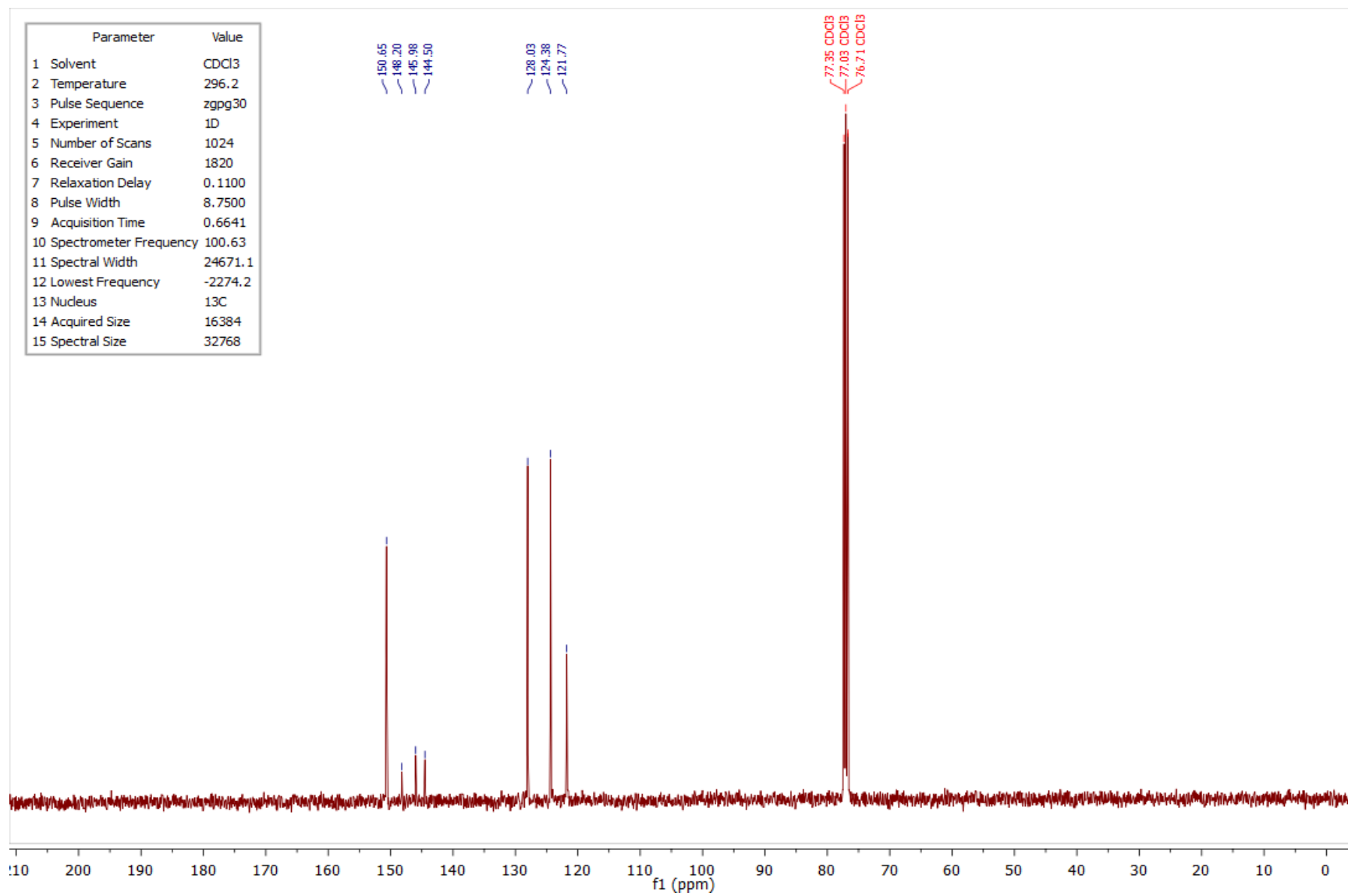


Figure 4.90 – ¹³C NMR spectrum of compound **2.22i** – **4 aryl** in CDCl₃.

4.2.18 ^1H and ^{13}C NMR spectra of compound 2.22j – 2 aryl

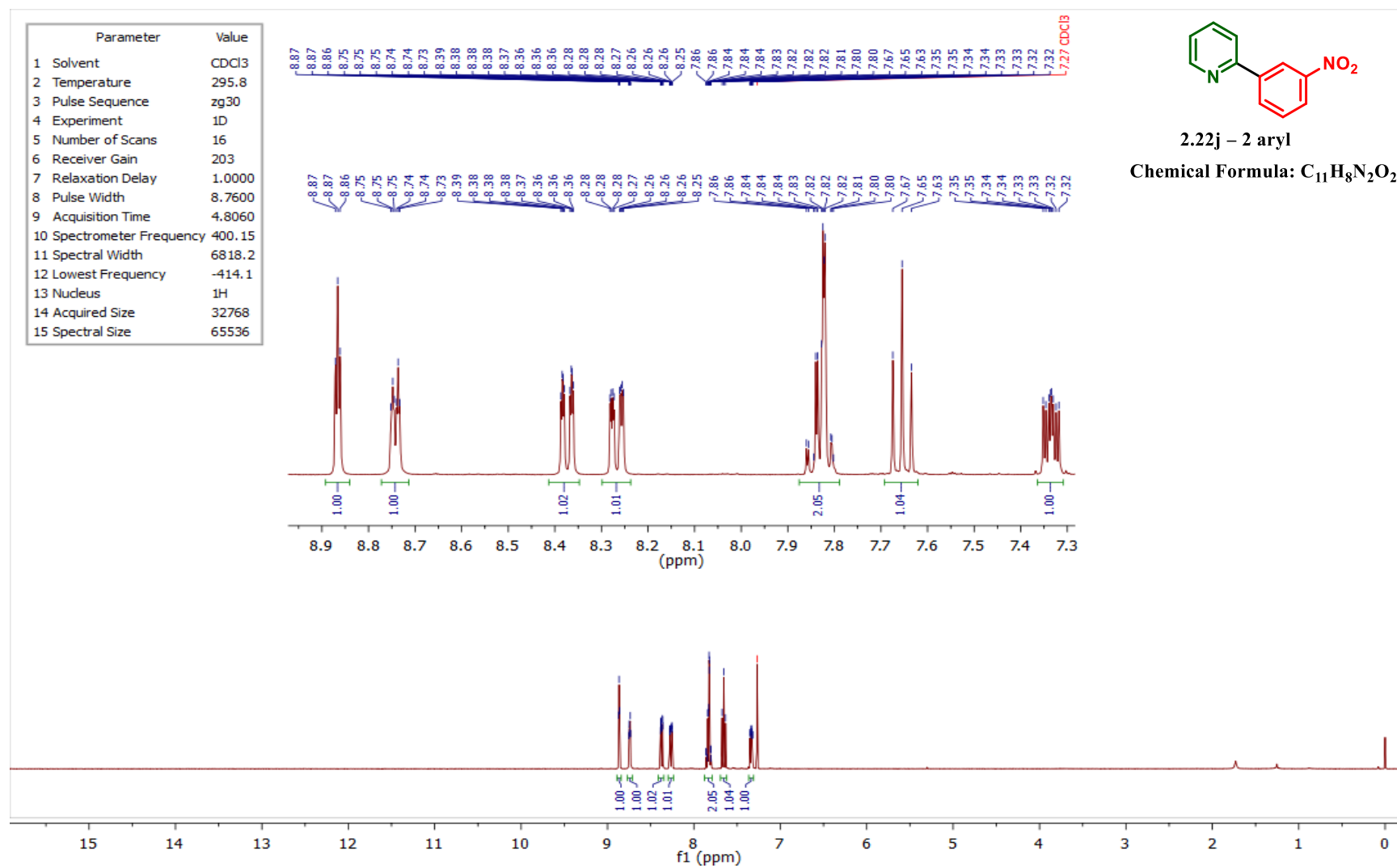


Figure 4.91 – ^1H NMR spectrum of compound 2.22j – 2 aryl in CDCl_3 .

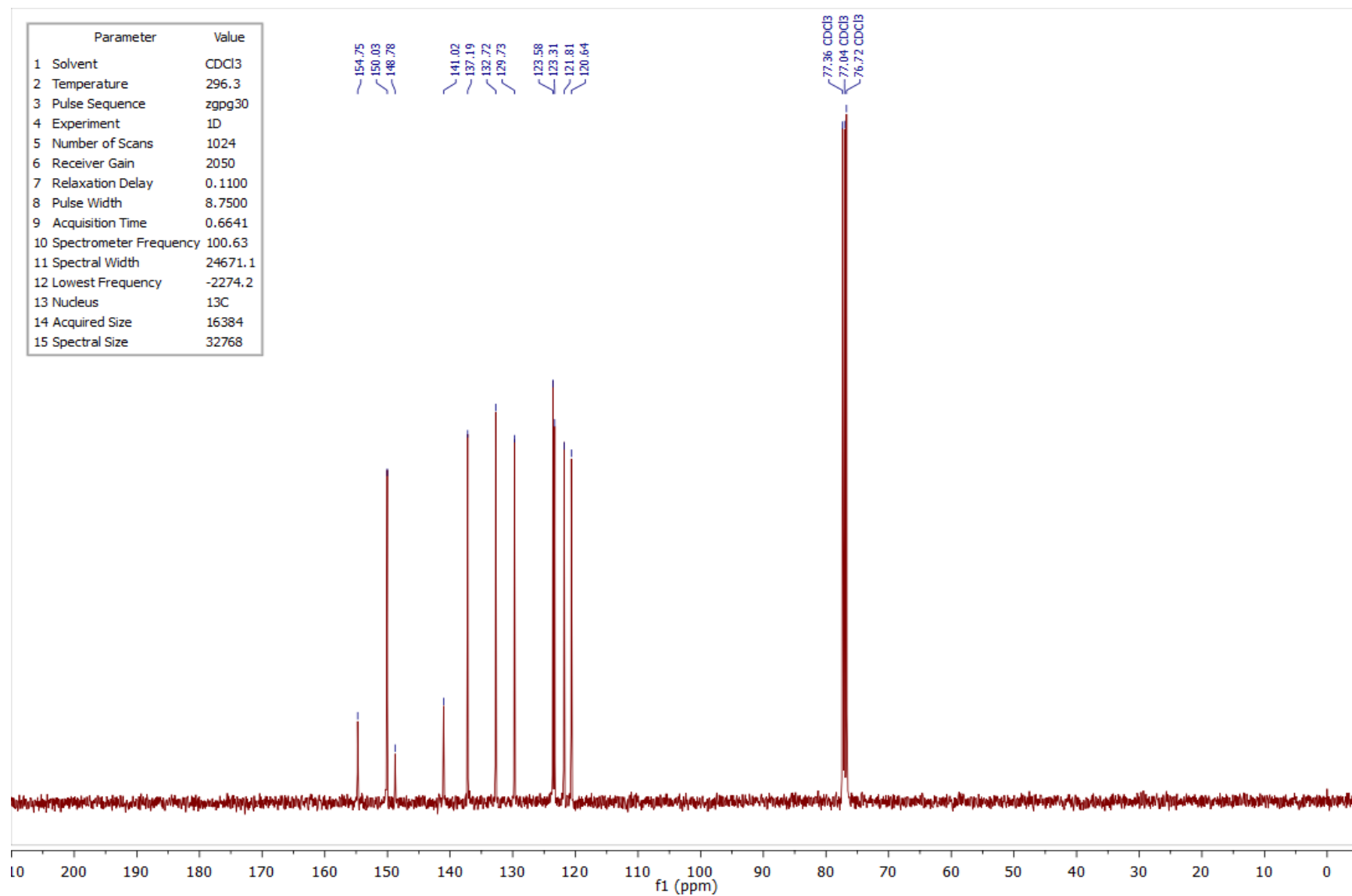


Figure 4.92 – ¹³C NMR spectrum of compound **2.22j** – **2 aryl** in CDCl₃.

4.2.19 ¹H and ¹³C NMR spectra of compound 2.22j – 4 aryl

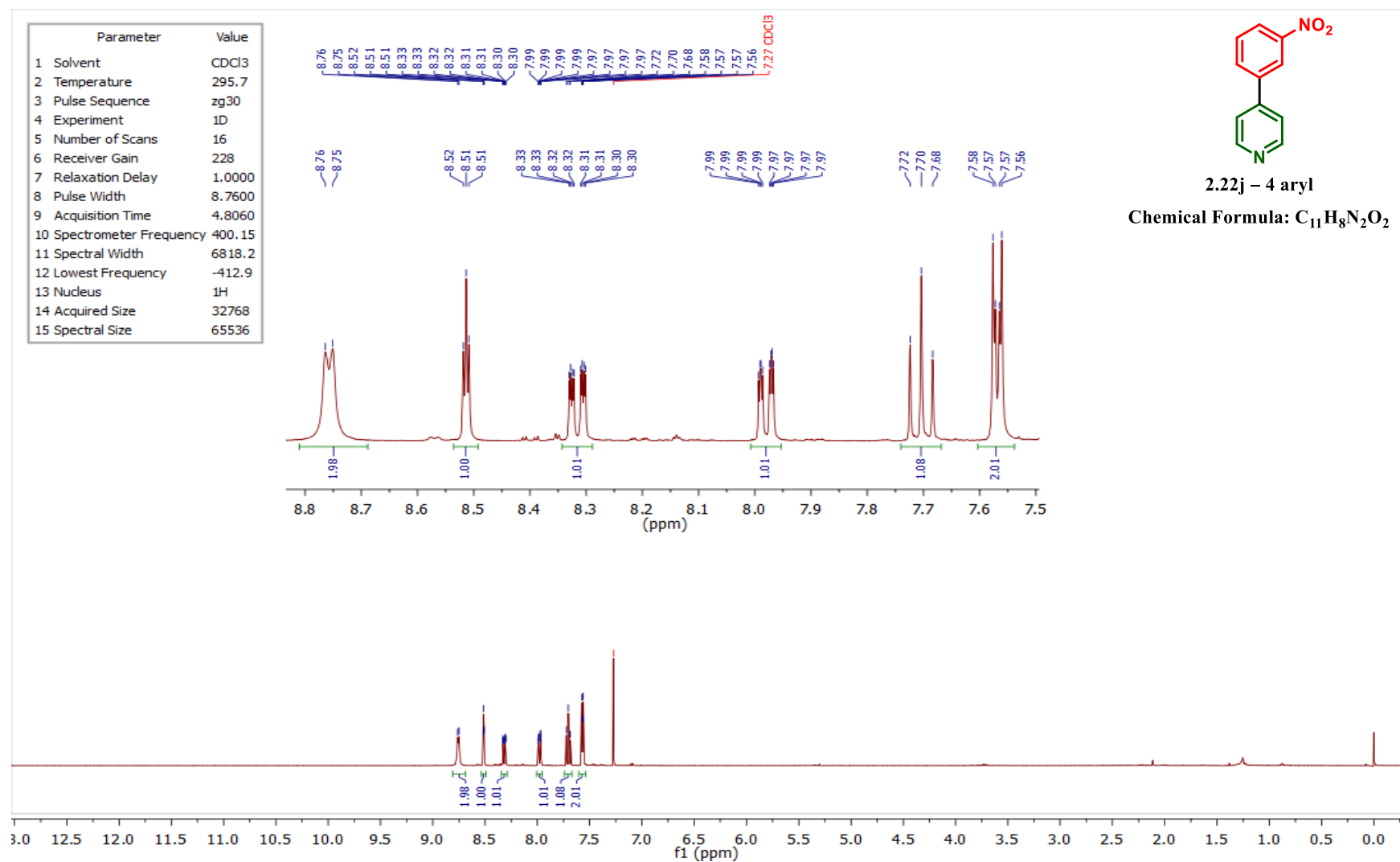


Figure 4.93 – ¹H NMR spectrum of compound 2.22j – 4 aryl in CDCl₃.

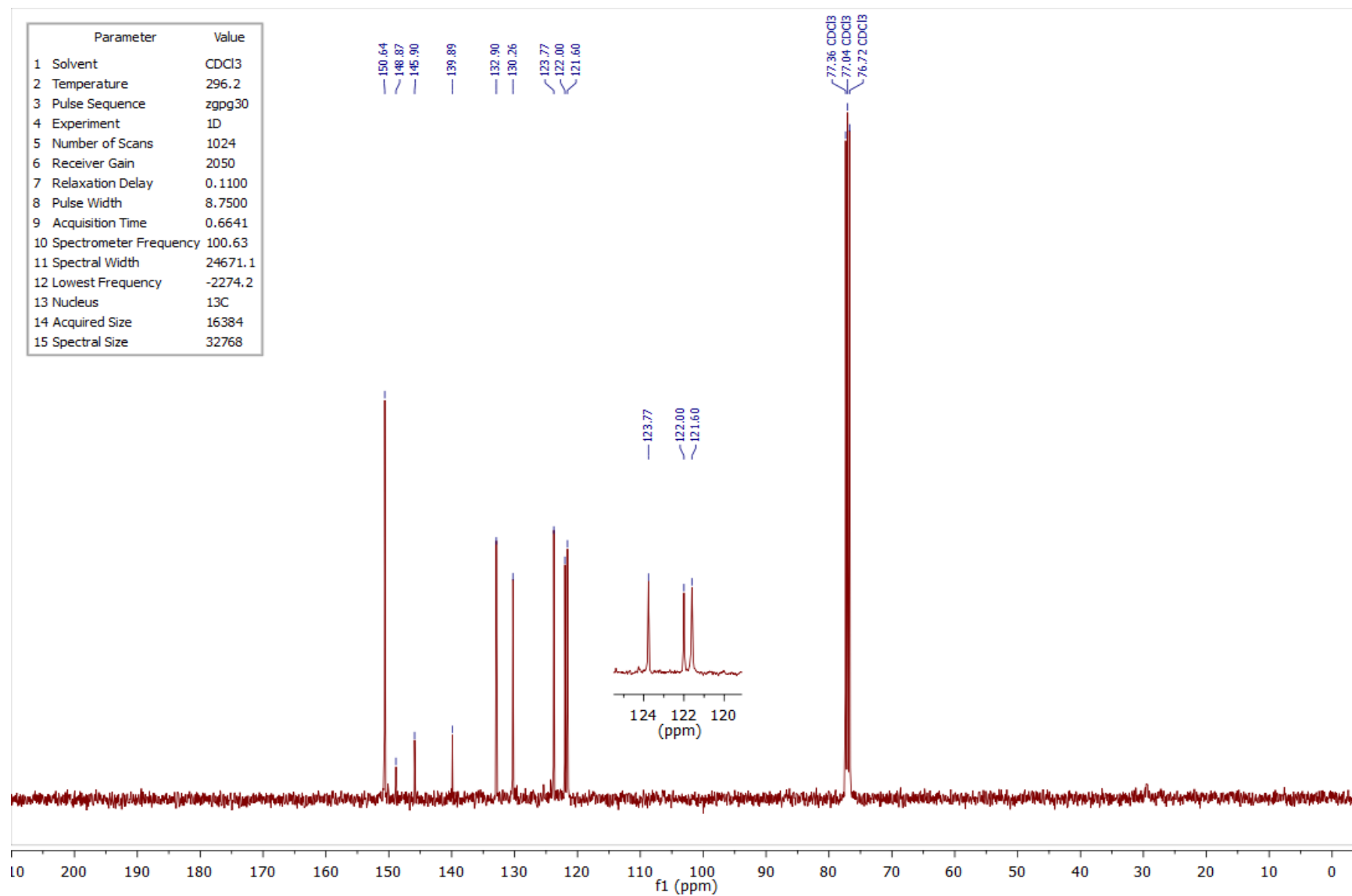


Figure 4.94 – ¹³C NMR spectrum of compound 2.22j – 4 aryl in CDCl₃.

4.2.20 ^1H and ^{13}C NMR spectra of compound 2.22k – 2 aryl

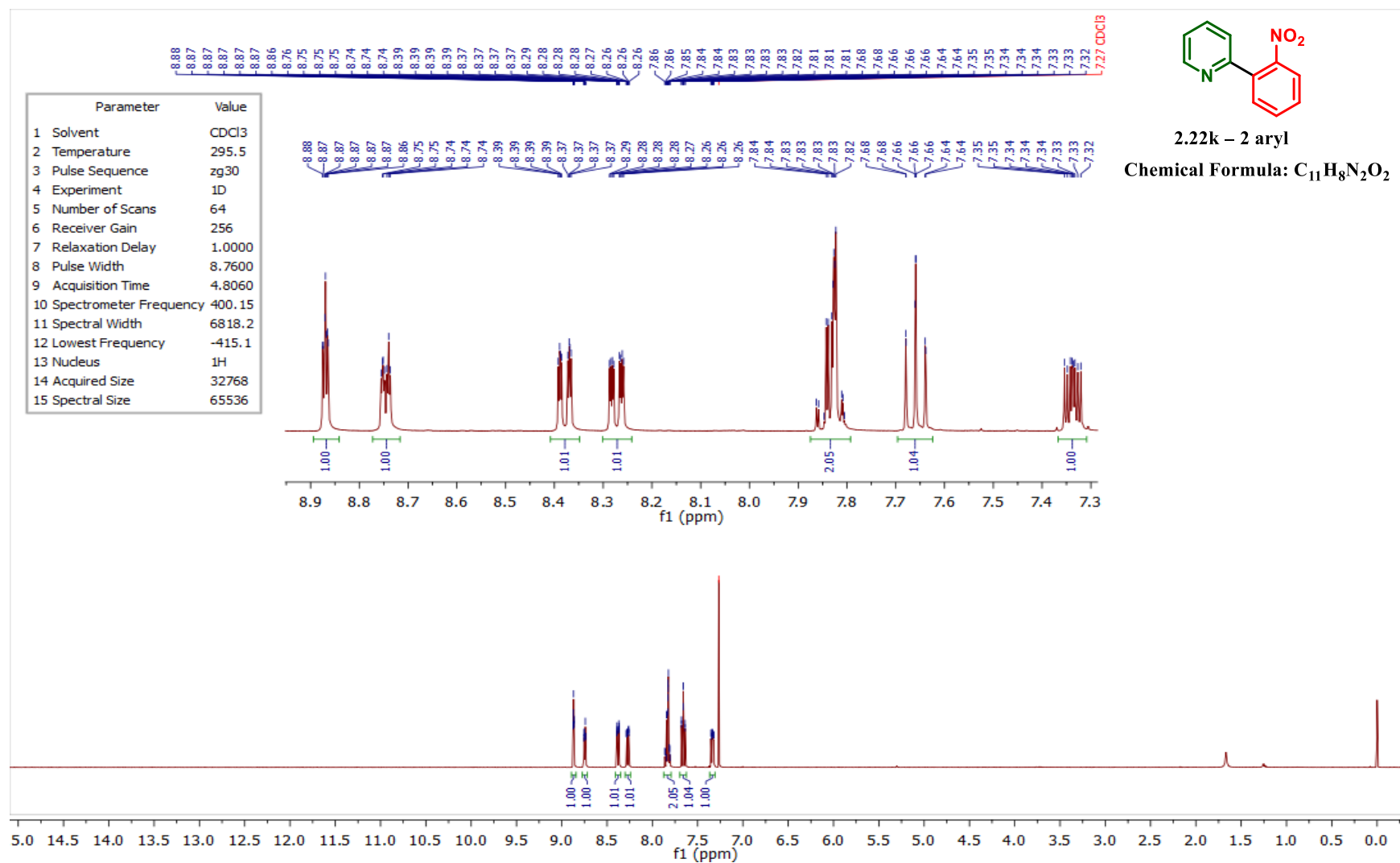


Figure 4.95 – ^1H NMR spectrum of compound 2.22k – 2 aryl in CDCl₃.

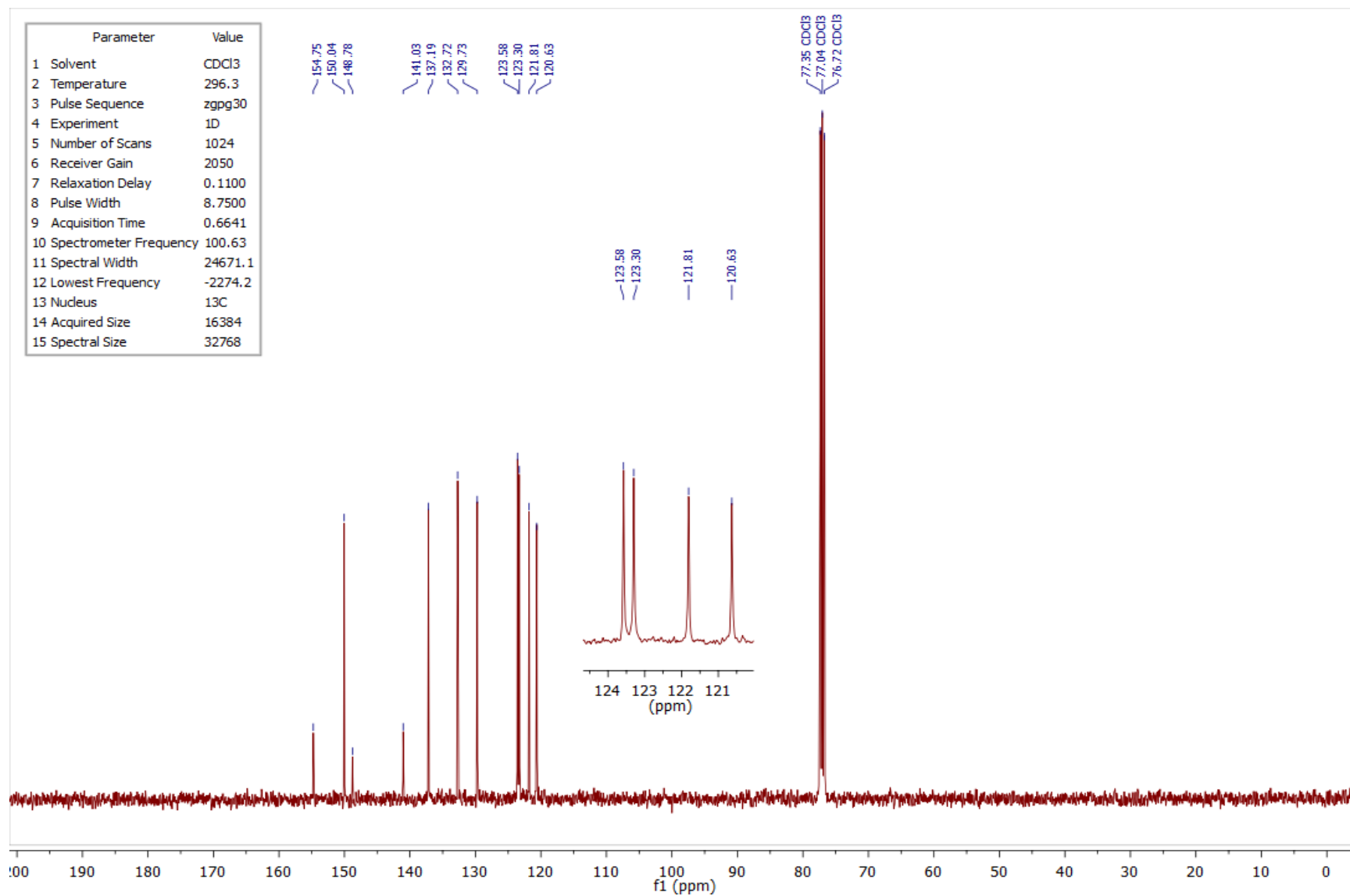


Figure 4.96 – ¹³C NMR spectrum of compound 2.22k – 2 aryl in CDCl₃.

4.2.21 ¹H and ¹³C NMR spectra of compound 2.22k – 4 aryl

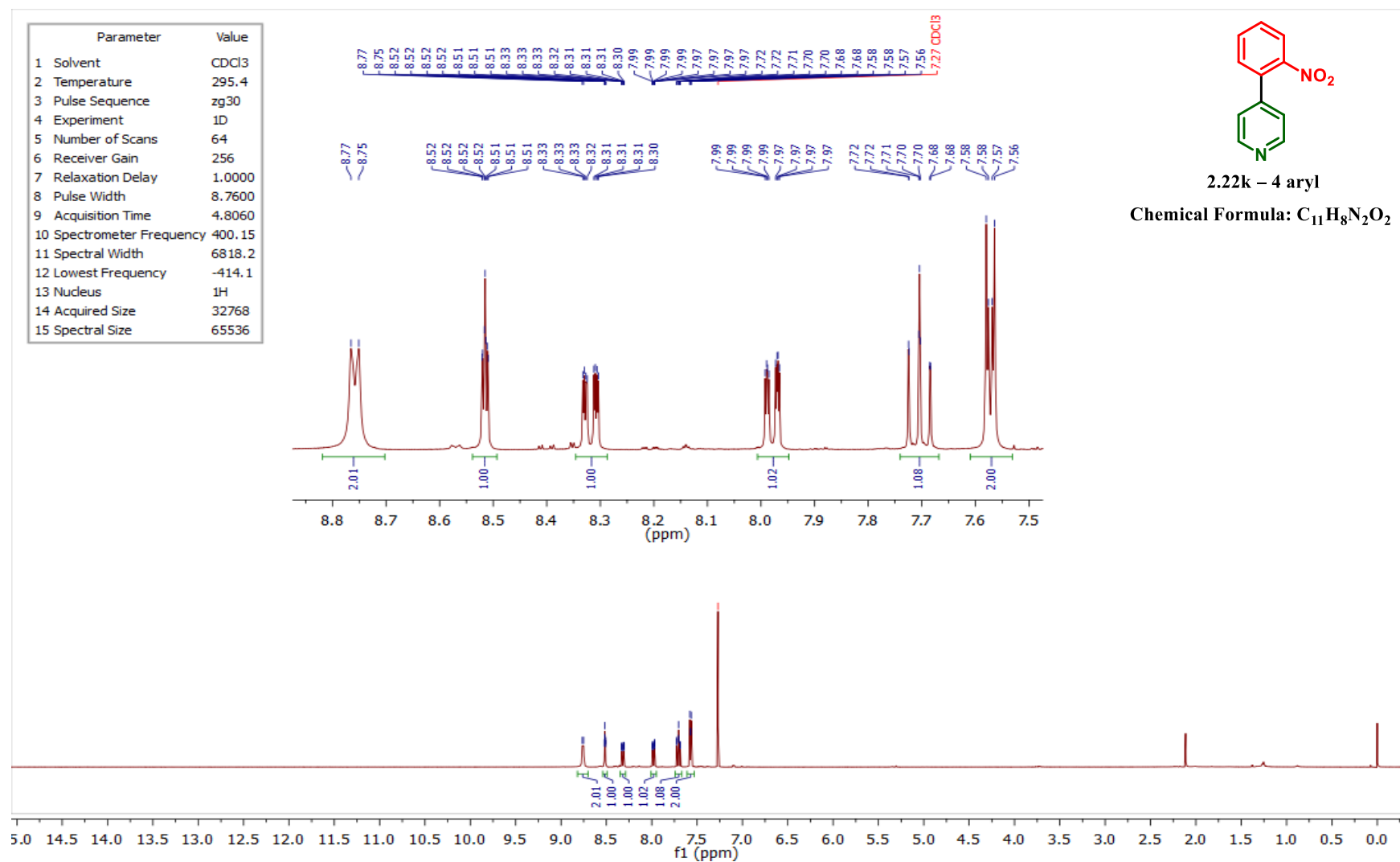


Figure 4.97 – ¹H NMR spectrum of compound 2.22k – 4 aryl in CDCl₃.

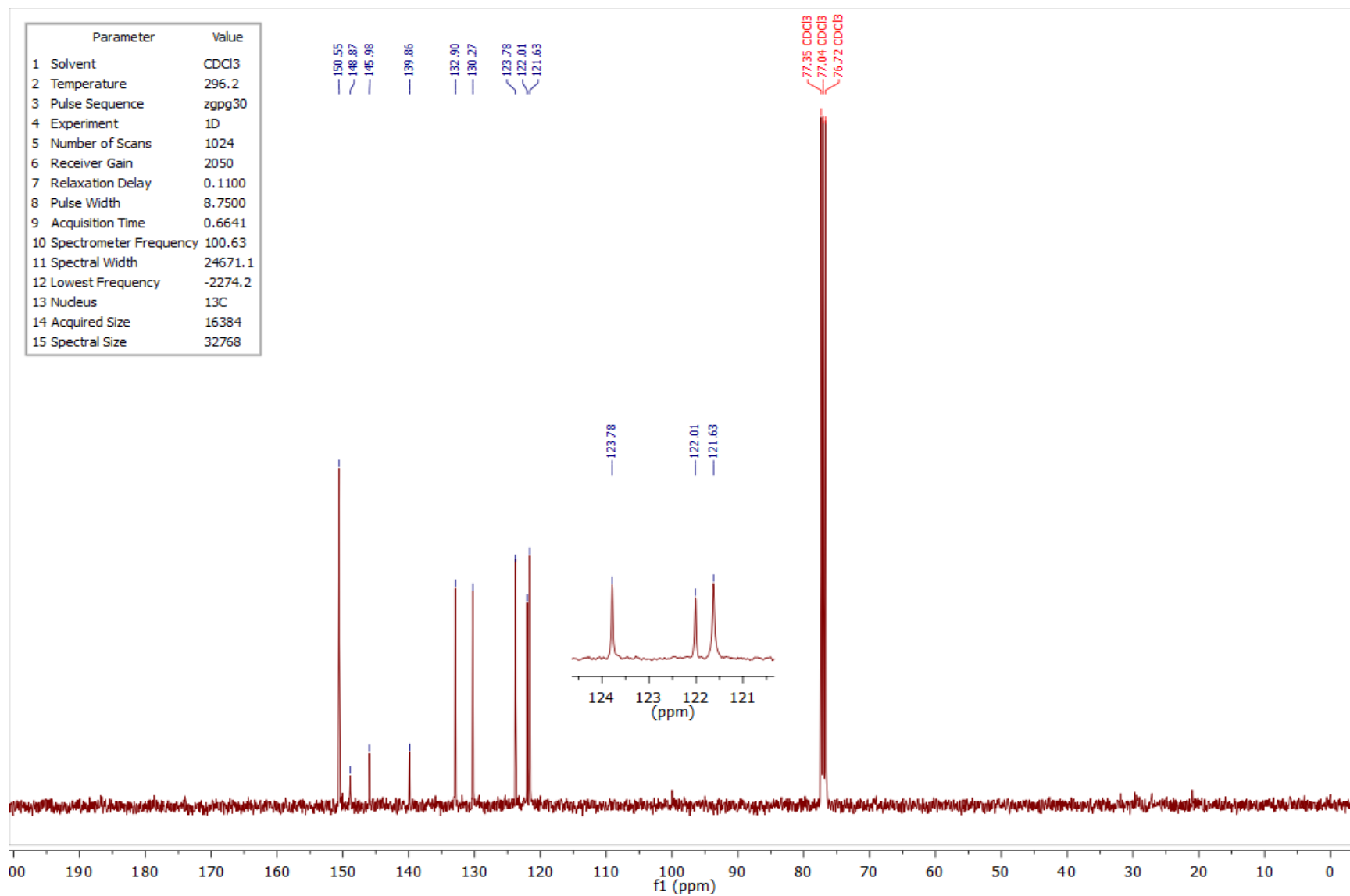


Figure 4.98 – ¹³C NMR spectrum of compound 2.22k – 4 aryl in CDCl₃.

4.2.22 ¹H and ¹³C NMR spectra of compound 2.221 – 2 aryl

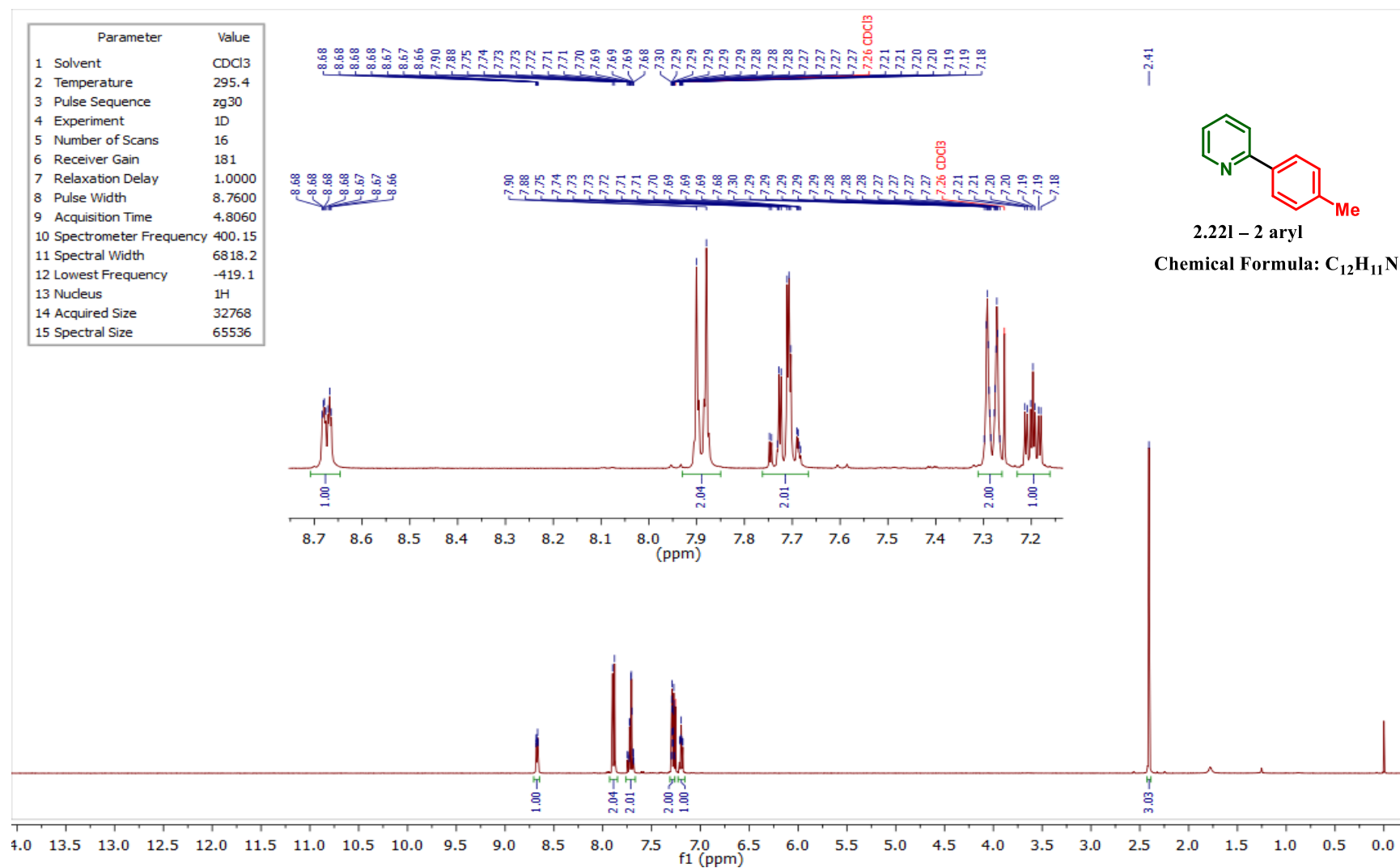


Figure 4.99 – ¹H NMR spectrum of compound 2.221 – 2 aryl in CDCl₃.

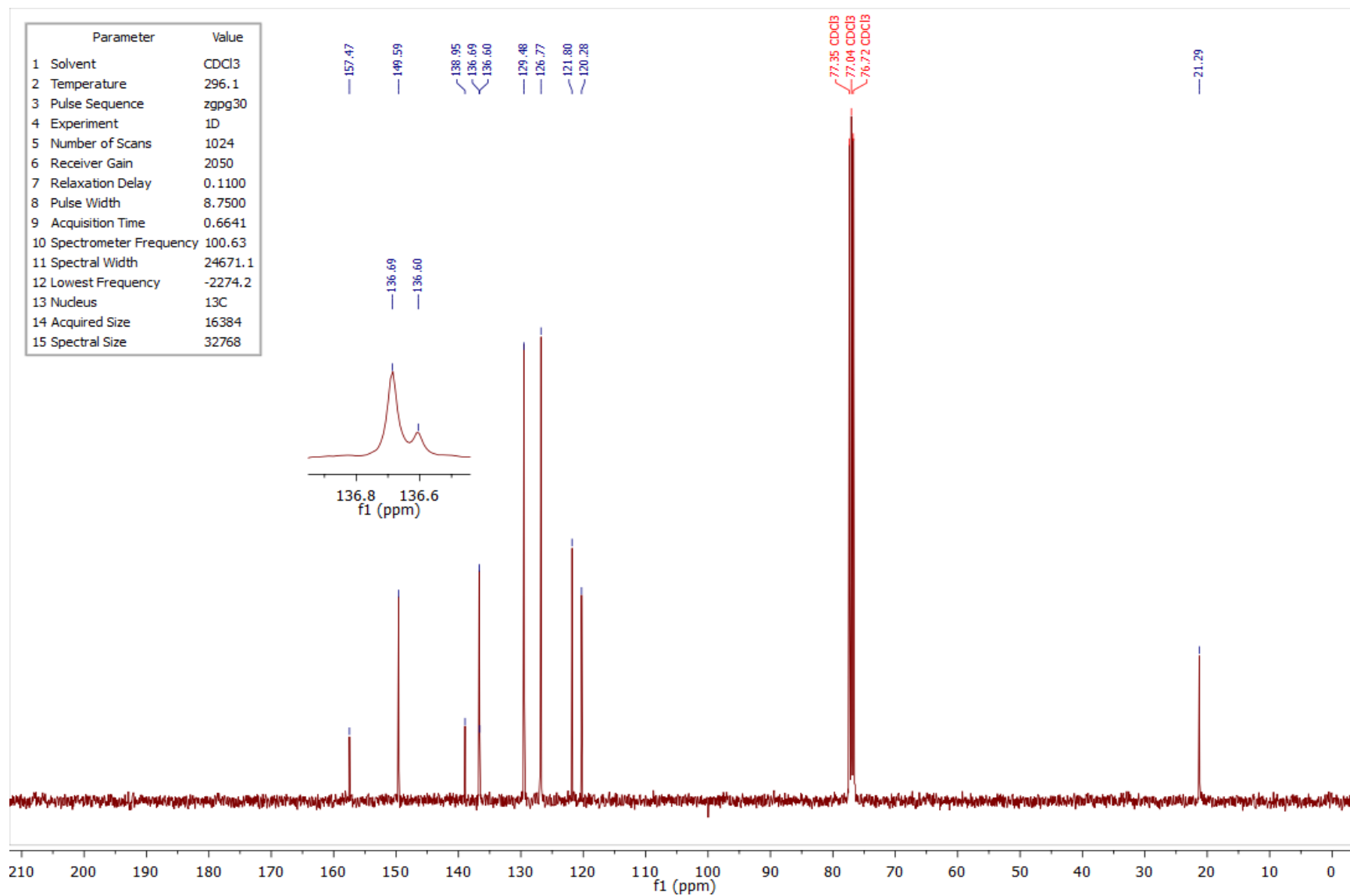


Figure 4.100 – ¹³C NMR spectrum of compound **2.221 – 2 aryl** in CDCl₃.

4.2.23 ^1H and ^{13}C NMR spectra of compound 2.221 – 4 aryl

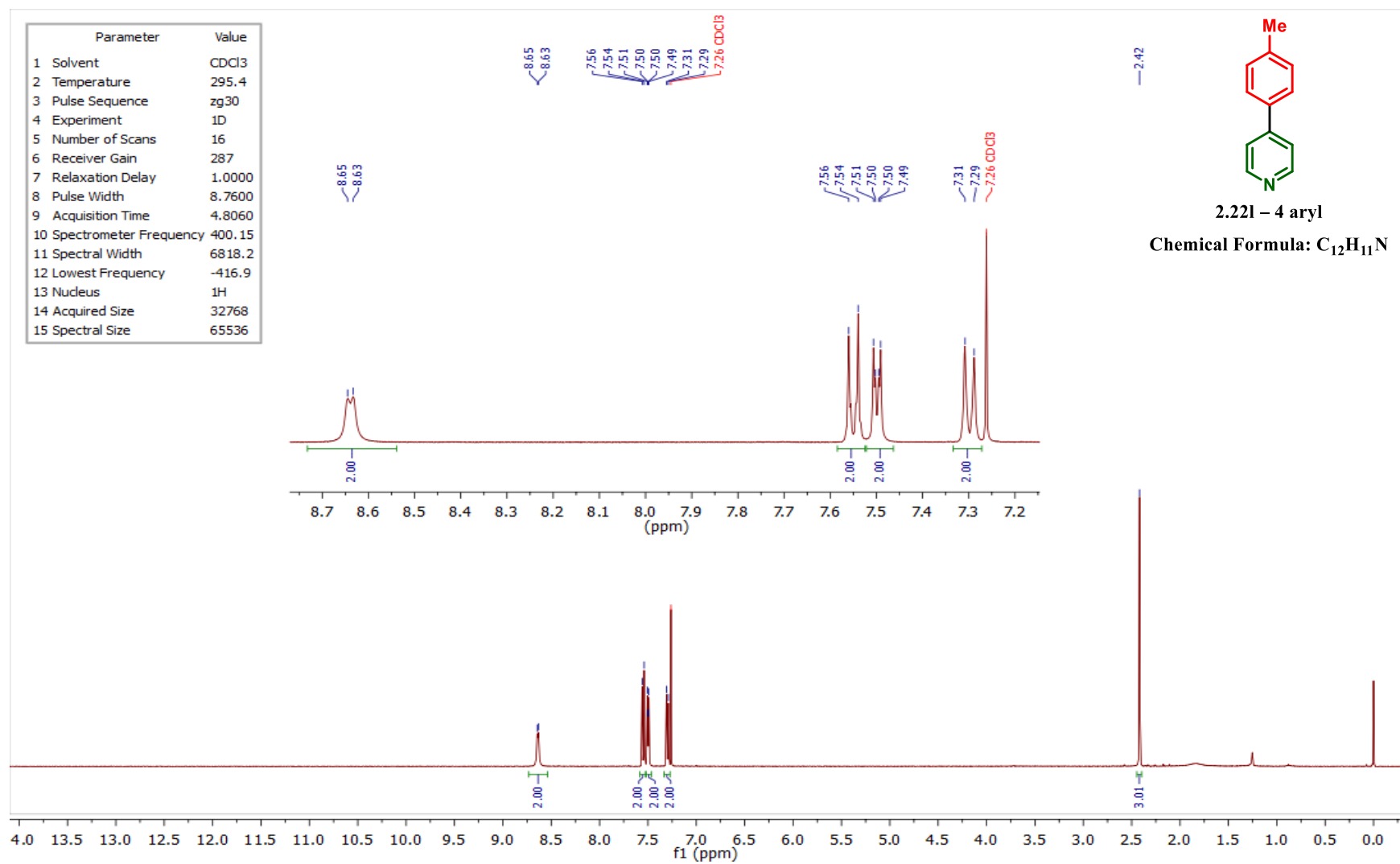


Figure 4.101 – ^1H NMR spectrum of compound 2.221 – 4 aryl in CDCl_3 .

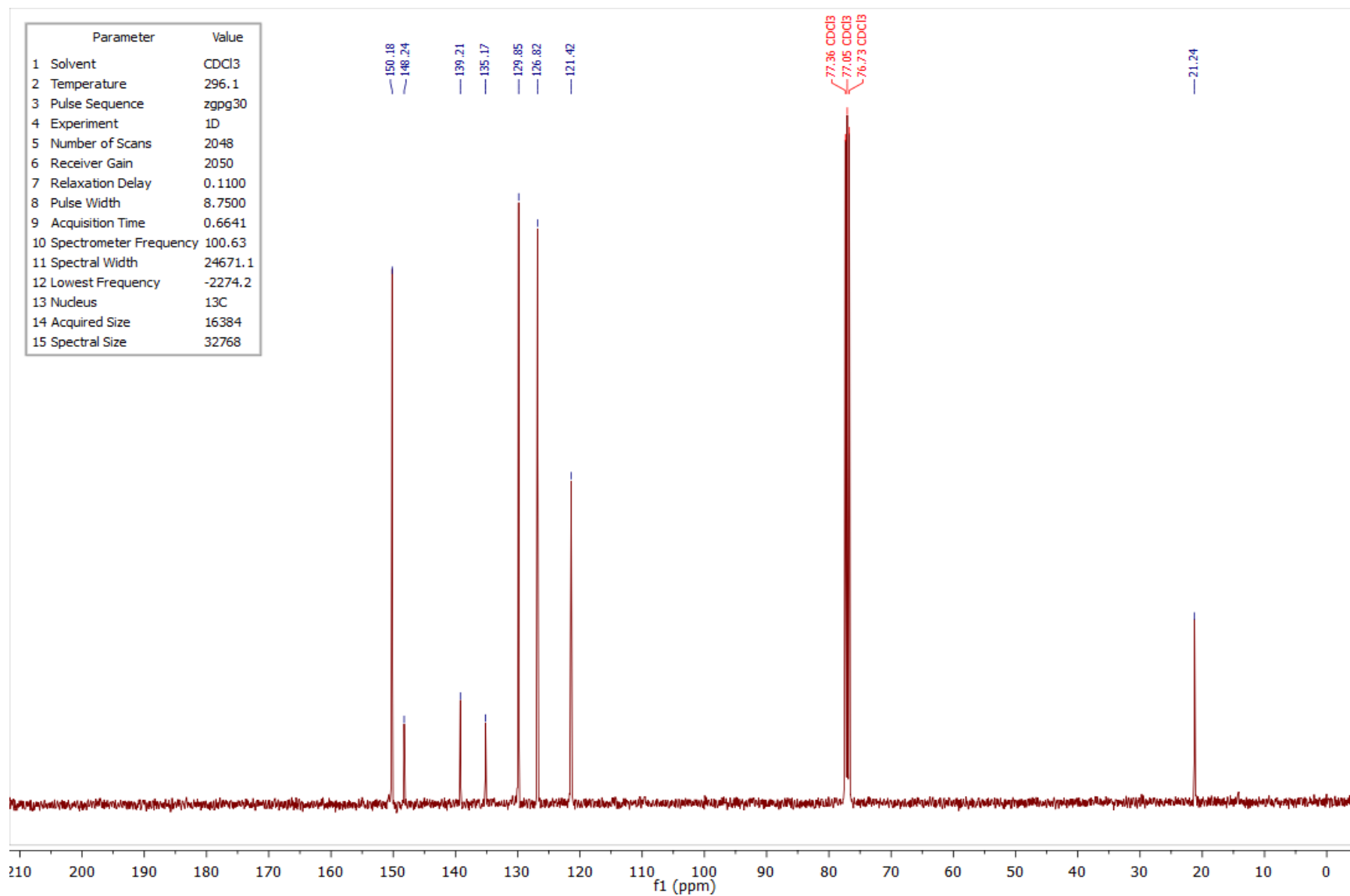


Figure 4.102 – ¹³C NMR spectrum of compound **2.221 – 4 aryl** in CDCl₃.

4.2.24 ^1H and ^{13}C NMR spectra of compound 2.22m – 2 aryl

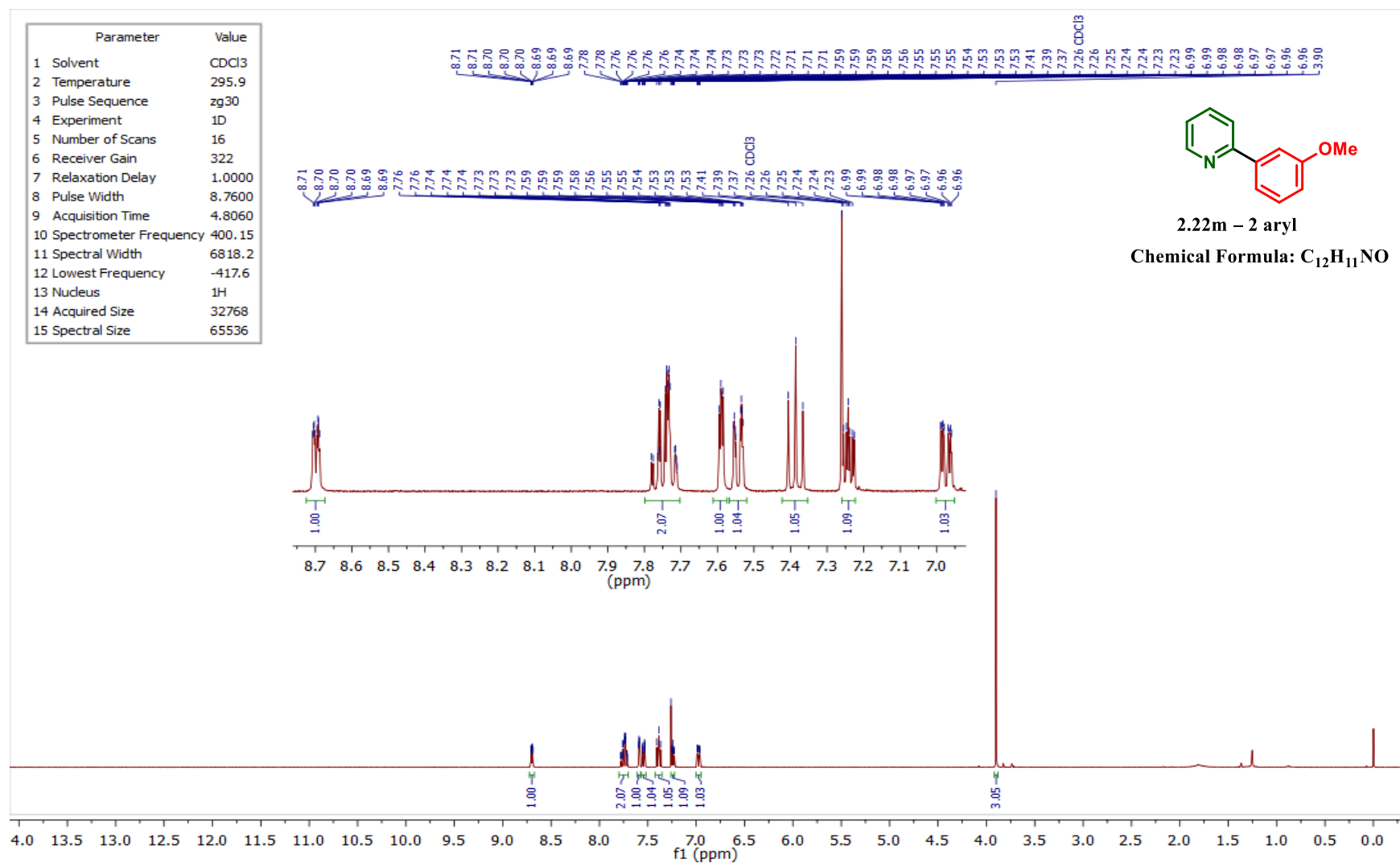


Figure 4.103 – ^1H NMR spectrum of compound 2.22m – 2 aryl in CDCl_3 .

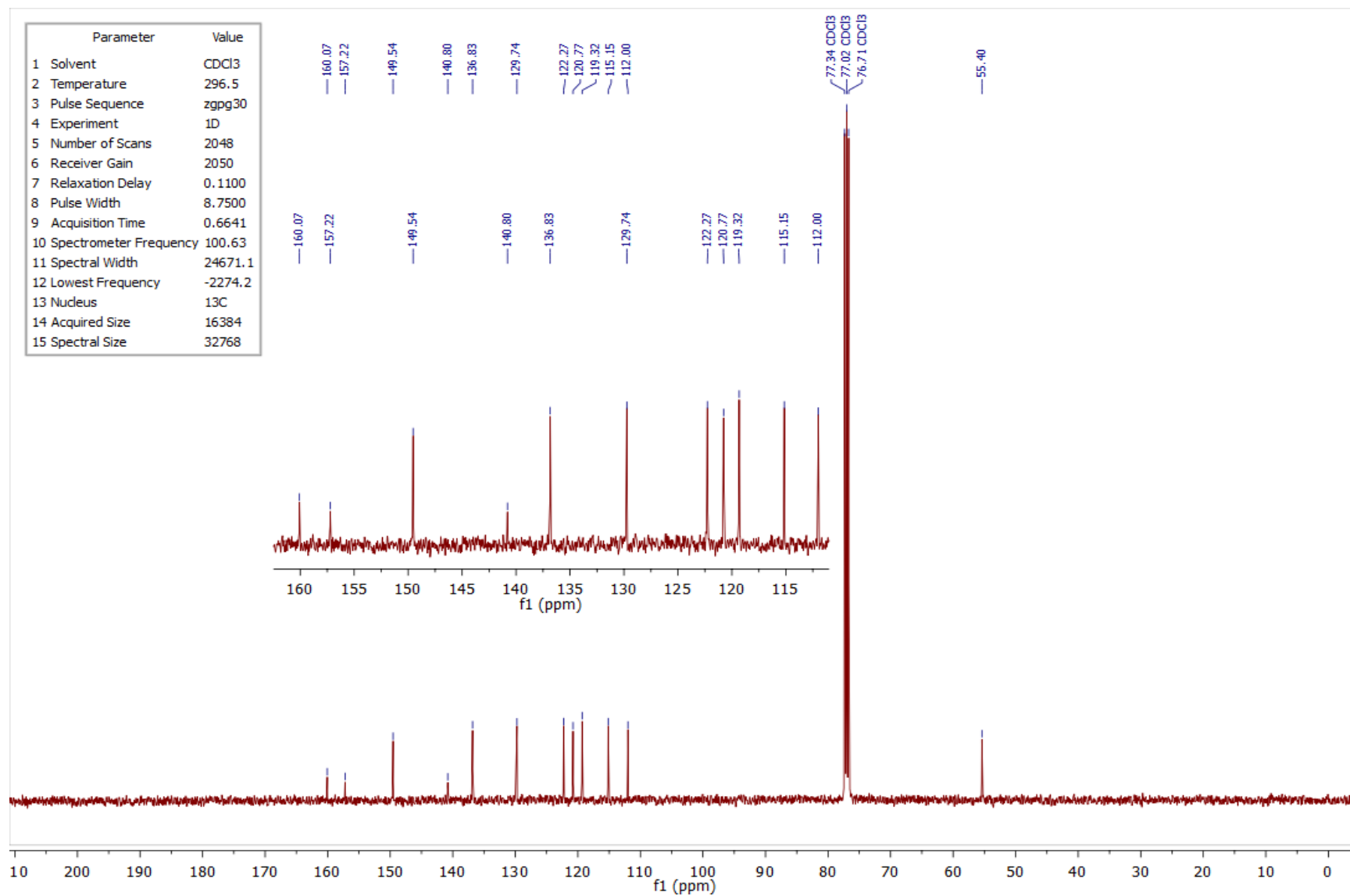


Figure 4.104 – ¹³C NMR spectrum of compound 2.22m – 2 aryl in CDCl₃.

4.2.25 ^1H and ^{13}C NMR spectra of compound 2.22m – 4 aryl

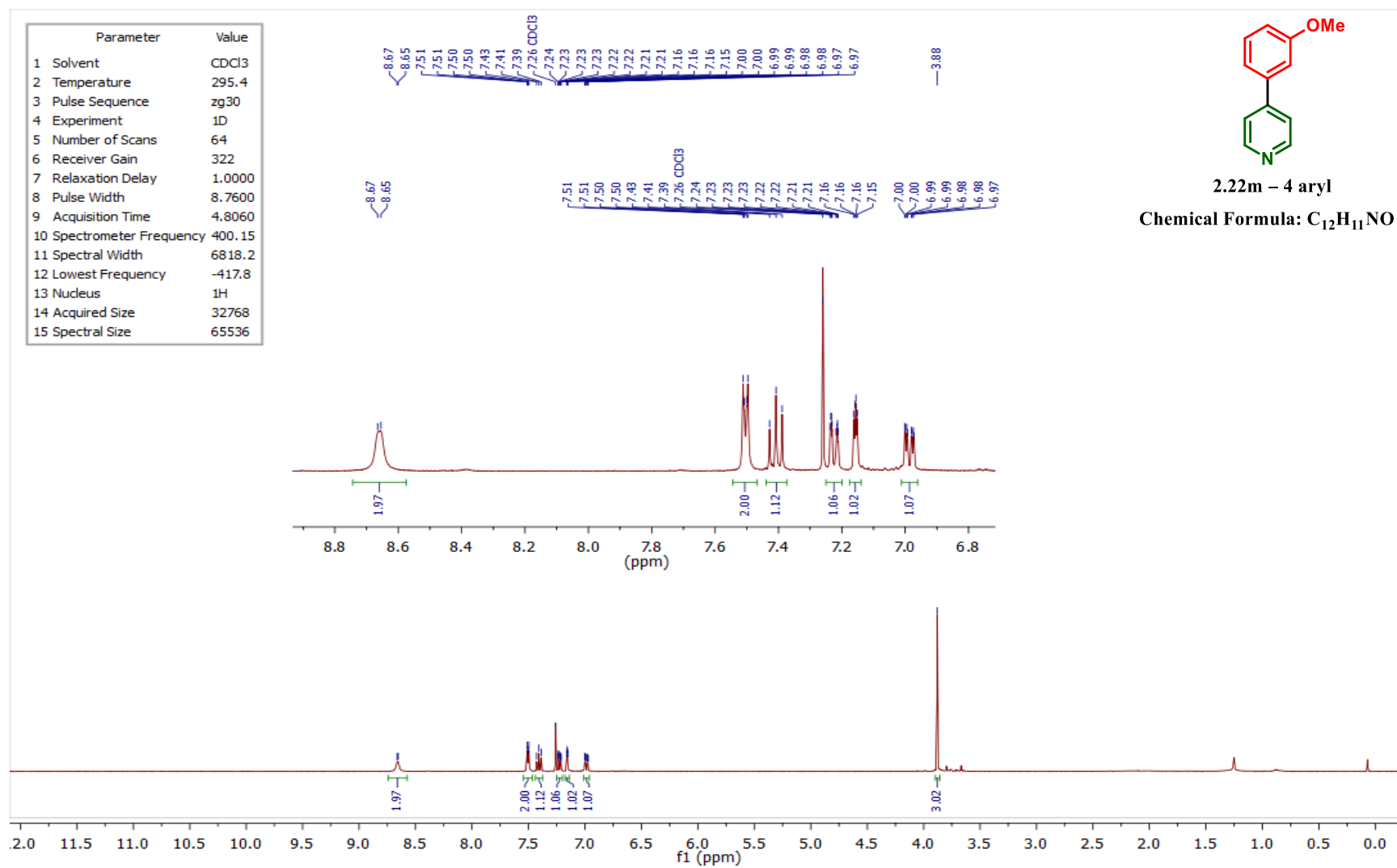


Figure 4.105 – ^1H NMR spectrum of compound 2.22m – 4 aryl in CDCl_3 .

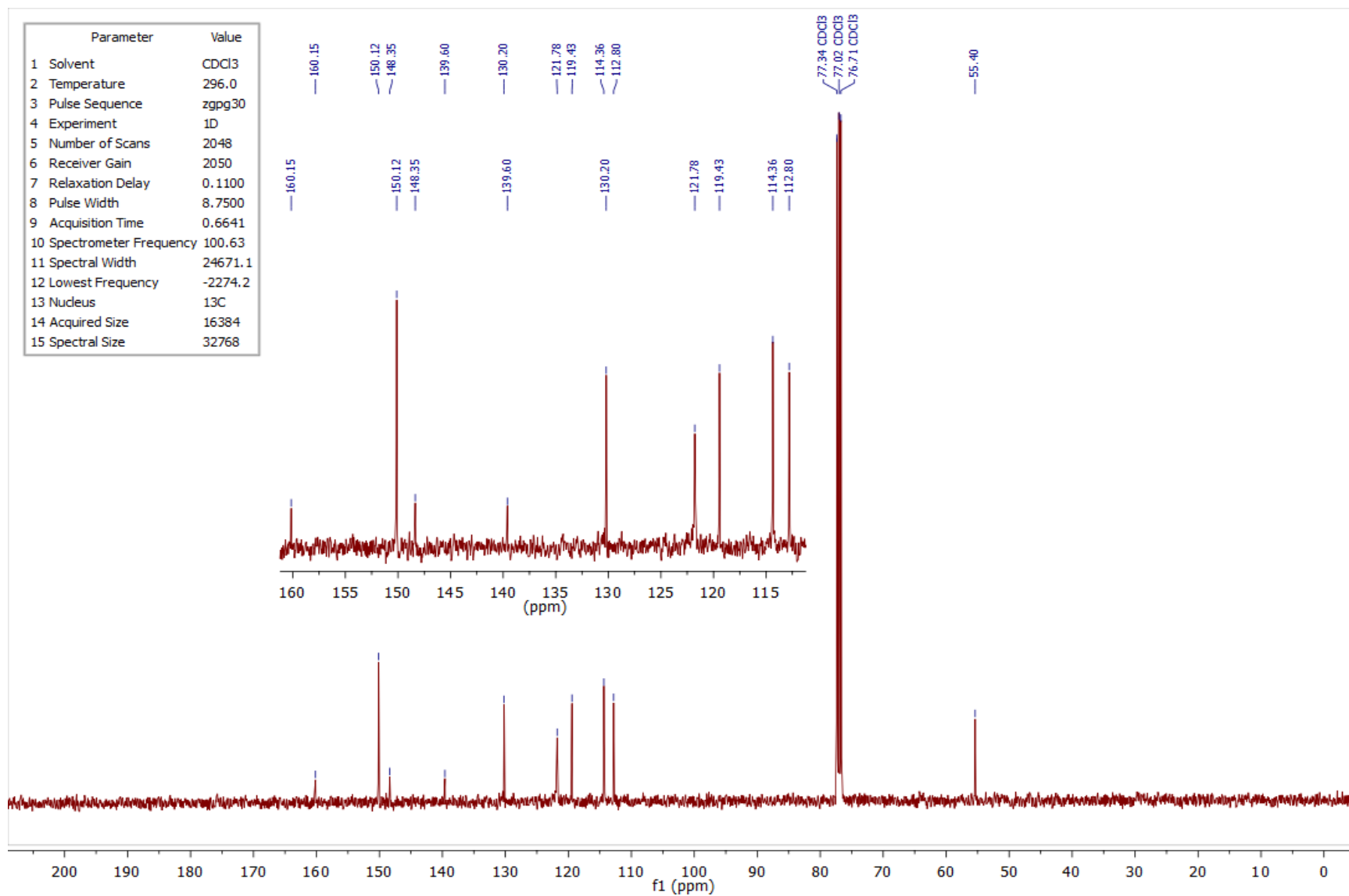


Figure 4.106 – ¹³C NMR spectrum of compound **2.22m – 4 aryl** in CDCl₃.

4.2.26 ^1H and ^{13}C NMR spectra of compound 2.22n – 2 aryl

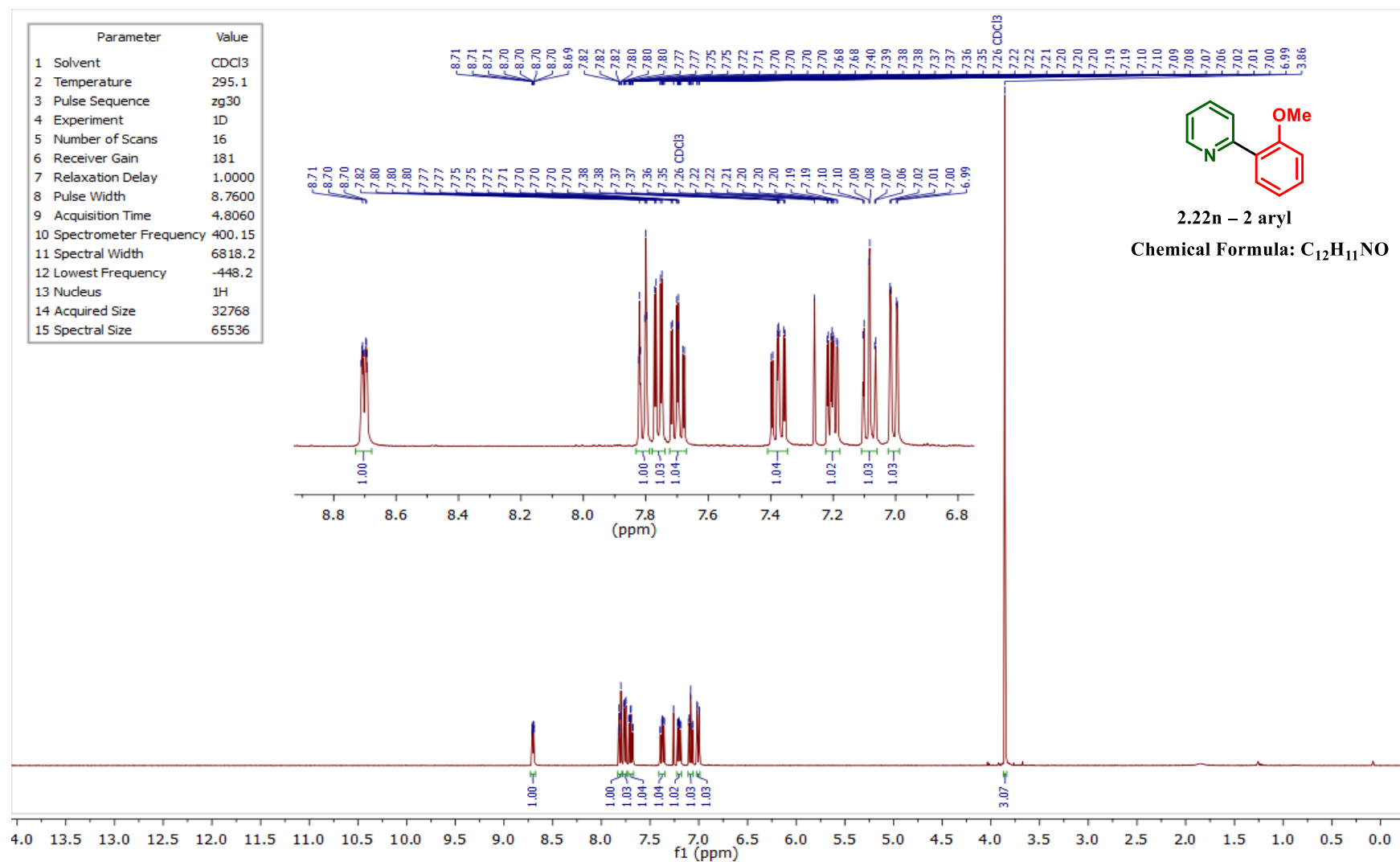


Figure 4.107 – ^1H NMR spectrum of compound 2.22n – 2 aryl in CDCl_3 .

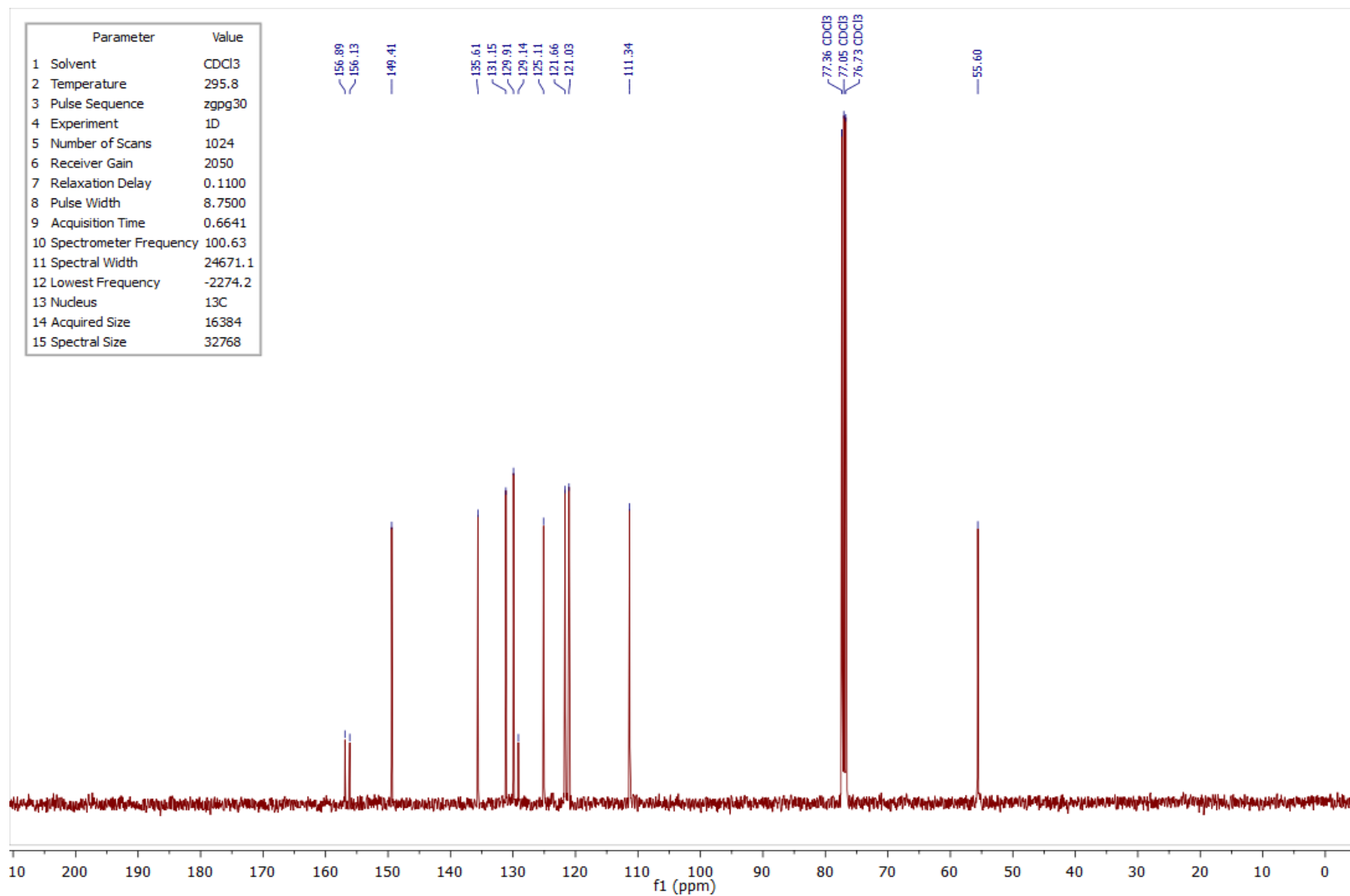


Figure 4.108 – ¹³C NMR spectrum of compound **2.22n – 2 aryl** in CDCl₃.

4.2.27 ¹H and ¹³C NMR spectra of compound 2.22n – 4 aryl

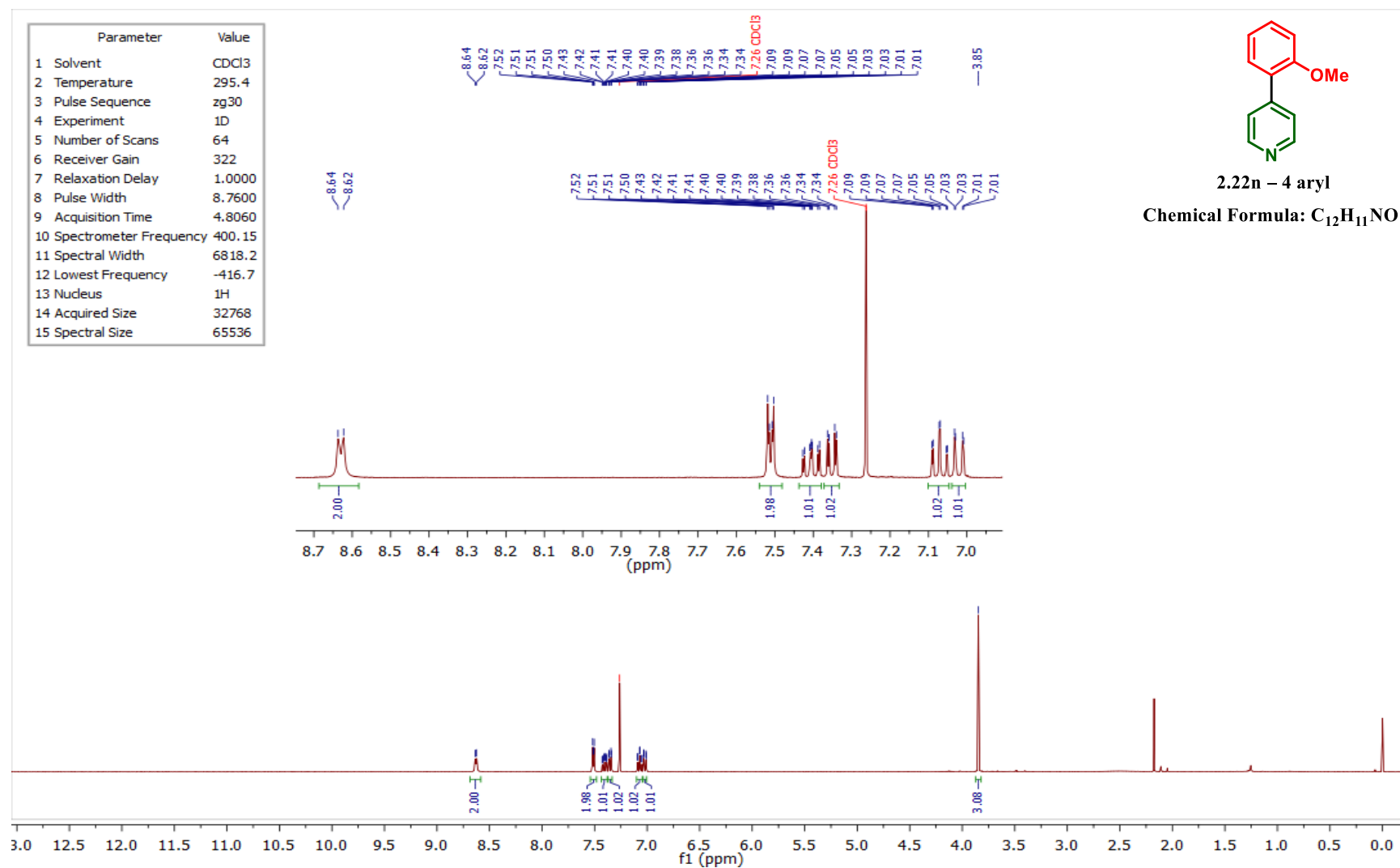


Figure 4.109 – ¹H NMR spectrum of compound 2.22n – 4 aryl in CDCl₃.

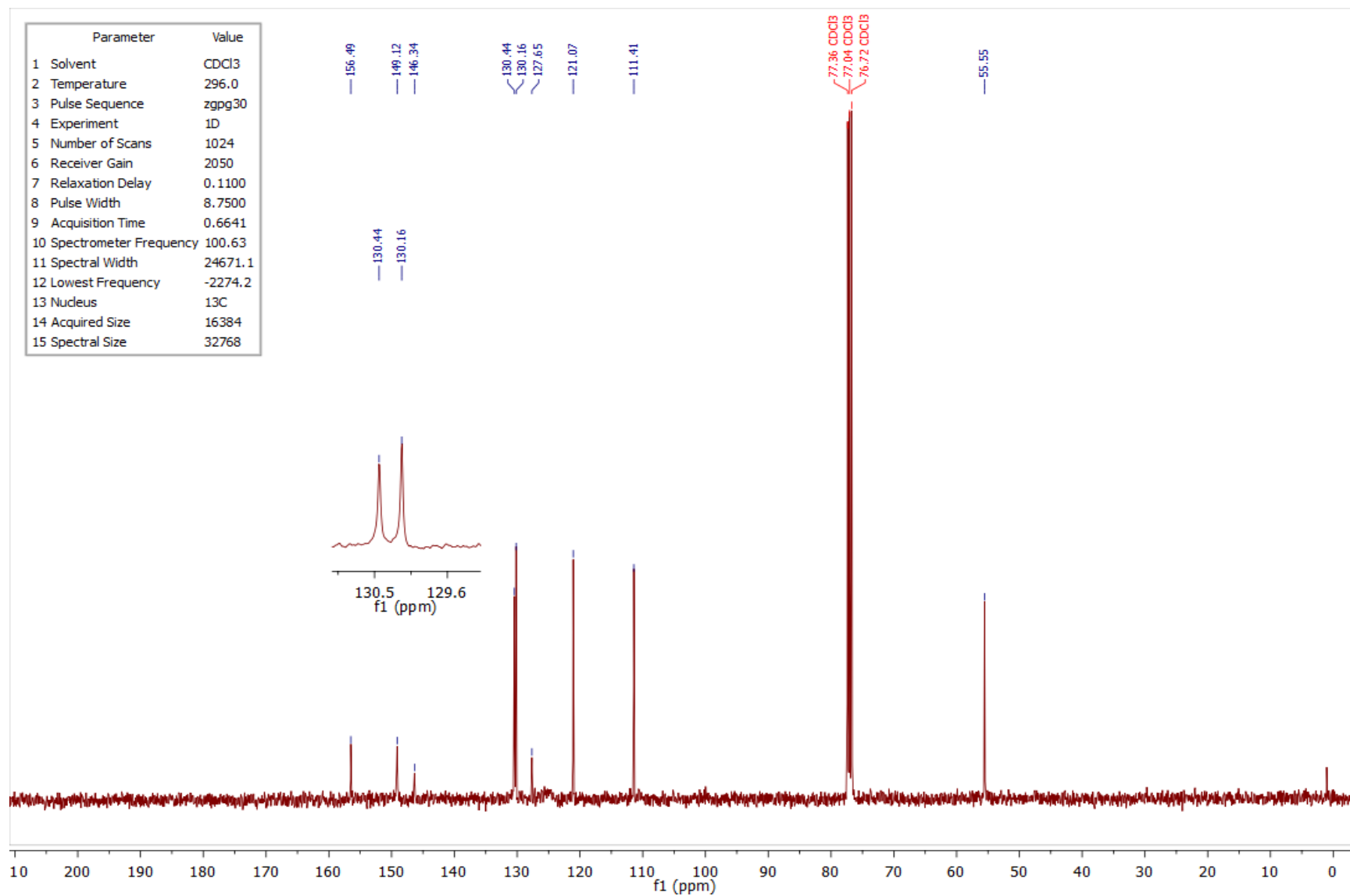


Figure 4.110 – ¹³C NMR spectrum of compound **2.22n – 4 aryl** in CDCl₃.

4.2.28 ¹H and ¹³C NMR spectra of compound 2.22o – 2 aryl

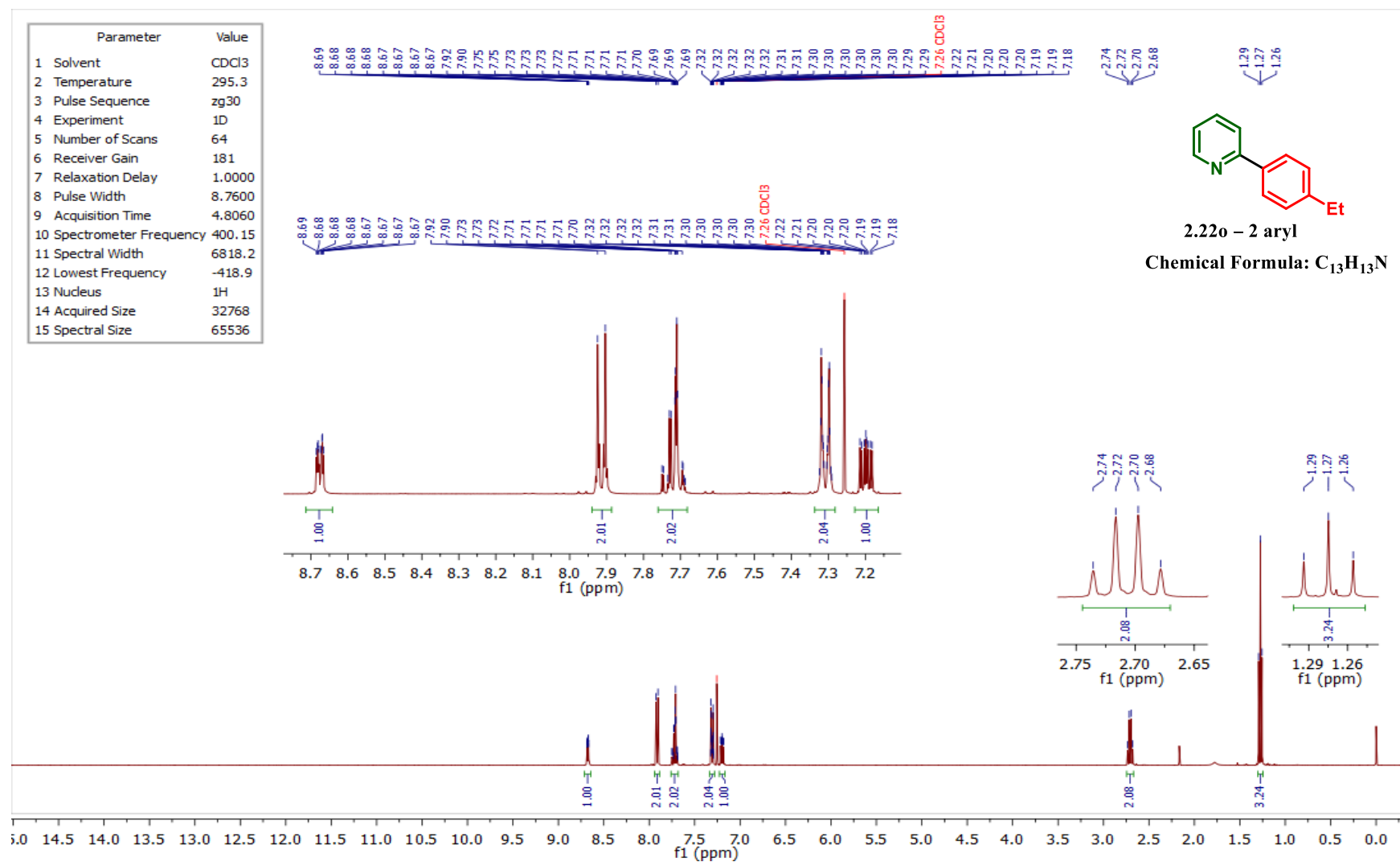


Figure 4.111 – ¹H NMR spectrum of compound 2.22o – 2 aryl in CDCl₃.

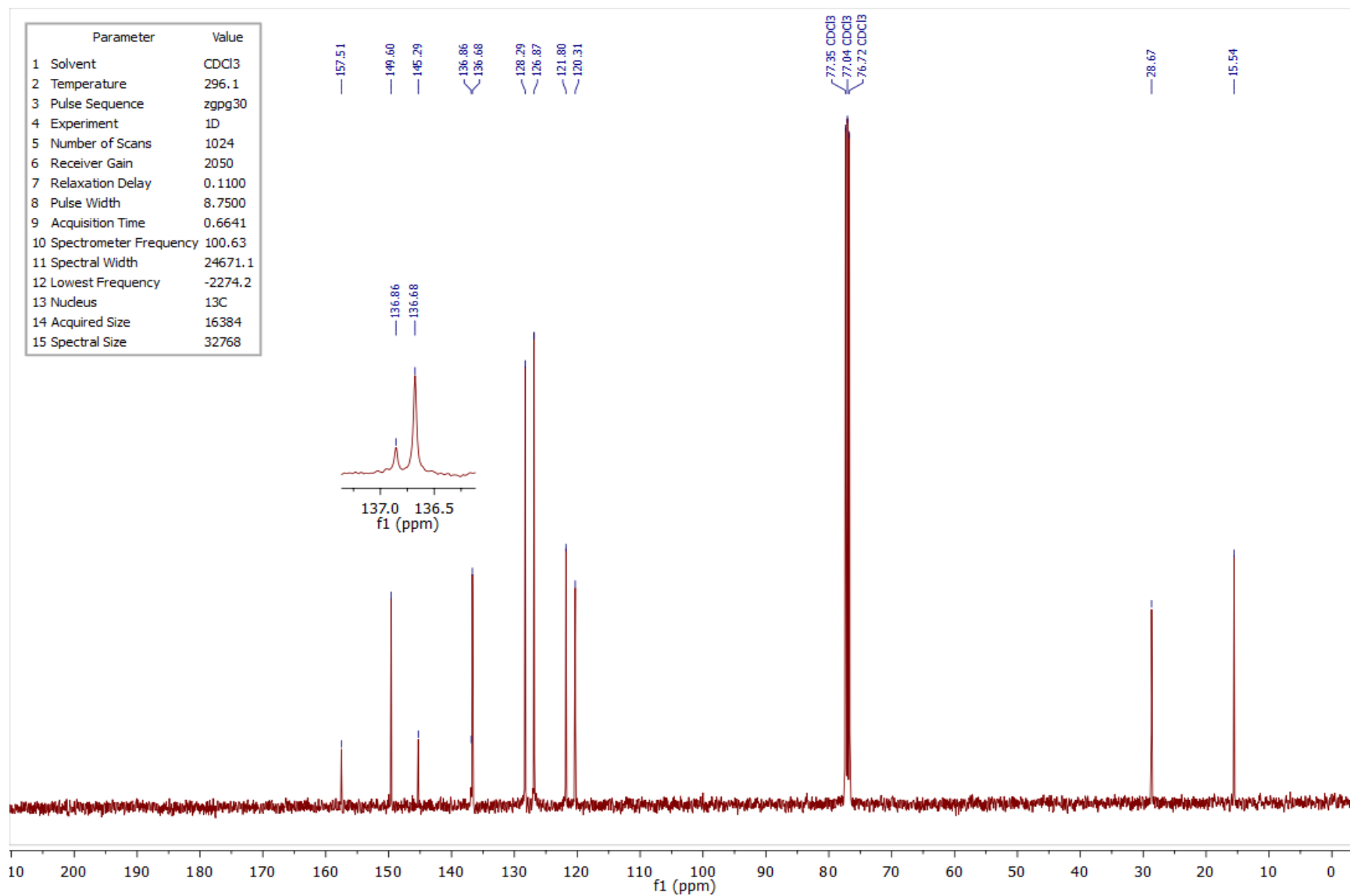


Figure 4.112 – ¹³C NMR spectrum of compound **2.22o** – **2 aryl** in CDCl₃.

4.2.29 ¹H and ¹³C NMR spectra of compound 2.22o – 4 aryl

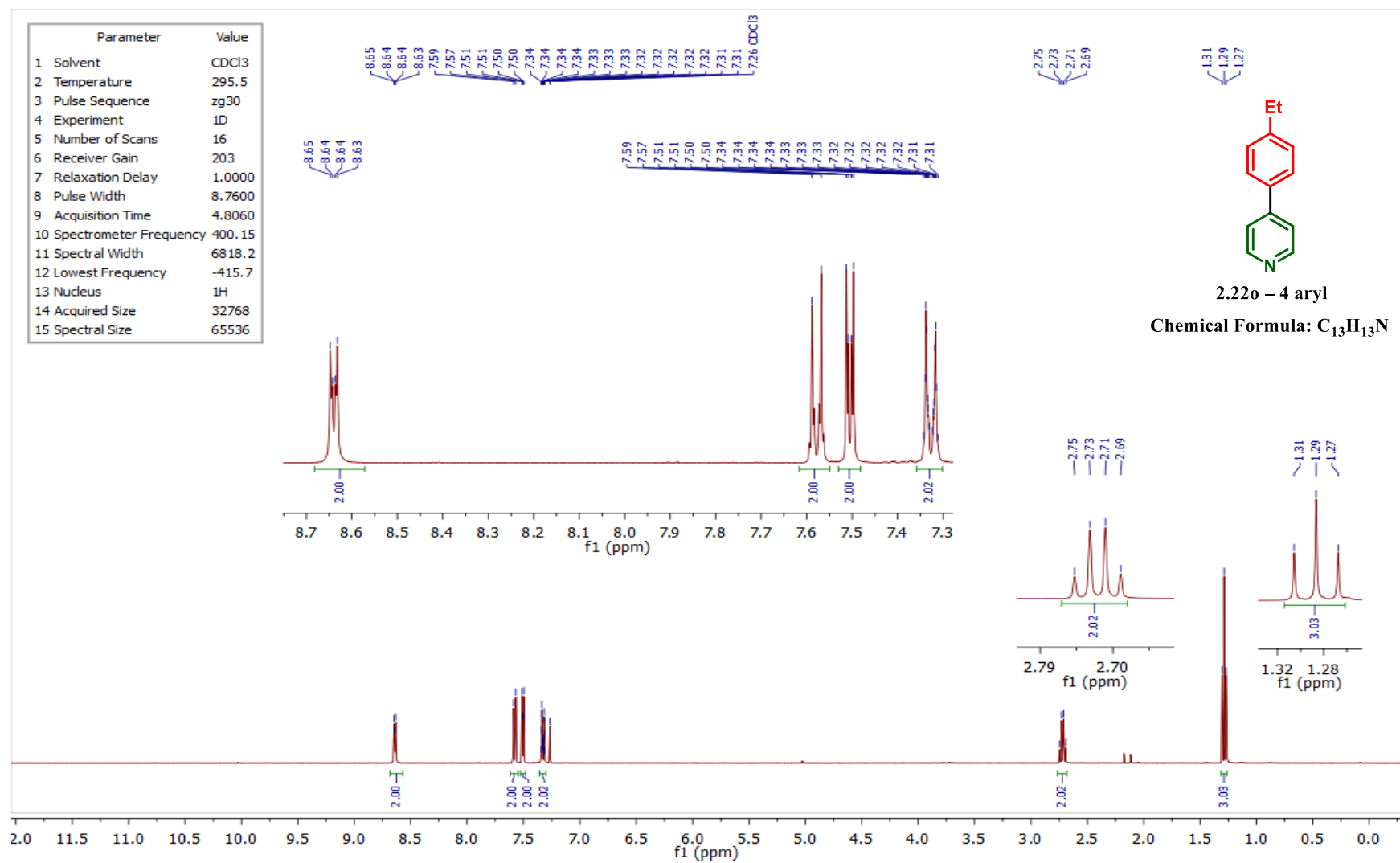


Figure 4.113 – ¹H NMR spectrum of compound 2.22o – 4 aryl in CDCl₃.

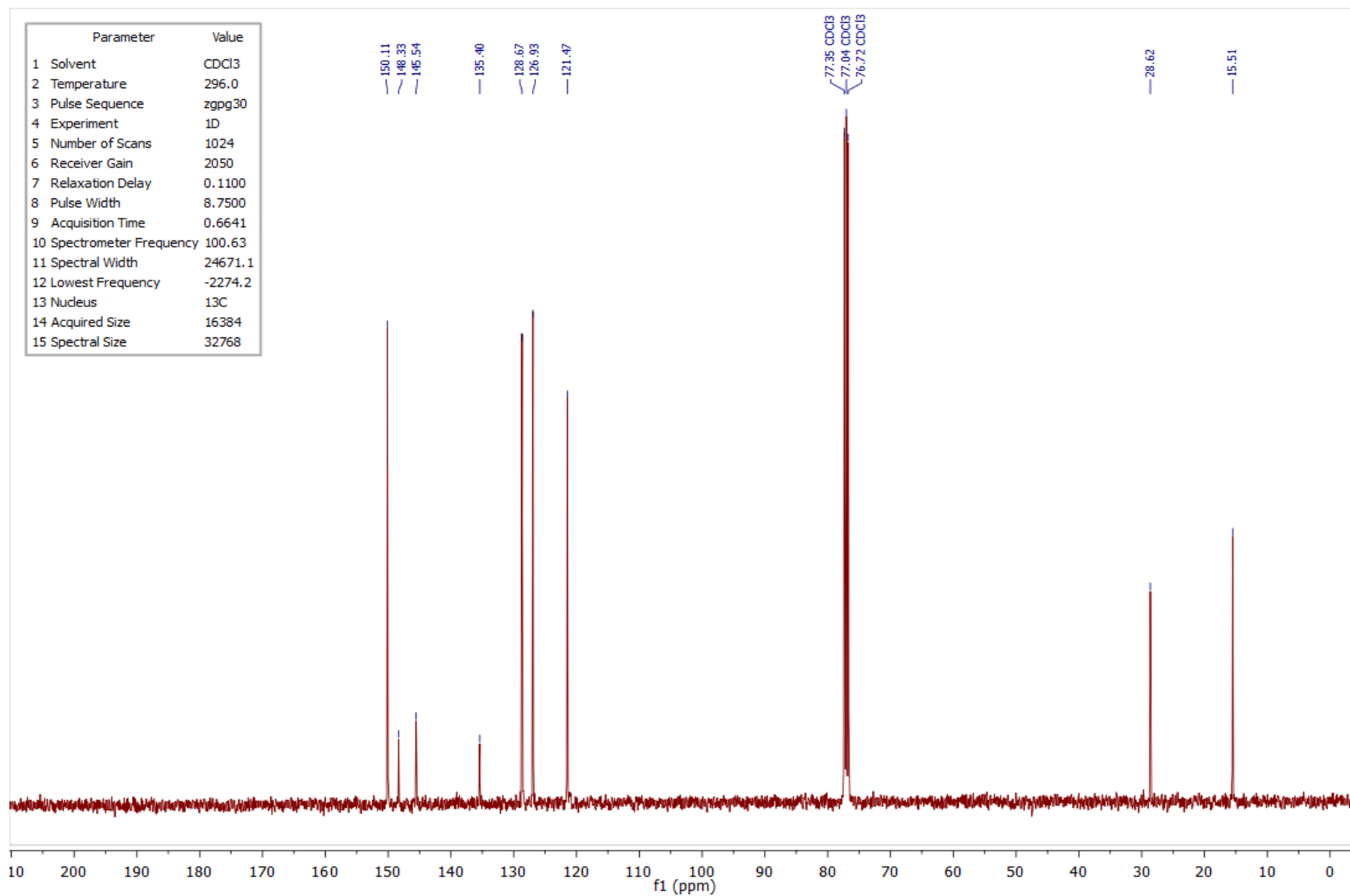


Figure 4.114 – ¹³C NMR spectrum of compound **2.22o** – **4 aryl** in CDCl₃.

4.2.30 ^1H and ^{13}C NMR spectra of compound 2.22r – 2 aryl

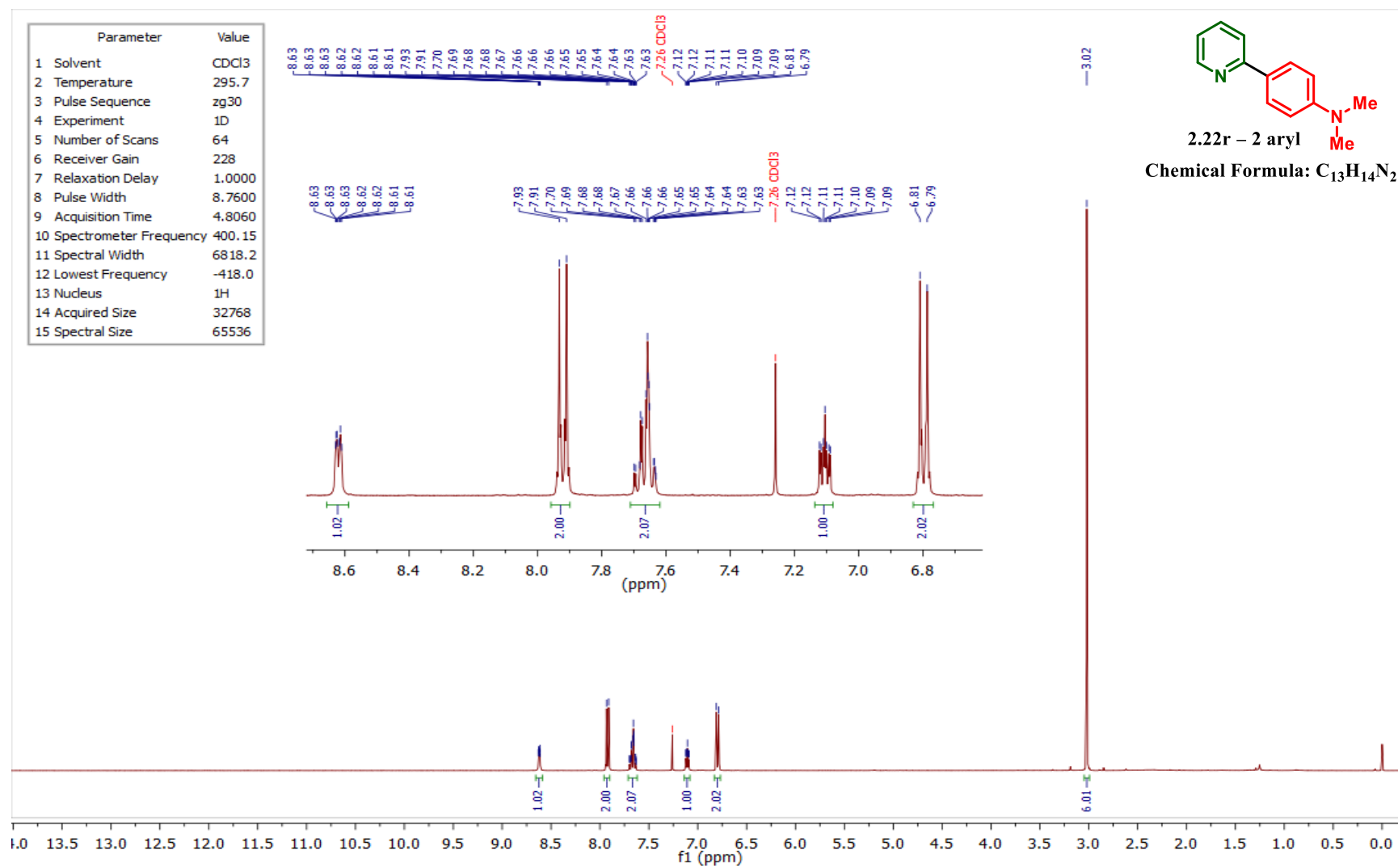


Figure 4.115 – ^1H NMR spectrum of compound 2.22r – 2 aryl in CDCl_3 .

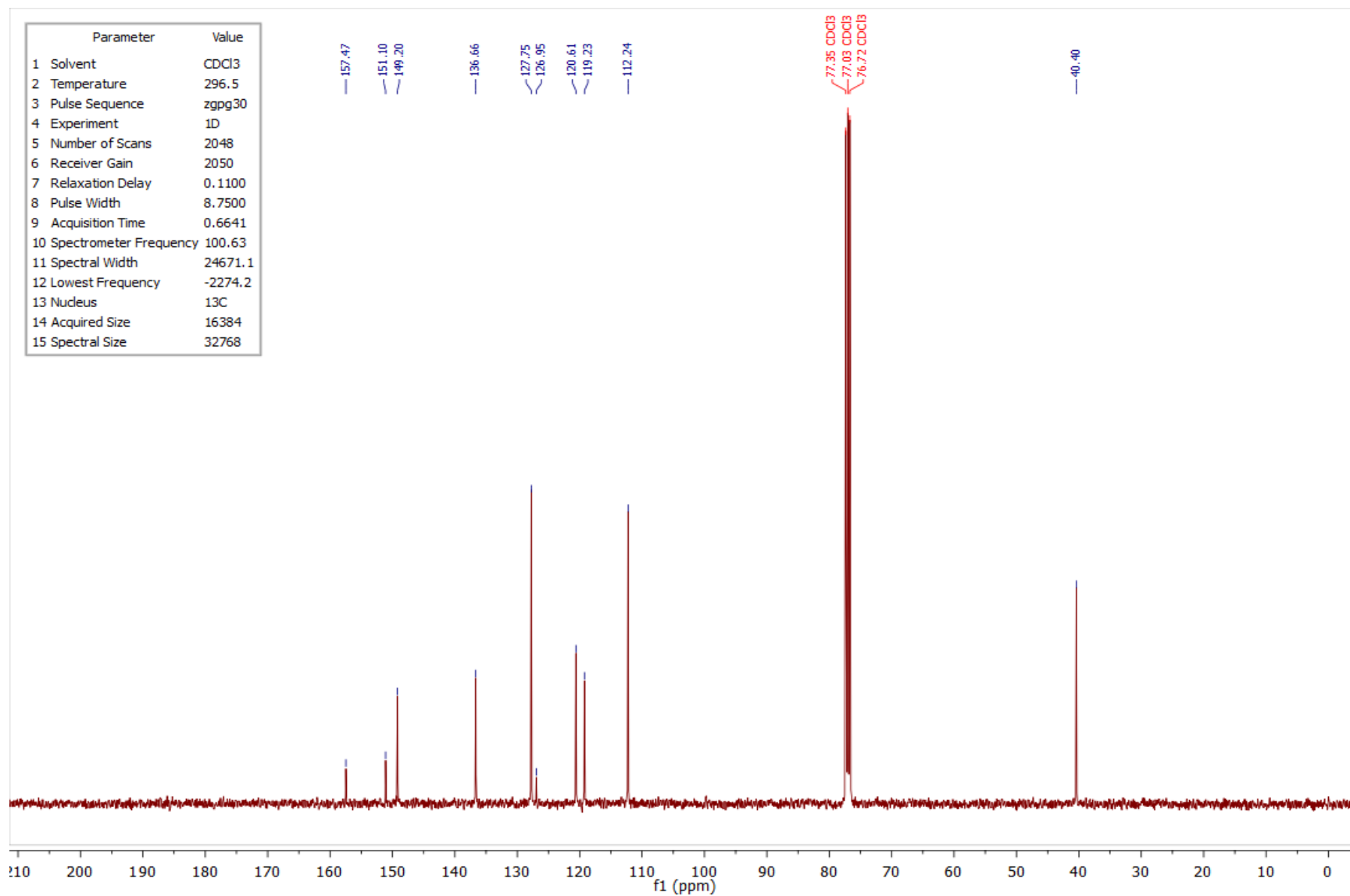


Figure 4.116 – ¹³C NMR spectrum of compound **2.22r** – **2 aryl** in CDCl₃.

4.2.31 ^1H and ^{13}C NMR spectra of compound 2.22s – 2 aryl

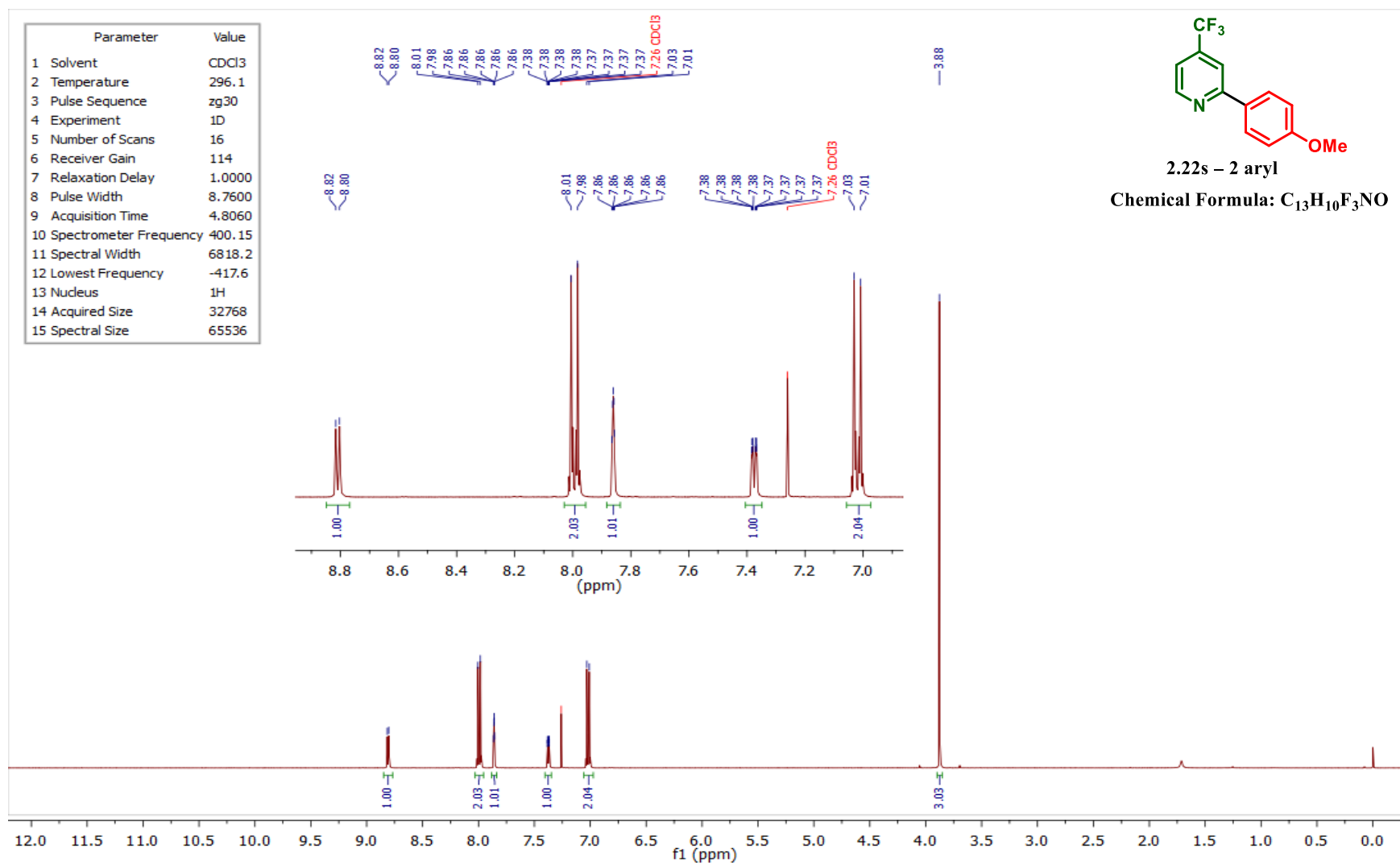


Figure 4.117 – ^1H NMR spectrum of compound 2.22s – 2 aryl in CDCl_3 .

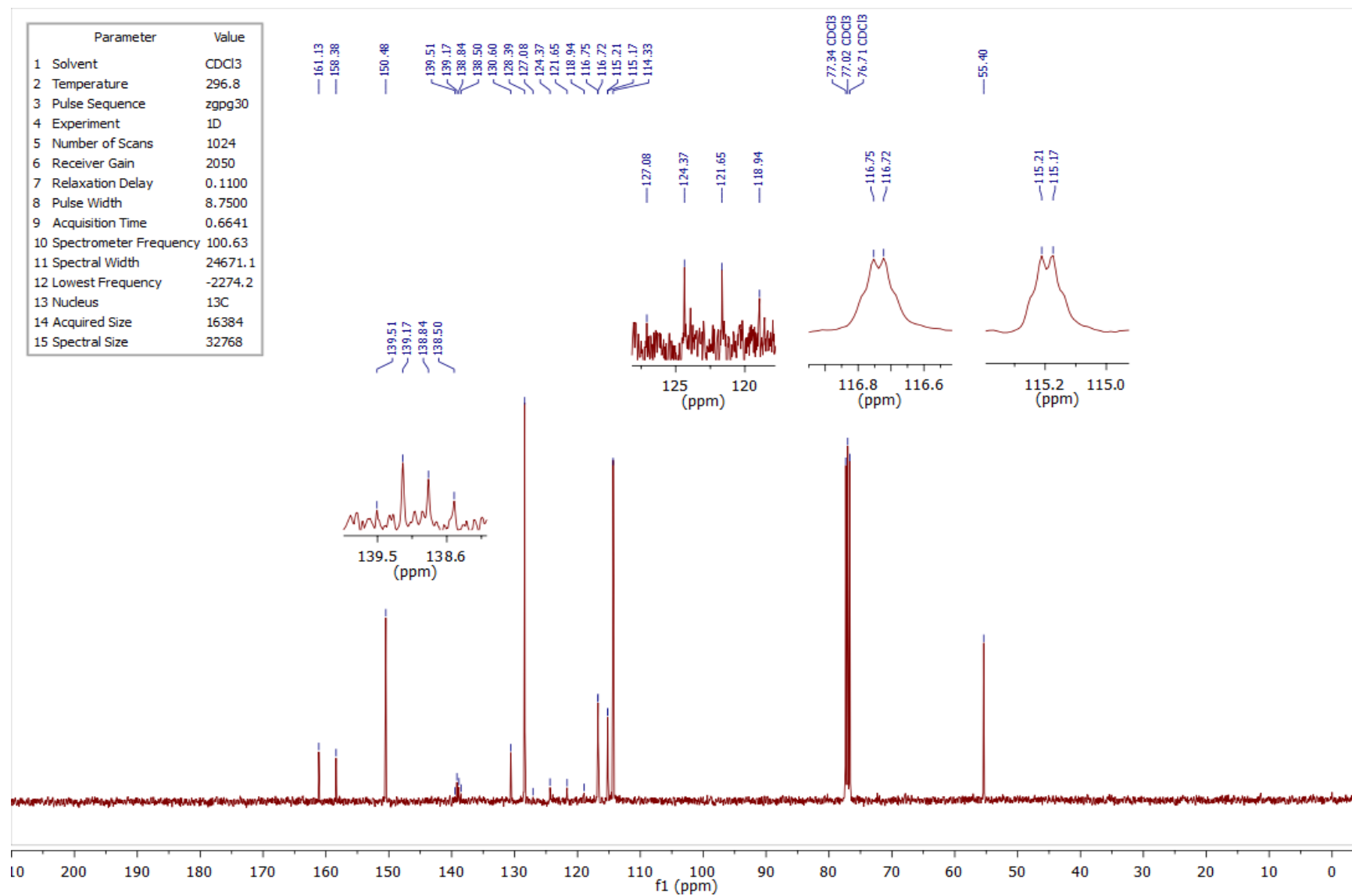


Figure 4.118 – ¹³C NMR spectrum of compound **2.22s – 2 aryl** in CDCl₃.

4.2.32 ^1H and ^{13}C NMR spectra of compound 2.22t – 2 aryl

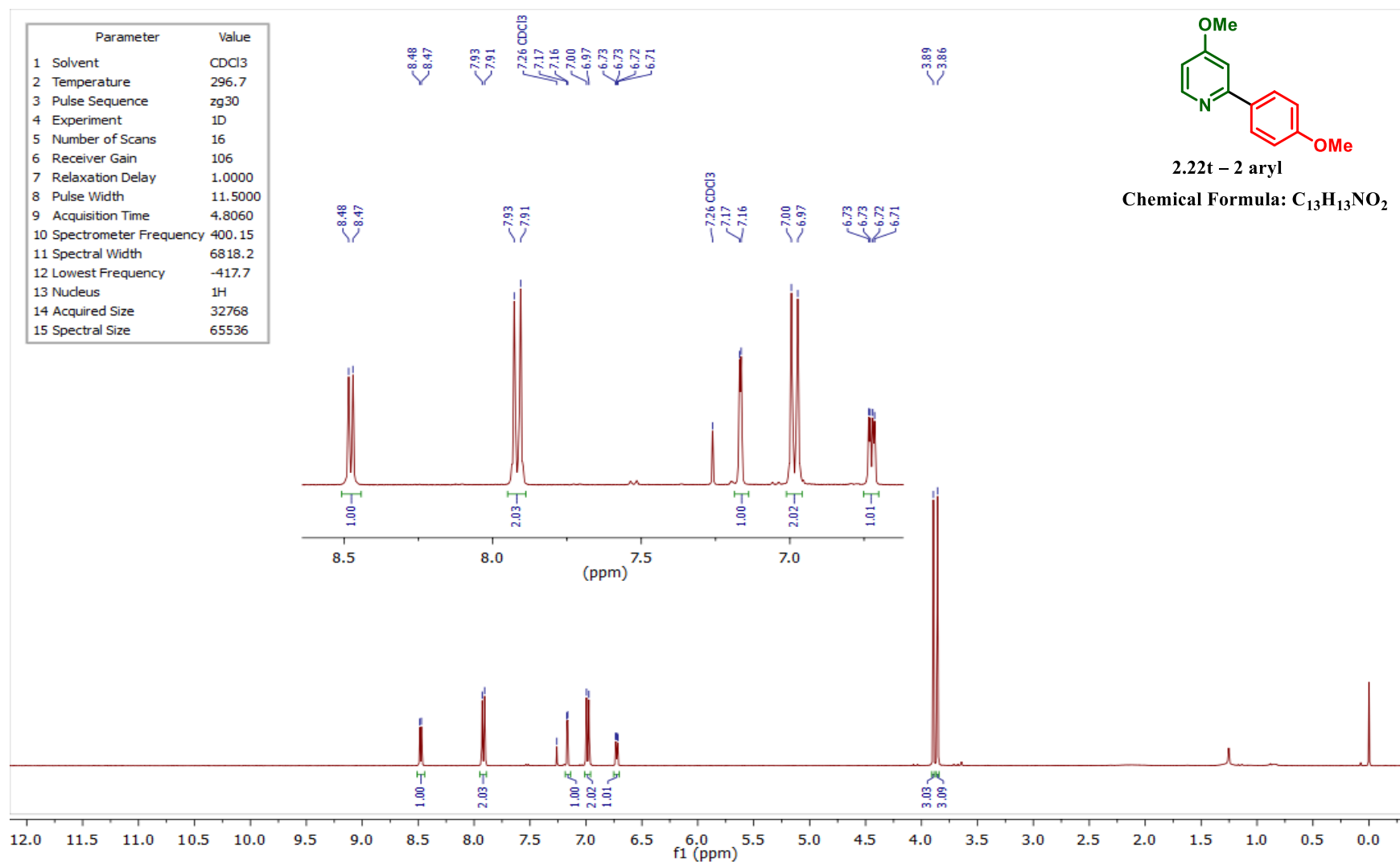


Figure 4.119 – ^1H NMR spectrum of compound 2.22t – 2 aryl in CDCl_3 .

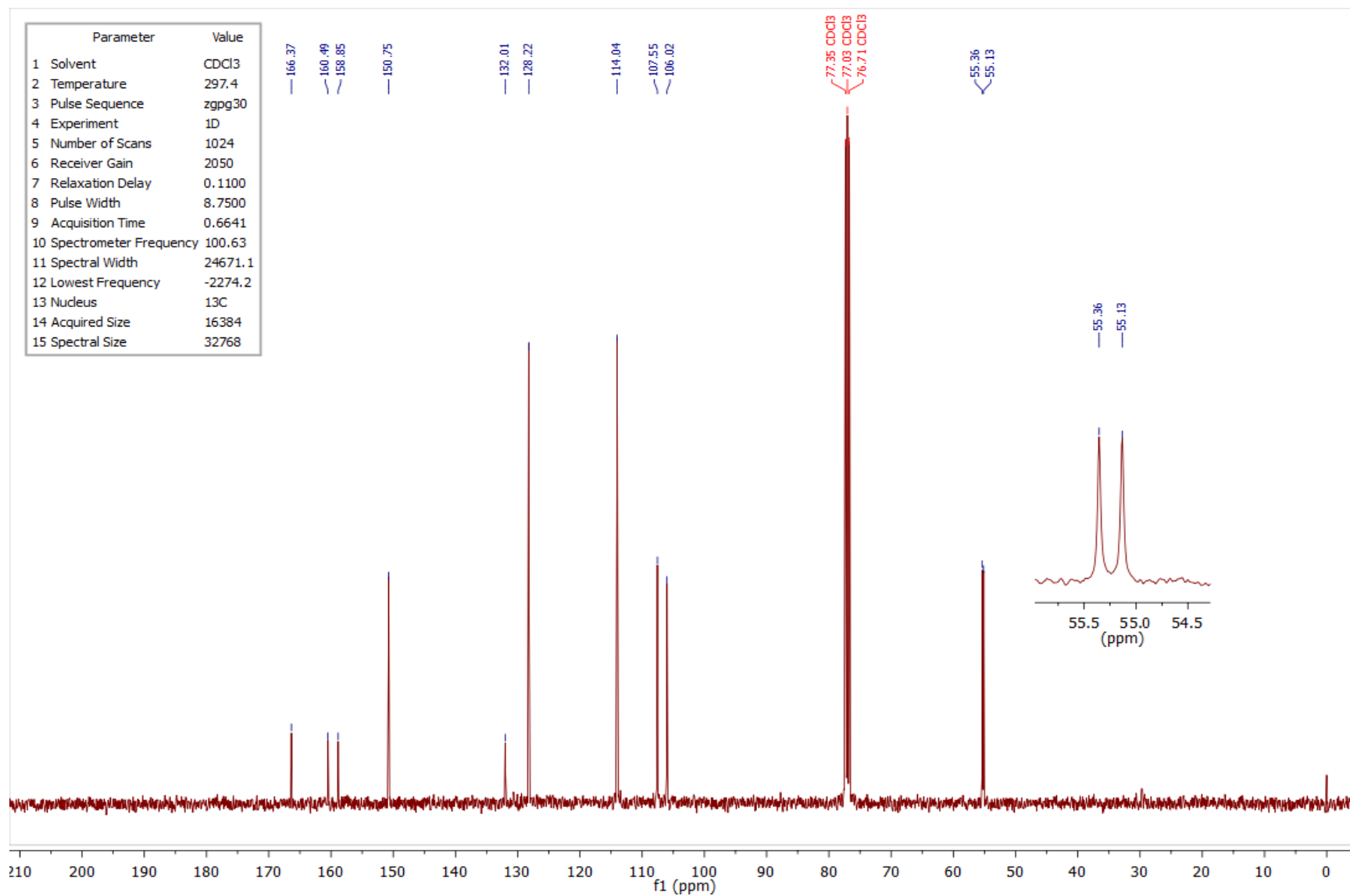


Figure 4.120 – ^{13}C NMR spectrum of compound **2.22t – 2 aryl** in CDCl_3 .

4.2.33 ¹H and ¹³C NMR spectra of compound 2.22u – 2 aryl

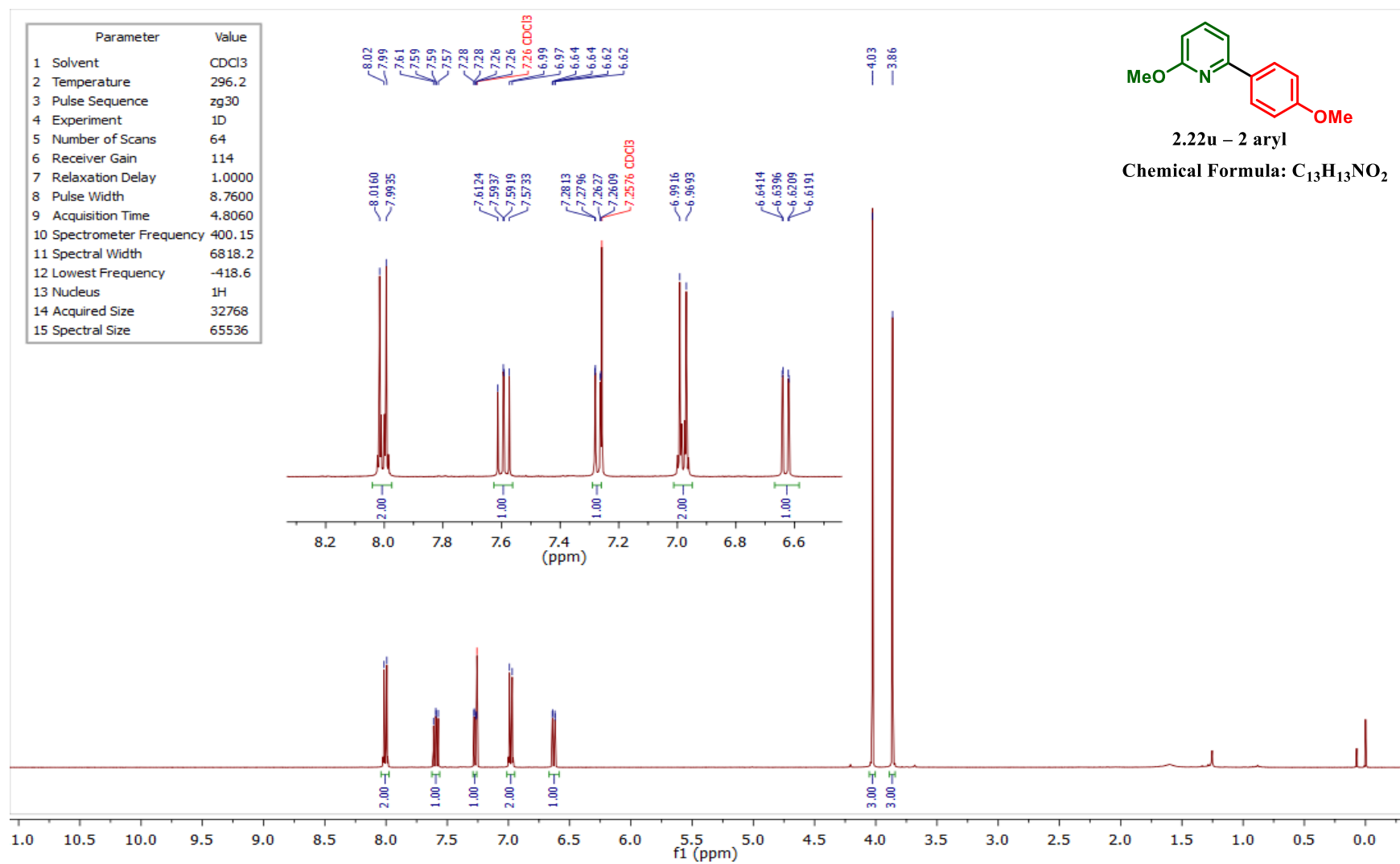


Figure 4.121 – ¹H NMR spectrum of compound 2.22u – 2 aryl in CDCl₃.

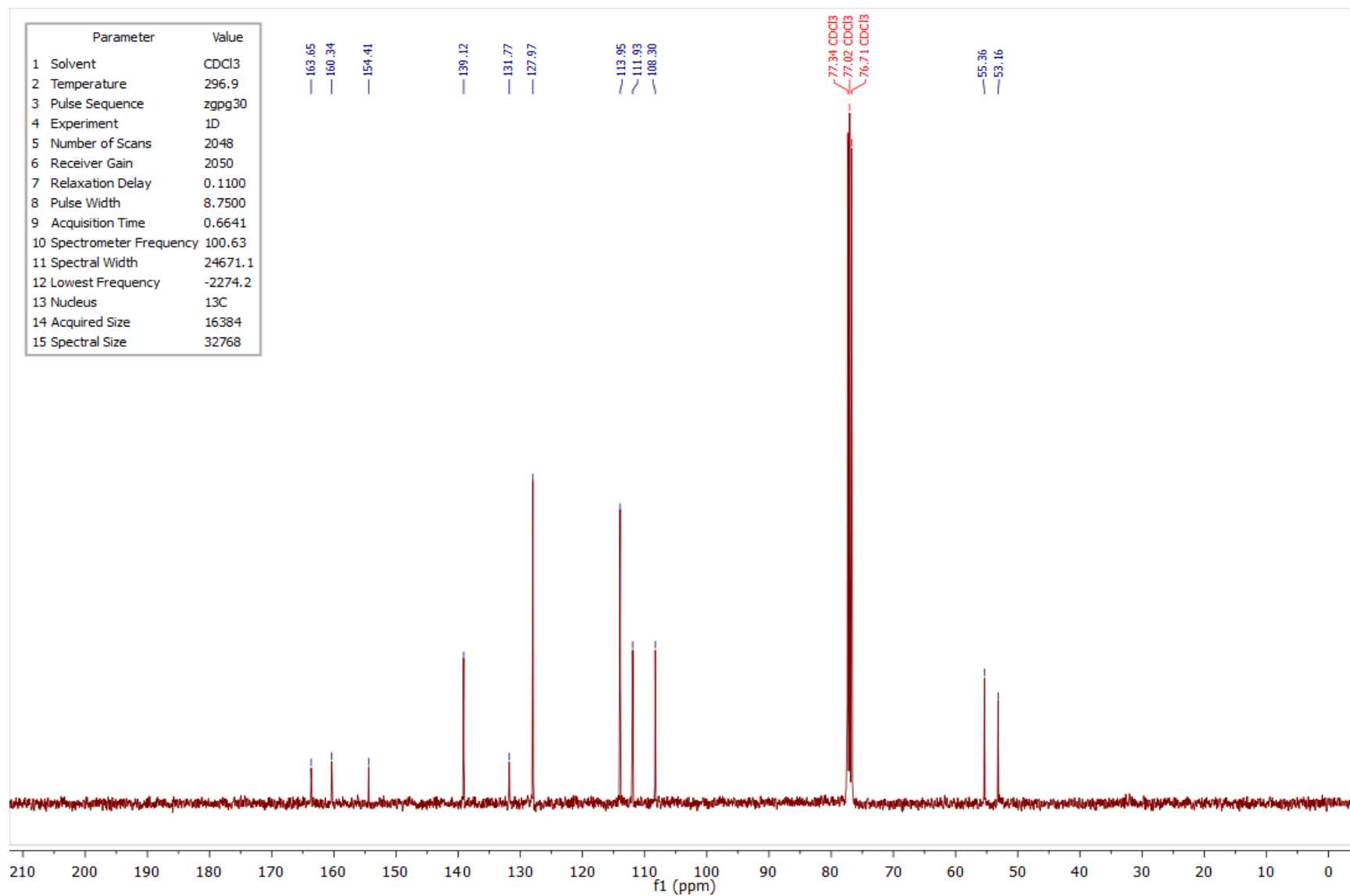


Figure 4.122 – ¹³C NMR spectrum of compound 2.22u – 2 aryl in CDCl₃.

4.2.34 ¹H and ¹³C NMR spectra of compound 2.22u – 4 aryl

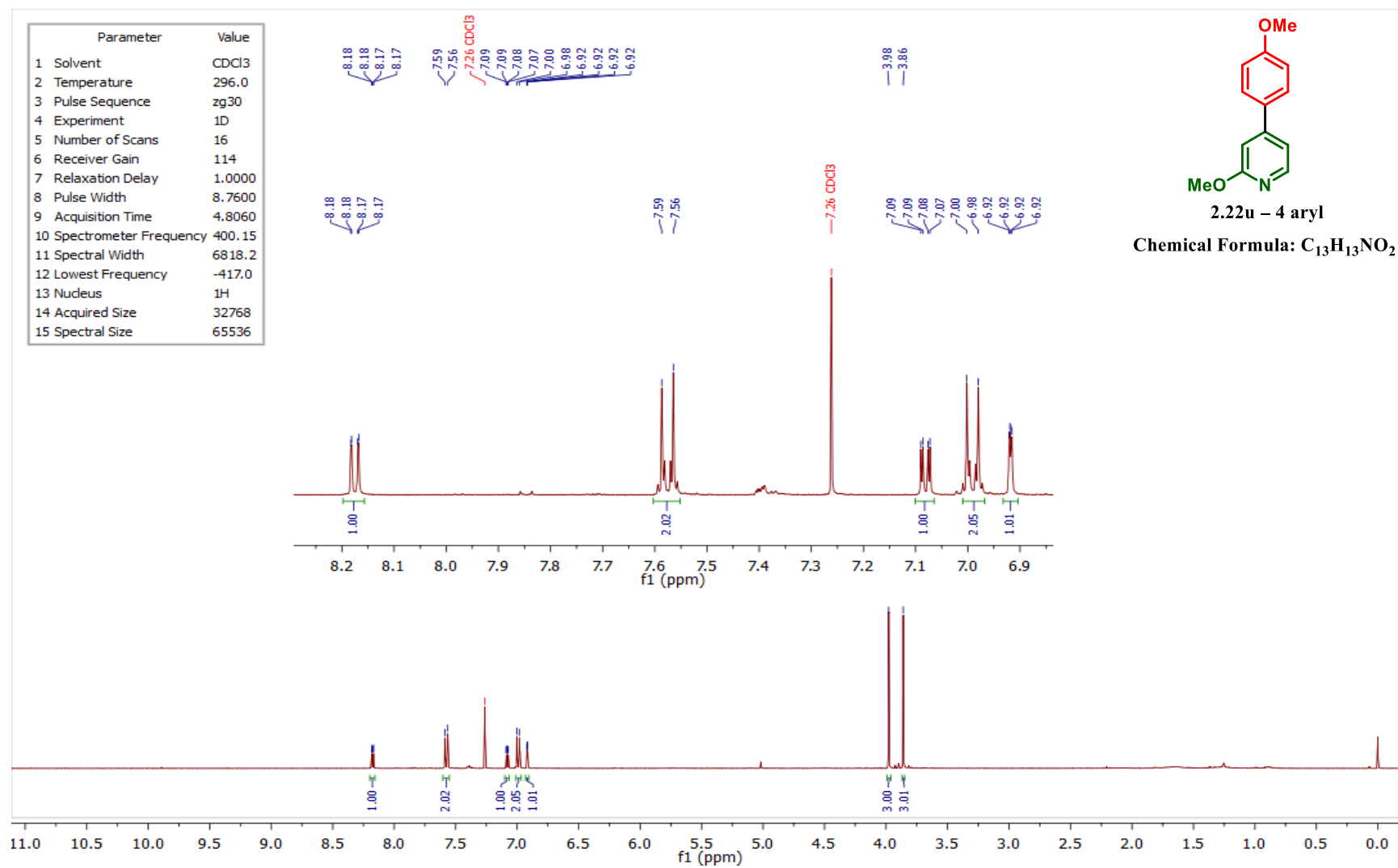


Figure 4.123 – ¹H NMR spectrum of compound 2.22u – 4 aryl in CDCl₃.

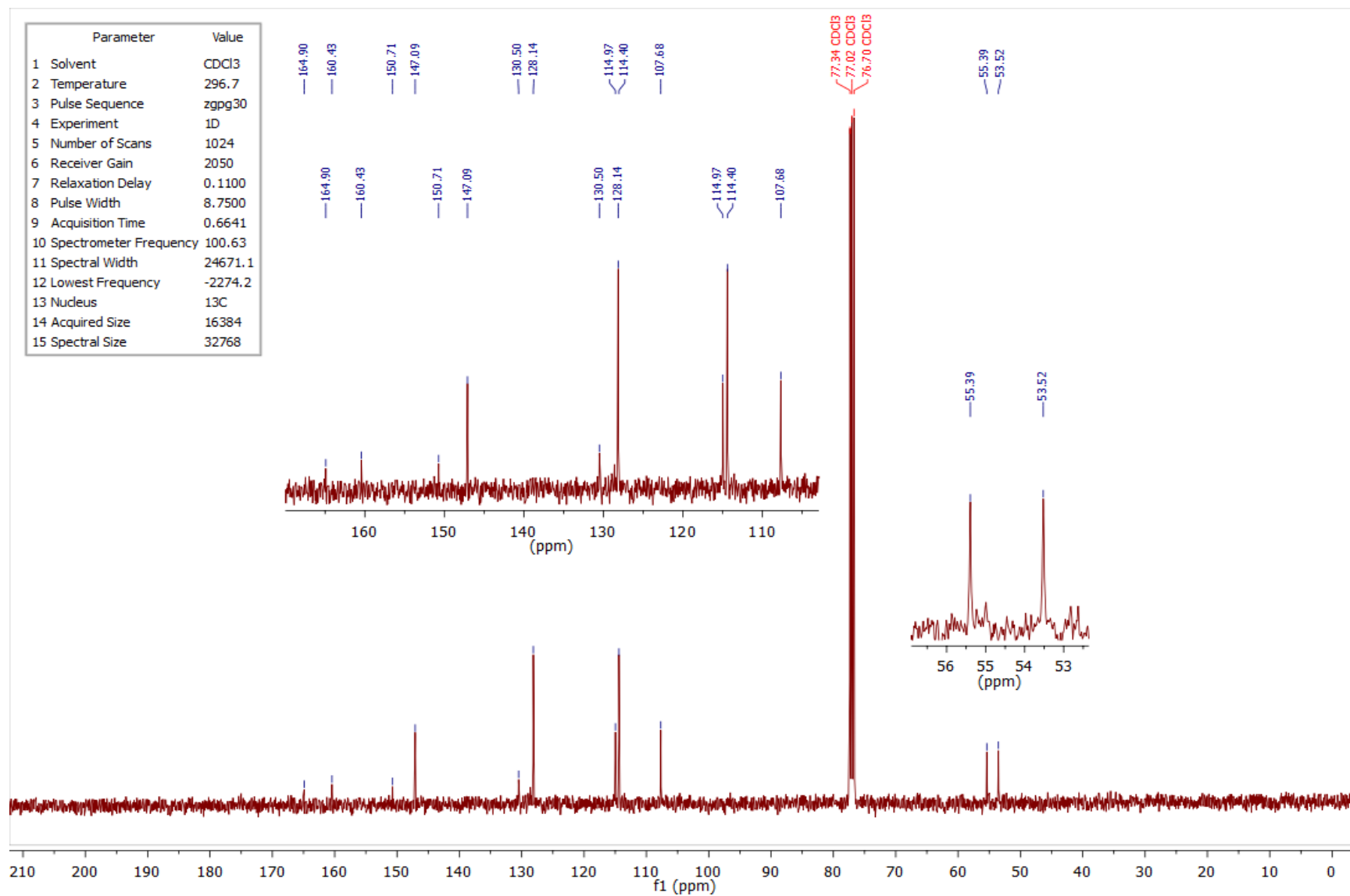


Figure 4.124 – ¹³C NMR spectrum of compound 2.22u – 4 aryl in CDCl₃.

4.2.35 ^1H and ^{13}C NMR spectra of compound 2.22v

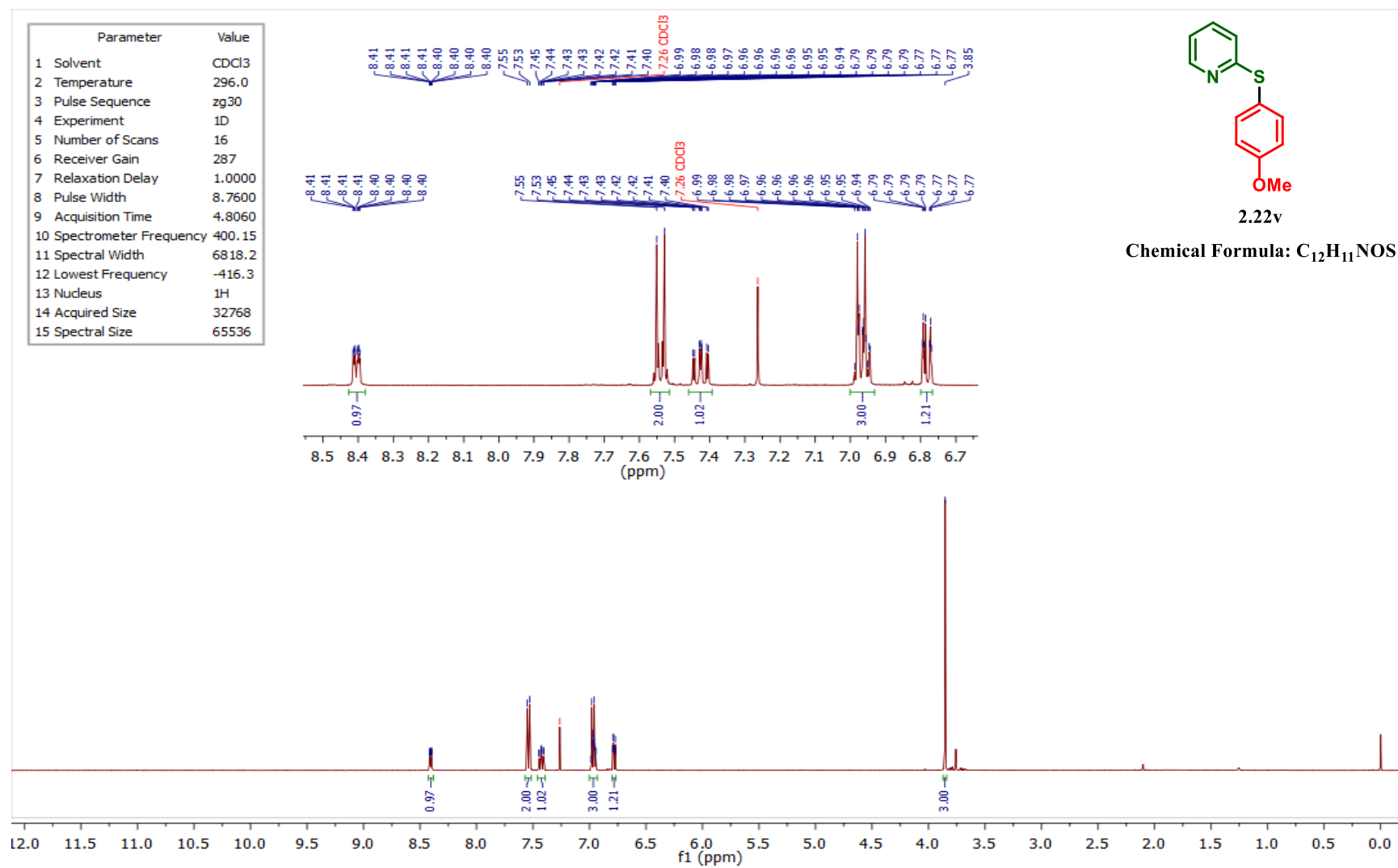


Figure 4.125 – ^1H NMR spectrum of compound 2.22v in CDCl_3 .

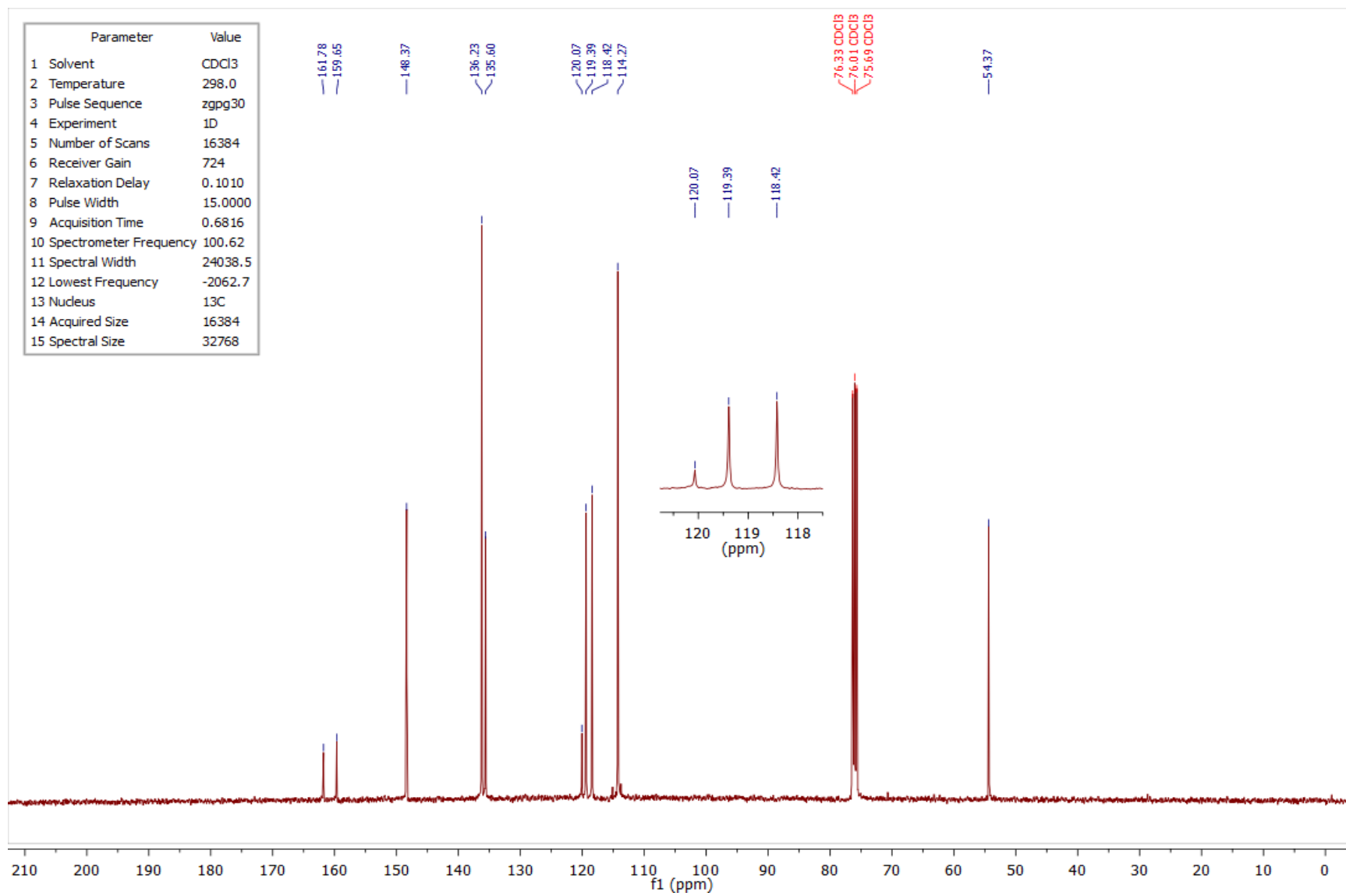


Figure 4.126 – ¹³C NMR spectrum of compound 2.22v in CDCl₃.

4.2.36 ^1H and ^{13}C NMR spectra of compound 2.22w – 2 aryl

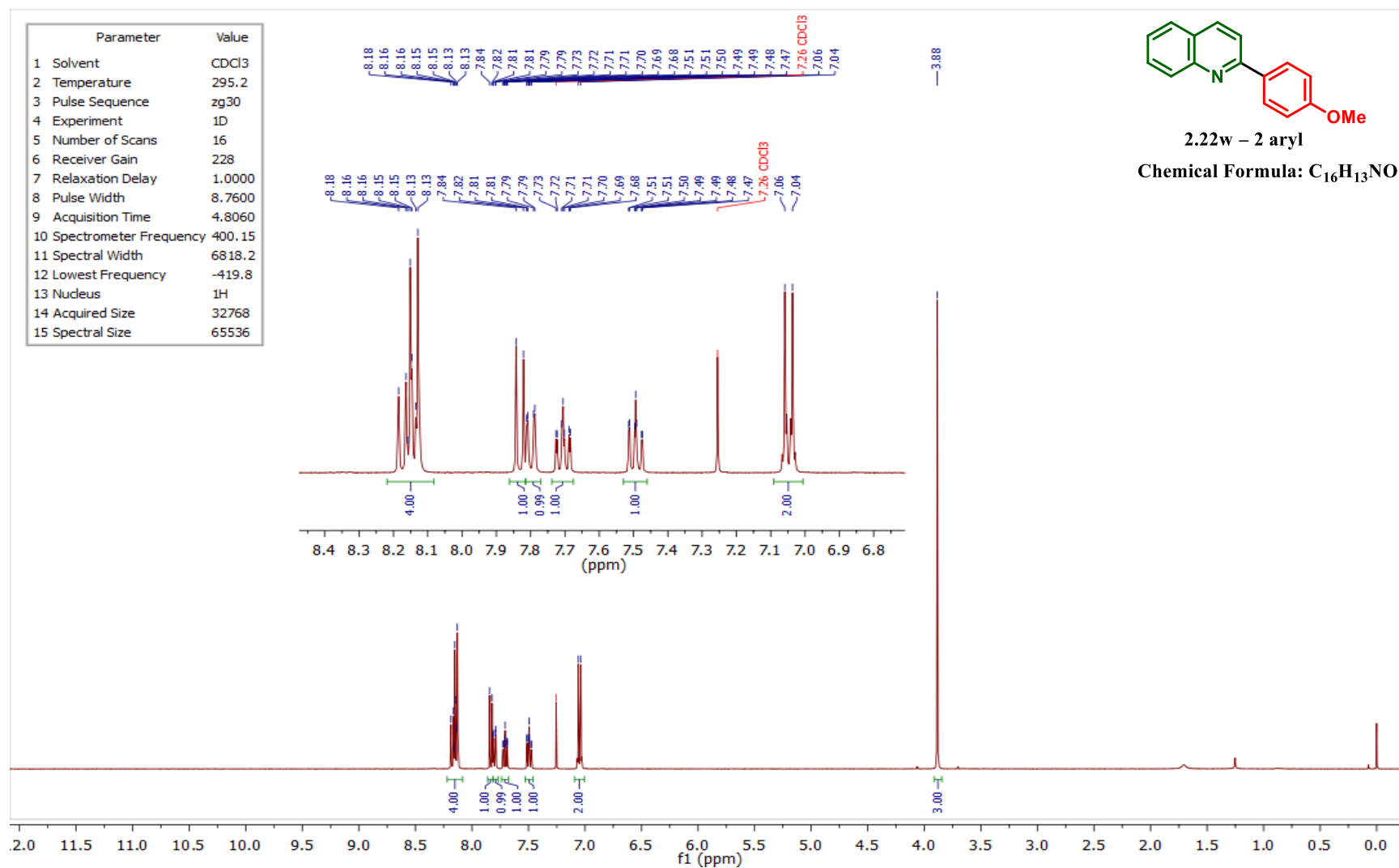


Figure 4.127 – ^1H NMR spectrum of compound 2.22w – 2 aryl in CDCl_3 .

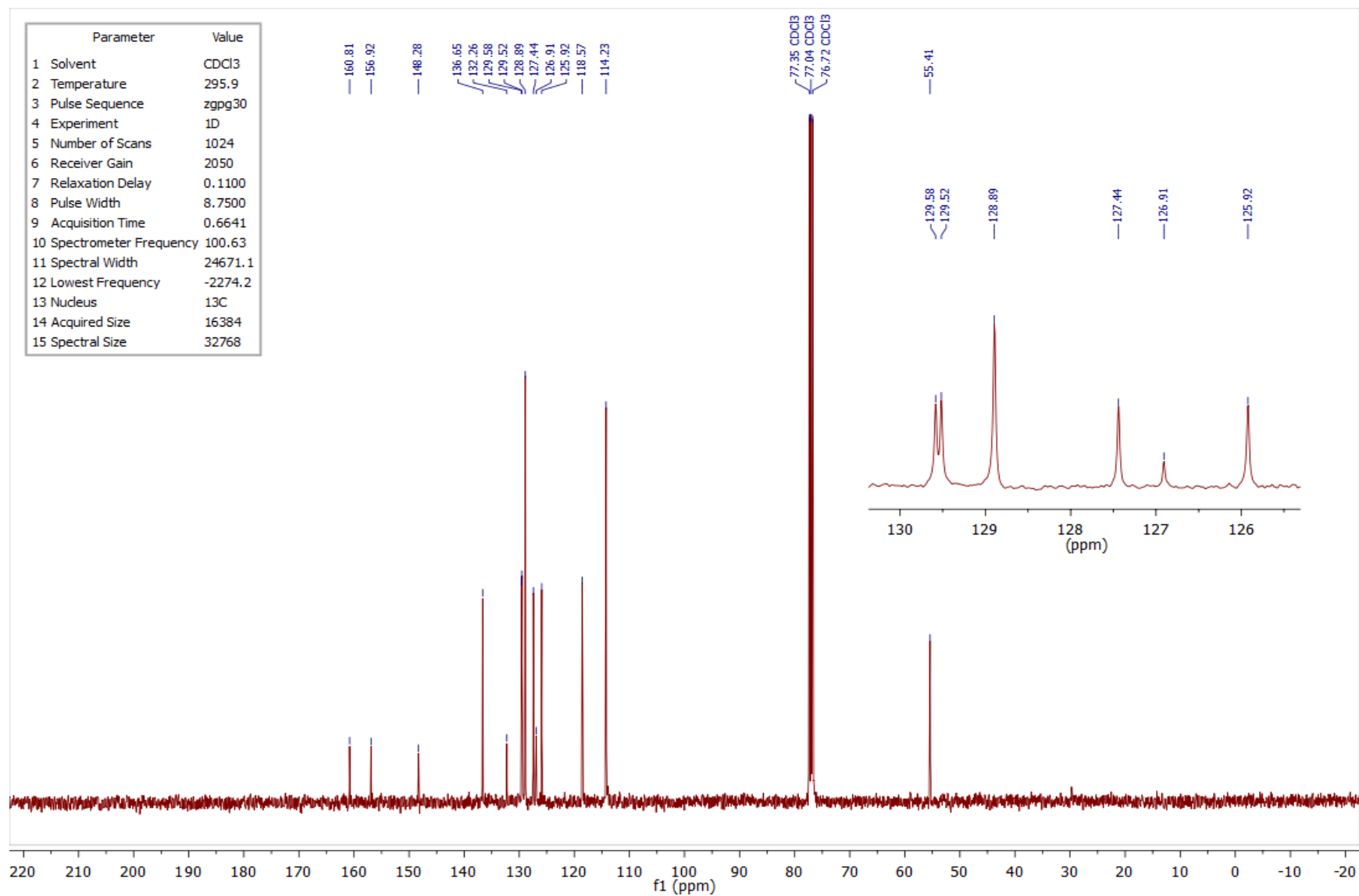


Figure 4.128 – ¹³C NMR spectrum of compound 2.22w – 2 aryl in CDCl₃.

4.2.37 ^1H and ^{13}C NMR spectra of compound 2.22w – 4 aryl

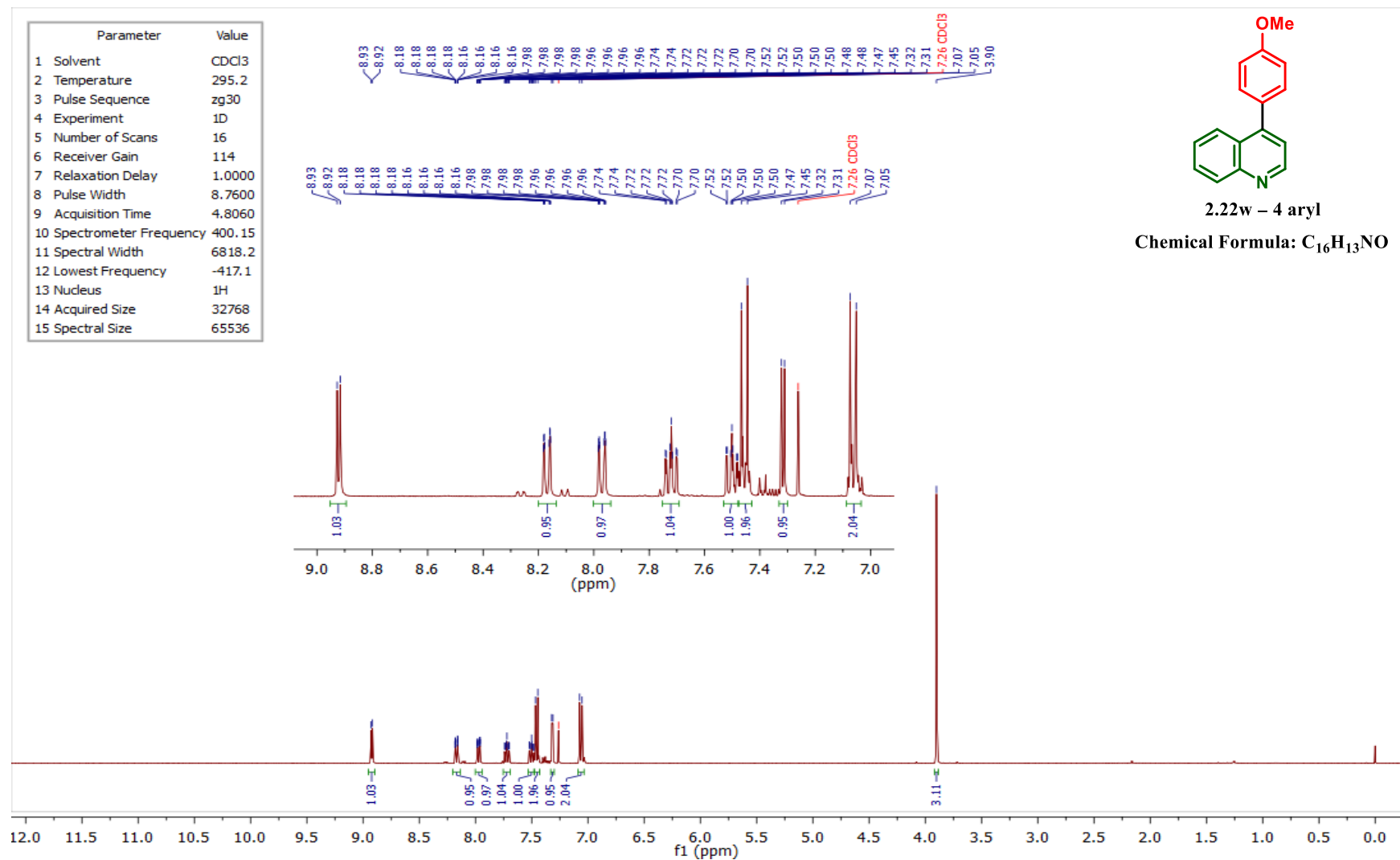


Figure 4.129 – ^1H NMR spectrum of compound 2.22w – 4 aryl in CDCl_3 .

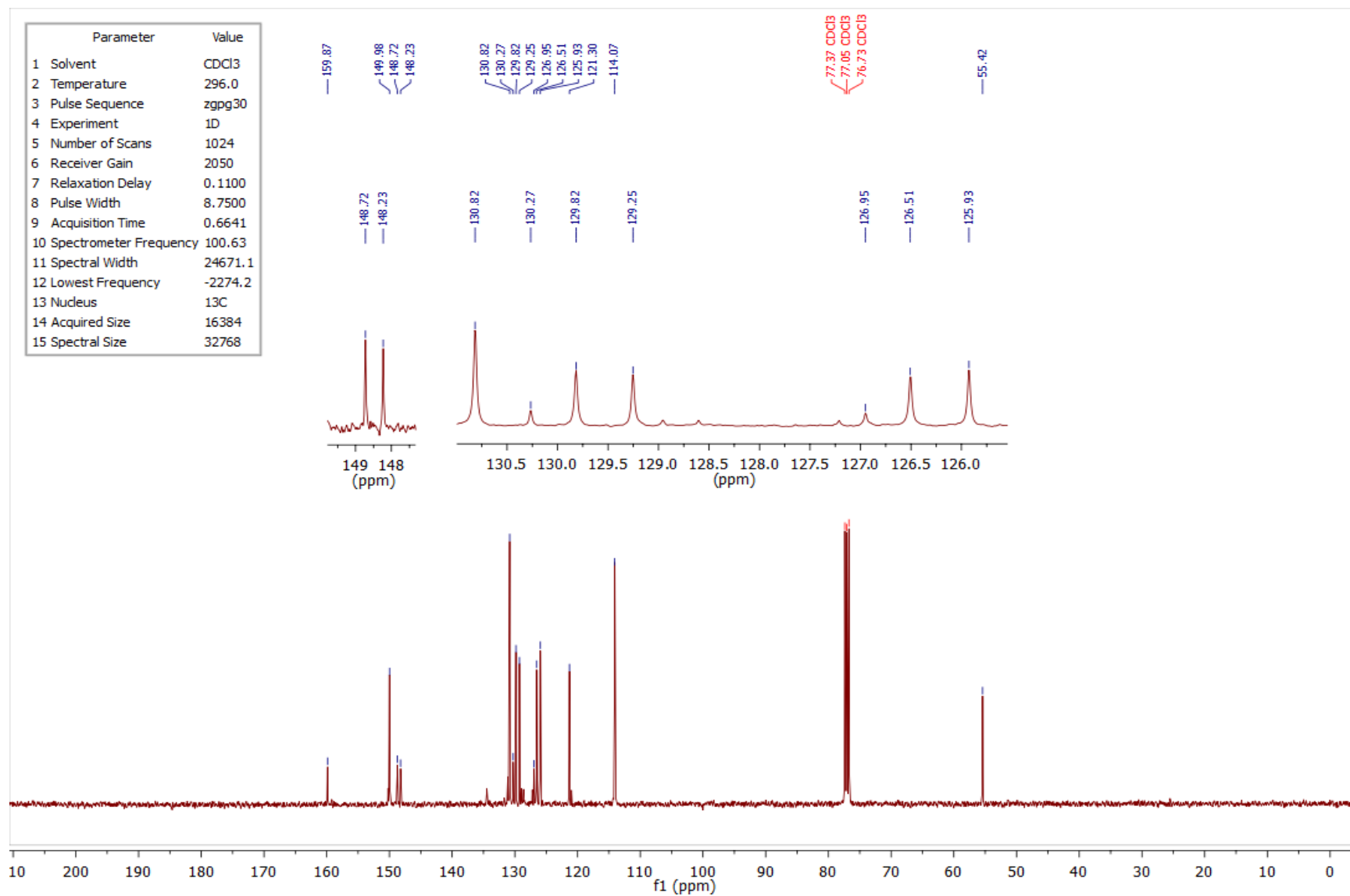


Figure 4.130 – ¹³C NMR spectrum of compound **2.22w** – **4 aryl** in CDCl₃.

4.2.38 ^1H and ^{13}C NMR spectra of compound 2.22x

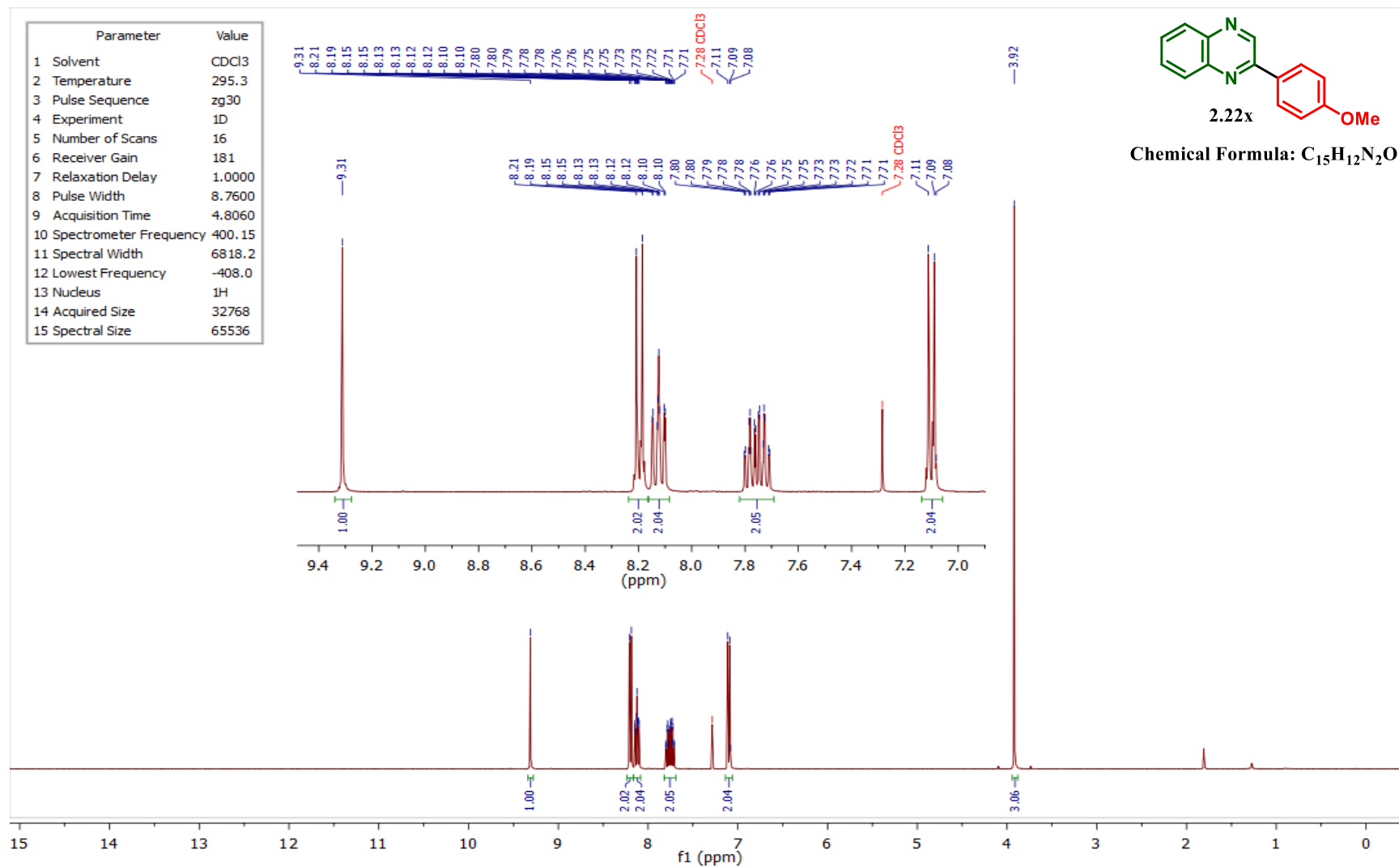


Figure 4.131 – ^1H NMR spectrum of compound 2.22x in CDCl_3 .

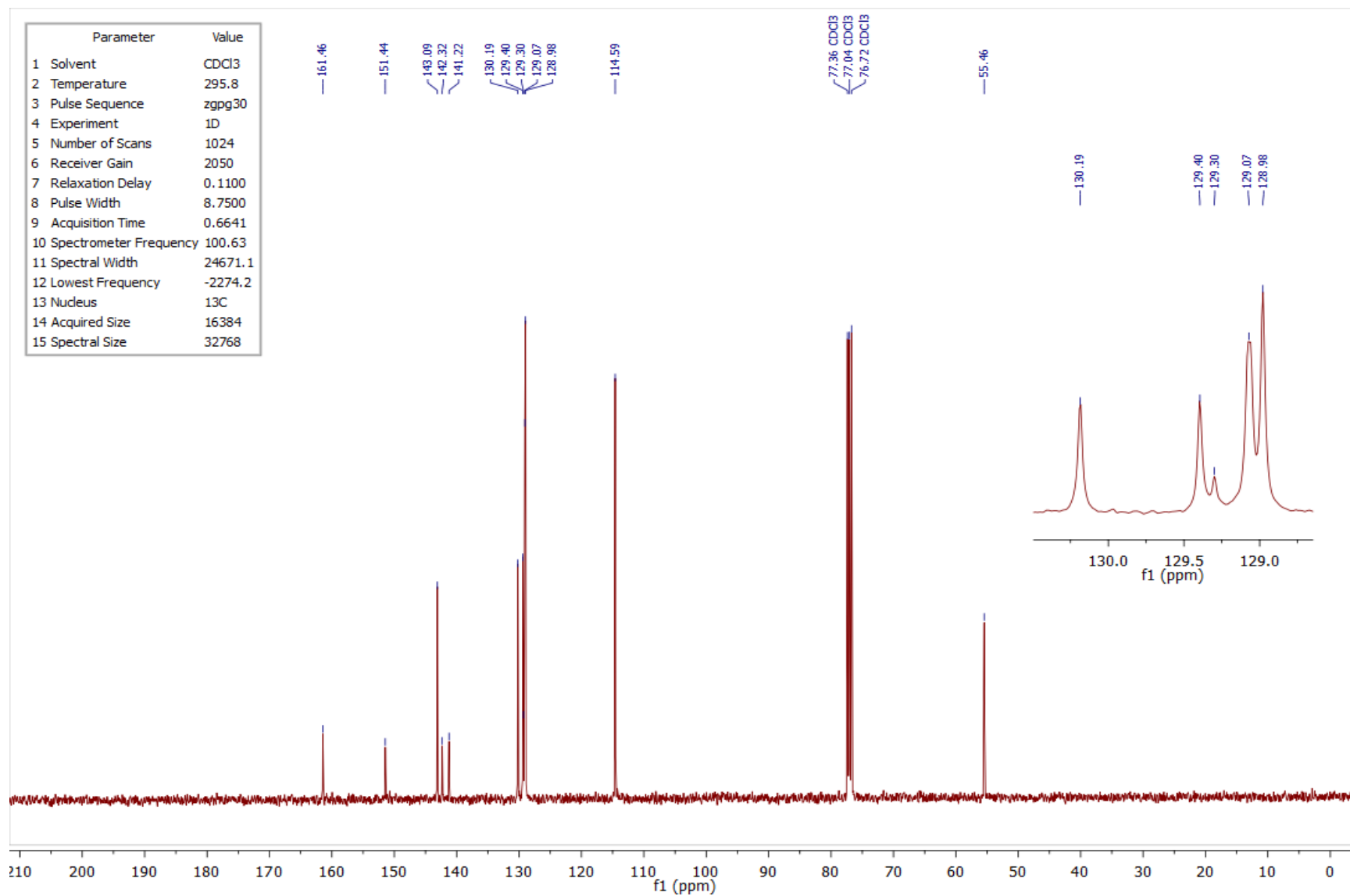


Figure 4.132 – ¹³C NMR spectrum of compound **2.22x** in CDCl₃.

4.3 Spectra of Chapter 3

4.3.1 ^1H , ^{13}C and ^{19}F NMR spectra of compound 3.26a

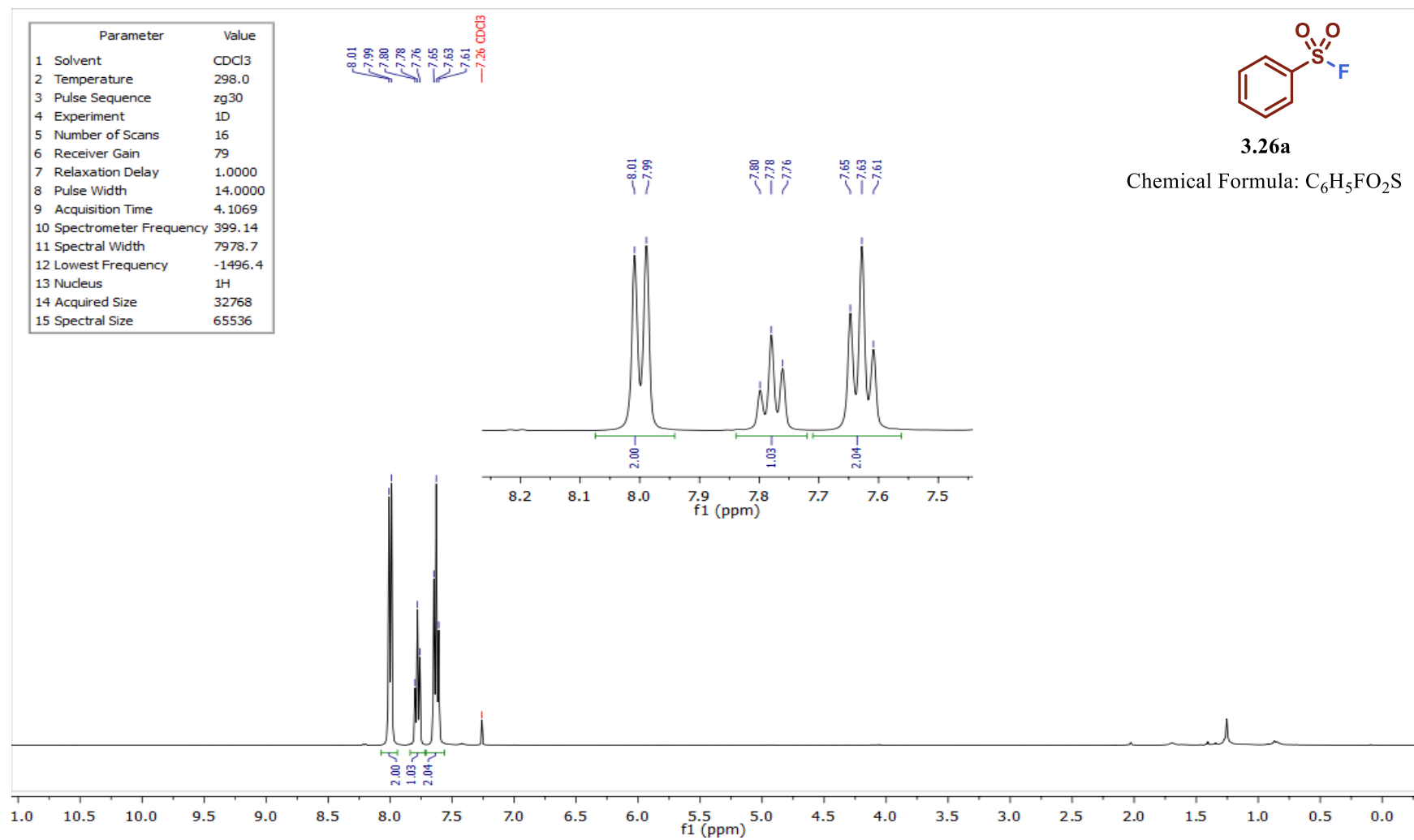


Figure 4.133 – ^1H NMR spectrum of compound 3.26a in CDCl_3 .

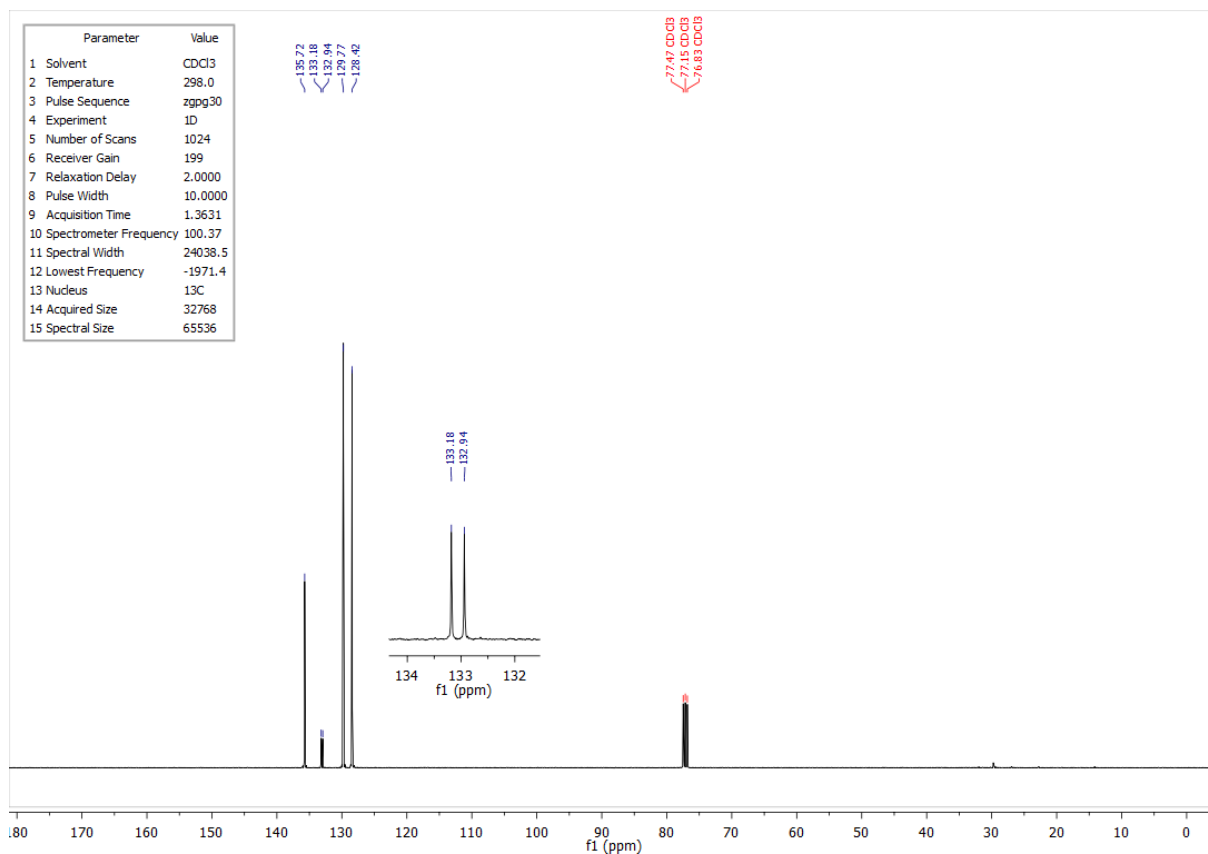


Figure 4.134 – ^{13}C NMR spectrum of compound **3.26a** in CDCl_3 .

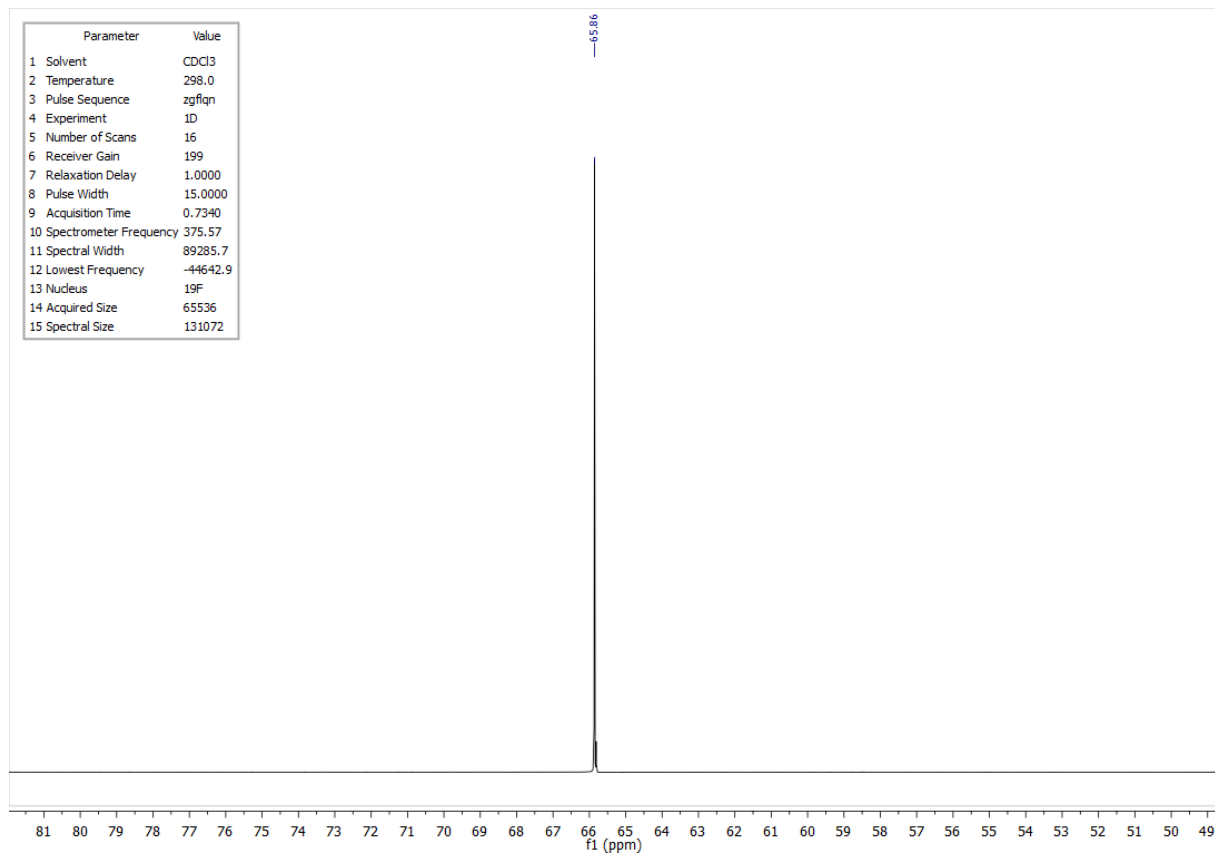


Figure 4.135 – ^{19}F NMR spectrum of compound **3.26a** in CDCl_3 .

4.3.2 ^1H and ^{13}C NMR spectra of compound 3.26a-der

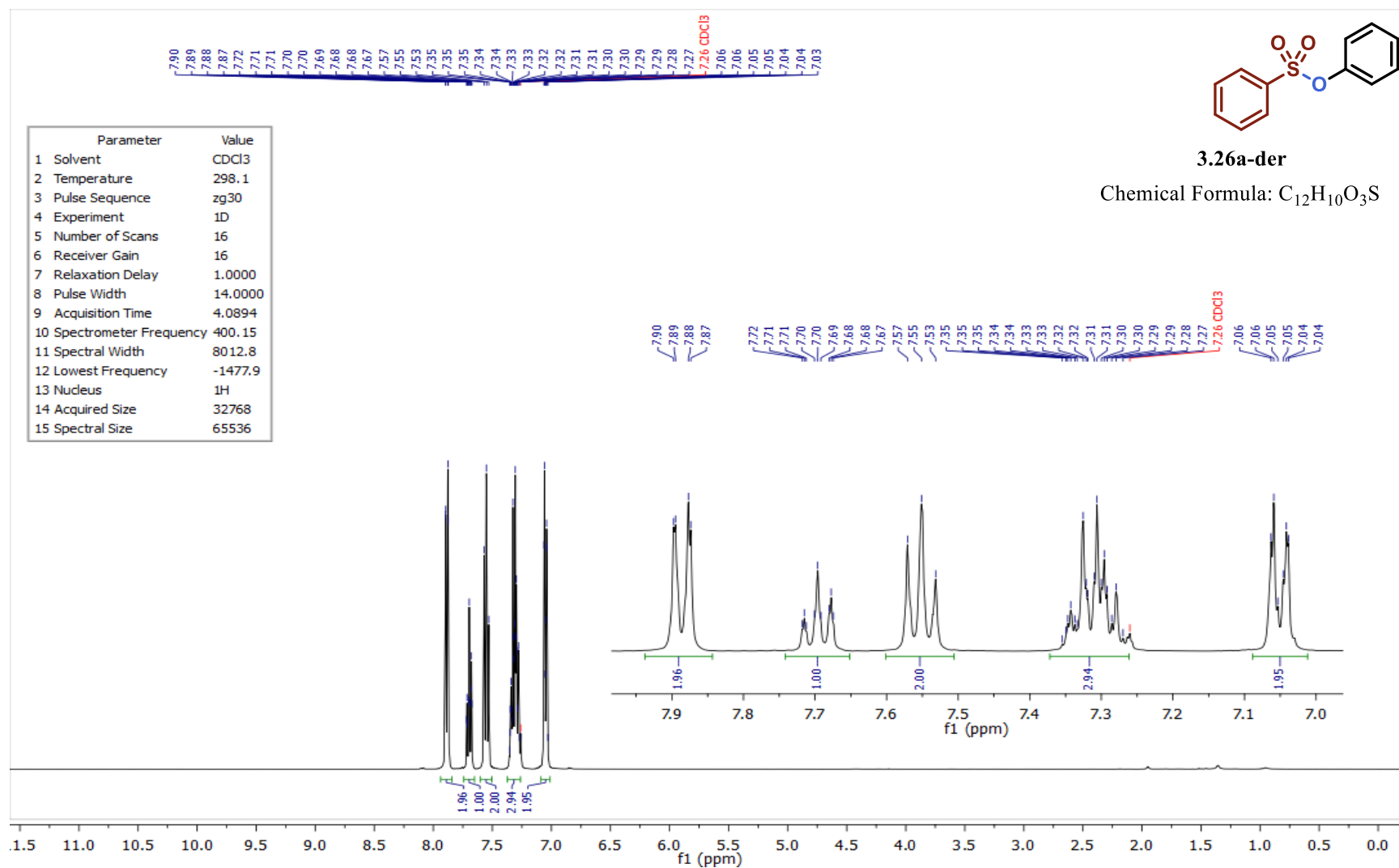


Figure 4.136 – ^1H NMR spectrum of compound 3.26a-der in CDCl_3 .

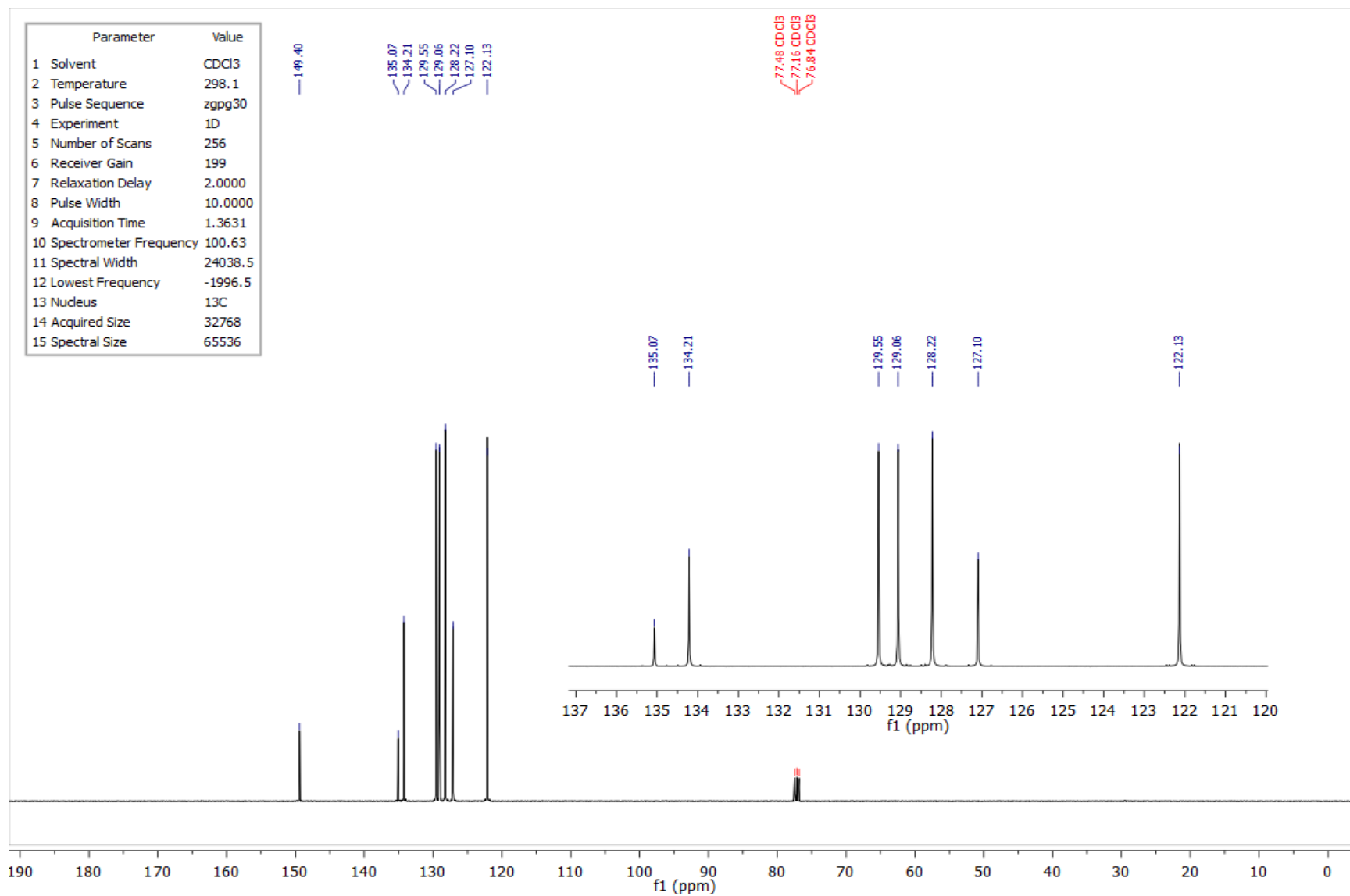


Figure 4.137 – ^{13}C NMR spectrum of compound **3.26a-der** in CDCl_3 .

4.3.3 ^1H , ^{13}C and ^{19}F NMR spectra of compound 3.26b

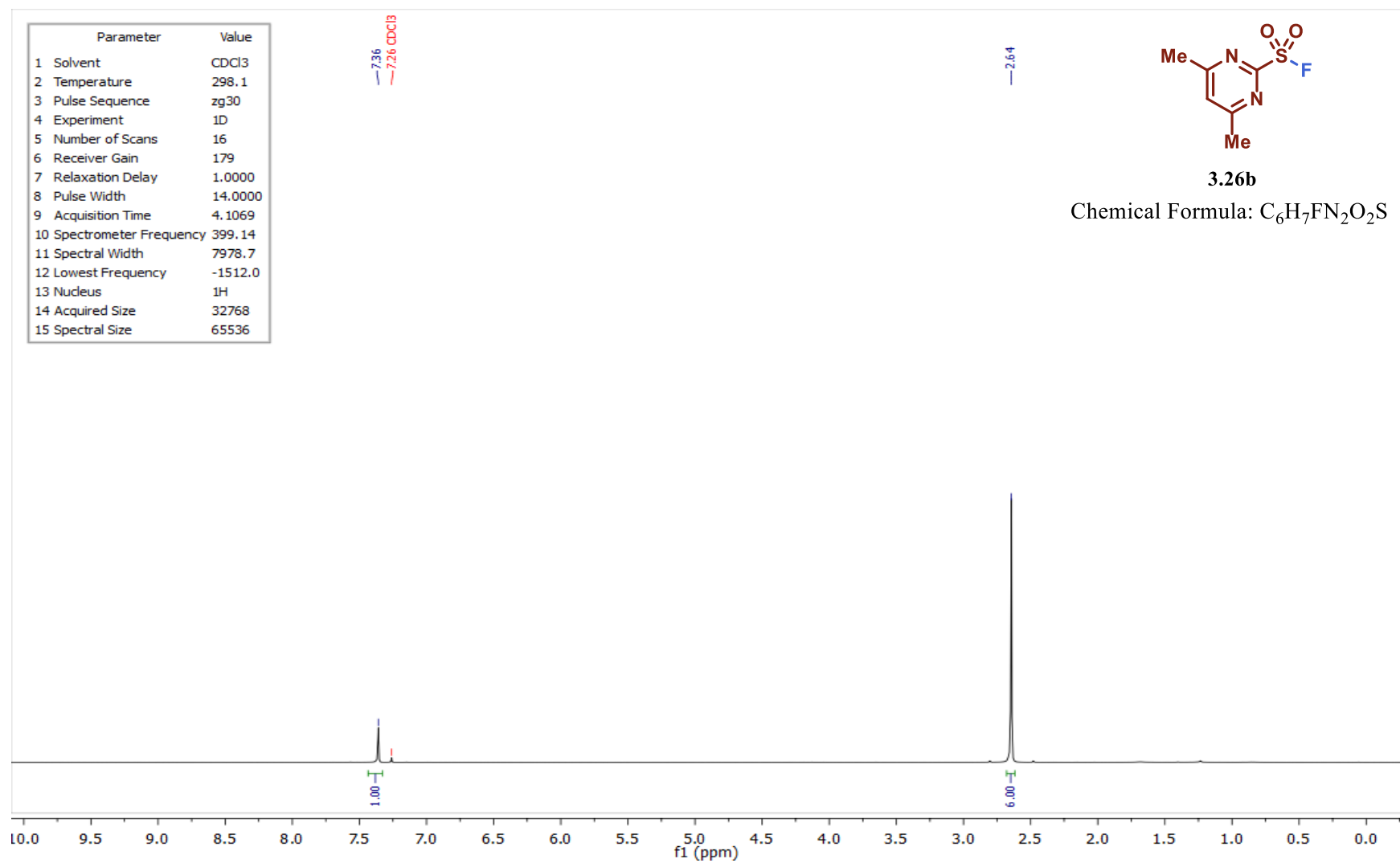


Figure 4.138 – ^1H NMR spectrum of compound 3.26b in CDCl_3 .

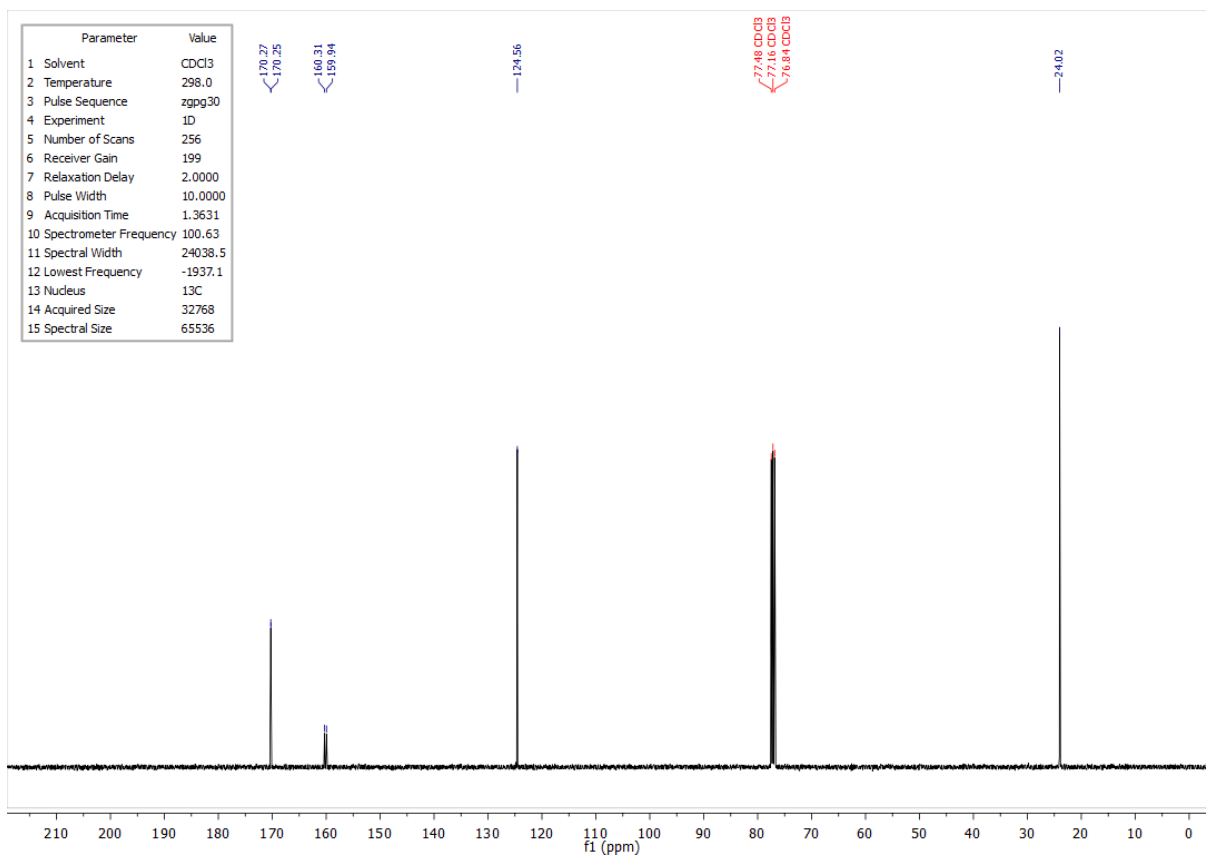


Figure 4.139 – ^{13}C NMR spectrum of compound **3.26b** in CDCl_3 .

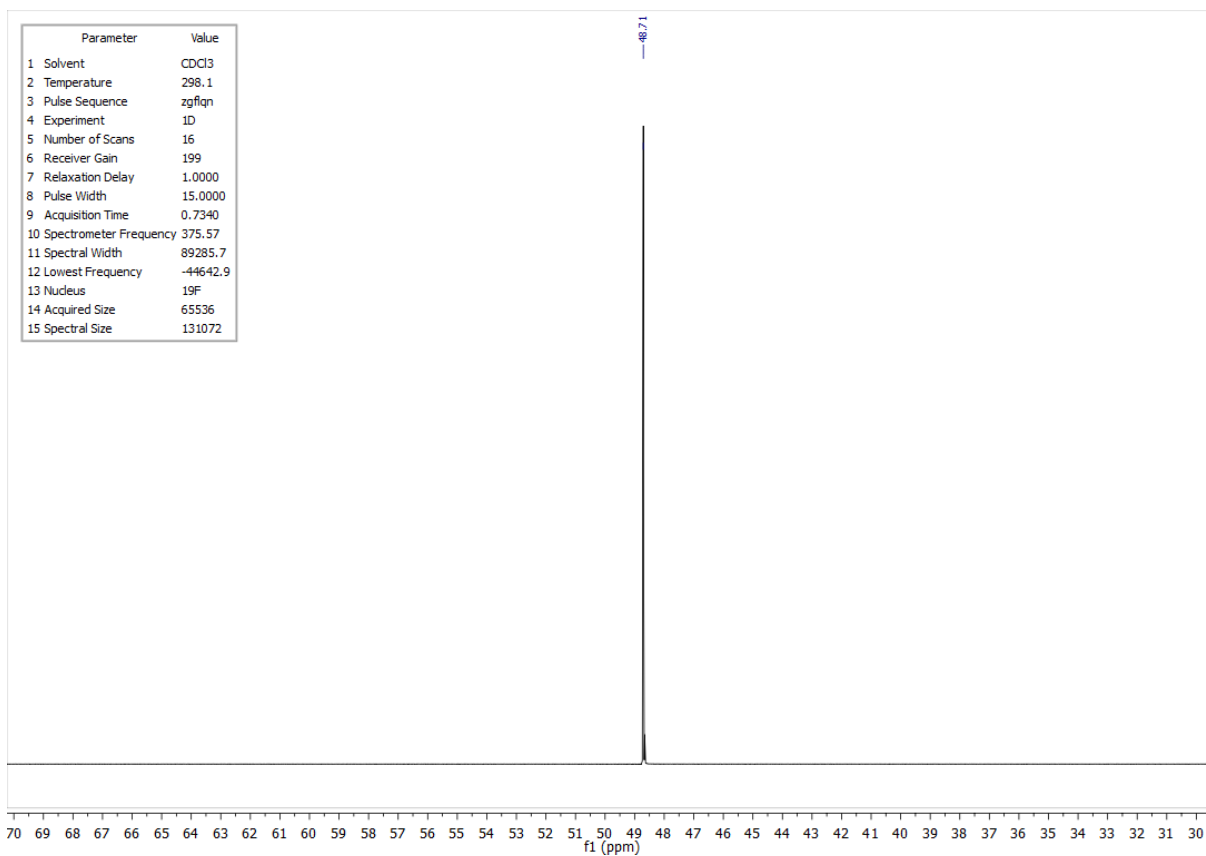


Figure 4.140 – ^{19}F NMR spectrum of compound **3.26b** in CDCl_3 .

4.3.4 ^1H , ^{13}C and ^{19}F NMR spectra of compound 3.26c

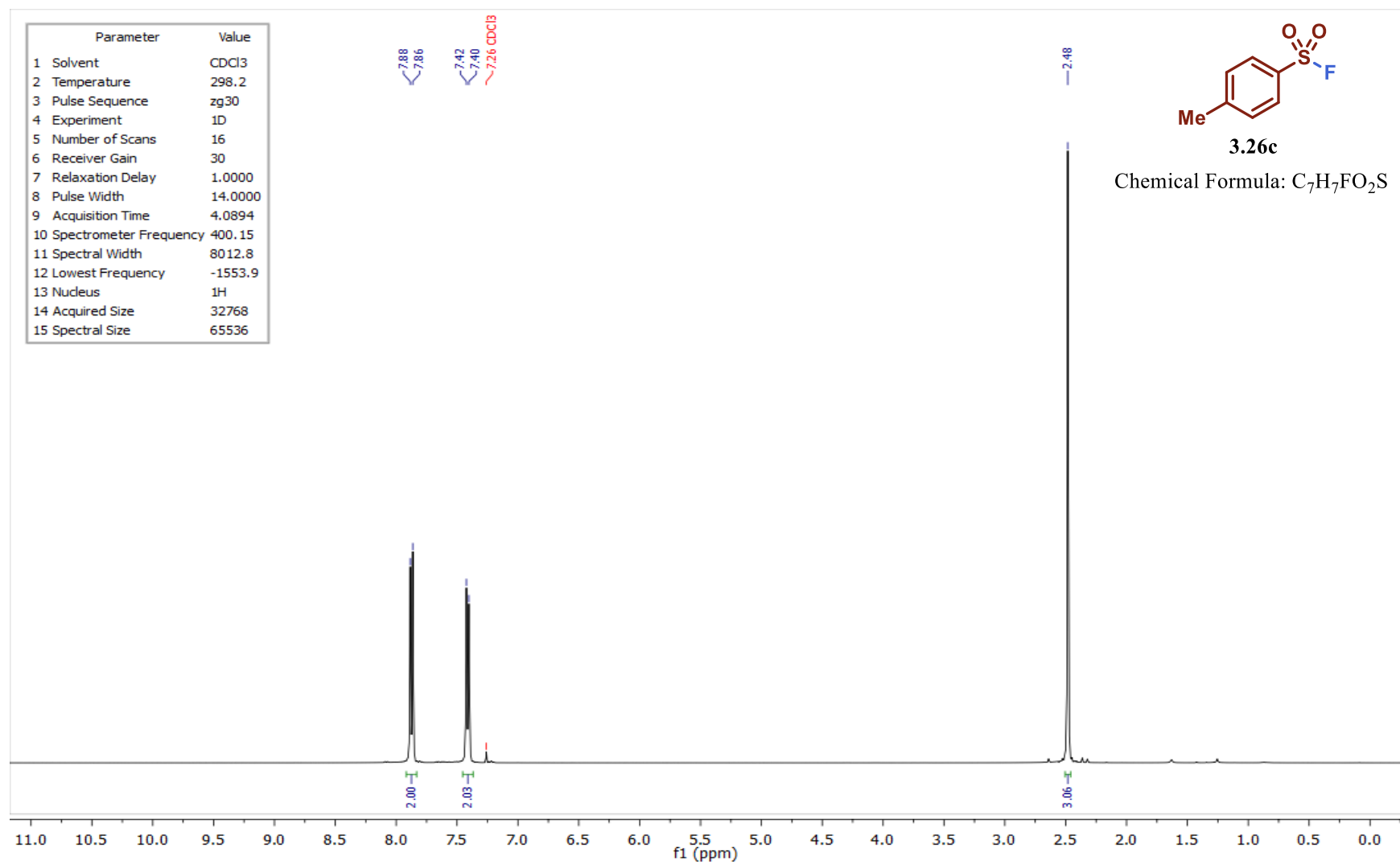


Figure 4.141 – ^1H NMR spectrum of compound 3.26c in CDCl_3 .

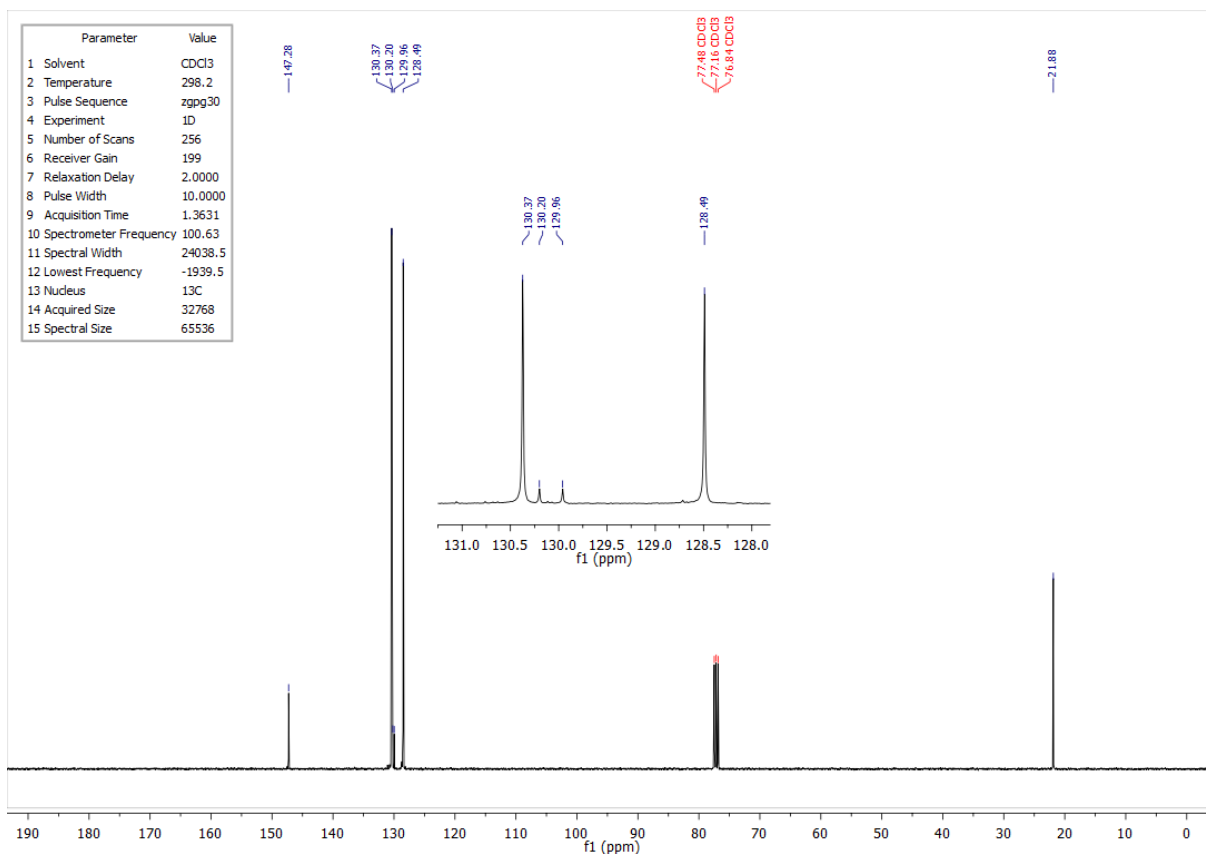


Figure 4.142 – ^{13}C NMR spectrum of compound **3.26c** in CDCl_3 .

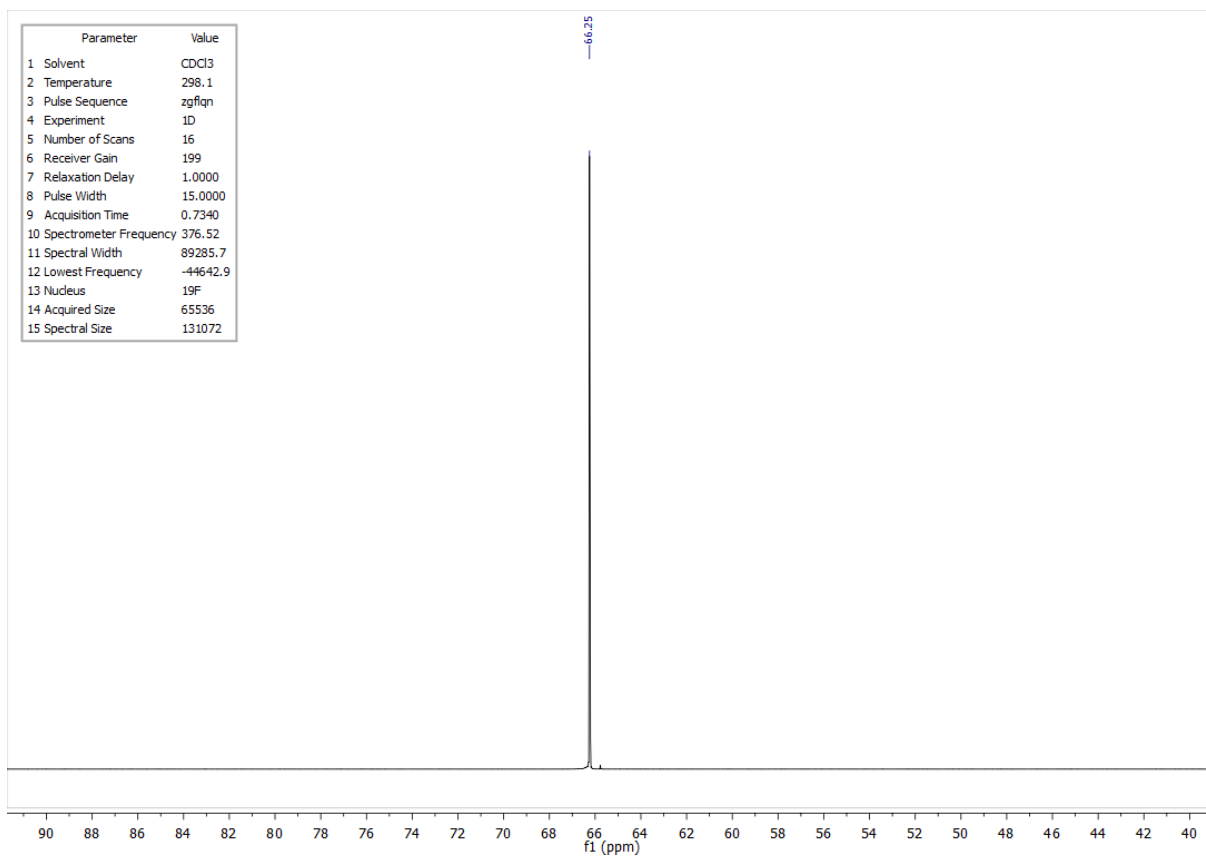


Figure 4.143 – ^{19}F NMR spectrum of compound **3.26c** in CDCl_3 .

4.3.5 ^1H , ^{13}C and ^{19}F NMR spectra of compound 3.26d

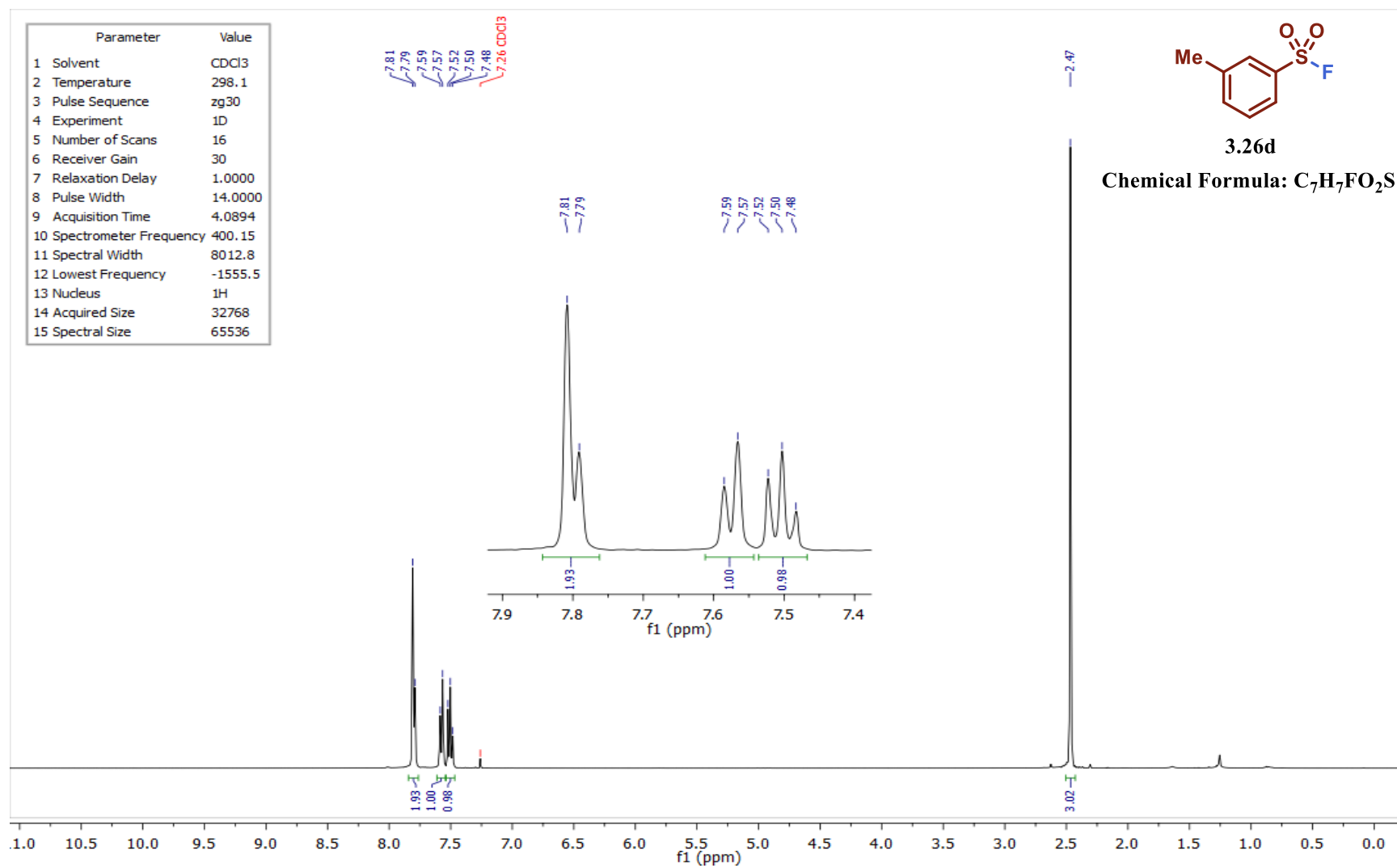


Figure 4.144 – ^1H NMR spectrum of compound 3.26d in CDCl_3 .

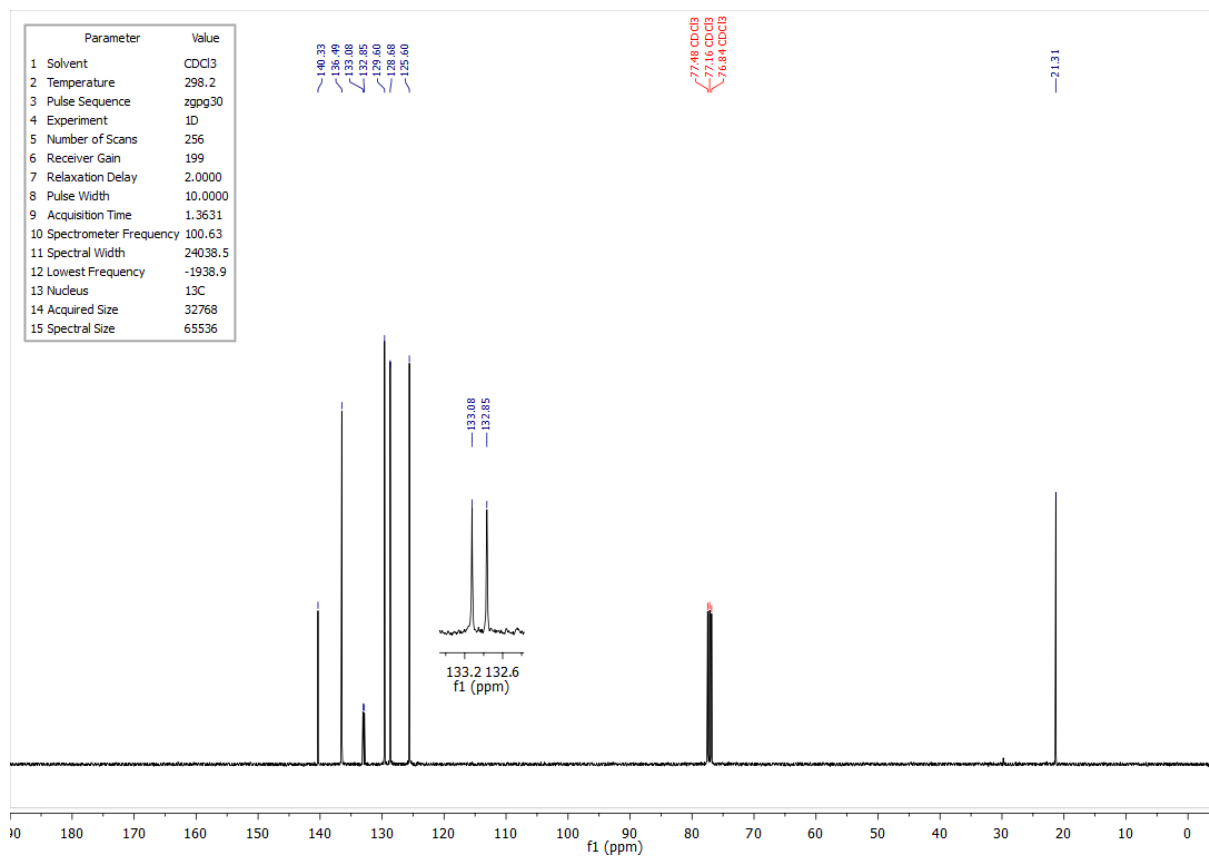


Figure 4.145 – ^{13}C NMR spectrum of compound **3.26d** in CDCl_3 .

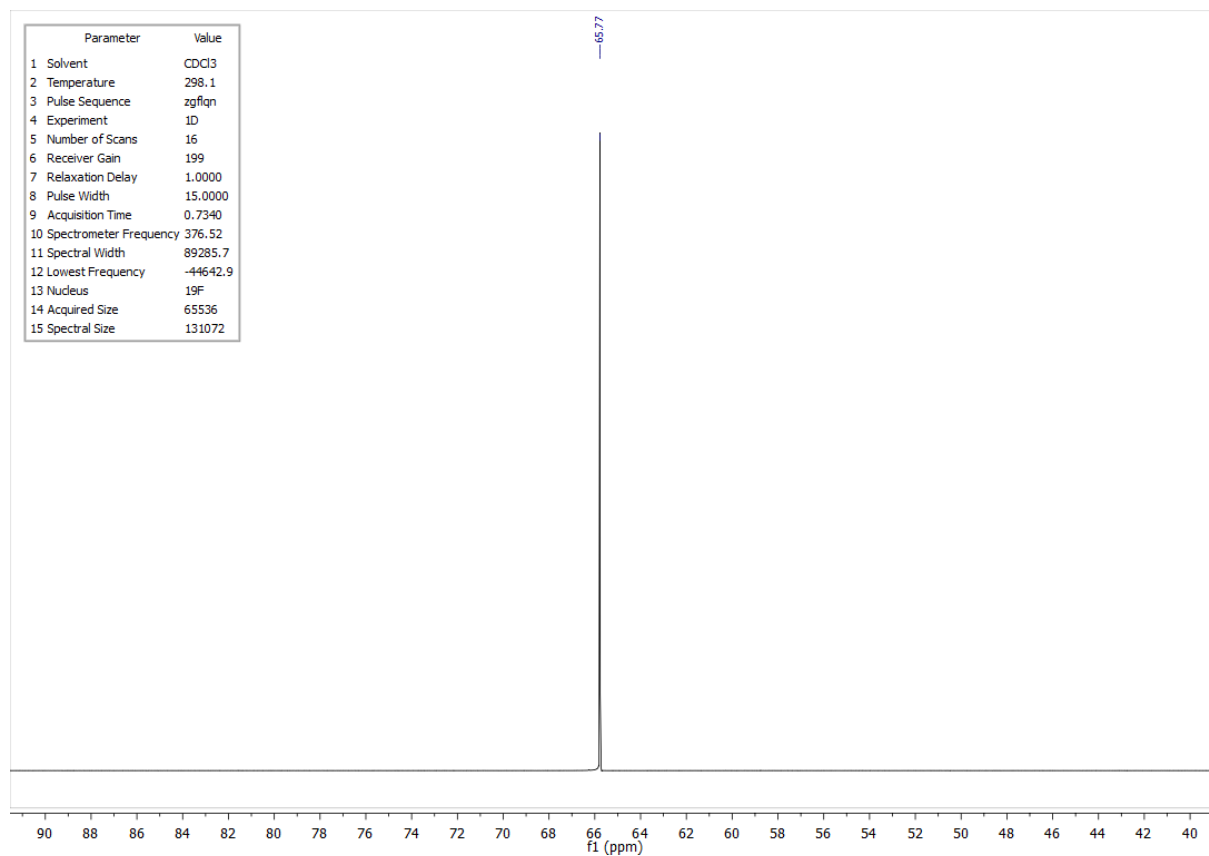


Figure 4.146 – ^{19}F NMR spectrum of compound **3.26d** in CDCl_3 .

4.3.6 ^1H , ^{13}C and ^{19}F NMR spectra of compound 3.26e

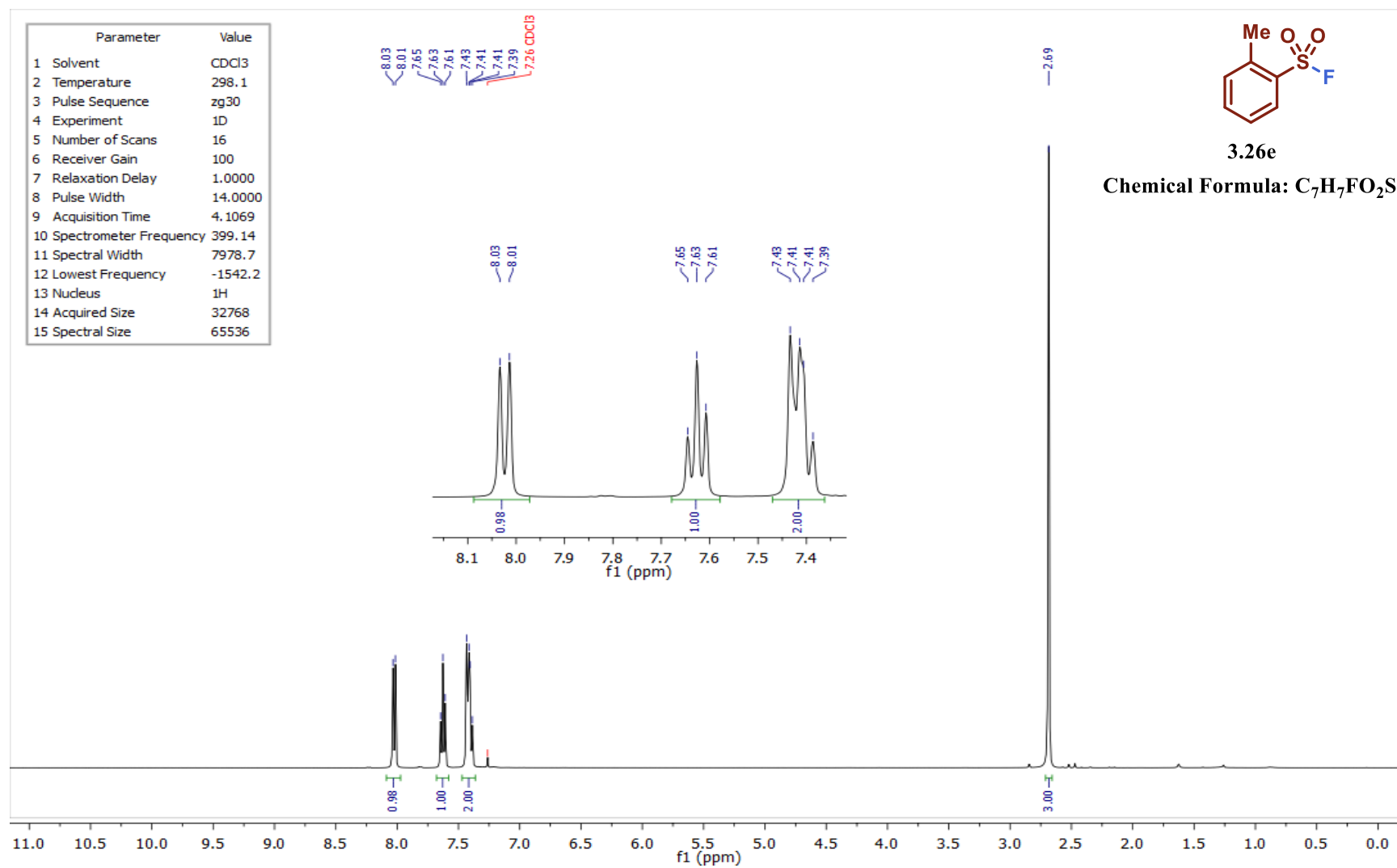


Figure 4.147 – ^1H NMR spectrum of compound 3.26e in CDCl_3 .

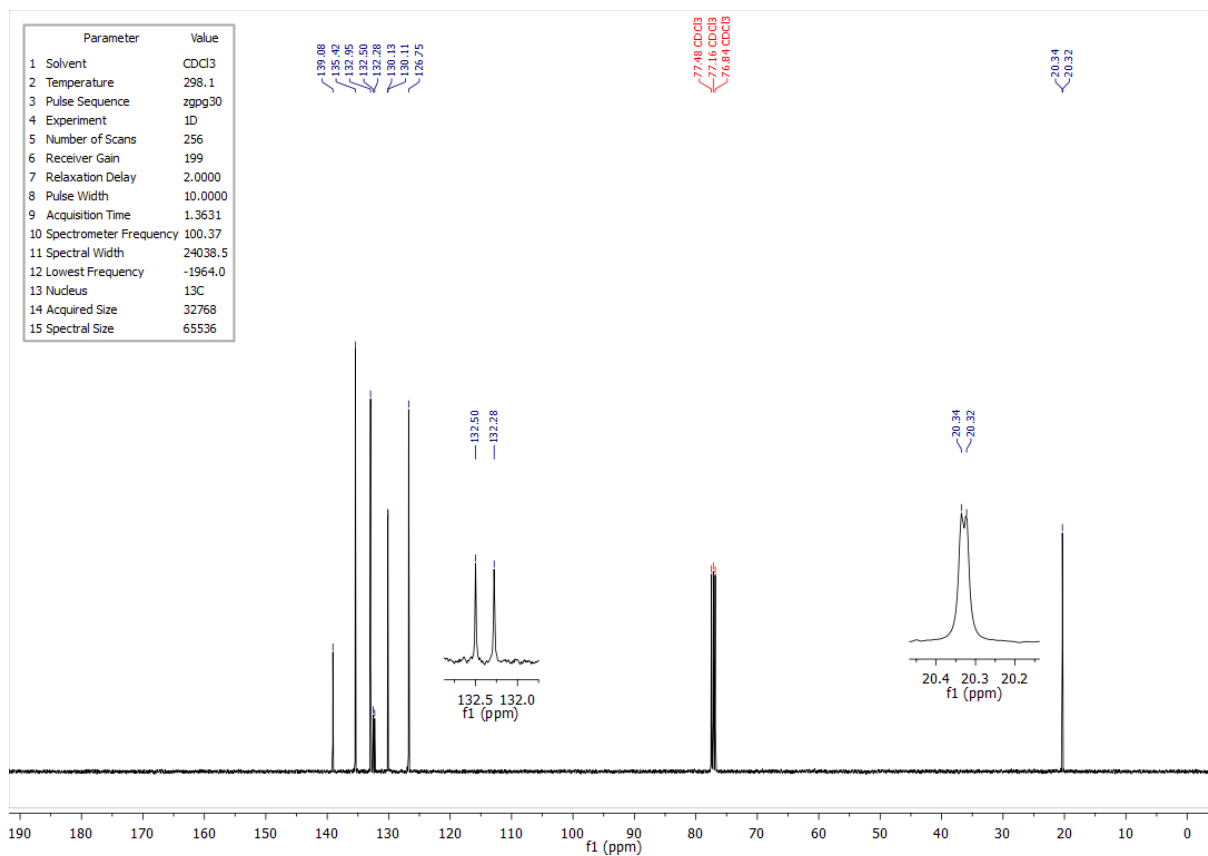


Figure 4.148 – ¹³C NMR spectrum of compound 3.26e in CDCl₃.

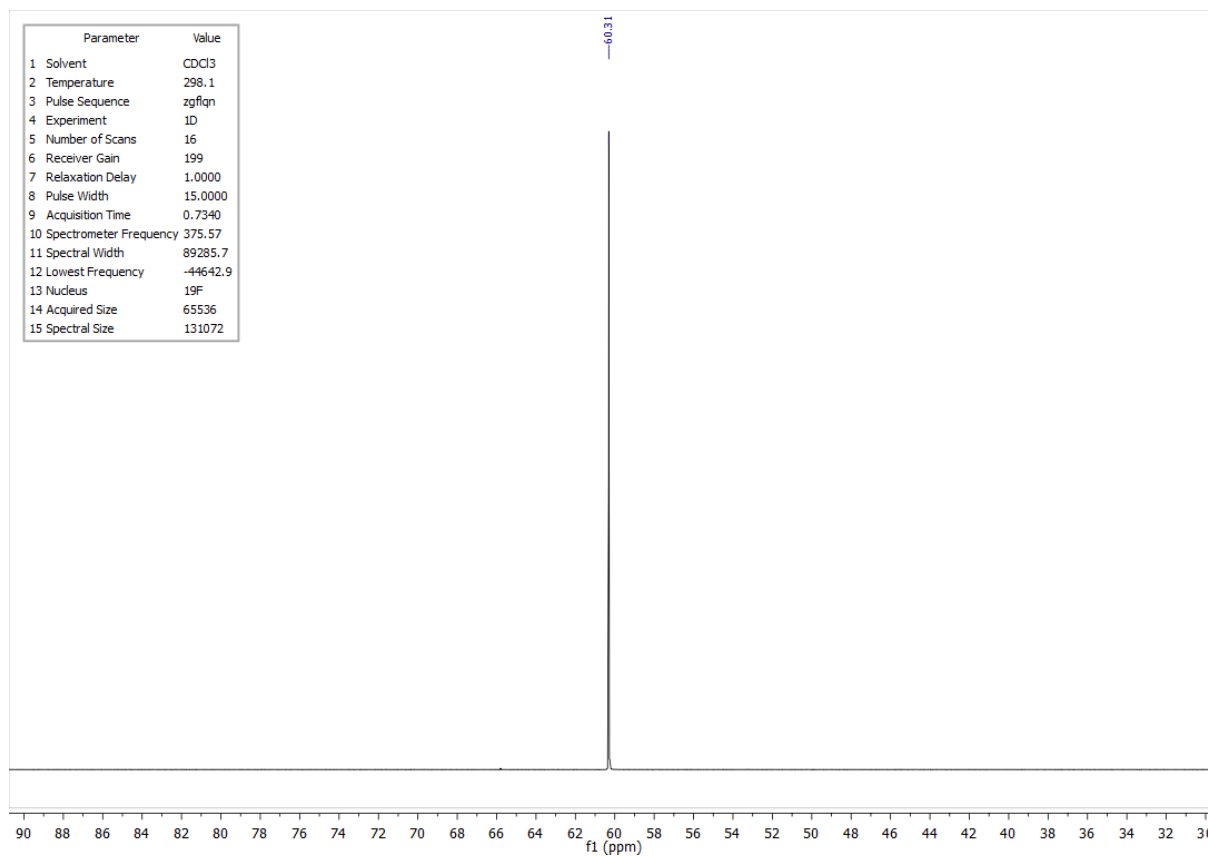


Figure 4.149 – ¹⁹F NMR spectrum of compound 3.26e in CDCl₃.

4.3.7 ^1H , ^{13}C and ^{19}F NMR spectra of compound 3.26f

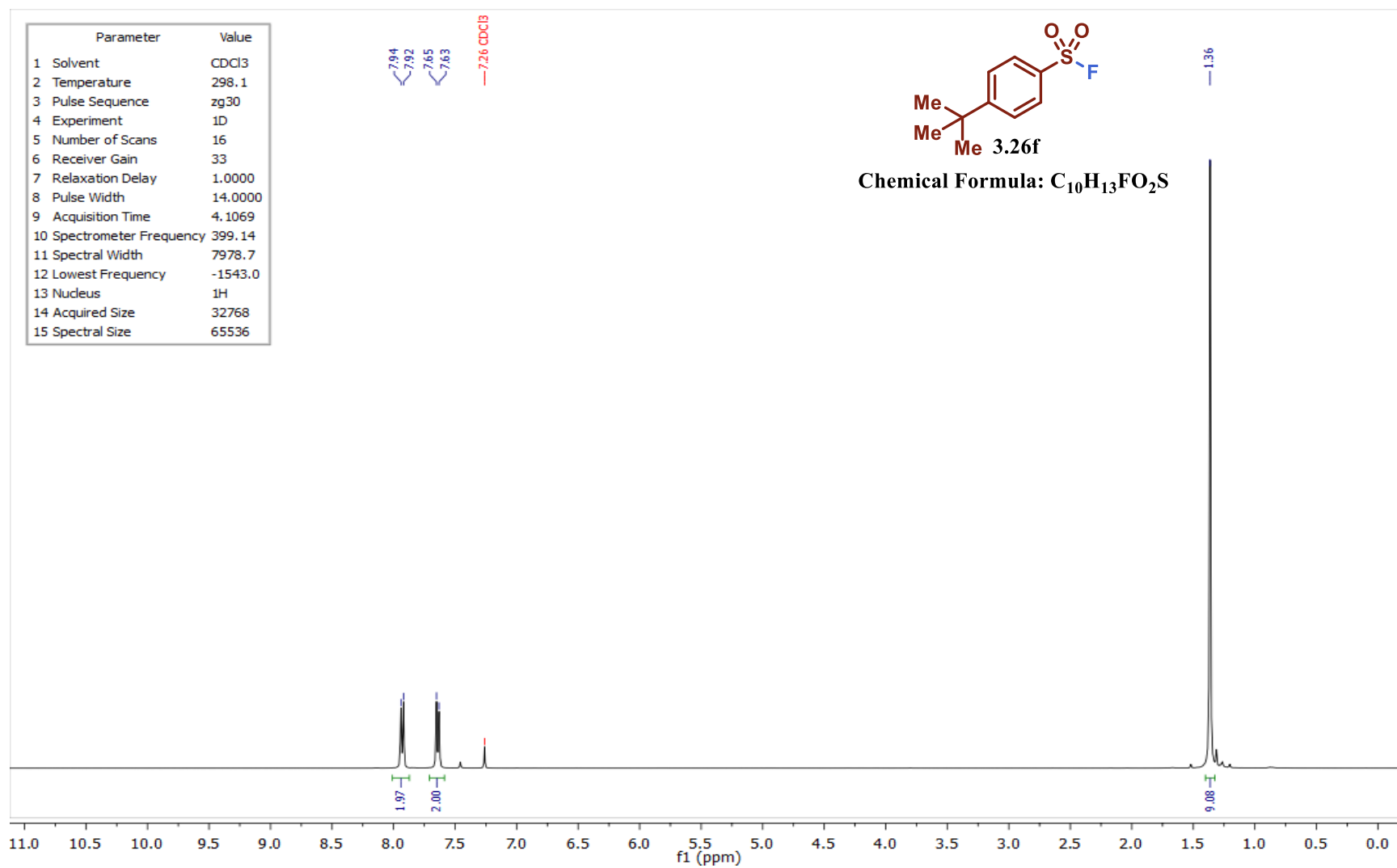


Figure 4.150 – ^1H NMR spectrum of compound 3.26f in CDCl_3 .

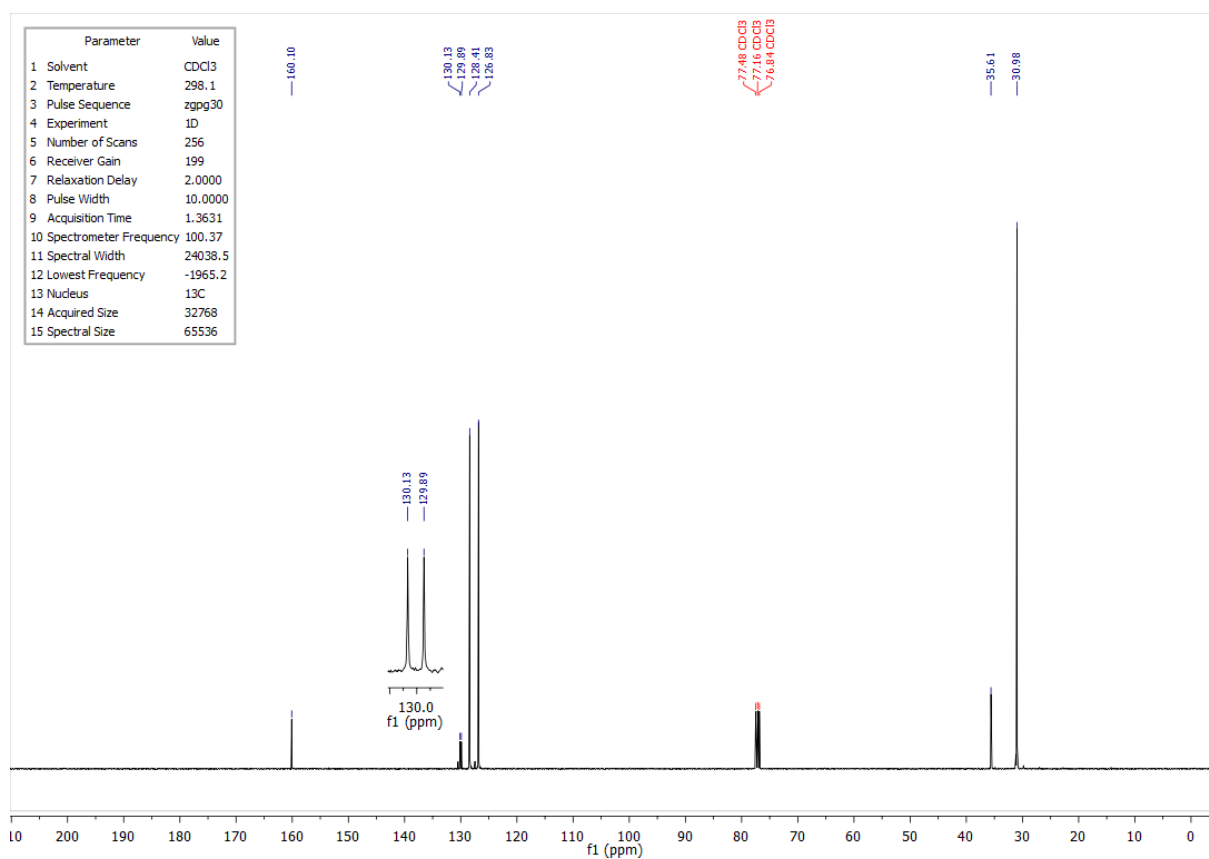


Figure 4.151 – ¹³C NMR spectrum of compound **3.26f** in CDCl₃.

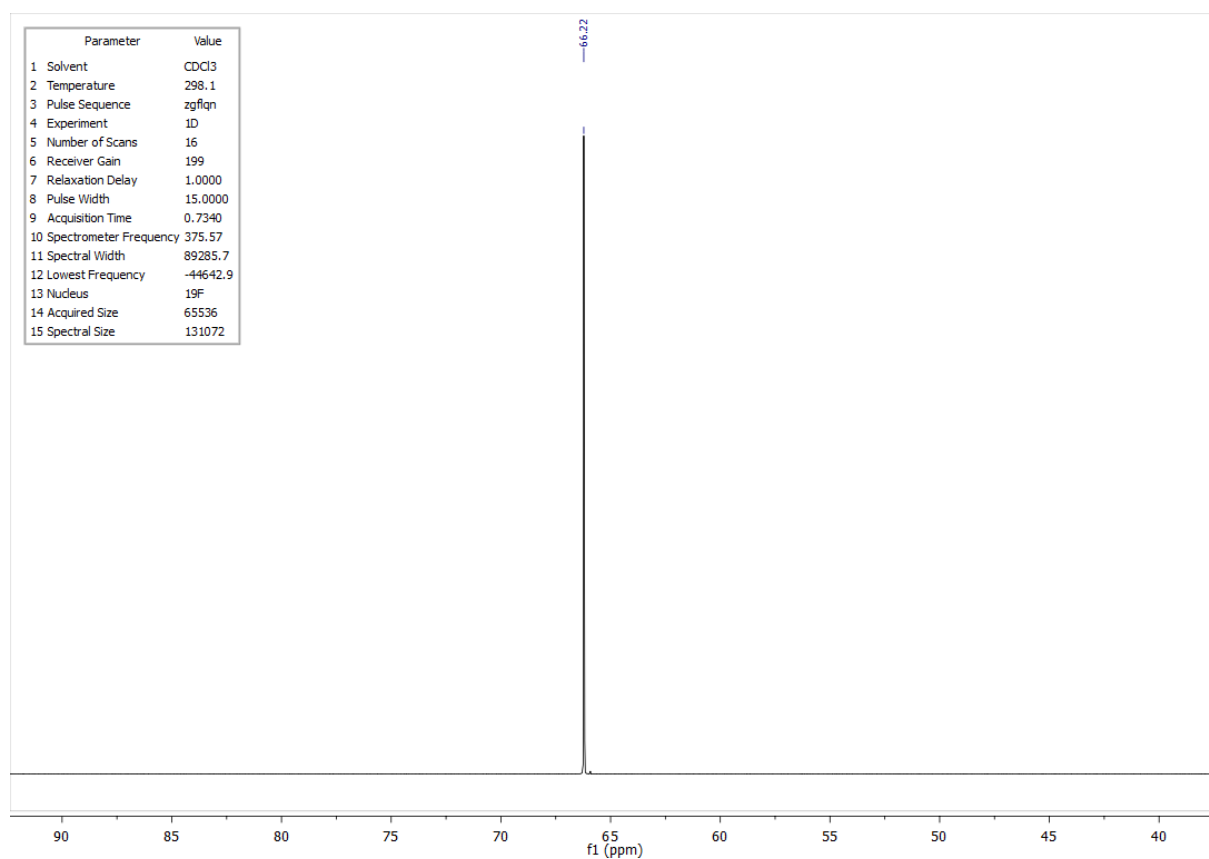


Figure 4.152 – ¹⁹F NMR spectrum of compound **3.26f** in CDCl₃.

4.3.8 ^1H , ^{13}C and ^{19}F NMR spectra of compound 3.26g

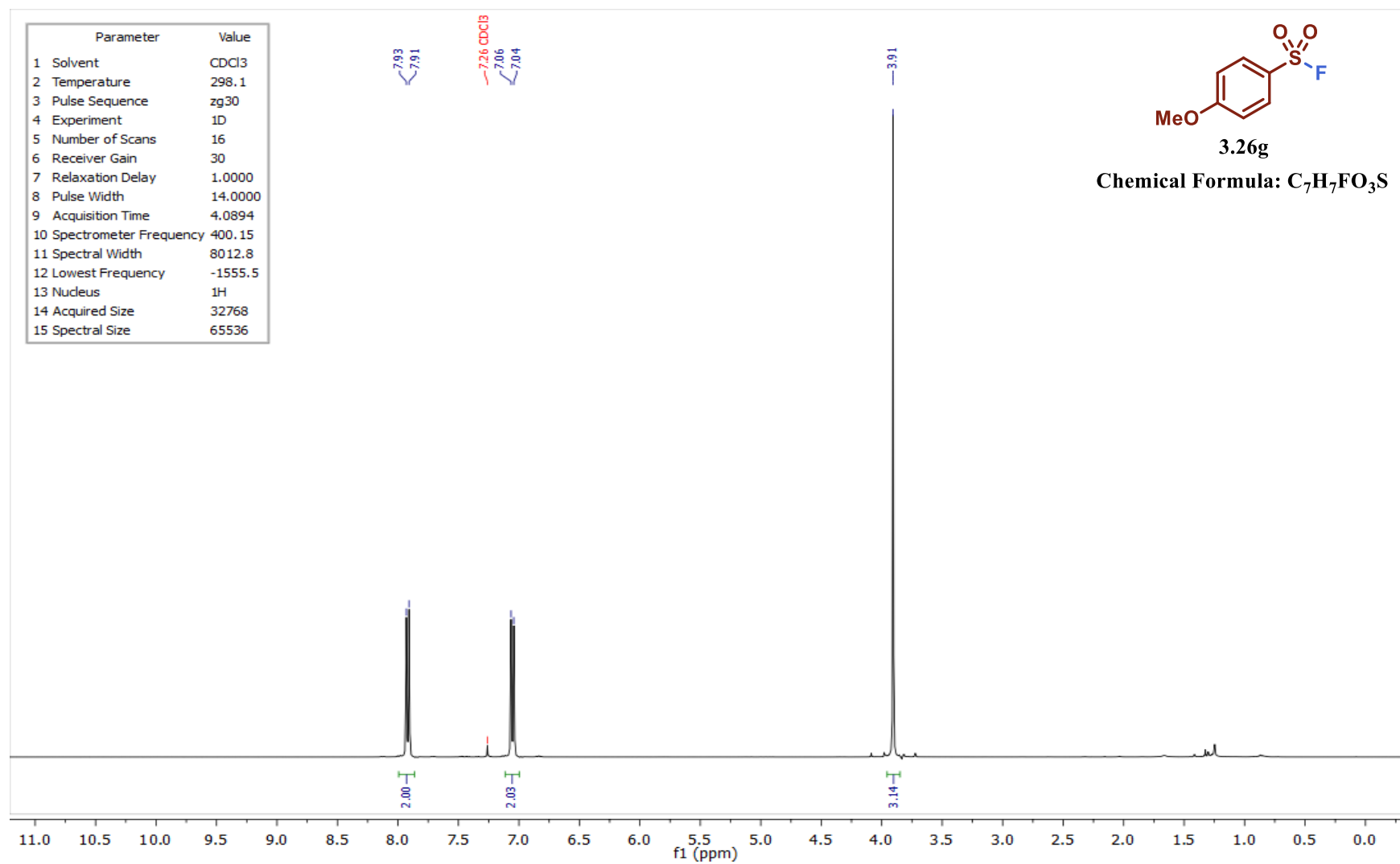


Figure 4.153 – ^1H NMR spectrum of compound 3.26g in CDCl_3 .

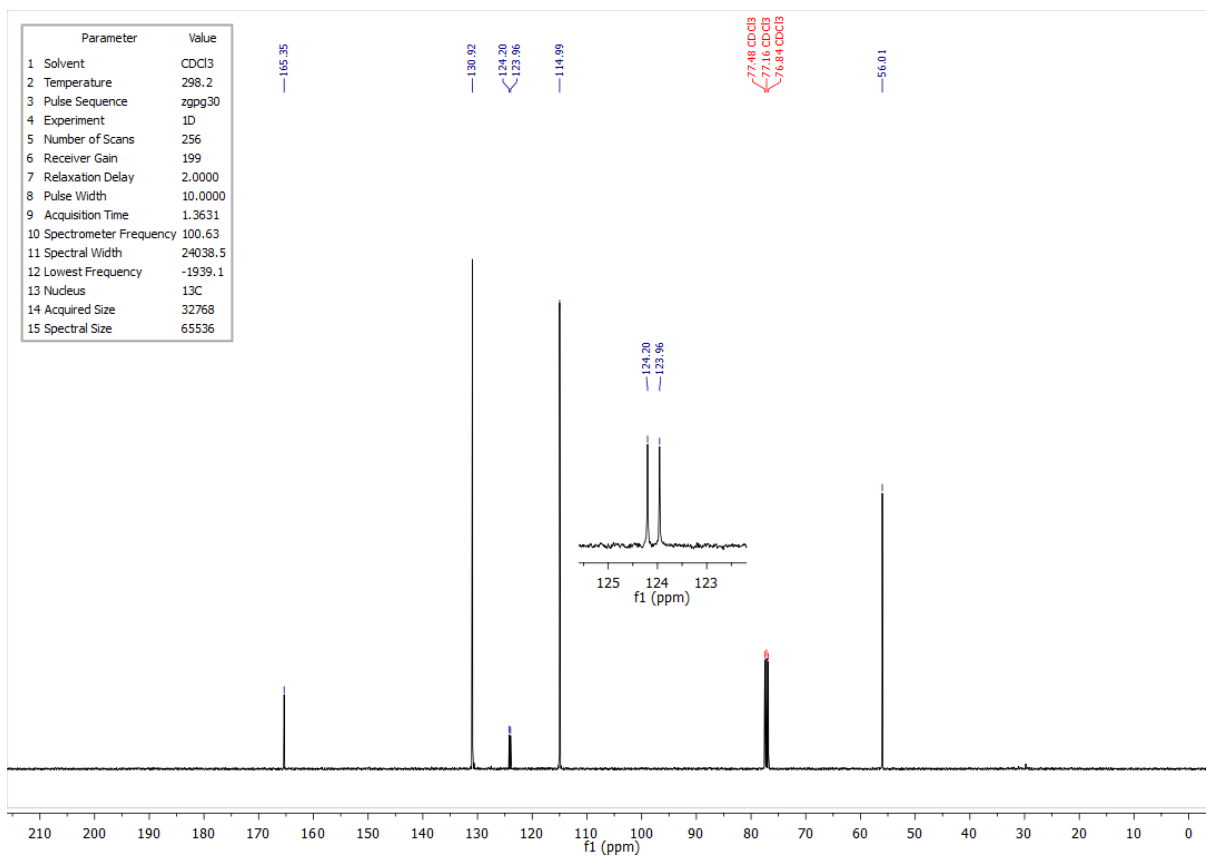


Figure 4.154 – ^{13}C NMR spectrum of compound **3.26g** in CDCl_3 .

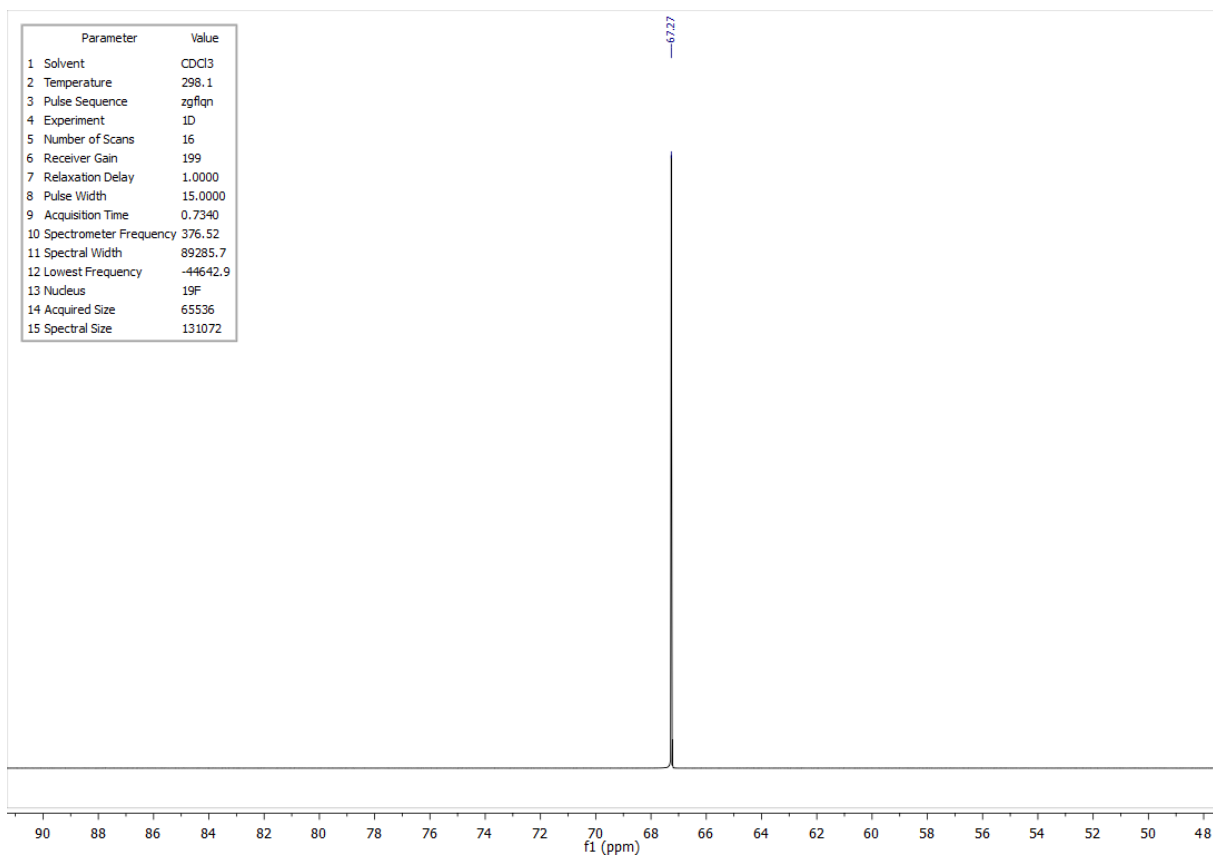


Figure 4.155 – ^{19}F NMR spectrum of compound **3.26g** in CDCl_3 .

4.3.9 ^1H , ^{13}C and ^{19}F NMR spectra of compound 3.26h

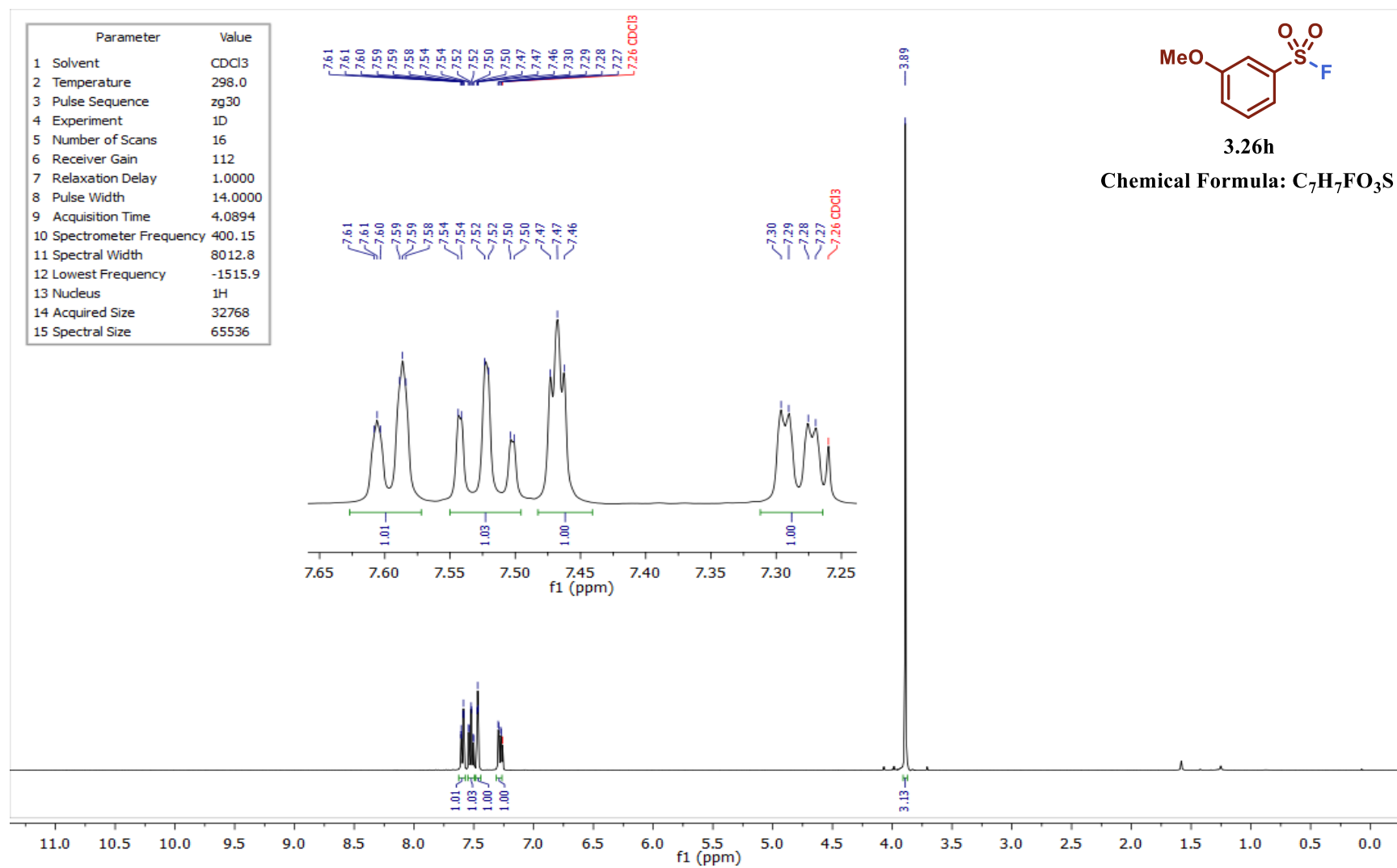


Figure 4.156 – ^1H NMR spectrum of compound 3.26h in CDCl_3 .

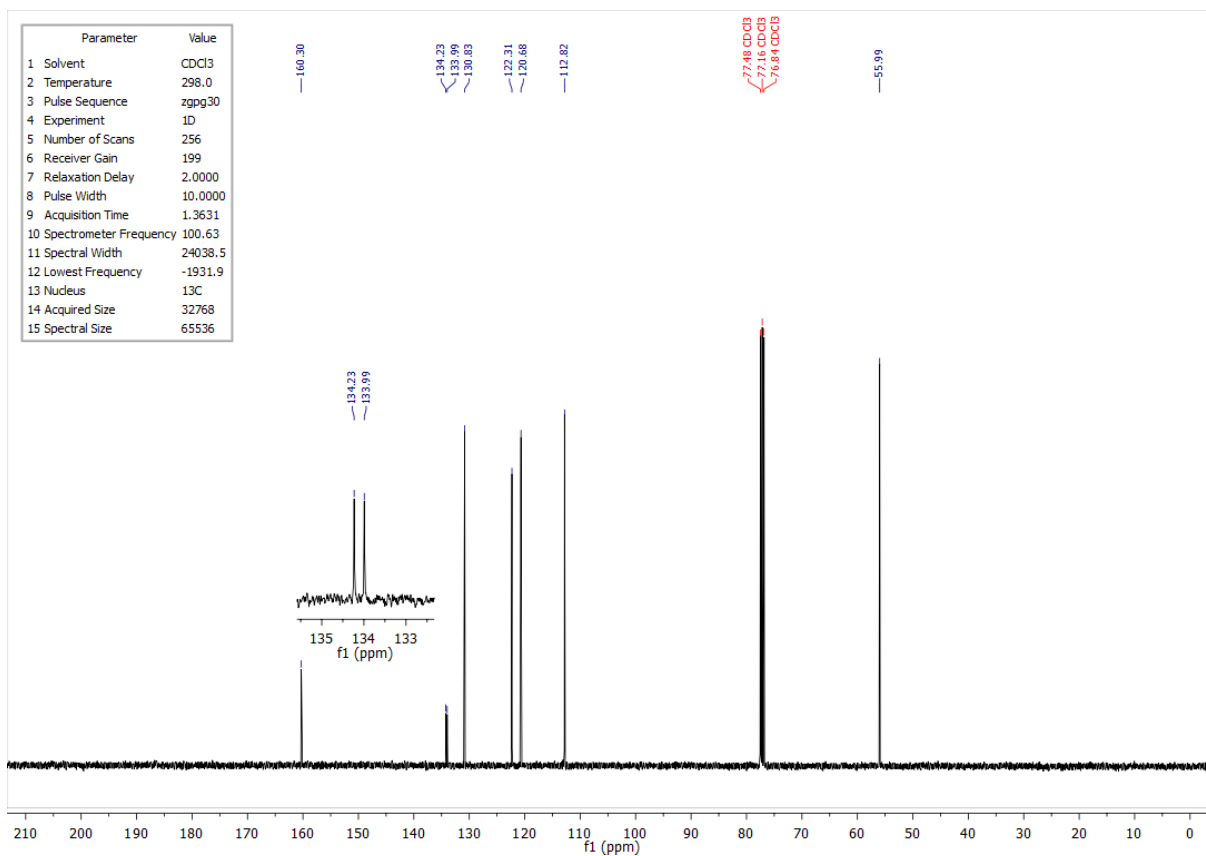


Figure 4.157 – ¹³C NMR spectrum of compound **3.26h** in CDCl₃.

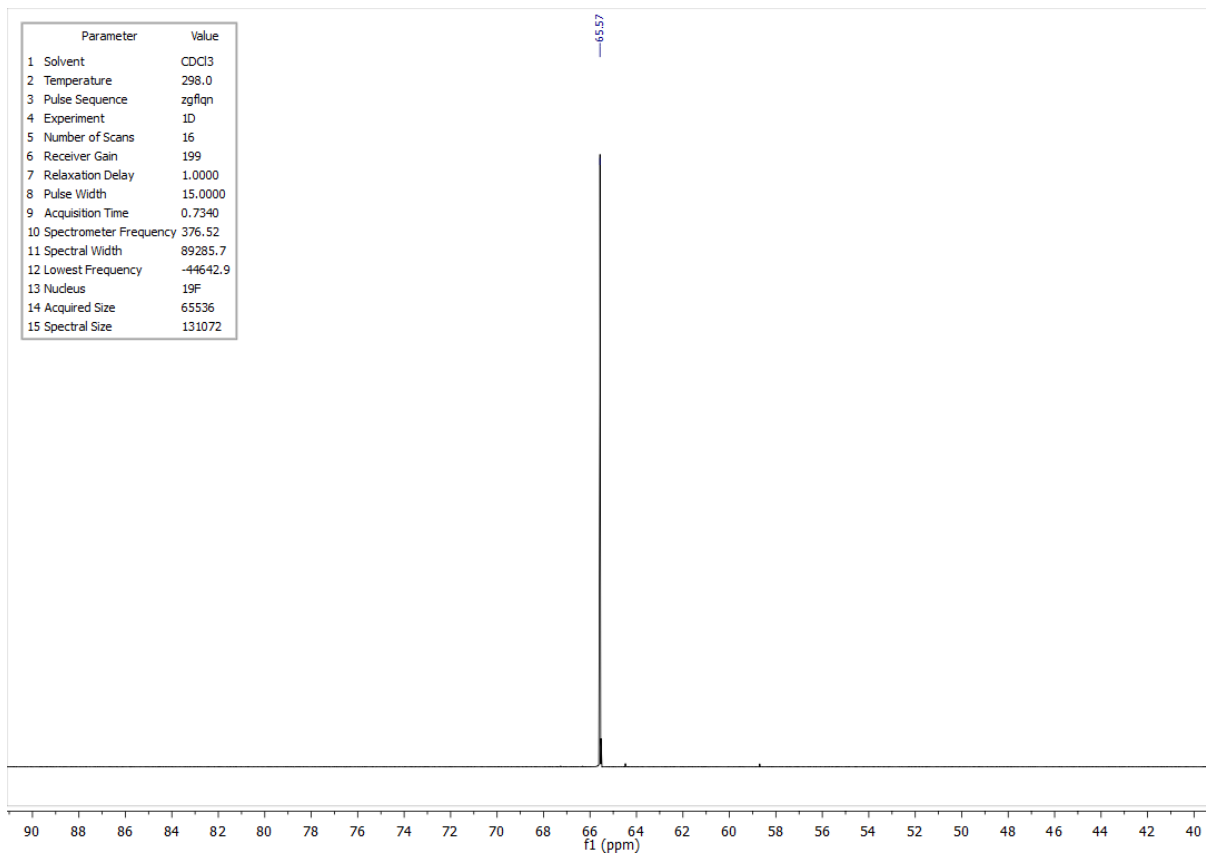


Figure 4.158 – ¹⁹F NMR spectrum of compound **3.26h** in CDCl₃.

4.3.10 ^1H , ^{13}C and ^{19}F NMR spectra of compound 3.26i

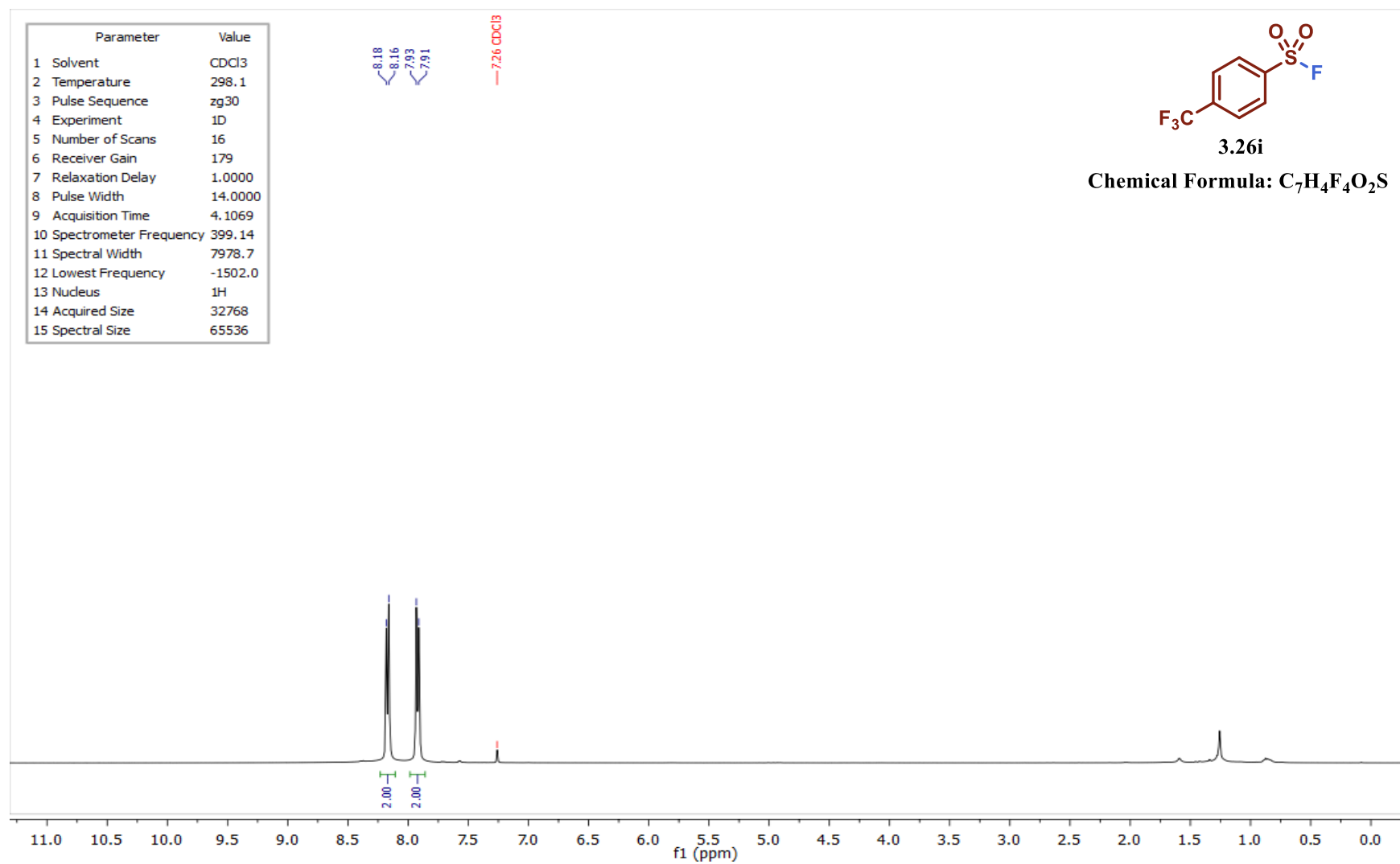


Figure 4.159 – ^1H NMR spectrum of compound 3.26i in CDCl_3 .

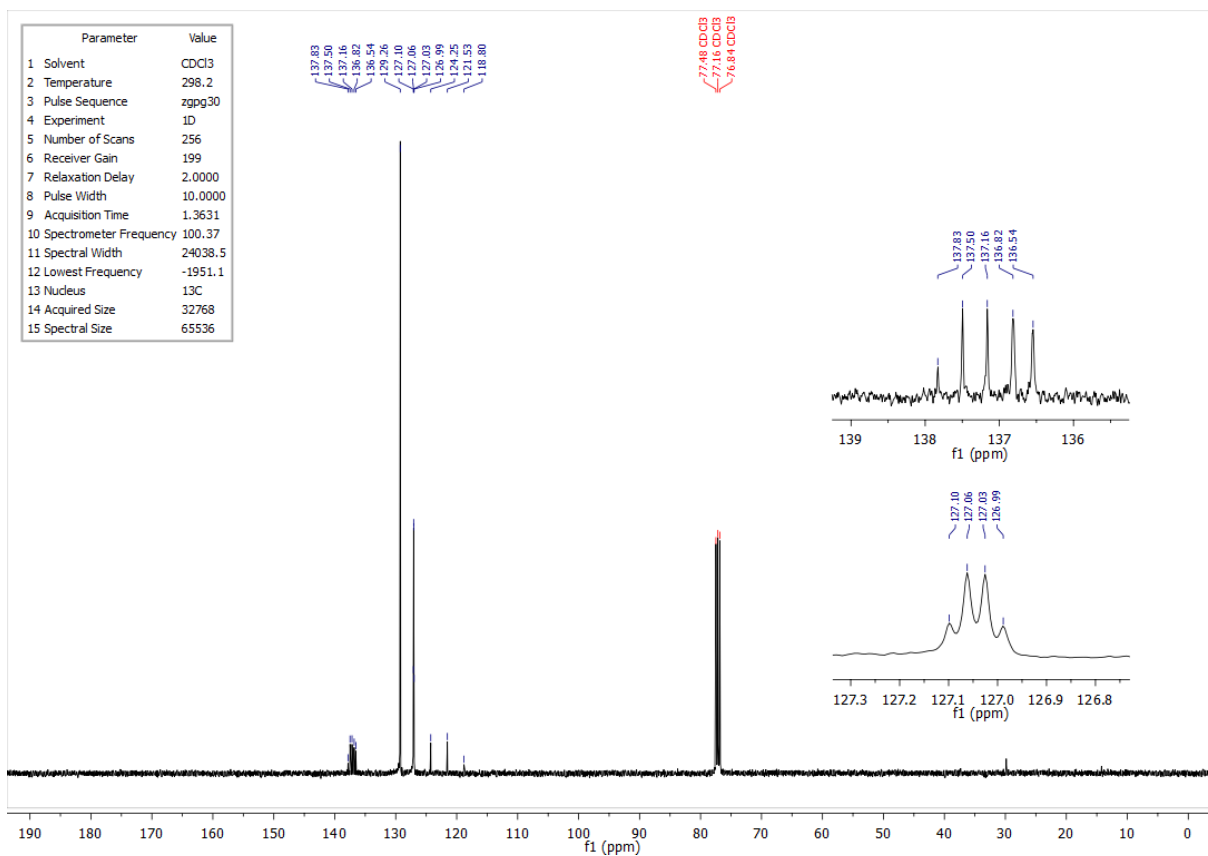


Figure 4.160 – ^{13}C NMR spectrum of compound **3.26i** in CDCl_3 .

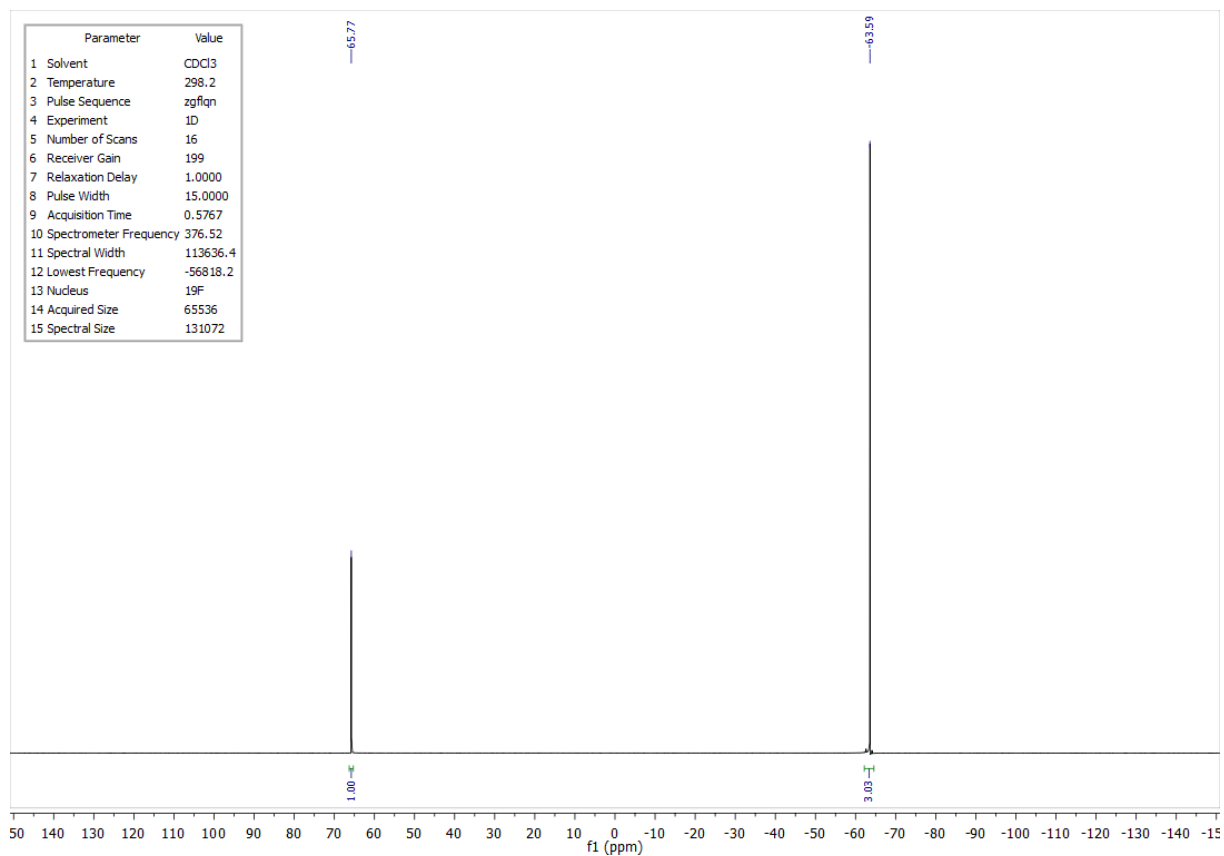


Figure 4.161 – ^{19}F NMR spectrum of compound **3.26i** in CDCl_3 .

4.3.11 ^{19}F and ^{13}C NMR spectra of compound 3.26j

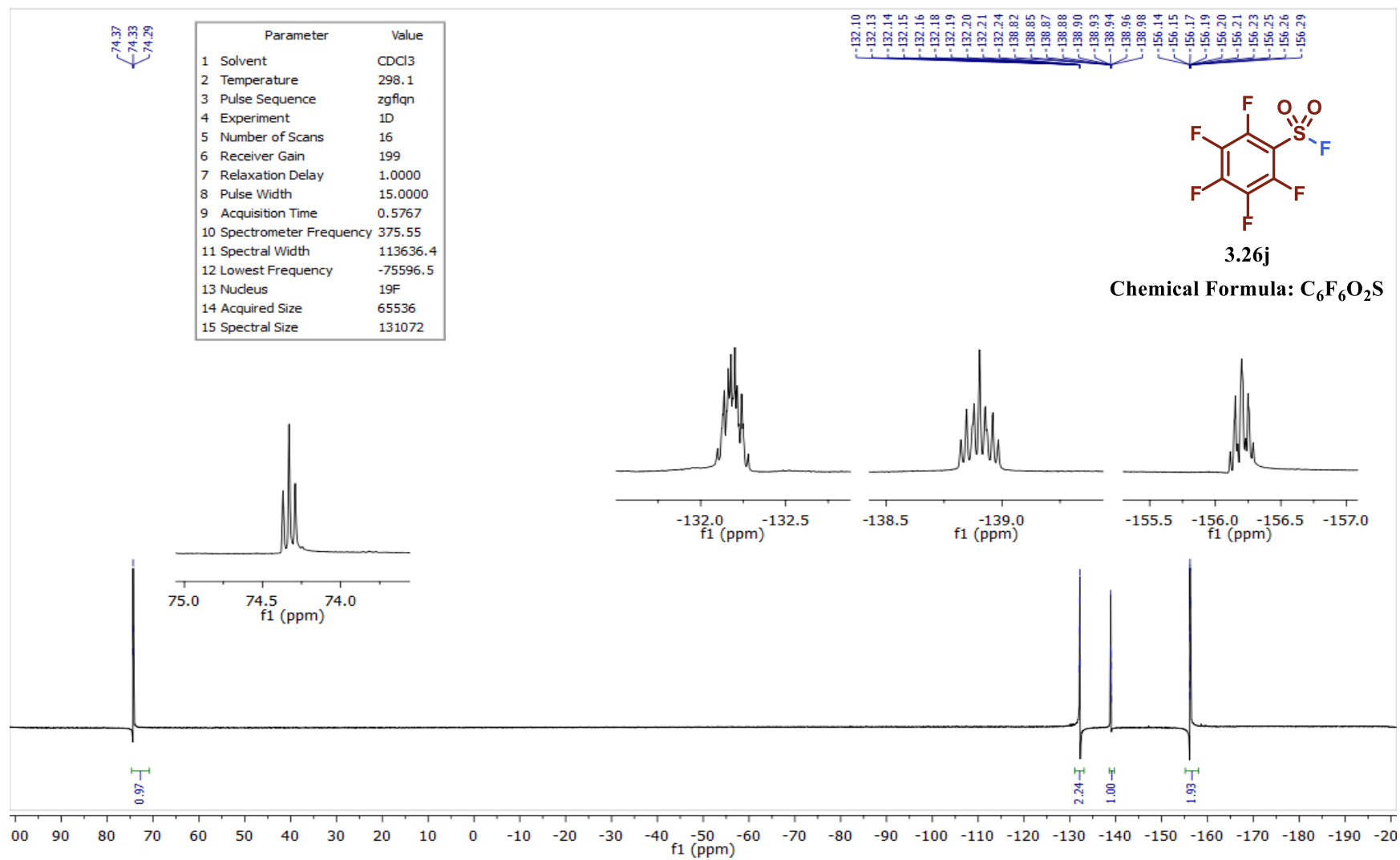


Figure 4.162 – ^{19}F NMR spectrum of compound 3.26j in CDCl_3 .

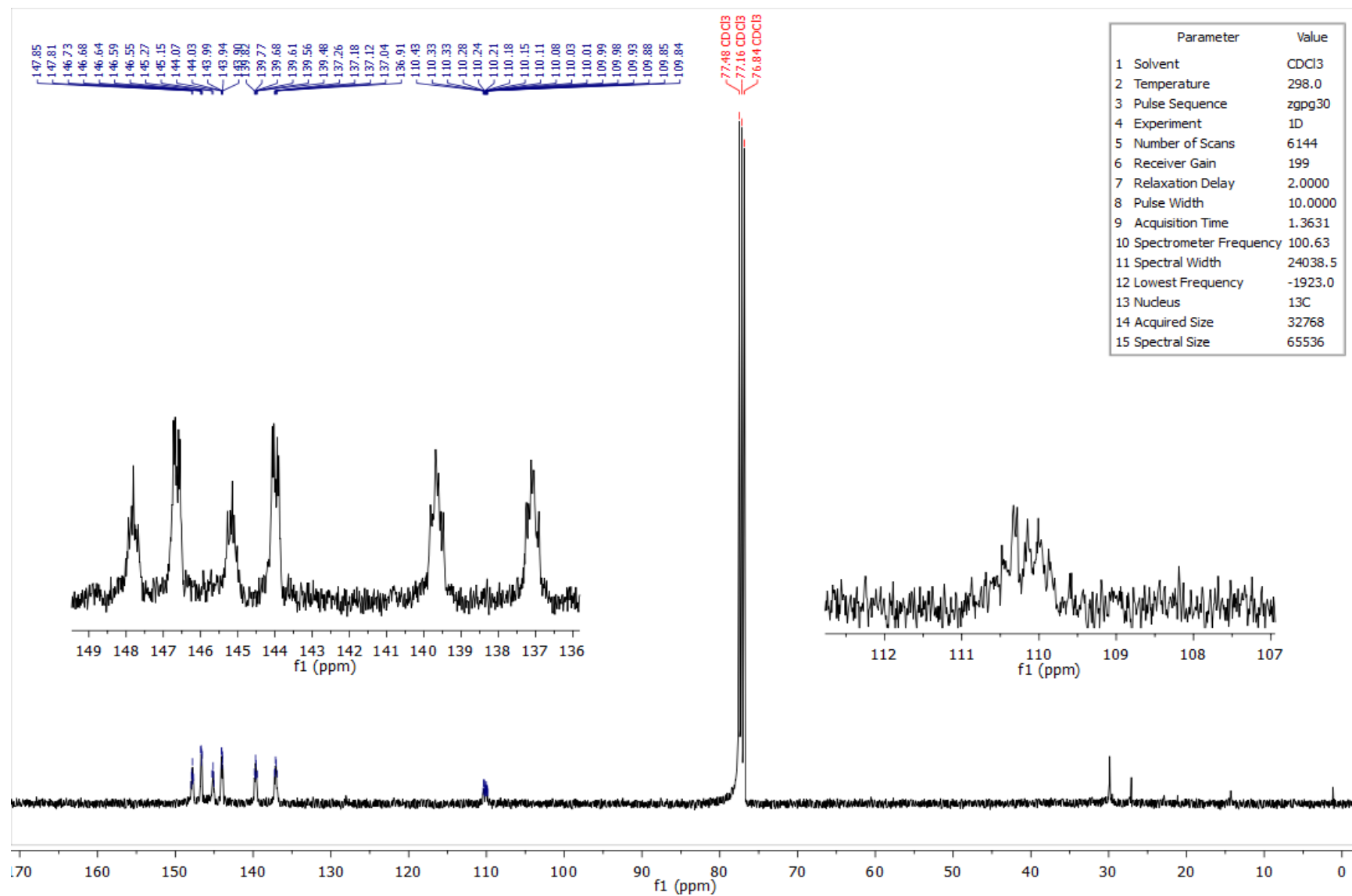


Figure 4.163 – ^{13}C NMR spectrum of compound 3.26j in CDCl_3 .

4.3.12 ^1H , ^{13}C and ^{19}F NMR spectra of compound 3.26j-der

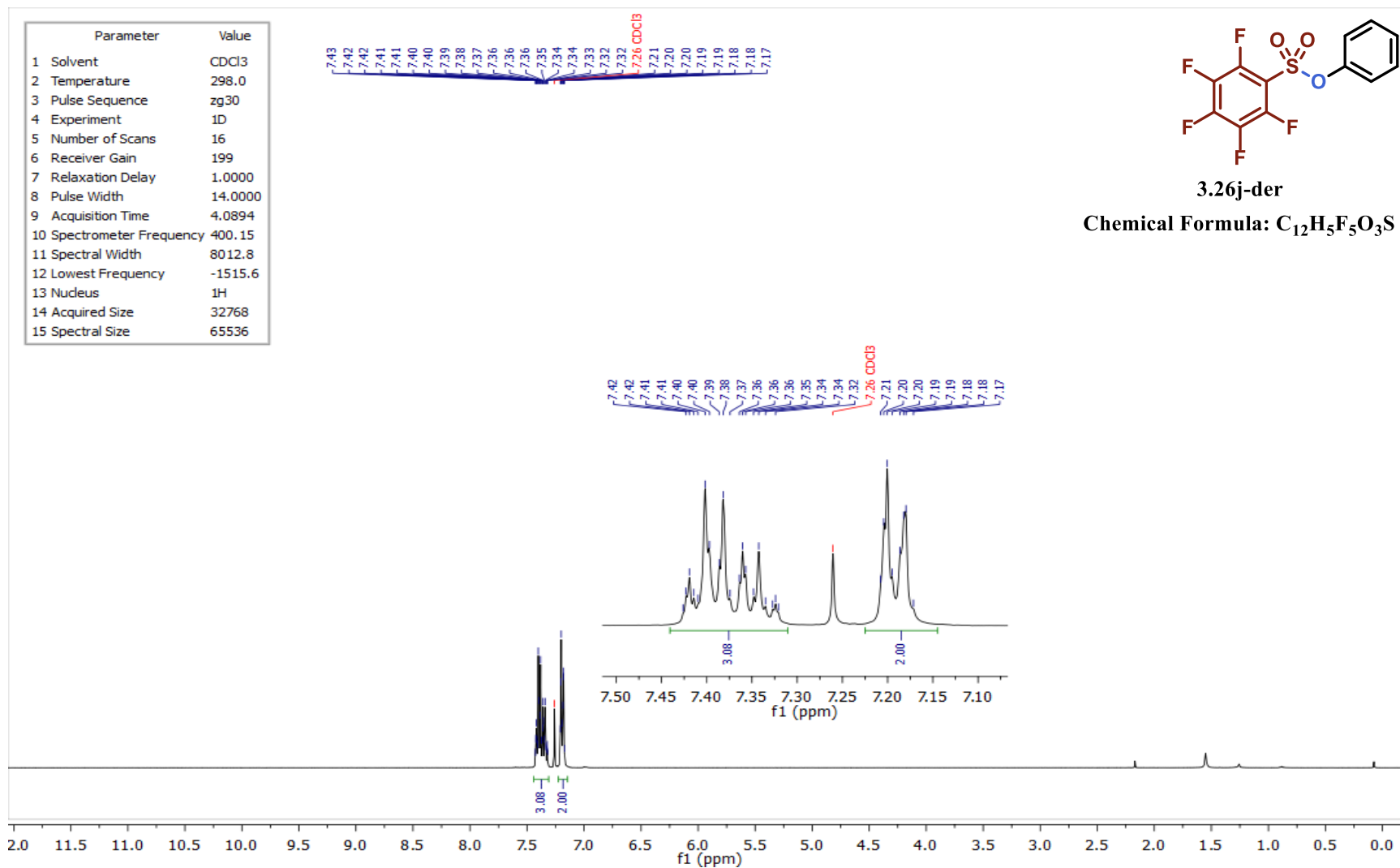


Figure 4.164 – ^1H NMR spectrum of compound 3.26j-der in CDCl_3 .

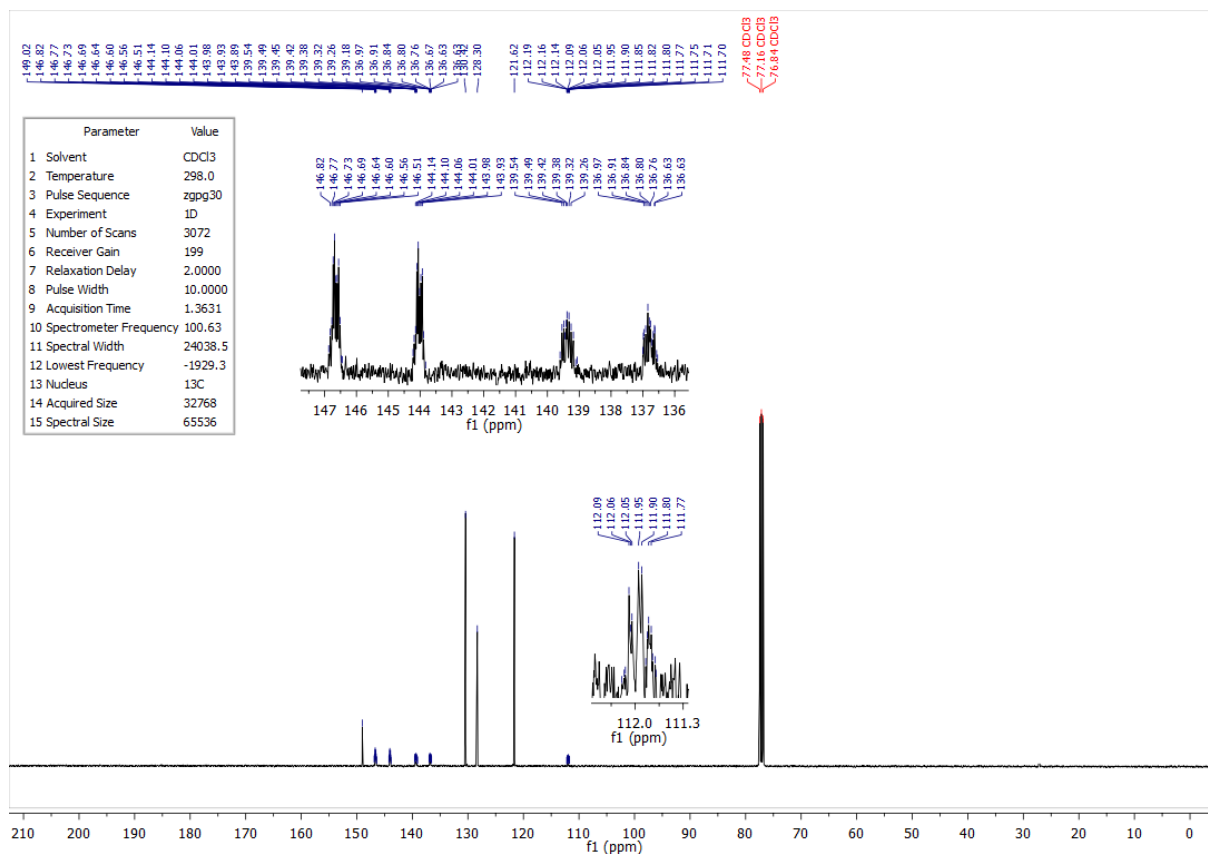


Figure 4.165 – ^{13}C NMR spectrum of compound **3.26j-der** in CDCl_3 .

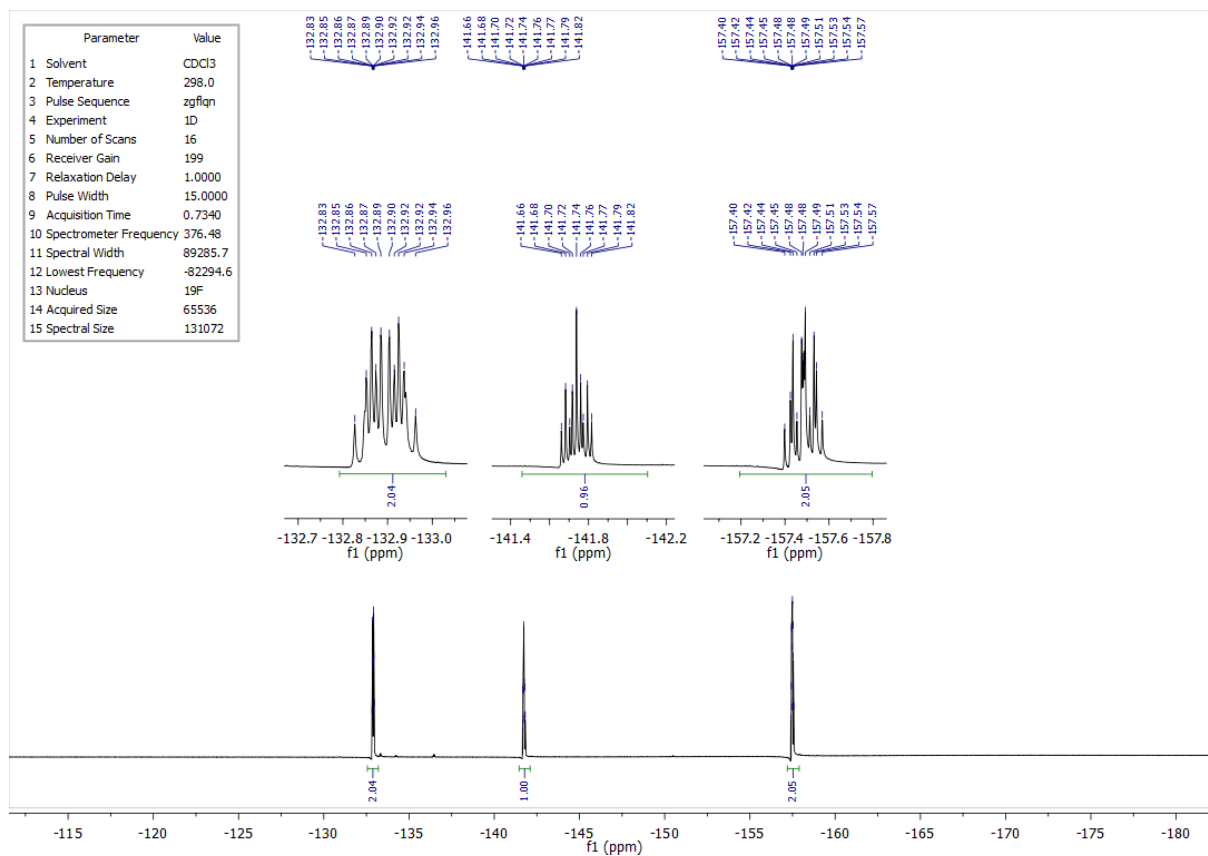


Figure 4.166 – ^{19}F NMR spectrum of compound **3.26j-der** in CDCl_3 .

4.3.13 ^1H , ^{13}C and ^{19}F NMR spectra of compound 3.26k

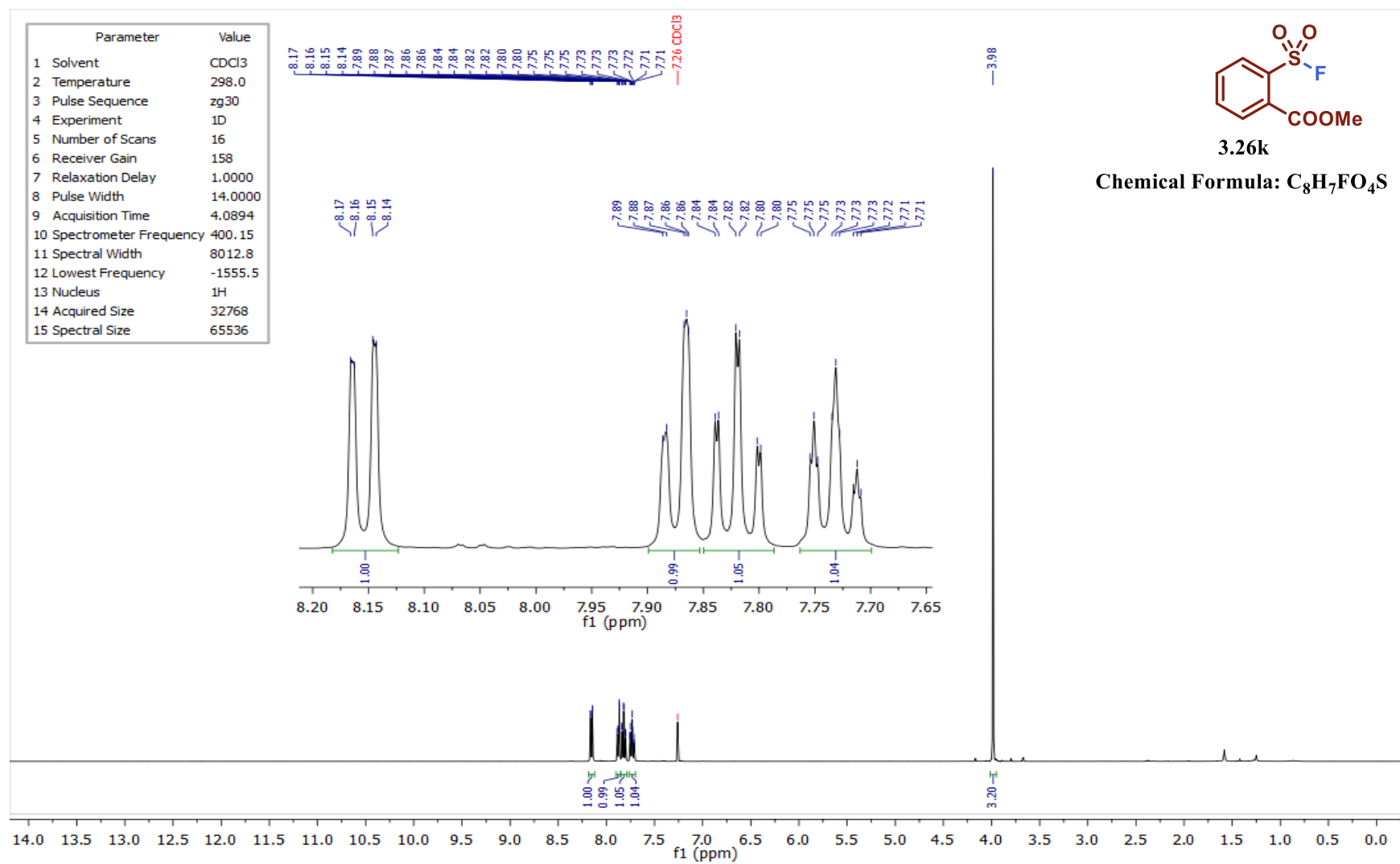


Figure 4.167 – ^1H NMR spectrum of compound 3.26k in CDCl_3 .

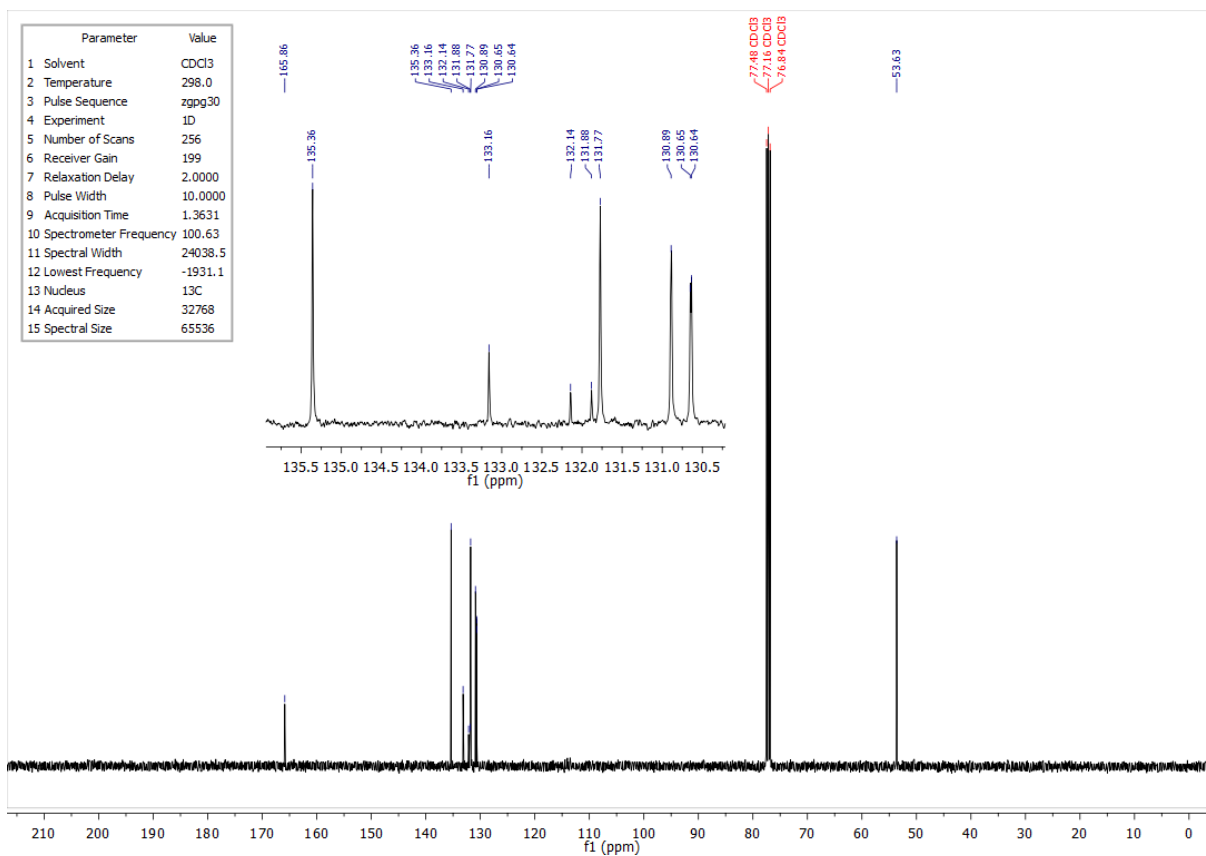


Figure 4.168 – ¹³C NMR spectrum of compound **3.26k** in CDCl₃.

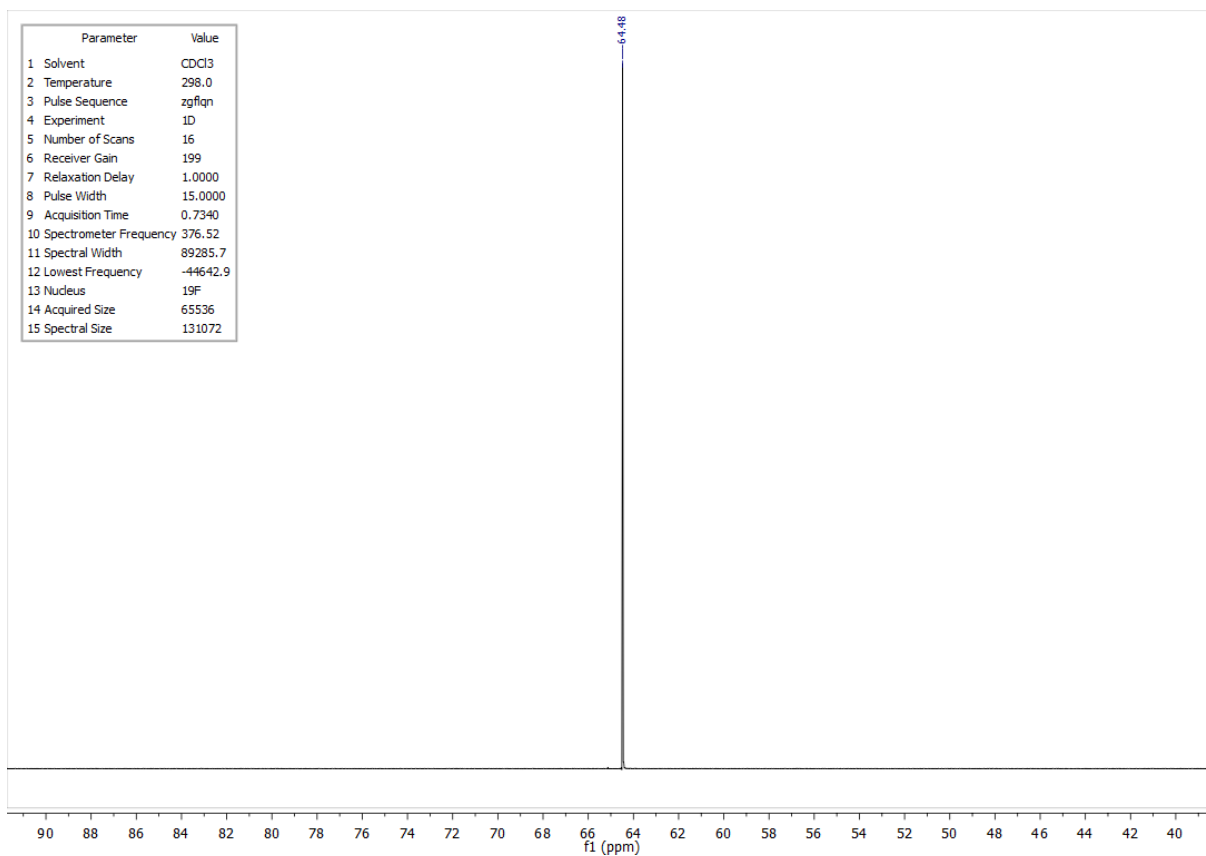


Figure 4.169 – ¹⁹F NMR spectrum of compound **3.26k** in CDCl₃.

4.3.14 ^1H , ^{13}C and ^{19}F NMR spectra of compound 3.26l

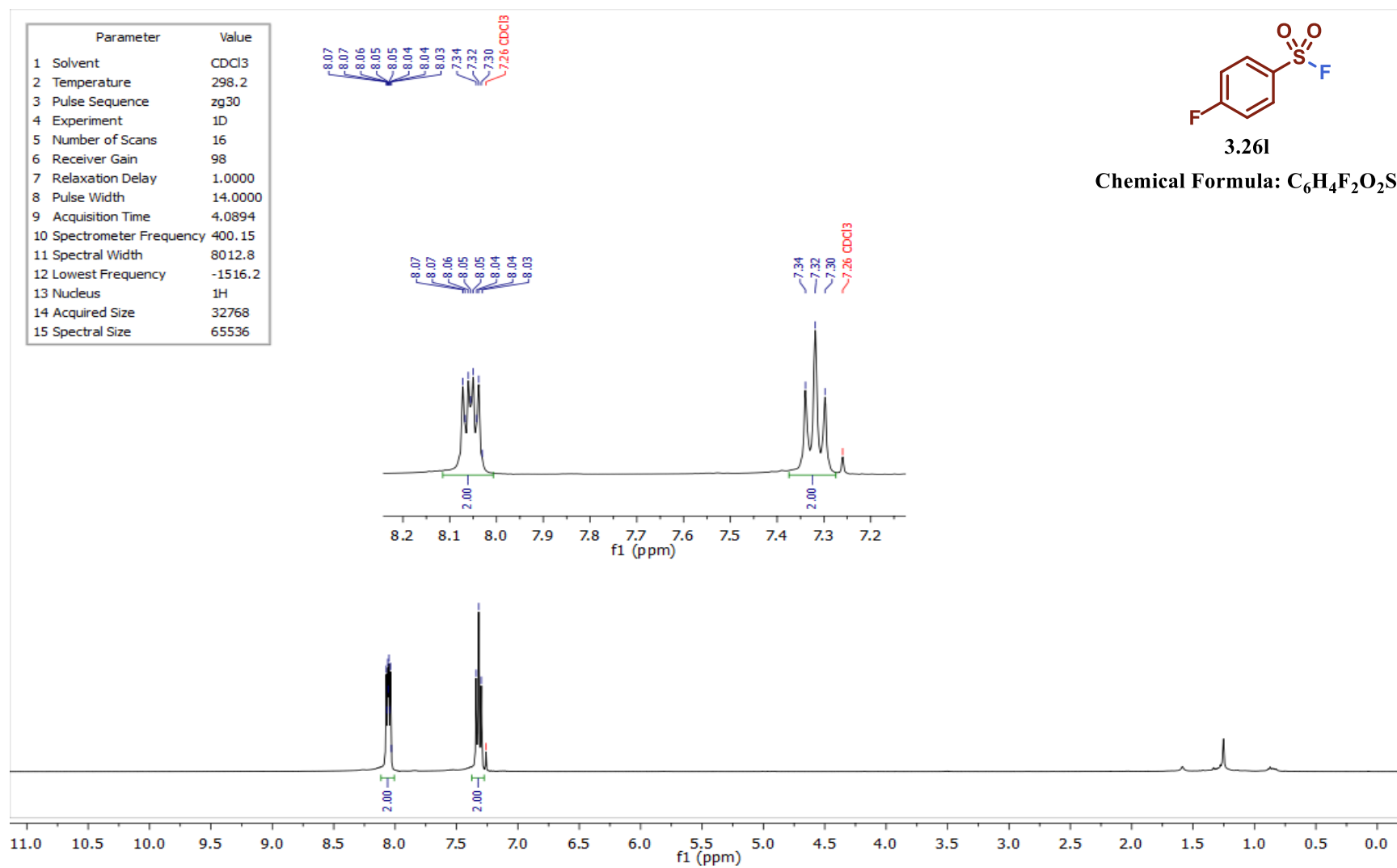


Figure 4.170 – ^1H NMR spectrum of compound 3.26l in CDCl_3 .

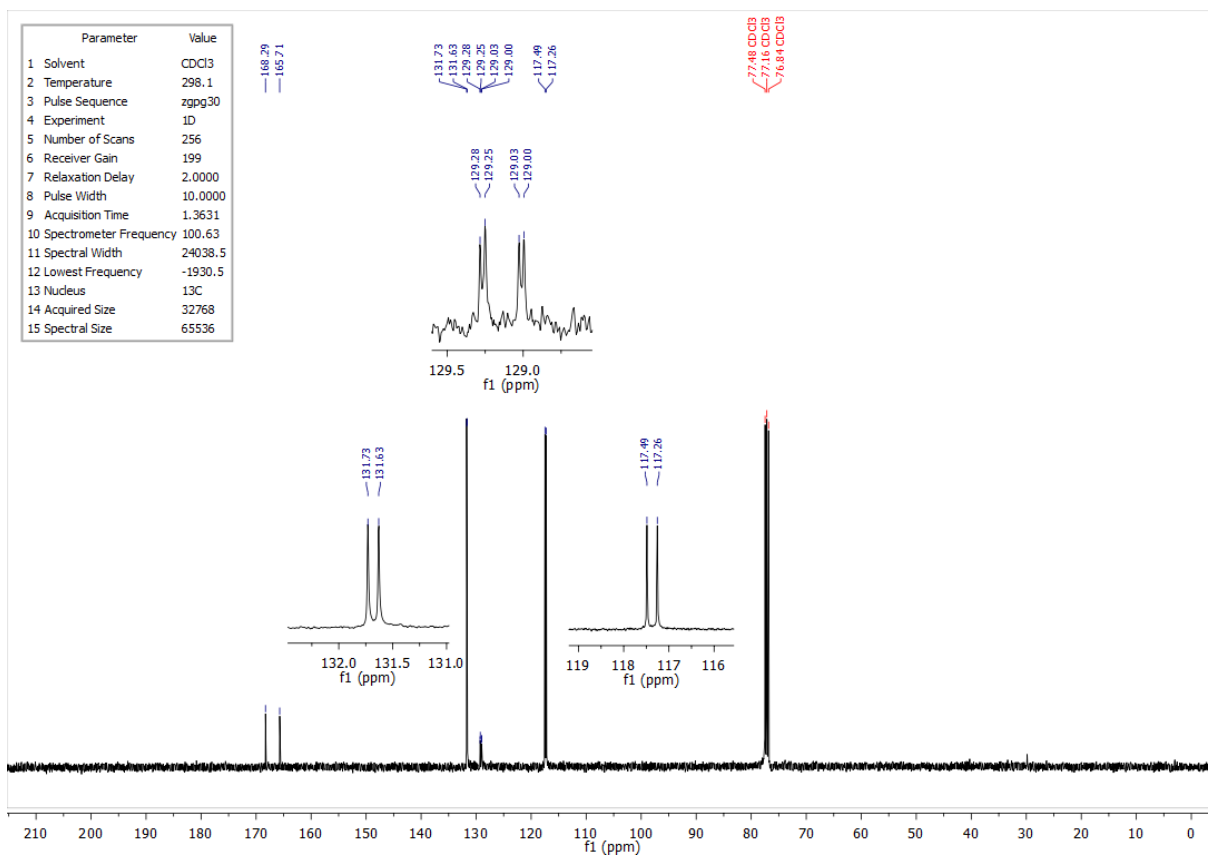


Figure 4.171 – ¹³C NMR spectrum of compound **3.261** in CDCl₃.

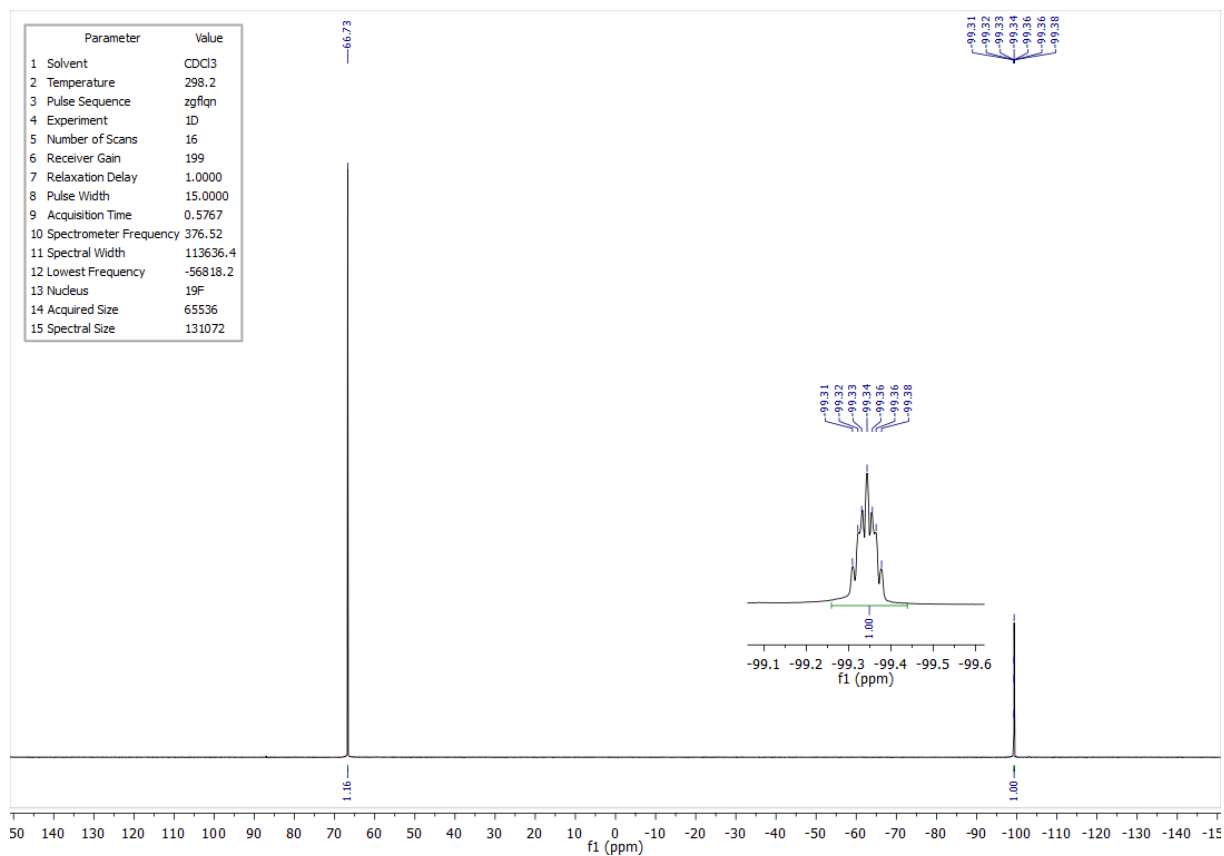


Figure 4.172 – ¹⁹F NMR spectrum of compound **3.261** in CDCl₃.

4.3.15 ^1H , ^{13}C and ^{19}F NMR spectra of compound 3.26m

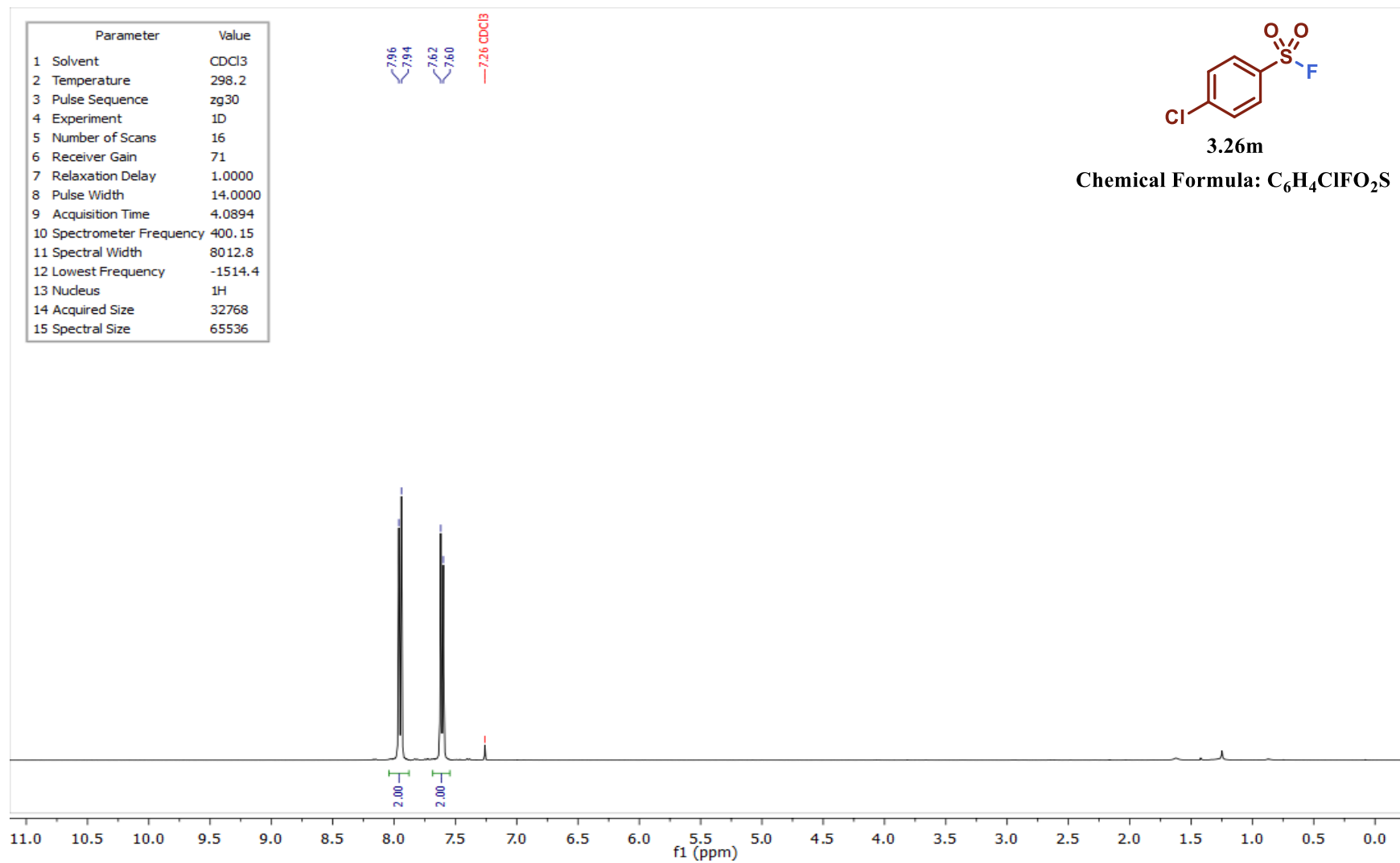


Figure 4.173 – ^1H NMR spectrum of compound **3.26m** in CDCl_3 .

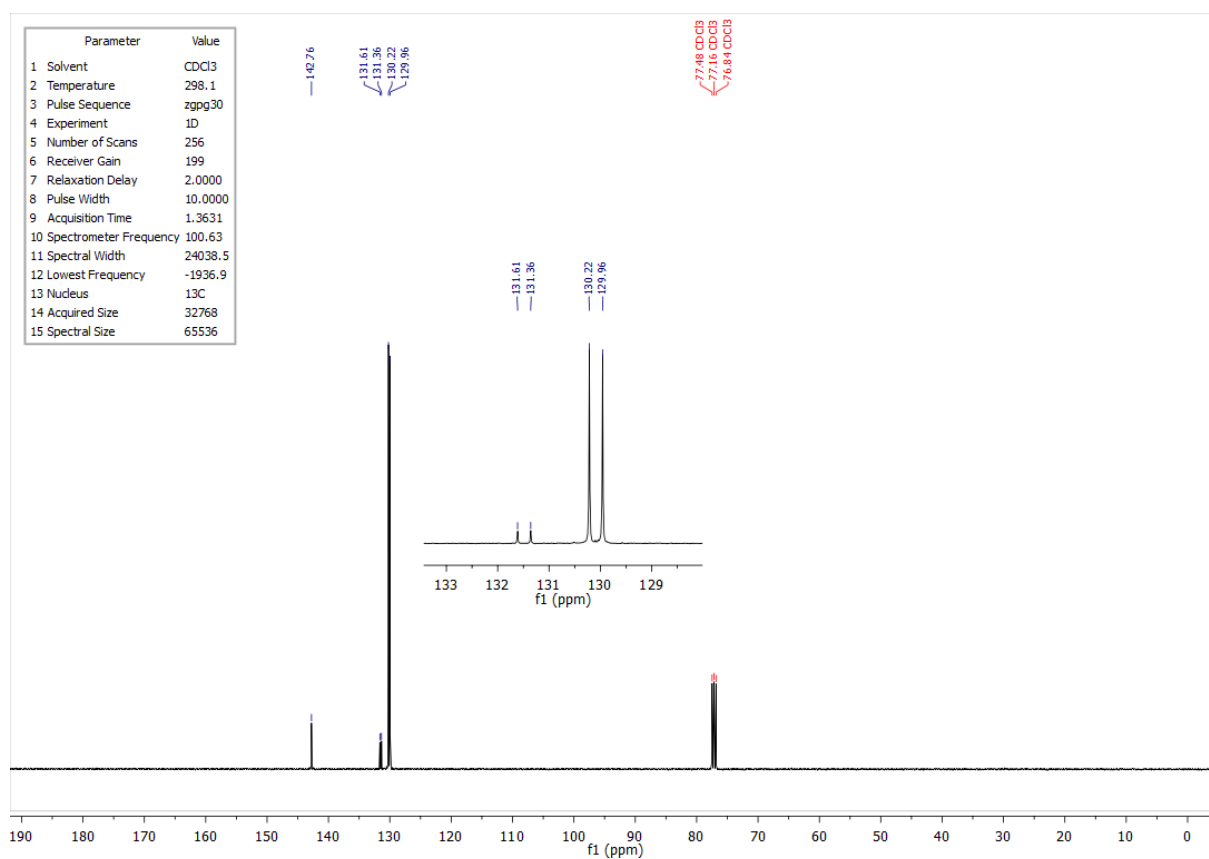


Figure 4.174 – ¹³C NMR spectrum of compound **3.26m** in CDCl₃.

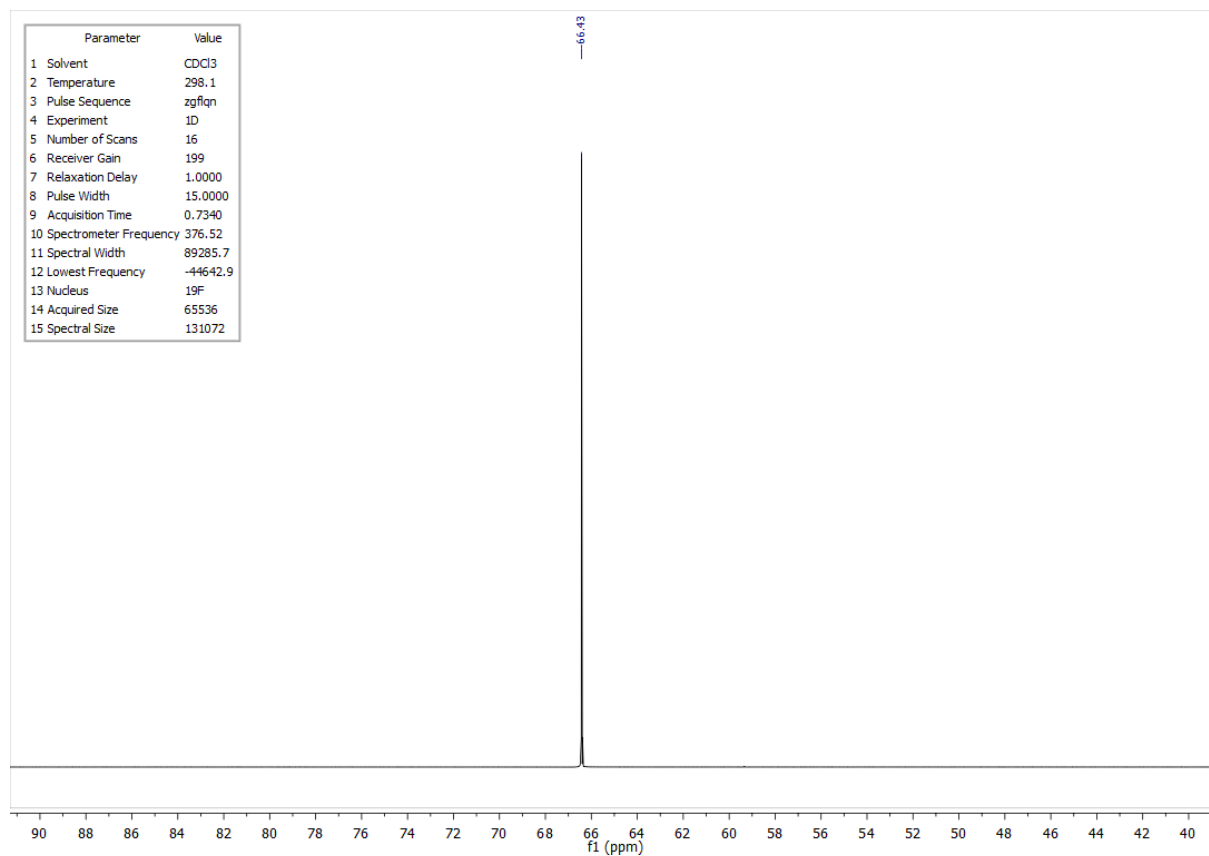


Figure 4.175 – ¹⁹F NMR spectrum of compound **3.26m** in CDCl₃.

4.3.16 ^1H , ^{13}C and ^{19}F NMR spectra of compound 3.26n

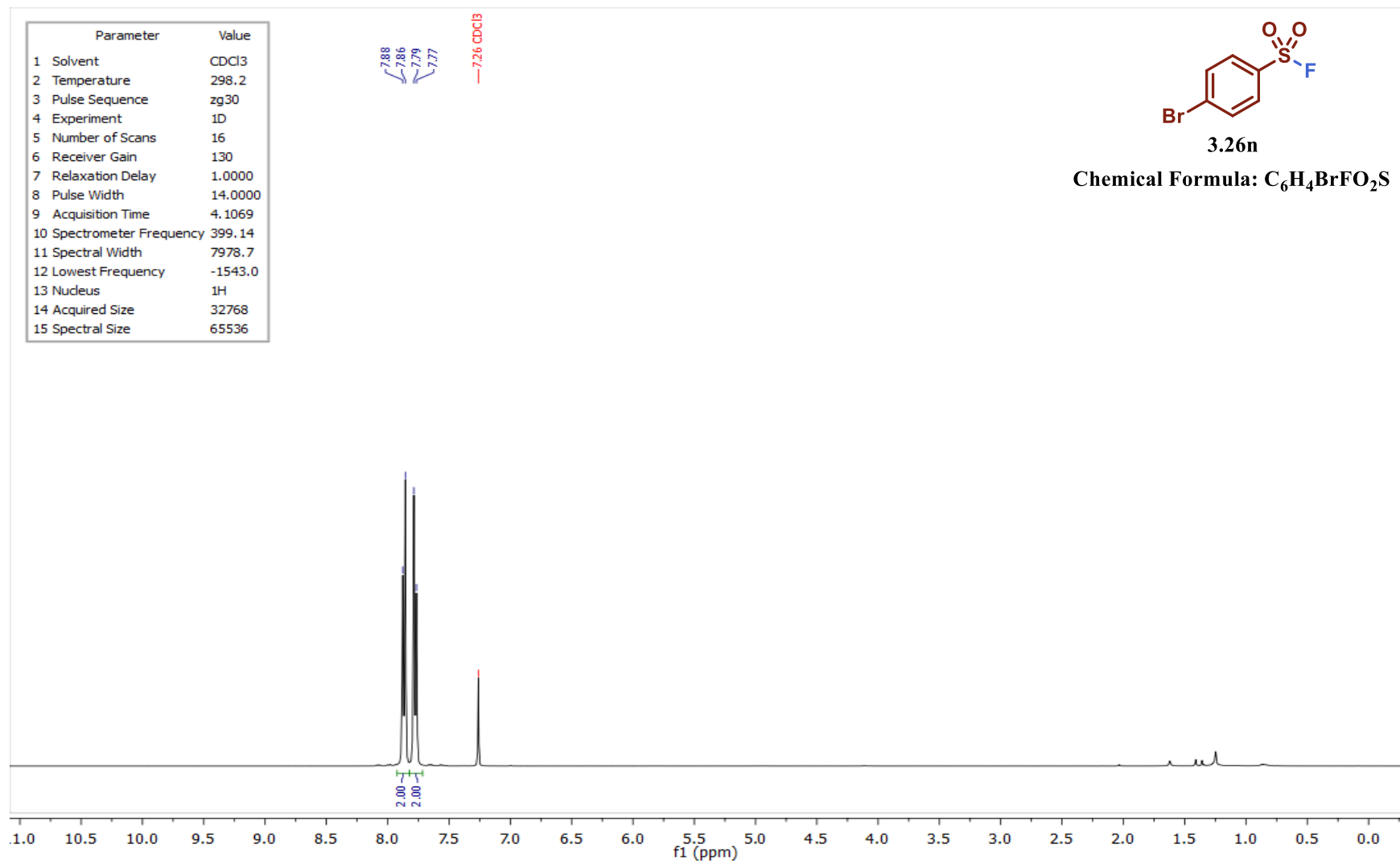


Figure 4.176 – ^1H NMR spectrum of compound 3.26n in CDCl_3 .

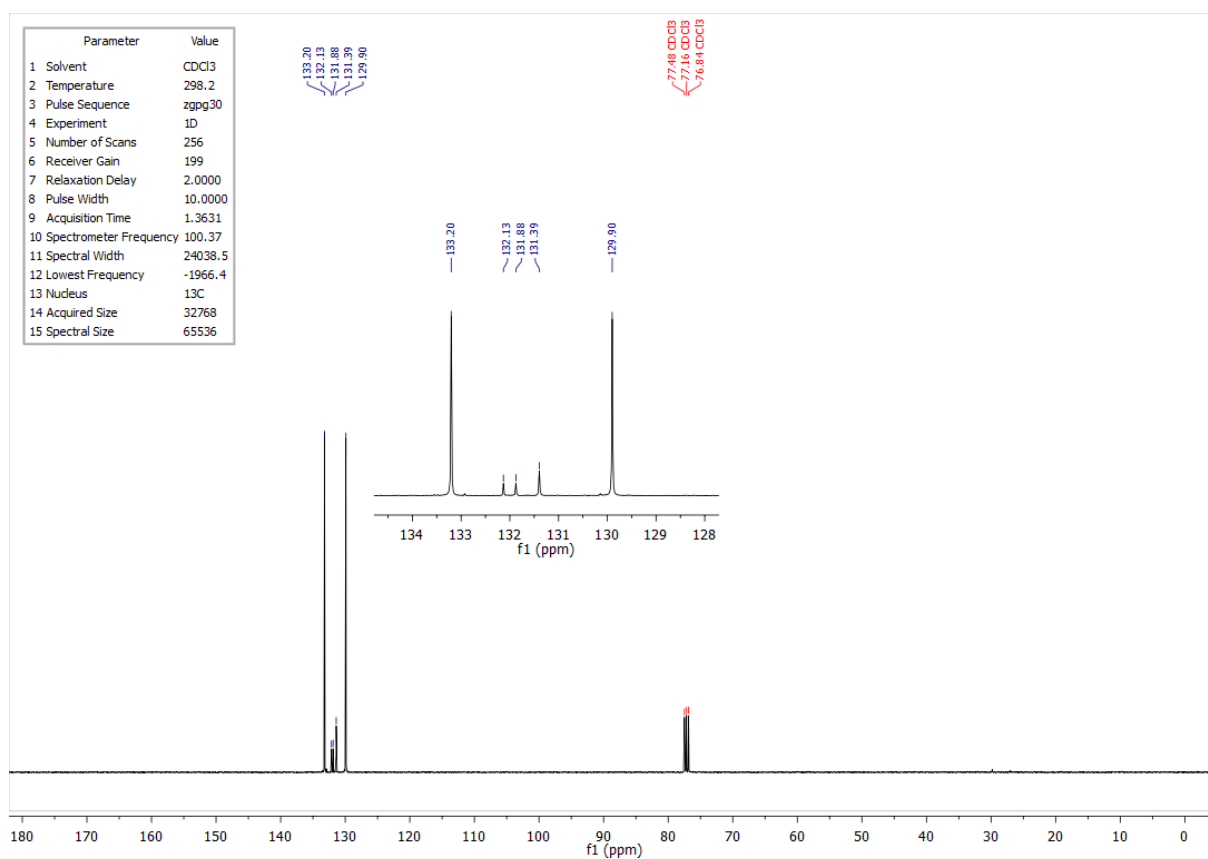


Figure 4.177 – ^{13}C NMR spectrum of compound **3.26n** in CDCl_3 .

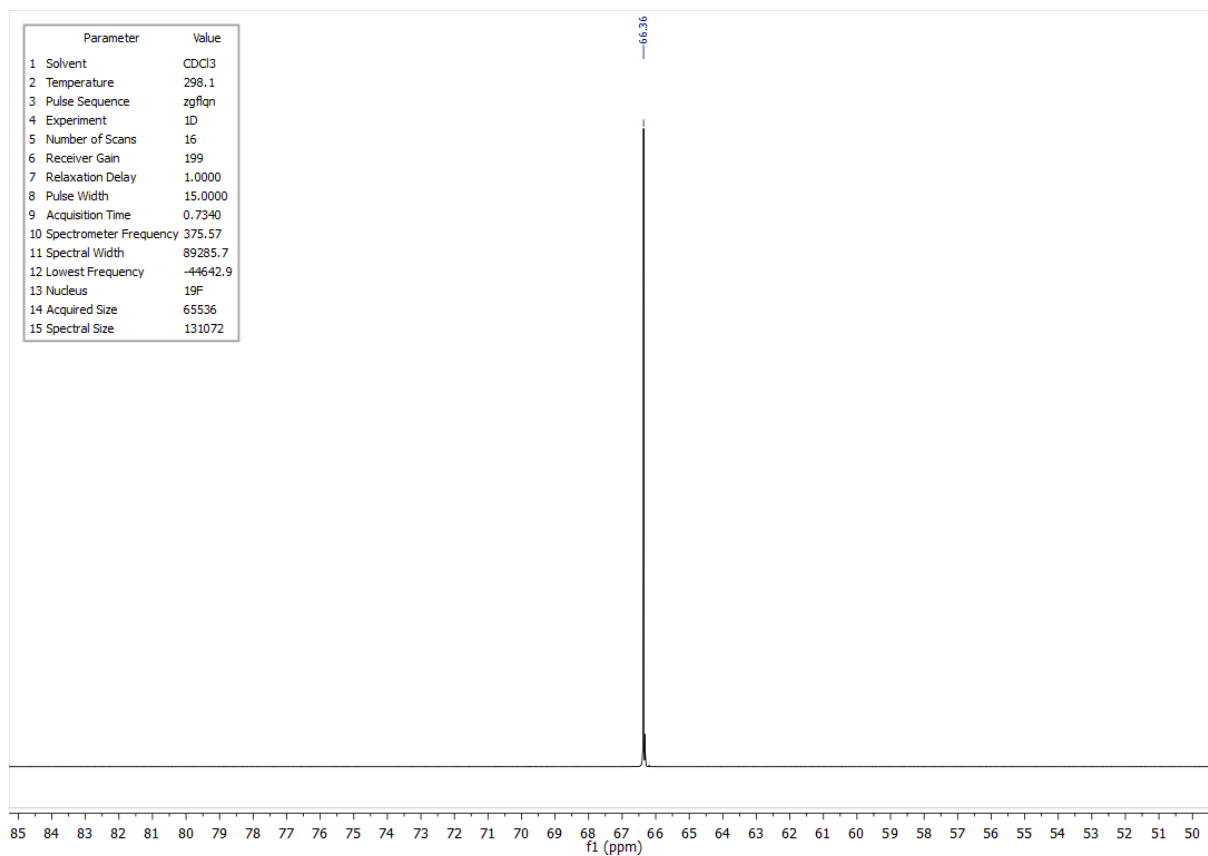


Figure 4.178 – ^{19}F NMR spectrum of compound **3.26n** in CDCl_3 .

4.3.17 ^1H , ^{13}C and ^{19}F NMR spectra of compound 3.26o

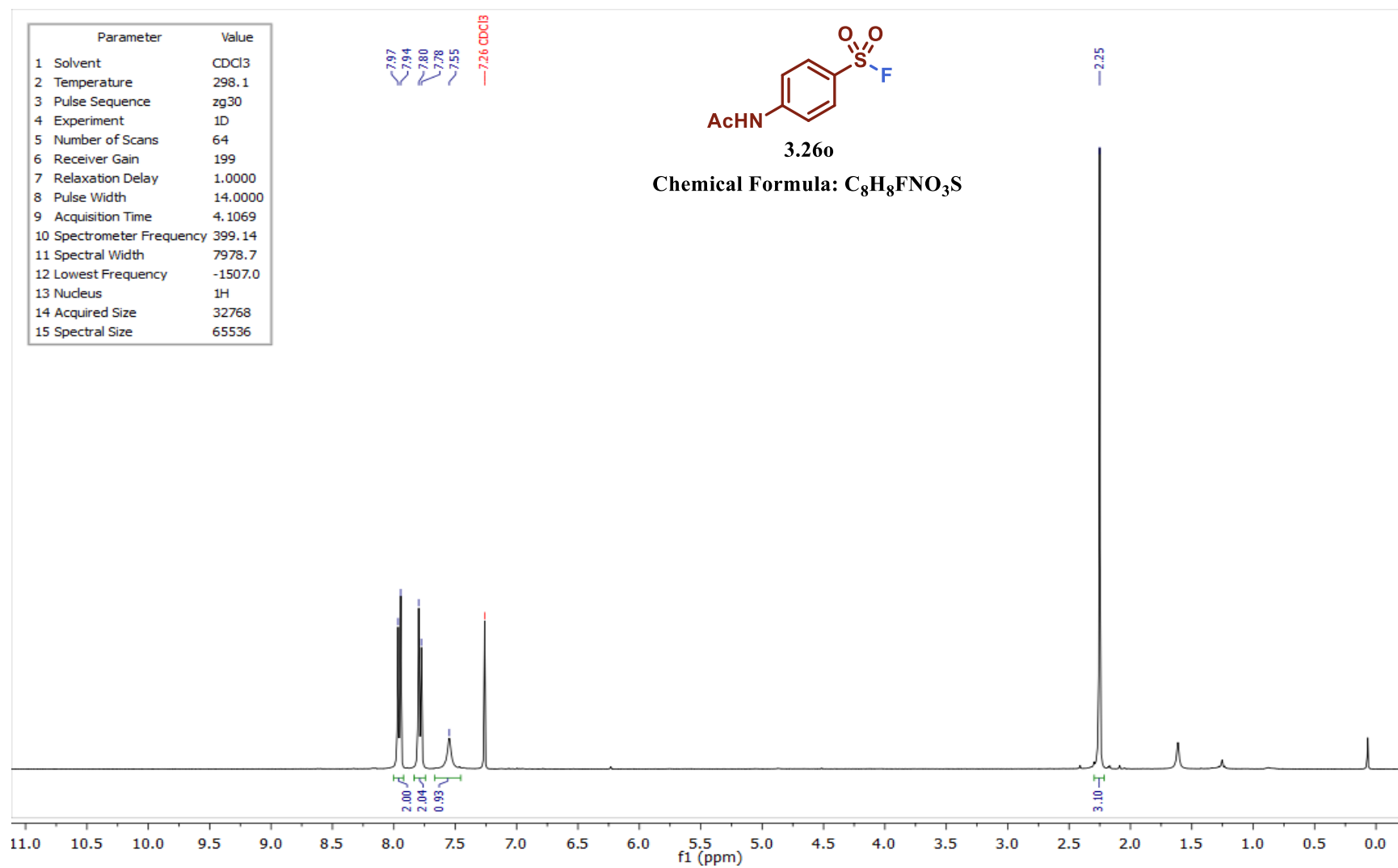


Figure 4.179 – ^1H NMR spectrum of compound 3.26o in CDCl_3 .

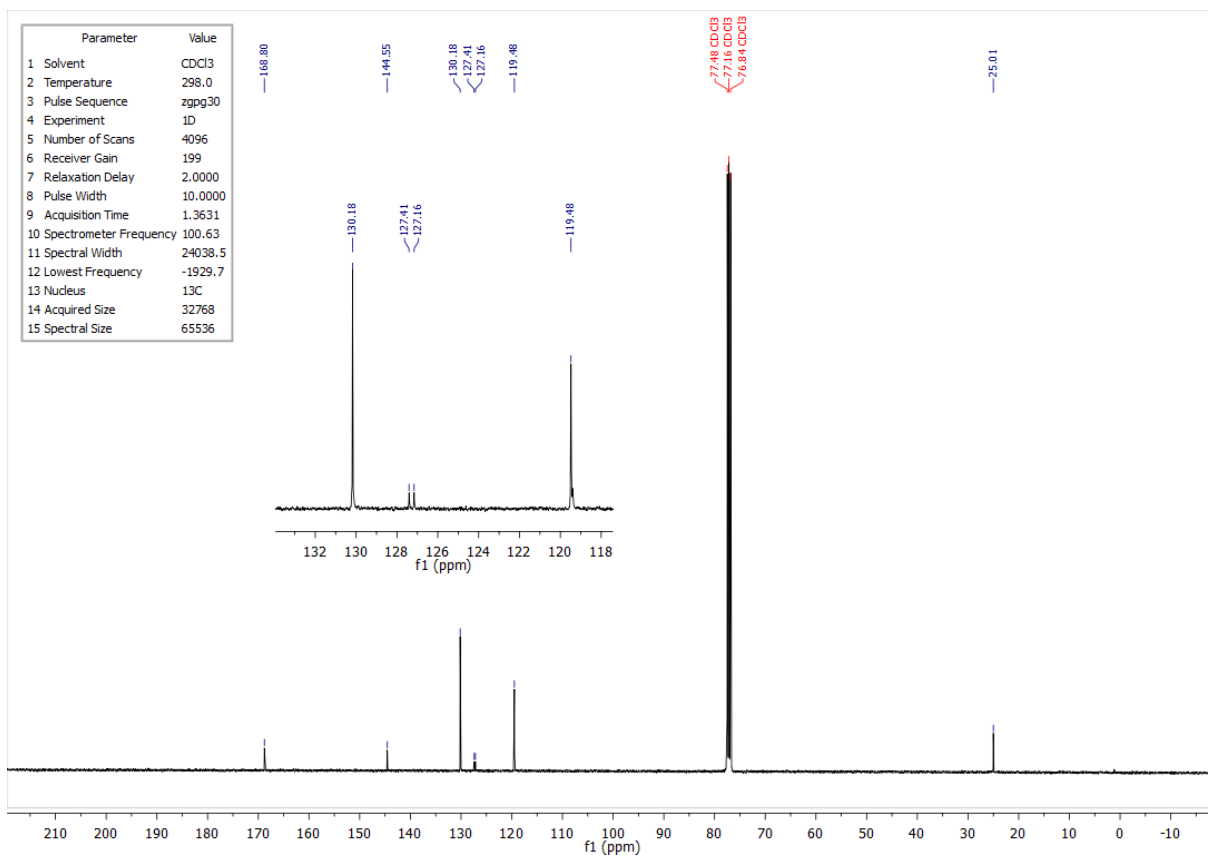


Figure 4.180 – ¹³C NMR spectrum of compound **3.260** in CDCl₃.

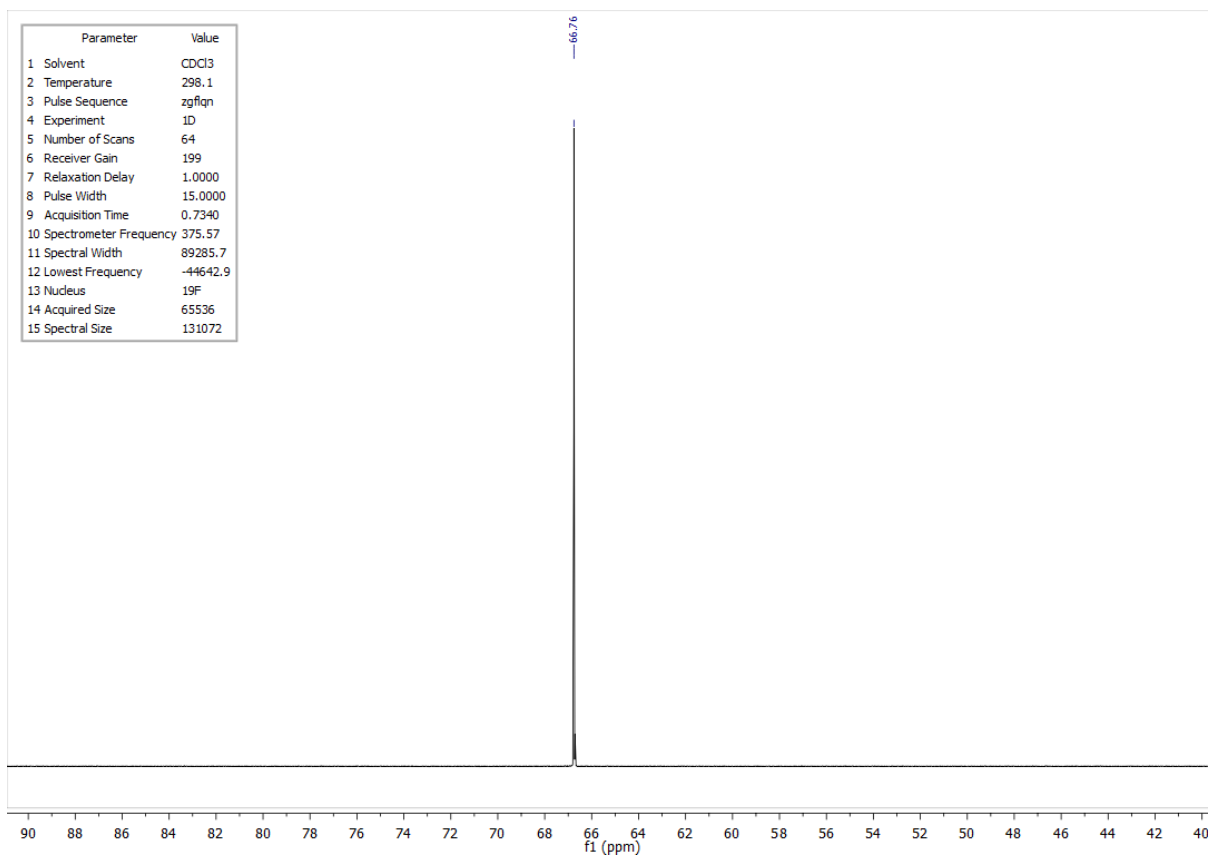


Figure 4.181 – ¹⁹F NMR spectrum of compound **3.260** in CDCl₃.

4.3.18 ^1H , ^{13}C and ^{19}F NMR spectra of compound 3.26p

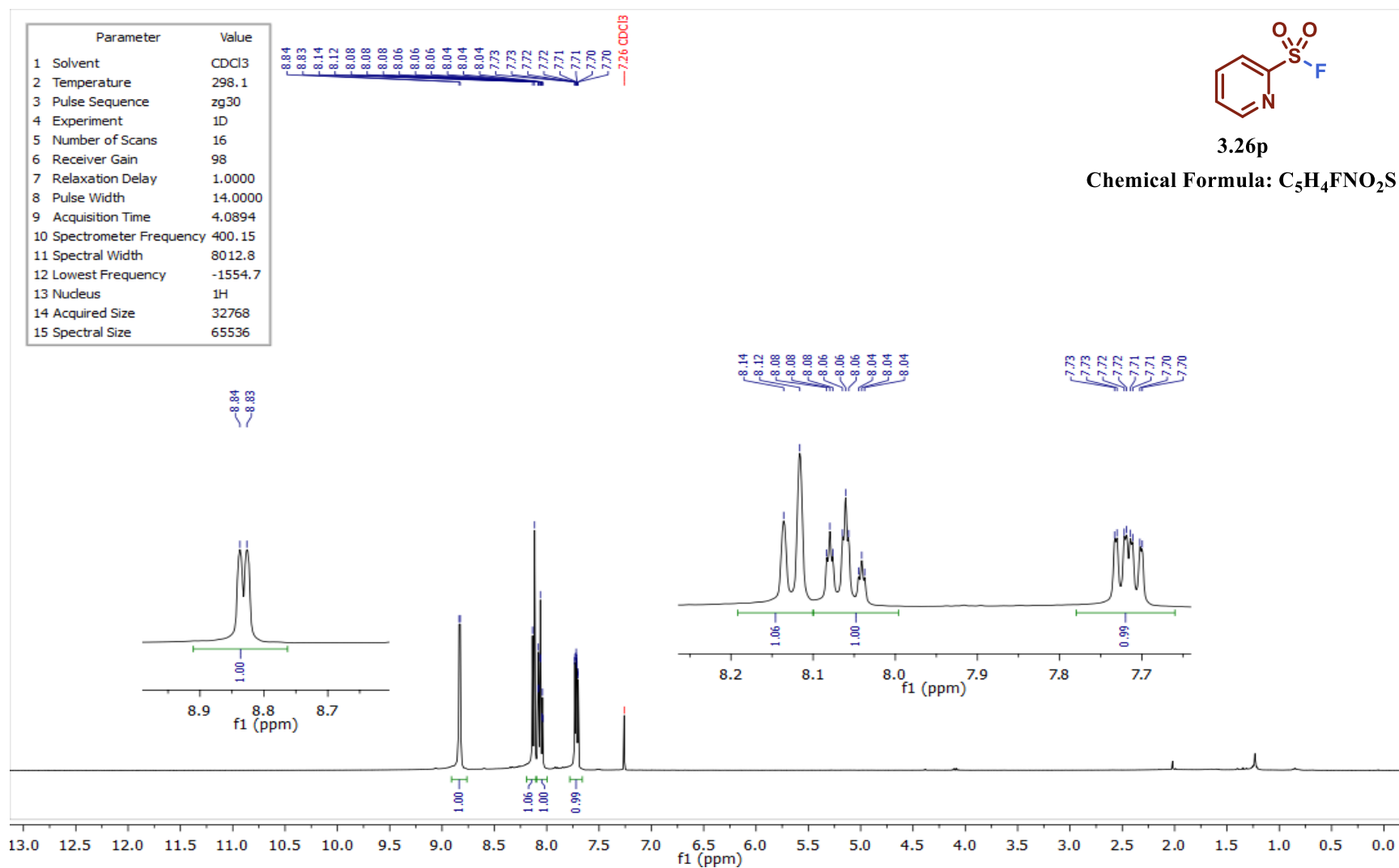


Figure 4.182 – ^1H NMR spectrum of compound 3.26p in CDCl_3 .

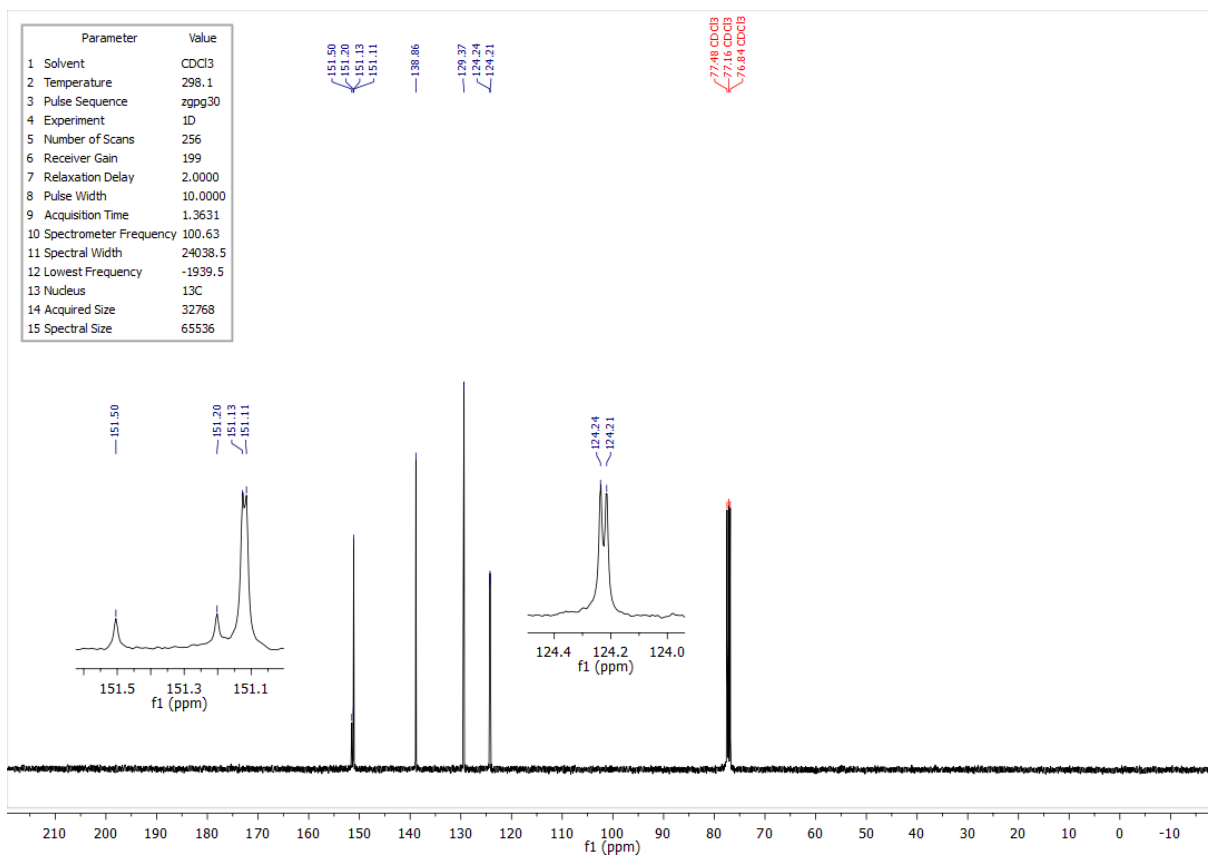


Figure 4.183 – ¹³C NMR spectrum of compound **3.26p** in CDCl₃.

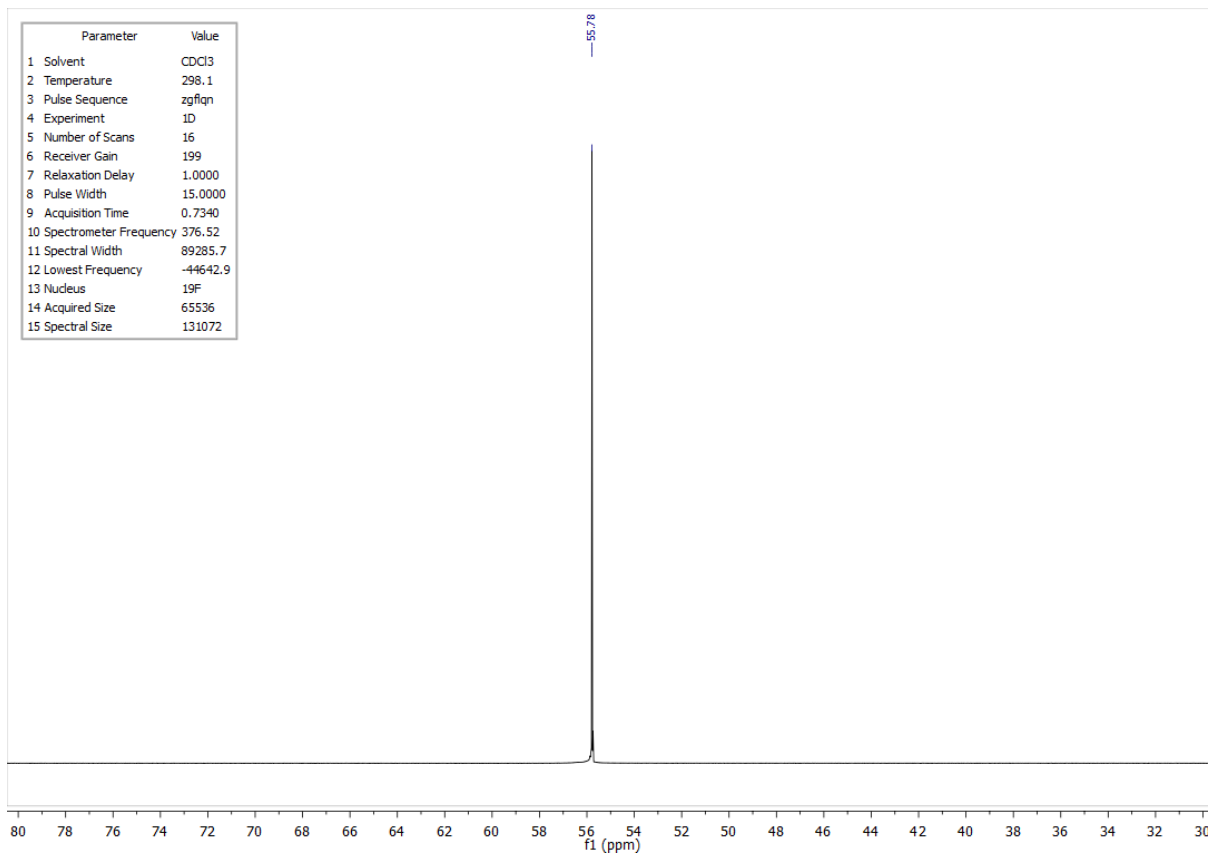


Figure 4.184 – ¹⁹F NMR spectrum of compound **3.26p** in CDCl₃.

4.3.19 ^1H , ^{13}C and ^{19}F NMR spectra of compound 3.26q

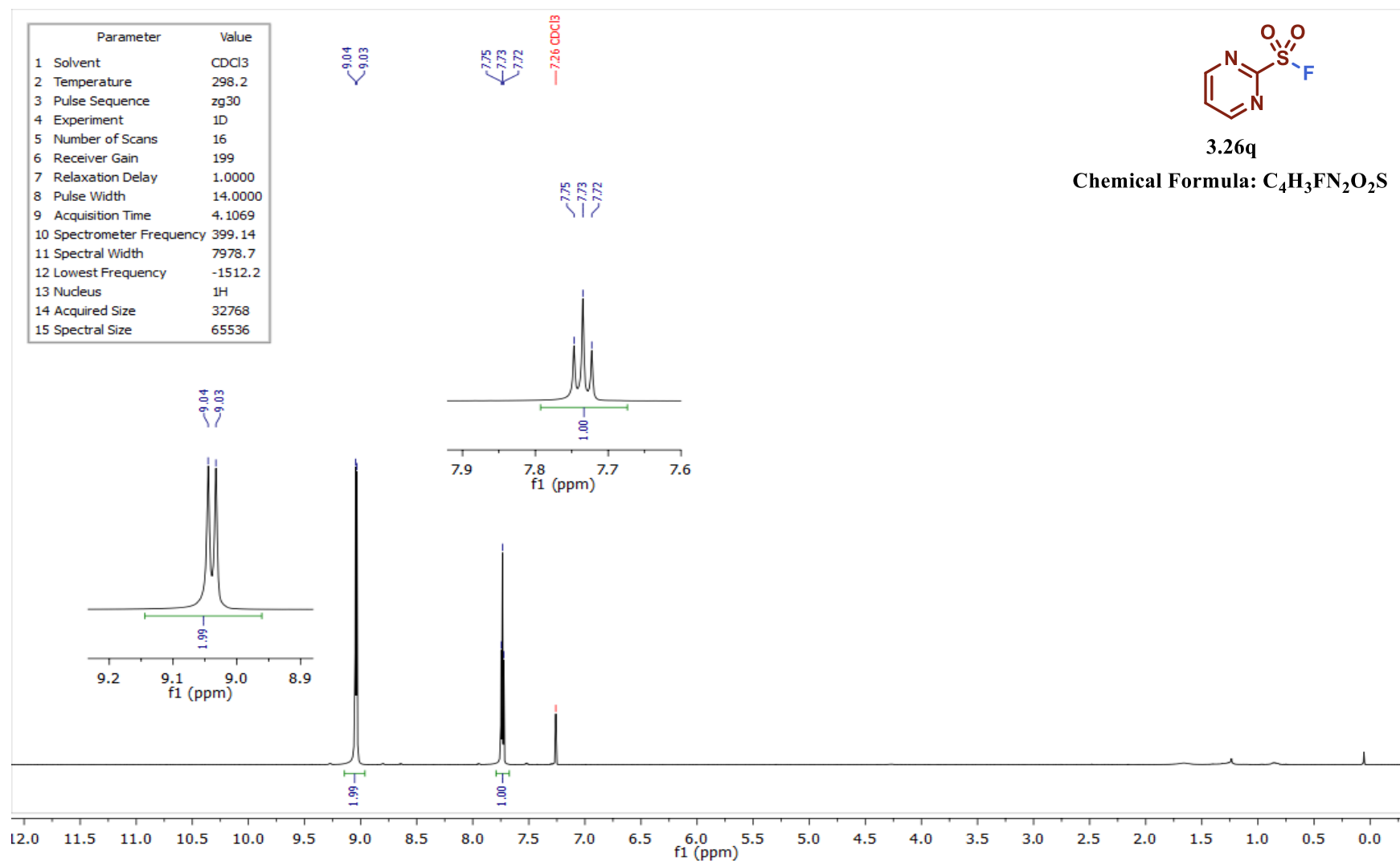
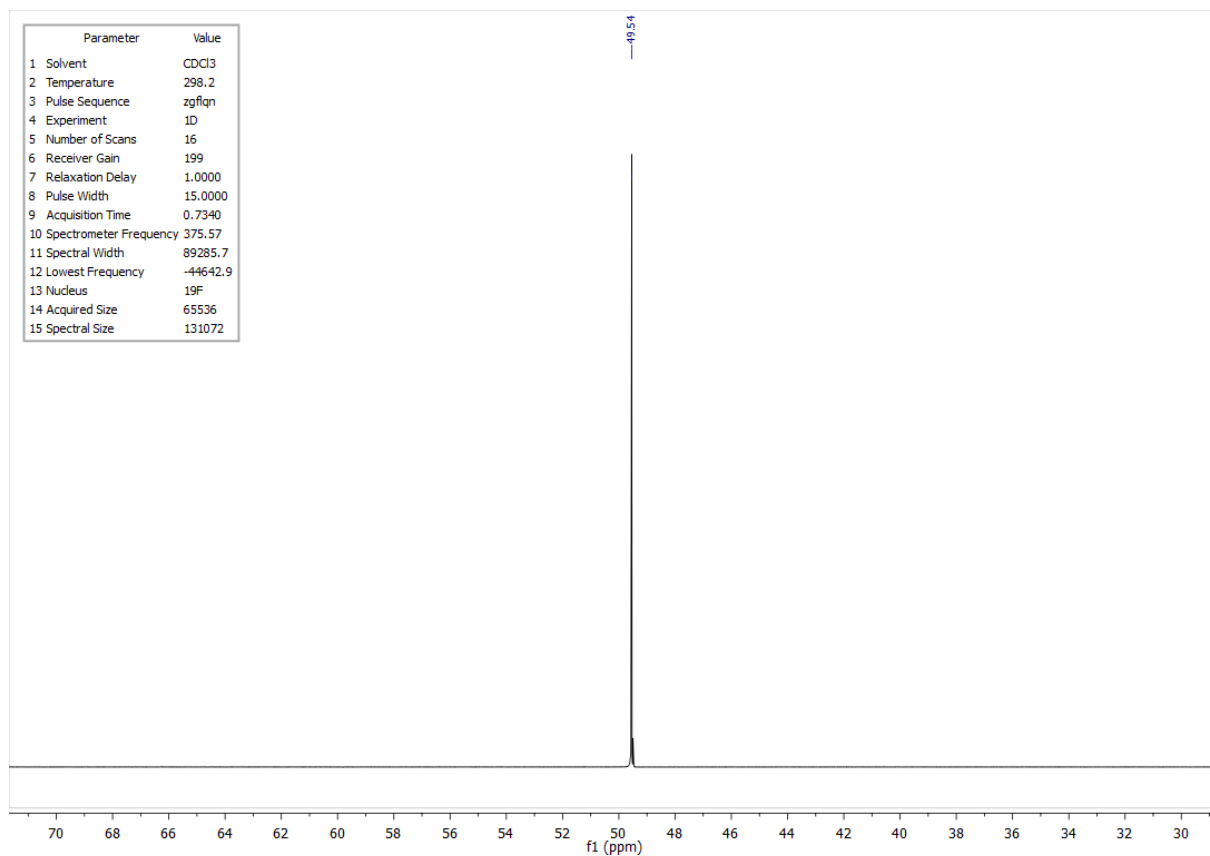
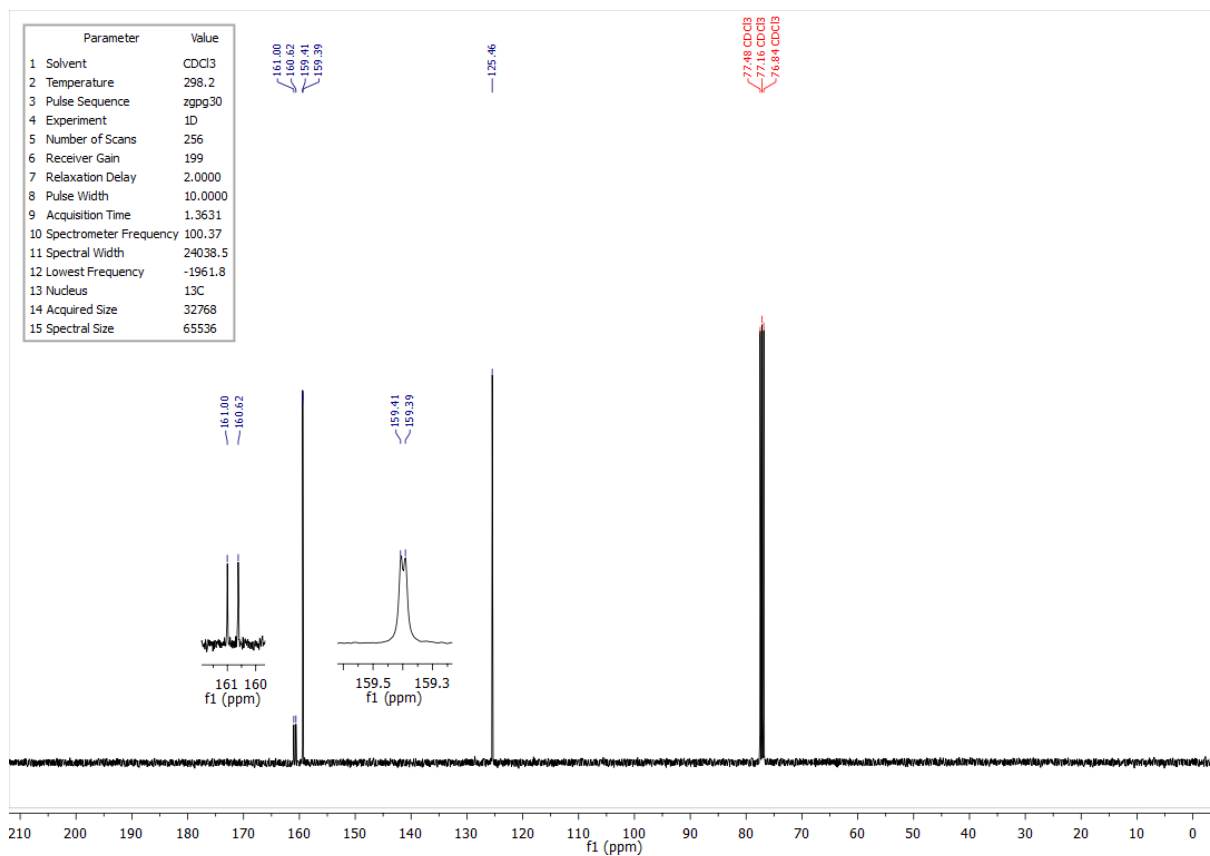


Figure 4.185 – ^1H NMR spectrum of compound 3.26q in CDCl_3 .



4.3.20 ^1H and ^{13}C NMR spectra of compound 3.26r-der

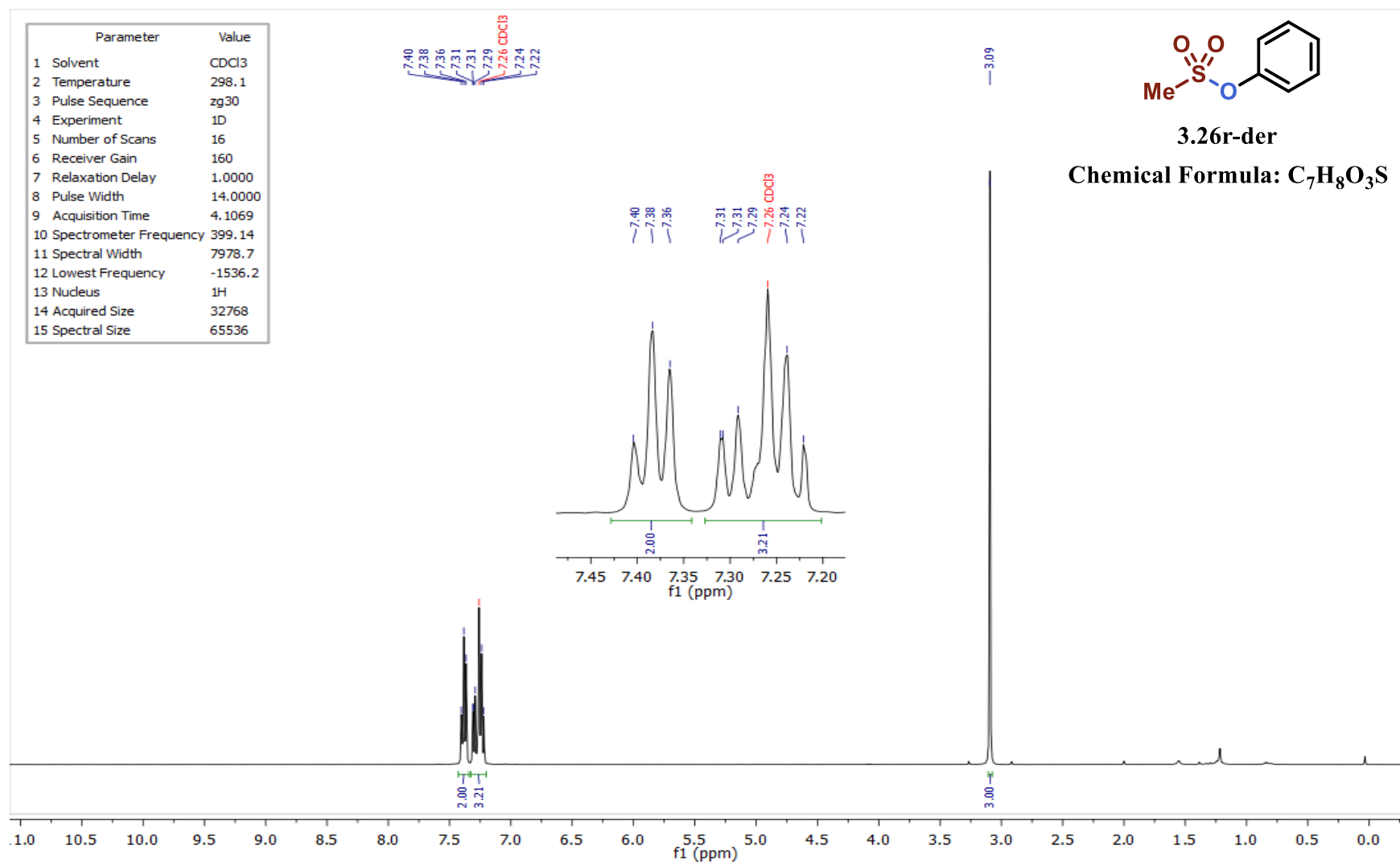


Figure 4.188 – ^1H NMR spectrum of compound 3.26r-der in CDCl_3 .

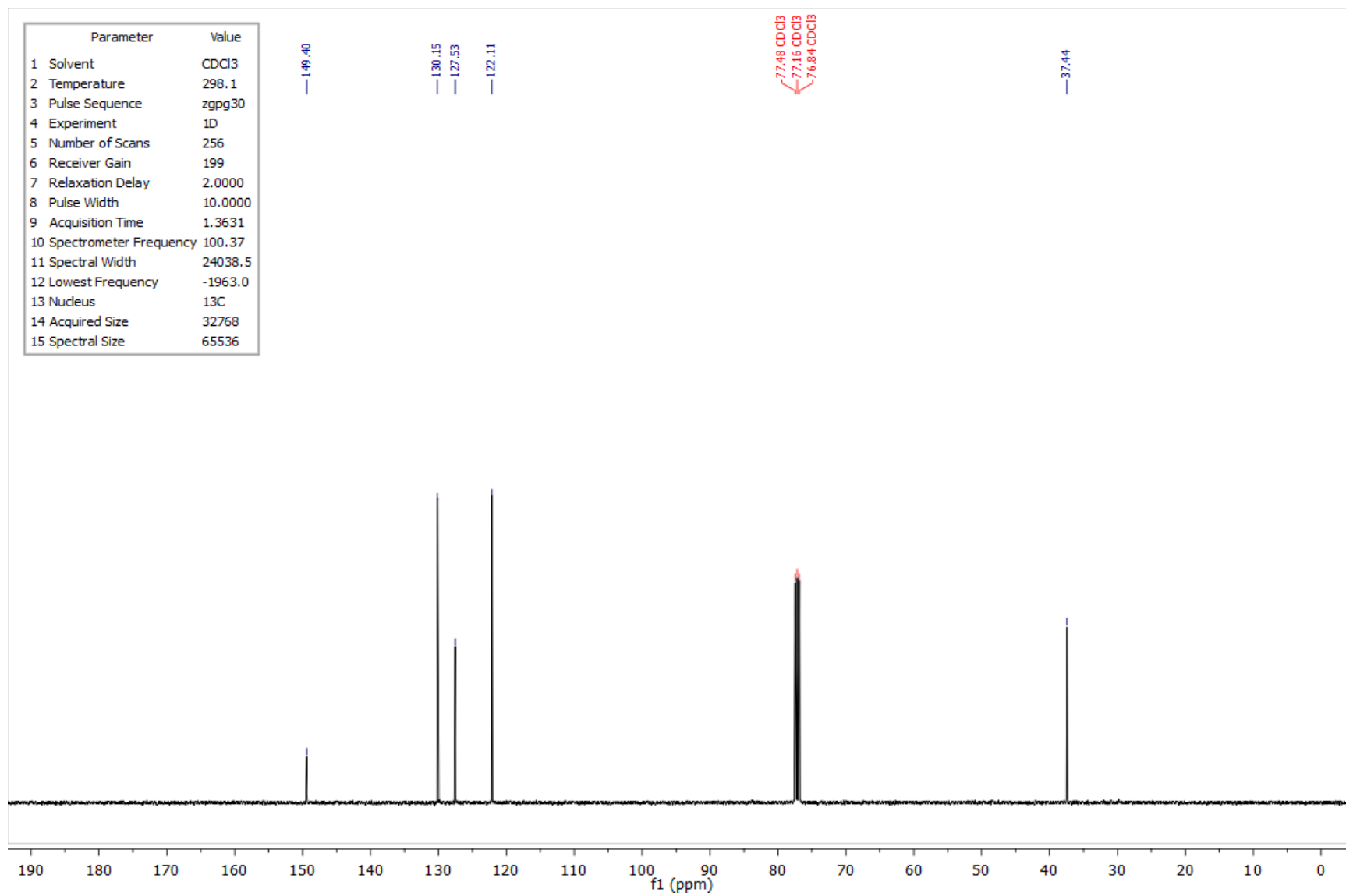


Figure 4.189 – ¹³C NMR spectrum of compound **3.26r-der** in CDCl₃.

4.3.21 ^1H and ^{13}C NMR spectra of compound 3.26s-der

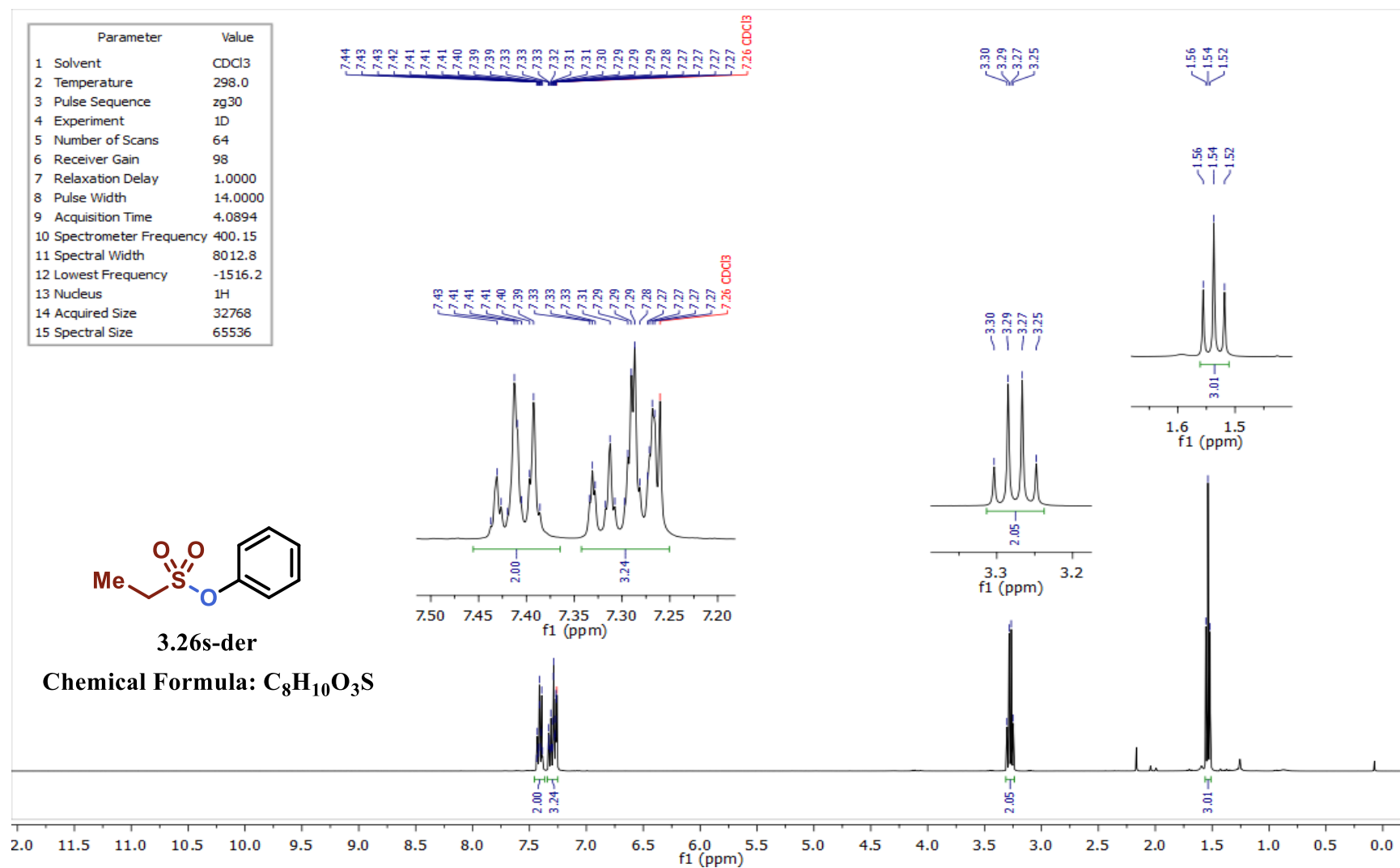


Figure 4.190 – ^1H NMR spectrum of compound 3.26s-der in CDCl_3 .

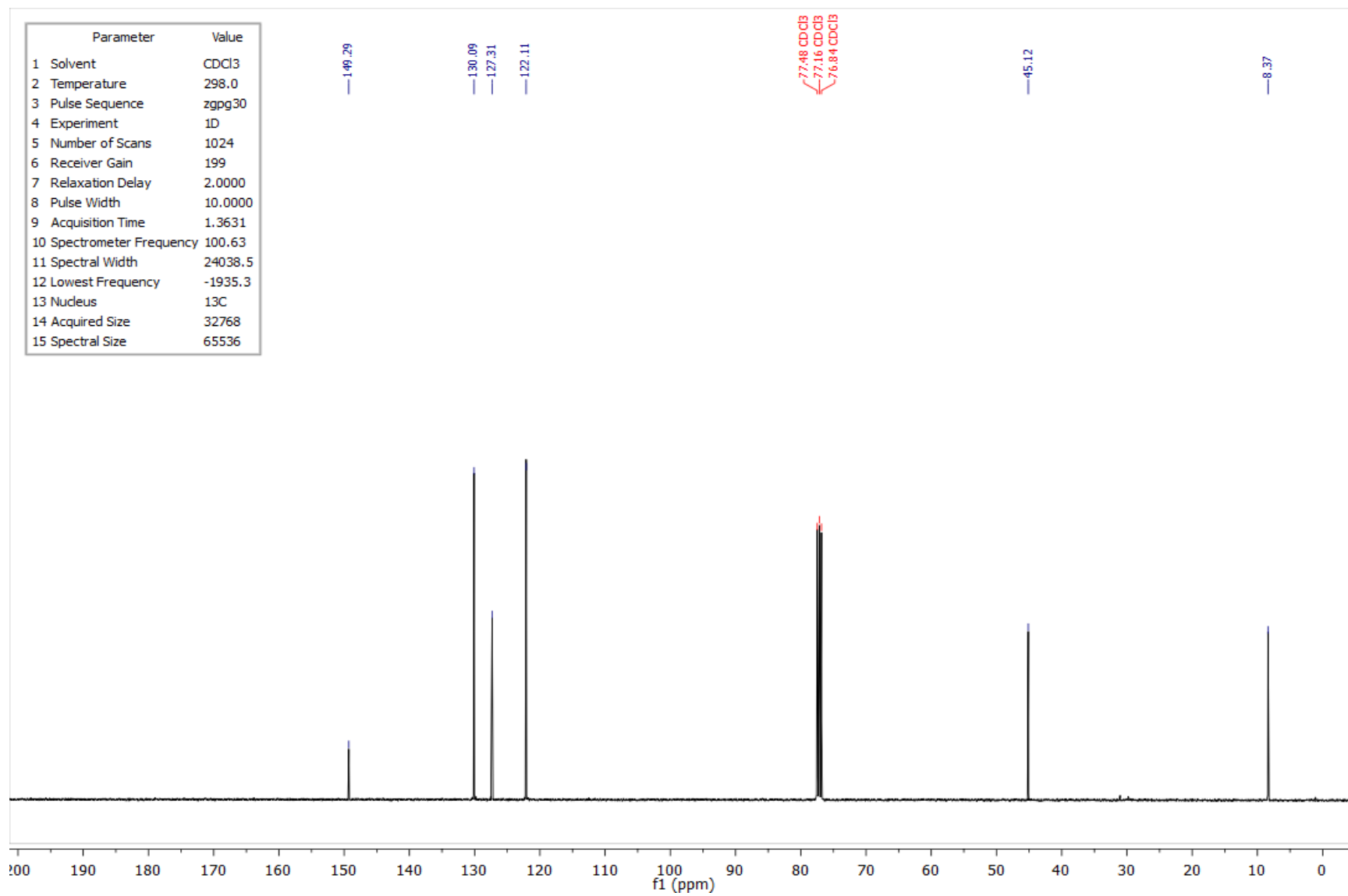


Figure 4.191 – ^{13}C NMR spectrum of compound **3.26s-der** in CDCl_3 .

4.3.22 ^1H and ^{13}C NMR spectra of compound 3.26t-der

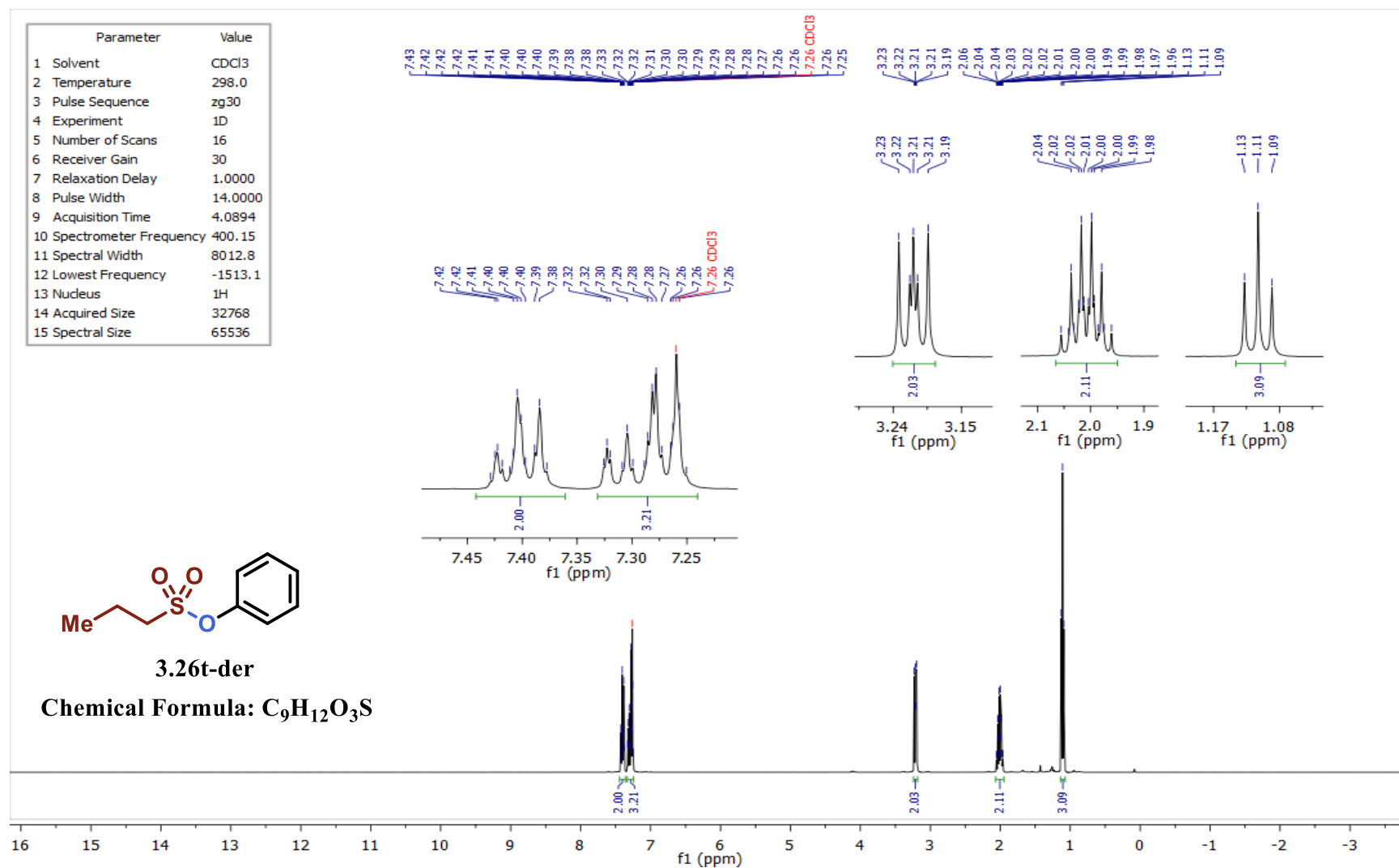


Figure 4.192 – ^1H NMR spectrum of compound 3.26t-der in CDCl_3 .

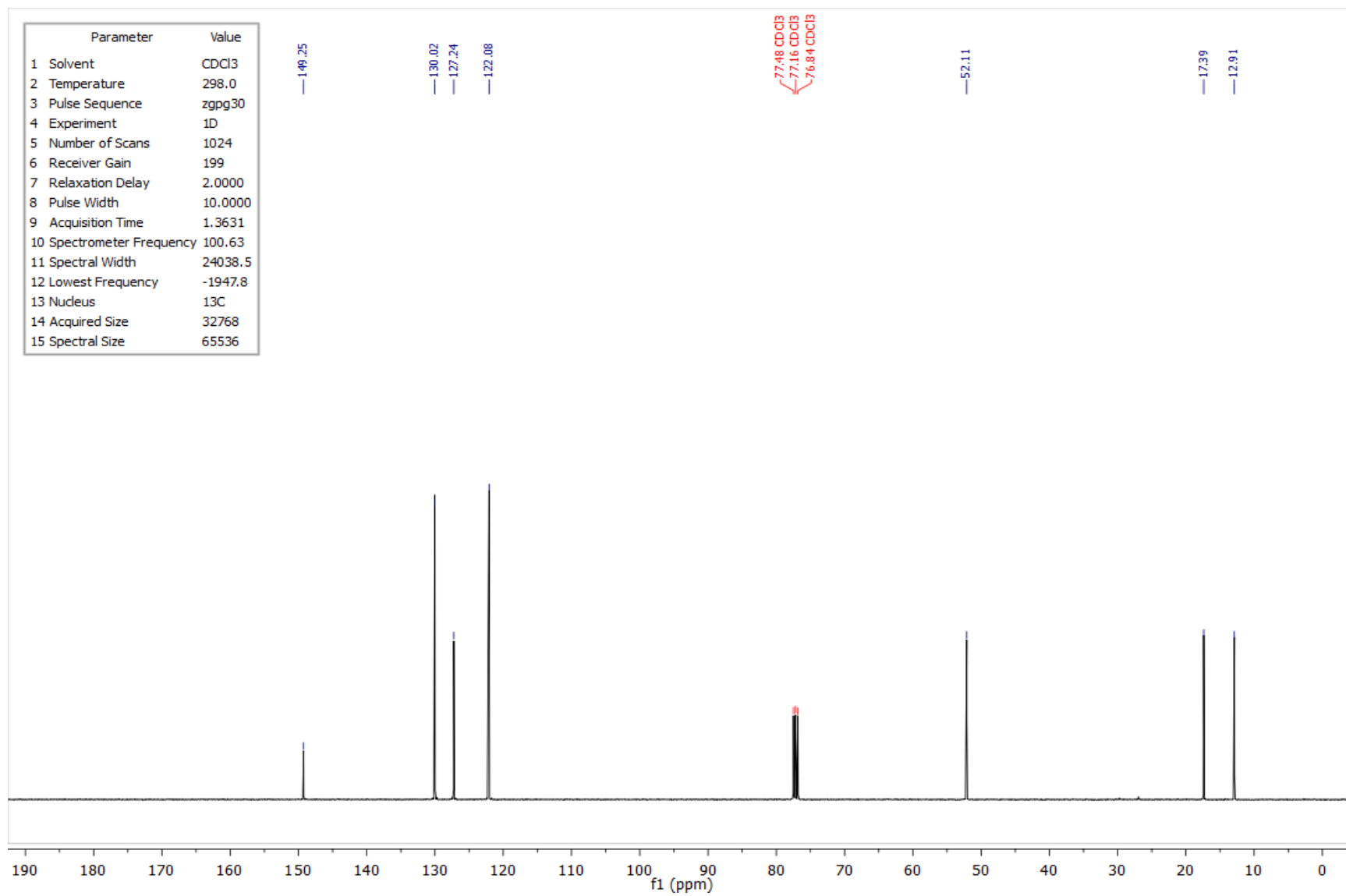


Figure 4.193 – ¹³C NMR spectrum of compound **3.26t-der** in CDCl₃.

4.3.23 ^1H , ^{13}C and ^{19}F NMR spectra of compound 3.26u

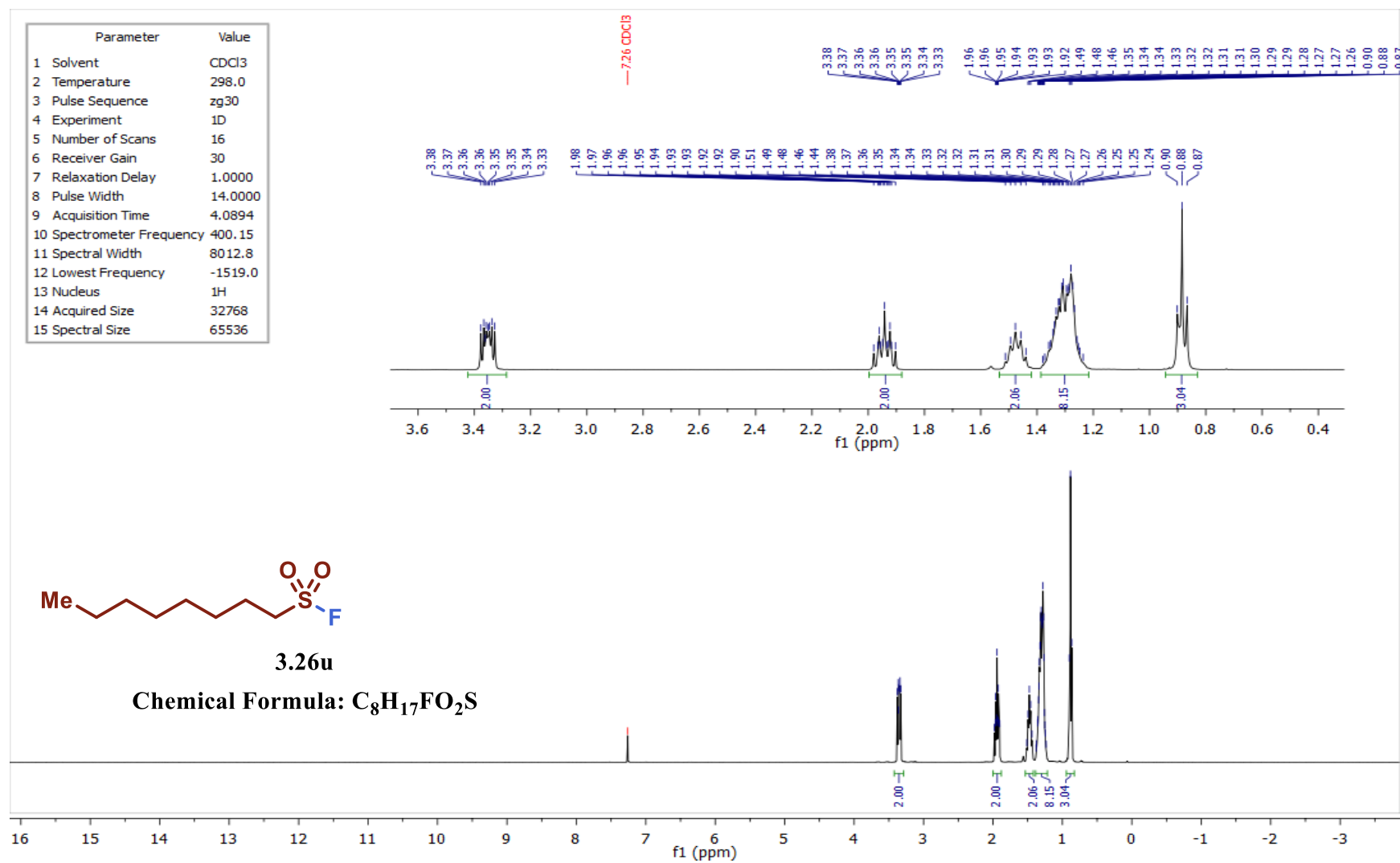


Figure 4.194 – ^1H NMR spectrum of compound 3.26u in CDCl_3 .

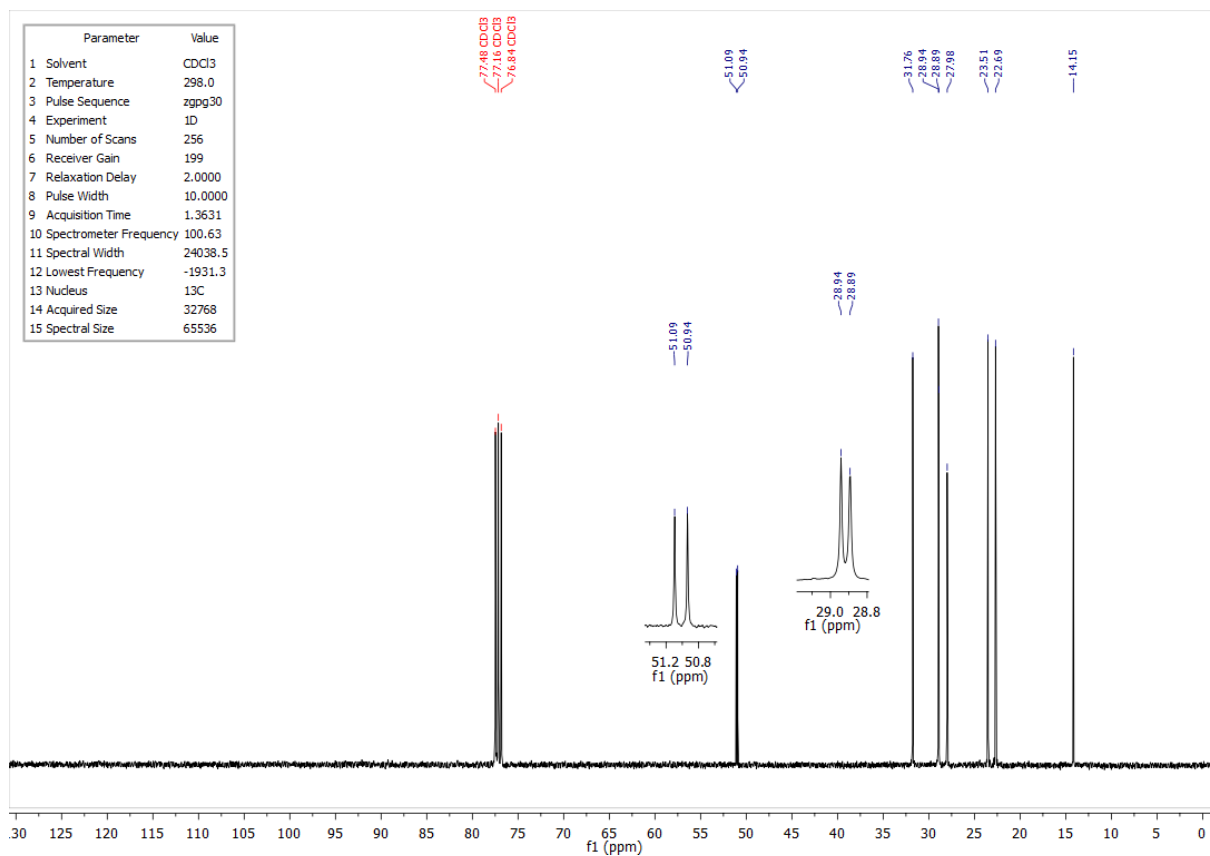


Figure 4.195 – ¹³C NMR spectrum of compound **3.26u** in CDCl₃.

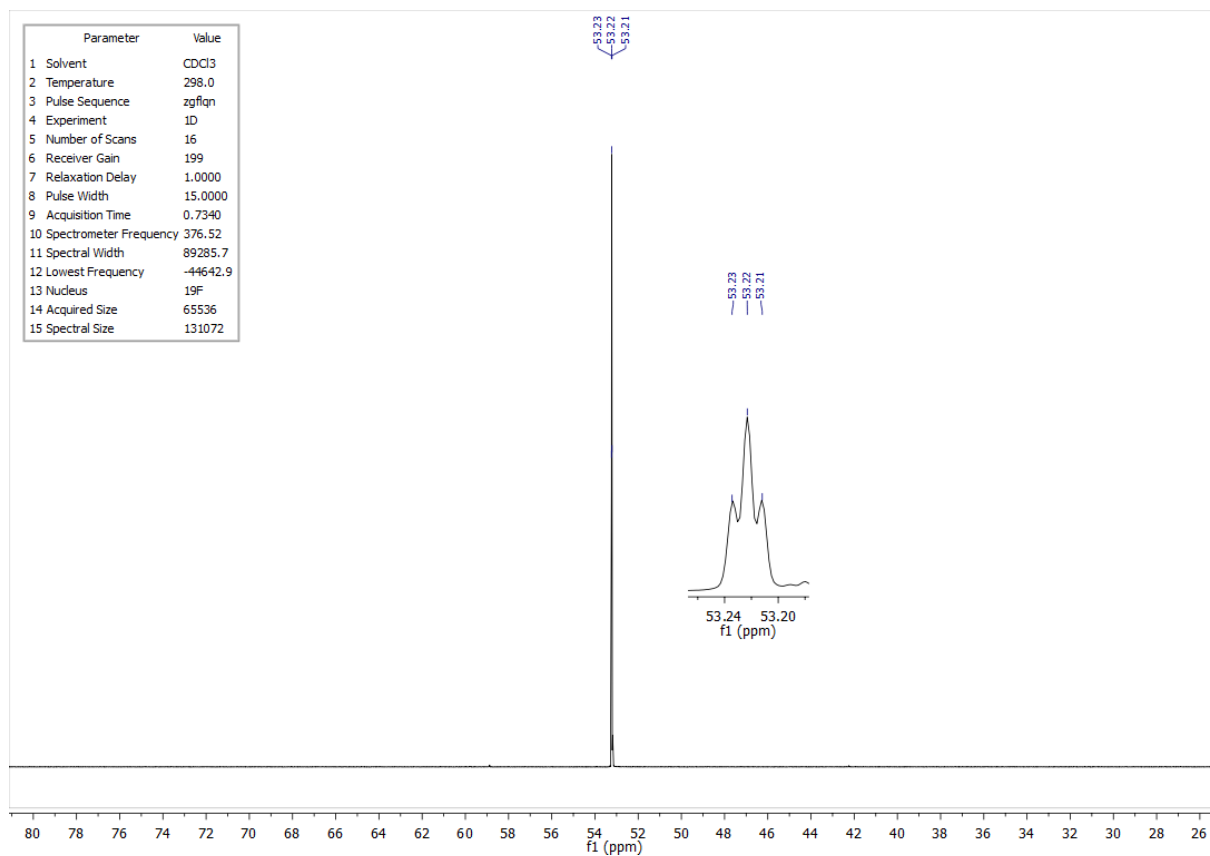


Figure 4.196 – ¹⁹F NMR spectrum of compound **3.26u** in CDCl₃.

4.3.24 ¹H and ¹³C NMR spectra of compound 3.26v-der

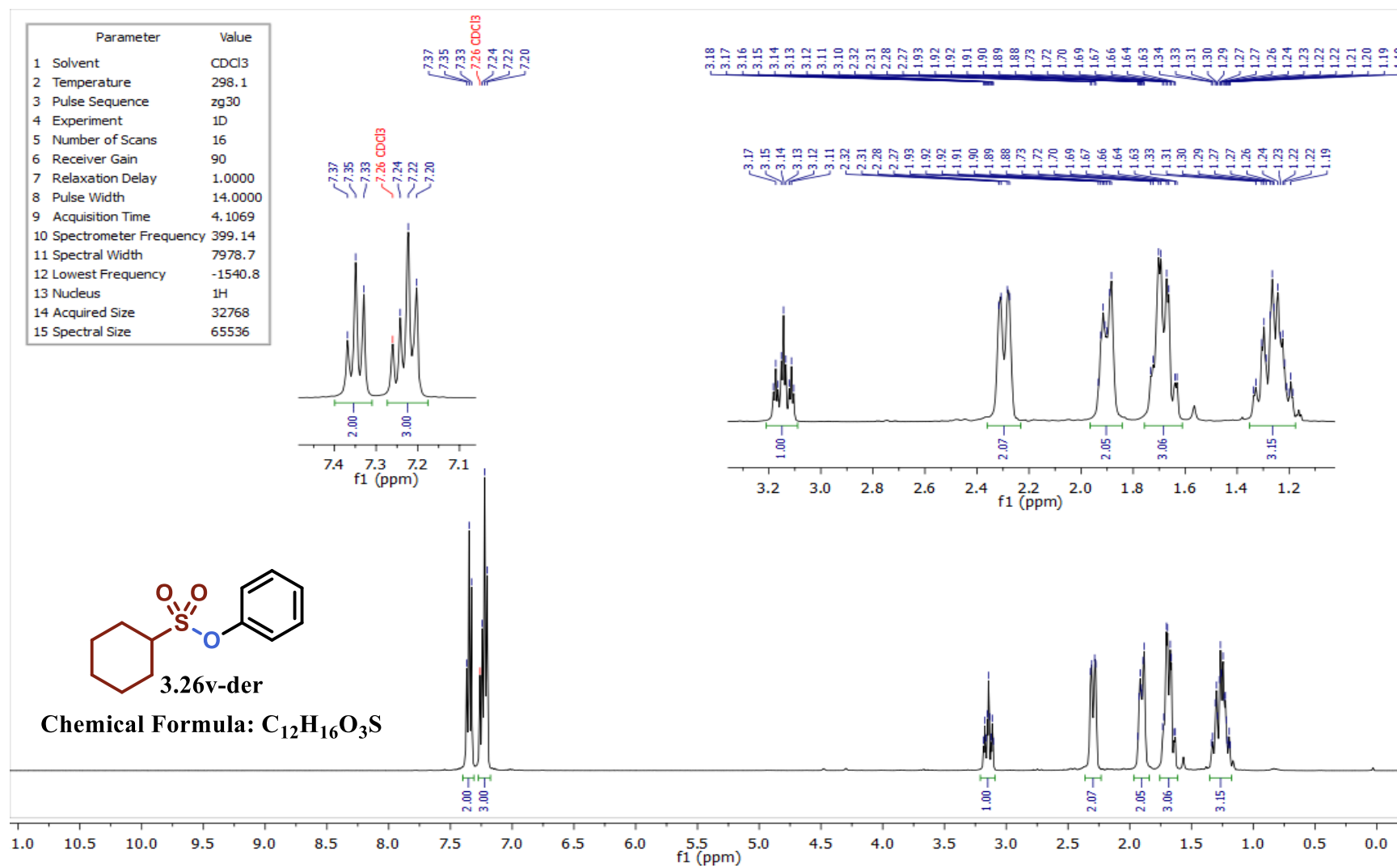


Figure 4.197 – ¹H NMR spectrum of compound 3.26v-der in CDCl₃.

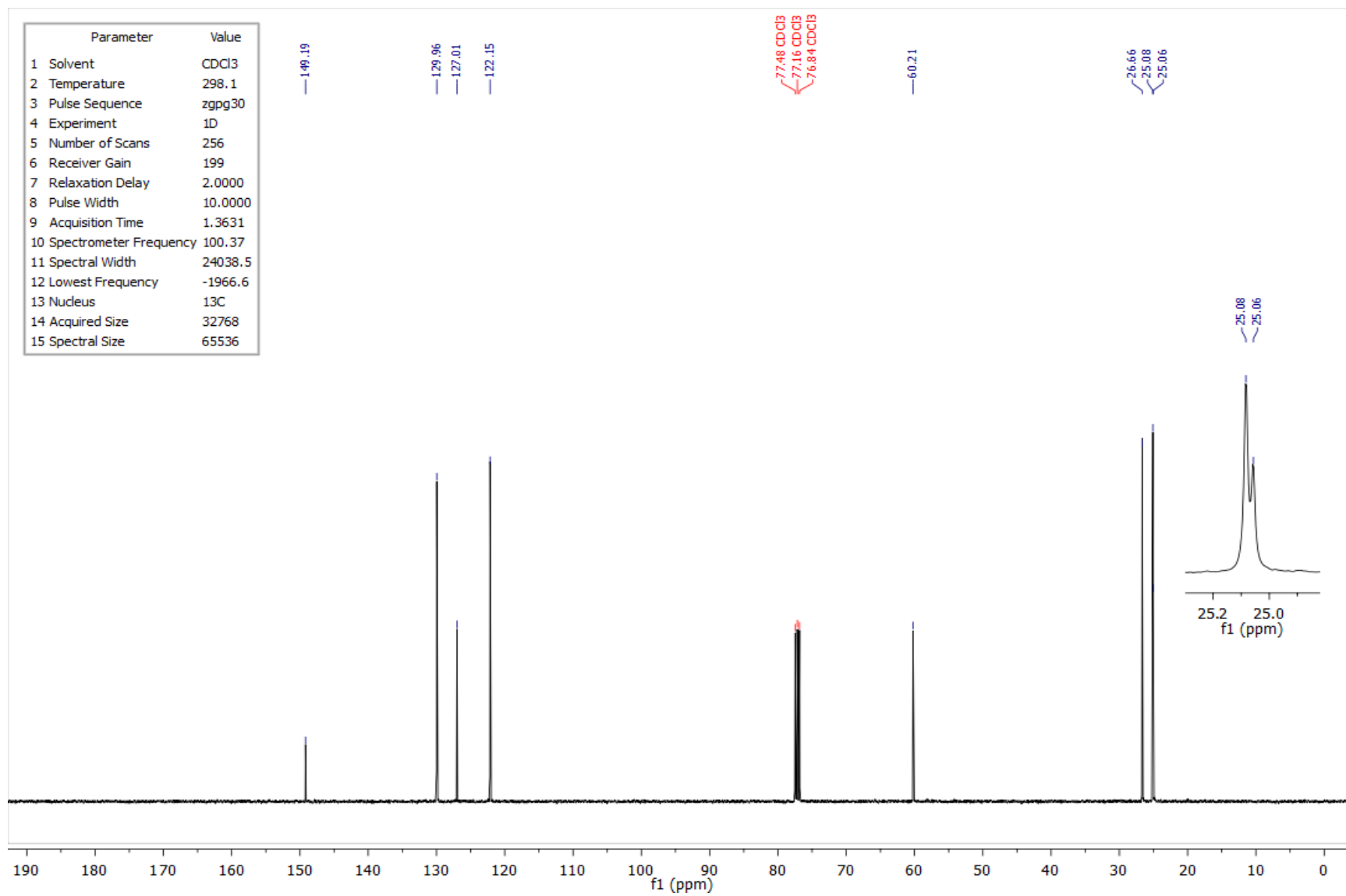


Figure 4.198 – ¹³C NMR spectrum of compound **3.26v-der** in CDCl₃.

4.3.25 ^1H , ^{13}C and ^{19}F NMR spectra of compound 3.26w

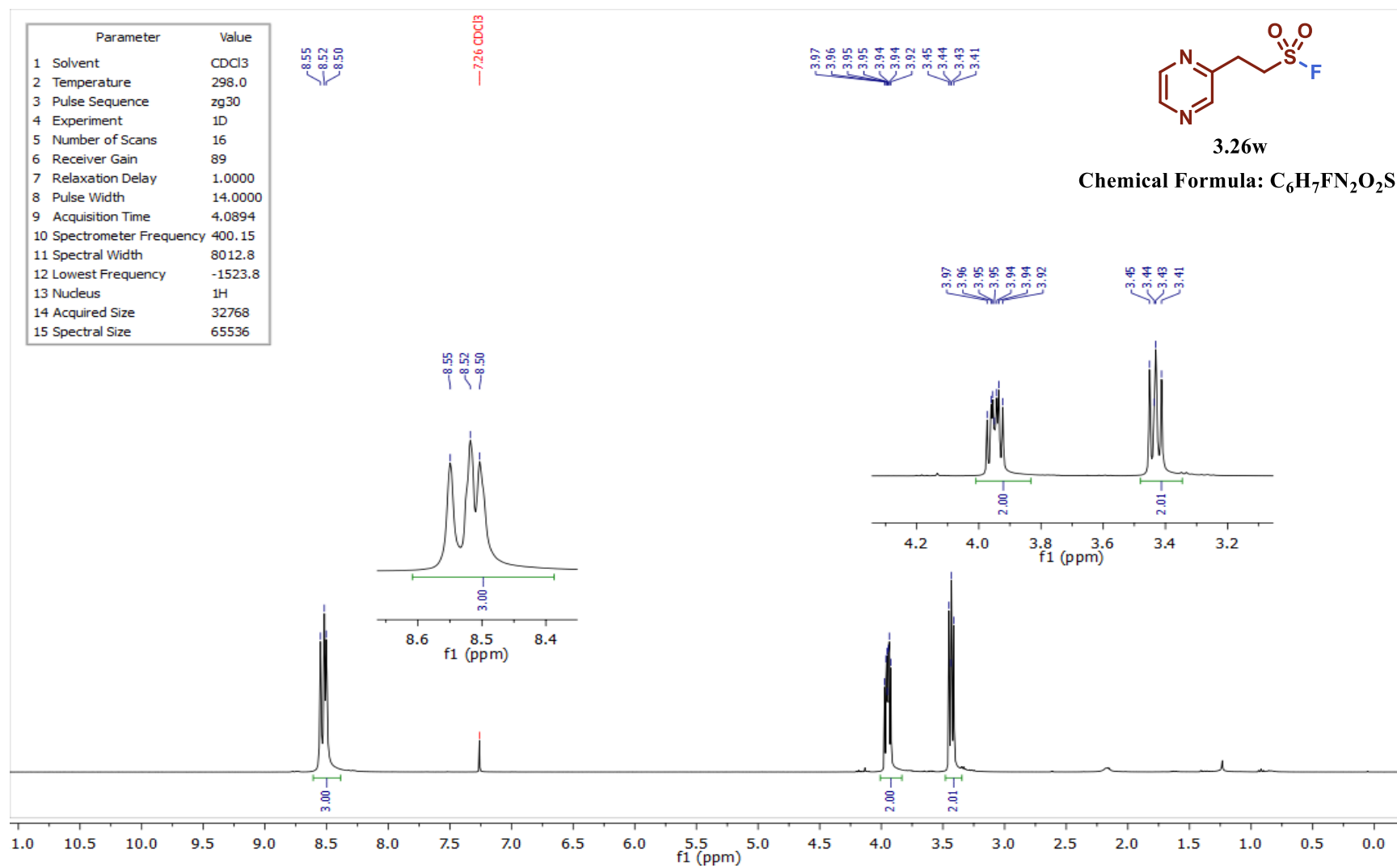


Figure 4.199 – ^1H NMR spectrum of compound 3.26w in CDCl_3 .

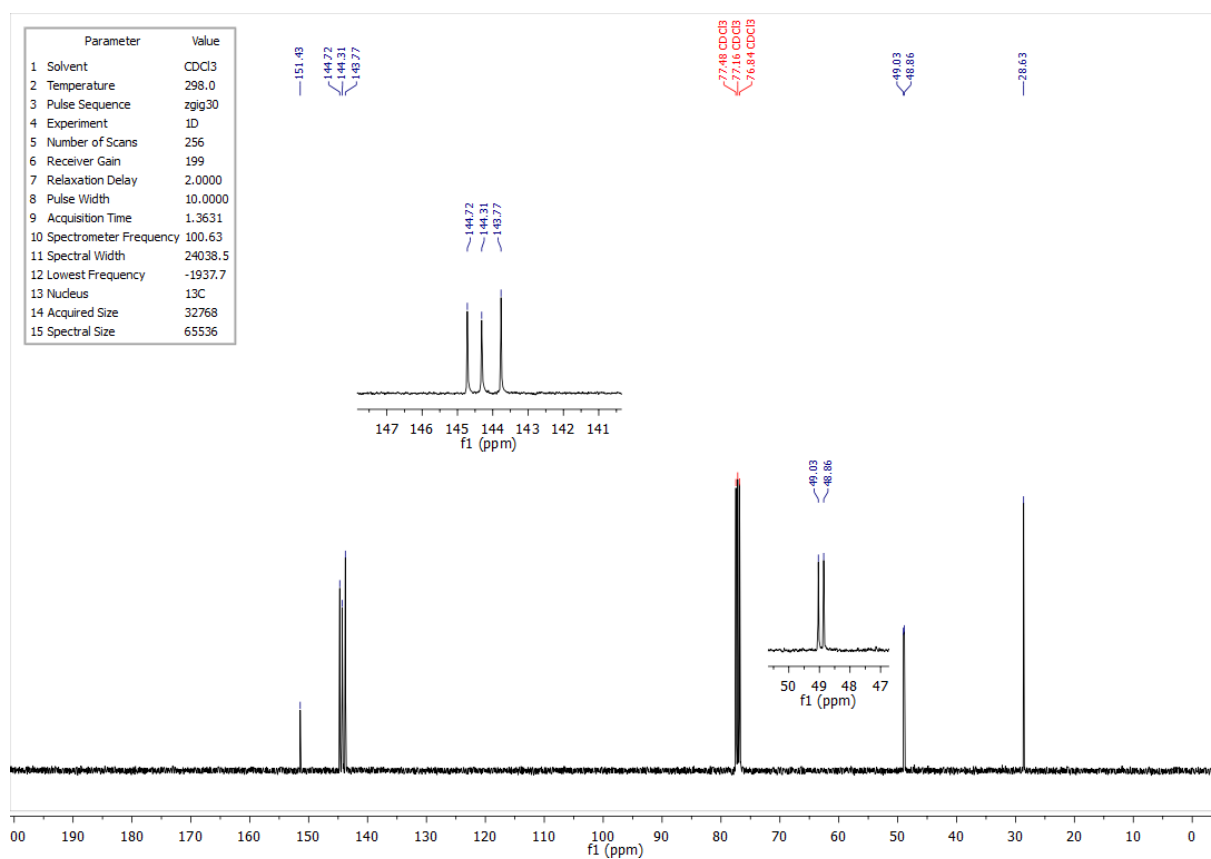


Figure 4.200 – ^{13}C NMR spectrum of compound **3.26w** in CDCl_3 .

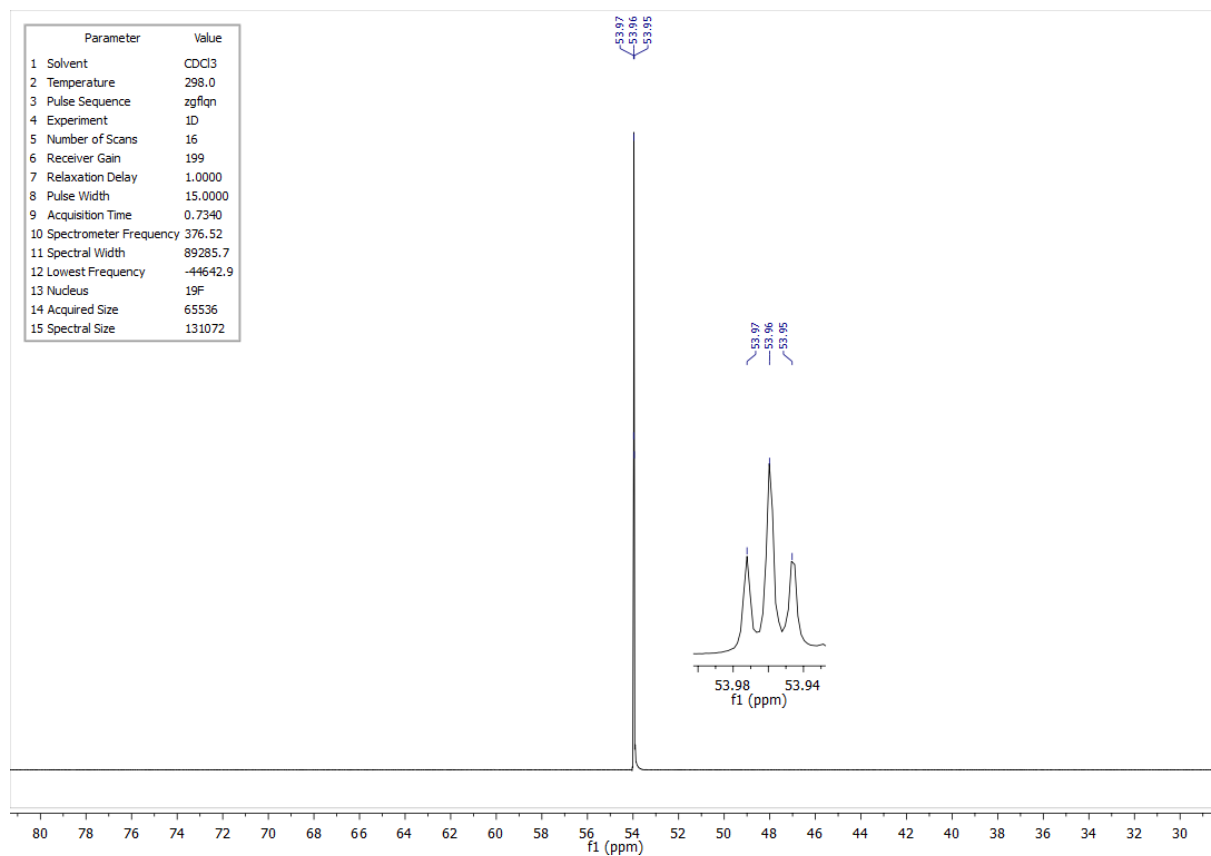


Figure 4.201 – ^{19}F NMR spectrum of compound **3.26w** in CDCl_3 .

4.3.26 ^1H , ^{13}C and ^{19}F NMR spectra of compound 3.26x

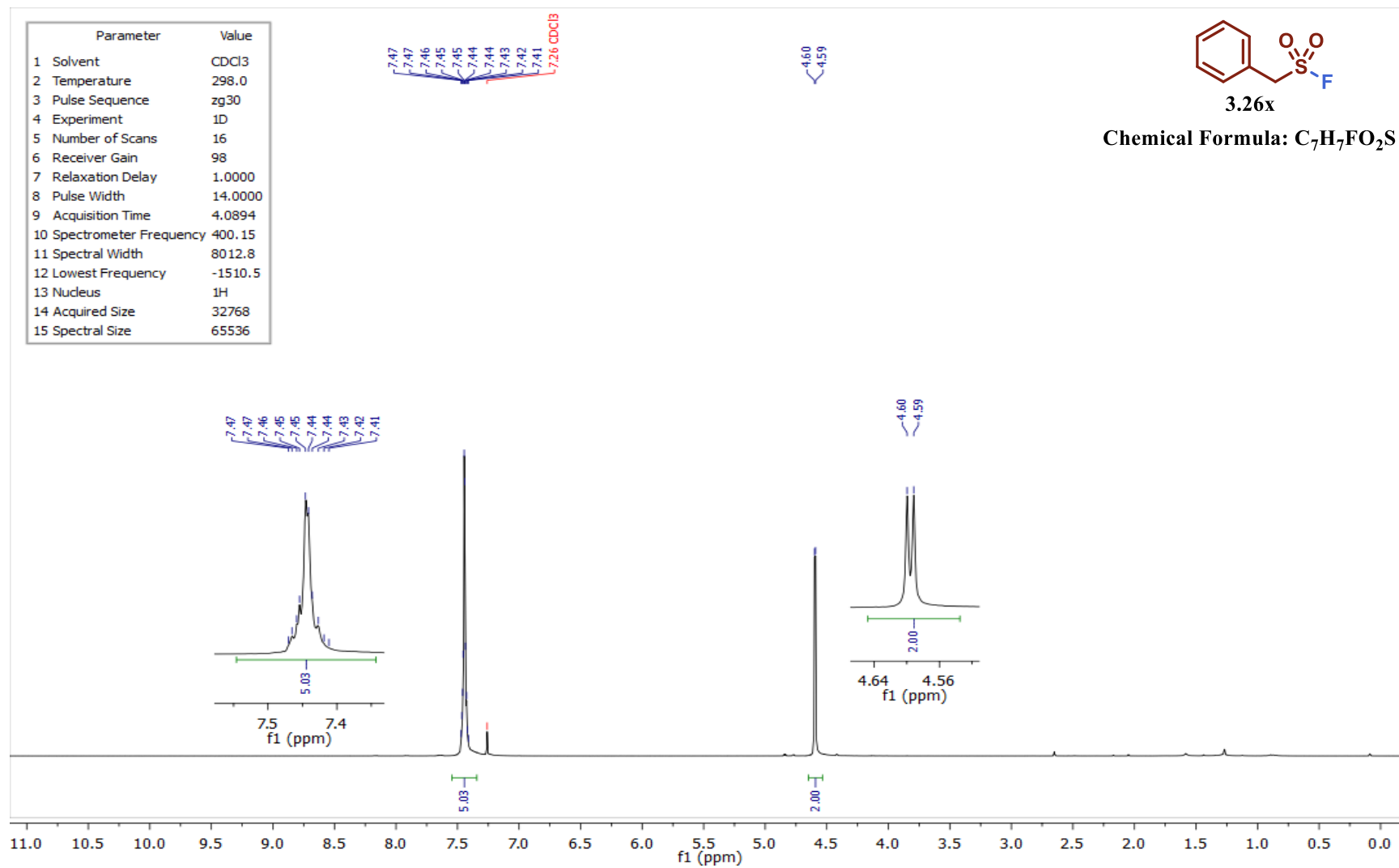


Figure 4.202 – ^1H NMR spectrum of compound 3.26x in CDCl_3 .

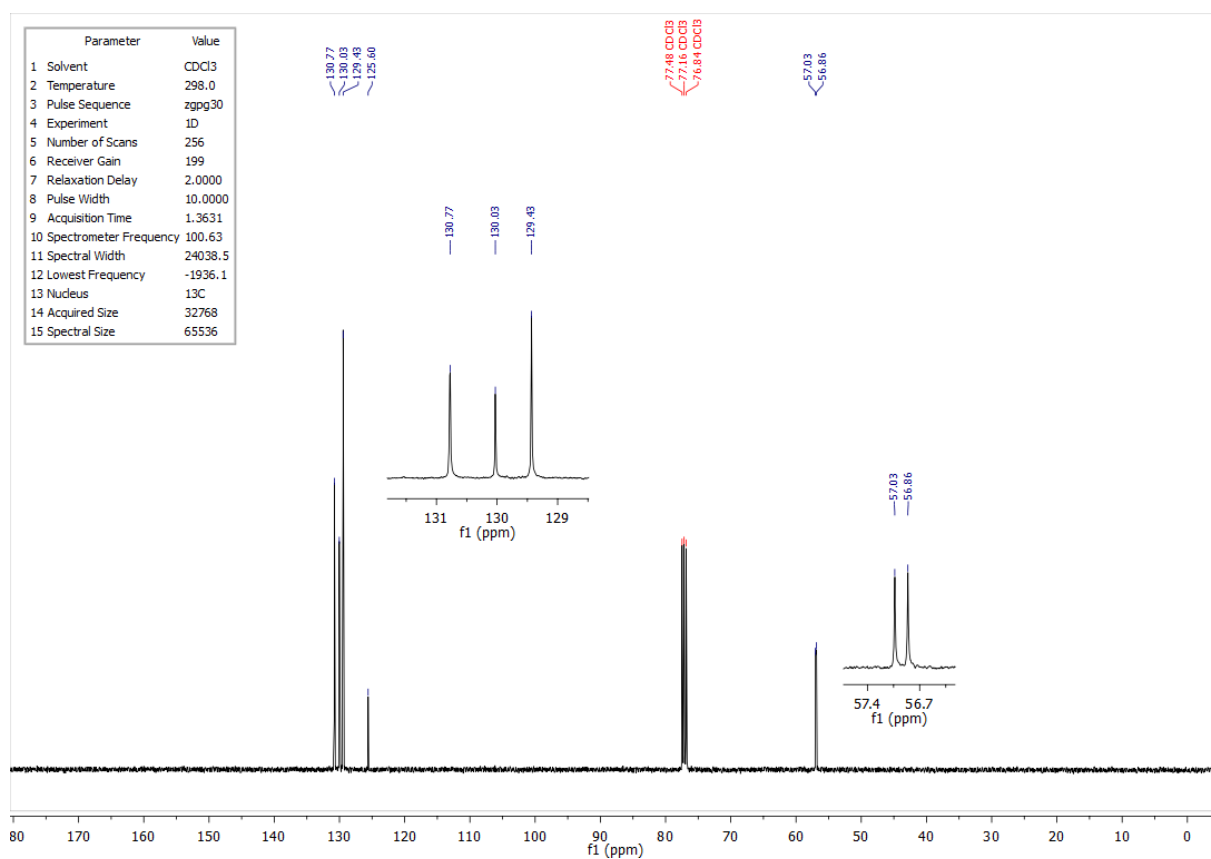


Figure 4.203 – ¹³C NMR spectrum of compound **3.26x** in CDCl₃.

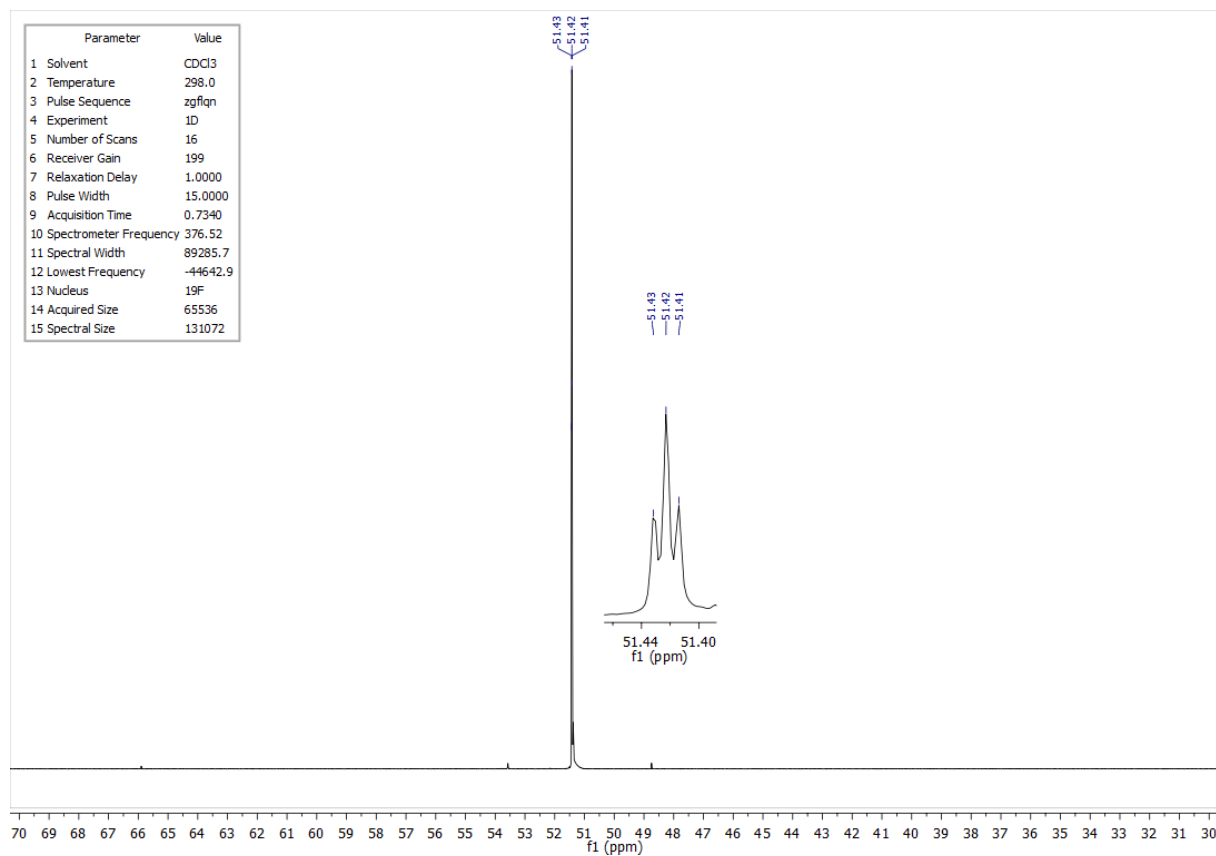


Figure 4.204 – ¹⁹F NMR spectrum of compound **3.26x** in CDCl₃.

4.3.27 ^1H , ^{13}C and ^{19}F NMR spectra of compound 3.26y

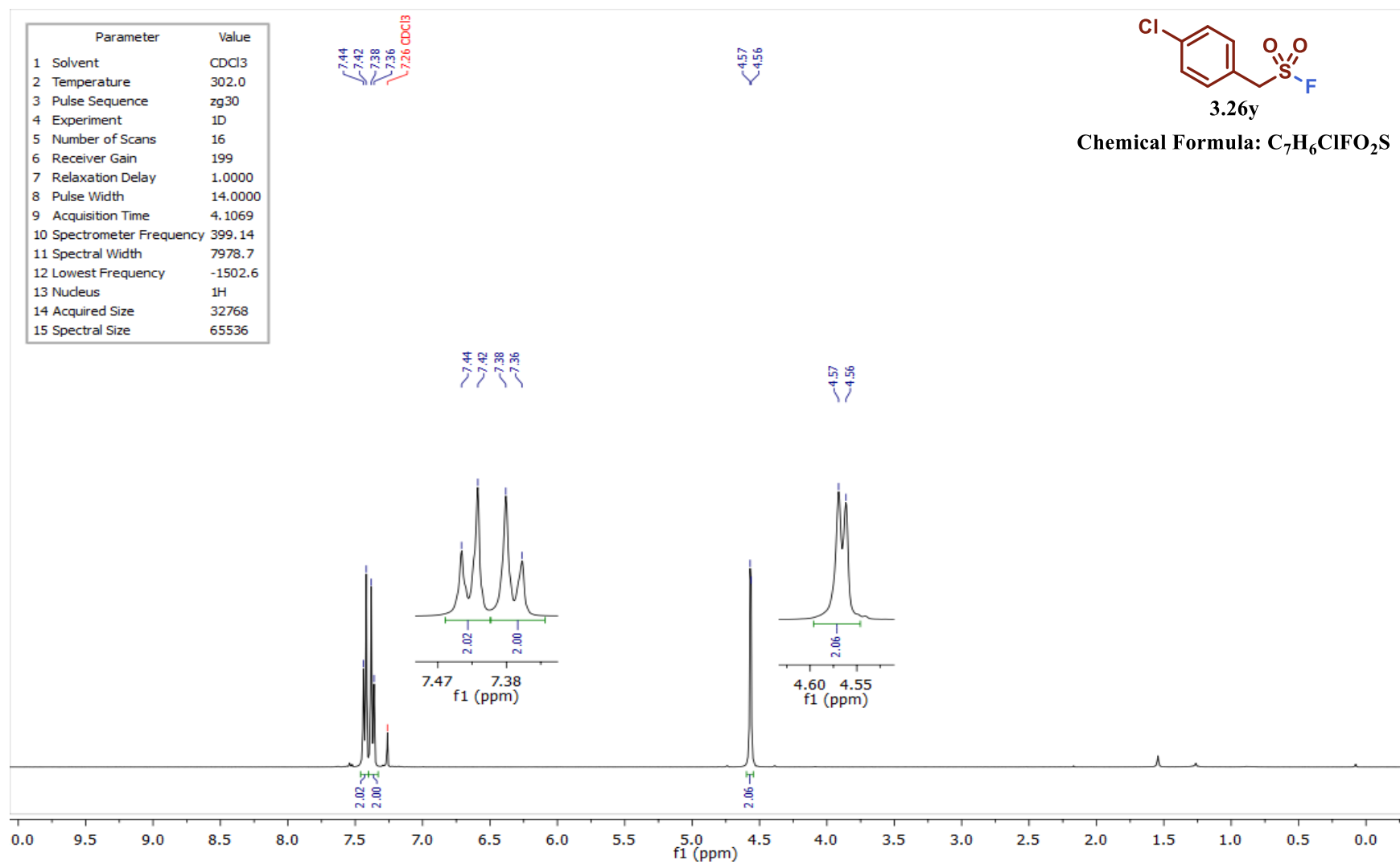


Figure 4.205 – ^1H NMR spectrum of compound 3.26y in CDCl_3 .

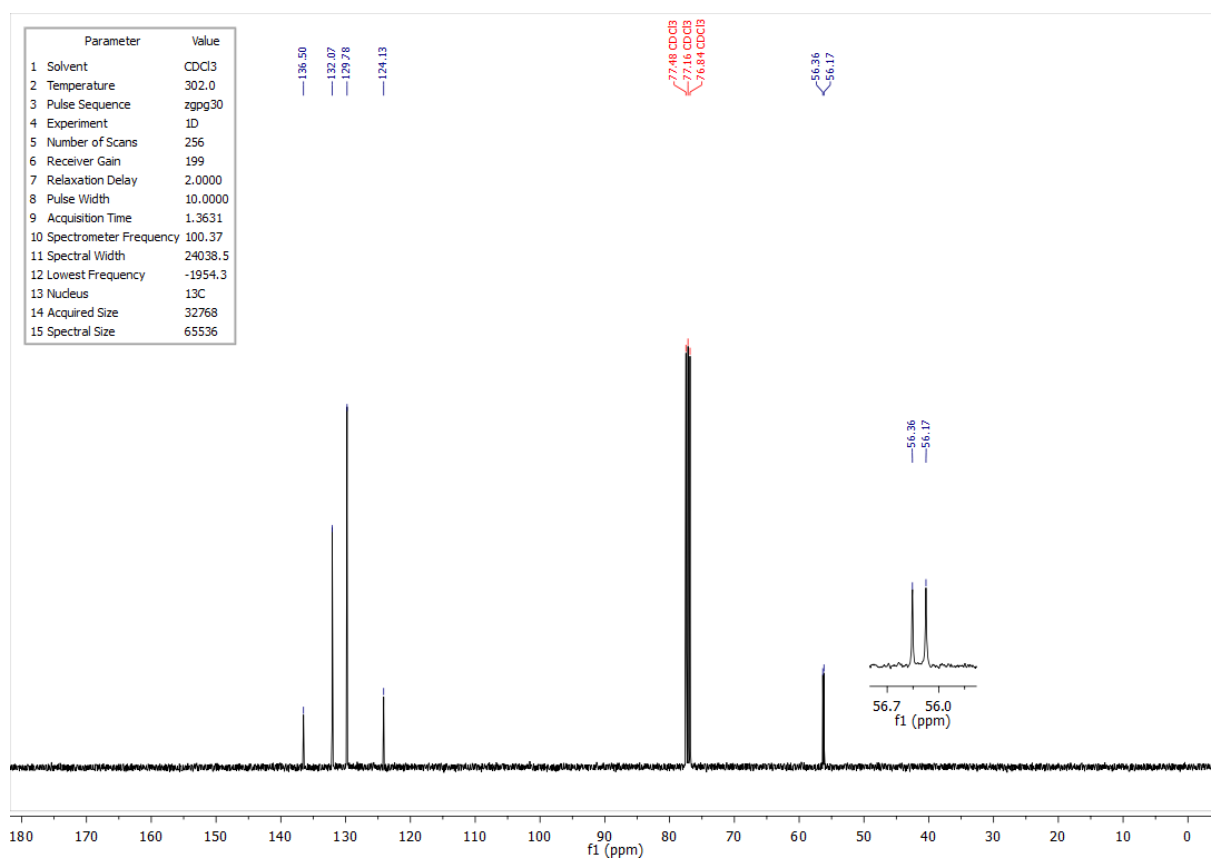


Figure 4.206 – ^{13}C NMR spectrum of compound **3.26y** in CDCl_3 .

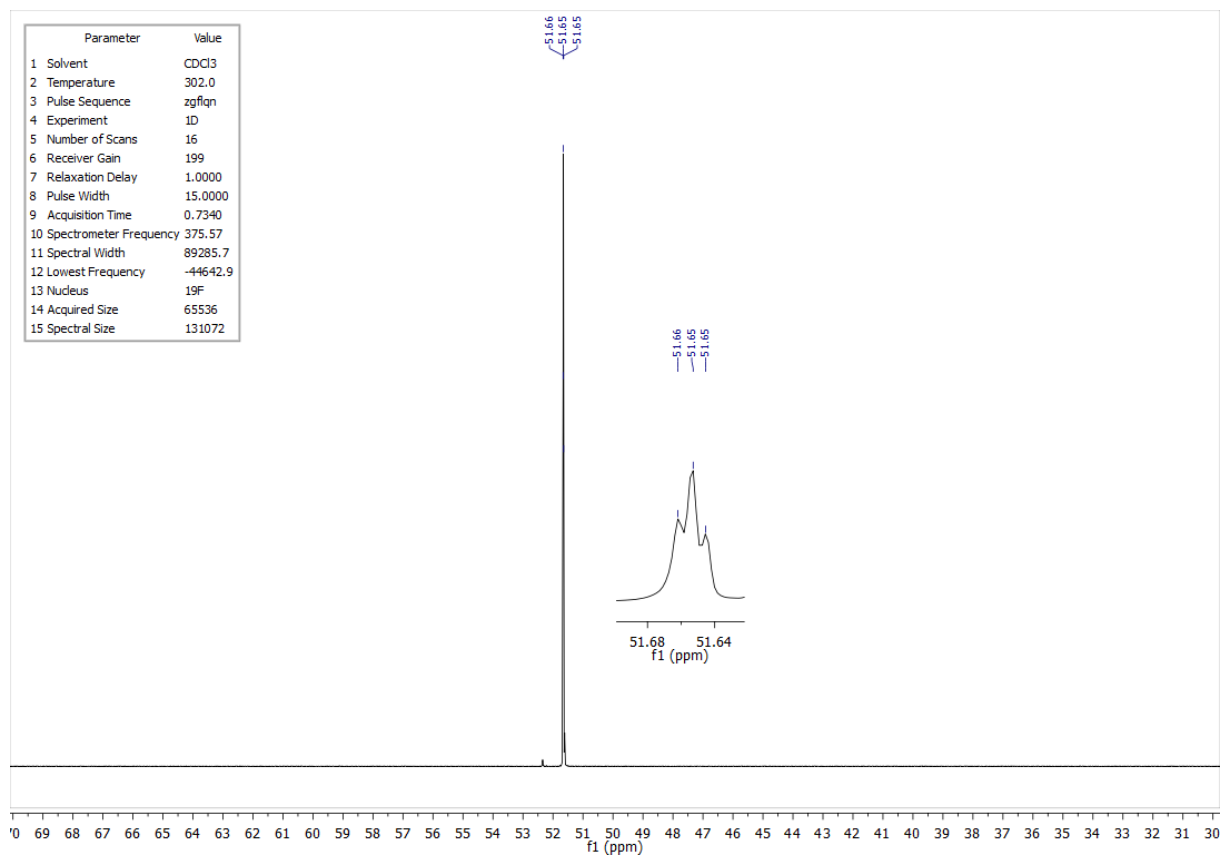


Figure 4.207 – ^{19}F NMR spectrum of compound **3.26y** in CDCl_3 .

4.3.28 ^1H , ^{13}C and ^{19}F NMR spectra of compound 3.26z

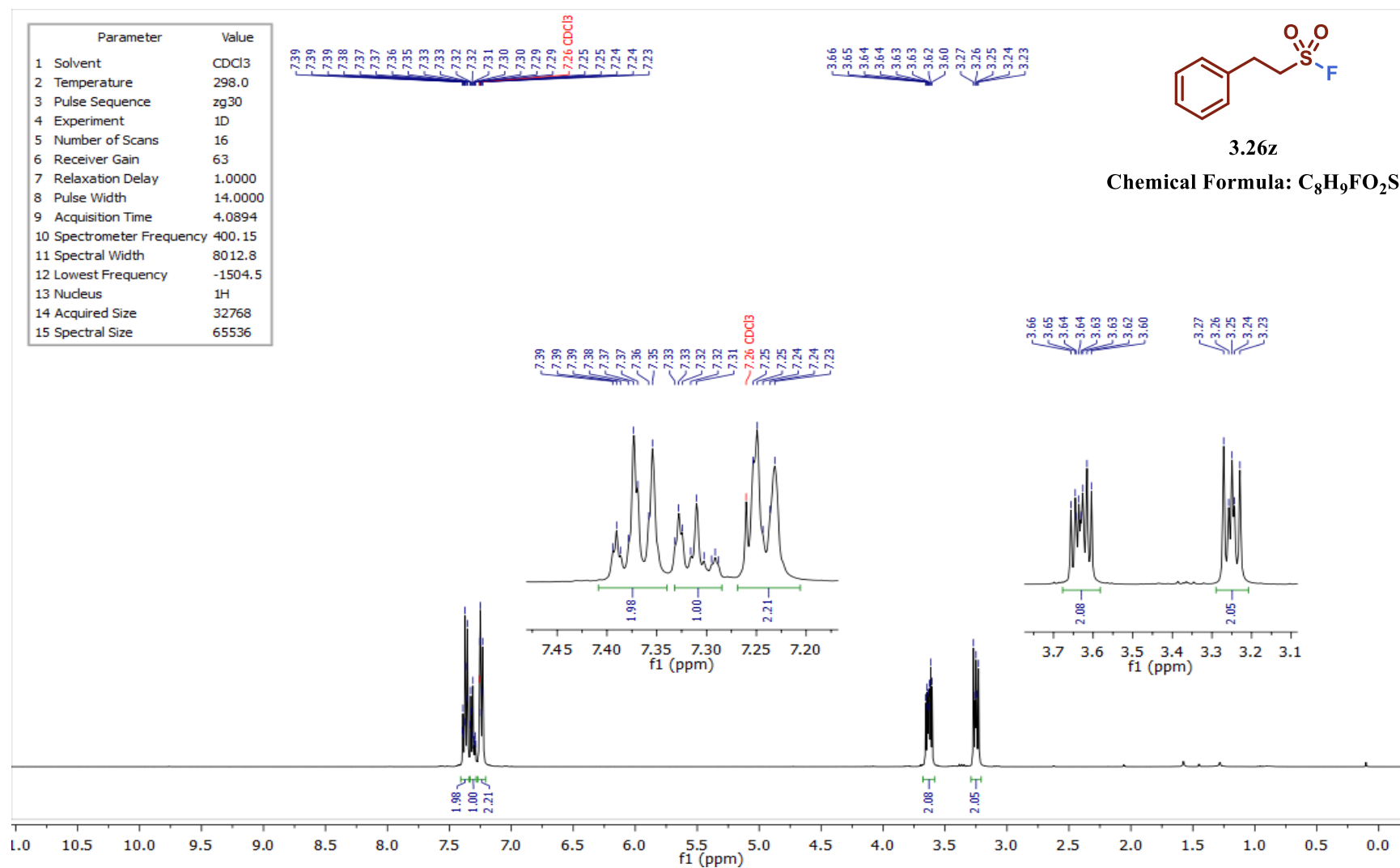


Figure 4.208 – ^1H NMR spectrum of compound 3.26z in CDCl_3 .

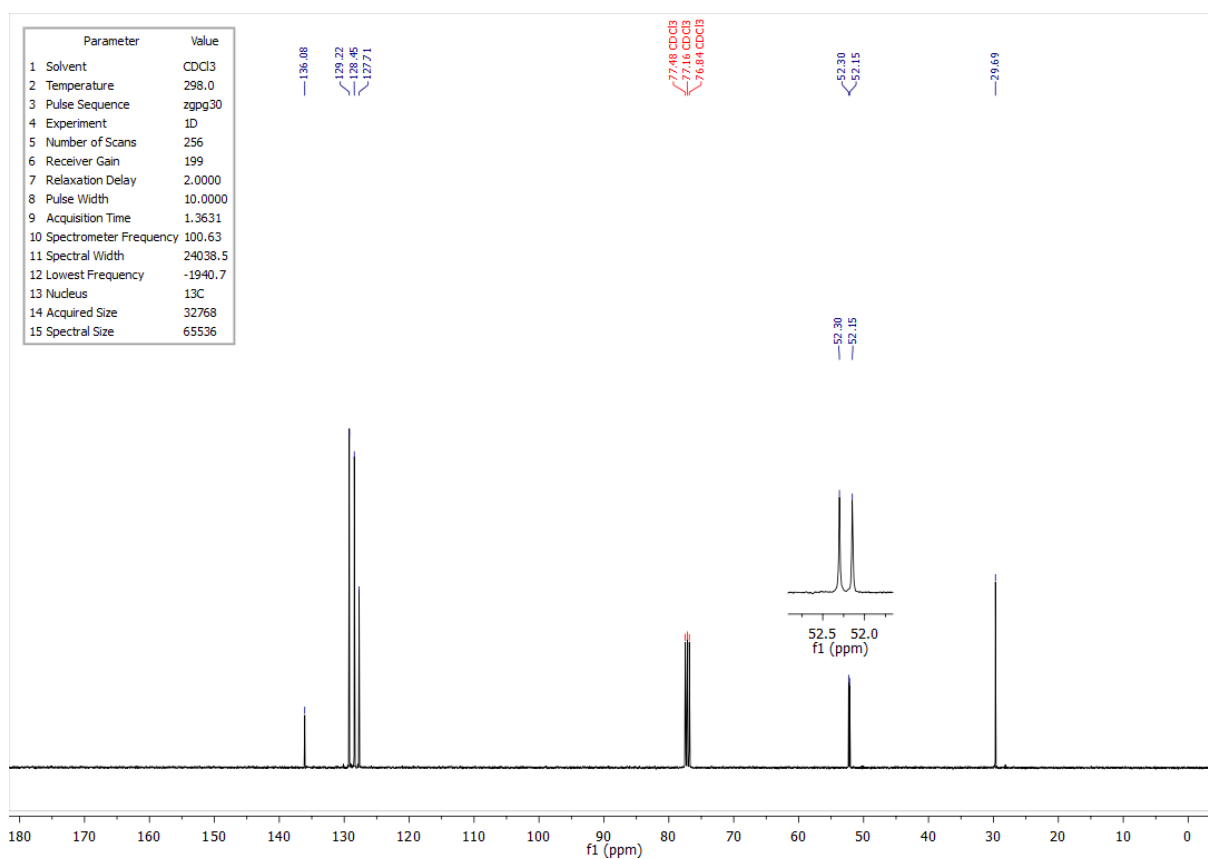


Figure 4.209 – ¹³C NMR spectrum of compound **3.26z** in CDCl₃.

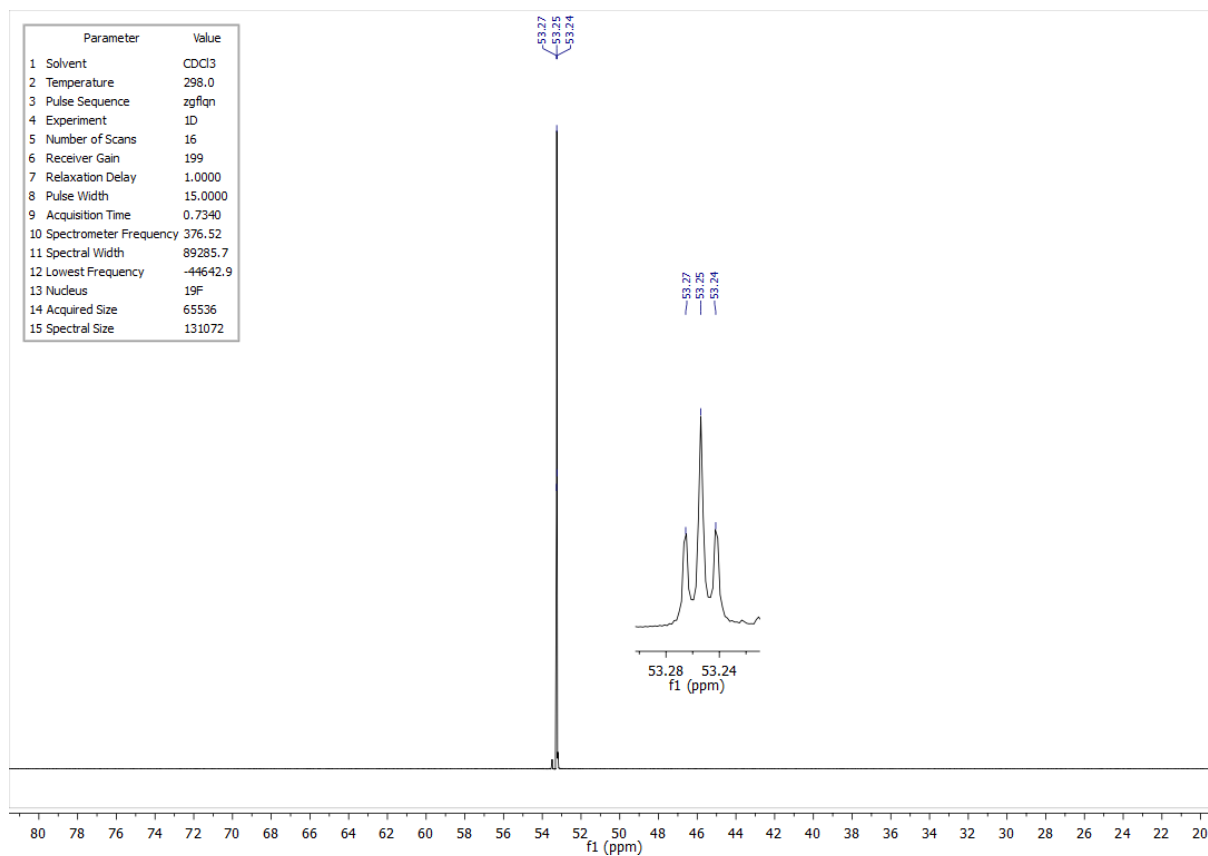


Figure 4.210 – ¹⁹F NMR spectrum of compound **3.26z** in CDCl₃.

4.3.29 ^1H , ^{13}C and ^{19}F NMR spectra of compound 3.26aa

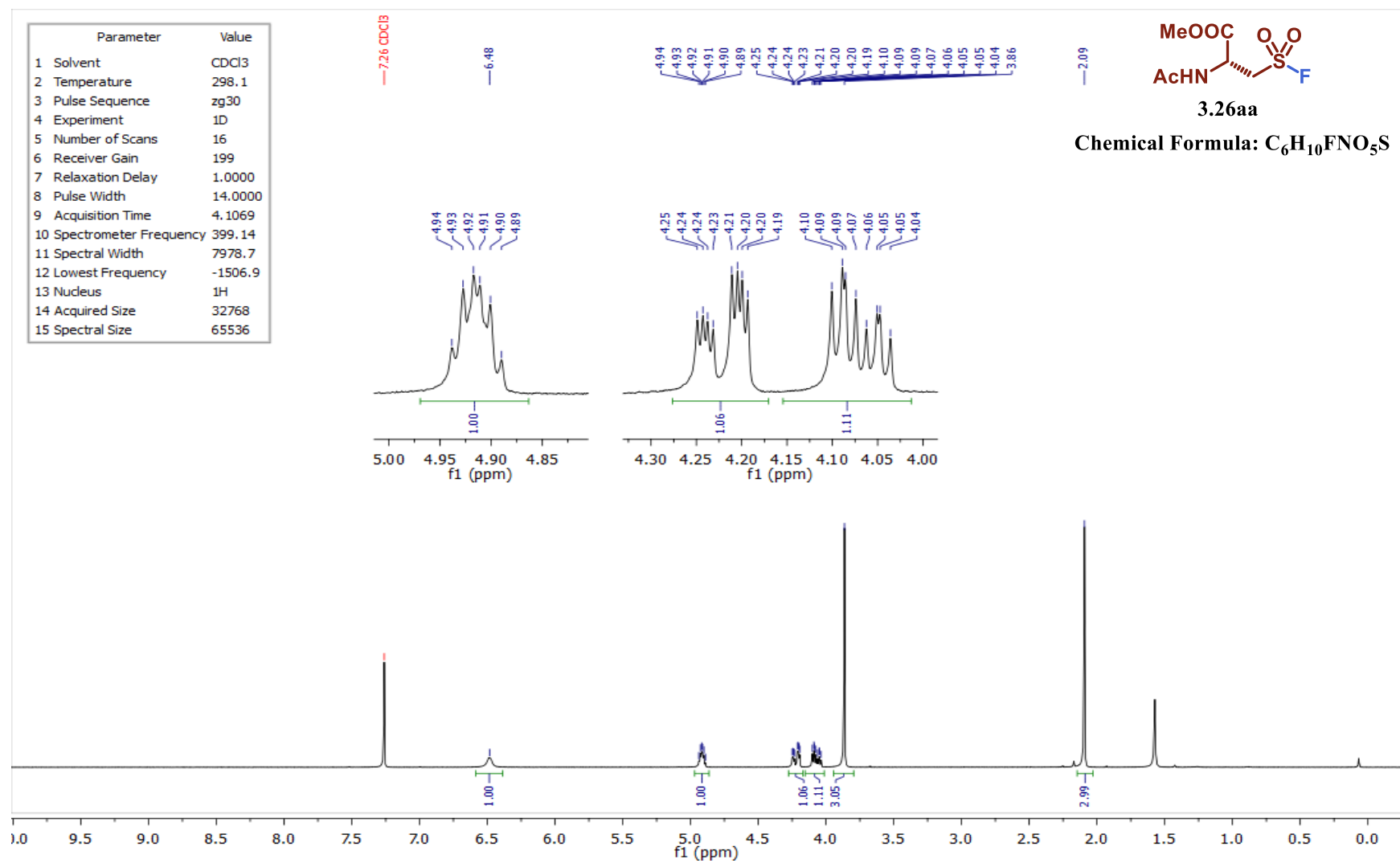
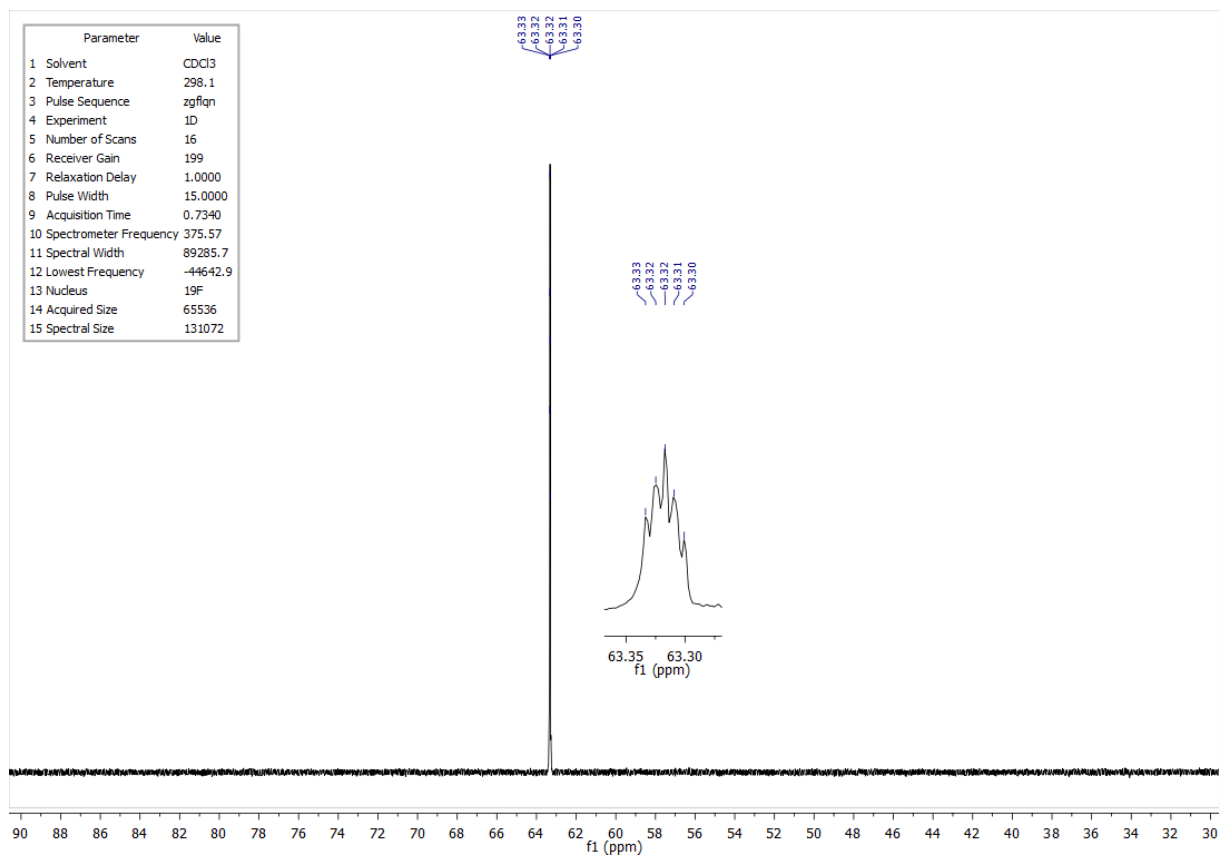
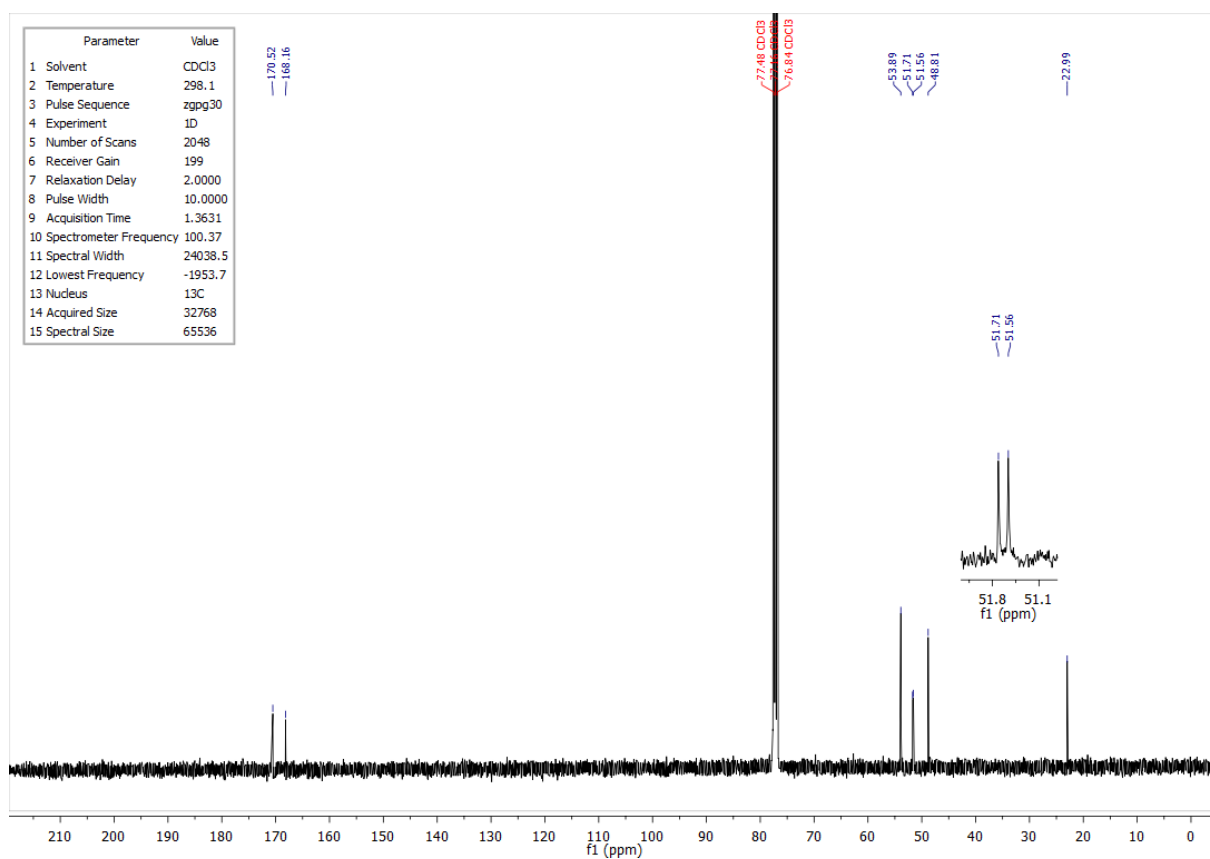


Figure 4.211 – ^1H NMR spectrum of compound 3.26aa in CDCl_3 .



5 Appendix

A List of publications

1. Papers included in the thesis:

BARTOLOMEU, A. A.; BROCKSOM, T. J.; DA SILVA-FILHO, L. C. & DE OLIVEIRA, K. T. “Multicomponent reactions mediated by NbCl₅ for the synthesis of phthalonitrile-quinoline dyads: methodology, scope, mechanistic insights and applications in phthalocyanine synthesis”. *Dyes Pigm.*, 151: 391, 2018.

BARTOLOMEU, A. A.; SILVA, R. C.; BROCKSOM, T. J.; NOËL, T. & DE OLIVEIRA, K. T. “Photoarylation of pyridines using aryldiazonium salts and visible light: an EDA approach”. *J. Org. Chem.*, 84 (16): 10459, 2019.

LAUDADIO, G.; BARTOLOMEU, A. A.; VERWIJLEN, L. M. H. M.; CAO, Y.; DE OLIVEIRA, K. T. & NOËL, T. “Sulfonyl fluoride synthesis through electrochemical oxidative coupling of thiols and potassium fluoride”. *J. Am. Chem. Soc.*, 141 (30): 11832, 2019.

2. Papers published during the Ph.D. period with my collaboration but not included in the thesis:

CAO, Y.; ADRIAENSSENS, B.; BARTOLOMEU, A. A.; LAUDADIO, G.; DE OLIVEIRA, K. T. & NOËL, T. “Accelerating sulfonyl fluoride synthesis through electrochemical oxidative coupling of thiols and potassium fluoride in flow”. *J. Flow Chem.*, 10: 191, 2020.

SILVA, T. L.; BARTOLOMEU, A. A.; DE JESUS, H. C.; DE OLIVEIRA, K. T.; FERNANDES, J. B.; BRÖMME, D. & VIEIRA, P. C. “New synthetic quinolines as Cathepsin K inhibitors”. *J. Braz. Chem. Soc.*, 31 (8): 1605, 2020.

SILVA, R. C.; DA SILVA, L. O.; **BARTOLOMEU, A. A.**; BROCKSOM, T. J. & DE OLIVEIRA, K. T. “Recent applications of porphyrins as photocatalysts in organic synthesis: batch and continuous flow approaches”. *Beilstein J. Org. Chem.*, 16: 917, 2020.

OŠEKA, M.; LAUDADIO, G.; VAN LEEST, N. P.; DYGA, M.; **BARTOLOMEU, A. A.**; GOOßEN, L. J.; DE BRUIN, B.; DE OLIVEIRA, K. T.; NOËL, T. “Electrochemical aziridination of internal alkenes with primary amines”. *J. Am. Chem. Soc.*, 2020. (submitted)

B Participation in events

BARTOLOMEU, A. A.; BROCKSOM, T. J. & DE OLIVEIRA, K. T. “Synthesis of phthalonitrile building blocks using a multicomponent reaction and niobium pentachloride as catalyst.” In: 39^a Reunião Anual da Sociedade Brasileira de Química (SBQ), 2016, Goiânia, Brazil. (Poster presentation)

6^a Escola Superior em Síntese Orgânica (ESSO), 2016, Juiz de Fora, Brazil.

BARTOLOMEU, A. A.; BROCKSOM, T. J.; DA SILVA-FILHO, L. C. & DE OLIVEIRA, K. T. “Synthesis of phthalonitrile building blocks using a multicomponent reaction promoted by niobium pentachloride”. In: 46th World Chemistry Congress (IUPAC) and 40^a Reunião Anual da Sociedade Brasileira de Química (SBQ), 2017, São Paulo, Brazil. (Poster presentation)

BARTOLOMEU, A. A.; NOËL, T. & DE OLIVEIRA, K. T. “Photoarylation of quinolines without photocatalysts by using aryldiazonium salts: and EDA complex approach”. In: Photo4Future Conference, 2018, Eindhoven, The Netherlands. (Poster presentation)

C Disciplines

Química Orgânica Avançada – Grade: A

Mecanismo de Reações Orgânicas – Grade: A

Estágio Supervisionado de Capacitação Docente em Química 1 – Grade: A

Síntese Orgânica – Grade: A